THE UNIVERSITY
of EDINBURGH

Assessing atmospheric composition impacts using a chemical climatology framework: Case studies at the UK monitoring supersites

Christopher Malley

A thesis submitted in fulfilment of the requirements
for the degree of Doctor of Philosophy
to the
University of Edinburgh

2015

Abstract

In the mid-1800s, monitoring networks were established to investigate atmospheric composition impacts, and the conditions giving rise to them. The development of these networks, in terms of coordination and standardisation between contributing sites, has resulted in large advances in knowledge of the nature of atmospheric composition. Currently thousands of sites collect high quality atmospheric composition measurements globally. This thesis contends that in order to maximise the information derived from these measurements, a further advancement in standardisation is required to encompass the interpretation of monitoring network data. Currently there are limited examples of a common interpretation of data applied across all sites in a monitoring network, especially in relation to specific atmospheric composition impacts. In this thesis, a 'chemical climatology' framework is outlined which provides a common basis for targeting analysis towards identifying the linkage between a specific atmospheric composition impact and its causal drivers. Case studies apply the chemical climatology framework to demonstrate its utility in deriving scientific and policy relevant conclusions using measurement data from the UK monitoring supersites located at Harwell and Auchencorth. Prior to this, the representativeness of each site is quantified through the application of cluster analysis to ozone data at 100 rural European sites to identify groupings of sites with similar ozone variation. Harwell was representative of rural locations within 120 km of London, while Auchencorth was representative of a larger, transboundary spatial domain including the remainder of the rural UK.

The first case study links the impact of ozone on human health (quantified by SOMO10 and SOMO35 metrics) and vegetation (flux-based POD_Y) to meteorological and emissions drivers. Between 1990 and 2013 at Harwell, there was a significant decrease in the contribution of European ozone to determining the impacts. Improvement in the human health impact was heavily dependent on the choice of metric (SOMO35 decreased, no change in SOMO10), and the vegetation impacts had not improved as

high ozone episodes frequently coincided with plant conditions which reduced ozone uptake. These chemical climates emphasise the need for ozone mitigation on larger (hemispheric) scales than currently implemented. Secondly, the impact of 27 measured VOCs on the extent of the regional ozone increment is assessed. The photochemical loss of VOCs is then linked to reported gridded VOC emissions using air mass back trajectory analysis. Ethene and m+p-xylene had the largest diurnal photochemical loss during maximum monthly regional ozone increment, but the key conclusion was the limitation introduced through the reporting of gridded VOC emissions in heavily aggregated source sectors. Finally, the conditions producing the long term health impact of particulate matter (quantified by annual average PM_{10} and $PM_{2.5}$ concentrations) at each site are derived through integration of measurements of PM_{10} and $PM_{2.5}$ with measurements of PM constituents. It is shown that the frequent, moderate PM_{10} and $PM_{2.5}$ concentrations made a larger contribution to annual average values compared to the relatively infrequent high, episodic concentrations. The contribution of PM constituents and the contribution of local vs regional emissions to the range of PM concentrations is investigated. It was concluded that similar reductions in the contribution of secondary inorganic aerosol to the moderate PM_{10} and $PM_{2.5}$ concentrations could be achieved from both the reduction of frequently traversed, smaller emissions sources, and less frequently traversed, larger emissions sources.

The final chapter demonstrates the benefits from the extension of this framework to an entire monitoring network. It is envisioned that for each atmospheric composition impact, a standard set of statistics would be calculated which quantify the ‘impact’, ‘state’ and ‘drivers’ of that chemical climate. Calculation of ozone human health chemical climates across 100 European monitoring sites demonstrate this concept. This standardised interpretation of monitoring network data not only allows consistent comparison of an impact, but the common basis for determining how the impact is derived allows for the consideration of novel mitigation strategies and their spatial applicability.

Lay Summary

This thesis presents a methodology, called ‘chemical climatology’, aimed at maximising the information derived from atmospheric composition monitoring networks. Currently thousands of sites collect high quality measurements globally to investigate atmospheric composition impacts (e.g. on human health or vegetation), and the conditions giving rise to them. In this thesis, the ‘chemical climatology’ framework is outlined which provides a common basis for targeting analysis towards identifying the linkage between a specific atmospheric composition impact and its causal drivers. Case studies apply the chemical climatology framework to demonstrate its utility in deriving scientific and policy relevant conclusions using measurement data from the UK monitoring supersites located at Harwell and Auchencorth. Prior to this, the geographic area for which each site is representative is calculated through comparison of measurement data across 100 rural European sites. Harwell was representative of rural locations within 120 km of London, while Auchencorth was representative of a larger, transboundary spatial domain including the remainder of the rural UK.

Ozone is not directly emitted into the atmosphere but is formed from the chemical reaction of nitrogen oxides (NO_x) and volatile organic compounds (VOCs), which are directly emitted from both natural and human activities. Once formed, ozone can have negative human health and vegetation impacts. The first case study links the impact of ozone on human health and vegetation to meteorological and emissions drivers. Between 1990 and 2013 at Harwell, there was a significant decrease in the contribution of European ozone to determining the impacts, but improvement in the human health impact was heavily dependent on the choice of metric, and the vegetation impacts had not improved. These chemical climates emphasise the need for ozone mitigation on larger (hemispheric) scales than currently implemented. Secondly, the contribution of 27 measured VOCs to the production of European ozone is quantified and then linked to spatially gridded VOC emissions. It was concluded emission controls of a large number of VOCs, and targeting VOCs with highest contribution, are both required to

reduce European ozone. Finally, the long term health impact of particulate matter (PM), and the conditions producing it are evaluated through the integration of PM measurements with measurement of the different components of PM. The frequent, moderate PM concentrations made a larger contribution to the long term health impact metrics compared to the relatively infrequent high, episodic concentrations. These moderate concentrations occured during a wide range of conditions, and hence to reduce the long term health impact of PM, a large number of different geographic emission sources must be mitigated.

The final chapter demonstrates the benefits from the extension of this framework to an entire monitoring network. It is envisioned that for each atmospheric composition impact, a standard set of statistics would be calculated which quantify the ‘impact’, ‘state’ and ‘drivers’ of that chemical climate. Calculation of chemical climates across 100 European monitoring sites for the human health impact of ozone demonstrates this concept. This standardised interpretation of monitoring network data not only allows consistent comparison of an impact, but the common basis for determining how the impact is derived allows for the consideration of novel mitigation strategies and their spatial applicability.

Declaration

I declare that this thesis has been composed by myself and is all my own work except where explicitly indicated otherwise. The work has not been submitted for any other degree or professional qualification.

Chris Malley
October 2015

Acknowledgements

Firstly I would like to thank my supervisors, Dr Mathew Heal and Dr Christine Braban. I owe them an enormous debt of gratitude for the help, support and guidance they have given me throughout my PhD, the highlight of which have been the regular, insightful discussions we have had which never failed to provide new ideas and perspective. I would also like to thank them for supporting my PhD financially, and encouraging my attendance at conferences and workshops.

Colleagues at CEH provided substantial help and insight at various points during my PhD. Specifically I would like to thank Dr Gina Mills for the large amount of guidance and expertise she provided to the analysis of ozone impacts at Harwell and Auchencorth, Professor Neil Cape for helpful insights regarding data interpretation, Dr Marsailidh Twigg for the useful discussions and suggestions regarding data analysis, Dr Mhairi Coyle for helpful discussions regarding ozone data analysis, and Professor David Fowler for insightful discussions on the policy-relevance of ozone analysis at Harwell and Auchencorth. . For the substantial help in running the PAN-GC instrument I would like to thank Professor Neil Cape, Dr Marsailidh Twigg, Dr Matt Jones, Ms Sarah Leeson, Dr Ben Langford and Dr Mhairi Coyle.

I would also like to thank all the staff and students from the University of Edinburgh School of Chemistry and School of Geosciences who make up the MACAQUE group. This provided an extremely useful forum for the initial presentation of results and their ideas informed the future direction of my work. Additionally, colleagues at Ricardo-AEA (Dr Peter Dumitrean, Dr Keith Vincent, Dr Justin Lingard) were extremely helpful in dealing with my requests for data.

Finally I would like to thank the University of Edinburgh School of Chemistry, the Centre for Ecology & Hydrology and the Department for the Environment, Food and Rural Affairs for funding this work.

Contents

List of Figures

List of Tables

Chapter 1: Introduction

The advances in understanding of atmospheric composition and its impacts has resulted in part from the development of coordinated and standardised atmospheric composition monitoring networks. An assessment of the historical development of these networks shows various step changes in coordination and standardisation which increased confidence that measurements made at different sites were comparable. To ensure that monitoring networks continue to make the maximum contribution to advancing our understanding of the atmosphere, this thesis proposes a new extension of network standardisation so that monitoring network data is subject to common interpretation. Specifically, a 'chemical climatology' framework is outlined, and demonstrated through specific case studies, which provides a clear method for construction of analyses which can be applied consistently across monitoring networks to assess changes in composition impacts spatially and temporally, comparison of different impacts and assessment of multi-pollutant impacts. The novelty of this approach is the linkage of a specific impact to the conditions producing it. When a standardised 'chemical climatology' analysis is applied to measurements across a network, it provides a common basis for assessment of variation in the conditions producing the impact, and hence the spatial applicability of mitigation strategies.

1.1 Atmospheric composition measurement

The atmosphere of the Earth is composed of nitrogen (78% by volume), oxygen (21%) and argon (1%) as well as hundreds of other molecules which make up the remaining small fraction. The concentrations of trace species can result in detrimental human health and environmental impacts. For centuries human activities have affected the composition of this small fraction and hence have been a driver in exacerbating these impacts (Brimblecombe, 1987). Since the industrial revolution of the 18th and 19th centuries and the associated increase in fossil fuel consumption, the spatial scale of

anthropogenic atmospheric composition change has increased substantially. Currently, the negative human health and environmental impacts resulting from this are experienced on local (e.g. health impacts in megacities (Gurjar et al., 2010)), regional (e.g. ozone vegetation damage across Europe (Mills et al., 2011) or acid deposition (Galloway et al., 2008)), and hemispheric/global scales (e.g. climate change (IPCC, 2014)).

During the 19th century there also developed interest in the investigation of atmospheric composition by direct measurement. For example, Victorian chemist Robert Angus Smith wrote, 'My object is to show that there are impurities in our atmosphere which may be discovered by chemical analyses and that the sense and general impression are not at fault when they speak of peculiarities of a town atmosphere' (Angus Smith, 1872). Development of measurement techniques means they are now a key method used to understand the chemical and physical processes of the atmosphere, the nature of impacts of atmospheric composition, and changes in composition resulting from changes in anthropogenic influence. Laboratory studies and atmospheric chemistry transport models (ACTMs) are two other methods also used for these purposes. While the three strands are mutually beneficial (Abbatt et al., 2014), atmospheric composition monitoring is especially important. Measurements of atmospheric composition (in-situ or remote sensing) yield information about the atmosphere directly, in contrast to laboratory studies and computer models which create a representation of the atmosphere in a controlled laboratory environment and computer code respectively. A suitable database of atmospheric composition measurements is required to validate the accuracy of these representations and the conclusions derived from them.

Since the first measurements, numerous advances have increased the suitability of monitoring to advance understanding of atmospheric composition, its impacts and their mitigation. Firstly, improvement of measurement techniques have resulted in the ability to measure and quantify the impact of a substantially larger number of atmospheric constituents, at higher time resolution, at lower cost and with greater

accuracy and precision. Instrumentation developments for gas-phase measurements are reviewed by Clemitshaw (2004), and Tanner (2003) analyses how historical development of measurement techniques impacted (positively and negatively) air quality.

The second type of advancement, which in part results from advances in instrumentation, is increasing coordination and standardisation between monitoring efforts across a city, region, nation and internationally. Coordination is the establishment of common goals to monitoring efforts across a spatial domain, for example measurement of atmospheric composition at various sites across a city for the protection of human health. Standardisation is the establishment of common methods to achieve the goals of the monitoring network. This includes protocols applied across the network of sites to ensure equivalent measurement techniques, site location representativeness, common quality assurance/quality control procedures and common data archiving. When consistently applied, this increases confidence that measurements obtained across the network are comparable with each other and with ACTM outputs and laboratory studies. Both coordination and standardisation are required to extract maximum information from measurements.

Advances in coordination and standardisation of monitoring efforts which have contributed to the development of the current state of national, regional and global monitoring networks are outlined in the following sections. Firstly, advances up to the 1940s are described (Section 1.2). Since the 1950s, there have been two parallel strands to atmospheric composition monitoring, both of which have resulted in increased coordination and standardisation. The first is the development of networks to evaluate human health-relevant exposure to air pollution (Section 1.3), and the second is the development of networks to advance scientific understanding of atmospheric chemistry and interaction between the atmosphere and the terrestrial environment (Section 1.4). Examples of monitoring networks which have advanced coordination and standardisation are shown in Table 1.1. An advancement in monitoring network standardisation to the interpretation of measurement data is proposed in Section 1.5,

and is centred on the concept of 'chemical climatology' first proposed by Robert Angus Smith. The remaining chapters of this thesis are reserved for a precise definition of the chemical climatology framework, its application to data collected at the UK's two monitoring 'supersites' to derive policy-relevant conclusions, and its future extension to data collected across monitoring networks.

1.2 Historical Measurements 1850s – 1940s

Measurement of atmospheric composition began in the mid-18th century, such as the detection of nitrate and chlorine in rain water samples collected in 1749 by German chemist Andreas Marggraf (Eriksson, 1952a; Miller, 1905). However, some of the first measurements on a large spatial scale were carried out in the 1850s to understand the chemical composition and impacts of ozone (Farrell, 2005). A method for measurement using colour changes in test papers impregnated with starch-iodine was developed by Christian Schoenbein. It was used at at over 300 sites across the globe, including locations in Europe (Anfossi and Sandroni, 1997; Anfossi et al., 1991; Bozo and Weidinger, 1995; Lisac et al., 2010; Nolle et al., 2005), North America (Bojkov, 1986), Central America, South America and Asia (Sandroni and Anfossi, 1994; Sandroni et al., 1992), yielding approximately 1 million measurements by the end of the 19th century (Colbeck and Mackenzie, 1994; Paneth and Edgar, 1938). However, deficiencies with the test papers prevented standardisation of monitoring efforts. Even when care was taken in the construction of test papers under the same conditions, they gave incomparable results due to sensitivity to humidity, wind speed and chemical interferents, and variation in test paper quality (Fox, 1886). The relatively recent application of corrections to a subset of this historic data has yielded semi-quantitative estimates of O_3 concentrations during the mid-late 19th century in various cities (Anfossi and Sandroni, 1997; Anfossi et al., 1991; Lisac and Grubisic, 1991; Lisac et al., 2010; Nolle et al., 2005; Sandroni and Anfossi, 1994; Sandroni et al., 1992).

Table 1.1: Summary of coordination and standardisation evident in key city, national, regional and global ground-level atmospheric monitoring networks.

Network	Location	Start Year	Measurements	Key Coordination of Network	Key Standardisation of Network
O_3 monitoring	300 sites globally	1850s	300 sites, 1 million measurements using Schoenbein test papers	Motivation to understand chemical composition and impacts of O_3	Common test paper method used but measurements were not comparable
Robert Angus Smith Precipitation Network	UK, Ireland, Germany	1869	4 components of precipitation at 59 sites	Coordinated by Robert Angus Smith to obtain 'careful observations' to investigate impacts of air pollution	Sites were classified and chemical analysis of samples performed using common methods
Paris O_3 network	Paris, France	1876	16 sites measuring O_3 with Schoenbein test papers, 1 site with additional method	*Prefecture du Departement de la Seine* wanted to map air quality across Paris	Intercomparison of two methods for measuring ozone concentration
Deposit Gauge Network	UK	1910	Deposit gauges measuring sootfall and sulphate deposition	Coordinated to quantitatively determine influence of soot deposit in 22 UK towns	Common method used but sites biased towards pollution hotspots
Air Pollution Disaster Prevention Program	Los Angeles County	1954	14 sites measuring O_3, CO_2, NO_x, SO_x and others	Sites designed to assess exposure to pollutants across LA in relation to legislated 'alert stage' standards	Sites chosen representatively, same instrumentation used at each site
European Air Chemistry Network (EACN)	North-west Europe	1954	Constituents in precipitation measured at a maximum of 120 sites in 1959	Coordinated by meteorologists to understand atmospheric circulation of chemical substances	Common measurement technique, but lack of standardisation in quality assurance so limited information gained
Global Ozone Observing System (GO3OS)	Global	1957	Measurement of total column ozone	Coordinated sites to measure total column ozone following work of International Ozone Commission	Standardised instrumentation, calibrated yearly against one instrument
National Survey	UK	1961	300 UK towns and cities, 1200 sites measuring SO_2 and black smoke	Coordinated to systematically determine spatial pattern of smoke and SO_2 concentrations across UK	Representative towns, sites within towns, same instruments used across network
Continuous Air Monitoring Program (CAMP)	USA	1963	6 cities in USA measuring 7 atmospheric constituents	Coordinated to investigate role of vehicle exhaust emissions on air pollution	Common data reporting as 4 key statistics across network
OECD programme on long-range transport of air pollutants	Europe	1972	Two-phase measurement period to determine local and transboundary contribution to acidity in precipitation.	Goal of programme achieved through coordination of measurements, emissions inventories and modelling	Common site selection measurement techniques, and data interpretation criteria applied across network
Background air pollution monitoring network (BAPMoN)	Global	1974	Measurement of background gaseous and precipitation constituents	Coordinated with other networks monitoring climate, health, terrestrial renewable resource and oceans through UNEP Global Environmental Monitoring System	Standardised instrumentation, site classification criteria (regional, continental, baseline)
European Monitoring and Evaluation Programme (EMEP)	Europe	1978	Measurement of atmospheric composition at sites with minimal local influence as part of UNECE Convention on Long-Range Transboundary Air Pollution	Measurement networks coordinated with emissions inventory calculations and modelling	EMEP manual outlines measurement methods, site locations, data quality and handling Regular method intercomparisons,
Global Atmospheric Watch (GAW)	Global	1989	Established from merging BAPMoN and GO3OS	Coordinated to establish global standards for monitoring of atmospheric composition	2 site classifications (regional and global), standardised methods and quality assurance procedures

The first national monitoring network, with the aim of investigating pollutant variation across a country, was constructed in the UK by Scottish chemist Robert Angus Smith in 1869 (Angus Smith, 1872). Born into near poverty and a member of the Health of Towns Commission, Angus Smith was familiar with the human health impact of air pollution (Gibson and Farrar, 1974). When chief inspector of the Alkali Act 1863 he minimised the environmental damage from Alkali works through reduction of hydrochloric acid emissions (Reed, 2012), but also noted that 'we are exposed to many changes of climate arising from the conditions of our civilisation; and although we cannot effect complete alterations, it is possible to do something. To learn the method we must by careful observation ascertain how we are affected' (Angus Smith, 1872). Angus Smith's network was therefore coordinated to identify how impacts arising from human changes to atmospheric composition could be mitigated.

In making 'careful observations', Angus Smith achieved a high level of standardisation compared to previous atmospheric precipitation measurements (Eriksson, 1952a; Eriksson, 1952b). Angus Smith set up 59 monitoring sites across the UK, Ireland and Germany by sending bottles to acquaintances along with instructions. Participants were to obtain half a bottle of rainwater, to take steps to avoid contamination, and to provide a description of the location of the bottle. Angus Smith performed the chemical analysis on the samples once returned. The monitoring sites were classified into categories such as towns or rural locations and 'inland country places' or 'seaside country places' (Angus Smith, 1872). The depth of the analysis Angus Smith was able to conduct highlights the advantage of the coordination of the 59 monitoring sites using a standardised chemical analysis and site classification (Gorham, 1982). For example, spatial patterns in chloride, sulphate, ammonium and nitrate precipitation concentrations were assessed across the UK, and compared with the German and Irish sites. Temporal trends in these constituents were monitored at one site (Manchester, UK) across the year through monthly sampling. The concurrent measurement of multiple constituents permitted covariance analysis and source apportionment (Angus Smith, 1872).

Angus Smith considered his monitoring studies to be a first step in the establishment of a continuous, comprehensive programme for the characterisation of atmospheric composition and its impacts (Angus Smith, 1872; Gorham, 1982). He was aware that the 1869 precipitation network suffered from deficiencies such as the characterisation of precipitation concentrations from a single sample from each site collected at different times of the year. However, despite Angus Smith's intentions, there are limited examples of advancement in composition monitoring during the rest of the 19th century. Continuous monthly measurements of precipitation composition were made at Rothamsted, south east England, between 1888 and 1916 using a standardised method (Miller, 1905; Russel and Richards, 1919), and long-term daily measurements of ozone were also recorded at the Montsouris Observatory, Paris between 1876 and 1910 (Volz and Kley, 1988). The extension of standardised monitoring towards production of long-term pollutant datasets increase the utility of measurements for the determination of inter-annual variability, and the presence of trends due to increases in emissions or interventions aimed at curbing impacts. Additionally, measurements at Montsouris contributed to a Paris-wide ozone monitoring network comprising 16 sites, where the Schoenbein test paper method was used (Anfossi and Sandroni, 1997). At Montsouris, concurrent measurements were made using two different methods, the test paper and an arsenic-based technique (Volz and Kley, 1988). This method inter-comparison allowed the unreliable Schoenbein method to be corrected based on the more accurate time series, and resulted in calculation of historical ozone concentrations from test paper measurements, detailed above, albeit with large uncertainties (±33%) (Anfossi and Sandroni, 1997; Anfossi et al., 1991).

In the mid-1800s, general interest in the atmosphere was due to detrimental human health impacts in towns, and mainly focussed on smoke and sulphur dioxide (SO_2) (Grainger, 1845; Playfair, 1845). However, assessment of the problems of smoke, attribution to sources and the proposal of solutions were undertaken largely without the quantification of atmospheric concentrations, even into the early 20th century (Smith, 1922). A World Health Organisation (WHO) review of air pollution noted that scientific papers published prior to 1900 were almost entirely concerned with the

effects and control of pollution, rather than development of measurement methods (Halliday, 1961). Reduction of smoke emissions and impacts was also limited partly because the cause and effect relationship was hard to establish due to the very large number of small smoke producers, and it was difficult to quantify the impact of individual emitters, as smoke pollution was so widespread in cities (Halliday, 1961). Subsequent monitoring efforts would demonstrate that these problems were exacerbated by the lack of a coordinated, standardised measurement network.

Some of the earliest efforts to measure smoke used the Ringelmann chart to quantify the 'blackness' of a plume of smoke emitted from a plant. A Ringelmann chart consisted of different, standardised shades of grey against which the shade of a smoke plume was compared. However, these measurements were subjective and could only gauge the blackness of direct emissions, rather than exposure across larger areas (Uekoetter, 2005). Measurement of smoke and SO_2 beginning in the 1910s provided comparison between locations within cities and across countries, producing a more accurate picture of the impact of air pollution and resulting in legislation for its mitigation (Brimblecombe, 1987; Halliday, 1961). In 1910, *The Lancet* installed 'deposit gauges' to measure monthly-averaged 'sootfall' at three urban locations in London, and a rural site in nearby Surrey (Anon., 1912). This was extended from March 1914 to a coordinated, standardised network of deposit gauges in 22 UK towns and cities (Anon., 1914). Despite limited standardisation, this network increased understanding of smoke pollution (Shaw and Owens, 1925), and measurements extended at some sites until the 1970s (Brimblecombe, 1982). However, the information obtained on smoke and sulphur pollution was limited due to the imprecision of the method (at best ± 20%), and the measurements often reflected deposited material from highly localised sources (Brimblecombe, 1987). The location of some sites in the most polluted areas of towns also made spatial comparisons difficult and reduced the willingness of local authorities to participate (Mosley, 2009). Similar limitations are revealed in monitoring in US cities (e.g. Pittsburgh (Davidson, 1979)). Hence, until the 1940s developments to advance coordination and standardisation of atmospheric composition monitoring were relatively few, and

substantial improvements to methodology were highlighted as being necessary (Cambi, 1961; Halliday, 1961; McCabe, 1961). In the UK, the relative lack of focus on advancement was due to two world wars and unfavourable economic conditions. In the US, in the 1930s, the price of oil and natural gas became comparable with coal and was adopted for heating on a large scale, reducing the emissions from coal burning, and leading to a perceived improvement in air pollution. Impacts of air pollution were observed in European cities but progress in monitoring networks was similarly limited. In some areas of continental Europe, smoke and SO_2 pollution was better than in the UK and the US, due to a proportionally larger rural population (Italy) and because domestic use of coal was lower, and industrial sources were of most interest (Germany, Austria, the Netherlands), and legislated against (Halliday, 1961).

1.3 Human Health Oriented Monitoring Networks 1950s - present

Increased coordination and standardisation of air pollution monitoring, principally for the protection of human health, emerged from two events. Firstly, three fatal air pollution disasters in Meuse Valley (Belgium, 1930), Donora (US, 1948) and London (UK, 1952) increased interest in air pollution research (Bell et al., 2004; Halliday, 1961; Heimann, 1961). Secondly, beginning in 1943, a different type of air pollution from smoke and SO_2 started to cause human health impacts in Los Angeles (Senn, 1948). The LA smog caused sore throats, watery eyes and headaches, and it was eventually shown to be composed of photochemical pollutants, including ozone, formed from reaction of volatile organic compounds with nitrogen oxides (Haagen-Smit, 1963). Following the fatal disasters, officials were concerned that similar events could occur in LA, and therefore the Air Pollution Disaster Prevention Program of LA County was established in 1954 (Chass et al., 1958). This program established a coordinated set of 14 monitoring stations designed to assess compliance with newly defined air quality concentration standards for carbon monoxide, nitrogen oxides, sulphur oxides and ozone (Maga and Goldsmith, 1960). These ‘alert stages’ specified concentrations above which control officers were required to take specific actions to

protect human health. To evaluate exceedance of alert stages, the monitoring sites were located so that measurements across the network 'would be most representative of general conditions throughout the basin' (Chass et al., 1958). Site locations were chosen based on wind flow patterns using measurements from 76 LA meteorological stations. Standardised instrumentation, which were inter-calibrated prior to installation, were used for each component, and measurements of hydrocarbons, particulate matter and other pollutants supplemented the 'alert stage' monitoring to improve research of fundamental atmospheric chemistry. This was the first modern monitoring network using continuous methods and facilitated research into spatial and temporal covariance between pollutants (Roger, 1958). The coordination of monitoring sites to investigate exposure relevant to human health, achieved through standardisation of site representativeness and instrumentation, has since been replicated globally on the back of city, national and international-scale air quality management plans implemented during the latter half of the 20th century.

The first nationally-coordinated monitoring response to the fatal air pollution disasters was The National Survey of air pollution established in the UK in 1961 (Clifton, 1964a). The National Survey comprised 1200 sites measuring smoke and sulphur dioxide to assess the impact of provisions within the Clean Air Act 1956, including the prohibition of dark smoke emissions from chimneys, the establishment of smoke control areas and increased use of smokeless furnaces. Daily smoke and SO_2 measurements were undertaken using the same method (Clifton, 1964b) in 150 UK towns and cities. To select representative sites, all towns in England and Wales were graded 'low', 'medium' or 'high' for domestic coal consumption per unit area, industrial coal consumption per unit area and natural ventilation. Within the resulting groups, towns were split by population and geographic region before a representative sample was selected (Clifton, 1964a). Within each conurbation, a maximum of five sites were then chosen to record characteristic concentrations for different districts, namely, high density terraced housing, moderate to low density housing (suburban), the commercial centre, industrial development and smoke controlled areas. The carefully constructed criteria for site locations ensured representativeness across the

UK and corrected a previous bias in measurements towards heavily industrialised areas (Mosley, 2009). The coordination and standardisation of the National Survey increased the information gained from UK smoke and SO_2 monitoring, including associations between human health and air pollution (Chinn et al., 1981; Walters et al., 1994), as well as the correlation between trends in pollutant concentration and emission reductions (Craxford and Weatherley, 1971). New methods to mitigate air pollution impacts, such as changes to town planning also directly resulted from this monitoring network (Craxford and Weatherley, 1971).

In 1963 the United States also established a national monitoring network, the continuous air monitoring program (CAMP) (Jutze and Tabor, 1963). Only six sites across six cities were coordinated to investigate the role of vehicle exhaust emissions on air pollution. This supplemented the National Air Sampling Network (NASN) which collected a single daily measurement of 'suspended particulate matter' once every two weeks at 260 sites (Anon., 1964; MacKenzie, 1958; McMullen and Smith, 1965). The low temporal resolution limited the information gained from NASN (Ludwig, 1960; Zimmer et al., 1959), and across the six chosen cities, CAMP provided a network to undertake substantially more detailed analysis, through the concurrent, continuous measurement of 7 atmospheric constituents.

The advancement in standardisation resulting from CAMP was to the reporting of data. Measurements across the CAMP sites were reported as four key statistics, derived from the use of automatic, computerised methods for recording, storing and disseminating measurements (Zimmer and Nehls, 1968). Computer programs were also used to process UK National Survey measurements which were reported in a monthly Bulletin (Clifton, 1964a). For CAMP, the higher time resolution of measurements afforded more options in the statistics reported. A punch-tape recording system automatically stored data, and a computer program extracted the daily average concentration, the monthly-averaged 24 hourly concentrations, the daily maximum hourly concentration and the daily maximum 5-min concentration of each pollutant (Jutze and Tabor, 1963). The standardised reporting of CAMP measurements using

these statistics was to permit analysis by relevant agencies, for investigation of 'inter-relationships between pollutants, concentration data, averaging period, dosage data etc.', and to identify specific pollutants which are a general indicator of air pollution severity. Lynn and McMullen (1966) evaluated concentrations, seasonal and diurnal variation of five pollutants across CAMP, demonstrating the utility of the standardised reporting procedure. This study is in contrast to those using NASN measurement, which are limited to discussion of frequency distributions between different classifications of sites (Zimmer et al., 1959). These days, the use of the internet in the storage of monitoring network data has extended the standardised reporting implemented by CAMP, and greatly increased the accessibility of monitoring data. Networks now commonly have consistent protocols for data archiving, often in publically accessible, internet-hosted databases.

The coordination and standardisation first implemented in the LA county network, the National Survey and CAMP has since extended to a large number of national human health-coordinated monitoring networks. For example, a comparison of 7 European countries and the USA showed a network in all countries, in part coordinated to evaluate compliance with legislated air quality standards (ATMO France, 2011). In six of the European countries, the requirements, standards and best practise of monitoring methods are standardised at a national level. In France, there is no national monitoring strategy and requirements are established at a local level. However, a detailed, standardised site classification scheme aids comparison between sites in different areas. In Switzerland and Austria there is no national oversight on monitoring site location, which has reduced site representativeness. In contrast to the earlier networks, this has mainly produced sites located where serious pollution problems are observed, due to the opportunity for funds from local authorities (ATMO France, 2011). In the USA, the Clear Air Act 1970 mandated states to undertake monitoring of air pollution (Bachmann, 2007), but there is significant national coordination through the Ambient Monitoring Technology Information Center (AMTIC, http://www.epa.gov/ttn/amtic/) which outlines reference and equivalent measurement methods (US EPA, 2014), and provides guidance to standardise quality assurance and data quality procedures (US

EPA, 2013). Australia has a similar system, in which individual states undertake monitoring in accordance with a national air quality strategy (EPA Victoria, 2014). The National Ambient Air Quality Standards in India are assessed by the National Air Quality Monitoring Programme (NAMP) which standardises the measurement of three pollutants at 503 sites in 209 cities, with additional composition measurements at some sites (Kamyotra et al., 2012). In Hong Kong, 14 sites are operated with common protocols for site representativeness, monitoring methods, and data quality and processing (Chow, 2014).

The 1996 European Council (EC) Air Quality Directive (European Council Directive 96/62/EC) directive, and the four subsequent 'daughter directives', mandate minimum pollutant concentration standards for which each EU member state is required to assess compliance with (European Council Directive 2008/50/EC). A key aim is to 'assess air quality in Member States on the basis of common methods and criteria' (van Aalst et al., 1998), hence extending coordination and standardisation of human health-relevant monitoring across national boundaries. Each Member State is required to divide their territory into 'zones' within which the spatial pattern of air quality is assessed through a measurement network combined with modelling (http://ec.europa.eu/environment/archives/air/pdf/guidanceunderairquality.pdf).

Across countries, site locations are similarly classified (Spangl et al., 2007), and a series of reference monitoring methods are used (European Council Directive 2008/50/EC). Quality control procedures are standardised through a forum, known as AQUILA, within which national air quality reference laboratories provide judgement on issues relating to measurements, and coordinate regular inter-comparisons of member state monitoring procedures (AQUILA, 2009). This helps to produce comparable, quality-assured measurements across Europe which are publically available in a standardised format through the AirBase data repository (http://acm.eionet.europa.eu/databases/airbase/). Finally, there is also standardised interpretation of measurement data, as Member States report an evaluation of data in relation to air quality standards (European Commission, 2013). The statistics differ for

each pollutant, and the time resolution of the measurements. For example, the statistics required for hourly measurements of SO_2 are the annual mean, no. of hours with concentrations greater than 350 μgm^{-3} and 500 μgm^{-3}, the winter mean and the 99.73 percentile. The standardised interpretation of data across this regional monitoring network provides a common comparison of air quality across Europe (EEA, 2014).

1.4 Environmental Monitoring Networks: 1950s - present

A second type of network, in addition to human health-coordinated monitoring, which have developed since the 1950s were 'not established as a result of concern about a gradual rise in atmospheric pollution but instead were created to gain a better scientific understanding of atmospheric chemistry and its implications for climate, soils and agriculture' (Wallen, 1980). The first was the European Air Chemistry Network (EACN) established in 1954 (Egner and Eriksson, 1955). This network resulted from an atmospheric chemistry conference in Sweden. Meteorologist Professor C. G. Rossby highlighted the need for atmospheric composition measurements in addition to conventional meteorological measurements to understand the atmospheric circulation of chemical substances. Plans were then formulated for a network to achieve this across the UK and Scandinavia (Eriksson, 1954). Monthly measurements of precipitation constituents were made at sites across Scandinavia and the UK, including the modification of an existing network in Sweden, which resulted in useful scientific information (Eriksson, 1959; Eriksson, 1960; Rossby and Egner, 1955). For example, it was shown that increasing acidity of precipitation in northern Europe was linked to long-range transport of air pollution (Granat, 1972; Granat, 1978; Kallend et al., 1983). However, the information gained from EACN was limited due to a lack of standardisation, as well as a flawed sampling method (Fowler and Cape, 1984). There was no systematic compilation of site conditions across the network, there were unquantifiable sources of error in the measurements and, after 25 years, there was no active coordination between sites in different countries (Paterson and Scorer, 1973; Rodhe and Granat, 1984).

In 1972, the findings of EACN were furthered by the Organisation for Economic Co-operation and Development (OECD) co-operative technical programme to measure long-range transport of air pollutants (LRTAP), which was coordinated to 'determine the relative importance of local and distant sources of sulphur compounds in terms of their contribution to the air pollution over a region'. This coordination led to the standardised measurement of sulphate in aerosol and precipitation and gaseous SO_2 between 1972 and 1975 at 76 sites across Europe chosen to minimise local influences on measurements (Ottar, 1978). The advancement in coordination specific to LRTAP was the use of direct measurement alongside other methods to achieve the goal of the programme, specifically the calculation of emission inventories and computer modelling. One of the main goals of the measurement network was the collection of atmospheric composition data to validate results from a Lagrangian dispersion model (Ottar, 1976). Gridded emission inventories were used as model input, and to assess the influence of local sources at each site. Finally, standardised interpretation of the measurement data using sector analysis showed that sulphur compounds could be transported hundreds of kilometres (Ottar, 1978). Importantly, the standardised LRTAP methods resulted in the identification of areas for improvement. These included the need to monitor over many years because of considerable inter-annually variability in meteorological conditions, and to monitor a wider array of constituents (e.g. nitrate) to fully evaluate the impact of atmospheric composition (in this case acidity in precipitation) on the environment.

Since 1977, the European Monitoring Evaluation Programme (EMEP) has continued and extended the work of the OECD LRTAP. The activities of EMEP were enshrined in Articles 9 and 10 of the United Nations Economic Commission for Europe (UNECE) Convention on Long Range Transboundary Air Pollution (CLRTAP) which was the first legally binding international framework for the protection of the environment (UNECE, 1979). The convention outlined the need for comparable and standardised measurement (initially of sulphur dioxide and related compounds) and data quality procedures, which was implemented by the chemical coordinating centre (CCC) based in Norway. The close coordination of measurements, emissions

inventories and atmospheric chemistry transport modelling in evaluating long-range transboundary air pollution was also continued. In the first EMEP measurement phase (1978-1980), 60 sites from 16 countries contributed (EMEP, 1980). Standardised results were achieved through regular laboratory inter-comparisons and meetings between experts to decide best practise (EMEP, 1979; Thrane, 1978). In 1981, comprehensive descriptions of site locations were collated by EMEP and the influence of local sources was calculated to ensure EMEP sites were representative of a large spatial domain (EMEP, 1981). The focus on coordination and standardisation of efforts across national boundaries has resulted in the successful incorporation of additional member states, and measurements of additional pollutants to the monitoring programme. For example, there have been workshops on heavy metals (EMEP, 1984), VOCs (EMEP, 1990), and nitrogen-containing compounds (EMEP, 1993) to synthesise best sampling and analysis techniques from world experts for implementation across the network.

To ensure comparability of EMEP data across a large and expanding number of sites, a procedure for quality assurance and data submission was developed. Presently, all data are submitted to the CCC in a standardised format, and then made publically available through a common data repository (ebas.nilu.no). The current standardised procedures for measurements and data handling required by EMEP are outlined in the EMEP Manual for Sampling and Analysis (EMEP, 2014). The manual contains the EMEP procedure for siting criteria (sites are classified into one of three 'levels' based on the extent of monitoring, and each level has specific requirements in terms of site density), sampling methods, chemical analysis, quality assurance, and data handling and data reporting. The implementation of the standardised EMEP methods has increased confidence in the scientific information produced, and provided substantial insight on the spatial and temporal trends in atmospheric composition across Europe (Torseth et al., 2012). The standardised methods have also identified potential improvements. For example, the 2004-2009 EMEP monitoring strategy background document identified shortcomings to EMEP monitoring such as contamination of ammonium and calcium samples, low sensitivity of SO_2 and NO_x measurement

techniques used in some countries, unsatisfactory laboratory performance, lack of sites in eastern Europe, and an insufficient number of background sites in Italy (Torseth and Hov, 2003).

The coordination and standardisation of EMEP has since been extended to other regional monitoring networks around the world, such as the network established in 1998 within the Male Declaration on Control and Prevention of Air Pollution and its Likely Transboundary Effects for South Asia (Nordberg and Hicks, 2013). This network comprises 15 sites in 8 countries in south Asia using standardised techniques and quality control procedures. The Acid Deposition Monitoring in East Asia (EANET) programme has guidelines directly influenced by EMEP protocols to ensure standardised measurements are taken at representative sites (EANET, 2000). EANET has two types of sites, deposition monitoring and ecological survey sites, which coordinate the investigation of atmospheric composition with its effects. Regional networks have also coordinated together. For example, to avoid duplication of monitoring, the 2010-2019 EMEP monitoring strategy recommends coordination between EMEP and other monitoring efforts such as Global Earth Observation System of Systems (GEOSS), Global Monitoring for Environment and Security (GMES), Male Declaration and EANET. The closer integration of regional monitoring efforts is also advocated by the Global Atmospheric Pollution Forum (GAP Forum, 2010).

Global monitoring networks began in 1957 with the Global Ozone Observing System (GO3OS), motivated by the work of the International Ozone Commission (Bojkov, 2010). Initially comprising 32 sites, the network used Dobson spectrophotometers to measure total column ozone which were calibrated against a single spectrophotometer to ensure comparable results (Komhyr and Grass, 1989; Stolarski et al., 1992). However, the location of sites within the network were biased towards the northern hemisphere (Stolarski et al., 1992). In 1974, a second global monitoring network measuring 8 constituents of precipitation and atmospheric turbidity at 109 sites (by 1980) was established, the Background Air Pollution Monitoring Network (BAPMoN) (Wallen, 1980). There were three levels of site classification, ‘regional’, ‘continental’

and ‘baseline (global)’ depending on the representativeness of measurements. Laboratory inter-comparisons ensured standardised chemical analyses and data was submitted to a centralised body for annual reporting. An advancement of BAPMoN was the explicit coordination with other networks monitoring climate, health, terrestrial renewable resource and ocean through the United Nations Environment Program (UNEP) Global Environment Monitoring System (GEMS) (Gwynne, 1982). BAPMoN therefore contributed to an ‘internationally coordinated effort to systematically collect, analyse and evaluate data variables that determine the state of the environment and the changes they undergo in space and time’ (Wallen, 1980).

In 1989 BAPMoN and GO3OS were merged at the 41st session of the World Meteorological Organization (WMO) executive council to create the Global Atmospheric Watch (GAW) programme. The aim of GAW was to produce long-term observations of atmospheric composition which are quality assured and controlled to reduce environmental risks to society, strengthen capabilities to predict climate, weather and air quality and to contribute to scientific assessments in support of air quality (Muller et al., 2007). This has resulted in a coordinated network of 436 GAW sites which are classified as regional or global, and meet criteria which demonstrate minimal local influence on measurements. GAW also produces a measurement guide to ensure standardisation and comparability of results (GAW, 2001). The standardisation of archiving and public availability of results is achieved through the publication of quality controlled data through GAW’s world data centres.

1.5 Standardised Interpretation of data

Atmospheric composition monitoring currently comprises city, national, regional and global-scale networks. The large volume of data collected by coordinated and standardised monitoring networks presents an unprecedented opportunity to investigate the interactions between the atmosphere, humans and the rest of the natural environment. This is aided by tools specifically designed for the interpretation of

atmospheric composition data, for example the *Openair* software package (Carslaw and Ropkins, 2012). However, to extract maximum information about atmospheric processes and impacts the large volume of high quality data collected requires interpretation. Monitoring network data is interpreted in two ways.

Data can be interpreted at sites individually, and tailored to extract information for which the station is appropriately positioned to provide. For example, Mace Head, the EMEP and GAW monitoring site on the west coast of Ireland, is located such that atmospheric composition measurements are often representative of hemispheric background concentrations. It was therefore useful to investigate trends and covariance in concentrations of trace species in air masses with minimal European influence (Derwent et al., 2013). Alternatively, spatial variation in pollutant concentrations and impacts can be investigated when common methods are applied to interpret data from multiple sites across a network. For example, the measurement of air quality across the EU in relation to the EC Air Quality Directive requires Member States to submit a standardised set of statistics which allows comparison of air quality across Europe (EEA, 2014; Guerreiro et al., 2014). Similarly, there are standardised interpretations of data across national (e.g. the UK Automatic Urban and Rural Network (AURN) (Harrison et al., 2012)) and regional (e.g. EMEP (Torseth et al., 2012)) monitoring networks. The disadvantage of these methods is that monitoring networks set up to achieve similar goals are often interpreted in different ways, making comparison between networks difficult. For example, differences in air quality standards between two monitoring networks make a determination of the relative air quality situation in each country difficult. Hence while the information gained from monitoring networks has been substantial (Monks et al., 2009), there is potential for even greater gains through a further advancement in the standardisation of monitoring network data interpretation. Other deficiencies in the interpretation of monitoring data have been highlighted. Chow and Watson (2008) note that ‘unfortunately the sole focus on compliance hinders the utility of data for a wider range of applications’ for those networks designed to evaluate against air quality standards. Among the additional applications listed are source apportionment, quantification of background levels and

investigation of pollution levels and adverse effects. Brook et al. (2009) conclude that current air quality management plans lack the mechanism by which improvements in health and environmental impacts can be documented and assessed.

Methods to improve monitoring network outputs include reporting data at higher time resolution and to the limit of precision, and calibrating instruments to lower concentrations (Chow and Watson, 2008). Brook et al. (2009) propose results-oriented, multi-pollutant air quality management strategies which aim to 'characterise the linkages in the accountability chain from emissions to [at least] exposure'. This requires improved knowledge of which pollutants cause effects, the effects of individual pollutants (making them hard to rank), and the effects of multi-pollutant exposure, as well as establishing objective metrics for prioritizing health vs ecosystem effects. Kuhlbusch et al. (2014) describe an 'information network' as part of the future of urban air quality monitoring in Europe which integrates atmospheric composition data from a diverse range of sources (e.g. fixed monitoring sites, remote sensing, mobile monitoring, urban scale modelling). To achieve closer integration of air quality and climate change mitigation, Schmale et al. (2014) suggest an 'information framework' where air quality and climate impacts are simultaneously evaluated by calculating a suite of metrics in order to identify co-beneficial strategies as well as identifying where trade-offs are needed.

This thesis outlines an additional method to improve monitoring network outputs. This 'chemical climatology' framework is a method by which the interpretation of atmospheric composition data could be standardised across networks. The framework is based on the philosophy of Victorian chemist Robert Angus Smith, and has been updated through analogy with the use of the term climate in other areas. When applied to atmospheric composition data (measurements or output from ACTMs), it links a specific impact of atmospheric composition, through the 'state' of composition variation (e.g. relevant diurnal, seasonal or exceedance above threshold variation in atmospheric components contributing to the impact), to its causal 'drivers' (e.g. meterology, emissions sources (spatial and activity), or long range transport). The

consistent application of the framework across networks would supplement analysis undertaken at individual sites and increase the information gained from monitoring networks about the spatial distribution of impacts and differences in conditions giving rise to them. Hence novel strategies to reduce deleterious impacts resulting from anthropogenic influence on the atmosphere could be derived. The widespread use of the chemical climatology framework would assist in reducing the identified deficiencies in current monitoring networks, and could also benefit solutions proposed by Brook et al. (2009), Kuhlbusch et al. (2014) and Schmale (2014).

1.6 Aim and structure of this thesis

The aim of this thesis is to demonstrate how a standardised interpretation of atmospheric composition measurements, derived using the chemical climatology framework, can increase the utility of monitoring networks, and maximise the information derived from them. To demonstrate this, the chemical climatology framework is applied to the assessment of spatial and temporal changes in atmospheric composition impacts, comparison of different impacts, and consideration of multi-pollutant impacts. The novelty of the approach outlined in this thesis is the ability of the standardised interpretation of data to not only quantify a particular impact using the same metric/method, but to provide a common basis for the quantification of the conditions producing the impact. This allows for the assessment of the spatial applicability of different mitigation strategies, hence identifying across a region the most effective methods to improve an atmospheric composition impact. The remainder of this thesis is structured as follows.

Chapter 2 outlines relevant historical background and definition of the chemical climatology framework. Chapter 3 defines the representativeness of the two UK EMEP monitoring supersites at Harwell (south-east England) and Auchencorth (south-east Scotland). The data collected at these sites is interpreted using the chemical climatology framework in Chapters 4-6. This produces three examples demonstrating

how the application of this framework links an impact to the conditions producing it and how this can be used to yield policy relevant conclusions and identify mitigation strategies. Chapter 4 analyses trends in human health and vegetation impacts of ozone temporally at Harwell between 1990 and 2013, and spatially between Harwell and Auchencorth, and links them to the changing relative contribution of regional and hemispheric processes as drivers of the impacts. Chapter 5 links the 'impact' of regionally produced ozone, through the 'state' of chemical loss of 27 measured volatile organic compounds (VOCs) to the VOC emission source sector 'drivers'. These linkages evaluate the limitations highly aggregated source sectors place on the identification of effective VOC emission reduction strategies. Chapter 6 assesses the contribution of individual constituents of particulate matter (PM) to the long term human health impact of PM, characterised by the annual average PM_{10} and $PM_{2.5}$ concentrations. The state of this chemical climate summarises the relative contribution of moderate vs high PM concentrations to the long term health metric, as well as the monthly and compositional contribution to different PM concentrations. This state is then linked to drivers through the proportion of time spent over of geographic regions during different PM concentrations, and the application of Principal Component Analysis (PCA) to quantify the contribution of short vs long range transport in determining the concentrations of major PM components. Finally, Chapter 7 proposes a route by which chemical climatology can be extended across monitoring networks. It is shown to facilitate comparison of the same impacts across a spatial domain, or comparison of different impacts in the same location on a common basis, and could increase the application of monitoring network data to assess linkages between atmospheric composition impacts and economic and societal issues.

References

Abbatt, J., George, C., Melamed, M., Monks, P., Pandis, S., Rudich, Y., 2014. New Directions: Fundamentals of atmospheric chemistry: Keeping a three-legged stool balanced. Atmos. Environ. 84, 390-391.

Anfossi, D., Sandroni, S., 1997. Ozone levels in Paris one century ago. Atmos. Environ. 31, 3481-3482.

Anfossi, D., Sandroni, S., Viarengo, S., 1991. Tropospheric ozone in the 19th Century - The Moncalieri series. J. Geophys. Res.-Atmos. 96, 17349-17352.

Angus Smith, R., 1872. Air and Rain: The Beginnings of a Chemical Climatology. Longmans, Green and co., London.

Anon., 1912. The Sootfall of London: Its Amount, Quality and Effects. Lancet 179, 47-50.

Anon., 1914. Atmospheric Pollution. Nature 94, 433-434.

Anon., 1964. New Cities in PHS Air Sampling Network. Public Health Rep. 79, 336.

AQUILA, 2009. National air quality reference laboratories and the European network - Aquila: Roles and requirements for measurement traceability, accreditation, quality assurance/quality control, and measurement comparisons, at national and European levels. European Council Report, available at: http://ec.europa.eu/environment/air/quality/legislation/pdf/aquila.pdf.

ATMO France, 2011. International comparison of air quality monitoring systems. ATMO France, available at http://www.airparif.asso.fr/_pdf/publications/comparaison-internationale-atmofrance-en.pdf.

Bachmann, J., 2007. Will the circle be unbroken: A history of the US national ambient air quality standards. J. Air Waste Manag. Assoc. 57, 652-697.

Bell, M. L., Davis, D. L., Fletcher, T., 2004. A retrospective assessment of mortality from the London smog episode of 1952: The role of influenza and pollution. Environ. Health Persp. 112, 6-8.

Bojkov, R. D., 1986. Surface ozone during the 2nd half of the 19th Century. J. Clim. Appl. Meteorol. 25, 343-352, doi:10.1175/1520-0450(1986)025<0343:sodtsh>2.0.co;2.

Bojkov, R. D., 2010. The International Ozone Commission (IO3C): Its history and activities related to atmospheric ozone. Academy of Athens Research Centre for Atmospheric Physics and Climatology Publication No 18, available at: http://ioc.atmos.illinois.edu/about/History%20of%20International%20Ozone%20Commission%203.pdf.

Bozo, L., Weidinger, T., 1995. Tropospheric ozone measurements over Hungary in the 19th Century. Ambio 24, 129-130.

Brimblecombe, P., 1982. Trends in the Deposition of Sulphate and Total Solids in London. Sci. Total Environ. 22, 97-103.

Brimblecombe, P., 1987. The Big Smoke: A History of Air Pollution in London Since Medieval Times. Methuen, London.

Brook, J. R., Demerjian, K. L., Hidy, G., Molina, L. T., Pennell, W. I., Scheffe, R., 2009. New Directions: Results-oriented multi-pollutant air quality management. Atmos. Environ. 43, 2091-2093.

Cambi, F., 1961. Sampling, Analysis and Instrumentation in the Field of Air Pollution. In: Air Pollution. World Health Organisation Monograph Series No. 46. Geneva, pp. 63-96.

Carslaw, D. C., Ropkins, K., 2012. openair - An R package for air quality data analysis. Environ. Modell. Softw. 27-28, 52-61.

Chass, R. L., Pratch, M., Atkinsson, A. A., 1958. The Air Pollution Disaster-Prevention Program of Los Angeles County. JAPCA J Air Waste Ma 8, 72-86.

Chinn, S., Florey, C. D., Baldwin, I. G., Gorgol, M., 1981. The relation of mortality in England and Wales 1969-73 to measurements of air pollution. J. Epidemiol. Commun. H. 35, 174-179.

Chow, C. F., 2014. Air Quality in Hong Kong 2013. Environmental Protection Department Report Number EPD/TR 1/14, Air Science Group, Hong Kong Environmental Protection Department, available at: http://www.aqhi.gov.hk/api_history/english/report/files/AQR2013e_final.pdf.

Chow, J. C., Watson, J. G., 2008. New directions: Beyond compliance air quality measurements. Atmos. Environ. 42, 5166-5168.

Clemitshaw, K. C., 2004. A review of instrumentation and measurement techniques for ground-based and airborne field studies of gas-phase tropospheric chemistry. Crit. Rev. Env. Sci. Tech. 34, 1-108.

Clifton, M., 1964a. The National Survey of air pollution. Proceedings of the Royal Society of Medicine-London 57, 1013-1015.

Clifton, M., 1964b. How air pollution is detected. Proceedings of the Royal Society of Medicine-London 57, 615-618.

Colbeck, I., Mackenzie, A., 1994. Air Pollution by Photochemical Oxidants, Elsevier, New York.

Craxford, S. R., Weatherley, M. P. M., 1971. Air Pollution in Towns in the United Kingdom. Philosophical Transactions of the Royal Society of London. Series A, Mathematical and Physical Sciences. 269, 503-513.

Davidson, C. I., 1979. Air Pollution in Pittsburgh: A Historical Perspective. JAPCA J. Air Waste Ma. 29, 1035-1041.

Derwent, R., Manning, A., Simmonds, P., Gerard Spain, T., O'Doherty, S., 2013. Analysis and interpretation of 25 years of ozone observations at the Mace Head Atmospheric Research Station on the Atlantic Ocean coast of Ireland from 1987 to 2012. Atmos. Environ. 80, 361-368.

EANET, 2000. Guidelines for Acid Deposition Monitoring in East Asia. Acid Deposition monitoring in East Asia (EANET) report, available at: http://www.eanet.asia/product/guideline/monitorguide.pdf.

EEA, 2014. Air Quality in Europe - 2014 Report. EEA Report No 5/2014, European Environment Agency, available at: http://www.eea.europa.eu/publications/air-quality-in-europe-2014.

Egner, H., Eriksson, E., 1955. Current Data on the Chemical Composition of Air and Precipitation. Tellus 7, 134-139.

EMEP, 1979. Expert Meeting on Chemical Matters Oslo, 3-5 December 1979. EMEP/CCC report 4/79, ECE Co-operative Programme for Monitoring and

Evaluation of the Long Range Transmission of Air Pollutants in Europe, available at: http://www.nilu.no/projects/ccc/reports/cccr4-79.pdf.

EMEP, 1980. Summary Report of the Chemical Coordinating Centre for the First Phase of EMEP. EMEP/CCC report 4/80, Co-operative programme for monitoring and evaluation of the transmission of air pollutants in Europe, available at: http://www.nilu.no/projects/ccc/reports/cccr4-80.pdf.

EMEP, 1981. EMEP Sampling Stations: Site Descriptions. EMEP/CCC Report 1/81, Co-operative Programme for monitoign and Evaluation of the Long Range Transmission of Air Pollutants in Europe, available at: http://www.nilu.no/projects/ccc/reports/cccr1-81.pdf.

EMEP, 1984. EMEP Workshop on Heavy Metals. EMEP/CCC Report 4/84, ECE Co-operative Programme for Monitoring and Evaluation of the Long Range Transmission of Air Pollutants in Europe, available at: http://www.nilu.no/projects/ccc/reports/cccr4-84.pdf.

EMEP, 1990. EMEP Workshop on Measurement of Hydrocarbons/VOC. Co-operative Programme for Monitoring and Evaluation of the Long Range Transmission of Air Pollutants in Europe, available at: http://www.nilu.no/projects/ccc/reports/cccr3-90.pdf.

EMEP, 1993. EMEP Workshop on Measurements of Nitrogen-Containing Compounds. EMEP/CCC Report 1/93, Co-operative Programme for Monitoring and Evaluation of the Long Range Transmission of Air Pollutants in Europe, available at: http://www.nilu.no/projects/ccc/reports/cccr1-93.pdf.

EMEP, 2014. Manual for Sampling and Analysis. EMEP/CCC Report 1/2014, Co-operative programme for monitoring and evaluation of the transmission of air pollutants in Europe, available at: http://www.nilu.no/projects/ccc/manual/index.html.

EPA Victoria, 2014. Air monitoring report 2013 - compliance with the National Environment Protection (Ambient Air Quality) Measure. EPA Victoria Publication number 1569, Environmental Protection Agency Victoria, available at: http://www.epa.vic.gov.au/~/media/Publications/1569.pdf.

Eriksson, E., 1952a. Composition of Atmospheric Precipitation: 1. Nitrogen compounds. Tellus 3, 215-232.

Eriksson, E., 1952b. Composition of Atmospheric Precipitation: 2. Sulphur, Chlorine, Iodine compounds. Tellus 4, 280-303.

Eriksson, E., 1954. Report in an informal conference in atmospheric chemistry held at the Meteorological Institute, University of Stockholm, May 24-26 1954. Tellus 6, 302-307.

Eriksson, E., 1959. The Yearly Circulation of Chloride and Sulfur in Nature: meteorological, Geochemical and Pedological Implications. Part 1. Tellus 11, 375-403.

Eriksson, E., 1960. The Yearly Circulation of Chloride and Sulfur in Nature: Meteorological, Geochemical and Pedological Implications. Part II. Tellus 12, 63-109.

European Commission, 2013. Guidance on the Commission Implementing Decision laying down rules for Directives 2004/107/EC and 2008/50/EC of the European Parliament and of the Council as regards the reciprocal exchange of

information and reporting on ambient air. European Commission Report, available at: http://ec.europa.eu/environment/air/quality/legislation/pdf/IPR_guidance1.pdf.

European Council Directive 96/62/EC, On ambient air quality assessment and management. 27th September 1996, No L 296/55.

European Council Directive 2008/50/EC, On ambient air quality and cleaner air for Europe. 21st May 2008, L 152/1.

Farrell, A. E., 2005. Learning to see the invisible: Discovery and measurement of ozone. Environ. Monit. Assess. 106, 59-80.

Fowler, D., Cape, J. N., 1984. The contamination of rain samples by dry deposition on rain collectors. Atmos. Environ. 18, 183-189.

Fox, C. B., 1886. Sanitary Examinations of Water, Air and Food. J & A Churchill, London.

Galloway, J. N., Dentener, F. J., Marmer, E., Cai, Z. C., Abrol, Y. R., Dadhwal, V. K., Murugan, A. V., 2008. The Environmental Reach of Asia. Ann. Rev. Environ. Resour., Vol. 33. Annual Reviews, Palo Alto, pp. 461-481.

GAP Forum, 2010. Atmospheric Pollution: Developing a Global Approach. Global Atmospheric Pollution Forum Discussion Paper 2, available at: http://www.sei-international.org/gapforum/reports/discussionpaper1.pdf.

GAW, 2001. Global Atmospheric Watch Measurements Guide. GAW Report No. 143, available at: ftp://ftp.wmo.int/Documents/PublicWeb/arep/gaw/gaw143.pdf.

Gibson, A., Farrar, W. V., 1974. Robert Angus Smith, F.R.S., and 'Sanitary Science'. Notes Rec. R. Soc. Lond. 28, 241-262.

Gorham, E., 1982. Robert Angus Smith, FRS and 'Chemical Climatology'. Notes Rec. Roy. Soc. 36, 267-272.

Grainger, R. D., 1845. Unhealthiness of Towns, Its Causes and Remedies. Charles Knight & Co., London.

Granat, L., 1972. On the relation between pH and the chemical composition in atmospheric precipitation. Tellus 14, 550-560.

Granat, L., 1978. Sulfate in Precipitation as Observed by the European Atmospheric Chemistry Network. Atmos. Environ., 413-424.

Guerreiro, C. B. B., Foltescu, V., de Leeuw, F., 2014. Air quality status and trends in Europe. Atmos. Environ. 98, 376-384.

Gurjar, B. R., Jain, A., Sharma, A., Agarwal, A., Gupta, P., Nagpure, A. S., Lelieveld, J., 2010. Human health risks in megacities due to air pollution. Atmos. Environ. 44, 4606-4613.

Gwynne, M. D., 1982. The Global Environment Monitoring System (GEMS) of UNEP. Environ. Conserv. 9, 35-41.

Haagen-Smit, A. J., 1963. Photochemistry and Smog. JAPCA J. Air Waste M. 13, 444-454.

Halliday, E. C., 1961. A Historical Review of Atmospheric Pollution. In: Air Pollution. World Health Organisation Monograph Series No. 46. Geneva, pp. 9-37.

Harrison, R. M., Laxen, D., Moorcroft, S., Laxen, K., 2012. Processes affecting concentrations of fine particulate matter (PM2.5) in the UK atmosphere. Atmos. Environ. 46, 115-124.

Heimann, H., 1961. Effects of Air Pollution on Human Health. In: Air Pollution. World Health Organisation Monograph Series No. 46. Geneva, pp. 159-220.

IPCC, 2014. Climate Change 2014: Impacts, Adaptation, and Vulnerability. IPCC Working Group II Contribution to Fifth Assessment Report (WGII AR5). Intergovernmental Panel on Climate Change, available at: http://www.ipcc.ch/report/ar5/wg2/.

Jutze, G. A., Tabor, E. C., 1963. The Continuous Air Monitoring Program. JAPCA J. Air Waste M. 13, 278-280.

Kallend, A. S., Marsh, A. R. W., Pickles, J. H., Proctor, M. V., 1983. Acidity of rain in Europe. Atmos. Environ. 17, 127-137.

Kamyotra, S. J. S., Basu, D. D., Agrawal, S., Darbari, T., Roychoudhury, S., Hagar, J. K., Sultan, R., 2012. National Ambient Air Quality Status and Trends in India - 2010. Central Pollution Control Board Report Number NAAQMS/35/2011-2012, Ministry of Environment & Forests, available at: http://www.cpcb.nic.in/upload/NewItems/NewItem_192_NAAQSTI.pdf.

Komhyr, W. D., Grass, R. D., 1989. Dobson Spectrophotometer 83: A Standard for Total Ozone Measurements 1962-1987. J. Geophys. Res. 94, 9847-9861.

Kuhlbusch, T., Quincey, P., Fuller, G., Kelly, F., Mudway, I., Viana, M., Querol, X., Alastuey, A., Katsouyanni, K., Weijers, E., Borowiak, A., Gehrig, R., Hueglin, C., Bruckmann, P., Favez, O., Sciare, J., Hoffmann, B., EspenYttri, K., Torseth, K., Sager, U., Asbach, C., Quass, U., 2014. New Directions: The future of European urban air quality monitoring. Atmos. Environ. 87, 258-260.

Lisac, I., Grubisic, V., 1991. An analysis of surface ozone data measured at the end of the 19th Century in Zagreb, Yugoslavia. Atmos. Environ. 25, 481-486.

Lisac, I., Vujnovic, V., Marki, A., 2010. Ozone measurements in Zagreb, Croatia, at the end of 19(th) century compared to the present data. Meteorol. Z. 19, 169-178.

Ludwig, J. H., 1960. Some Ramifications of Air Contamination. Public Health Rep. 75, 413-419.

Lynn, D. A., McMullen, T. B., 1966. Air Pollution in Six Major U.S. Cities as Measured by the Continuous Air Monitoring Program. JAPCA J. Air Waste M. 16, 186-190.

MacKenzie, V. G., 1958. Progress Report on Air Pollution. Public Health Rep. 73, 39-41.

Maga, J. A., Goldsmith, J. R., 1960. Standards for Air Quality in California. JAPCA J. Air Waste M. 10, 453-467.

McCabe, L. C., 1961. The Identification of an Air Pollution Problem. In: Air Pollution. World Health Organisation Monograph Series No. 46. Geneva, pp. 39-47.

McMullen, T. B., Smith, R., 1965. The trend of suspended particulates in urban air: 1957-1964. Environmental Health Series: Air Pollution Public Health Service Publication No. 999-AP-19, U.S. Department of Health, Education and Welfare: Public Health Service, available at: http://nepis.epa.gov/Adobe/PDF/9100K7RY.PDF.

Miller, N. H. J., 1905. The amounts of nitrogen as ammonia and as nitric acid and of chlorine in the rain water collected at Rothamsted. J. Agric. Sci. 1, 280-303.

Mills, G., Hayes, F., Simpson, D., Emberson, L., Norris, D., Harmens, H., Bueker, P., 2011. Evidence of widespread effects of ozone on crops and (semi-)natural vegetation in Europe (1990-2006) in relation to AOT40-and flux-based risk maps. Global Change Biol. 17, 592-613.

Monks, P. S., Granier, C., Fuzzi, S., Stohl, A., Williams, M. L., Akimoto, H., Amann, M., Baklanov, A., Baltensperger, U., Bey, I., Blake, N., Blake, R. S., Carslaw, K., Cooper, O. R., Dentener, F., Fowler, D., Fragkou, E., Frost, G. J., Generoso, S., Ginoux, P., Grewe, V., Guenther, A., Hansson, H. C., Henne, S., Hjorth, J., Hofzumahaus, A., Huntrieser, H., Isaksen, I. S. A., Jenkin, M. E., Kaiser, J., Kanakidou, M., Klimont, Z., Kulmala, M., Laj, P., Lawrence, M. G., Lee, J. D., Liousse, C., Maione, M., McFiggans, G., Metzger, A., Mieville, A., Moussiopoulos, N., Orlando, J. J., O'Dowd, C. D., Palmer, P. I., Parrish, D. D., Petzold, A., Platt, U., Poeschl, U., Prevot, A. S. H., Reeves, C. E., Reimann, S., Rudich, Y., Sellegri, K., Steinbrecher, R., Simpson, D., ten Brink, H., Theloke, J., van der Werf, G. R., Vautard, R., Vestreng, V., Vlachokostas, C., von Glasow, R., 2009. Atmospheric composition change - global and regional air quality. Atmos. Environ. 43, 5268–5350.

Mosley, S., 2009. 'A Network of Trust': Measuring and Monitoring Air Pollution in British Cities, 1912-1960. Environment and History 15, 273-302.

Muller, G., Artz, R., Baltensperger, U., Carmichael, G., Dlugokencky, E., Penkett, S., Stahelin, J., Webb, A., Hov, O., Klausen, J., Sturges, B., Barrie, L., Braathen, G., Jalkanen, L., Nickovic, S., 2007. WMO Global Atmospheric Watch (GAW) Strategic Plan: 2008-2015. GAW Report 172, available at: ftp://ftp.wmo.int/Documents/PublicWeb/arep/gaw/gaw172-26sept07.pdf.

Nolle, M., Ellul, R., Ventura, F., Gusten, H., 2005. A study of historical surface ozone measurements (1884-1900) on the island of Gozo in the central Mediterranean. Atmos. Environ. 39, 5608-5618.

Nordberg, L., Hicks, K., 2013. Male Declaration 1998-2013: a Synthesis: Progress and Opportunities. Male Declaration Report, available at: http://www.rrcap.ait.asia/male/uploadedfiles/file/Synthesis%20Report.pdf.

.

Ottar, B., 1976. Monitoring Long-Range Transport of Air Pollutants: The OECD Study. Ambio 5, 203-206.

Ottar, B., 1978. An Assessment of the OECD study on Long Range Transport of Air Pollutants (LRTAP). Atmos. Environ. 12, 445-454.

Paneth, F. A., Edgar, J. L., 1938. Concentration and measurement of atmospheric ozone. Nature 142, 112-113.

Paterson, M. P., Scorer, R. S., 1973. Data Quality and the European Air Chemistry Network. Atmos. Environ. 7, 1163-1171.

Playfair, L., 1845. Report on the State of Large Towns in Lancashire. W. Clowes and Sons, London.

Reed, P., 2012. The Alkali Inspectorate 1874-1906: Pressure for Wider and Tighter Pollution Regulation. Ambix 59, 131-151.

Rodhe, H., Granat, L., 1984. An Evaluation of Sulfate in European Precipitation 1955-1982. Atmos. Environ. 18, 2627-2639.

Roger, L. H., 1958. Nitric Oxide and Nitrogen Dioxide in the Los Angeles Atmosphere. JAPCA J. Air Waste M. 8, 124-128.

Rossby, C. G., Egner, H., 1955. On the Chemical Climate and its Variation with the Atmospheric Circulation Pattern. Tellus 7, 119-133.

Russel, E. J., Richards, E. H., 1919. The amounts and composition of rain and snow falling at Rothamsted. J. Agr. Sci. 9, 309-337.

Sandroni, S., Anfossi, D., 1994. Historical data of surface ozone at tropical latitudes. Sci. Total Environ. 148, 23-29.

Sandroni, S., Anfossi, D., Viarengo, S., 1992. Surface ozone levels at the end of the 19th Century in South America. J. Geophys. Res.-Atmos. 97, 2535-2539.

Schmale, J., van Aardenne, J., von Schneidemesser, E., 2014. New Directions: Support for integrated decision-making in air and climate policies – Development of a metrics-based information portal. Atmos. Environ. 90, 146-148.

Senn, C. L., 1948. General Air Pollution: Los Angeles "Smog". Am. J. Public Health 38.

Shaw, N., Owens, J. S., 1925. The Smoke Problem of Great Cities. Constable and Company Ltd., London.

Smith, W. B., 1922. Should we Longer Tolerate the Pollution of the Air? Brit. Med. J. 2, 361-362.

Spangl, W., Schneider, J., Moosmann, L., Nagl, C., 2007. Representativeness and classification of air quality monitoring stations. Umweltbundesamt report, available at: http://ec.europa.eu/environment/air/quality/legislation/pdf/report_uba.pdf.

Stolarski, R., Bojkov, R., Bishop, L., Zerefos, C., Staehelin, J., Zawodny, J., 1992. Measured Trends in Stratospheric Ozone. Science 256, 342-349.

Tanner, R. L., 2003. Measurements in support of air quality improvement - some historical insights. Atmos. Environ. 37, 1271-1276.

Thrane, K. E., 1978. Report on the First Intercomparison of Analytical Methods Within the EMEP, EMEP/CCC report 2/78, Co-operative Programme for Monitoring and Evaluation of the Long Range Transmission fo Air Pollutants in Europe, available at: http://www.nilu.no/projects/ccc/reports/cccr2-78.pdf.

Torseth, K., Hov, O., 2003. The EMEP monitoring strategy 2004-2009: Background document with justification and specification of the EMEP monitoring programme 2004-2009. EMEP/CCC Report 9/2003, Co-operative Programme for Monitoring and Evaluation of the Long-range Transmission of Air Pollutants in Europe, available at: http://www.nilu.no/projects/ccc/reports/cccr9-2003.pdf.

Torseth, K., Aas, W., Breivik, K., Fjaeraa, A. M., Fiebig, M., Hjellbrekke, A. G., Myhre, C. L., Solberg, S., Yttri, K. E., 2012. Introduction to the European Monitoring and Evaluation Programme (EMEP) and observed atmospheric composition change during 1972-2009. Atmos. Chem. Phys. 12, 5447-5481.

Uekoetter, F., 2005. The strange career of the Ringelmann smoke chart. Environ. Monit. Assess. 106, 11-26.

UNECE, 1979. Convention on Long-Range Transboundary Air Pollution. United Nations Economic Commission for Europe, 13th November 1979.

US EPA, 2013. QA Handbook for Air Pollution Measurement Systems. Volume II: Ambient Air Quality Monitoring Program. US EPA report number EPA-454/B-13-003, United States Environmental Protection Agency, available at: http://www.epa.gov/ttn/amtic/files/ambient/pm25/qa/QA-Handbook-Vol-II.pdf.

US EPA, 2014. List of designated reference and equivalent methods. United State Environmental Protection Agency, available at: http://www.epa.gov/ttn/amtic/files/ambient/criteria/reference-equivalent-methods-list.pdf.

van Aalst, R., Edwards, L., Pulles, T., De Saeger, E., Tombrou, M., Tonnesen, D., 1998. Guidance report on preliminary assessment under EC air quality directives. EEA Technical Report No 11, European Environment Agency, available at: http://www.eea.europa.eu/publications/TEC11a.

Volz, A., Kley, D., 1988. Evaluation of the Montsouris series of ozone measurements made in the 19th Century. Nature 332, 240-242.

Wallen, C. C., 1980. Monitoring Potential Agents of Climatic Change. Ambio 9, 222-228.

Walters, S., Griffiths, R. K., Ayres, J. G., 1994. Temporal associations between hospital admissions for asthma in Birmingham and ambient levels of sulfur dioxide and smoke. Thorax 49, 133-140.

Zimmer, C. E., Nehls, G. J., 1968. The Impact of Computers Upon Air Pollution Research. JAPCA J. Air Waste M. 18, 383-386.

Zimmer, C. E., Tabor, E. C., Stern, A. C., 1959. Particulate Pollutants in the Air of the United States. JAPCA J. Air Waste M. 9, 136-143.

Chapter 2: The definition and framework for chemical climatology

The work outlined in this chapter has been adapted from a research paper which was published in 'Atmospheric Environment' as a shortened, New Directions article (Malley, C. S., Braban, C. F., & Heal, M. R. (2014). New Directions: Chemical climatology and assessment of atmospheric composition impacts. Atmospheric Environment, 87, 261-264. 10.1016/j.atmosenv.2014.01.027, see Appendix II). My supervisors Dr Mathew Heal and Dr Christine Braban contributed to the determination of the theoretical basis and practical definition of chemical climatology. Following an initial draft, their editing of the article upon which this chapter is based improved the clarity with which the chemical climatology framework and its rationale were presented.

2.1 Historical Background

The term *chemical climatology* was conceived by British chemist Robert Angus Smith (1817–1884) who established an early coordinated and standardised monitoring network (Chapter 1). The context within which Angus Smith developed his vision of chemical climatology was a desire to alleviate the problems in urban Victorian Britain, including air pollution: 'Having given considerable attention to the inquiry into the causes affecting the health of towns, I was anxious to find what the real evil in their polluted atmosphere consisted of' (Angus Smith, 1845). From 1843 Angus Smith was an assistant commissioner to the Health of Towns Commission and witnessed at first-hand urban poverty and mortality. In 1863 Angus Smith was appointed the inaugural chief inspector of the Alkali Act, aimed at curbing hydrochloric acid emissions from the British chemical industry (Reed, 2012). Angus Smith recognised that a precursor

to achieving the goals of the Act, and of mitigation of health effects caused by anthropogenic influence on the atmosphere, was systematic observation and characterisation of the atmospheric constituents, which he undertook himself. Through his 1872 book *Air and rain: The beginnings of a chemical climatology* (Angus Smith, 1872), Angus Smith both laid the foundations for similar studies conducted decades later (Gorham, 1982) and sought to popularise chemical climatology as a scientific endeavour.

Angus Smith's approach in *Air and rain* was the first systematic study presented in one volume (Gorham, 1982). Although Angus Smith explained that 'peculiarities' in urban air can be recognised by one's senses his aim was to use chemical analysis to characterise these peculiarities (Angus Smith, 1872). To achieve this, Angus Smith applied methodologies still commonly found in modern air pollution studies, i.e. the establishment of a coordinated and standardised monitoring network collecting rain water samples (see Chapter 1). Analysis of the collected data highlighted spatial patterns across the UK, e.g. highest chloride concentrations in samples collected close to the coast, and highest ammonium concentrations in urban areas, particularly in central Scotland and north-west England (Figure 2.1). In addition, Angus Smith attempted basic pollutant covariance analysis. For example, the sulphate to chloride ratio in each rainwater sample was calculated to demonstrate the increase in sulphate inland, even in rural locations, due to 'the decomposition of vegetable and animal matter' (Angus Smith, 1872) (Figure 2.2).

Although the reliability of Angus Smith's analyses has been questioned, because of poor temporal resolution and lack of multiple samples collected at each site (Gibson and Farrar, 1974; Gorham, 1982), his concept and approach are enduring (Figures 2.1 & 2.2 highlight the commonality of methods employed by Angus Smith with those still used today, rather than focus on quality of the underlying data). Angus Smith's work represented the first steps in attempts to establish a new branch of environmental science which he called chemical climatology. He advocated for 'the establishment of a department at some Observatories for Chemical Climatology and Meteorology'

(Angus Smith, 1870). The driving force behind Angus Smith's work was concern regarding an impact of atmospheric composition (i.e. health effects) and the human reasons for these (Angus Smith, 1872). The linkage between health (and other negative) impacts and the chemical state of the atmosphere remains relevant today.

For the century after the publication of *Air and Rain*, chemical climatology was described as being an 'abandoned field' (Landsberg, 1983). However, aspects of impact-driven investigations are evident through the literature, despite the term itself not finding widespread usage as Angus Smith had envisaged. Crowther and Ruston (1911) for example similarly collected and analysed monthly rainwater samples over 3 years to examine the effect of atmospheric pollutants on vegetation in Leeds, UK. Different types of sites were sampled and spatial and temporal patterns in rainwater composition examined. Analyses of the meteorological data revealed light rain to contain proportionally more chloride than heavy downpours. In subsequent investigations, the visual impact of air pollution on leaves was shown to be considerably more pronounced in the 'industrial-rural' regions south of Leeds than in the agricultural land to the north (Crowther and Steuart, 1913). As noted in Chapter 1, the three fatal air pollution disasters in the 1940s and 1950s increased monitoring of atmospheric composition and provided greater impetus to the application of chemical climatology principles. For example, subsequent to the 1952 London smog, the UK National Survey ensured representativeness of sites measuring black smoke and SO_2 to assess exposure relevant to human health. Similar processes were occurring elsewhere. For example, in 1977 the US National Atmospheric Deposition Program was established for the benefit of scientists and agencies concerned with environmental effects, albeit of atmospheric deposition, with 288 monitoring sites (Lamb and Bowersox, 2000).

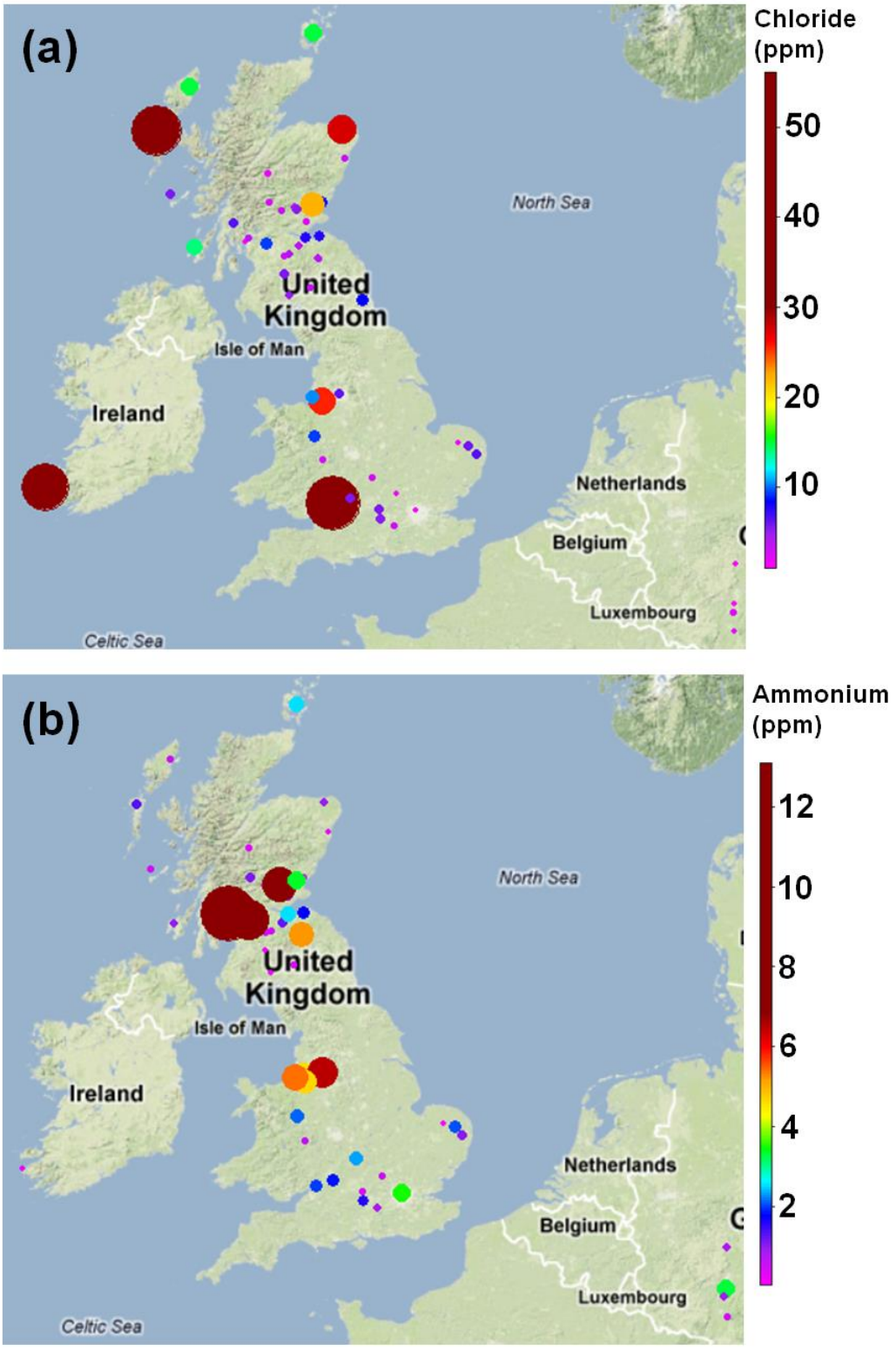

Figure 2.1: Concentrations in rainwater of (a) chloride and (b) ammonium, for 1869-70, presented by Angus Smith (1872) (Map data: Google, Geobasis-DE/BKG).

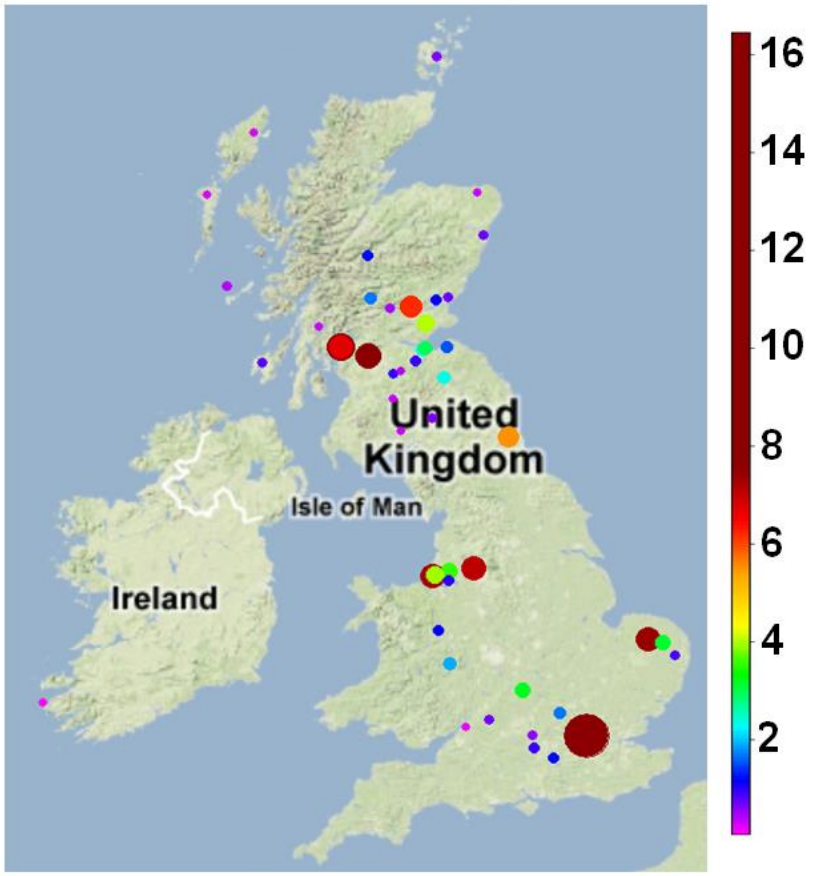

Figure 2.2: Sulphate to chloride ratios in rainwater samples calculated by Angus Smith for his 1869-1870 network (Angus Smith, 1872) (Map data: Google, Geobasis-DE/BKG).

Landsberg (1983) updated the role of chemical climatology, describing it as 'central' to the 'complex questions' on atmospheric composition that climate research programmes should address. However, use of the term chemical climatology in the literature of the last couple of decades has been varied and inconsistent. For example, it has been applied to multiple atmospheric constituent studies (Aneja et al., 1992; Bigi and Harrison, 2010; Fuzzi et al., 1996; Kasper and Puxbaum, 1998), to a single chemical component (Tarasova et al., 2007; Tilmes et al., 2012; Wuttke et al., 2012) and also to atmospheric modelling studies (Al-Saadi et al., 2004; Kelly et al., 2012). Consequently, the following universally-applicable framework for the definition and application of chemical climatology is proposed.

2.2 A framework for chemical climatology

A glossary of the terms used in our definition of chemical climatology is given in Table 2.1, and an illustration of the framework is shown in Figure 2.3. The word climate is used in its general sense, as in for example 'political climate', rather than its more specific use as a descriptor of the physical state of the atmosphere. Nevertheless, parallels with meteorological climate are useful and relevant. The meteorological climate has been defined as the 'composite of the day-to-day weather conditions' (Lamb, 1972). More recently it has been defined as 'the thermodynamic/hydrodynamic status of the global boundary conditions that determine the current array of weather patterns' (Bryson, 1997). McGregor (2006) further explains that this definition of climate 'describes the conditions under which "things" are "possible"', and advocated for greater focus on the drivers of climate state, where the climate state bounds the 'possible' weather patterns (the impacts). Therefore, in general a climate consists of three elements: the 'drivers', the 'state' and the 'impact' (Figure 2.3). Examples of these elements are provided in Table 2.2 for three different examples of climates (meteorological, chemical and political).

The assessment of a climate requires clear demarcation of the temporal and spatial boundaries (time period and geographical location) encompassed. Where there is identification of a significant change in the impact, resulting from significant change to the drivers and state, then these may be classified as different phases of the climate (Figure 2.3). Practically, the identification of different climate phases might arise in two ways: either the assessment of a large dataset might lead to the conclusion of different blocks (phases) of time or space within the climate; or separate climates may be derived for a given impact, e.g. for different time periods or different geographical areas, which might subsequently be incorporated as different phases of a single overarching climate. Both approaches end up with phases that encapsulate the variation in climate over time and/or space.

Table 2.1: A glossary of terms in chemical climatology.

Term	Definition
Chemical climatology	The overarching framework within which the three elements (drivers, state and impact) of the chemical climate are investigated.
Chemical climate	The holistic characterisation of the atmospheric composition, through the three elements of drivers, state and impact, for a specified spatial and temporal domain. The identification of significant differences in the three elements in space or time leads to the concept of different phases of the chemical climate. A given domain has as many climates as impacts identified.
Impact	An identified effect or metric of atmospheric composition, for which it is sought to determine the underlying contributing sources and processes. Different impacts are associated with different chemical climates. An impact may also be influenced by non-chemical climate factors.
State	The description of the composition and conditions producing the identified impact. Atmospheric constituents contributing to the impact (or metric) are identified. This includes consideration of the relevant temporal variations for the impact (metric), for example diurnal, annual, peak over threshold, etc. An individual chemical climate contains one state, incorporating all relevant variation.
Drivers	The sources and influences on the atmospheric composition that determine the state, and hence the impact (metric). Different combinations of drivers and processes can contribute to the state. A chemical climatology therefore describes the relative importance of the different drivers to the production of the state.
Phase	A distinct instance in space or time of the chemical climate. Different phases are demarcated by significant change in the drivers and state leading to significant change in the impact (metric). Phases may be defined by the segmentation of the temporal or spatial domain of a chemical climate derived using all available data, or by merging climates derived separately for a given impact over smaller temporal or spatial domains.

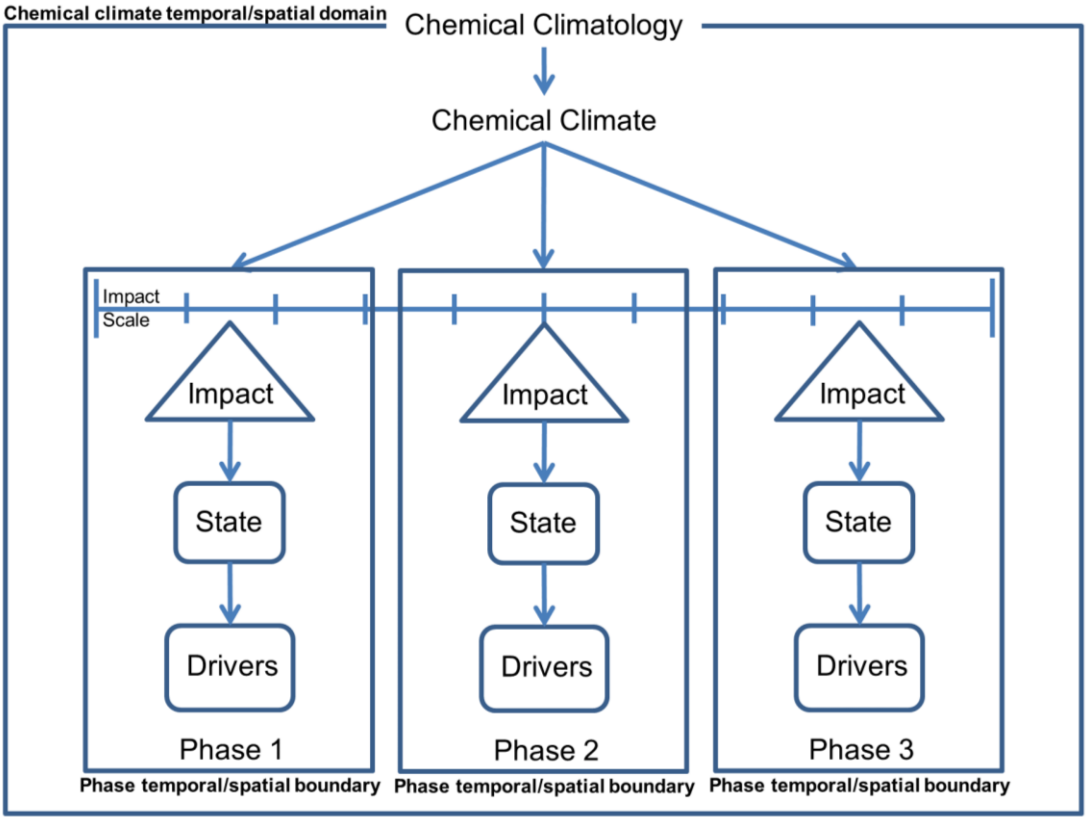

Figure 2.3: An illustration of the chemical climatology framework. A glossary of the terms is given in Table 2.1. For a particular chemical climate description, only a single phase might be identified.

Some examples provide illustration of application of this climatology framework. A regional climate classification scheme devised by Köppen and Geiger in 1900 is a useful illustration of a meteorological climatology. Wladimir Köppen sought to link impacts of climates, specifically the variable types of natural global vegetation cover (inspired by the global vegetation classification of Grisebach (1866)), to the state of climate associated with each type of vegetation cover (Koppen, 1884). Consequently the number of classifications in the Köppen-Geiger system (30) and the vegetation map by Grisebach (33) are very similar. Each classification represents a different climate state, defined through maximum and minimum seasonal temperatures and amounts of seasonal rainfall, assessing a different impact (vegetation cover classification). Each climate is bound within a defined spatial domain, as shown in the Köppen-Geiger climate-type map of the world (Peel et al., 2007). Subsequent studies

assessing different climate impacts have found it necessary to redefine the parameters governing the climate classifications, highlighting the impact-specific nature of the climatology (Ackerman, 1941; Kesseli, 1942).

Table 2.2: Examples of the three elements of climate – impact, state and drivers – that characterise three different examples of a climate (meteorological, chemical, political).

	Impact	**State**	**Drivers**
Meteorological	Vegetation type and growth, population distributions, atmospheric composition	Averaged weather conditions: e.g. annual, seasonal, daily average, max & min temperature, precipitation etc.	Solar variability, hydrosphere, biosphere, cryosphere interactions
Chemical	Ecosystem effects, human health, atmospheric oxidising capacity, radiative forcing	Chemical composition of the atmosphere: e.g. annual, seasonal, daily concentrations, concentration ranges, covariance between atmospheric constituents, etc.	Meteorological conditions, proximity to sources, atmospheric chemistry, transport patterns
Political	Legislation, economic prosperity, conflicts, distribution of wealth	Political system: e.g. democracy, dictatorship, monarchy. As characterised by political parties, voting rights, freedom of speech, etc.	International relations, civil unrest, quality of life, public perception

The study by Kubicka et al. (1998) into Czech men's drinking between 1983-93 illustrates the features and analysis of a political climate. The impact – alcohol consumption habits – was assessed for three temporal political climate phases: communist rule (mid-80s); an anti-alcohol regime (1988 to early 1990s) which decreased alcohol consumption; and the re-establishment of democracy (early-1990s), which led to a 16% increase in alcohol consumption. These phases of differing alcohol consumption are demarcated by significant changes in the political climate state and its drivers.

A chemical climate can be derived either from the observation of an impact attributable to atmospheric composition or from the interpretation of atmospheric composition measurements (or model output) from which impacts may occur. The chemical climatology is then derived, within the stated spatial and temporal boundary conditions, by describing the chemical climate state that produces instances of the impact, i.e. the 'conditions' under which 'things' are possible. The state details the 'what', 'when' and 'where', of pollutant variation contributing to the impact. 'What' refers to the pollutant, or suite of pollutants, responsible for the impact. 'When' details the temporal variation in pollutant concentration relevant to the chemical climate impact, including pollutant covariance. For example, the photochemical nature of ozone production dictates that the chemical climate state relating to ozone's acute health impact includes diurnal variation. Finally, 'where' describes spatial variation of pollutant concentration relevant to the chemical climate impact, for example over a region covered by a policy-making body, or between classifications of regions e.g. urban vs. rural. When the chemical climate state is sufficiently detailed, assessment of the different combination of drivers leading to the state and impact can then be undertaken. Drivers address 'why' and 'how' a chemical climate state occurs and may include proximity of emission sources, meteorological conditions, atmospheric photochemistry, long-range transport, etc. Additionally, an identified chemical climate impact may be influenced by non-chemical climate factors, which may in turn act to influence the chemical climate state and relevant drivers producing instances of the impact. For example, a chemical climate describing the impact of SO_2 on ecosystems would consider dry deposition rates of SO_2 to terrestrial surfaces (among other processes e.g. wet deposition) (RoTAP, 2012). Non-chemical climate factors influencing dry deposition rates include meteorology (wind velocity) which regulates turbulent transfer within the atmosphere, and landscape features (e.g. vegetation type, soils, water and bark) which determine the rates of reaction with which SO_2 is deposited. Hence when the chemical climate state and drivers have been described, correlation with non-chemical climate factors can be used to assess temporal/spatial periods at which the combination of chemical climate and non-chemical climate factors produces maximum/minimum SO_2 ecosystem impact.

The requirement for identification of an atmospheric composition impact in the derivation of a chemical climate prior to the assessment of the state and drivers specific to that impact can result in differences in the categorisation of atmospheric composition phenomena as impact, state or drivers for different chemical climates. For example, in the chemical climates specific to the impact of ozone on human health and vegetation (Chapter 4), the state statistics (diurnal and monthly ozone variation relevant to the health and vegetation impact) linked the impact to the relative contribution from hemispheric background, and regional (European) ozone production (see Chapter 4 for definition of these terms). However, in Chapter 5, the aim was to investigate the impact of Volatile Organic Compounds (VOCs) measured at the UK EMEP supersites. VOCs are precursors to ozone, and therefore the impact of interest in this chemical climate was that of the measured VOCs on regional ozone production. The state and drivers of this chemical climate assess variation in measured VOC concentrations, and VOC emissions, in the production of regional ozone. The requirement that state and drivers are defined for a specific impact results in a chemical climatology framework flexible enough to investigate a wide range of atmospheric composition impacts, and the conditions producing them. This enhances the information derived from measurement data, in this case by facilitating assessment of the impacts of regional ozone production (when defined as a driver) in one chemical climate, and the conditions producing it in another (when defined as the impact), separate chemical climate.

Applying this framework, *a posteriori*, to the National Survey following the 1952 London smog (described in Chapter 1), the chemical climate specific to the health impact of smog was investigated through increased measurement of black smoke and SO_2. Representative sites allowed assessment of spatial variation, and suitably high time resolution measurements (daily) were specified (Clifton, 1964). This combination of ‘what’, ‘when’ and ‘where’ meant the chemical climate drivers became better understood, including meteorology, emissions and social factors, the latter underlying pronounced regional differences exacerbated by the measures within the Clean Air Act 1956 (Craxford and Weatherley, 1971). New mitigation strategies could therefore be

developed; specifically relating to emissions reductions, and town planning that better segregated industrial, residential and commercial areas. In this example, the chemical climate was confined to the UK, but within the UK spatial variation of the impact, state and drivers was described. Different temporal phases are evident from the significant change in the impact due to changes in the state and drivers. For example, the phase prior to the Clean Air Act was characterised by the greatest health impact. Curtailment of a principal driver (black smoke emissions) resulted in a different phase: same impact but significantly lower severity.

A locality or an atmospheric component(s) has as many chemical climates associated with it as there are identified impacts. Each chemical climate is defined by a distinct state and combination of drivers, although considerable overlap of these drivers may occur. For example, chemical climatology principles assessed the linkage between childhood exposure to lead pollution and increased violent crime in adulthood (Mielke and Zahran, 2012). The mass of 'air Pb' emitted described the state for this impact, and the state had both a spatial dimension through incorporation of geographically-diverse cities (within the USA) and a temporal component through use of annual averages. The state was assessed in relation to relevant drivers: state gasoline usage, city traffic volume, average miles per gallon, and the lead content of different fuels. 85% of the temporal variation in the aggravated assault rate in New Orleans was explained by variation in air Pb with a 22 year lag. Thus this chemical climate explicitly linked an observed impact to a chemical climate state and its drivers. However, lead pollution has other adverse impacts not adequately explained by this state and set of drivers. Johansson et al. (2001) studied the adverse impact of long-range atmospheric transport and deposition of lead on biological processes in forest soils in Sweden. A different state and set of drivers were required to construct the chemical climate in this case.

Finally, the framework is as applicable to atmospheric model output as to measurements. Modelling studies have the advantage of being able to simulate the

effect that variation of drivers may have on state and impact (e.g. policy actions, climate change, etc.).

2.3 Application of the chemical climatology framework

2.3.1 Practical steps

Six practical steps to define a chemical climate are summarised in Table 2.3 and Figure 2.4. Step 1 identifies the impact; for example, studies link acute exposure to elevated ozone concentrations and respiratory conditions (WHO, 2006). Step 2 defines the relevant metric; e.g. maximum daily 8-h average concentration above 35 ppb, which is associated with a statistically significant increase in mortality (Amann et al., 2008). Step 3 defines the temporal and spatial boundaries to the dataset. Step 4 is the description of the state. This involves relevant temporal and spatial patterns of ozone variation above 35 ppb, e.g. diurnal and seasonal variation, and covariance with precursor molecules. Step 5 identifies drivers, for example the relative importance of local, regional and hemispheric transport, and source activities emitting ozone precursors. Step 6 assesses the presence of different phases within the chemical climate, e.g. significantly different patterns of ozone metric exceedance in different regions, or significant changes to ozone precursor emissions over time. Different phases may be identified during steps 2-5 or through independent application of steps 2-5 for different spatial/temporal domains, followed by collation into a single chemical climate. Were a different impact being investigated, for example the ozone impact on vegetation (assessed by a cumulative deposition flux over a season) or the human health impact of particulate matter, the state and drivers would be different, and a separate chemical climate would be derived. Steps 1-3 are usually integral to impact studies, while steps 4-6 are key components of atmospheric chemistry studies. The need for integration is emphasised here.

Table 2.3 also highlights the chemical climatology steps covered by four illustrative studies concerning ground-level ozone. Derwent et al. (2013) is a good recent example of a study featuring full chemical climates assessing the contribution of a driver (hemispheric background ozone concentrations) to different ozone impacts (vegetation and human health). Three examples of the majority of studies which assess a subset of the steps are also included in Table 2.3. WHO (2006) assess the health impact of ozone and define a relevant metric (steps 1 and 2), but do not evaluate the state and drivers of ozone variation in particular locations; Malley et al. (2014) describe changes in ozone variation at rural sites across Europe (steps 3 and 4), but do not link to ozone impacts or causal drivers; Gerasopoulos et al. (2006) assess the state and drivers of ozone variation at Finokalia, Crete (steps 4 and 5), but do not link this variation to ozone impacts, nor evaluate the temporal and spatial representativeness of ozone variation at the location.

Covering a subset of the chemical climatology steps is not a shortcoming of studies, and neither should every investigation aim to cover every step in the chemical climatology framework. However, increased awareness of the steps within the framework covered by isolated studies means that they can be combined to produce full impact-led chemical climate assessments focussing on relevant local, regional and global scale issues. This would better facilitate consideration of impact mitigation strategy development where needed. A standard output from chemical climate studies, such as those outlined in Chapter 7, summarises the statistical features of the chemical climate, as well as the temporal and spatial boundaries and scientific uncertainties. This could allow collation and linkage between chemical climates and promote a consistent and accessible interpretation of atmospheric pollutant datasets.

Table 2.3: Chemical climatology framework: component steps and example studies identifying which component steps were described.

		Example chemical climatology	Example studies			
Step	**Description**	**Ozone**	***Gerasop-oulos et al. (2006)***	***WHO (2006)***	***Derwent et al. (2013)***	***Malley et al. (2014)***
1	Identify **impact**	Human health; Vegetation damage		✓	✓	
2	Define relevant chemical climate metric(s) for the **impact**	Sum of means over 35 ppb (SOMO35); Accumulated ozone over 40 ppb (AOT40)		✓	✓	
3	Define the chemical climate's temporal and spatial boundaries	Representivity of time period and location			✓	✓
4	Describe the chemical climate **state**	Statistical analysis of measured/modelled dataset	✓		✓	✓
5	Identify the chemical climate **driver(s)**	Relative contribution of meteorology, source apportionment, atmospheric chemistry	✓		✓	
6	Assess for phases within the chemical climate	Significant temporal/spatial changes in impact severity			✓	

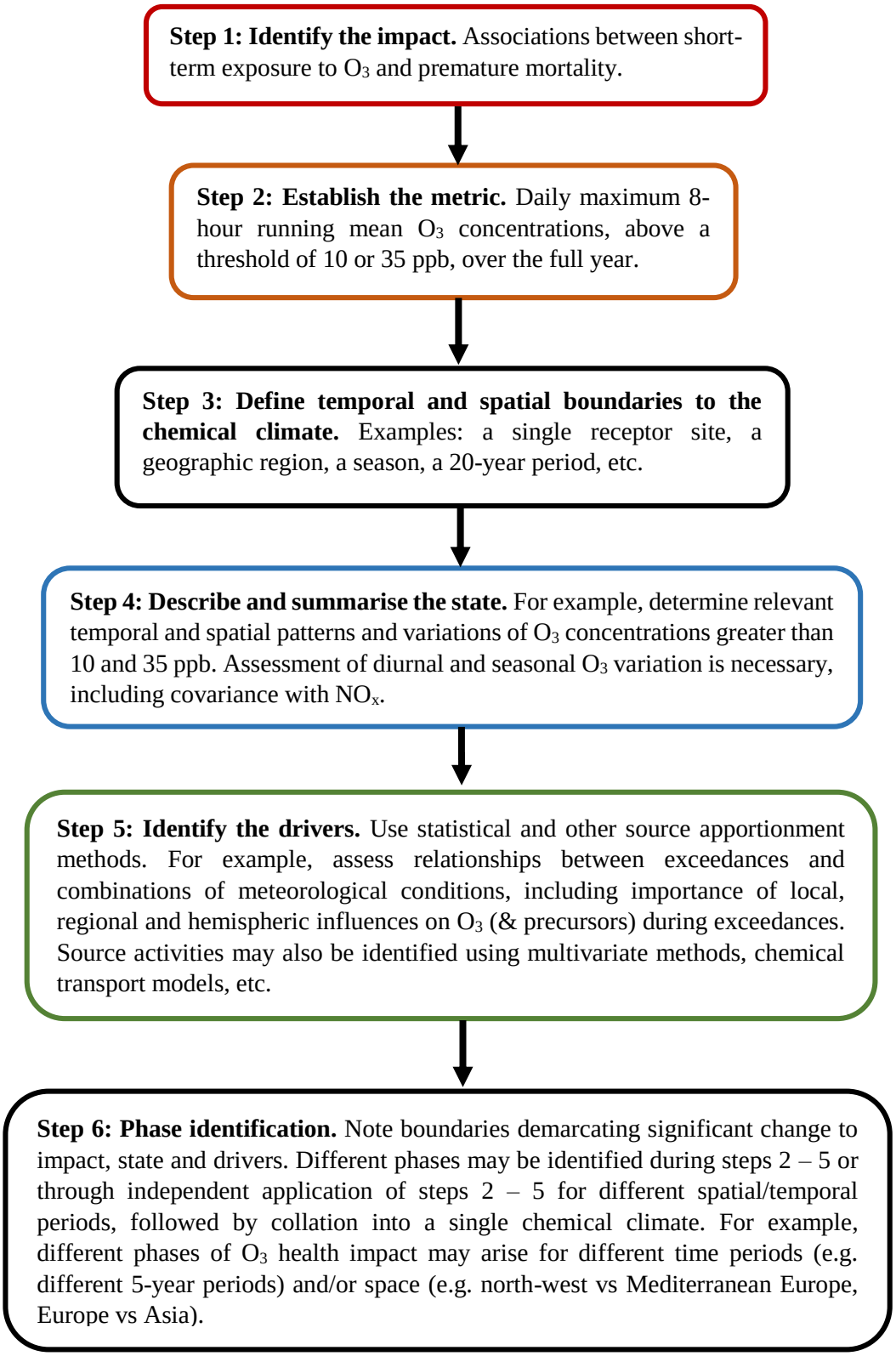

Figure 2.4: Flow diagram showing practical steps for derivation of a chemical climate. The impact of premature mortality associated with short-term exposure to O_3 is used as an example.

2.3.2 Scientific methods

A wide range of possible data analysis approaches are available to investigate and summarise the state and drivers of a chemical climate. To describe a particular state will usually require temporal and/or spatial trend analysis, for which many techniques and examples exist (Chandler and Scott, 2011; RoTAP, 2012). Since other atmospheric constituents can influence the concentration of a given pollutant, assessment of covariance can aid understanding of a chemical climate state and drivers (Monks et al., 2009). In considering the drivers of a chemical climate, it is important to identify the source of a component, whether from primary emissions, secondary formation or bi-directional fluxes. The geographical origin may be probed through the construction of air-mass histories using a variety of meteorological approaches, e.g. wind direction, back trajectories, dispersion modelling. These histories may then be categorised based on pollutant concentrations at the receptor site when the trajectory arrives (e.g. using geographic sector analyses or cluster analyses). Air mass histories and their application have been extensively reviewed by Fleming et al. (2012). Finally, many multivariate techniques such as principal component analysis, positive matrix factorization and chemical mass balance can be used to identify the source activity of atmospheric components (Song et al., 2008).

The common basis for analysis afforded by the chemical climatology framework can aid in the selection of the most appropriate tool to assess a particular impact of atmospheric composition, given the wide array of possible analytical tools, including specific software targeted towards atmospheric composition data interpretation, e.g. the Openair R software package (Carslaw and Ropkins, 2012). Additionally, a standardised method for data interpretation allows for comparison between analyses utilising different analytical methods.

2.4 Conclusions

In the context of monitoring networks, history has shown success is achieved when they are coordinated and standardised. For example, compilation of site conditions, and standardised measurement methods contribute to producing high quality, comparable measurement data. The chemical climatology framework provides a pathway to extend network standardisation to data interpretation. The first application of atmospheric chemical climatology, compiled by Robert Angus Smith in the 1870s, comprised a systematic investigation of the state of the atmosphere with the overall aim of mitigating the deleterious air pollution experienced by the urban population of Victorian Britain. The impact-led approach of Angus Smith is conserved in this modern definition. In a field where there is an abundance of measured (and modelled) datasets, a clear, modern definition of chemical climatology and practical steps to its application could facilitate better interpretation of atmospheric chemistry measurements with respect to impacts. Based on the principle that any climate system consists of the impact, state and the drivers – the chemical climatology framework investigates these three elements within defined temporal and spatial boundaries. The existence of different phases of a chemical climate within a larger temporal and spatial domain can be demarcated when significant changes to the impact occur. Application of the chemical climatology principles could allow many atmospheric chemistry studies to be defined in a more holistic context and focus on relevant scientific questions at local, regional and global scales, followed by, if appropriate, a more considered development of mitigation strategies.

References

Ackerman, E., 1941. The Koppen Classification of Climates in North America. Geographical Review 31, 105-111.

Al-Saadi, J. A., Pierce, R. B., Natarajan, M., Fairlie, T. D., Grose, W. L., 2004. Chemical climatology of the middle atmosphere simulated by the NASA Langley Research Center Interactive Modeling Project for Atmospheric Chemistry and Transport (IMPACT) model. Journal of Geophysical Research 109, D17301, doi:10.1029/2003jd004354.

Amann, M., Derwent, D., Forsberg, B., Hanninen, O., Hurley, F., Krzyzanowski, M., de Leeuw, F., Liu, S., Mandin, C., Schneider, J., Schwarze, P., Simpson, D., 2008. World Health Organization: Health risks of ozone from long-range transboundary air pollution. WHO Regional Office for Europe. http://www.euro.who.int/__data/assets/pdf_file/0005/78647/E91843.pdf.

Aneja, V. P., Robarge, W. P., Claiborn, C. S., Murthy, A., Sookim, D., Zheng, L., Cowling, E. B., 1992. Chemical climatology of high elevation spruce fir forests in the southern appalachian mountains. Environmental Pollution 75, 89-96.

Angus Smith, R., 1845. Some Remarks on the Air and Water of Towns. Mem. Proc. Chem. Soc. 3, 311-315.

Angus Smith, R., 1870. Chemical Climatology. Journal of the Scottish Meteorological Society.

Angus Smith, R., 1872. Air and Rain: The Beginnings of a Chemical Climatology. Longmans, Green and co., London.

Bigi, A., Harrison, R. M., 2010. Analysis of the air pollution climate at a central urban background site. Atmospheric Environment 44, 2004-2012.

Bryson, R. A., 1997. The paradigm of climatology: An essay. Bulletin of the American Meteorological Society 78, 449-455.

Carslaw, D. C., Ropkins, K., 2012. openair - An R package for air quality data analysis. Environ. Modell. Softw. 27-28, 52-61.

Chandler, R. E., Scott, E. M., 2011. Statistical Methods for Trend Detection and Analysis in Environmental Sciences, Wiley, Chichester.

Clifton, M., 1964. How air pollution is detected. Proceedings of the Royal Society of Medicine-London 57, 615-618.

Craxford, S. R., Weatherley, M. P. M., 1971. Air Pollution in Towns in the United Kingdom. Philosophical Transactions of the Royal Society of London. Series A, Mathematical and Physical Sciences. 269, 503 - 513.

Crowther, C., Ruston, A., 1911. The Nature, Distribution and Effects upon Vegetation of Atmospheric Impurities in and near an Industrial Town. The Journal of Agricultural Science 4, 25-55.

Crowther, C., Steuart, D., 1913. The Distribution of Atmospheric Impurities in the Neighbourhood of an Industrial City. The Journal of Agricultural Science 5, 391-408.

Derwent, R., Manning, A., Simmonds, P., Gerard Spain, T., O'Doherty, S., 2013. Analysis and interpretation of 25 years of ozone observations at the Mace Head

Atmospheric Research Station on the Atlantic Ocean coast of Ireland from 1987 to 2012. Atmos. Environ. 80, 361-368.

Fleming, Z. L., Monks, P. S., Manning, A. J., 2012. Review: Untangling the influence of air-mass history in interpreting observed atmospheric composition. Atmospheric Research 104, 1-39.

Fuzzi, S., Facchini, M. C., Orsi, G., Bonforte, G., Martinotti, W., Ziliani, G., Mazzali, P., Rossi, P., Natale, P., Grosa, M. M., Rampado, E., Vitali, P., Raffaelli, R., Azzini, G., Grotti, S., 1996. The NEVALPA project: A regional network for fog chemical climatology over the Po Valley basin. Atmospheric Environment 30, 201-213.

Gerasopoulos, E., Kouvarakis, G., Vrekoussis, M., Donoussis, C., Mihalopoulos, N., Kanakidou, M., 2006. Photochemical ozone production in the eastern Mediterranean. Atmos. Environ. 40, 3057-3069.

Gibson, A., Farrar, W. V., 1974. Robert Angus Smith, F.R.S., and 'Sanitary Science'. Notes Rec. R. Soc. Lond. 28, 241-262.

Gorham, E., 1982. Robert Angus Smith, FRS and 'Chemical Climatology'. Notes and Records of the Royal Society of London 36, 267-272, doi:10.1098/rsnr.1982.0016.

Grisebach, A., 1866. Vegetation der Erde (Vegetation of the Earth). Petermanns Geogr. Mitt. 12, 45-53.

Johansson, K., Bergback, B., Tyler, G., 2001. Impact of Atmospheric Long Range Transport of Lead, Mercury and Cadmium on the Swedish Forest Environment. Water, Air and Soil Pollution: Focus 1, 279 - 297.

Kasper, A., Puxbaum, H., 1998. Seasonal variation of SO2, HNO3, NH3 and selected aerosol components at Sonnblick (3106 m asl). Atmospheric Environment 32, 3925-3939.

Kelly, J., Makar, P. A., Plummer, D. A., 2012. Projections of mid-century summer air-quality for North America: effects of changes in climate and precursor emissions. Atmospheric Chemistry and Physics 12, 5367-5390.

Kesseli, J., 1942. The Climates of California According to the Koppen Classification. Geographical Review 32, 476-480.

Koppen, W., 1884. Die Waermezonen der Erde, nach der Dauer der heissen, gemaessigten und kalten Zeit und nach der Wirkung der Waerme auf die organische Welt betrachtet (The thermal zones of the earth according to the duration of hot, moderate and cold periods and to the impact of heat on the organic world). – Meteorol. Z. 1, 215–226. (translated and edited by Volken, E. and S. Bronnimann. – Meteorol. Z. 20 (2011), 351–360).

Kubicka, L., Csemy, L., Duplinsky, J., Kozeny, J., 1998. Czech men's drinking in changing political climates 1983-93: a three-wave longitudinal study. Addiction 93, 1219-1230.

Lamb, D., Bowersox, V., 2000. The national atmospheric deposition program: an overview. Atmospheric Environment 34, 1661–1663.

Lamb, H. H., 1972. Climate: Past, Present, and Future, Volume 1: Fundamentals and Climate Now, Methuen and Co.

Landsberg, H. E., 1983. Climatology - The future. International Journal of Environmental Studies 20, 159-165.

Malley, C. S., Braban, C. F., Heal, M. R., 2014. The application of hierarchical cluster analysis and non-negative matrix factorization to European atmospheric monitoring site classification. Atmos. Res. 138, 30-40.

McGregor, G. R., 2006. Climatology: Its scientific nature and scope. International Journal of Climatology 26, 1-5.

Mielke, H. W., Zahran, S., 2012. The urban rise and fall of air lead (Pb) and the latent surge and retreat of societal violence. Environment International 43, 48-55.

Monks, P. S., Granier, C., Fuzzi, S., Stohl, A., Williams, M. L., Akimoto, H., Amann, M., Baklanov, A., Baltensperger, U., Bey, I., Blake, N., Blake, R. S., Carslaw, K., Cooper, O. R., Dentener, F., Fowler, D., Fragkou, E., Frost, G. J., Generoso, S., Ginoux, P., Grewe, V., Guenther, A., Hansson, H. C., Henne, S., Hjorth, J., Hofzumahaus, A., Huntrieser, H., Isaksen, I. S. A., Jenkin, M. E., Kaiser, J., Kanakidou, M., Klimont, Z., Kulmala, M., Laj, P., Lawrence, M. G., Lee, J. D., Liousse, C., Maione, M., McFiggans, G., Metzger, A., Mieville, A., Moussiopoulos, N., Orlando, J. J., O'Dowd, C. D., Palmer, P. I., Parrish, D. D., Petzold, A., Platt, U., Poeschl, U., Prevot, A. S. H., Reeves, C. E., Reimann, S., Rudich, Y., Sellegri, K., Steinbrecher, R., Simpson, D., ten Brink, H., Theloke, J., van der Werf, G. R., Vautard, R., Vestreng, V., Vlachokostas, C., von Glasow, R., 2009. Atmospheric composition change - global and regional air quality. Atmospheric Environment 43, 5268–5350.

Peel, M. C., Finlayson, B. L., McMahon, T. A., 2007. Updated world map of the Koppen-Geiger climate classification. Hydrology and Earth System Sciences 11, 1633-1644.

Reed, P., 2012. The Alkali Inspectorate 1874-1906: Pressure for Wider and Tighter Pollution Regulation. Ambix 59, 131-151.

RoTAP, 2012. Review of Transboundary Air pollution: Acidification, Eutrophication, Ground Level Ozone and Heavy metals in the UK. Contract Report to the Department for Environment, Food and Rural Affairs. Centre for Ecology and Hydrology. http://www.rotap.ceh.ac.uk/sites/rotap.ceh.ac.uk/files/CEH%20RoTAP.pdf.

Song, Y., Dai, W., Shao, M., Liu, Y., Lu, S., Kuster, W., Goldan, P., 2008. Comparison of receptor models for source apportionment of volatile organic compounds in Beijing, China. Environmental Pollution 156, 174-183.

Tarasova, O. A., Brenninkmeijer, C. A. M., Joeckel, P., Zvyagintsev, A. M., Kuznetsov, G. I., 2007. A climatology of surface ozone in the extra tropics: cluster analysis of observations and model results. Atmospheric Chemistry and Physics 7, 6099-6117.

Tilmes, S., Lamarque, J. F., Emmons, L. K., Conley, A., Schultz, M. G., Saunois, M., Thouret, V., Thompson, A. M., Oltmans, S. J., Johnson, B., Tarasick, D., 2012. Technical Note: Ozonesonde climatology between 1995 and 2011: description, evaluation and applications. Atmospheric Chemistry and Physics 12, 7475-7497.

WHO, 2006. Air Quality Guidelines. Global update 2005. Particulate matter, ozone, nitrogen dioxide and sulfur dioxide., World Health Organisation Regional Office for Europe, Copenhagen. ISBN 92 890 2192 6. http://whqlibdoc.who.int/hq/2006/WHO_SDE_PHE_OEH_06.02_eng.pdf.

Wuttke, S., Kreuter, A., Blumthaler, M., 2012. Aerosol climatology in an Alpine valley. Journal of Geophysical Research **117**, D20202, doi:10.1029/2012JD017854.

Chapter 3: The UK EMEP supersites: site representativeness in a European context

This chapter is based on a research paper published in 'Atmospheric Research' (Malley, C. S., Braban, C. F., & Heal, M. R. (2014). The application of hierarchical cluster analysis and non-negative matrix factorization to European atmospheric monitoring site classification. Atmospheric research, 138, 30-40. 10.1016/j.atmosres.2013.10.019, See Appendix III). I undertook all data analysis, but Dr Mathew Heal and Dr Christine Braban also contributed to the methodology, and the presentation of results through discussions and manuscript editing.

3.1 Introduction

Monitoring sites that contribute to a network are usually classified into different groups that internally share similar atmospheric composition variation. A balance is required which captures the major variations in composition across the network but in as few groups as possible so as to retain the ability to generalise. Various grouping methodologies have been applied (Joly and Peuch, 2012). These range from the relatively subjective use of metadata (Spangl et al., 2007), traditionally used in monitoring networks, to more objective techniques such as rankings based on statistical indicators (Kovac-Andric et al., 2010), linear discriminant analysis (Joly and Peuch, 2012), principal component analysis (Lau et al., 2009), and non-hierarchical (Ignaccolo et al., 2008) and hierarchical cluster analysis (Flemming et al., 2005; Henne et al., 2010; Tarasova et al., 2007). The latter is a multivariate approach that

encompasses many separation/agglomeration techniques which aims to identify natural groupings, or clusters, amongst objects in a dataset through minimisation of the within-cluster variance and maximisation of the between-cluster variance (Kaufman and Rousseeuw, 1990). Clustering methods require user-defined parameters which may impact the objectivity of the analysis. For example, a method for calculating 'distance' between individual members needs to be specified (Dabboor et al., 2013), as must a method for calculating the separation between different groups of members (Mangiameli et al., 1996). Nevertheless, as cited above, clustering techniques have been widely applied to grouping atmospheric monitoring sites.

The aim of this study was to place the two UK European Monitoring and Evaluation Programme (EMEP) Level 2 'supersites', located at Harwell (SE England) and Auchencorth (SE Scotland) in a European context, and assess whether the sites are representative of UK background conditions. These sites do not fully meet the EMEP criteria for non-locally influenced 'background' sites (this is also the case at other EMEP sites, as acknowledged in Torseth et al. (2012), see Section 3.2 for site descriptions). Effective site classification is important to ensure that the spatial domain across which conclusions derived from the interpretation of monitoring site data is appropriately defined. This analysis defines the spatial domain for the chemical climates (defined in Chapter 2) derived in Chapters 4-6 using measurement data from Harwell and Auchencorth. Hence the spatial scale of conclusions derived from these chemical climates, e.g. insights into the mitigation of deleterious air pollution impacts, is extended beyond the confines of the immediate site location to larger geographic areas and human populations. Effective site classification is particularly important for EMEP Level 2 'supersites' across Europe because these are few in number yet subject to much investment in composition monitoring capability.

In this chapter, sites across the EMEP domain were classified according to the annual and daily patterns in ground-level ozone (O_3) concentrations. Ozone was chosen for two reasons. First, it is the most widely measured constituent across the EMEP network – between 2007 and 2010, 113 sites measured hourly O_3 concentrations and

49 sites have continuous O_3 time series since 1991. Second, measured O_3 concentrations are a result of the combination of a wide variety of drivers which are also relevant to many aspects of atmospheric composition, including precursor emissions, photochemistry, deposition, meteorological and climatic conditions and long-range transport (AQEG, 2009; Royal Society, 2008). A major driver of temporal O_3 variation is hemispheric background concentrations (AQEG, 2009). Regional and local-scale processes lead to modification of these values. Under suitable conditions, efficient photochemical processing of NO_x and volatile organic compounds (VOCs) lead to additional O_3 formation and high O_3 episodes, while local-scale depletion of O_3 occurs due to reaction with NO, an effect which increases with higher NO concentrations (Jenkin, 2008).

Hierarchical clustering was applied to the monthly-diurnal O_3 concentrations (average diurnal cycle for each month of the year) at each EMEP site over 4-year periods. Although hierarchical clustering has been applied previously to monitoring site classification (Tarasova et al., 2007), the novelty here was the subsequent application of non-negative matrix factorisation (NMF) (Lee and Seung, 2001) to order the sites across the dendrogram according to an extracted factor. In this case the factor represented the extent of anthropogenic influence on O_3 concentrations. Hierarchical cluster analysis was chosen in preference to non-hierarchical techniques as the robustness and suitability of the cluster assignment is more objectively investigated through the resulting dendrogram, particularly when this is combined with NMF. By using NMF, the O_3 concentrations at the two UK EMEP supersites were placed more precisely in the European context. The analysis was carried out separately for five 4-year periods spanning 1991-2010 to assess the consistency of site representativeness over time.

3.2 Harwell and Auchencorth: UK supersite context and description

The data collected at the Harwell and Auchencorth monitoring sites are a key component of UK atmospheric composition monitoring contributing to the European Monitoring and Evaluation Program (EMEP). EMEP provides scientific information required to evaluate the effect of the current protocols of the Convention on long-range transboundary transport of air pollution (LRTAP), and to develop future protocols within the convention to reduce the impacts of air pollution. EMEP activities include the measurement of atmospheric composition at a network of sites with minimal local emission sources (in addition to calculation of emissions inventories and development and application of atmospheric chemistry transport models).

The EMEP measurement guidance outlines methods intended to ensure that air sampled at a monitoring site is representative of air not directly affected by local emission sources, i.e. data obtained is standardised and comparable (see Chapter 1) (EMEP, 2014). These methods include: sites located 50 km from major pollution sources (towns, power plants etc.), 2 km from the application of manure, and consideration of meteorological and topographical features. More than 200 European sites have contributed data to EMEP and are classified into three categories, Level 1, Level 2 and Level 3. The specific components required for each level are outlined in the EMEP monitoring strategy 2010-2019 (UNECE, 2009). Level 1 sites require measurement of atmospheric constituents at a basic level to understand the chemistry and temporal trends of particulate matter, O_3, acidifying and eutrophying pollutants and heavy metals. There is a target of a minimum of two Level 1 sites per 100,000 km^2. Level 2 sites require measurement of a larger number of constituents and a greater degree of speciation, and nations greater than 50,000 km^2 should aim to operate at least one Level 2 site. Level 3 sites are research-oriented, and include campaign-type data. Sites meeting the criteria for the latter two classifications are called ‘supersites’.

In the UK, 45 sites have contributed measurement data to the EMEP network. These sites range from 'supplemental' Level 1 sites, which measure a subset of the required Level 1 species (e.g. GB0035 Great Dun Fell, where only O_3 is continuously measured) to the two Level 2 monitoring supersites located at Harwell and Auchencorth (Figure 3.1). Harwell is located in rural Oxfordshire, England (lat: 51.571, lon: –1.325, altitude: 126 m) and is 70 km west of London. Potential local influences include a power station, 6 km from the monitoring station. The combined coal and oil power station ceased operation in 2013, while the natural gas power plant continues to operate. Additionally, a dual carriageway road is approximately 2 km from the site. The site has been described previously (Abdalmogith 2006), and measurement began in the late 1970s (Brice et al., 1982). Auchencorth is located on an ombotrophic bog (dependent on atmospheric moisture for its nutrients), 17 km south of Edinburgh, Scotland (lat: 55.792, lon: –3.243, altitude: 260 m) and started as a monitoring site in the mid-1990s. Despite a relatively close proximity to a 487,000 population city to the north-east of the site, the dominant south-westerly wind direction results in the sampling of air with low local influence during the majority of the year. The site location, conditions and typical meteorology have also been described previously (Twigg et al., 2015).

Currently, each supersite measures approximately 120 components of the air, rain and particulate matter, summarised in Table 3.1. The measurements made at the UK supersites, and at sites throughout the EMEP network contribute to the achievement of EMEP's objectives, which include: 1) provide data on air pollutant concentrations, deposition rates, emissions and fluxes, and identify trends in time, 2) identify sources of pollution concentrations and the effects of changes in emissions, 3) improve understanding of physical and chemical processes relevant to vegetation and human health to support the mitigation of these impacts, and 4) explore concentrations of new chemical substances (UNECE, 2012).

The large number of concurrent measurements, including components not measured at other UK sites, result in a disproportionately large contribution from Harwell and

Auchencorth data to achieving the EMEP objectives for the UK, compared to the Level 1 sites. Hence the utility of the supersite concept as part of a strategy to address air quality research issues has recently been reinforced (Kuhlbusch et al., 2014). This thesis uses the UK supersite measurement data to derive case studies which demonstrate the additional value added to measurements collected in a standardised and coordinated way resulting from the standardised interpretation of the data. These sites were chosen to show the utility of a standardised interpretation of data because it was possible to: a) compare different impacts of atmospheric composition at the same site (Chapter 4), b) investigate an impact resulting from multiple constituents (Chapters 5 & 6), c) compare impacts in different spatial domains (Chapters 4, 5 & 6), and d) analyse temporal changes in impact (Chapters 4 & 5). Applying the chemical climatology framework (Chapter 2) as this standardised interpretation of data extends analysis beyond a simple comparison of the impact severity. It instead allows for comparison of the differing conditions producing each impact through the calculation of statistics which highlight the 'state' and 'drivers' associated with different impacts.

Figure 3.1: Location of the UK EMEP supersites at Auchencorth and Harwell.

Table 3.1: Summary of the routine measurements of atmospheric composition made at Auchencorth and Harwell.

Gases	**Particulate matter**	**Precipitation**
NO	$PM_{2.5}$	Ammonium
NO_2	PM_{10}	Nitrate
NH_3	Black carbon	Chloride
HNO_3	UV particulate matter	Sulphate
HONO	Particle size and number	Sodium
HCl	Ammonium (PM_{10} & $PM_{2.5}$)	Potassium
O_3	Nitrate (PM_{10} & $PM_{2.5}$)	Magnesium
SO_2	Chloride (PM_{10} & $PM_{2.5}$)	Calcium
Volatile Organic Compounds (VOCs)	Sulphate (PM_{10} & $PM_{2.5}$)	Phosphate
Mercury (speciated)	Sodium (PM_{10} & $PM_{2.5}$)	Heavy metals
	Potassium (PM_{10} & $PM_{2.5}$)	PAHs
	Magnesium (PM_{10} & $PM_{2.5}$)	
	Calcium (PM_{10} & $PM_{2.5}$)	
	Heavy metals (PM_{10})	
	Polycyclic aromatic hydrocarbons (PAH)	
	Elemental/Organic carbon	

3.3 Methodology

Data arrays of 4-year averaged monthly-diurnal O_3 concentrations were calculated for each EMEP site across Europe included in the analysis, i.e. 288 (= 24 hours × 12 months) O_3 concentrations per site where, for example, the O_3 concentration for 'Jan-00.00' was the average of the 00.00-01.00 hourly O_3 on all days in January in the 4-year period under consideration (1991-1994, 1995-1998, 1999-2002, 2003-2006 and 2007-2010) (Measured data from http://ebas.nilu.no). Four-year averages of monthly-

diurnal concentrations were considered a reasonable compromise between long enough to smooth out inter-annual variability whilst short enough to avoid incorporation of long term trends. The number of sites included in each time period, and the number of countries within which these sites are located is summarised in Table 3.2. 154 sites contributed O_3 data to at least one 4-year period, of which 49 contributed to every 4-year time period.

Table 3.2: Number of EMEP sites across Europe used in cluster analysis for each four year period. The increasing number of countries with sites indicates the increasing geographical coverage across Europe with time. 49 sites are common to all time periods.

Time period	No. of sites	No. of countries
1991-1994	76	14
1995-1998	100	20
1999-2002	117	27
2003-2006	117	27
2007-2010	113	26

The choice of clustering parameters can impact the clustering result. In this study, the standard Euclidean distance (*d*) between two *n*-dimensional data arrays (represented by *x* and *y*) was used and in this case *n* = 288 (Equation 3.1).

$$d(x, y) = \sqrt{\sum_{i=1}^{n}(x_i - y_i)^2} \quad (3.1)$$

In hierarchical clustering each object (here each site's monthly-diurnal O_3 concentrations) initially constitutes its own cluster. The two nearest clusters are then combined and this process is continued until there is one cluster containing all objects. The process of agglomeration is summarised in a dendrogram. Hierarchical clustering techniques differ in how the separation of clusters is quantified, and hence how the linkages of the dendrogram are constructed. A number of linkage methods can be applied, e.g. single, complete, average or centroid linkage, or Ward's method (Kaufman and Rousseeuw, 1990). Mangiameli et al. (1996) applied these linkage

methods to model datasets of known cluster assignments to assess their effectiveness under a range of conditions, e.g. with dispersed datasets and large disparities in cluster density. In general, Ward's method resulted in a higher percentage of objects assigned to their correct cluster. Ward's method has also been used previously with pollutant concentration data (e.g. Dillner et al. (2005) and Lu et al. (2006)) and was chosen here. At each step (i.e. reduction in the number of clusters by 1 through the merging of 2 clusters), Ward's method calculates the within-cluster sum of squares (WCSS) for every cluster (Kaufman and Rousseeuw, 1990; Ward, 1963), where WCSS is the squared Euclidean distance between an object in the cluster (x_j) and the mean of that cluster ($\bar{x}$), summed over all (m) objects in that cluster (Equation 3.2).

$$WCSS = \sum_{j=1}^{m}(x_j - \bar{x})^2 \quad (3.2)$$

The two clusters merged at that step are those which after merging produce the smallest increase in the sum of WCSS over all clusters.

The branches of the dendrogram are rotatable, allowing the members to be weighted and reordered according to those weightings within the confines of the dendrogram branches. Here, non-negative matrix factorisation (NMF) was used to reorder the monitoring sites based on the range of monthly-diurnal O_3 profiles observed across Europe. This facilitated investigation into the variability of monthly-diurnal O_3 between sites within the produced clusters (see Section 3.4). The 288 O_3 concentrations for all monitoring sites are combined into a $n \times m$ matrix, **V**, where n is the number of dimensions (288), and m is the number of monitoring sites (113 for 2007-2010). NMF decomposes **V** into two output matrices, an $n \times r$ matrix, **W**, and an $r \times m$ matrix, **H**, whose product **WH** approximates the input matrix **V** (Figure 3.2). This approximation is achieved such that the Euclidean distance between the input matrix and output matrix product (i.e. $(\mathbf{V} - \mathbf{WH})^2$) is minimized. Variable r is the number of factors with which to simplify **V**, **H** contains the contribution of each factor at each monitoring site, and **W** details the composition of each factor (Lee and Seung, 1999). Although a locally minimised Euclidean distance between **V** and **WH** resulted

from the NMF algorithm, and therefore **W** and **H** varied between runs, this did not cause significant variation in the composition of each factor (matrix **W**), or the dendrogram reordering results (Lee and Seung, 2001).

Two factors were used in the NMF here; hence **W** described two O_3 monthly-diurnal cycles (visualised in Figure 3.3), from which the monthly-diurnal cycle at each site is reconstructed by considering the contribution of each from **H**. The appearance of the monthly-diurnal cycle of Factor 1 is consistent with an air mass significantly influenced by regional anthropogenic emissions of O_3 precursor (nitrogen oxides (NO_x) and volatile organic compounds (VOCs)) and depleting (NO_x) species. It features pronounced variation in diurnal (max ~40 µg m^{-3}) and annual (max ~40 µg m^{-3}) O_3 concentration, and a summer maximum in O_3 concentration, consistent with regional-scale O_3 production, as shown in Jenkin (2008). Factor 2 exhibits greater uniformity in monthly-diurnal O_3 concentrations, with the absence of a summer maximum and substantially reduced diurnal O_3 variation in each month, and hence the contribution from Factor 2 does not represent a proxy for the extent of anthropogenic influence at a site. The choice of two factors was semi-arbitrary, but allows an estimation of the anthropogenic influence at each site to be encapsulated via the contribution from a single factor (Factor 1). Each site was weighted with this contribution, and at each node in the dendrogram, where two branches meet, the mean weight of sites on each branch was calculated. The branch with the higher value was placed on the right hand side of the node, producing a dendrogram reordered based on each site's relative anthropogenic pollution influence.

The hierarchical cluster analysis, NMF and map plotting were undertaken with the R statistical software (R Core Development Team, 2008), using respectively the 'NMFN' (Liu, 2012), 'Cluster' (Maechler et al., 2013) and 'Openair' (Carslaw and Ropkins, 2013) packages.

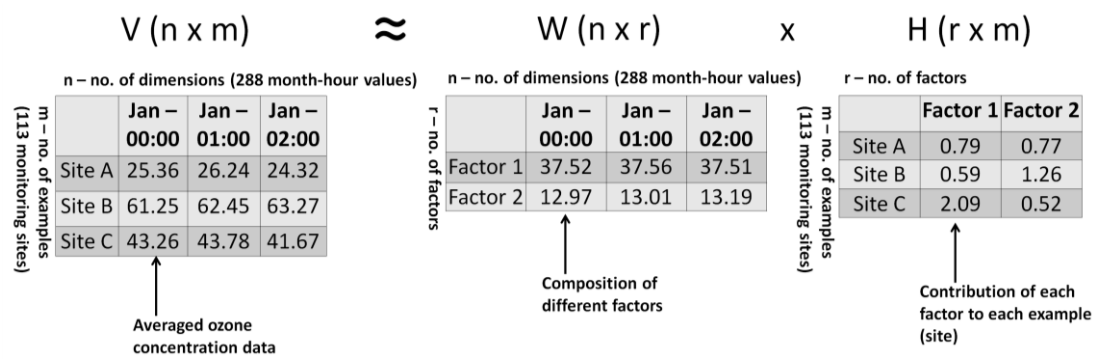

Figure 3.2: Illustration of the process of non-negative factorization as applied to the ozone data in this work.

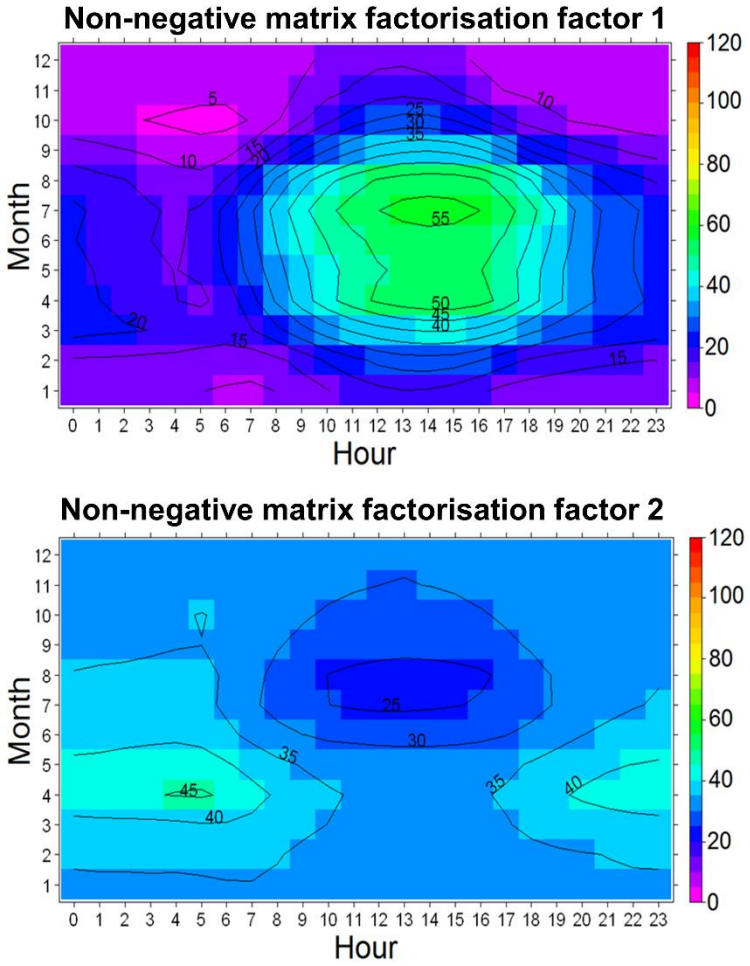

Figure 3.3: Average ozone monthly-diurnal cycles of two factors produced during non-negative matrix factorisation of data for 2007 – 2010. Concentrations are µg m^{-3}.

3.4 Results

Figure 3.4 shows the dendrogram for the EMEP sites recording O_3 data for the period 2007-2010, including site reordering based on NMF Factor 1 (Figure 3.3). The progression of the average monthly-diurnal O_3 cycles across the dendrogram is shown across the bottom of the diagram for selected sites, and illustrates the dramatic change in characteristics of these cycles. Figure 3.5 shows the proportion of explained within-cluster variance (Equation 3.2) as a function of the number of clusters, and ranges from 100% when all sites were located in individual clusters to zero when all sites were located in one cluster. In selecting the optimal number of clusters, the aim is to maximise the explained inter-site O_3 variability using a small number of clusters, allowing key features of O_3 variation across Europe to be summarised. The statistics in Figure 3.5 clearly show that decreasing from 113 to 4 clusters yields relatively small decreases in explained variance (four clusters still explains 75% of within cluster variance) but that a further decrease in cluster number results in substantial disbenefit to explained variance. The natural break into four clusters is also clearly evident in the dendrogram of Figure 3.4. These four clusters were designated as Remote, Polluted, Elevated and Mountain going from left to right across the dendrogram, and contained 39, 39, 25 and 10 of the EMEP sites, respectively. The average monthly-diurnal cycles and locations of sites in each cluster are shown in Figures 3.6 and 3.7 respectively.

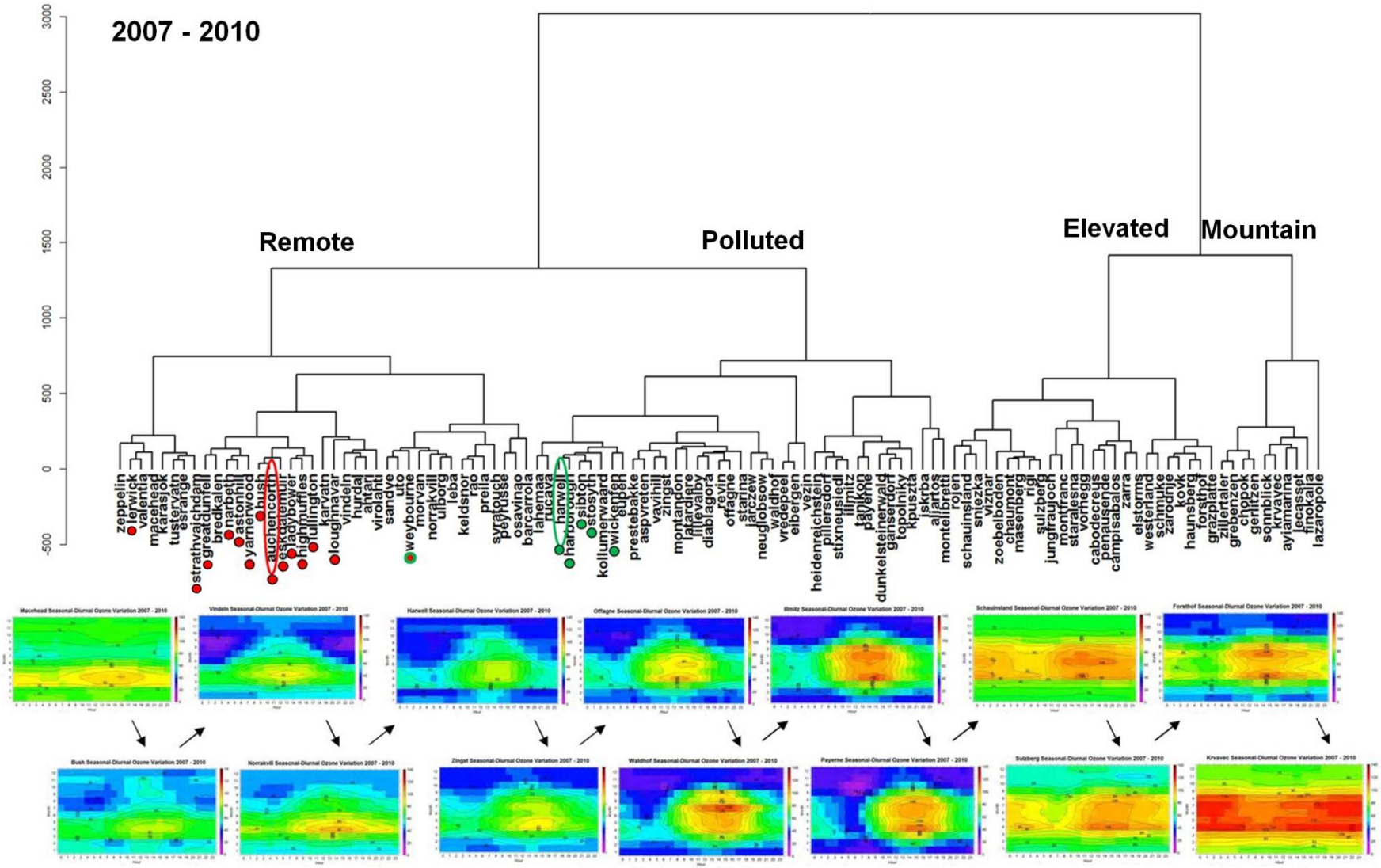

Figure 3.4: Dendrogram of 2007-2010 EMEP sites derived by Ward's method of hierarchical clustering and reordered using non-negative matrix factorisation with the two factors whose monthly-diurnal ozone concentrations are illustrated in Figure 3.3. The UK EMEP sites are identified with a red dot for those classified as Remote and a green dot for those classified as Polluted. The two UK EMEP supersites of Harwell and Auchencorth are circled. The 14 average monthly-diurnal cycles for example sites show the progression of monthly-diurnal O_3 variation across the dendrogram, and between the different clusters.

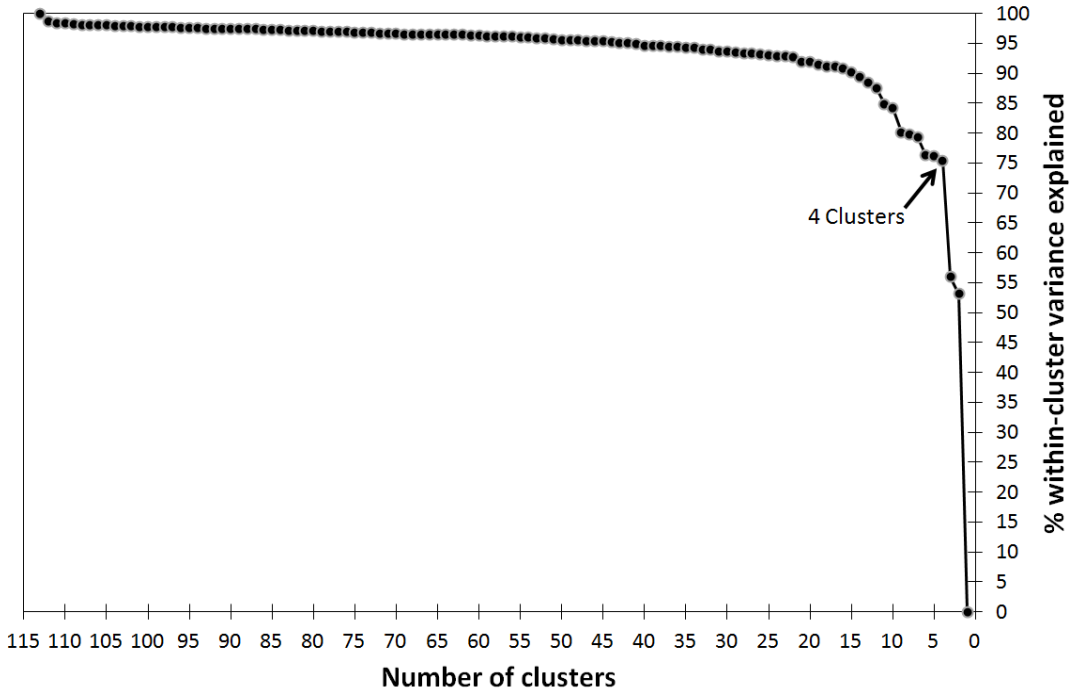

Figure 3.5: The proportion of within-cluster variance explained as a function of number of clusters (2007-2010 dataset).

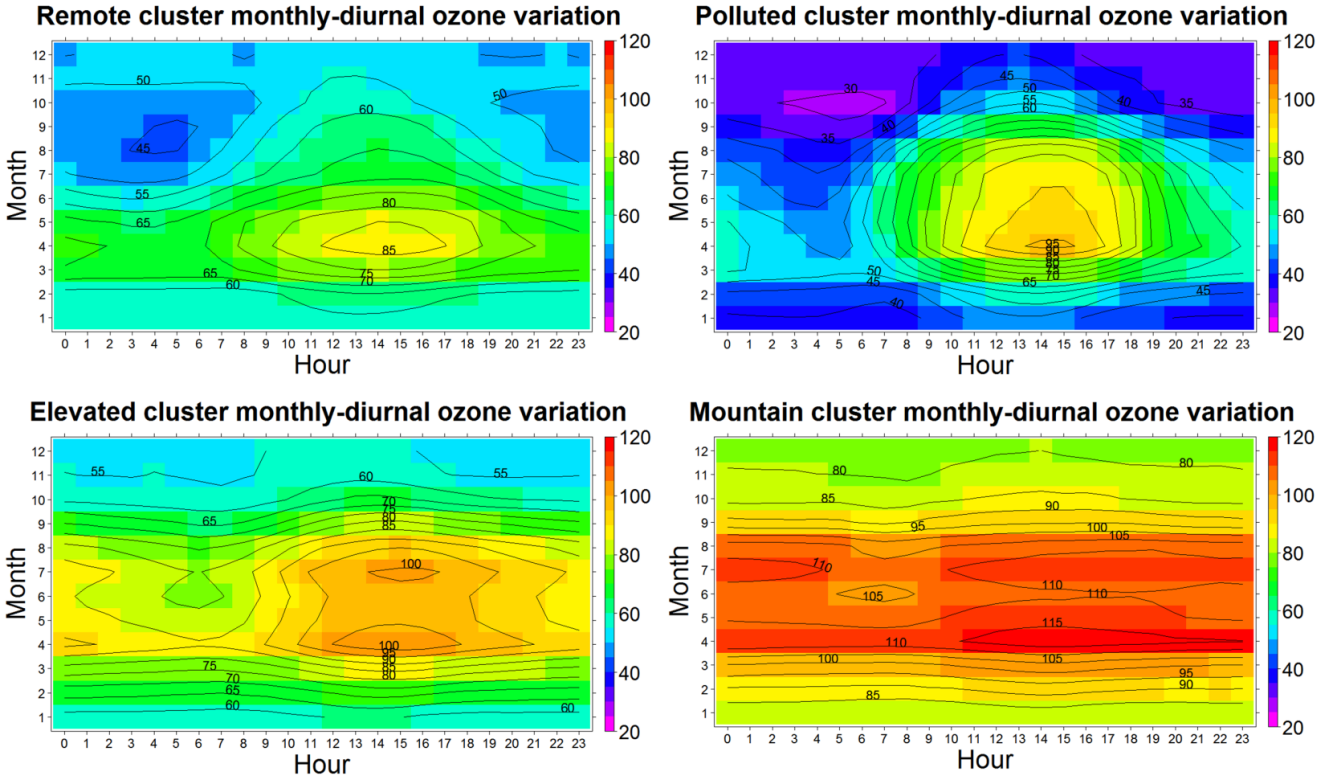

Figure 3.6: Average ozone monthly-diurnal cycle for the four clusters assigned for 2007-2010. Concentrations are µg m^{-3}.

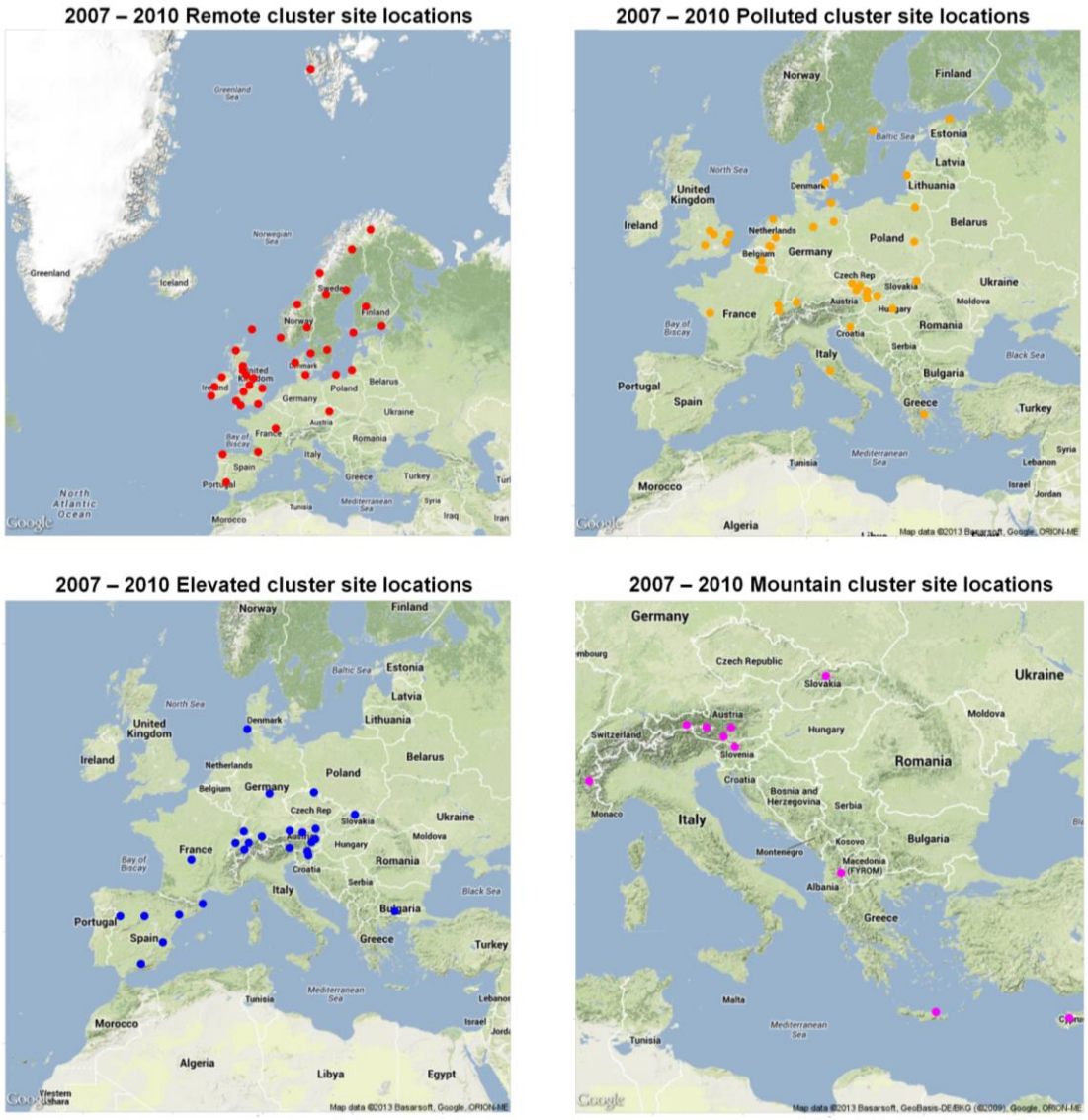

Figure 3.7: Locations of the 113 EMEP sites separated according to the four clusters assigned for 2007 – 2010 monthly-diurnal ozone cycles (Map data: Google, Basarsoft, GeoBasis-DE/BKG, ORION-ME).

The Remote cluster's average monthly-diurnal cycle comprised an annual maximum in April (~85 µg m^{-3}) and a diurnal maximum during the early afternoon (Figure 3.6). However, diurnal and annual variations in O_3 concentrations were not large. The minimum O_3 concentration was ~44 µg m^{-3} and maximum amplitudes in diurnal and annual O_3 variation were 23 and 37 µg m^{-3} respectively. The majority of the sites in the Remote cluster are on the north and west fringes of Europe, predominantly in Scandinavia and the UK (Figure 3.7). In comparison, the Polluted cluster contained

significantly more O_3 concentration variation. Maximum average O_3 concentrations (96 µg m^{-3}) occurred in April and elevated afternoon concentrations persisted through summer before decreasing in August and September. Maximum amplitudes in diurnal and annual O_3 variation of 49 and 59 µg m^{-3}, respectively, produced the lowest concentrations across all clusters (minimum concentration: 27 µg m^{-3}). Sites contributing to this cluster were predominantly in central and southern Europe, including central and eastern England (Figure 3.7). The majority of sites in the Elevated and Mountain clusters are located at altitude. The Mountain cluster contained a greater proportion of mountain-top sites, as opposed to the mix of mountain-top, mountain-side and valley sites found in the Elevated cluster. Diurnal O_3 variation was considerably lower in these two clusters than in the Remote and Polluted clusters (maximum amplitude of Mountain cluster diurnal cycle = 5 µg m^{-3}), and the Mountain cluster showed highest O_3 concentrations (maximum 119 µg m^{-3}). The average O_3 monthly-diurnal cycle of the Elevated cluster had similar features to that of the Mountain cluster, but with lower concentrations and greater annual/diurnal O_3 variation. These statistics summarise variation for the period 2007-2010; however, due to numerous factors, including long-term trends and inter-annual variability, these values vary for the other four time periods spanning 1990-2006.

Though the four major clusters explained 75% of the variability in monthly-diurnal O_3 variation between EMEP sites for 2007-2010, application of NMF dendrogram reordering allowed the remaining 25% to be investigated. From left to right in Figure 3.4 sites within each cluster are ordered according to increasing anthropogenic influence. All 19 UK EMEP sites (which are highlighted in Figure 3.4 and shown geographically in Figure 3.8) were apportioned to the Remote and Polluted clusters. Of these, 17 sites grouped closely with each other within the two clusters (Figure 3.4). The two exceptions were Lerwick and Weybourne. Lerwick, on the Shetland Islands, is much further north and double the distance from a city than any other UK site and was ordered in the dendrogram as considerably more remote than other UK sites in the Remote cluster, i.e. significantly less anthropogenically influenced (Figure 3.4 shows the change in monthly-diurnal O_3 variation between sites within the Remote cluster).

Weybourne, on England's east coast, was clustered midway between the two groupings of UK sites, suggesting the site experienced both types of O_3 regimes. The Auchencorth EMEP supersite was in the middle of the grouping of twelve UK sites within the Remote cluster, whilst the Harwell supersite grouped with the five UK sites in the Polluted cluster, and was the least anthropogenically influenced of this grouping (Figure 3.4). It is a highly relevant result that the cluster analysis showed two dominant O_3 regimes in the UK and each was well represented by one of the two UK EMEP supersites.

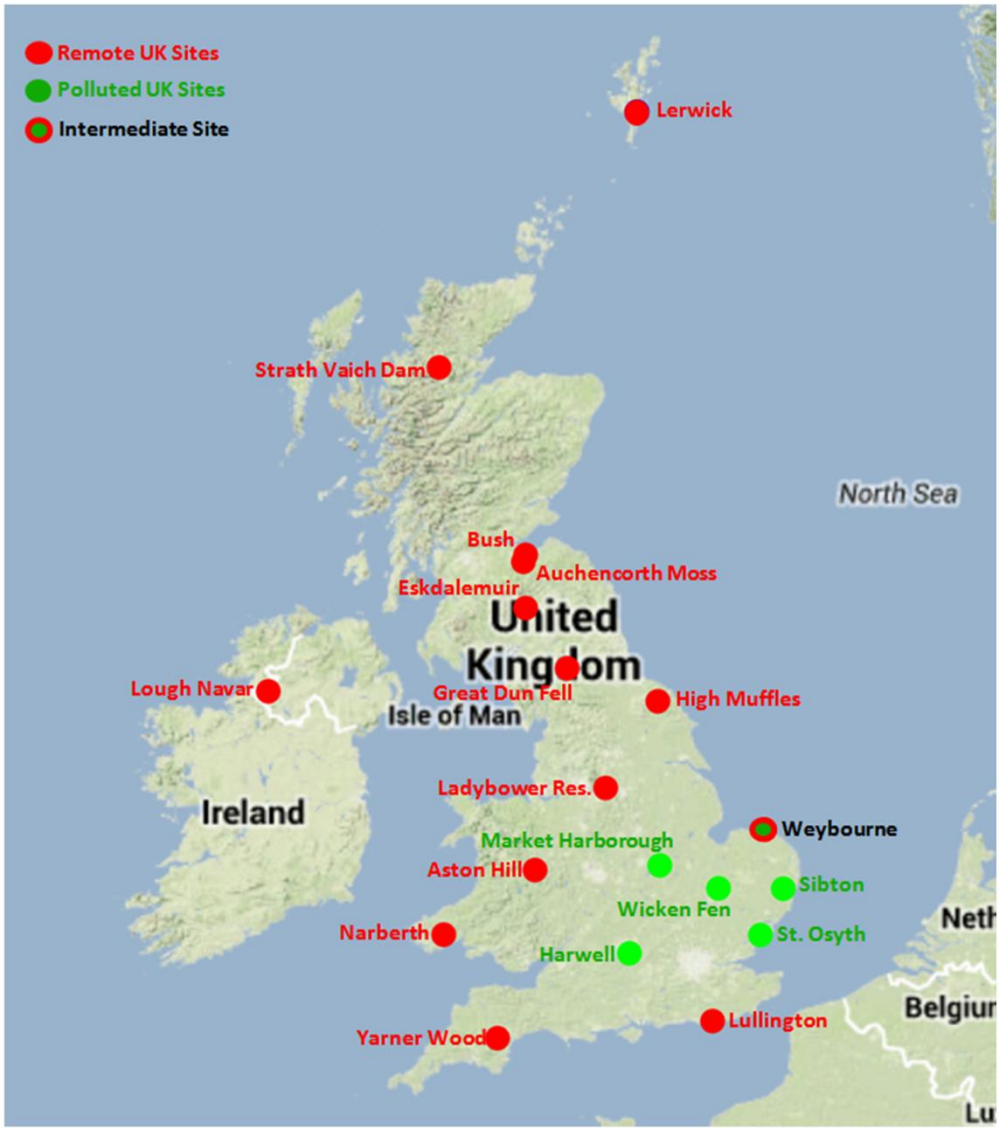

Figure 3.8: Location of UK EMEP sites operational for 2007 – 2010. Sites clustered as Remote are shown in red, and those clustered as Polluted are shown in green (Map data: Google, GeoBasis-DE/BKG).

For the other four 4-year periods spanning 1991-2006, sites were included in the clustering if monitoring data was available for the 4-year period under consideration. The number of clusters produced for each 4-year time period were not fully consistent. The periods 2007-2010 and 1999-2002 yielded a Remote, Polluted, Elevated, Mountain cluster set. For 2003-2006, the nine least anthropogenically-influenced Remote cluster sites formed an additional, distinct cluster. For 1995-1998, four clusters were produced, but three of these groups were of non-elevated sites, with Mountain and Elevated sites combined into one cluster. For 1991-1994 there were only three clusters: a Remote, Polluted and combined Mountain and Elevated cluster.

The Harwell EMEP supersite was consistently amongst the least anthropogenically-influenced sites of the Polluted cluster in every 4-year period except 2003-2006 (see Figure 3.4 for 2007-2010). For 2003-2006, the clustering assigned Harwell to the Remote cluster. This shift in classification also occurred for the four other UK sites which clustered tightly with Harwell in 2007-2010 (Market Harborough, Sibton, St Osyth and Wicken Fen). This indicated a change in this UK O_3 regime, relative to O_3 variation across Europe. This regime, for which Harwell was representative, was characterised by greater diurnal and annual O_3 variation than the rest of the UK, and its spatial domain encompassed sites within 120 km of London. In a European context, however, this regime was not the most anthropogenically influenced.

Data submission to EMEP for Auchencorth commenced in 2006, so O_3 concentrations from a neighbouring site at Bush, only 8 km from Auchencorth, were used as a proxy for Auchencorth prior to 2006. While small changes to the state and drivers of atmospheric composition can result in relatively large changes in O_3 variation, both sites are south of Edinburgh and similarly influenced by local and regional-scale meteorology. In 2011, hourly wind direction between the two sites differed by more than 45^o only 3% of the time. For the period 2007-2010, Auchencorth and Bush grouped immediately adjacent in the dendrogram (Figure 3.4), and the mean difference in hourly O_3 concentrations was 6.48 µg m^{-3}. Bush maintained a consistent assignment across the 20-year period, grouping immediately after sites including Zeppelin (on the

Arctic island of Svalbard), Mace Head (on the west coast of Ireland), and other more Remote sites. However, the other Remote UK sites exhibited greater variability in their position relative to Bush with time than was the case for the other UK Polluted sites relative to Harwell. For example, in 2003-2006, five UK sites grouped with Bush, however, four were less tightly grouped but remained assigned to the Remote cluster, and one site, Lullington Heath, was assigned to the Polluted cluster. Similar variability was found for the remaining time periods. The Remote UK sites were located in the north and west of the UK, with the exception of Lullington Heath on England's south coast.

3.5 Discussion

Sites within the Remote cluster are further from the largest sources of O_3 precursor (NO_x and VOCs) and depleting (NO) species as shown by their locations predominantly on the north-west fringe of Europe. This leads to lower perturbation of larger scale, continental and hemispheric background O_3 levels, and hence relatively low amplitude monthly-diurnal O_3 cycles. Ozone variation in the Polluted cluster show greater diurnal and annual variation, and sites are closer to major sources of O_3 precursor/depleting species which facilitate greater photochemical production during the day and removal through reaction with NO. In the Elevated (average altitude = 1098 ± 625 m, excluding coastal sites (see below)) and Mountain (1931 ± 521 m, excluding coastal sites (see below)) clusters, higher concentrations and less diurnal variability are observed due to O_3 transport in the free troposphere. Ozone formed in polluted areas with high concentrations of VOCs and NO_x ventilates from the boundary layer to the free troposphere where lower temperatures reduce O_3 loss through reaction with species such as NO (Guo et al., 2013). The greater atmospheric motions at altitude also rapidly replenish any O_3 loss by deposition. The lower average altitude of sites in the Elevated cluster possibly leads to a greater degree of local O_3 production/depletion, increasing diurnal variability compared with the Mountain cluster.

These results reflect previous analysis of O_3 spatial trends across the UK and Europe. Tarasova et al. (2007) used cluster analysis to group 114 extra-tropical sites globally based on O_3 variation between 1990 and 2004. Of the six clusters derived, European sites were assigned to five, with only a 'polar/remote' classification not found in Europe. The additional cluster in Tarasova et al. (2007) compared to this study was because sites assigned to the Remote cluster (for 2007-2010) were separated into Clean Background and Rural clusters. Inspection of Figures 3.4 and 3.5 show that this subsidiary separation is not borne out by the application of the clustering algorithm applied here. Ozone variation at monitoring sites in North America, Japan and Argentina was classified in the five clusters containing European sites. Henne et al. (2010) reported an 'observation-independent' Ward's method hierarchical cluster analysis to differentiate 34 rural European sites. Parameters characterising emissions, deposition and transport were included and six clusters ranging from 'generally remote' to 'agglomeration' were identified. The Harwell site grouped in the most polluted 'agglomeration' cluster along with Weybourne. The clustering result explained 55% of the inter-site variability in daily median O_3 concentrations, compared with 75% of inter-site variability explained by the methodology adopted here. Comparison of the results from Henne et al. (2010) with the results obtained in this study show one main difference. In the former clustering there was no differentiation between elevated sites (e.g. Jungfraujoch, Switzerland, 3578 m) and non-elevated remote sites. A study of 97 'non-urban' US sites used principal component analysis to identify 14 groups of sites with similar summer O_3 variation (Chan and Vet, 2010). Comparison of the monthly O_3 variation revealed a spectrum of sites similar to that found in the cluster analysis of European sites, from those with high summer concentrations and a strong influence of regional photochemistry, to those without such regional photochemical influences.

Variation in the clusters produced for each four-year period may be a result of numerous factors. One is long-term trends in O_3 variation from the reduction of O_3 precursor emissions, as recently highlighted across 158 EMEP sites by Wilson et al. (2012), and globally by Parrish et al. (2013) who found long-term shifts in seasonal

O_3 cycles at sites in Europe and North America. Another factor is changes in the number and distribution of EMEP monitoring sites (Table 1). In 1991-1994, there was only one site in southern Europe (Portugal) and one in eastern Europe (Czech Republic). The rest were located in central Europe, Scandinavia and the UK. Hence there was less variability in monthly-diurnal O_3 variation overall and only three major clusters formed. By 2010, more sites had been established in Mediterranean regions and eastern Europe providing data across a more varied O_3 landscape. A third factor is anomalous characteristics for some time periods. In one 4-year period, 2003-2006, half of the years (2003 and 2006), contained periods when 'heat-wave' conditions affected significant areas across Europe. Lee et al. (2006) detail the significant increase in photochemical activity during these conditions, including an approximate doubling of VOC reactivity with the OH radical. Hence this change in drivers provides another potential method for changes in site classification. In the cluster results from 2003-2006, nine Remote sites formed an additional cluster, suggesting O_3 variation at these sites was more different from the other Remote sites than at any other time between 1991 and 2010. Similarly, Polluted UK sites, including Harwell, grouped in the Remote cluster, and therefore showed most difference in O_3 variation compared to Polluted sites in central and southern Europe during this period. Conversely, Lullington Heath, on England's south coast, clustered in the Polluted cluster. Its closer proximity to mainland Europe, relative to other UK sites may have led to a greater exposure to the anomalous O_3 variation during the two 'heat-wave' periods in 2003 and 2006.

AQEG (2009) reported annual mean O_3 concentrations were highest in the north and west UK, but the propensity for prolonged exceedance of health-based O_3 metrics was higher in the south and east (based on daily maximum 8 hr average concentrations with various cutoffs between 70 and 120 µg m^{-3}). This is explained by a greater influence of hemispheric background levels in the UK towards the north-west (Jenkin, 2008), and leads to the separation of UK EMEP sites found in this analysis. Modification of hemispheric background O_3 concentrations occurs through formation of additional O_3 on a regional scale due to reaction of NO_x and VOCs, and local-scale depletion of O_3

by reaction with NO. Remote UK sites, generally towards the north and west UK, are less susceptible to transport of primary emissions from major pollution sources such as southern England and continental Europe (RoTAP, 2012). Hence lower NO concentrations at Remote UK sites lead to less O_3 depletion, and greater influence of hemispheric background concentrations. Ozone concentrations at many EMEP sites across Europe, such as in Scandinavia, are similarly influenced by hemispheric background concentrations. The geographic domain for which monthly-diurnal O_3 variation at Auchencorth is representative is therefore large and transboundary in nature. Non-UK sites falling within this international domain also cluster tightly with Auchencorth, leading to greater variability in the position of UK Remote sites relative to Auchencorth within the ordered dendrograms.

Conversely, Polluted UK sites, in south-east England, are closer to major sources of VOCs and NO_x and have higher diurnal and annual variability due to greater modification of hemispheric background O_3 concentrations. Higher NO concentrations facilitate greater O_3 depletion, while the proximity of O_3 precursor sources increase the prevalence of regional-scale, elevated O_3 episodes. Ozone variation within the entire Polluted cluster is less homogeneous than in the Remote cluster due to differences in emission patterns and other drivers (e.g. solar intensity) between sites. For example, the southern UK has a variety of different drivers determining O_3 concentrations compared with sites in central Europe. Depending on meteorological conditions air masses entering this region can contain relatively high or low concentrations of O_3 production and loss species (see e.g. (Jenkin, 2008)). Hence these UK sites, in close proximity to London, cluster more tightly with Harwell between 1991 and 2010. Harwell is therefore representative of a smaller geographic area than Auchencorth. UK EMEP sites provide an excellent case study for this effect, due to their large number (19) and density. However it is also apparent elsewhere: for example, six sites within 120 km of Vienna all cluster tightly together in the 2007-2010 dendrogram, along with Topolniky, Slovakia, a similar distance from Vienna. These sites (Heidenreichstein, Pillersdorf, Ganserdorf, Stixneusiedl, Illmitz,

Dunkelsteinerwald and Topolniky) are located at the more anthropogenically influenced end of the Polluted cluster.

Europe-wide, the clustering produced a number of anomalous classifications. For example, Finokalia, a coastal site on Crete, grouped in the Mountain cluster (Figure 3.4). It has been shown that significant incursion and entrainment of the free troposphere into the boundary layer occurs at Finokalia producing a monthly-diurnal O_3 profile typically found at sites at much higher elevations (Gerasopoulos et al., 2005; Gerasopoulos et al., 2006). Other coastal sites, such as Westerland, Denmark and Cabo de Creus, Spain, were grouped in the Elevated cluster. The NMF reordering facilitated evaluation of other anomalous sites. For example, Lazaropole in Macedonia was a member of the mountain cluster, but the classification was relatively weak and it could be construed as its own cluster. Ozone concentrations at Lazaropole were significantly higher than the 112 other sites in the analysis, with 51% of the monthly-hourly averaged concentrations exceeding 120 μg m^{-3}. The source of this anomaly remains unexplained. There are no other EMEP sites within 300 km of Lazaropole, and only two sites within 500 km, so to examine the geographic extent of the high O_3 concentrations reported at Lazaropole, and the O_3 regime across south-eastern Europe in general, requires a greater number of sites.

Few pollutants are monitored as widely as O_3, with some not routinely measured at all, making pollutant-specific site representativeness studies impractical. For example, peroxyacetyl nitrates (PAN), which provide a mechanism for NO_x storage and long range transport, are not continuously monitored at EMEP sites (McFadyen and Cape, 2005), but it is nevertheless important to assess the spatial relevance of conclusions of sporadic PAN measurement. Since O_3 is influenced by a wide variety of drivers, site classifications based on O_3 may be anticipated to be representative for many other atmospheric species – particularly secondary components, including PAN. Hence, as a consequence of demonstrating the representativeness of the UK EMEP supersites based on O_3 variation, comprehensive chemical climatologies derived for the impacts of O_3 and other atmospheric components at the sites can be placed in a European

context (see Chapters 4-6). Application of this methodology to different pollutant datasets could be used to assess changes in site classification as a function of pollutant. For example, a recent study applies a k-means clustering algorithm to differentiate US sites based on five-year averaged concentrations of $PM_{2.5}$ components (Austin et al., 2013).

3.6 Conclusions

Two major ground-level O_3 regimes over the UK have been identified through the use of hierarchical cluster analysis of monthly-diurnal O_3 datasets from 154 EMEP monitoring sites across Europe. The application of non-negative matrix factorization (NMF) reordered the summary dendrogram based on the relative anthropogenic influence on O_3 at each site. This allows the 25% within-cluster variability in O_3 concentrations across Europe not explained by the identification of four major clusters to be interpreted. For 2007-2010, all 19 UK EMEP sites were assigned to two of the Europe-wide clusters, with 17 sites apportioned into two groups in these two clusters. One cluster is comparatively less anthropogenically influenced, with O_3 concentrations featuring less modification from hemispheric background levels; the other cluster is of sites closer to O_3 precursor/depleting emissions and features more pronounced diurnal and annual O_3 cycles. The UK EMEP supersites of Auchencorth and Harwell grouped tightly with the other UK sites in these 'Remote' and 'Polluted' clusters respectively. For the other four, four-year periods considered between 1991 and 2006, a similar separation of UK sites occurred, with relatively tighter clustering of Polluted UK sites to Harwell than Remote UK sites to Auchencorth/Bush due to the larger, transboundary spatial domain for which Auchencorth is representative. Hence the UK background O_3 conditions are well represented by the location of the UK EMEP supersites at Auchencorth and Harwell. Both supersites currently monitor 120 different chemicals in air, precipitation and particulate matter; this work shows that conclusions derived from the application of the chemical climatology framework (Chapter 2) are likely appropriately applied to a wider geographic area.

References

AQEG, 2009. Ozone in the United Kingdom: Air Quality Expert Group, Defra Publications,
London. http://www.defra.gov.uk/environment/quality/air/airquality/publications/ozone/documents/aqeg-ozone-report.pdf.

Austin, E., Coull, B., Zanobetti, A., Koutrakis, P., 2013. A framework to spatially cluster air pollution monitoring sites in US based on the PM2.5 composition. Environ. Int. 59, 244-254.

Brice, K. A., Derwent, R. G., Eggleton, A. E. J., Penkett, S. A., 1982. Measurements of CCL3F and CCL4 at Harwell over the period January 1975 - June 1981 and the Atmospheric Lifetime of CCL3F. Atmos. Environ. 16, doi:10.1016/0004-6981(82)90334-1.

Carslaw, D. C., Ropkins, K., 2013. openair: Open-source tools for the analysis of air pollution data. R package version 0.8-5.

Chan, E., Vet, R. J., 2010. Baseline levels and trends of ground level ozone in Canada and the United States. Atmos. Chem. Phys. 10, 8629-8647.

Dabboor, M., Yackel, J., Hossain, M., Braun, A., 2013. Comparing matrix distance measures for unsupervised POLSAR data classification of sea ice based on agglomerative clustering. Int. J. Remote Sens. 34, 1492-1505.

Dillner, A. M., Schauer, J. J., Christensen, W. F., Cass, G. R., 2005. A quantitative method for clustering size distributions of elements. Atmos. Environ. 39, 1525-1537.

EMEP, 2014. Manual for Sampling and Analysis. EMEP/CCC Report 1/2014, Co-operative programme for monitoring and evaluation of the transmission of air pollutants in Europe, available at: http://www.nilu.no/projects/ccc/manual/index.html.

Flemming, J., Stern, R., Yamartino, R. J., 2005. A new air quality regime classification scheme for O-3, NO2, SO2 and PM10 observations sites. Atmos. Environ. 39, 6121-6129.

Gerasopoulos, E., Kouvarakis, G., Vrekoussis, M., Kanakidou, M., Mihalopoulos, N., 2005. Ozone variability in the marine boundary layer of the eastern Mediterranean based on 7-year observations. J. Geophys. Res. 110, D15309, doi:10.1029/2005JD005991.

Gerasopoulos, E., Kouvarakis, G., Vrekoussis, M., Donoussis, C., Mihalopoulos, N., Kanakidou, M., 2006. Photochemical ozone production in the eastern Mediterranean. Atmos. Environ. 40, 3057-3069.

Guo, H., Ling, H., Cheung, K., Jiang, F., Wang, D. W., Simpson, I. J., Barletta, B., Meinardi, S., Wang, T. J., Wang, X. M., Saunders, S. M., Blake, D. R., 2013. Characterization of photochemical pollution at different elevations in mountainous areas in Hong Kong. Atmos. Chem. Phys. 13, 3881 - 3898.

Henne, S., Brunner, D., Folini, D., Solberg, S., Klausen, J., Buchmann, B., 2010. Assessment of parameters describing representativeness of air quality in-situ measurement sites. Atmos. Chem. Phys. 10, 3561-3581.

Ignaccolo, R., Ghigo, S., Giovenali, E., 2008. Analysis of air quality monitoring networks by functional clustering. Environmetrics 19, 672-686.

Jenkin, M. E., 2008. Trends in ozone concentration distributions in the UK since 1990: Local, regional and global influences. Atmos. Environ. 42, 5434-5445.

Joly, M., Peuch, V. H., 2012. Objective classification of air quality monitoring sites over Europe. Atmos. Environ. 47, 111-123.

Kaufman, L., Rousseeuw, P. J., 1990. Finding Groups in Data: An Introduction to Cluster Analysis. Wiley, New York.

Kovac-Andric, E., Sorgo, G., Kezele, N., Cvitas, T., Klasinc, L., 2010. Photochemical pollution indicators-an analysis of 12 European monitoring stations. Environ. Monit. Assess. 165, 577-583.

Lau, J., Hung, W. T., Cheung, C. S., 2009. Interpretation of air quality in relation to monitoring station's surroundings. Atmos. Environ. 43, 769–777.

Lee, D. D., Seung, H. S., 1999. Learning the parts of objects by non-negative matrix factorization. Nature 401, 788-791.

Lee, D. D., Seung, H. S., 2001. Algorithms for non-negative matrix factorization. Adv. Neural Inf. Process. Syst. 13, 556-562.

Lee, J. D., Lewis, A. C., Monks, P. S., Jacob, M., Hamilton, J. F., Hopkins, J. R., Watson, N. M., Saxton, J. E., Ennis, C., Carpenter, L. J., Carslaw, N., Fleming, Z., Bandy, B. J., Oram, D. E., Penkett, S. A., Slemr, J., Norton, E., Rickard, A. R., Whalley, L. K., Heard, D. E., Bloss, W. J., Gravestock, T., Smith, S. C., Stanton, J., Pilling, M. J., Jenkin, M. E., 2006. Ozone photochemistry and elevated isoprene during the UK heatwave of August 2003. Atmos. Environ. 40, 7598-7613.

Liu, S., 2012. NMFN: Non-negative Matrix Factorization. R package version 2.0. http://CRAN.R-project.org/package=NMFN.

Lu, H. C., Chang, C. L., Hsieh, J. C., 2006. Classification of PM10 distributions in Taiwan. Atmos. Environ. 40, 1452-1463.

Maechler, M., Rousseeuw, P., Struyf, A., Hubert, M., Hornik, K., 2013. cluster: Cluster Analysis Basics and Extensions. R package version 1.14.4.

Mangiameli, P., Chen, S. K., West, D., 1996. A comparison of SOM neural network and hierarchical clustering methods. Eur. J. Oper. Res. 93, 402-417.

McFadyen, G. G., Cape, J. N., 2005. Peroxyacetyl nitrate in eastern Scotland. Sci. Total Environ. 337, 213-222.

Parrish, D. D., Law, K. S., Staehelin, J., Derwent, R., Cooper, O. R., Tanimoto, H., Volz-Thomas, A., Gilge, S., Scheel, H. E., Steinbacher, M., Chan, E., 2013. Lower tropospheric ozone at northern midlatitudes: Changing seasonal cycle. Geophys. Res. Lett. 40, 1631-1636.

R Core Development Team, 2008. R: A language and environment for statistical computing. R Foundation for Statistical Computing, Vienna, Austria. ISBN 3-900051-07-0, URL http://www.R-project.org. .

RoTAP, 2012. Review of Transboundary Air pollution: Acidification, Eutrophication, Ground Level Ozone and Heavy metals in the UK. Contract Report to the Department for Environment, Food and Rural Affairs. Centre for Ecology and Hydrology. http://www.rotap.ceh.ac.uk/sites/rotap.ceh.ac.uk/files/CEH%20RoTAP.pdf.

Royal Society, 2008. Ground-level ozone in the 21st century: future trends, impacts and policy implications. The Royal Society, London. (Science Policy, 15/08). http://royalsociety.org/uploadedFiles/Royal_Society_Content/policy/publications/2008/7925.pdf.

Spangl, W., Schneider, J., Moosmann, L., Nagi, C., 2007. Representativeness and Classification of Air Quality Monitoring Stations, Umweltbundesamt Report. http://www.umweltbundesamt.at/fileadmin/site/publikationen/REP0121.pdf.

Tarasova, O. A., Brenninkmeijer, C. A. M., Joeckel, P., Zvyagintsev, A. M., Kuznetsov, G. I., 2007. A climatology of surface ozone in the extra tropics: cluster analysis of observations and model results. Atmos. Chem. Phys. 7, 6099-6117.

Torseth, K., Aas, W., Breivik, K., Fjaeraa, A. M., Fiebig, M., Hjellbrekke, A. G., Myhre, C. L., Solberg, S., Yttri, K. E., 2012. Introduction to the European Monitoring and Evaluation Programme (EMEP) and observed atmospheric composition change during 1972-2009. Atmos. Chem. Phys. 12, 5447-5481.

Twigg, M. M., Di Marco, C. F., Leeson, S., van Dijk, N., Jones, M. R., Leith, I. D., Morrison, E., Coyle, M., Proost, R., Peeters, A. N. M., Lemon, E., Frelink, T., Braban, C. F., Nemitz, E., Cape, J. N., 2015. Water soluble aerosols and gases at a UK background site – Part 1: Controls of PM2.5 and PM10 aerosol composition. Atmos. Chem. Phys. Discuss. 15, 3703-3743.

UNECE, 2009. Steering Body to the Cooperative Programme for Monitoring and Evaluation of the Long-range Transmission of Air Pollutants in Europe (EMEP): Draft Revised Monitoring Strategy 2010-2019. United Nations Economic Commission for Europe, ECE/EB.AIR/GE.1/2009/15, 23rd June 2009, available at: http://www.unece.org/fileadmin/DAM/env/documents/2009/EB/ge1/ece.eb.air.ge.1.2009.15.e.pdf.

UNECE, 2012. Revised Strategy for EMEP 2010-2019. United Nations Economic Commission for Europe, ECE/EB.AIR/2009/16/Rev.1, 17th September 2012, available at: http://www.unece.org/fileadmin/DAM/env/documents/2013/air/emep/Informal_document_no_20_Revised_Strategy_for_EMEP_for_2010-2019_clean_text.pdf.

Ward, J., 1963. Hierarchical Grouping to Optimize an Objective Function. J. Am. Stat. Assoc. 58, 236 - 244.

Wilson, R. C., Fleming, Z. L., Monks, P. S., Clain, G., Henne, S., Konovalov, I. B., Szopa, S., Menut, L., 2012. Have primary emission reduction measures reduced ozone across Europe? An analysis of European rural background ozone trends 1996-2005. Atmos. Chem. Phys. 12, 437-454.

Chapter 4: Trends and drivers of ozone human health and vegetation impact metrics at Harwell and Auchencorth

This chapter is based on a research paper published in 'Atmospheric Chemistry and Physics' (Malley, C. S., Heal, M. R., Mills, G., & Braban, C. F. (2015). Trends and drivers of ozone human health and vegetation impact metrics from UK EMEP supersites measurements (1990-2013). Atmospheric Chemistry & Physics, 15, 4025-4042. 10.5194/acp-15-4025-2015. See Appendix IV). I undertook all data analysis, but co-authors Dr Mathew Heal, Dr Christine Braban and Dr Gina Mills made valuable contributions to the methodology, and the presentation of results through discussions and manuscript editing. In addition, Dr Mhairi Coyle provided insight into the calculation of AOT40 and Professor David Fowler assisted in discussions on the calculation of POD_Y and the policy relevance of this work.

4.1 Introduction

This chapter presents analysis of measurement data from the Harwell and Auchencorth supersites (described in Chapter 3.2), using the chemical climatology framework outlined in Chapter 2. The distinct impacts of groud-level ozone (O_3), one of the constituents measured at Harwell and Auchencorth, on human health and vegetation have been widely studied (REVIHAAP, 2013; RoTAP, 2012). However, changes in the recommended metrics used to quantify O_3 exposure relevant to these impacts (see below) necessitates new analyses of supersite measurement data. The utility of the chemical climatology framework in conducting these analyses is the linkage of the

human health and vegetation impact metrics to the causal drivers through the state of relevant O_3 (and precursor) variation.

In this study the six steps in the construction of a chemical climate described in Figure 2.4, and outlined in Chapter 2 and Malley et al. (2014b) were applied to characterise the exposure of ground-level O_3 concentrations measured at Harwell and Auchencorth relevant to human health and four vegetation types. The O_3 measured at these sites has been shown to be representative of rural O_3 concentrations in the larger geographical areas of south-east England and northern UK, respectively (Chapter 3 and Malley et al., 2014a).

Ozone exposure relevant to short-term health impacts is quantified using the SOMO10 and SOMO35 metrics, which are the annual sums of daily maximum running 8-h average O_3 concentrations above 10 and 35 ppb thresholds, respectively. These metrics are in line with the recent World Health Organisation Review of evidence on health aspects of air pollution (REVIHAAP, 2013) report which recommends quantifying acute O_3 health impacts using both these measures of daily O_3 concentration and across the full year. In earlier syntheses of human health effects of O_3, importance was attached to the peak O_3 concentrations (WHO, 2006). The recent REVIHAAP synthesis shows important O_3 effects on human health down to very small concentrations, and a suggestion that there is no specific threshold for effects. The inclusion of SOMO10 reflects this recent synthesis. To quantify vegetation impacts of O_3, the species-specific metric of phytotoxic O_3 dose above a threshold flux Y (POD_Y) is used (LRTAP Convention, 2010). This parameter represents the modelled accumulated stomatal uptake of O_3 over a fixed time period based on hourly variations in climate (temperature (T), vapour pressure deficit (VPD), photosynthetically active radiation (PAR)), soil moisture (soil water potential (SWP) or plant available water (PAW)), O_3 and plant phenology (Emberson et al., 2000). Stomatal flux metrics are increasingly used to assess O_3 vegetation impacts, as they more accurately reflect the spatial pattern of O_3 damage across Europe compared with concentration-based metrics such as AOT40, the sum of hourly O_3 concentrations above 40 ppb during

daylight hours during the growing season (Mills et al., 2011a; RoTAP, 2012). Statistical analyses of O_3 and NO_x variation provide characterisation of the 'state' of atmospheric composition at the two sites for the different impacts, while analysis of meteorology, air mass history and NO_x emissions provide insight into the relevant 'drivers' of the chemical climates.

The focus of this study is characterisation of the variation in O_3 impacts with time at Harwell, and spatially between Harwell and Auchencorth, and of the contributions of regional and hemispheric O_3-modifying processes in determining each impact. Hemispheric background O_3 concentrations are defined here as O_3 formed from anthropogenic and natural precursor emissions outside of Europe (Derwent et al., 2013). Superimposed on this background, regional net O_3 production or loss derives from the balance of processes such as emissions, deposition and meteorological conditions occurring on a regional scale. Photochemical reactions between NO_x and volatile organic compounds (VOCs) emitted in Europe produces O_3 regionally, but high NO_x environments (regionally and locally) limit O_3 formation (Jenkin, 2008; Munir et al., 2013). Spatial and temporal variation of these processes in the UK context have been discussed previously (AQEG, 2009). Studies have also quantified both human health (EMEP, 2014; Gauss et al., 2014; Guerreiro et al., 2014; Stedman and Kent, 2008) and vegetation O_3 impacts (Mills et al., 2011b; RoTAP, 2012) within the spatial domain of each supersite. However, consideration of both impacts at each site using a common chemical climatology approach links the impacts studies with the analyses of temporal and spatial O_3 variation, and allows identification of differences and similarities in the drivers of each impact which inform the development of co-beneficial O_3 mitigation strategies.

An important aspect of this study is to also compare impacts quantified through the updated metrics with previously-used metrics. For the health impact the contrast is between health-relevant exposure quantified by SOMO10 and SOMO35 compared with that quantified using the higher thresholds of the WHO guideline (50 ppb) and the EU target value (60 ppb) (Derwent et al., 2013; EEA, 2014b). For the vegetation

impact the contrast is between the POD_Y metric and the concentration-based crop AOT40 metric (Coyle et al., 2002; Jenkin, 2014; Klingberg et al., 2014). In addition, comparison is made between POD_Y calculated using on-site measured O_3 and meteorological data (used in this study and previously (Karlsson et al., 2007)) and analyses which have used gridded modelled O_3 and meteorological data to calculate POD_y (Emberson et al., 2007; Klingberg et al., 2011; Mills et al., 2011a; Mills et al., 2011b; Simpson et al., 2007).

The ambition to integrate data (such as measured concentrations) with knowledge (such as the adverse impacts of O_3) to advance both science and policy is currently an area of intense research interest (Abbatt et al., 2014; Kuhlbusch et al., 2014; Schmale et al., 2014). This chemical climatology-based example presents a clear methodology for achieving this and shows a simple categorisation for summarising information which could be more widely adopted.

4.2 Methods

A chemical climate is based on an identified impact (Figure 2.4, Step 1), which is linked to atmospheric composition variation through a suitable metric (Step 2). For assessment of O_3 acute health impact, REVIHAAP (2013) recommends the use of all-year metrics based on the value by which the daily maximum 8-hour average O_3 concentration exceeds either 10 ppb or 35 ppb. The annual sum of the daily exceedances of these thresholds yields the SOMO10 and SOMO35 metrics respectively. The POD_Y metric for the vegetation chemical climates was calculated using the DO_3SE model version 3.0.5 (http://www.sei-international.org/do3se, Emberson et al. (2000)). POD_Y values were calculated for two crops (wheat and potato) and two forest trees (beech and Scots pine), accumulated across their respective growing seasons. The length of the growing seasons, and phenological limitation on stomatal conductance throughout the growing season (limitation on O_3 uptake during different stages of the growing season) were derived according to methods detailed in

LRTAP Convention (2010). The growing seasons for wheat (late April – early August) and potato (late May – early September), were calculated by accumulated temperature and therefore varied inter-annually based on meteorological conditions. For beech, the growing season was calculated using a latitude model (19/04-20/10 at Harwell, 26/04-10/10 at Auchencorth). The Scots pine growing season was the full year.

The DO_3SE model calculates the stomatal flux for each species using parameterisations which quantify the sensitivity of each species to modification of stomatal conductance due to the effects of phenology, O_3, PAR, T, VPD and soil moisture (SWP for potato, beech and Scots pine and PAW for wheat) (LRTAP Convention, 2010). For this study, the DO_3SE model used as input hourly measured O_3 concentrations at Harwell and Auchencorth, and the following hourly meteorological data from the Met Office stations closest to each monitoring site: wind speed, rainfall, vapour pressure deficit, temperature, global radiation and pressure (UK Meteorological Office, 2012). For Harwell, the station at Benson (SRC ID: 613), 13 km distance, provided all meteorological data except global radiation which was obtained from Bracknell (SRC ID: 838, 1990-2002) and Rothamsted (SRC ID: 471, 2003-2013). For Auchencorth, all meteorological data were obtained from the station at Gogarbank (SRC ID: 19260), 14 km distance. The location of all sites used in the analysis is shown in Figure 4.1. All archived data from these stations undergoes documented quality control procedures (http://badc.nerc.ac.uk/data/ukmo-midas/ukmo_guide.html). The DO_3SE model calculated hourly O_3 concentrations at the top of the canopy and stomatal conductance for each vegetation type (Emberson et al., 2000; LRTAP Convention, 2010). SWP and PAW were calculated in the DO_3SE model using the measured meteorological data based on the Penman-Monteith model of evapotranspiration (Bueker et al., 2012). In addition to meteorological conditions, the evaporation of moisture from soil is dependent on the hydraulic properties of the soil texture. Statistics were therefore calculated for four different soil textures, sandy loam (soil texture classification = coarse), silt loam (medium coarse), loam (medium)

and clay loam (fine). The properties of these soil textures are detailed in Bueker et al. (2012).

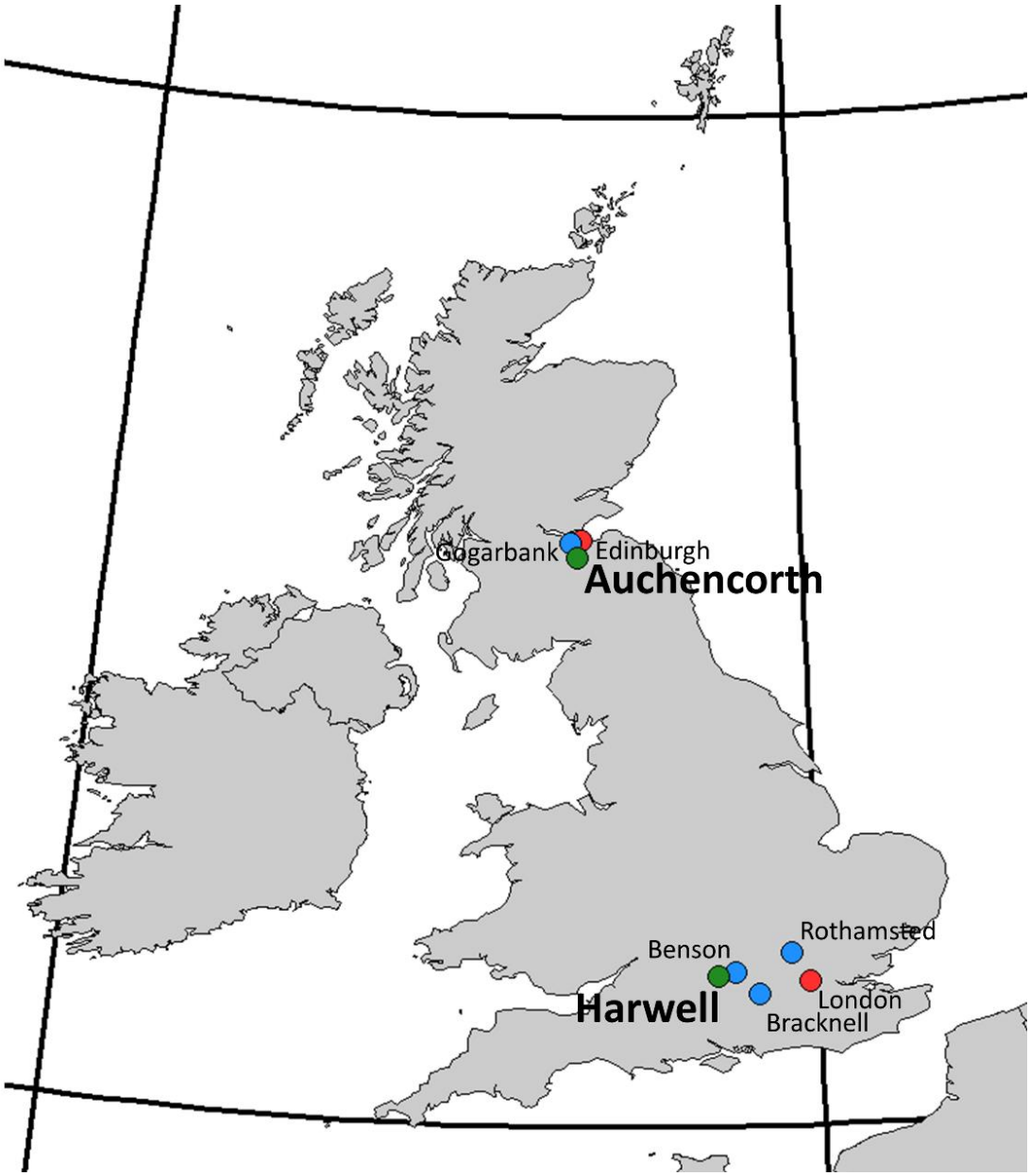

Figure 4.1: Map of the United Kingdom and Ireland showing the location of the two UK EMEP supersites (green circles) at Auchencorth and Harwell, and the location of the UK Met Office stations from which meteorological data was used (blue circles).

POD_Y was accumulated when this stomatal flux was above a plant-specific threshold flux set at 6 nmol m^{-2} s^{-1} for crops and 1 nmol m^{-2} s^{-1} for forest trees. The thresholds were calculated to be those that produced the strongest correlation between POD_Y and yield loss (LRTAP Convention, 2010), and represent the detoxification capacity of the vegetation. Response functions were applied to wheat, potato and beech to convert POD_Y into grain yield, tuber weight and whole-tree biomass reduction estimates respectively (Mills et al., 2011c). As the representative coniferous species in the 'Atlantic central Europe' geographic zone (LRTAP Convention, 2010), Scots pine was included despite no published response function, with increasing POD_Y assumed to indicate increasing potential damage. In addition, the crop-specific AOT40 metric for May to July was calculated (Fuhrer et al., 1997) to allow for comparison with previous studies that used AOT40 to estimate the impact of O_3 on crops (e.g. Derwent et al., 2013; Jenkin, 2014).

The spatial domain (Figure 2.4, Step 3) in this analysis was the area of representativeness of each monitoring site. In the context of European O_3 variation evaluated across all EMEP sites measuring O_3, Harwell was shown to be representative of rural sites within 120 km of London, and Auchencorth representative of rural locations in a larger domain including the rest of the UK (Chapter 3 and Malley et al., 2014a). The temporal domain investigated was 1990-2013 for Harwell (NO_x data available from 1996) and 2007-2013 for Auchencorth. The NO_x and O_3 measurements were co-located at Harwell, but the NO_x data for analyses at Auchencorth were obtained from Bush (UK-AIR ID: UKA00128), 8 km from Auchencorth. The suitability of Bush as a proxy site for Auchencorth has been outlined previously, and O_3 variation was found to be similar at both sites (Chapter 3). The chemical data were downloaded from the UK-Air data repository (http://uk-air.defra.gov.uk) and the Automatic Urban and Rural Network (AURN) reports provide further details on these measurements (Eaton and Stacey, 2012).

A minimum data capture of 75% across the year for SOMO10/35 calculations, and across the relevant growing season for POD_Y and AOT40 calculations, was imposed

for inclusion of a particular year in the summary statistics for the particular metric. This resulted only in the exclusion of statistics at Harwell for potato in 1995 and Scots pine in 1993. As data capture was generally very high, no adjustment of summary statistics for missing data was applied. At Harwell, average annual data capture for 1990-2013 was 94%. The lowest annual data capture was 76% (1993). When the missing hourly O_3 data were estimated through linear interpolation, 1993 SOMO35 and SOMO10 increased by no more than 2% compared with no interpolation. For the four vegetation types, the 1990-2013 average data capture during the respective growing seasons at Harwell was between 92 and 94%. Sensitivity to missing O_3 and meteorological data during the years of lowest data capture (above 75%) for wheat (1994, 75%), potato (1993, 80%), beech (1995, 82%) and pine (2007, 81%) was also evaluated through linear interpolation. POD_Y values were 19%, 19% and 18% higher for wheat, beech and pine, respectively, compared with no linear interpolation, and 6% lower for potato. These sensitivities illustrate an estimate of the greatest extent of impact metrics not included due to missing data. For the majority of years biases will be much smaller, as data capture was substantially higher. As estimation of missing data introduces new sources of uncertainty, the impacts calculated using measured data only are considered here.

The state (Figure 2.4, Step 4) of the human health chemical climates was characterised using the following statistics for the SOMO10 and SOMO35 metrics: the number of accumulation days (ADs), i.e. days on which the maximum 8-hour O_3 concentration exceeded 10 or 35 ppb; percentage contribution per season to annual number of ADs; the percentage contribution per season to SOMO10/35; the average diurnal amplitudes in O_3, NO and NO_2 concentrations on ADs and non-accumulation days (NADs); and the contributions to SOMO10/35 from 13 daily maximum 8-h O_3 concentration bins (10 ppb to >70 ppb in 5 ppb groups). The state for the vegetation chemical climates was characterised by the following statistics for the POD_Y metric for each vegetation type: the number of POD_Y accumulation days; the percentage monthly contributions to POD_Y across the growing season; the contributions to POD_Y from 15 hourly O_3 concentration bins (0 ppb to >70 ppb in 5 ppb groups); and the average diurnal

amplitudes of O_3, NO and NO_2 on ADs and NADs. For the AOT40 metric, the contributions from May, June and July were calculated as well as the average diurnal amplitudes in May, June and July of O_3, NO and NO_2.

Three potential drivers of the state (Step 5) were investigated. First, the effect of temperature was investigated using data from Benson (SRC ID: 613), 13 km from Harwell, and Gogarbank (SRC ID: 19260), 14 km from Auchencorth (UK Meteorological Office, 2012). The mean daily temperature on ADs and NADs for SOMO10/35 and POD_Y were compared. Monthly averaged temperatures during the AOT40 growing season were calculated.

Secondly, the association of the state (Step 4) with air-mass history was investigated by grouping back trajectories based on the similarity of their pathway. The proportion of trajectories arriving from each group during SOMO10/35 and POD_Y ADs and NADs, and over the AOT40 growing season, was then compared. Pre-calculated 4-day HYSPLIT air-mass back trajectories arriving at 3 hour intervals (2920 trajectories per year) (Carslaw and Ropkins, 2013; Draxler and Rolph, 2013; R Core Development Team, 2008) were grouped using Ward's linkage hierarchical cluster analysis which has been shown through simulations to perform effectively (Mangiameli et al., 1996). The similarity between trajectories was quantified using the measure of their 'angle' from the receptor (Equation 4.1):

$$d_{1,2} = \frac{1}{n}\sum_{i=1}^{n} cos^{-1}\left(0.5\frac{A_i+B_i+C_i}{\sqrt{A_i B_i}}\right) \quad (4.1)$$

where

$$A_i = (X_1(i) - X_0)^2 + (Y_1(i) - Y_0)^2$$
$$B_i = (X_2(i) - X_0)^2 + (Y_2(i) - Y_0)^2$$
$$C_i = (X_2(i) - X_1(i))^2 + (Y_2(i) - Y_1(i))^2$$

$d_{1,2}$ is the variance between trajectory 1 and trajectory 2, X_0 and Y_0 are the latitude and longitude coordinates of the origin of the back trajectory (i.e. the supersite), and X_1,

Y_1, and X_2, Y_2 are the coordinates of back trajectories 1 and 2, respectively, at a common time point *i* along the trajectory (n = 96). In Ward's method each object (back trajectory) initially constitutes its own cluster. At each step, the two clusters are merged that give the smallest increase in total within-cluster variance. This process is repeated until all trajectories are located in one cluster (Kaufman and Rousseeuw, 1990). The summary dendrogram was then 'cut' to produce a set of four clusters in which the back trajectories were predominantly 'westerly', 'easterly', 'northerly' and 'southerly'. This cluster analysis is a more appropriate method for the grouping of back trajectories compared to assignment based on arbitrary boundaries, e.g. 90 ° about N, E, S and W, as the cluster analysis attempts to create clusters based on the natural groupings within the data, and the similarity of the pathway taken. With boundary groupings, e.g. trajectories grouped as 'Northerly', and approaching a site from between 315 ° and 45 °, trajectories approaching from the opposite extremes of these boundaries would be given the same classification, but may have greater commonality with trajectories in a different boundary group.

Thirdly, the 2920 4-day back trajectories arriving each year were combined with reported gridded NO_x emissions to investigate the contribution of NO_x emissions as a chemical climate driver. Each 1 h time point along a trajectory was associated with the relevant 0.5° × 0.5° grid square NO_x emissions reported by EMEP (Mareckova et al., 2013; Simpson et al., 2012). This grid encompasses the region 30.25°N to 75.25°N and 29.75°W to 60.25°E. The associated annual NO_x gridded emissions were adjusted using month, day of week and hour of day time factors (Simpson et al., 2012) to obtain an estimate of the hourly NO_x emissions during the hour in which the trajectory passed over the grid cell. The 96 hourly emissions estimates for each trajectory were summed, and averaged across the 8 trajectories arriving each day, producing a daily average trajectory NO_x emissions estimate which was compared on SOMO10/35 and POD_Y ADs and NADs. The monthly average trajectory NO_x emissions estimate was calculated for the May-July AOT40 growing season.

The chemical climate statistics derived were compared between Harwell and Auchencorth for evidence of different spatial phases in the O_3 impacts (Figure 2.4, Step 6). Evidence for a different temporal phase in the O_3 impact chemical climate at Harwell was investigated by Theil-Sen trend analysis of the 24-year time series of chemical climate statistics. This non-parametric test selects the median of all the slopes between pairs of points in a time series as the estimate of the trend, and calculates statistical significance using bootstrap re-sampling (Carslaw and Ropkins, 2013). The 7-year dataset from Auchencorth was of insufficient duration to evaluate significant changes in either the health or vegetation impacts.

The terminology spring, summer, autumn and winter refer to the 3-month periods Mar-Apr-May, Jun-Jul-Aug, Sep-Oct-Nov and Dec-Jan-Feb, respectively.

4.3 Results and Discussion

The chemical climate statistics derived for the O_3 human health and vegetation impacts at Harwell and Auchencorth are presented as datasheets in Supplementary Information Tables S4.1-S4.12 (Appendix I). For Harwell, the statistics are averaged across six time periods (1990-1993, 1994-1997, 1998-2001, 2002-2005, 2006-2009, 2010-2013). These tables contain a lot of statistics and exemplify a resource which could be replicated and collated for different impacts, locations and time periods to identify key linkages between chemical climates and aid in the development of more holistically-considered mitigation strategies. The main features which support the key conclusions from the human health and vegetation O_3 chemical climates at the UK supersites are presented in Figures 4.2-4.13 and discussed in the following subsections.

4.3.1 O_3 human health impact chemical climates

The detailed statistics describing the O_3 human health chemical climates at Harwell and Auchencorth are presented in Tables S4.1 and S4.2, respectively. This section

presents two analyses of the impact, state and drivers of the chemical climatology framework (Figure 2.4, steps 1-5); specifically, changes in chemical climate phase (Figure 2.4, Step 6) temporally at Harwell between 1990 and 2013 (Section 4.3.1.1) and spatially between Auchencorth and Harwell (Section 4.3.1.2).

4.3.1.1 Long-term changes at Harwell

When characterised by the SOMO35 metric, the short-term O_3 exposure associated with human health impact at Harwell decreased significantly between 1990-2013 (Figure 4.2), with a median trend of –2.2% y^{-1} (p = 0.001). The annual number of SOMO35 accumulation days (ADs) did not vary significantly during this period, averaging 148 ± 28 days y^{-1}. In contrast, when characterised by the SOMO10 metric, O_3 exposure associated with human health impact at Harwell showed no statistically significant trend (1990-2013 mean (±sd) = 8329 ± 802 ppb.d) (Figure 4.2). However, the annual number of SOMO10 ADs has increased significantly with a median trend of +1.7 days y^{-1} (p = 0.01). In the more recent years, the additional ADs occurred in winter, and SOMO10 was accumulated on almost every day of the year (Table S4.1).

The majority of SOMO35 accumulation at Harwell occurred in spring and summer (Figure 4.3). Between 1990 and 2013 the spring contribution to SOMO35 increased significantly (+1.1% y^{-1}, p = 0.01), whilst the summer contribution decreased significantly (–1.2% y^{-1}, p = 0.01). The spring and summer contributions to SOMO35 values were considerably larger, and showed larger inter-annual variation, compared with those for SOMO10 (Figure 4.3). Between 1990 and 2013 there was a significant decrease in contribution to SOMO10 during summer (trend –0.4% y^{-1}, p = 0.01) and a significant increase during winter (+0.3% y^{-1}, p = 0.001).

Figure 4.4 shows the contributions from thirteen 5-ppb daily maximum 8-h O_3 concentration bins to SOMO10 and SOMO35 at Harwell. The majority of SOMO10 was accumulated on days when the O_3 concentration was between 25 and 45 ppb

(Figure 4.4a). Contributions to SOMO10 from days with the highest concentrations (60-70 ppb and >70 ppb) decreased significantly between 1990 and 2013 (–0.2 and –0.4 % y^{-1} respectively), while contributions from more moderate O_3 concentrations (20-30 ppb and 40-50 ppb) increased significantly (+0.3% y^{-1} and +0.2% y^{-1} respectively). Ozone concentrations between 10 and 35 ppb, i.e. included in SOMO10 but not in SOMO35, contributed on average 40 ± 8% across the whole 24-year period. The contribution to SOMO35 from the higher concentration bins was larger than for SOMO10, but also decreased significantly (Figure 4.4b): the 1990-2013 trends in SOMO35 contributions from O_3 concentrations between 60-70 ppb and >70 ppb were –0.4 and –1.4 % y^{-1} respectively. There were significant increases in contributions to SOMO35 from concentrations between 35 and 50 ppb (trends in the range +0.4 to +1.5% y^{-1}). At Harwell the amplitude of the diurnal O_3 cycle was consistently greater (by 7-18 ppb) on SOMO35 ADs compared with SOMO35 NADs (Table S4.1), while the diurnal NO and NO_2 cycles were substantially lower on ADs than on NADs. Figure 4.5 shows that the mean diurnal amplitudes of O_3, NO_2 and NO on SOMO35 ADs decreased significantly between 1990 and 2013 (trends of –1.8% y^{-1}, –2.8% y^{-1}, –3.6% y^{-1}, respectively). There was also a significant decrease in mean diurnal cycle amplitudes of O_3, NO_2 and NO on SOMO10 ADs (trends of –1.4, –2.6, and –3.9% y^{-1}, respectively, NO_x data only from 1996). Trends of decreasing diurnal amplitudes were also observed on SOMO35 NADs (note that SOMO10 NADs were rare, and in 2010-2013 there were essentially no SOMO10 NADs).

The largest change in the O_3 human health chemical climate drivers between 1990 and 2013 at Harwell was the decrease in the estimated daily averaged NO_x emissions along the air-mass back trajectories (Figure 4.6). For SOMO35 ADs and NADs, the decreases were –3.1% y^{-1} and –3.0% y^{-1} respectively, while the decrease on SOMO10 ADs was –2.9% y^{-1} (all p = 0.001). For SOMO10 and SOMO35, temperatures on NADs were lower than on ADs. For SOMO35, the average temperature was 2.3 ± 1.5 °C higher on ADs than on NADs between 2010-2013, smaller than the corresponding differential of 3.9 ± 1.3 °C between 1990 and 1993. The median trend in this

temperature differential was −2.5% y^{-1} (p = 0.001). The proportion of air-mass back trajectories classified into the four geographic groupings through cluster analysis did not vary significantly between ADs and NADs for SOMO35, or across the whole 1990-2013 period. In 2003, the effects of long-term changes in the emissions drivers were temporarily offset and SOMO10 and SOMO35 values were elevated (Figure 4.2). This was due to the 'heat-wave' period experienced across south-east England during summer that year. The elevated temperatures enhanced O_3 concentrations by leading to greater biogenic VOC emissions and increased reactivity of VOCs with OH, and to reduced O_3 dry deposition (Lee et al., 2006; Vieno et al., 2010).

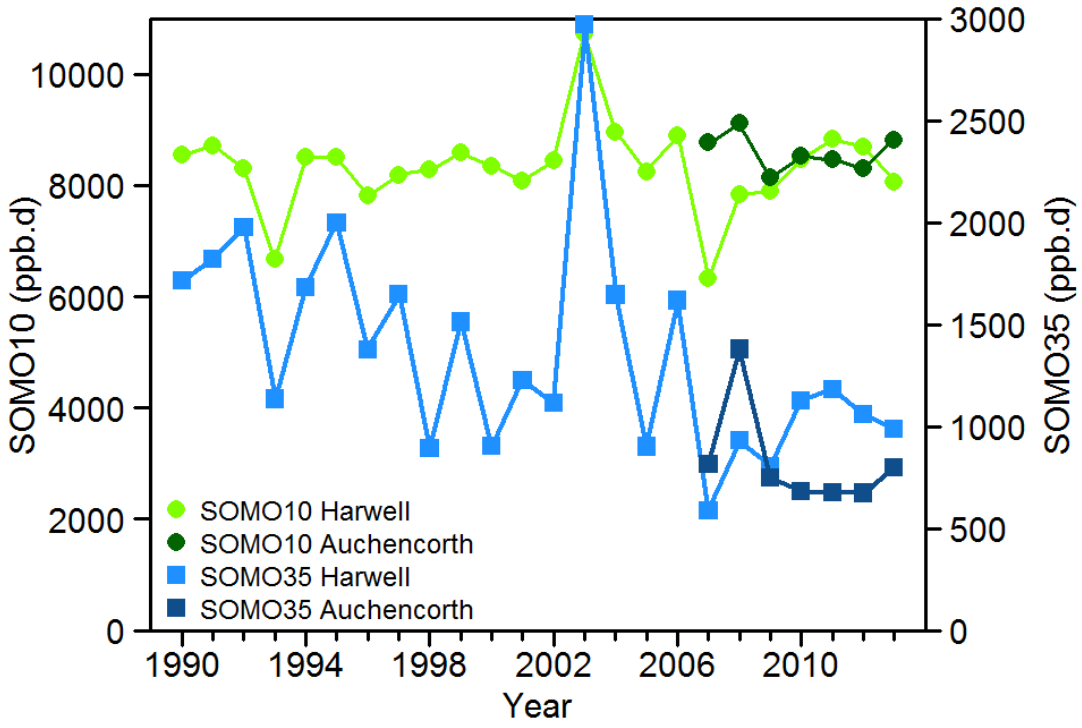

Figure 4.2: Human health relevant exposure to O_3 at Harwell (1990-2013) and Auchencorth (2007-2013), as characterised by the SOMO10 and SOMO35 metrics.

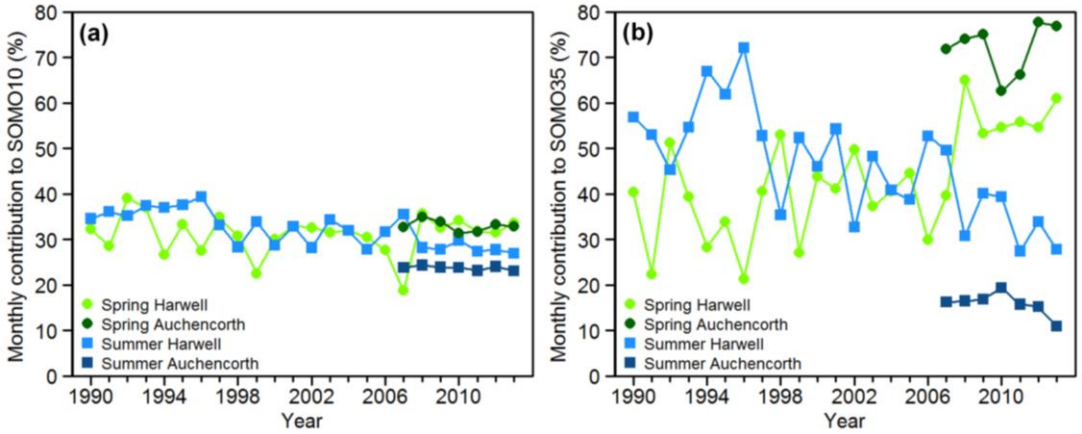

Figure 4.3: Relative annual contributions from spring (MAM) and summer (JJA) to (a) SOMO10 and (b) SOMO35.

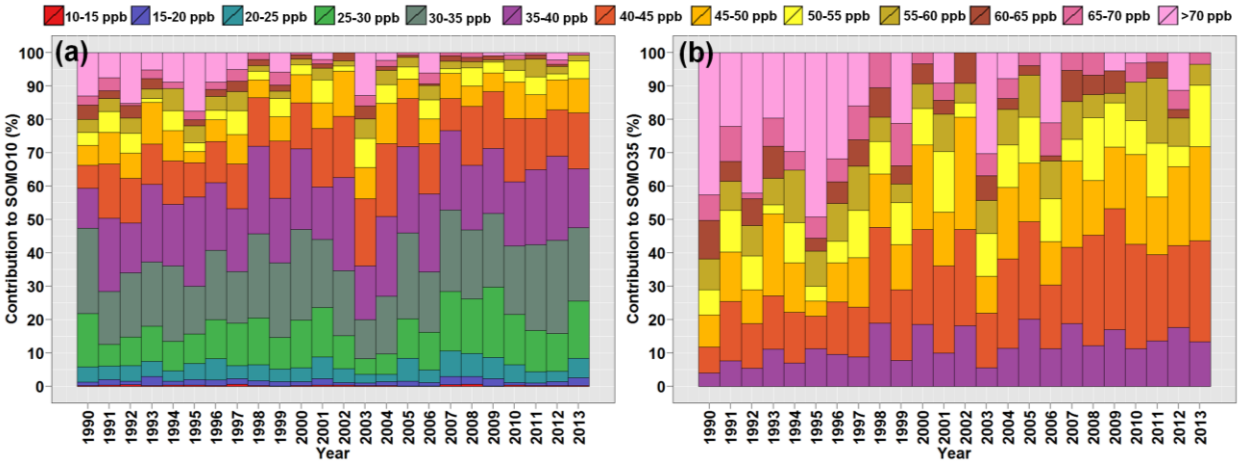

Figure 4.4: Relative annual contributions to (a) SOMO10 and (b) SOMO35 at Harwell from different O_3 concentration bins. Concentrations are separated into thirteen 5 ppb bins spanning daily maximum 8-h mean O_3 concentrations between 10 ppb and >70ppb. Note: these concentration bins are contributing to a decreasing long-term trend in SOMO35 and to a constant trend in SOMO10, as illustrated in Figure 4.2.

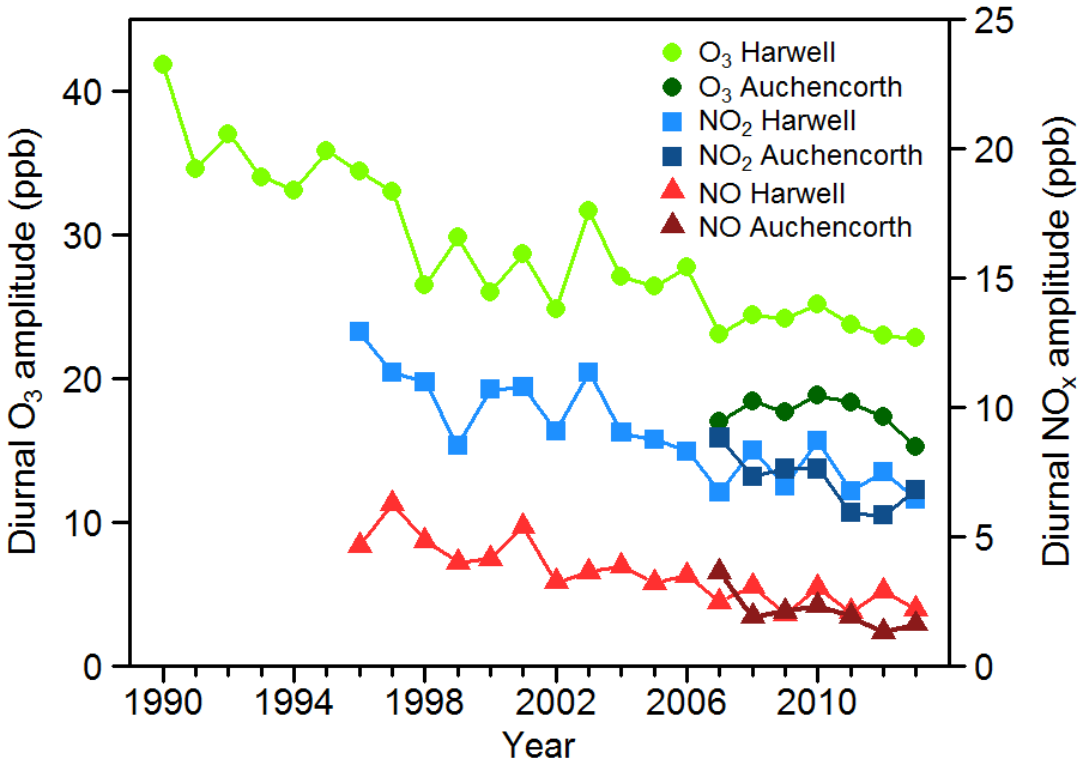

Figure 4.5: Amplitude of the diurnal O_3, NO_2 and NO cycles at Harwell and Auchencorth during SOMO35 accumulation days (ADs).

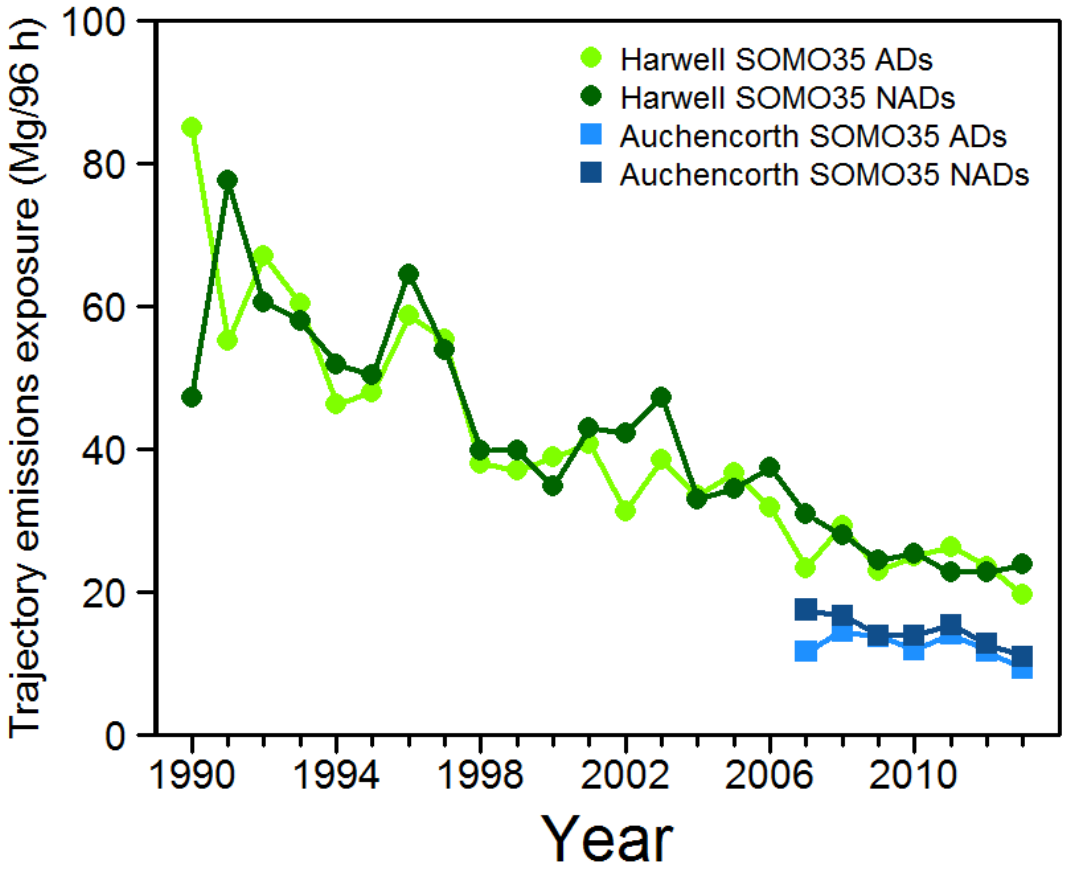

Figure 4.6: Estimate of the hourly European NO_x emissions emitted from the EMEP 0.5° grids over which 96-h back trajectories passed prior to arrival at Harwell and Auchencorth for SOMO35 accumulation days (ADs) and non-accumulation days (NADs).

The trends and differences in the statistics presented for the SOMO10 and SOMO35 metrics for 1990-2013 at Harwell reveal changes in the relative importance to O_3 concentrations of hemispheric, regional and local-scale processes in determining the health-relevant O_3 exposure at Harwell. Hemispheric background levels of O_3 over Europe, as represented by Mace Head, Ireland, feature a pronounced spring maximum and summer minimum (Derwent et al., 2013; Parrish et al., 2013). Hence during spring the SOMO35 threshold is exceeded on the majority of days. Derwent et al. (2013) analysed O_3 concentrations in non-European influenced air masses and found an increasing trend up to 2008, most strongly observed in winter and spring, followed by a levelling off and decrease. Wilson et al. (2012) also calculated a significant positive trend between 1996 and 2005 in monthly 5th percentile O_3 concentrations, taken as a measure of background concentrations, at 82 out of 158 European monitoring sites,

including the majority of sites in the UK. This increase in hemispheric background concentrations has led to the increases in the number of winter SOMO10 ADs and in the spring contribution to SOMO35.

Regional O_3 production is greatest in summer when solar intensity and temperatures are highest, so the contribution to the O_3 exposure associated with the health impact during summer is predominantly of European origin (Jenkin, 2008). Autumn and winter have far fewer SOMO35 ADs because of lower hemispheric background levels and lower solar intensity for regional production; however, the consistent exceedance of 10 ppb during autumn and winter leads to a significant contribution to SOMO10 (approximately 40% in 2010-2013 (Table S4.1)). The decrease in summer contribution to SOMO35 results from reduced regionally-produced O_3 episodes. This is evidenced by the reduced contribution from the highest O_3 concentration days, the decreased amplitude of diurnal O_3 variation during SOMO35 and SOMO10 ADs and the decreased temperature difference between SOMO35 AD and NADs (regionally-generated O_3 exhibits a pronounced diurnal cycle due to its photochemical production and is therefore determined to a greater extent by European meteorological conditions than is hemispheric background O_3). Jenkin (2008) and Munir et al. (2013) likewise attributed long-term decreases in high percentile O_3 concentrations at UK monitoring sites to reduced regional photochemical O_3 episodes, and increases in lower percentile concentrations due to increased hemispheric background, and reduced depletion due to reaction of O_3 with NO.

The decrease in regional O_3 production is due to the decreasing trend in precursor emissions affecting Harwell (Figure 4.6). The European Environment Agency (EEA) estimate that, across the EU28 countries, NO_x emissions have decreased by 51% between 1990 and 2012 and volatile organic compound (VOC) emissions have decreased by 60% (EEA, 2014a). Unlike SOMO35, the SOMO10 metric did not decline between 1990 and 2013 because of the lower contribution to SOMO10 from the highest O_3 concentrations, which derive from regional photochemical episodes. SOMO10 was therefore less sensitive to decreases in the magnitude of these episodes,

and the decrease was offset by an increase in contribution from 20-30 ppb daily maximum 8-hour ADs, which were not included in SOMO35.

In summary, whether it is concluded there has been a decline or no decline in O_3 exposure associated with human health impact between 1990 and 2013 at Harwell differs according to the choice of a 35 ppb or 10 ppb threshold, both of which are recommended in the recent WHO review (REVIHAAP, 2013). Although the absolute health impact apportioned to O_3 is sensitive to the choice of threshold (Heal et al., 2013; Stedman and Kent, 2008), the analyses presented here have shown that, irrespective of whether a 35 or 10 ppb threshold is selected, the extent, timing and severity of the human health impact of O_3 is increasingly driven by more frequent, modest exceedances of the respective threshold, rather than short-lived extreme episodic exceedances.

4.3.1.2 Spatial differences between Auchencorth and Harwell (2007-2013)

In the comparison between Auchencorth (representative of much of the rural west and north of the UK) and Harwell (representative of SE England), annual mean and 75th percentile O_3 concentrations were greater at Auchencorth between 2007 and 2013, while maximum values were substantially greater at Harwell (Tables S4.1 and S4.2). Between 2007 and 2013, the average SOMO35 was 14% lower at Auchencorth, while the average SOMO10 was 7% higher compared with Harwell. The proportion of SOMO10 accumulated in spring was similar at both sites, but the proportion accumulated in summer was on average 5.3 ± 2.9% lower at Auchencorth. The contribution to SOMO35 from spring was greater at Auchencorth, but smaller for summer compared with Harwell (Figure 4.3). Auchencorth also had a smaller contribution from days with >60 ppb daily maximum 8-hour O_3 concentrations (Table S4.2). Mean amplitudes of diurnal O_3 variation on SOMO10 and SOMO35 ADs were also smaller at Auchencorth than at Harwell (see Figure 4.5 for the data relating to SOMO35 ADs). In addition, the difference in mean amplitudes of diurnal O_3, NO_2 and

NO variation on SOMO10/35 ADs and NADs was smaller at Auchencorth than at Harwell. For example, diurnal O_3 amplitude was 2.2-4.5 ppb greater on SOMO35 ADs than on NADs at Auchencorth (Table S4.2), which was smaller than the 5.6-8.2 ppb differential at Harwell between 2007 and 2013 (Table S4.1).

The estimated daily averaged NO_x emissions along the air-mass back trajectories were substantially lower at Auchencorth than at Harwell (Figure 4.6) and generally lower (13 ± 9% on average in 2007-2013) on SOMO35 ADs compared with NADs. The temperature difference between SOMO35 ADs and NADs at Auchencorth was less than at Harwell, ranging between 1.7 °C higher on average on ADs in 2010 to 1.4 °C lower on ADs in 2013. Elevated SOMO10 (6% above 2007-2013 average) and SOMO35 (67%) values in 2008 at Auchencorth (as also reported by Gauss et al. (2014) using the EMEP/MSC-W model) resulted from an increased contribution from days with maximum 8-h concentrations above 50 ppb (12% and 36% contributions to SOMO10 and SOMO35 respectively). In addition, 28% of trajectories were grouped in an 'easterly' cluster on SOMO35 ADs in 2008, compared with 13% on NADs. Patterns were similar in 2009, 2012 and 2013, but without the elevated SOMO35 compared to 2008. The larger O_3 and NO_2 diurnal amplitudes on SOMO10 and SOMO35 ADs in 2008, and the elevated temperatures on SOMO35 ADs (Table S4.2) suggests regional O_3 production was a substantially stronger driver of SOMO35 in 2008 compared to other years at Auchencorth.

The chemical climate state and driver statistics for Auchencorth indicate that O_3 concentrations at this location are less modified from the hemispheric background than at Harwell, consistent with spatial patterns reported in Jenkin (2008). The larger contribution from spring to SOMO35 at Auchencorth compared to Harwell shows that the hemispheric spring maximum in O_3 produces the majority of SOMO35, and the lower contribution to SOMO35 from high O_3 concentration ADs indicates lower influence from regional photochemical O_3 production. Since SOMO10 is determined to a lesser extent by high O_3 concentration ADs, this explains why calculated SOMO35

are lower at Auchencorth, yet SOMO10 values are similar at Auchencorth and Harwell.

4.3.1.3 Comparison between SOMO10/SOMO35 and higher threshold metrics

In spite of these spatial differences between the SOMO10 and SOMO35 metrics, both provide a substantially different picture of the extent (proportion of year over which impact metric is accumulated), timing (particular periods when impact metric is accumulated) and severity (magnitude of impact metric) of human health relevant O_3 exposure at Harwell and Auchencorth compared with use of higher threshold metrics such as the WHO air quality guideline (50 ppb) or the EU target value (60 ppb). For example, in 2013, the extent of exceedance of the 60 ppb EU target value across the UK was only 19 days (at least 1 of 81 UK sites exceeding threshold), and the timing of these exceedances was mainly in summer (EEA, 2014b). In contrast, at Harwell in 2013, there were 356 and 130 ADs for SOMO10 and SOMO35 respectively, of which only 27% and 28% was accumulated in summer. In respect of severity, at Harwell in 2010-2013, on average 91% and 66% of SOMO10 and SOMO35 respectively was accumulated on days with maximum 8-h O_3 concentrations below the WHO guideline of 50 ppb, compared to 76% and 38% in 1990-1993 (Table S4.1). At Auchencorth, an even larger proportion of SOMO10 and SOMO35 were accumulated below 50 ppb, on average 96% and 84% respectively during the 2007-2013 monitoring period (Table S4.2).

The overall impression from these statistics showing a decline in exposure to concentrations in excess of 35 ppb is that the threat to human health has declined between 1990 and 2013 in south-east England. The comments from the EEA (2014b) on the very few episodes in excess of 50 or 60 ppb in 2013 are consistent with this view. However, the recent REVIHAAP (2013) synthesis shows that the lower percentiles of O_3 are also important and it is hard to define a precise threshold below which O_3 is not harmful. Thus the dose of O_3 to humans through respiration may be

the more important guide to the potential threat, and as the SOMO10 (and the mean values) have changed little with time, the suggested improvement in air quality from the EEA may be more apparent than real. An important policy implication of these trends is the degree to which local, regional or global policies are required to decrease the threat to human health from O_3. In the case of exposures to O_3 in excess of 60 ppb, controls at the European and national scales can be effective, as the measurements demonstrate. However, if the mean or lower percentiles are important, as suggested in recent syntheses, then controls at much larger (hemispheric) scales are required.

4.3.2 O_3 vegetation impact chemical climates

The detailed statistics describing the impacts of O_3 on crops at Harwell and Auchencorth, as derived using the POD_Y metric are presented in Tables S4.3 and S4.4 for potato, Tables S4.5 and S4.6 for wheat, and as derived using the generic crop AOT40 metric for a May-July growing season in Tables S4.7 and S4.8. The statistics for the POD_Y metric for forest trees are presented in Tables S4.9 and S4.10 for beech, and Tables S4.11 and S4.12 for Scots pine (Appendix IV). The POD_Y statistics presented in Tables S4.5-S4.12, and Figures 4.6-4.12 were calculated for the loam (medium) soil texture (Bueker et al., 2012). The representativeness of the conclusions derived from the interpretation of these statistics to other soil textures is discussed in Section 4.3.2.1 and 4.3.2.2. This section presents two analyses of the impact, state and drivers of the chemical climatology framework (Figure 2.4, steps 1-5); specifically, changes in chemical climate phase (Figure 2.4, Step 6) temporally at Harwell between 1990 and 2013 (Section 4.3.2.1) and spatially between Auchencorth and Harwell (Section 4.3.2.2).

4.3.2.1 Long-term changes in vegetation impact at Harwell (1990-2013)

Figure 4.7 shows the impact of O_3 on vegetation at Harwell, as quantified by the relevant POD_Y and response (grain yield for wheat, tuber weight for potato and biomass reduction for beech). The 1990-2013 average POD_Y values calculated using sandy loam (coarse), silt loam (medium coarse), loam (medium) and clay loam (fine) soil texture properties are shown in Table 4.1. The ratio between the largest and smallest average POD_Y due to differences in soil moisture for the different soil textures was 1.57 (wheat), 1.32 (potato), 1.14 (beech) and 1.10 (Scots pine), but the annual pattern of POD_Y accumulation was consistent across the four soil textures. The statistics in the following sections are those calculated for the loam soil texture, unless otherwise stated, which has intermediate hydraulic properties compared with the three other soil textures.

For crops, there has not been a statistically significant change in POD_Y between 1990 and 2013, across all soil textures (Figure 4.7). Using the critical levels for adverse vegetation damage agreed by the UN Convention on Long Range Transboundary Air Pollution (LRTAP) (Mills et al., 2011c), O_3 has a greater impact on wheat than potato at Harwell, with 13 of the 24 years exceeding the 5% yield reduction critical level for wheat, compared to 6 years exceeding the 5% tuber weight reduction critical level for potato. Mills et al (2011b), using modelled O_3 and meteorological data to assess the impact of O_3 on vegetation across the UK in 2006 and 2008, also reported a smaller impact on potato than wheat, due to the lower sensitivity of potato to O_3.

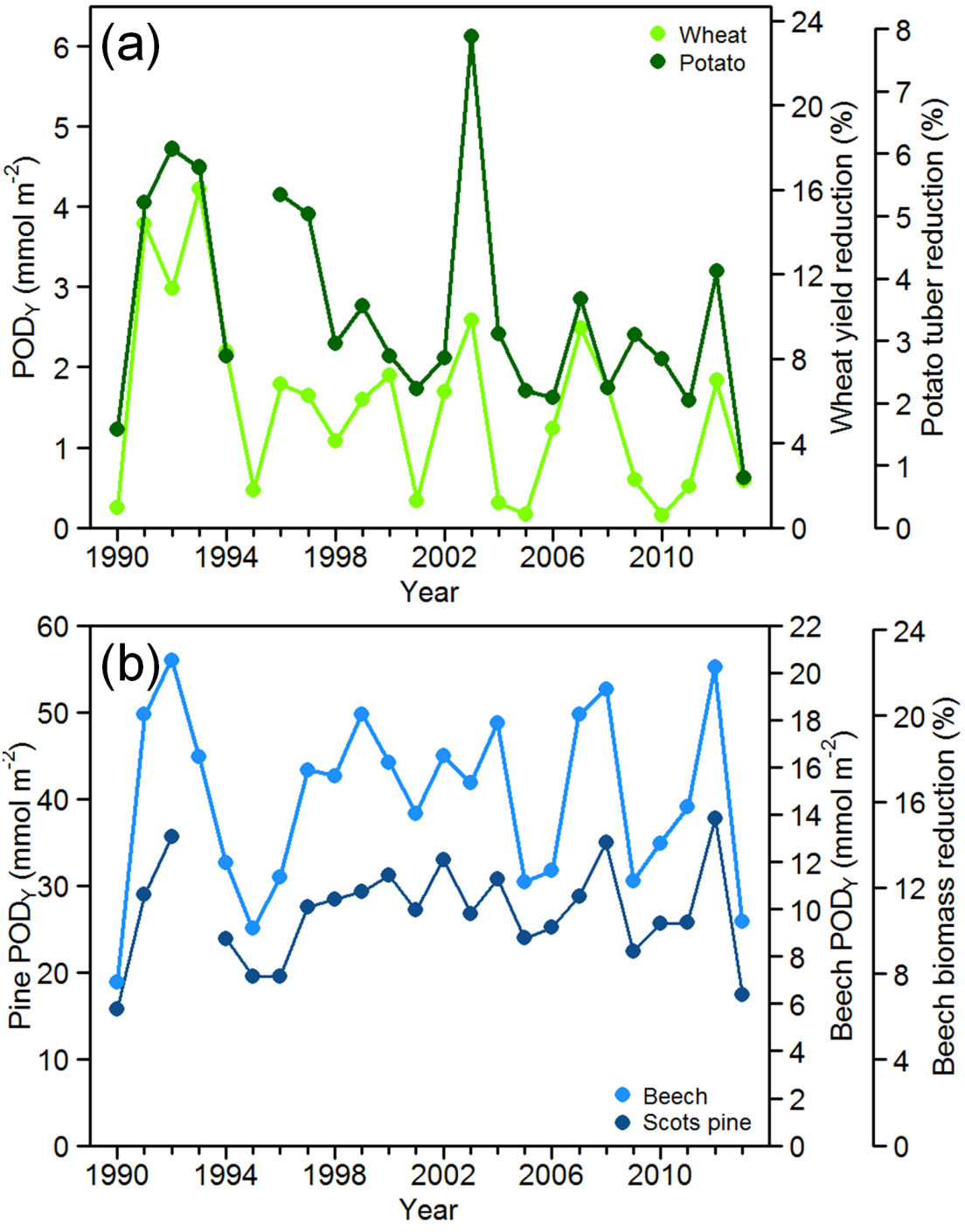

Figure 4.7: Impact of O_3 characterised by the POD_Y metric (and associated response) for (a) wheat (grain yield reduction) and potato (tuber weight reduction), and (b) beech (biomass reduction) and Scots pine at Harwell between 1990 and 2013.

Table 4.1: Average ± SD wheat, potato, beech and Scots pine POD_Y calculated for 4 different soil textures (see Bueker et al. (2012) for a description of their hydraulic properties) over the monitoring periods at Harwell and Auchencorth.

Harwell 1990-2013 average	**Sandy loam (coarse)**	**Silt loam (medium coarse)**	**Loam (medium)**	**Clay loam (fine)**
Wheat POD_Y (mmol m^{-2}) (grain yield % reduction)	1.21 ± 1.07 (4.61%)	1.75 ± 1.19 (6.64%)	1.51 ± 1.14 (5.72%)	1.90 ± 1.19 (7.22%)
Potato POD_Y (mmol m^{-2}) (tuber yield % reduction)	2.35 ± 1.27 (3.03%)	3.10 ± 1.42 (3.99%)	2.64 ± 1.32 (3.40%)	3.10 ± 1.46 (4.00%)
Beech POD_Y (mmol m^{-2}) (biomass % reduction)	14.0 ± 3.7 (15.4%)	16.0 ± 3.5 (17.6%)	14.7 ± 3.7 (16.2%)	16.1 ± 3.4 (17.7%)
Pine POD_Y (mmol m^{-2})	26.2 ± 5.5	28.7 ± 5.3	27.0 ± 5.6	28.8 ± 5.3
Auchencorth 2007-2013 average				
Wheat POD_Y (mmol m^{-2}) (grain yield % reduction)	0.85 ± 0.45 (3.23%)	1.01 ± 0.38 (3.86%)	0.96 ± 0.39 (3.65%)	1.05 ± 0.37 (3.99%)
Potato POD_Y (mmol m^{-2}) (tuber yield % reduction)	0.95 ± 0.41 (1.22%)	1.08 ± 0.46 (1.39%)	0.99 ± 0.41 (1.28%)	1.09 ± 0.47 (1.40%)
Beech POD_Y (mmol m^{-2}) (biomass % reduction)	16.6 ± 1.6 (18.3%)	16.9 ± 1.2 (18.6%)	16.7 ± 1.5 (18.4%)	16.9 ± 1.2 (18.6%)
Pine POD_Y (mmol m^{-2})	35.9 ± 3.6	36.5 ± 2.7	36.2 ± 3.3	36.6 ± 2.7

The majority of POD_Y accumulation for potato and wheat occurred in June (Tables S4.3 and S4.5). Between 1990 and 2013 there were significant decreases in diurnal O_3, NO_2 and NO amplitudes on June ADs (Figure 4.8, Tables S4.3 and S4.5). The median trend in diurnal O_3 amplitude on June ADs was –2.0% y^{-1} and –2.4% y^{-1} for potato and wheat respectively ($p = 0.001$), and, in the latter period (2010-2013), the difference in diurnal O_3 amplitude between June ADs and NADs was small (Tables S4.3 and S4.5). Figure 4.9 shows the percentage of POD_Y accumulated during different measured hourly O_3 concentration ranges. There were significant decreasing trends in the contribution from the highest concentration bins (65-70 ppb and >70 ppb) for potato (–0.4 to –1.4 % y^{-1}), and from the 55-60 and 65-70 ppb concentrations bins for wheat. In contrast, there were increasing trends in POD_Y contribution from the 25-45 ppb O_3 concentration bins for potato (+0.1 to +0.8% y^{-1}) and from the 30-45 ppb concentration bins for wheat (+0.5 to +1.1% y^{-1}). These trends were due to a decreasing frequency of hours with O_3 concentrations in the range 55 to >70 ppb during the

growing seasons of potato (–3.0 to –4.3% y^{-1}) and wheat (–2.1 to –4.8% y^{-1}) and increasing frequency of hourly O_3 concentrations in the range 25-45 ppb (wheat) and 20-35 ppb (potato). For both crops, the estimated back-trajectory NO_x emissions on ADs decreased significantly in the period 1990-2013 for each month of the growing season (Figure 4.8 shows this decrease for ADs in June), with trends ranging from –2.5 to –4.3% y^{-1}. Other drivers such as temperature, global radiation and back-trajectory pathway did not change significantly between 1990 and 2013 (Tables S4.3 and S4.5).

For beech and Scots pine, there was no significant trend in POD_Y between 1990 and 2013 across all soil types (Figure 4.7). The average POD_Y for beech (Table 1) was four times the critical level (Mills et al., 2011c). Beech and Scots pine PODy values were substantially higher than for the crops, due to a lower threshold for exceedance, a longer growing season and other differences in the stomatal conductance response to T, PAR, VPD and SWP. The average beech POD_Y value calculated here is comparable with the estimate for beech POD_Y modelled by Simpson et al. (2007) for the south east of England (8-16 mmol m^{-2}), but both values were higher than the values estimated in Emberson et al. (2007) for three European climate regions (not including UK) in 1997.

The low 1 nmol m^{-2} s^{-1} threshold for POD_Y accumulation for beech and Scots pine was exceeded during the majority of days during the respective growing seasons. The major contributions by month to POD_Y were consistently May and June for beech, and April, May and June for Scots pine (Tables S4.9 and S4.11). During 1990-2013 diurnal O_3 amplitude decreased significantly on beech and Scots pine ADs between May and September, with median monthly AD trends between –1.5% and –2.3% y^{-1} for beech, and –1.3% and –2.4% y^{-1} for Scots pine. Across the 24 year period there was a more consistent, major contribution to POD_Y during hourly O_3 concentrations in the range 25-50 ppb compared with wheat and potato, especially for Scots pine (Figure 4.9c and 4.9d). For beech and Scots pine, the trends in contribution from different concentration bins were smaller compared with crops. Decreasing trends in POD_Y contribution were significant for concentration bins between 50 and >70 ppb (–0.1 to –0.4 % y^{-1} for

beech and –0.1 to –0.2 % y^{-1} for Scots pine), and significant increasing trends in more moderate concentration bins (25-40 ppb) were only apparent for beech. During the growing season of each tree, the frequency of high O_3 concentrations (55 to >70 ppb) decreased significantly (–2.5 to –5.3% y^{-1} for both trees), and there was an increase in the frequency of concentrations between 25-35 ppb (+1.4 to +2.2% y^{-1} for both trees). Karlsson et al. (2007) calculated a similar result for Norway spruce in Sweden, where between 2002-2004 approximately 80% of POD_Y was accumulated during O_3 concentrations between 30 and 50 ppb. The estimated NO_x emissions into the air-mass trajectories also decreased significantly during beech and Scots pine ADs, with median monthly trends ranging from –3.2 to –3.6% y^{-1} for beech, and –1.9 to –3.7% y^{-1} for Scots pine.

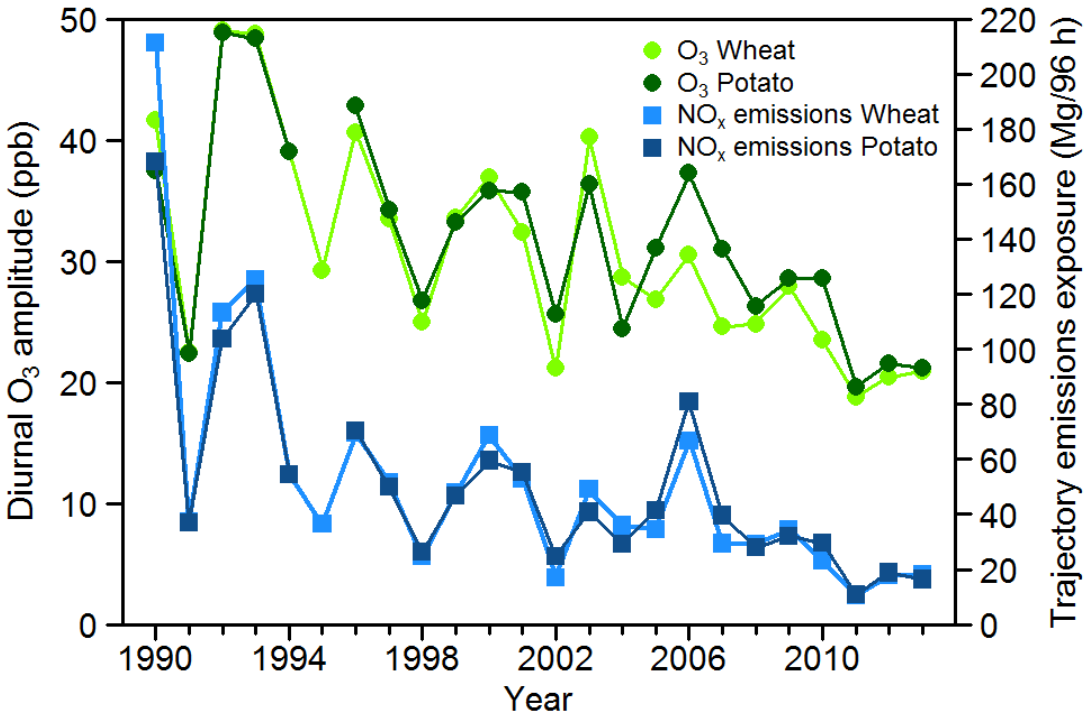

Figure 4.8: Amplitude of the diurnal O_3 cycle at Harwell during June POD_Y accumulation days for wheat and potato and hourly European NO_x emissions estimate for the EMEP 0.5° grids over which 96-h back trajectories passed prior to arrival at Harwell during June POD_Y accumulation days for wheat and potato.

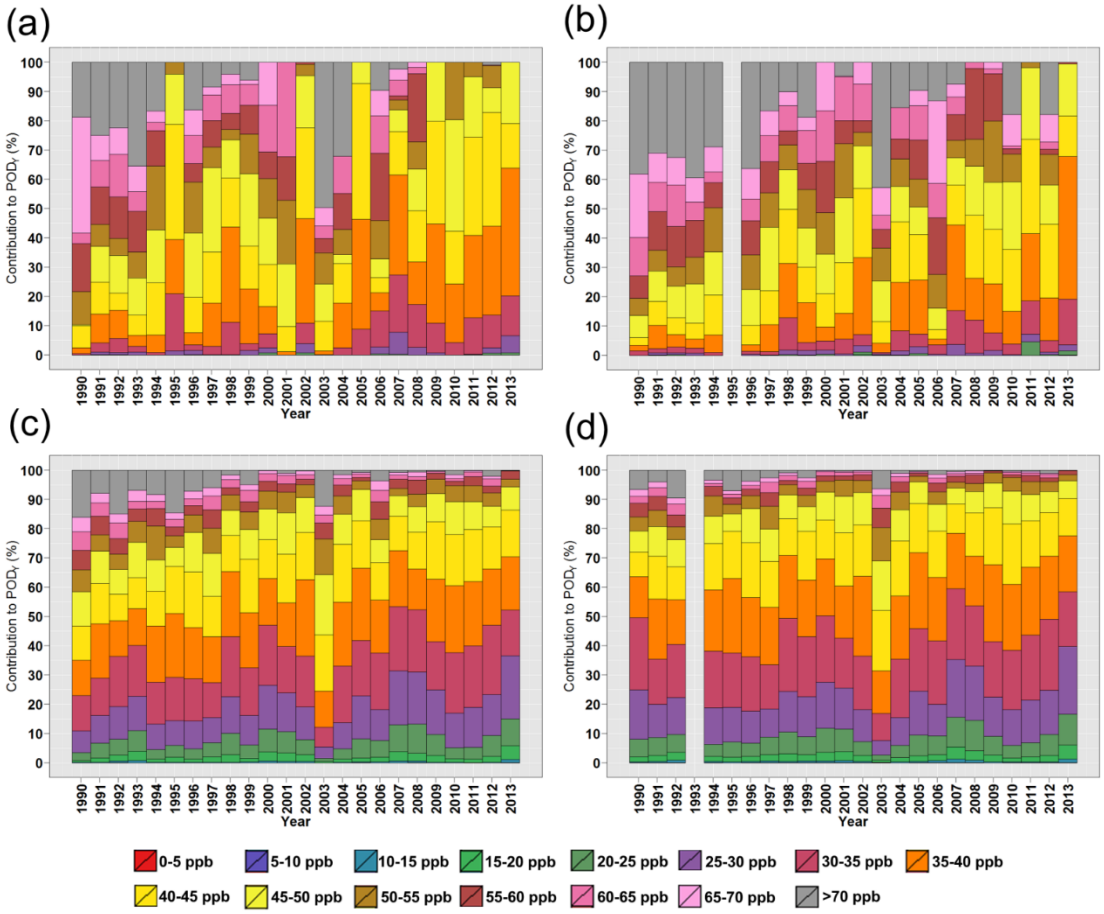

Figure 4.9: Relative annual contributions to (a) wheat POD_Y, (b) potato POD_Y, (c) beech POD_Y and (d) Scots pine POD_Y at Harwell from different O_3 concentration bins. Concentrations are separated into fifteen 5 ppb groups spanning hourly O_3 concentrations between 0 ppb and >70ppb. Note: these concentration bins are contributing to constant trends in POD_Y for each vegetation type – see Figure 4.7.

The significant trends in state (pollutant diurnal variation and concentration bin contributions) and drivers (trajectory emissions estimates) for the four vegetation types (Figure 4.8 and Tables S4.3, S4.5, S4.9 and S4.11) indicate an increase in the relative importance of hemispheric background O_3 concentrations in determining POD_Y. Despite this change, POD_Y values have not decreased, in contrast to SOMO35 for which decreased contribution from high O_3 concentrations (produced during regional O_3 episodes) resulted in a decreasing trend. This was due to non-O_3 factors such as stomatal response to VPD and soil moisture which also determine the severity of a vegetation impact by limiting the O_3 flux during high O_3 concentration episodes, reducing the sensitivity of POD_Y values to decreases in regional O_3 production. For

example, during the potato growing season the median stomatal conductance during hours with O_3 concentrations in the ranges 60-65, 65-70 and >70 ppb were 86, 90 and 65 mmol m^{-2} s^{-1} respectively (median across 1990-2013). These are significantly lower than the maximum stomatal conductance for potato of 750 mmol m^{-2} s^{-1} (LRTAP Convention, 2010), and similar to the median stomatal conductances calculated during more moderate O_3 concentrations, such as 35-40 ppb (54 mmol m^{-2} s^{-1}), 40-45 ppb (68 mmol m^{-2} s^{-1}) and 45-50 ppb (87 mmol m^{-2} s^{-1}).

Soil water potential (SWP) is a soil texture dependent determinant of potato stomatal conductance in the DO_3SE model, which decreases when SWP is lower than −0.5 MPa (Bueker et al., 2012; LRTAP Convention, 2010). Changes in soil moisture status (represented and linked to stomatal conductance by SWP in the DO_3SE model) are dependent on evaporative loss which in turn depends on meteorological conditions, including temperature, and net radiation at the top of the canopy, and input of moisture through precipitation (Bueker et al., 2012). The 1990-2013 average SWP during hours when O_3 concentrations at Harwell were in the concentration ranges 60-65 ppb, 65-70 ppb and >70 ppb were −1.50 ± 1.32 MPa, −1.14 ± 0.93 MPa and −1.10 ± 0.90 MPa respectively for the clay loam (fine) soil texture. The average SWP during these O_3 concentration ranges were lower, and even more limiting for the other three soil textures. These are substantially lower than the average SWP for the O_3 concentration ranges between 25 and 50 ppb, all of which are above the −0.5 MPa cut-off except 45-50 ppb for sandy loam, silt loam and loam soil textures (average SWP of −0.65, −0.52 and −0.58 MPa respectively). Across all soil textures, reduction in the frequency of elevated O_3 concentrations produced during regional photochemical episodes has therefore not reduced POD_Y, as these elevated O_3 concentrations coincided with other factors (e.g. SWP) which limit stomatal conductance and hence any potential increase in O_3 accumulation resulting from increased O_3 concentrations. Decreasing regional O_3 production resulted in the largest change in concentration bin contributions for potato POD_Y (Figure 4.9b). This is due to a later growing season compared with wheat, and a shorter accumulation period and higher maximum stomatal conductance compared with forest trees (150 and 180 mmol m^2 s^{-1} for beech and Scots pine

respectively compared to 750 mmol m^2 s^{-1} for potato), limiting the O_3 flux during high O_3 episodes.

These non-O_3 factors, such as SWP, also determine the annual pattern of POD_Y accumulation. For example, between 2010 and 2013 at Harwell, the average SWP on potato ADs in June was –0.11 MPa, compared to –0.72 MPa on NADs (loam soil texture). Hence in June, O_3 concentrations were sufficient that, when plant conditions were favourable, accumulation of POD_Y occurred. In July, SWP was substantially higher due to increased temperatures (2010-2013 average SWP on potato ADs was –1.02 MPa). This, combined with decreasingly favourable potato and wheat phenology, reduced potato and wheat stomatal conductance, leading to a smaller contribution to total POD_Y in July compared to June. Higher O_3 concentrations were therefore needed to accumulate POD_Y; these occurred during regional photochemical O_3 production, hence the larger difference between diurnal O_3 amplitude on AD and NADs in July compared with June for the two crops.

For beech and Scots pine, the proportion of POD_Y accumulated in May and June was higher than in July and August, despite no change in phenology used in the DO_3SE model from May-August, and exceedance of the 1 nmol m^{-2} s^{-1} threshold on the majority of days. For beech, reduction in stomatal conductance occurs when SWP is lower than –0.8 MPa (LRTAP Convention, 2010). Between 2010 and 2013, across the four soil textures, on average 0% and 0-9% of hourly SWP values in May and June, respectively, were below this value, compared with 23-51% and 18-31% in July and August respectively. The reduction in stomatal conductance of O_3 due to soil moisture begins at SWP < –0.7 MPa for Scots pine, and therefore has a larger limiting effect on O_3 accumulation. SWP was also found to be one of the most important limiting factors in determining the impact of O_3 on forests across Europe (Emberson et al., 2007). Clay loam had the highest SWP of the four soil textures, and therefore the lowest limitation to stomatal conductance, followed by silt loam, loam and sandy loam. However, the variation in soil moisture between different soil textures due to differences in the extent

of evaporation is sufficiently small that the lack of long-term trend in POD_Y and annual pattern of accumulation is consistent across the soil textures.

4.3.2.2 Spatial differences between Auchencorth and Harwell (2007-2013)

The 2007-2013 average POD_Y calculated for the four soil textures is shown in Table 1, and the variation between soil textures is less than at Harwell. The ratio between the largest and smallest average POD_Y due to differences in soil moisture for the different soil textures was 1.24 (wheat), 1.15 (potato), 1.02 (beech) and 1.02 (Scots pine). The pattern of accumulation, and spatial differences between Harwell and Auchencorth, were consistent across soil textures. Annual POD_Y for potato at Auchencorth (Table S4.4) were consistently lower than at Harwell, while, for wheat, POD_Y were higher at Auchencorth (Table S4.6) for 3 of the 7 years. The LRTAP critical level for impact (Mills et al., 2011c) was only exceeded at this site in 2008 for wheat (5.04% yield reduction). These observations, determined using measured O_3 and meteorological data, are consistent with the spatial patterns identified by Mills et al. (2011b) in which modelled O_3 and meteorological variables were used to model POD_Y in 10 km × 10 km grids across the UK. However, the calculated 2008 tuber weight reduction of 1.4% for potato at Auchencorth is higher than the 0% reduction estimated for the grids containing Auchencorth. Simpson et al. (2007) also modelled wheat POD_Y across Europe for 2000, and calculated POD_Y in south-east Scotland of 0.5-1 mmol m^{-2}, and in south-east England of 1-3 mmol m^{-2}, which are similar to those determined here using the measurement data at Harwell and Auchencorth. In general, diurnal amplitudes of O_3, NO_2 and NO and back-trajectory NO_x emissions estimates were lower at Auchencorth (shown in Figure 4.10b for wheat and potato POD_Y ADs in June), which indicates a greater importance of hemispheric background concentrations in determining the O_3 impact at Auchencorth on wheat and potato.

Periods with elevated regional O_3 influence at Auchencorth can lead to a larger effect on POD_Y compared with Harwell. For example, in 2008 across all soil textures, July

contributed 0.47 mmol m^{-2} (36% total) to wheat POD_Y (Figure 4.11a). In this month, O_3 concentrations at Auchencorth had a significant regional photochemical contribution, evidenced by elevated diurnal O_3 and NO_2 variation and 71% higher back-trajectory NO_x emissions on ADs compared to the 2007-2013 average (Figure 4.11b). POD_Y in July 2011 at Auchencorth was also influenced by regional O_3 production. Diurnal O_3 amplitude in July 2011 was 6 ppb higher on ADs than on NADs and global radiation during ADs was 26% higher than the AD average. July 2011 contributed 80% of the annual wheat POD_Y at Auchencorth across all soil textures. At Harwell in July 2008, wheat POD_Y was less than half the Auchencorth value, and in July 2011, there was no POD_Y accumulation, despite elevated regional O_3 influence in both cases. These two examples demonstrate that elevated regional photochemical O_3 production can have a larger crop impact, characterised through POD_Y, in south-east Scotland than in south-east England, despite being further from major sources of O_3 precursor emissions. The meteorological conditions conducive to regional photochemical O_3 production (higher temperature and global radiation) at Harwell resulted in unfavourable conditions for high O_3 stomatal conductance in crops compared with Auchencorth, due to reduction in soil moisture through increased evaporative loss. The median daytime O_3 stomatal conductance at Harwell was 58 mmol m^{-2} s^{-1} and 63 mmol m^{-2} s^{-1} in July 2008 and 2011 respectively for loam soil texture, compared to 94 mmol m^{-2} s^{-1} and 95 mmol m^{-2} s^{-1} at Auchencorth. Average SWP in July 2008 and 2011 was –0.03 MPa and –0.02 MPa respectively at Auchencorth, and –0.63 MPa and –1.17 MPa at Harwell. In addition lower temperatures at Auchencorth result in a longer accumulated temperature growing season. In July 2008 and 2011, the phenological limitation on wheat stomatal conductance was similar for the first three weeks of the month at both sites, but in the final week diverged and was substantially more limiting at Harwell at the end of July (40% and 50% lower in 2008 and 2011, respectively), also resulting in less favourable conditions for POD_Y accumulation in south-east England.

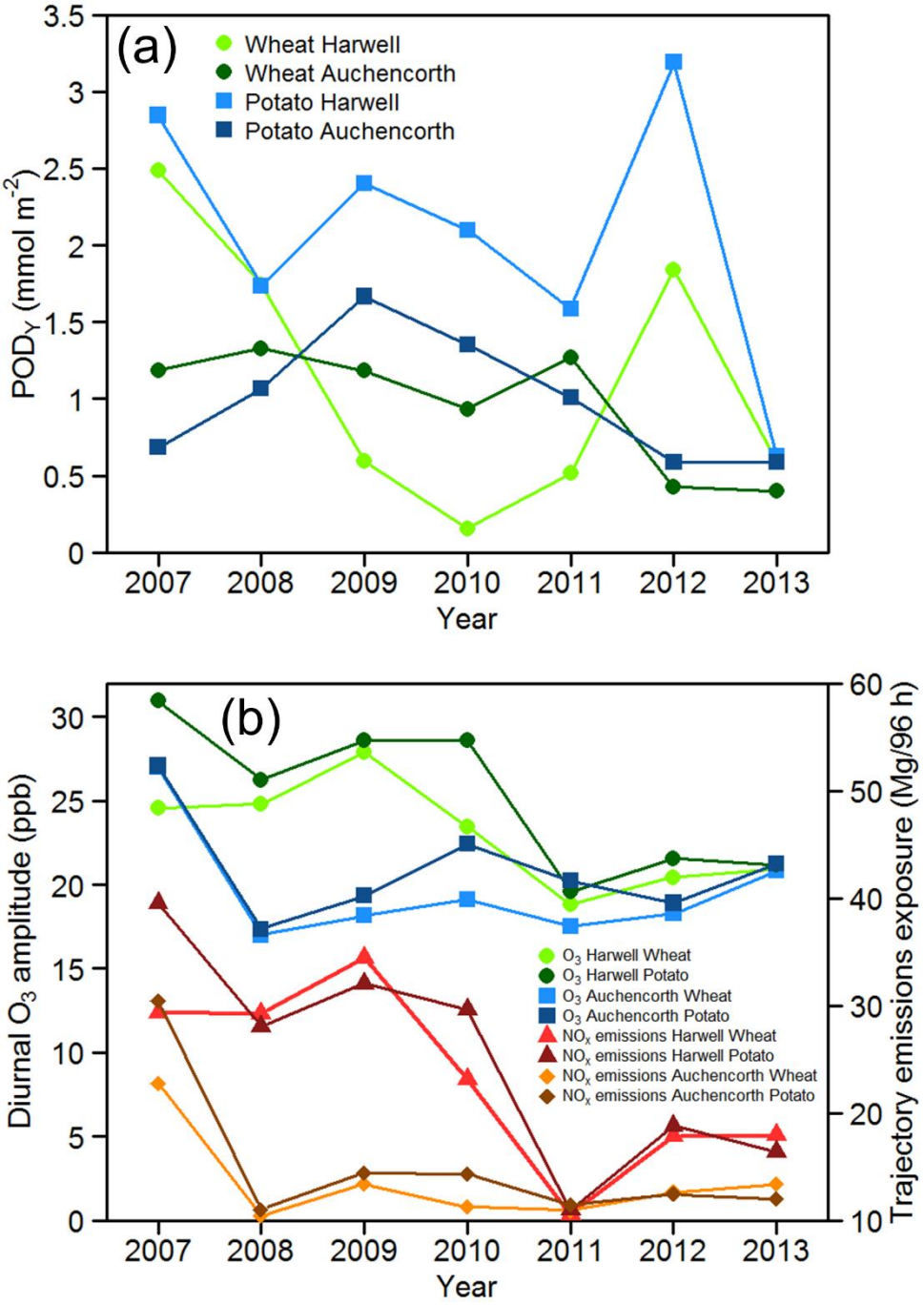

Figure 4.10: Comparison of O_3 vegetation impact chemical climates for wheat and potato 2007-2013. (a) Annual POD_Y for wheat and potato, (b) Diurnal O_3 amplitude during June accumulation days (ADs) at Harwell and Auchencorth, and trajectory NO_x emissions estimates at Harwell and Auchencorth.

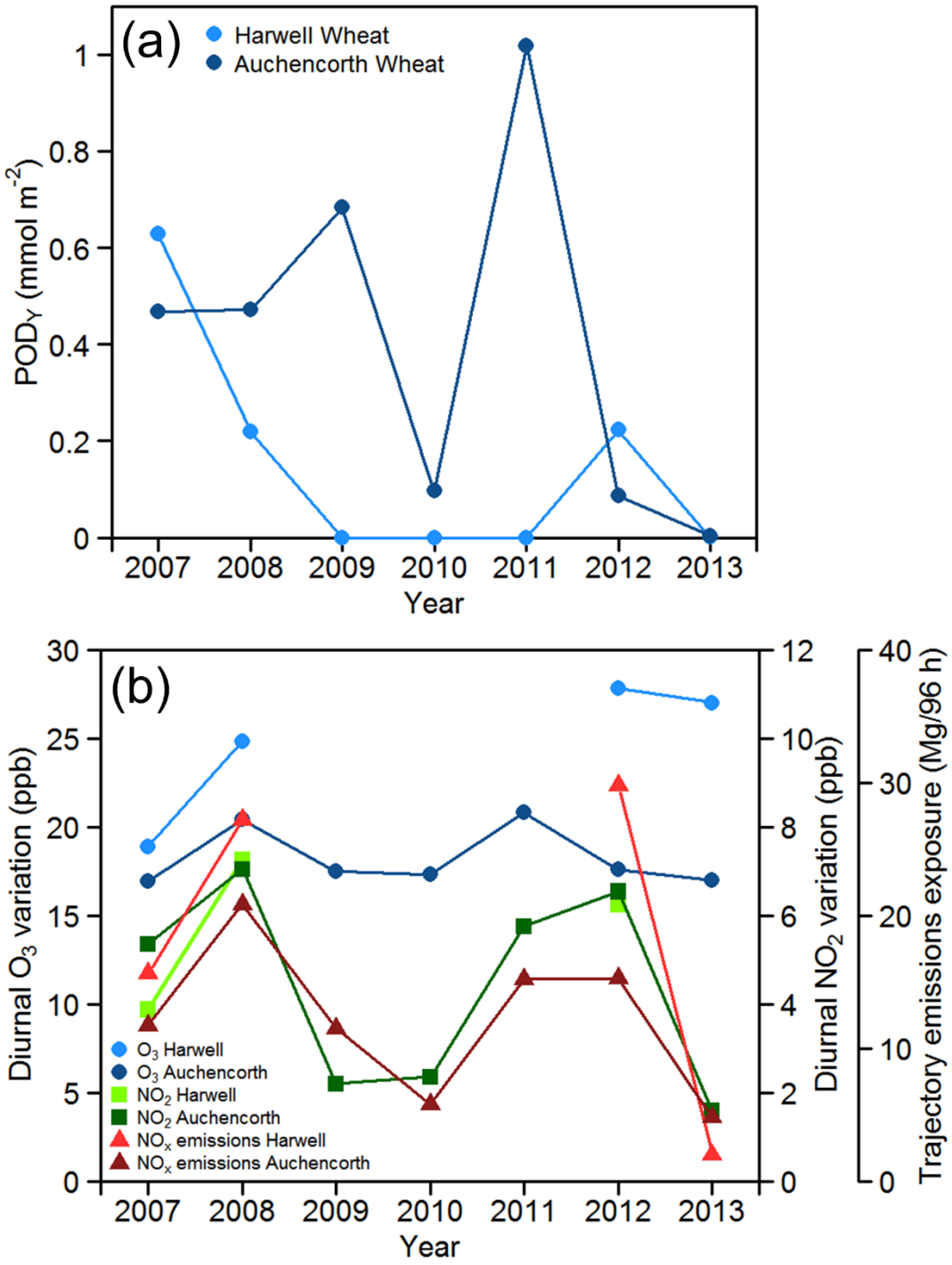

Figure 4.11: (a) Wheat POD_Y accumulated during July at Harwell and at Auchencorth, 2007-13. (b) Diurnal cycle amplitude of O_3 and NO_2, and back-trajectory NO_x emissions estimates during wheat accumulation days (ADs) in July at Harwell and at Auchencorth, 2007-13.

Between 2007 and 2013 across the soil textures, Scots pine and beech POD_Y were on average 27-37% and 5-19% higher at Auchencorth compared to Harwell (Table 4.1 and Figure 4.12a). These larger values were due to larger contributions from July and August at Auchencorth (Tables S4.10 and S4.12). In these months, higher temperatures at Harwell produced conditions which reduced stomatal conductance. For example, in 2007-2013 at Harwell for loam soil texture, SWP was on average 59% higher in July and 82% higher in August than at Auchencorth.

Elevated regional photochemical O_3 production also had varying impacts on forest trees at the two sites. In May 2008 across all soil textures, accumulated POD_Y was elevated at Auchencorth for both Scots pine and beech (Figure 4.12b). Larger diurnal O_3 variation (28% higher than the 2007-2013 average) and back-trajectory NO_x emissions (53% higher) during May 2008 indicate regional photochemical O_3 production made a significant contribution to measured O_3 concentrations at Auchencorth (Figure 4.12c). Despite larger increases in these variables at Harwell, the accumulated POD_Y in May 2008 was 14% and 29% less than at Auchencorth for beech and Scots pine, respectively across all soil textures (Figure 4.12b), and the frequency of hours with high POD_Y accumulation was lower at Harwell. For example, the maximum hourly POD_Y accumulated at Harwell and Auchencorth in May 2008 were 0.027 mmol m^{-2} and 0.033 mmol m^{-2} respectively and there were 21 fewer hours when hourly POD_Y accumulated was above 0.02 mmol m^{-2} compared with Auchencorth. Hence the conditions during this regional O_3 episode at Harwell, e.g. a 12% increase in monthly average temperature, also produced less favourable plant conditions for POD_Y accumulation.

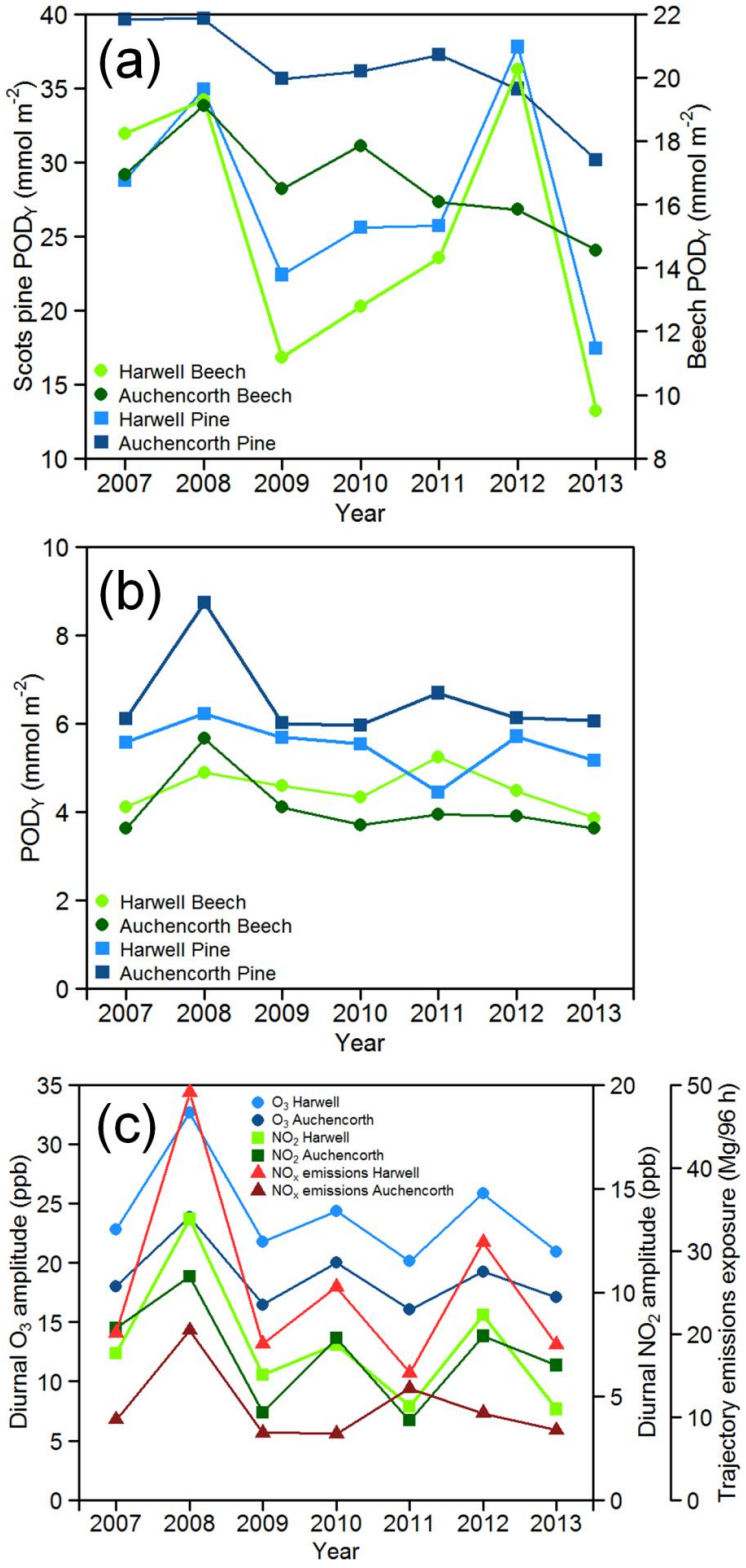

Figure 4.12: Comparison of O_3 vegetation impact chemical climates for beech and Scots pine 2007-2013 at Harwell and Auchencorth. (a) Annual POD_Y for beech and Scots pine. (b) POD_Y accumulated in May for beech and Scots pine. (c) May monthly average diurnal amplitude of O_3 and NO_2, and back-trajectory NO_x emissions estimates.

4.3.2.3 Comparison between POD_Y and AOT40

The chemical climates based on the AOT40 metric (Tables S4.7 and S4.8) were derived for the crop-based AOT40 definition and are therefore most comparable with the wheat and potato POD_Y chemical climates. At Harwell, there was a significant long-term decrease in AOT40 from an average of 6533 ppb.h in 1990-1993 to an average of 2623 ppb.h in 2010-2013 (trend: –3.6% y^{-1}, p = 0.001, Figure 4.13, Table S4.7). This decrease in AOT40 is in contrast to the trends in wheat and potato POD_Y at Harwell, which showed no significant trend across the 24 year period (Figure 4.7a). However, the AOT40 climate showed similar decreases in diurnal pollutant amplitudes and back-trajectory NO_x emissions estimates compared with the crop POD_Y climates, indicating increased importance of hemispheric background concentrations. This is in line with Derwent et al. (2013) which reported an increase between 1989-2012 in AOT40 when selecting hemispheric background air arriving at Mace Head, Ireland. AOT40 at Auchencorth was lower than at Harwell, and the magnitude of the difference was much larger than for POD_Y. This was similar to the spatial differences in Jenkin (2014), where estimated regional background AOT40 was twice as large at Harwell compared to a rural site in central Scotland (EMEP site GB0033R: Bush).

The spatial difference between sites was less for POD_Y than for AOT40 because the latter does not account for modification of stomatal conductance, especially during summer months when SWP at Harwell can be low. Hence the average contribution from July in 2010-2013 to AOT40 was 35%, but only 3% for wheat POD_Y (Tables S4.5 and S4.7). Conversely, the contribution from July to AOT40 at Auchencorth is lower than the contribution to wheat and potato POD_Y (Tables S4.6 and S4.8), indicating that O_3 concentrations below the 40 ppb threshold determine the wheat and potato POD_Y to a large extent during this month. The limitations of the fixed growing season in the AOT40 concept have been detailed previously (Coyle et al., 2003; RoTAP, 2012), including the observation that there can be significant impact on vegetation below the 40 ppb threshold. For forest trees, Gauss et al. (2014) reported forest-based AOT40 across the UK from 2007-2012 to be between 5 and 50% lower

than that calculated in 2000. In addition Klingberg et al. (2014) found a much smaller decline in forest-specific POD_Y than AOT40 between 1960 and 2100 using modelled O_3 and meteorological data at 14 sites across Europe.

In summary, the crop-based AOT40 trend at Harwell showed an improvement in O_3 crop impact which is not shown when the interaction between plant and O_3 climates are modelled using biological process based POD_Y metric.

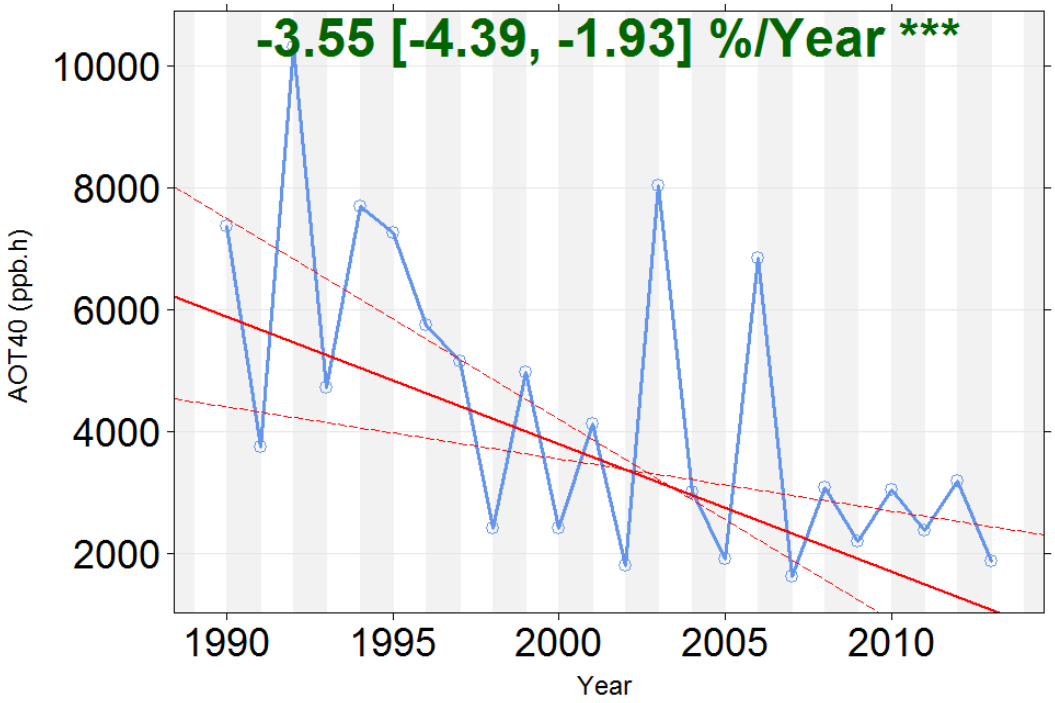

Figure 4.13: Crop-relevant AOT40 (calculated between May and July) at Harwell for the period 1990 to 2013. The Theil-Sen trend estimate of median trend (shown in red) is –3.6 % y^{-1} (p = 0.001).

4.4 Conclusions

The chemical climatology framework outlined in Chapter 2 was applied to characterise O_3 exposure associated with human health and vegetation impacts using measured data at the Harwell and Auchencorth UK EMEP supersites. These sites have been shown to be representative of rural O_3 over the wider geographic areas of south-east England and northern UK, respectively (Chapter 3).

At Harwell, each chemical climate analysis indicated a decrease over the period 1990-2013 in the relative importance of regional photochemical O_3 production, associated with NO_x emissions reductions, and increasing relative importance of hemispheric background concentrations. However trends in the human health and vegetation metrics associated with these changes were different.

As quantified by the SOMO35 metric, the human health-relevant O_3 exposure at Harwell decreased significantly over the period 1990-2013 (–2.2% y^{-1}), while quantification using the SOMO10 metric showed no trend due to its lower dependence on the highest O_3 concentrations, which have decreased due to declining regional photochemical production. Hence the choice of these two O_3 concentration thresholds, which are both recommended by WHO REVIHAAP for health impact assessments, determines both the perceived annual pattern of health burden and whether there has been improvement in time. The policy significance of these findings is important since the regional policies adopted to date, of controls on NO_x and VOC emissions in Europe, have been effective in reducing peak concentrations and exposure. The growth in these emissions elsewhere has increased the importance of background contribution to O_3 exposure in the UK. The effective controls for background O_3 would be controls at hemispheric scales on O_3 precursors, and in methane emissions especially (Fiore et al., 2009).

The POD_Y metrics used to quantify the impact of O_3 on vegetation showed no change over the period 1990-2013 at Harwell for wheat and potato crops, and beech and Scots

pine trees, in contrast to a decreasing trend in potential impact if quantified by the crop AOT40 metric. The contrast highlights the need to model vegetation impacts using the biologically more relevant POD_Y metrics. The potential reductions in vegetation impact (i.e. POD_Y), due to decreases in regional photochemical O_3 production decreases (as reflected in the decrease in crop AOT40 at Harwell), did not occur due to the other factors that reduce plant stomatal conductance and hence accumulated O_3 uptake (e.g. changing plant phenology and low soil water potential). Thus the long-term decrease in regional O_3 production evident at Harwell led to a lower beneficial effect on POD_Y than on SOMO35.

The chemical climates indicate a greater influence of hemispheric background concentrations at Auchencorth compared to Harwell (for the period 2007-2013). SOMO10 values were similar at both sites, but SOMO35 was lower at Auchencorth. POD_Y values were larger for vegetation species with longer growing seasons and lower thresholds for exceedance compared to Harwell (i.e. for beech and Scots pine). In addition, more favourable plant conditions (higher SWP, longer accumulated temperature derived growing season) during periods of elevated regional O_3 production resulted in exacerbation of vegetation impacts at Auchencorth compared to Harwell. Hence the potential for O_3 vegetation impact reduction from future reductions in regional O_3 is greater at Auchencorth than at Harwell, despite being further from the major sources of O_3 precursors. However, the policies required to substantially reduce exposure of vegetation in the UK to damage from O_3, like those for human health, are measures that reduce the background O_3 concentrations, hence the need for hemispheric control measures on O_3 precursors.

References

Abbatt, J., George, C., Melamed, M., Monks, P., Pandis, S., Rudich, Y., 2014. New Directions: Fundamentals of atmospheric chemistry: Keeping a three-legged stool balanced. Atmos. Environ. 84, 390-391.

AQEG, 2009. Ozone in the United Kingdom: Air Quality Expert Group, Defra Publications, London. http://www.defra.gov.uk/environment/quality/air/airquality/publications/ozone/documents/aqeg-ozone-report.pdf.

Bueker, P., Morrissey, T., Briolat, A., Falk, R., Simpson, D., Tuovinen, J. P., Alonso, R., Barth, S., Baumgarten, M., Grulke, N., Karlsson, P. E., King, J., Lagergren, F., Matyssek, R., Nunn, A., Ogaya, R., Penuelas, J., Rhea, L., Schaub, M., Uddling, J., Werner, W., Emberson, L. D., 2012. DO3SE modelling of soil moisture to determine ozone flux to forest trees. Atmos. Chem. Phys. 12, 5537-5562.

Carslaw, D. C., Ropkins, K., 2013. openair: Open-source tools for the analysis of air pollution data. R package version 0.8-5.

Coyle, M., Fowler, D., Ashmore, M., 2003. New directions: Implications of increasing tropospheric background ozone concentrations for vegetation. Atmos. Environ. 37, 153-154.

Coyle, M., Smith, R. I., Stedman, J. R., Weston, K. J., Fowler, D., 2002. Quantifying the spatial distribution of surface ozone concentration in the UK. Atmos. Environ. 36, 1013-1024.

Derwent, R., Manning, A., Simmonds, P., Gerard Spain, T., O'Doherty, S., 2013. Analysis and interpretation of 25 years of ozone observations at the Mace Head Atmospheric Research Station on the Atlantic Ocean coast of Ireland from 1987 to 2012. Atmos. Environ. 80, 361-368.

Draxler, R. R., Rolph, G. D., 2013. HYSPLIT (HYbrid Single-Particle Lagrangian Integrated Trajectory) Model access via NOAA ARL READY Website (http://www.arl.noaa.gov/HYSPLIT.php). NOAA Air Resources Laboratory, College Park, MD.

Eaton, S., Stacey, B., 2012. QA/QC Data Ratification Report for the Automatic Urban and Rural Network, October-December 2011, and Annual Report 2011. AEAT/ENV/R/3284 Issue 1. Contract Report to the Department for Environment, Food and Rural Affairs. AEA. http://uk-air.defra.gov.uk/assets/documents/reports/cat05/1207040912_AURN_2011_Q4_Issue_1.pdf.

EEA, 2014a. EU emission inventory report 1990-2012 under the UNECE Convention on long-range transboundary air pollution (LRTAP). EEA technical report No 12/2014. European Environment Agency. http://www.eea.europa.eu/publications/eu-emission-inventory-report-lrtap.

EEA, 2014b. Overview of exceedances of EC ozone threshold values: April–September 2013. EEA technical report No 3/2014. European Environment

Agency. http://www.eea.europa.eu/publications/air-pollution-by-ozone-across-1.

Emberson, L. D., Buker, P., Ashmore, M. R., 2007. Assessing the risk caused by ground level ozone to European forest trees: A case study in pine, beech and oak across different climate regions. Environ. Pollut. 147, 454-466.

Emberson, L. D., Ashmore, M. R., Cambridge, H. M., Simpson, D., Tuovinen, J. P., 2000. Modelling stomatal ozone flux across Europe. Environ. Pollut. 109, 403-413.

EMEP, 2014. Transboundary particulate matter, photo-oxidants, acidifying and eutrophying components. EMEP Status Report 1/2014. European Monitoring and Evaluation Programme. http://emep.int/publ/reports/2014/EMEP_Status_Report_1_2014.pdf.

Fiore, A. M., Dentener, F. J., Wild, O., Cuvelier, C., Schultz, M. G., Hess, P., Textor, C., Schulz, M., Doherty, R. M., Horowitz, L. W., MacKenzie, I. A., Sanderson, M. G., Shindell, D. T., Stevenson, D. S., Szopa, S., Van Dingenen, R., Zeng, G., Atherton, C., Bergmann, D., Bey, I., Carmichael, G., Collins, W. J., Duncan, B. N., Faluvegi, G., Folberth, G., Gauss, M., Gong, S., Hauglustaine, D., Holloway, T., Isaksen, I. S. A., Jacob, D. J., Jonson, J. E., Kaminski, J. W., Keating, T. J., Lupu, A., Marmer, E., Montanaro, V., Park, R. J., Pitari, G., Pringle, K. J., Pyle, J. A., Schroeder, S., Vivanco, M. G., Wind, P., Wojcik, G., Wu, S., Zuber, A., 2009. Multimodel estimates of intercontinental source-receptor relationships for ozone pollution. J. Geophys. Res. 114, 21.

Fuhrer, J., Skarby, L., Ashmore, M. R., 1997. Critical levels for ozone effects on vegetation in Europe. Environ. Pollut. 97, 91-106.

Gauss, M., Semeena, V., Benedictow, A., Klein, H., 2014. Transboundary air pollution by main pollutants (S, N, Ozone) and PM: The United Kingdom. MSC-W Data Note 1/2014. http://emep.int/publ/reports/2014/Country_Reports/report_GB.pdf.

Guerreiro, C. B. B., Foltescu, V., de Leeuw, F., 2014. Air quality status and trends in Europe. Atmos. Environ. 98, 376-384.

Heal, M. R., Heaviside, C., Doherty, R. M., Vieno, M., Stevenson, D. S., Vardoulakis, S., 2013. Health burdens of surface ozone in the UK for a range of future scenarios. Environ. Int. 61, 36-44.

Jenkin, M., 2014. Investigation of an oxidant-based methodology for AOT40 exposure assessment in the UK. Atmos. Environ. 94, 332-340.

Jenkin, M. E., 2008. Trends in ozone concentration distributions in the UK since 1990: Local, regional and global influences. Atmos. Environ. 42, 5434-5445.

Karlsson, P. E., Tang, L., Sundberg, J., Chen, D., Lindskog, A., Pleijel, H., 2007. Increasing risk for negative ozone impacts on vegetation in northern Sweden. Environ. Pollut. 150, 96-106.

Kaufman, L., Rousseeuw, P. J., 1990. Finding Groups in Data: An Introduction to ClusterAnalysis. Wiley, New York. Wiley, New York.

Klingberg, J., Engardt, M., Uddling, J., Karlsson, P. E., Pleijel, H., 2011. Ozone risk for vegetation in the future climate of Europe based on stomatal ozone uptake calculations. Tellus A 63, 174-187.

Klingberg, J., Engardt, M., Karlsson, P. E., Langner, J., Pleijel, H., 2014. Declining ozone exposure of European vegetation under climate change and reduced precursor emissions. Biogeosciences 11, 5269-5283.

Kuhlbusch, T., Quincey, P., Fuller, G., Kelly, F., Mudway, I., Viana, M., Querol, X., Alastuey, A., Katsouyanni, K., Weijers, E., Borowiak, A., Gehrig, R., Hueglin, C., Bruckmann, P., Favez, O., Sciare, J., Hoffmann, B., EspenYttri, K., Torseth, K., Sager, U., Asbach, C., Quass, U., 2014. New Directions: The future of European urban air quality monitoring. Atmos. Environ. 87, 258-260.

Lee, J. D., Lewis, A. C., Monks, P. S., Jacob, M., Hamilton, J. F., Hopkins, J. R., Watson, N. M., Saxton, J. E., Ennis, C., Carpenter, L. J., Carslaw, N., Fleming, Z., Bandy, B. J., Oram, D. E., Penkett, S. A., Slemr, J., Norton, E., Rickard, A. R., Whalley, L. K., Heard, D. E., Bloss, W. J., Gravestock, T., Smith, S. C., Stanton, J., Pilling, M. J., Jenkin, M. E., 2006. Ozone photochemistry and elevated isoprene during the UK heatwave of August 2003. Atmos. Environ. 40, 7598-7613.

LRTAP Convention, 2010. In: Mills, G., et al. (Eds.). Chapter 3 of the LRTAP Convention Manual of Methodologies for Modelling and Mapping Effects of Air Pollution. Available at: http://icpvegetation.ceh.ac.uk/.

Malley, C. S., Braban, C. F., Heal, M. R., 2014a. The application of hierarchical cluster analysis and non-negative matrix factorization to European atmospheric monitoring site classification. Atmos. Res. 138, 30-40.

Malley, C. S., Braban, C. F., Heal, M. R., 2014b. New Directions: Chemical climatology and assessment of atmospheric composition impacts. Atmos. Environ. 87, 261-264.

Mangiameli, P., Chen, S. K., West, D., 1996. A comparison of SOM neural network and hierarchical clustering methods. Eur. J. Oper. Res. 93, 402-417.

Mareckova, K., Wankmueller, R., Whiting, R., Pinterits, M., 2013. Review of emission data reported under the LRTAP Convention and NEC Directive, Stage 1 and 2 review, Review of emission inventories from shipping, Status of Gridded and LPS data, EEA and CEIP technical report, 1/2013, ISBN 978-3-99004-248-9. Available at: http://www.ceip.at/review-of-inventories/review-2013/.

Mills, G., Hayes, F., Simpson, D., Emberson, L., Norris, D., Harmens, H., Bueker, P., 2011a. Evidence of widespread effects of ozone on crops and (semi-)natural vegetation in Europe (1990-2006) in relation to AOT40-and flux-based risk maps. Global Change Biol. 17, 592-613.

Mills, G., Hayes, F., Norris, D., Hall, J., Coyle, M., Cambridge, H., Cinderby, S., Abbott, J., Cooke, S., Murrells, T., 2011b. Impacts of Ozone Pollution on Food Security in the UK: a Case Study for Two Contrasting Years, 2006 and 2008. Defra contract AQ0816, London.

Mills, G., Pleijel, H., Braun, S., Bueker, P., Bermejo, V., Calvo, E., Danielsson, H., Emberson, L., Gonzalez Fernandez, I., Gruenhage, L., Harmens, H., Hayes, F., Karlsson, P.-E., Simpson, D., 2011c. New stomatal flux-based critical levels for ozone effects on vegetation. Atmos. Environ. 45, 5064-5068.

Munir, S., Chen, H., Ropkins, K., 2013. Quantifying temporal trends in ground level ozone concentration in the UK. Sci. Total Environ. 458, 217-227.

Parrish, D. D., Law, K. S., Staehelin, J., Derwent, R., Cooper, O. R., Tanimoto, H., Volz-Thomas, A., Gilge, S., Scheel, H. E., Steinbacher, M., Chan, E., 2013. Lower tropospheric ozone at northern midlatitudes: Changing seasonal cycle. Geophys. Res. Lett. 40, 1631-1636.

R Core Development Team, 2008. R: A language and environment for statistical computing. R Foundation for Statistical Computing, Vienna, Austria. ISBN 3-900051-07-0, URL http://www.R-project.org.

REVIHAAP, 2013. Review of evidence on health aspects of air pollution – REVIHAAP Project technical report. World Health Organization (WHO) Regional Office for Europe, Bonn. http://www.euro.who.int/__data/assets/pdf_file/0004/193108/REVIHAAP-Final-technical-report-final-version.pdf.

RoTAP, 2012. Review of Transboundary Air pollution: Acidification, Eutrophication, Ground Level Ozone and Heavy metals in the UK. Contract Report to the Department for Environment, Food and Rural Affairs. Centre for Ecology and Hydrology. http://www.rotap.ceh.ac.uk/sites/rotap.ceh.ac.uk/files/CEH%20RoTAP.pdf.

Schmale, J., van Aardenne, J., von Schneidemesser, E., 2014. New Directions: Support for integrated decision-making in air and climate policies – Development of a metrics-based information portal. Atmos. Environ. 90, 146-148.

Simpson, D., Ashmore, M. R., Emberson, L., Tuovinen, J. P., 2007. A comparison of two different approaches for mapping potential ozone damage to vegetation. A model study. Environ. Pollut. 146, 715-725.

Simpson, D., Benedictow, A., Berge, H., Bergstrom, R., Emberson, L. D., Fagerli, H., Flechard, C. R., Hayman, G. D., Gauss, M., Jonson, J. E., Jenkin, M. E., Nyiri, A., Richter, C., Semeena, V. S., Tsyro, S., Tuovinen, J. P., Valdebenito, A., Wind, P., 2012. The EMEP MSC-W chemical transport model - technical description. Atmos. Chem. Phys. 12, 7825-7865.

Stedman, J. R., Kent, A. J., 2008. An analysis of the spatial patterns of human health related surface ozone metrics across the UK in 1995, 2003 and 2005. Atmos. Environ. 42, 1702-1716.

UK Meteorological Office, 2012. Met Office Integrated Data Archive System (MIDAS) Land and Marine Surface Stations Data (1853-current), [Internet]. NCAS British Atmospheric Data Centre, 2014. Available from http://badc.nerc.ac.uk/view/badc.nerc.ac.uk__ATOM__dataent_ukmo-midas.

Vieno, M., Dore, A. J., Stevenson, D. S., Doherty, R., Heal, M. R., Reis, S., Hallsworth, S., Tarrason, L., Wind, P., Fowler, D., Simpson, D., Sutton, M. A., 2010. Modelling surface ozone during the 2003 heat-wave in the UK. Atmos. Chem. Phys. 10, 7963-7978.

WHO, 2006. Air Quality Guidelines. Global update 2005. Particulate matter, ozone, nitrogen dioxide and sulfur dioxide., World Health Organisation Regional Office for Europe, Copenhagen. ISBN 92 890 2192 6. http://www.euro.who.int/__data/assets/pdf_file/0005/78638/E90038.pdf?ua=1.

Wilson, R. C., Fleming, Z. L., Monks, P. S., Clain, G., Henne, S., Konovalov, I. B., Szopa, S., Menut, L., 2012. Have primary emission reduction measures

reduced ozone across Europe? An analysis of European rural background ozone trends 1996-2005. Atmos. Chem. Phys. 12, 437-454.

Chapter 5: The impact of 27 VOCs on the regional ozone increment at Harwell and Auchencorth

This chapter is based on a research paper published in 'Atmospheric Chemistry and Physics Discussions' (Malley, C. S., Braban, C. F., Dumitrean, P., Cape, J.N., and Heal, M.R. (2015). The impact of speciated VOCs on regional ozone increment derived from measurements at the UK EMEP supersites between 1999 and 2012. Atmospheric Chemistry & Physics Discussions, 15, 7267-7308. 10.5194/acpd-15-7267-2015. See Appendix V). I undertook all data analysis, but co-authors Dr Mathew Heal, Dr Christine Braban and Professor Neil Cape made valuable contributions to the methodology, and the presentation of results through discussions and manuscript editing. In addition, Dr Peter Dumitrean collected and processed the measurements on which the analysis is based.

5.1 Introduction

Production of ground-level ozone (O_3) is dependent on concentrations of NO_x (NO and NO_2), methane, carbon monoxide, and volatile organic compounds (VOCs) (Jenkin and Clemitshaw, 2000). The formation of O_3 causes substantial deleterious human health and environmental impacts worldwide (REVIHAAP, 2013; RoTAP, 2012). Development of policies for the mitigation of these impacts requires understanding of the influences on O_3 concentrations from local, regional and hemispheric scale processes. The range in VOC atmospheric lifetimes from a few hours to several days (Atkinson, 2000) means that the major fraction of the VOC impact on O_3 production occurs on the regional scale of air-mass movements. At the regional scale, Gauss et al.

(2014) modelled the reductions in O_3 impacts across Europe on human health (using the SOMO35 metric) and vegetation (using the deciduous forest POD_Y metric) resulting from 15% reductions in NO_x and VOC emissions across the EU and showed that VOC emissions reductions were more effective than NO_x emissions reductions in reducing the O_3 impact metrics across much of north-west Europe. Hence knowledge of the contribution of individual VOCs to O_3 production on the European (regional) scale will enable targeting of the most effective VOC reductions for reducing regionally-derived O_3 exposure relevant to O_3 impacts.

In this chapter, chemical climates (defined in Chapter 2) are derived to quantify the impact of measured VOCs on the regional increment of O_3 concentrations (the difference between regional background and hemispheric background O_3 concentrations) measured at Harwell and Auchencorth. Full definitions of each of these O_3 quantities are given in Section 5.2.1. At Harwell and Auchencorth hourly concentrations of O_3, NO_x and 27 VOCs (summarised in Table 5.1) are measured. Ozone variation at the EMEP supersites has previously been shown to be representative of wider geographical areas, namely rural background air of south-east England and northern UK for the Harwell and Auchencorth UK supersites, respectively (Chapter 3).

The interpretation of VOC measurements at rural sites has previously been undertaken using Positive Matrix Factorisation (PMF) to identify contribution from different source categories (Lanz et al., 2009), trajectory analysis (Sauvage et al., 2009), VOC variability as a measure of source proximity (Jobson et al., 1999), winter/summer VOC ratios to indicate changing emissions sources (Jobson et al., 1999), and the ratio of VOCs with similar reactivity to highlight changes in emission sources (Yates et al., 2010). These studies identified VOC emissions sources based on measured VOC concentrations. However, the ‘state’ of atmospheric composition variation producing a regional O_3 increment above hemispheric background concentrations is more rigorously evaluated by considering the chemical loss of the measured VOCs, since it is the VOC chemical loss in the air mass that drives the production of a regional O_3

increment, not the VOC concentration remaining in the air mass. In urban environments, the chemical loss of VOCs has been calculated through the estimation of initial emission ratios of two VOCs, and calculation of photochemical age through parameters such as 'OH exposure' or 'VOC consumption' (Shao et al., 2009; Yuan et al., 2012). This method is not appropriate for rural studies since it assumes that local sources dominate emissions.

In this analysis, monthly-averaged diurnal variations of individual VOC concentrations relative to ethane were used to assess the photochemical loss of each VOC and its contribution to the regional O_3 increment at Harwell and Auchencorth. Monthly-diurnal averaging was chosen as the annual and daily cycles are key features of O_3 variability associated with the driving processes on its concentrations and on its impact. For example, the monthly and diurnal variation in O_3 is central to determining the extent and spatiotemporal trends in health and vegetation-relevant O_3 metrics (Malley et al., 2015). Ozone variability at hundreds of monitoring sites globally has also been characterised based on monthly-diurnal variation (Tarasova et al., 2007). Monthly-diurnal averaging was therefore also appropriate for setting this work in the wider context, especially given the relative scarcity of hourly VOC measurements. The magnitude of VOC chemical loss at each site was linked to anthropogenic emissions by estimating the integrated VOC emissions along 96-hour air-mass back trajectories. These emissions, from the 11 Selected Nomenclature for Air Pollution (SNAP, EEA (2013)) source sectors, were speciated to compare observed VOC variation with an estimate of individual VOC integrated back-trajectory emissions. Integration of emissions, VOC chemistry and O_3 production has been reported previously for one location in the UK using a photochemical trajectory model with a near-explicit chemical mechanism for a large suite of VOCs (Derwent et al., 2007b; Derwent et al., 2007c). The advantage of the methodology presented here, based on measurement data, is that uncertainties associated with the speciation of VOC emission source categories can be identified. A country-specific disaggregation of emissions into 91 more narrowly defined Nomenclature for Reporting (NFR, EEA (2013)) source sectors was used to determine more precisely the activities contributing to VOC back-

trajectory emissions estimates. This current work presents a clear methodology for achieving a coherent VOC regional-O_3-impact chemical climate. It explores how the application of the chemical climatology framework can be used to assess the effect of limited emission and measurement species on the understanding of the regional contribution to O_3 concentrations.

5.2 Methodology

The methodology is separated into the three elements of a chemical climate, the impact (here, the regional O_3 increment), state (VOC diurnal photochemical depletion) and drivers (meteorology and emissions) as defined in Chapter 2 and Malley et al. (2014). The Methods and Results sections are subdivided into impact (Section 5.2.1 and 5.3.1 for Methods and Results respectively), state (Section 5.2.2 and 5.3.2) and drivers (Section 5.2.3 and 5.3.3) to emphasise the analyses used to derive the components of the chemical climate. Analyses were undertaken for the periods 1999-2001 and 2010-2012 at Harwell and 2010-2012 at Auchencorth. Measured data were obtained from UK-AIR (http://uk-air.defra.gov.uk/) and EMEP (http://ebas.nilu.no/). For each year, the monthly-averaged diurnal cycles of each atmospheric component were calculated, i.e. 24×12 = 288 values per year.

Table 5.1: Summary data for the measured VOCs at Auchencorth and Harwell (note that m-xylene and p-xylene are reported as a single measurement). The rate coefficients at 298 K for reactions of each VOC with OH are taken from Atkinson and Arey (2003), and the POCPs are from Derwent et al. (2007a). The 'main source' column gives the SNAP sector with the largest contribution of that VOC to UK annual anthropogenic emissions in 2011 with the exception of isoprene which is mainly of biogenic origin (defined in Section 5.2.3). The listed SNAP sectors are SNAP 2: Non-industrial combustion plants, SNAP 4: Production processes, SNAP 5: Extraction and distribution of fossil fuels, SNAP 6: Solvent use, SNAP 7: Road transport and SNAP 8: Non-road transport.

VOC	Class	Chemical Formula	Main source	OH reaction rate constant (10^{12} x k (298 K) (cm^3 $molecule^{-1}$ s^{-1}))	POCP
ethane	alkane	C_2H_6	SNAP 5 (65%)	0.248	8
propane	alkane	C_3H_8	SNAP 5 (36%)	1.09	14
n-butane	alkane	C_4H_{10}	SNAP 6 (44%)	2.36	31
isobutane	alkane	C_4H_{10}	SNAP 5 (61%)	2.12	28
n-pentane	alkane	C_5H_{12}	SNAP 5 (42%)	3.80	40
isopentane	alkane	C_5H_{12}	SNAP 5 (41%)	3.60	34
n-hexane	alkane	C_6H_{14}	SNAP 6 (42%)	5.20	40
2-methylpentane	alkane	C_6H_{14}	SNAP 6 (43%)	5.20	41
n-heptane	alkane	C_7H_{16}	SNAP 5 (43%)	6.76	35
n-octane	alkane	C_8H_{18}	SNAP 5 (64%)	8.11	34
isooctane	alkane	C_8H_{18}	SNAP 4 (100%)	3.34	25
ethene	alkene	C_2H_4	SNAP 8 (27%)	8.52	100
propene	alkene	C_3H_6	SNAP 4 (36%)	26.3	117
1-butene	alkene	C_4H_8	SNAP 7 (26%)	31.4	104
cis-2-butene	alkene	C_4H_8	SNAP 5 (87%)	56.4	113
trans-2-butene	alkene	C_4H_8	SNAP 5 (90%)	64.0	116
1,3-butadiene	alkene	C_4H_6	SNAP 8 (57%)	66.6	89
isoprene	alkene	C_5H_8	biogenic	100	114
ethyne	alkyne	C_2H_2	SNAP 7 (46%)	0.78	7
benzene	aromatic	C_6H_6	SNAP 2 (35%)	1.22	10
toluene	aromatic	C_7H_8	SNAP 6 (63%)	5.63	44
ethylbenzene	aromatic	C_8H_{10}	SNAP 6 (54%)	7.0	46
o-xylene	aromatic	C_8H_{10}	SNAP 6 (50%)	13.6	78
m-xylene	aromatic	C_8H_{10}	SNAP 6 (71%)	23.1	86
p-xylene	aromatic	C_8H_{10}	SNAP 6 (50%)	14.3	72
1,2,3-trimethylbenzene	aromatic	C_9H_{12}	SNAP 6 (79%)	32.7	105
1,2,4-trimethylbenzene	aromatic	C_9H_{12}	SNAP 6 (74%)	32.5	110
1,3,5-trimethylbenzene	aromatic	C_9H_{12}	SNAP 6 (71%)	56.7	107

5.2.1 Regional O_3 increment impact

The regional O_3 increment is defined as the regional background O_3 concentrations minus the hemispheric background O_3 concentration. Here, regional background O_3 concentration is defined as that which is imported into a local spatial domain following modification of hemispheric background O_3 concentrations by European emissions. Examples of local spatial domains are south-east England and northern UK for which, based on monthly-diurnal O_3 variation, Harwell and Auchencorth respectively were shown previously to be representative (Malley et al., 2014b). The hemispheric background O_3 concentration is in turn defined as that which is imported into the European domain, with minimal influence from European emissions.

Hemispheric background O_3 concentrations were derived by applying Ward's method hierarchical cluster analysis to pre-calculated 96-h air-mass back trajectories arriving at 3-h intervals at Mace Head, Ireland (Carslaw and Ropkins, 2012; Draxler and Rolph, 2013; R Core Development Team, 2008), to identify periods with no European influence. Mace Head is on the west coast of Ireland and frequently experiences conditions (air masses arriving from the Atlantic) during which atmospheric composition has minimal influence from European emissions. The discrimination achieved by cluster analysis may be influenced by user choices but the method used here was shown to be the most accurate of commonly used clustering techniques (Mangiameli et al., 1996). In addition, the use of cluster analysis avoids the subjective choice of a boundary to segment non-European influenced air masses. In Ward's method, each object (back trajectory) initially constitutes its own cluster. The algorithm then calculates which two clusters, when merged, gives the smallest increase in total within-cluster variance. The process is repeated until all trajectories are located in one cluster (Kaufman and Rousseeuw, 1990). The dendrogram summarising the cluster merging process is then 'cut' at an appropriate level to produce the cluster set. The aim is to maximise explained inter-trajectory variability using a small number of clusters to highlight major distinctions between trajectory paths. The distance between a trajectory and its cluster mean was quantified using the two-dimensional 'angle' of

each trajectory (or cluster mean trajectory) from the origin (i.e. the supersite) at common time points along the trajectory:

$$d_{1,2} = \frac{1}{n}\sum_{i=1}^{n} cos^{-1}\left(0.5\frac{A_i+B_i+C_i}{\sqrt{A_iB_i}}\right) \quad (5.1)$$

where

$$A_i = (X_1(i) - X_0)^2 + (Y_1(i) - Y_0)^2$$
$$B_i = (X_2(i) - X_0)^2 + (Y_2(i) - Y_0)^2$$
$$C_i = (X_2(i) - X_1(i))^2 + (Y_2(i) - Y_1(i))^2$$

$d_{1,2}$ is the distance between trajectory 1 and trajectory 2, X_0,Y_0 are the latitude and longitude coordinates of the origin of the trajectory, and $X_1(i)$,$Y_1(i)$, and $X_2(i)$,$Y_2(i)$ are the coordinates at time *i* of trajectories 1 and 2 respectively. The 2920 back trajectories arriving at Mace Head each year were separated into four clusters. The monthly-diurnal cycles of O_3 concentrations for the westerly trajectory cluster were used as the estimate of hemispheric background O_3. These values showed excellent agreement with the monthly average hemispheric background estimates derived by Derwent et al. (2007a) using Mace Head O_3 data and a combination of pollutant tracers and atmospheric modelling to select 'clean' air masses ($r = 0.93$, $p < 0.001$, Figure 5.1).

Regional background O_3 concentrations were estimated using the method of Clapp and Jenkin (2001). In the region of south-east England characterised by the Harwell supersite nine locations, ranging from rural background to kerbside, had hourly measurements of O_3, NO and NO_2. Clapp and Jenkin (2001) used the linear fit to a plot of total oxidant (O_3 + NO_2) vs NO_x (NO + NO_2) to investigate the relationship between O_3, NO_2 and NO in South East England. As NO_x concentration increased, the total oxidant also increased, as NO_2 is a constituent of both NO_x and oxidant. However, at low NO_x concentrations, the *y*-intercept of the linear fit was positive, indicating a NO_x-independent contribution to oxidant. This yields the regional background O_3 concentration, i.e. in this case the contribution to O_3 within south-east England from

processes occurring outside south-east England. Application of this method assumes that the NO_x is locally emitted, which is likely to be the case for the majority of NO_x in south-east England due to substantial local emission sources such as the megacity of London. An advantage of the application of the oxidant vs NO_x plot for estimation of regional background concentrations in this study is that Clapp and Jenkin (2001) showed this method to be appropriately applied within the spatial domain of Harwell. Extraction of the *y*-intercept from an oxidant vs NO_x plot based on the data from the sites in south-east England for each of the 288 'month-hour' averages yielded the monthly-diurnal cycle of regional background O_3 variation in south-east England. The difference between the hemispheric background and regional background O_3 concentrations provided the magnitude and direction of the regional modification to hemispheric background O_3 concentration. A positive regional O_3 increment indicates additional O_3 formation regionally in excess of hemispheric background concentrations, and vice versa.

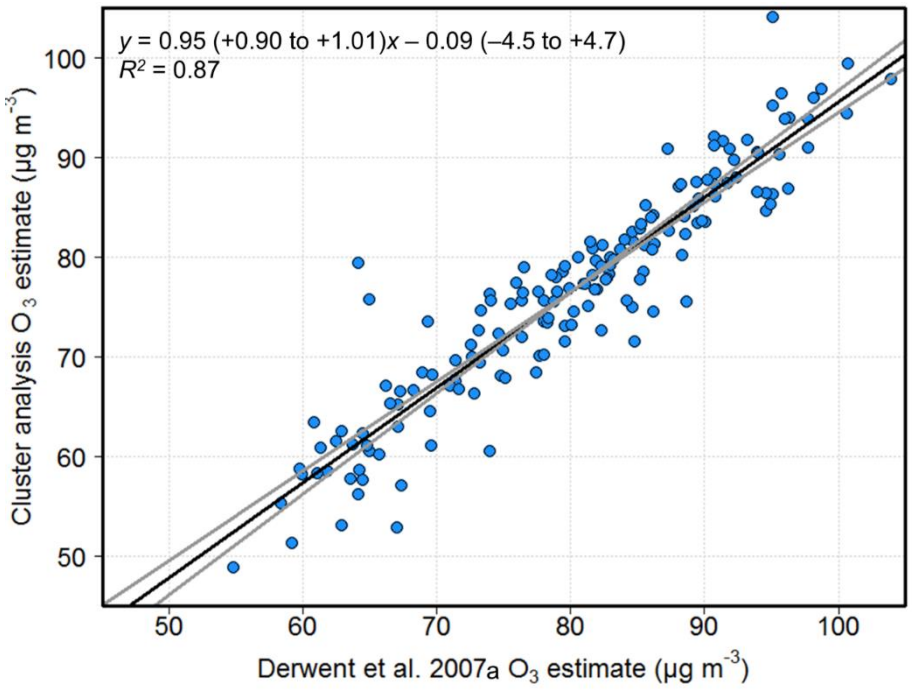

Figure 5.1: Correlation between monthly hemispheric background O_3 concentrations derived by Derwent at al. (2007a) using pollutant tracers and atmospheric modelling to select 'clean' air masses, and derived by the method described in Section 5.2.1 using cluster analysis. Black regression line is calculated by the ordinary least squares (OLS) method, with confidence intervals (95th percent) shown in grey.

Regional background O_3 concentrations were estimated using the method of Clapp and Jenkin (2001). In the region of south-east England, characterised by the Harwell supersite, nine locations, ranging from rural background to kerbside, had hourly measurements of O_3, NO and NO_2. The *y*-intercept of the linear fit to a total oxidant ($O_3 + NO_2$) vs NO_x ($NO + NO_2$) plot yields the NO_x-independent oxidant contribution, interpreted as the regional background O_3 concentration, i.e. the contribution to O_3 within south-east England from processes occurring outside south-east England. Extraction of the *y*-intercept from an oxidant vs NO_x plot for each of the 288 'month-hour' averages yielded the monthly-diurnal cycle of regional background O_3 variation in south-east England. The difference between the hemispheric background and regional background O_3 concentrations provided the magnitude and direction of the regional modification to hemispheric background O_3 concentration. A positive regional O_3 increment indicates additional O_3 formation regionally in excess of hemispheric background concentrations, and vice versa.

The spatial domain for which Auchencorth is representative does not have sufficient co-located NO_x and O_3 monitoring sites to derive regional background O_3 concentrations by the above method. The regional O_3 increment at Auchencorth was therefore estimated by subtracting the Mace Head hemispheric background estimates directly from the Auchencorth monthly-averaged diurnal concentrations. In Chapter 3, Auchencorth was shown to be representative of a large, transboundary spatial domain, and therefore it was assumed that local O_3 depletion due to NO_x was low, and that estimation of regional background O_3 concentrations using this method did not introduce significant underestimation of regional background O_3 concentrations when averaged over the monthly-diurnal periods.

5.2.2 State

VOC concentrations were determined by automated gas chromatography (Dernie and Dumitrean, 2013). For 2010-2012, data were available for 27 species at both Harwell

and Auchencorth. Concentrations of 6 VOCs at Auchencorth during this period were not above the reported limit of detection (LOD) so their contribution to the regional O3 increment was not evaluated. For 1999-2001, data were available for 21 VOCs at Harwell only.

The VOC datasets had extensive periods during which concentrations were below LOD, particularly at Auchencorth (e.g. between 6% and 81% below LOD at Harwell in 2011, and between 11% and 82% at Auchencorth). Therefore maximum likelihood estimation (MLE) was used to fit three positively-skewed distributions (lognormal, gamma and Weibull) to the dataset for each VOC (Gardner, 2012; Helsel, 2006). MLE adjusts the parameters of a given distribution such that the probability of obtaining the dataset from that distribution is maximised. The Akaike Information Criterion (AIC) was then used to select the distribution which best fitted the data; this provides a relative estimate of the information lost when a given distribution is used to represent a dataset (Akaike, 1974). This process was performed on data for each month of the year, and separately for the 288 monthly-diurnal time periods. The fitted distributions estimated the probability that a 'non-detect' (below the LOD) was a concentration in the range 0 $\mu g\ m^{-3}$ to the LOD.

When non-detects occurred for all VOCs in a particular hour, these were excluded from the MLE analysis on the assumption that this was due to instrument failure. To avoid the unnecessary omission of valid concentration measurements, all other data were used, and consequently all remaining non-detects were assumed to be values below LOD. A number of non-detects due to the selective failure of the instrument to measure a particular VOC may be falsely considered to be below the LOD. However, the following evidence indicates that any bias introduced is likely to be small. Annual medians were calculated twice using MLE for Harwell in 2011, first, with the non-detects unique to each VOC, secondly with their omission (i.e. assuming all these non-detects were due to reasons other than LOD). The increase when omitted was below 10% for 11 of the 27 VOCs, including the VOCs with concentrations consistently well above the LOD. For example, the 5^{th} percentile concentrations (of all valid

concentrations) of propane, ethane and toluene were 1200%, 800% and 175% above the LOD, and consequently the number of unique non-detects was relatively low (4%, 2% and 1% of values respectively). The increase when the unique non-detects were omitted was 10%, 8% and 3% for propane, ethane and toluene respectively. Other VOCs had a 5^{th} percentile concentration much closer to the LOD, increasing the likelihood of periods during which concentrations were below LOD. For nine of the 10 VOCs with the largest annual median increase, the 5^{th} percentile concentration was the LOD.

In summary, for those VOCs with few unique non-detects, the potential inclusion of non-LOD-related non-detects resulted in a small change in calculated concentration, while VOCs with a larger proportion of non-detects had concentrations more frequently close to the LOD, increasing the likelihood that the unique non-detects resulted from concentrations below the LOD. This indicates that the decision to assign all unique non-detects as values below the LOD was justified, as the potential bias introduced was small, and therefore that the maximum of valid VOC concentration data was preserved and used in the MLE distribution calculations. Intra-annual and monthly-diurnal variation in VOC concentrations were summarised using the monthly median concentrations and the 24 hourly median concentrations for each month from the best-fit distributions respectively.

For each VOC, each of the 288 median monthly-diurnal concentrations was multiplied by the corresponding model-derived Photochemical Ozone Creation Potential (POCP) (Derwent et al., 2007c), to weight the observed diurnal variation of VOCs according to their different propensities for O_3 formation. In Derwent et al. (2007c), a VOC POCP was defined as the ratio (multiplied by 100) of the increase in O_3 due to increased emissions of the VOC simulated in a Lagrangian model along a trajectory traversing from central Europe to the UK, relative to the modelled increase in O_3 from the same mass increase in emissions of ethene (the reference POCP VOC assigned a value of 100). Multiple studies have calculated reactivity scales of O_3 production potential (OPP) for a range of VOCs using incremental reactivity methods (Derwent

et al., 2007c; Hakami et al., 2004; Luecken and Mebust, 2008; Martien et al., 2003), multi-parent assignment (Bowman, 2005) and 'tagging' of VOC degradation sequences (Butler et al., 2011). These varying methods were shown to be generally well correlated (Butler et al., 2011; Derwent et al., 2010; Luecken and Mebust, 2008). The Derwent et al. (2007c) POCPs are appropriate to use in this study as they were calculated under simulated north-western European conditions. Previous comparison with other VOC reactivity scales indicated uncertainty in POCP values up to ± 5 POCP units which equates to an average of ± 15% for the measured VOCs in this study (Derwent et al., 2007b).

The diurnal variation of individual VOCs due to photochemical depletion was summarised by calculating the ratio of each POCP-weighted VOC concentration to the POCP-weighted ethane concentration. Ethane has the second smallest POCP of the measured VOCs, 87 % smaller than the average, and 20 % smaller than the next smallest POCP (benzene), so using this ratio removed the effect on diurnal VOC concentration of changes in boundary layer mixing depth. The diurnal cycle of VOC concentrations is determined in part by the expansion of the boundary layer mixing depth at sunrise due to increased surface temperatures, and its collapse at night which decreases the mixing depth. Removing this variability using VOC ratios meant that remaining VOC diurnal variability is isolated from boundary layer mixing depth variation. When the remaining VOC diurnal variability showed a reduction in VOC concentration (relative to ethane) during the afternoon, this was assumed to be due to photochemical depletion (see Section 5.3.2 for further discussion). The VOC with smallest POCP, ethyne, had low data capture at Harwell between 1999 and 2001 (maximum 57% in 2001). Additionally, ethane has a smaller rate coefficient for reaction with OH compared with ethyne (Table 1), and the POCPs were similar (7 for ethyne vs 8 for ethane). Ratios of VOC/ethane have been used previously to estimate the photochemical loss of VOCs (Helmig et al., 2008; Honrath et al., 2008; Yates et al., 2010).

It is also assumed that the diurnal variation of VOC at the site is not driven by differences in the magnitude of VOC emissions along the trajectories contributing VOC to that site during the day and at night. This can be verified by the similar monthly median VOC emissions emitted along the path of 96-h trajectories (outlined in Sect. 2.3) arriving at night (3 a.m.) and afternoon (3 p.m.). For example, at Harwell in 2011, night trajectory VOC emissions were no more than ±12 % different from afternoon. Hence a daytime decrease in POCP-weighted VOC/ethane ratio indicates greater photochemical depletion of the VOC relative to ethane. The magnitude of diurnal photochemical variability for each VOC was derived from the difference between the average POCP-weighted VOC/ethane ratio at night (1 am – 5 am) and in the afternoon (1 pm – 5 pm). A positive value indicates daytime photochemical depletion of the VOC relative to ethane. The sum of positive daytime photochemical depletion of individual VOCs produces the total VOC diurnal photochemical depletion for each month. The monthly pattern of total VOC diurnal photochemical depletion was compared with the monthly pattern of the regional O_3 increment. During those months with a positive regional O_3 increment, the relative contribution of each VOC to total VOC photochemical depletion was used as an estimate of the relative contribution of each VOC to the VOC chemical loss which contributed to the production of the positive regional O_3 increment.

At Auchencorth, the analysis of VOC diurnal photochemical depletion was not possible in 2010 and 2011 due to low data capture, which compromises the ability of MLE to accurately estimate median VOC concentrations. This is particularly important for ethane, as a large error in the fitted distribution for ethane propagates to all VOC/ethane ratios. In 2011, the average proportion of non-detects for the measured VOCs was 56% when the 6 VOCs with no measurements above LOD were excluded (34% for ethane). In 2012 this decreased to 34% (10% for ethane), and VOC diurnal photochemical depletion was calculated. For comparison, at Harwell, there were on average 26% non-detects for each VOC species in 2011 (7% for ethane).

5.2.3 Drivers

The two main drivers producing the 'state' of this chemical climate, i.e. VOC diurnal photochemical depletion, which are considered here are meteorology and anthropogenic VOC emissions. Other drivers such as biogenic VOC emissions, and NO_x concentrations are drivers of the regional O_3 increment. Meteorology and anthropogenic VOC emissions are the focus due to the benefits previously outlined in improvement in health and vegetation-relevant O_3 impacts that result from anthropogenic VOC emission reductions. The meteorology was characterised by monthly mean, maximum and minimum temperature, and number of hours of sunshine for Harwell and Auchencorth obtained from the UK Met Office climate summaries for 'South East and Central South England' and 'East Scotland', respectively (http://www.metoffice.gov.uk/climate/uk/datasets/#) (Perry and Hollis, 2005).

To investigate geographical emissions sources, the locations of each of the 96 hourly time points of the 2920 HYSPLIT 96-h back trajectories arriving at 3 h intervals per year were mapped to the 0.5° × 0.5° gridded VOC emissions reported by EMEP and used in the EMEP model (Mareckova et al., 2013; Simpson et al., 2012). This grid encompasses the region 30.25°N − 75.25°N and 29.75°W – 60.25°E, and the emissions in each grid square are disaggregated into 11 SNAP source sectors (http://ceip.at/ms/ceip_home1/ceip_home/webdab_emepdatabase/emissions_emepmodels/).When the location of the trajectory during a particular hour fell within the gridded domain, the annual emissions and country of the grid square over which the trajectory was located were assigned to that time point. Emissions were assigned to the country which had the greatest emissions when the grid square straddled an international border. Annual emissions were modified by prescriptive month, day-of-week and hour-of-day time factors (Simpson et al., 2012) to obtain an estimate of the hourly emissions from each SNAP sector during the hour in which the trajectory passed over the grid cell. The monthly average hourly SNAP emission estimates at each of the 96 1 h time points were summed to give the average European VOC emissions estimate of all the trajectories arriving in that month (henceforth the VOC

trajectory emissions estimate (TEE)), and the proportions derived from individual countries.

The total VOC TEE from the 11 SNAP sectors were speciated using the 114 VOC speciated profiles from Passant (2002) to quantify the proportion of emissions emitted as one of the 27 measured VOCs. The profiles were first applied to UK annual emissions to obtain speciated profiles for each SNAP sector which could be applied to the VOC TEEs. Each year, at the most disaggregated level, the UK National Atmospheric Emissions Inventory (NAEI) reports total VOC emissions for 337 source activities (http://naei.defra.gov.uk/data/) (Passant et al., 2013). In Passant (2002), each of these activities is assigned one of the 114 speciation profiles which in total consider the contribution from 630 VOCs, including aggregated groups of VOCs, for example, 'C7 alkanes'. For example, the speciation profile for total VOC emissions from the NAEI source 'catalyst cars (exhaust) – urban driving', specifies the proportion of emissions emitted as 62 VOCs, with toluene (11.0%), ethene (7.3%) and 2-methylbutane (6.8%) the largest proportion. The total annual UK emissions for each activity were apportioned between the VOCs in the assigned profile. This resulted in a matrix of 337 columns of source activities, and 630 rows of VOCs. Activities were then grouped into the 55 NFR codes used by NAEI, and then into SNAP sectors 1-9 based on the NFR-SNAP conversion recommended by the EMEP Centre for Emission Inventories and Projections (CEIP, http://www.ceip.at/fileadmin/inhalte/emep/pdf/nfr09_to_snap-.pdf). There were no reported VOC emissions from activities falling under SNAP 10 (agriculture) and SNAP 11 (other). The relative contribution of each VOC to total annual UK SNAP emissions was calculated to provide speciated emissions profiles which were used to speciate the monthly SNAP sector VOC TEEs. For example, in 2011, the proportion of UK SNAP 7 (road transport) emissions emitted as toluene was 7.6%, and hence 7.6% of the SNAP 7 total VOC TEE were apportioned to toluene for each month. This produced an estimate of the contribution to total monthly VOC TEE from 630 VOCs (Figure 5.2). This contribution was then multiplied by the VOC's POCP to weight it according to O_3 formation potential.

The EU emissions inventory disaggregates annual emissions from SNAP sectors 1-9 into 91 NFR codes for each EU member state (EEA, 2014). For example, 7 more narrowly defined NFR codes contribute to SNAP 7 (road transport). In each Member State, the proportion of SNAP 7 emissions emitted from each NFR code is different. For example in the UK 62% of SNAP 7 emissions in 2011 were from NFR code 1A3bi (Passenger cars), compared to 34% for France. The monthly change in the SNAP sector VOC TEE was attributed to changes in the contribution from the more narrowly defined NFR codes, based on the country-specific contributions of each NFR sector to annual SNAP sector emissions. The VOC TEE from each of the 91 NFR codes for each country were summed across all countries to obtain the contribution of each NFR code to the total VOC TEE for each month (Figure 5.3).

The emission inventories used in this study have several sources of uncertainty (EEA, 2013; Koohkan et al., 2013). The 0.5° × 0.5° grid squares mean that numerous distinct sources, each with uncertainties in emission factors and activity rates, are aggregated together to produce the estimate of emissions from a particular SNAP or NFR source sector. The size of the grid square also does not necessarily reflect the size of the area from which emissions influence the atmospheric composition of the trajectory air mass as it passes over. The VOC TEE is therefore used as a relative comparison spatially and temporally, rather than a definitive quantification of the VOC emissions emitted into an air mass. In addition, there are uncertainties in the speciation of total VOC emissions to individual components (Borbon et al., 2013). However, the emissions inventories used here are the best estimate of the spatial distribution of anthropogenic VOC emissions across Europe. While studies have shown discrepancies between the EMEP emission inventory and other estimates of European emissions (Koohkan et al., 2013), EMEP gridded emissions have also been shown previously to capture variation in VOC measurement data (Derwent et al., 2014; Sauvage et al., 2009)

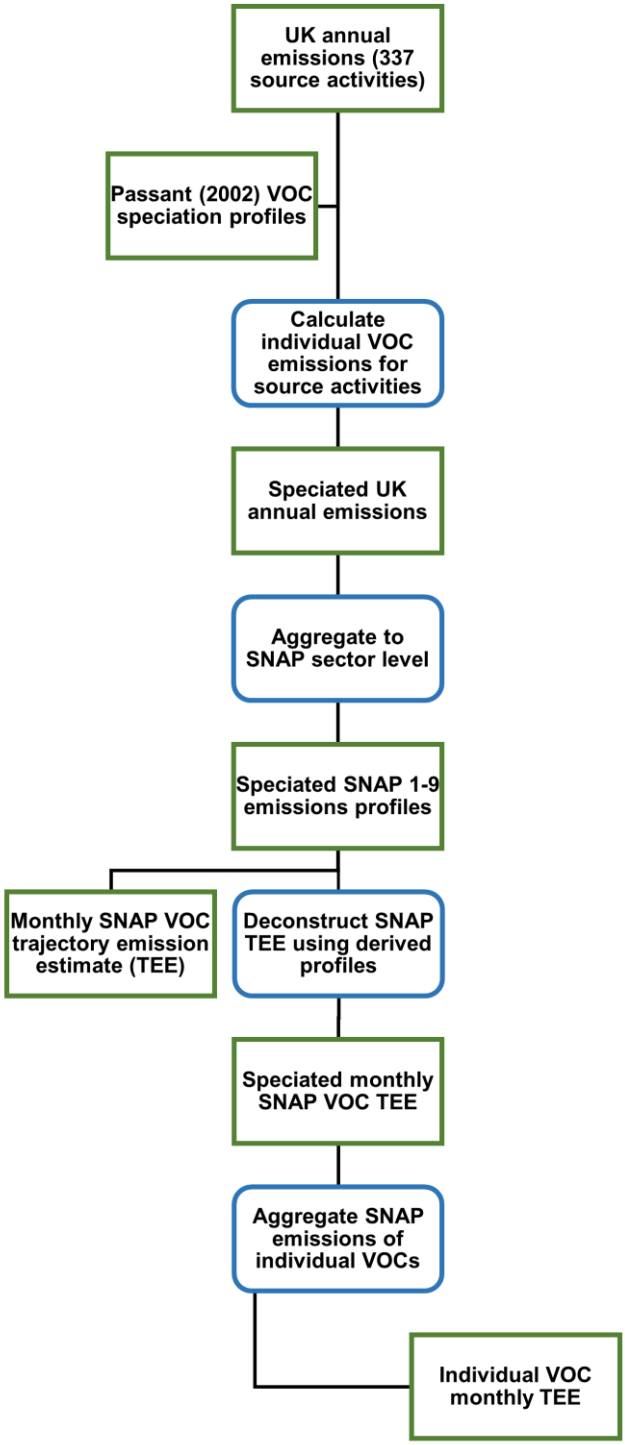

Figure 5.2: Flowchart demonstrating the process used to calculate the contribution of 630 individual VOCs to the monthly total VOC trajectory emissions estimate (TEE, defined in Section 5.2.3). The green rectangles represent products or datasets, and the blue rounded rectangles represent processes applied to transform a dataset. Further explanation is provided in Section 5.2.3.

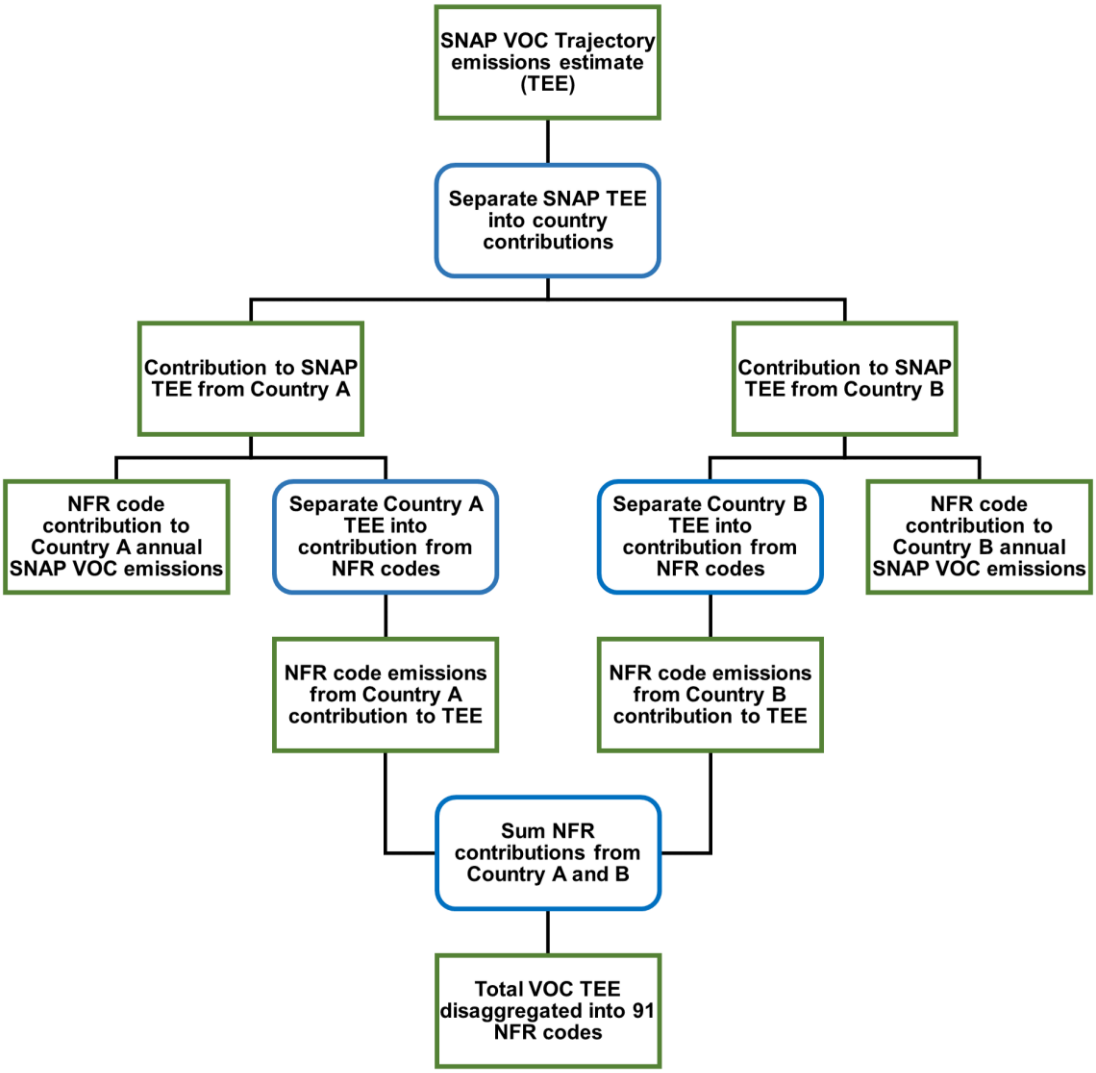

Figure 5.3: Flowchart representing the process used to derive the contribution from NFR codes to monthly trajectory emissions estimates (TEE, defined in Section 5.2.3). The green rectangles represent products or datasets, and the blue rounded rectangles represent processes applied to transform a dataset. Note that the separation of the TEE into contributions from two countries is illustrative, and in most cases a greater number of countries contributed to the TEE in a given month. Further explanation is provided in Section 5.2.3.

5.3 Results and Discussion

5.3.1 Impact: regional O_3 production/destruction assessment

The difference between hemispheric background O_3 concentrations and regional background O_3 concentrations relevant for Harwell for 2001 (representative of 1999-2001), 2011 (representative of 2010-2012) and for Auchencorth in 2012 is shown in Figure 4. Although there was inter-annual variability within each time period, the data for these years illustrate the main differences between three different phases of the regional O_3 increment chemical climate both temporally at Harwell (1999-2001 vs 2010-2012) and spatially (Harwell vs Auchencorth). At Harwell in 2001, a positive regional O_3 increment occurred in each month between May and September (Figure 5.4a). The annual maximum regional O_3 increment (i.e. the difference between hemispheric background and regional background O_3 concentrations) occurred in the afternoon in July 2001 (42 µg m^{-3}), while monthly regional O_3 increments peaked in excess of 20 µg m^{-3} in June and August, and in excess of 10 µg m^{-3} in May and September. A similar pattern occurred in 2000, but with a lower annual maximum (26 µg m^{-3} in July). In 1999, regional ozone production was greater, extending from April to September with the annual maximum in July (53 µg m^{-3}), and production in excess of 30 µg m^{-3} in June and August. In 2011 at Harwell positive regional O_3 increments occurred between April and September (Figure 5.4b), but their magnitudes were reduced compared with the 1999-2001 phase. Only two months, April and July, had maximum regional O_3 increments >10 µg m^{-3} (11 µg m^{-3} and 32 µg m^{-3}, respectively). In 2012, the monthly regional O_3 increment exceeded 10 µg m^{-3} in May (12 µg m^{-3}), July (28 µg m^{-3}) and August (11 µg m^{-3}), and occurred more modestly in April, June and September. In 2010, the regional O_3 increment in June was 24 µg m^{-3}, which then decreased in July (19 µg m^{-3}). Reductions in regional O_3 have been reported in the UK previously, using high percentile O_3 concentrations as an indicator of regionally-derived episodes, rather than calculation of the average monthly-diurnal regional O_3 increment. For example, Munir et al. (2013) attributed negative trends in highest O_3

concentrations calculated at 22 UK monitoring sites (13 sites with significant trends) to regional reduction in O_3 precursor emissions between 1993 and 2011.

The regional O_3 increments at Auchencorth were substantially lower than at Harwell. Between 2010 and 2012, the maximum regional O_3 increment observed was 14 µg m^{-3} in July 2011. In 2012 (Figure 5.4c), the maximum regional O_3 increment was 4 µg m^{-3}. The spatial differences in the extent of regional contribution to O_3 variation at Harwell and Auchencorth are consistent with a previous study of rural UK O_3 spatial variability (Jenkin, 2008).

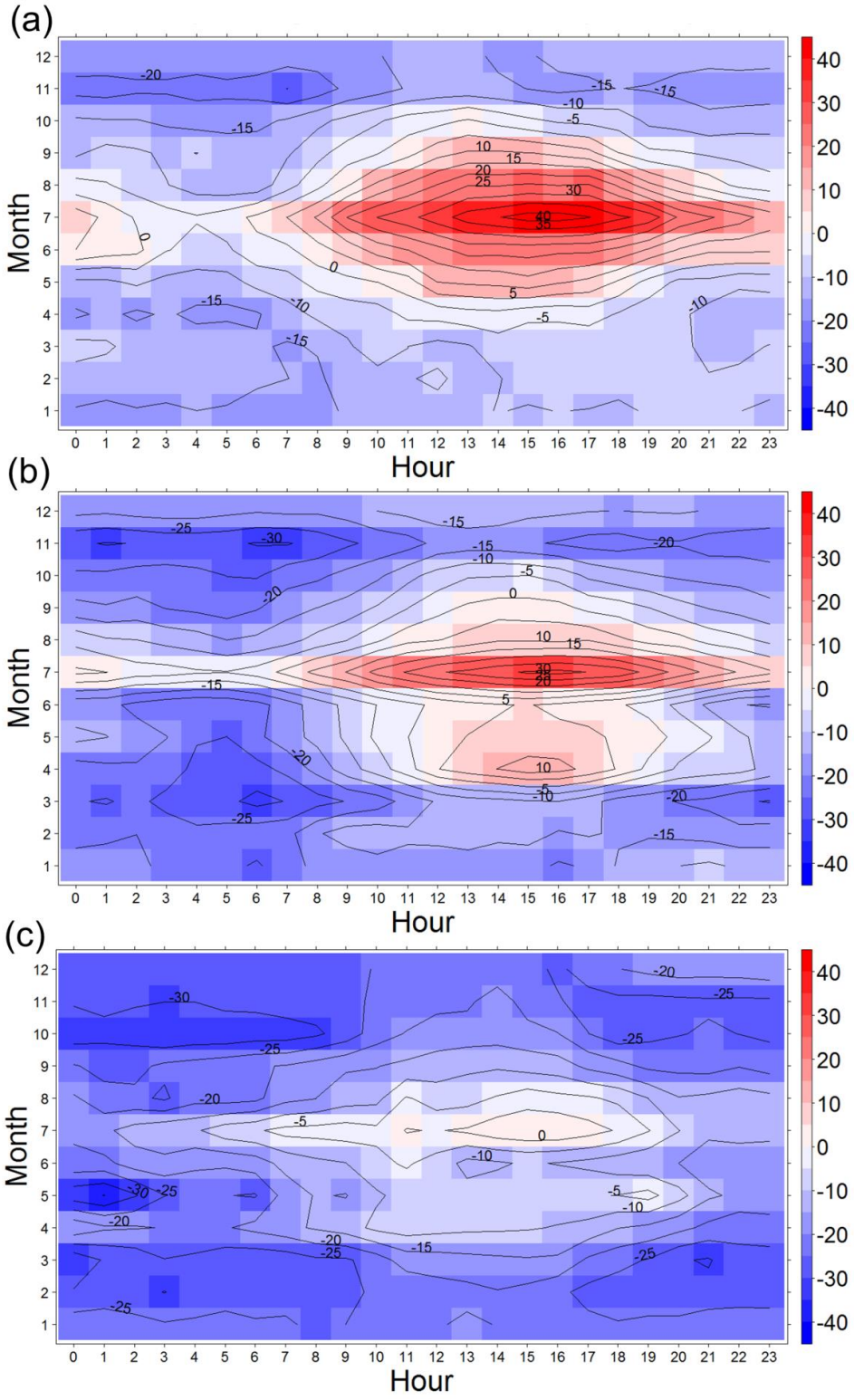

Figure 5.4: Monthly-hourly average differences between hemispheric background O_3 and regional background O_3 concentrations (µg m^{-3}) for (a) 2001 and (b) 2011 in south-east England, the area for which Harwell is representative, and (c) the difference between hemispheric and measured O_3 concentrations for 2012 at Auchencorth.

5.3.2 State: VOC concentration and chemical depletion

The monthly median concentrations of the 27 VOCs measured at Harwell and Auchencorth have a pronounced seasonal cycle with highest total summed VOC concentrations in winter at each site, albeit with concentrations at Auchencorth substantially lower than at Harwell (Figure 5.5 shows an example year for each of the three periods). Monthly variation was lower at Auchencorth: the difference between minimum and maximum monthly total median VOC concentrations at Auchencorth in 2012 was 6.2 µg m^{-3}, compared with 9.5 µg m^{-3} and 13.1 µg m^{-3} at Harwell in 2011 and 2001 respectively. Monthly median total VOC concentrations at Harwell in 1999-2001 and 2010-2012 were similar in winter months (Jan, Feb, Dec), and generally ranged between 6 µg m^{-3} and 18 µg m^{-3}. In summer (Jun, Jul, Aug) between 1999 and 2001, total VOC concentrations were between 5 and 13 µg m^{-3}, but between 2010 and 2012, concentrations were lower, between 3 and 6 µg m^{-3}. Only in June 2010 were total VOC concentrations higher than the lowest total VOC concentration in the summer months in 1999-2001. In addition, in 2001, six VOCs were not measured, and these constituted between 2.1% and 7.4% of monthly total measured VOC concentrations in 2011. The non-measurement of these VOCs does not alter the conclusions relating to the differences in total VOC concentrations observed between 1999-2001 and 2010-2012.

The relative composition of total measured VOCs showed differences between 2001 and 2011 at Harwell. Ethane, propane and n-butane had the largest measured concentrations. Ethane contributed on average 22 ± 4% of total monthly measured VOC concentrations in 2001, compared with 33 ± 6% in 2011 (annual average monthly measured ethane concentration had a small increase from 2.0 ± 0.8 µg m^{-3} in 2001 to 2.3 ± 1 µg m^{-3} in 2011), while the relative contribution from propane did not vary (15% in each year, average monthly concentrations in 2001 and 2011 were 1.5 ± 0.9 and 1.2 ± 0.8 µg m^{-3} respectively) and that from n-butane decreased from 11 ± 2% to 8 ± 1% (1.1 ± 0.6 µg m^{-3} in 2001 and 0.6 ± 0.4 µg m^{-3} in 2011). Although these differences are not large, they may result from differences in the reduction of VOC

emission sources between 1999-2001 and 2010-2012. The aim of this work, however, was not the determination of long-term trends in absolute VOC concentrations, and the reader is referred to Dollard et al. (2007), von Schneidemesser et al. (2010) and Derwent et al. (2014) which have undertaken analyses of trends in VOC concentrations at multiple UK sites, including Harwell and Auchencorth.

The extent of diurnal photochemical loss of VOCs over the year is shown in Figure 5.6. At Harwell, periods of increased VOC diurnal photochemical depletion mirror the monthly magnitude of regional O_3 increments (Figure 5.4 *c.f.* Figure 5.6). In 2001 at Harwell, both the regional O_3 increment and VOC diurnal photochemical depletion increased from June to July, before declining in August. In 2011, there was a local maximum in the regional O_3 increment in April, followed by the annual maximum in July, mirrored by VOC diurnal photochemical depletion. During 2012 the regional O_3 increment was minimal at Auchencorth, and the magnitude of VOC diurnal photochemical depletion was low, with a small peak in August.

The association between the monthly variation in the regional O_3 increment and total VOC diurnal photochemical depletion at Harwell indicates that the variation in VOC chemical loss contributing to the regional O_3 increment is represented by the VOC diurnal photochemical depletion. The relative contribution of each measured VOC to total VOC diurnal photochemical depletion during months of enhanced regional O_3 increment therefore indicates where emissions reductions should be targeted to most effectively reduce VOC chemical loss and hence to reduce the magnitude of the regional O_3 increment. The contributions of each measured VOC to total VOC diurnal photochemical depletion during the month of maximum regional O_3 increment in 2010, 2011 and 2012 at Harwell are shown in Figure 5.7. A positive value indicates lower POCP-weighted VOC/ethane during the afternoon compared to night (i.e. photochemical depletion). A higher POCP-weighted VOC/ethane ratio during the afternoon results in the negative value. Ethene had the largest contribution during these months (34%, 29% and 45% of total measured VOC diurnal reactivity in 2010, 2011 and 2012 respectively). The sum of m+p-xylene also made a major positive

contribution during 2010 (15%) and 2011 (13%). The majority of the remaining measured VOCs made smaller, positive contributions. In July 2011, 71 % of the remaining VOCs (i.e. all VOCs excluding ethene and m+p-xylene) contributed on average 3.4% ± 2.5 % to total positive VOC diurnal variation. In July 2012, the maximum regional O_3 increment was 12% lower than July 2011, and only 58% of remaining VOCs made positive contributions. In June 2010, the maximum regional O_3 increment was 25% lower than July 2011, and 54% of the remaining VOCs contributed. VOCs with larger VOC/ethane ratios in the afternoon included isoprene, which is predominantly of biogenic origin (von Schneidemesser et al., 2011). Laurent and Hauschild (2014) modelled the impact on O_3 formation of speciated VOC emissions from 31 countries, and also reported m-xylene and ethene to have the largest impact of 270 VOCs on regional O_3 formation.

Figure 5.8 is the analogous plot to Figure 5.7 for 1999-2001 at Harwell. In 1999-2001, m+p-xylene had the largest diurnal photochemical depletion, followed by ethene. However, there were much larger negative VOC/ethane diurnal variations for some anthropogenic VOCs compared to 2010–2012 (Fig. 6), i.e. afternoon POCP-weighted VOC/ethane ratios were substantially higher than at night. This indicates that processes other than photochemical depletion, e.g. local emission patterns, contributed to diurnal variation in POCP-weighted VOC/ethane ratios for these VOCs in 1999-2001. Iso-pentane had the largest negative difference, but had a consistent positive contribution in 2010-2012. Toluene also had a negative value in 1999 and 2000. Therefore from 1999-2001 to 2010-2012 there was a change in the balance between emissions of iso-pentane and toluene and their photochemical removal to the point where photochemical depletion dominated during the day, and VOC/ethane ratios were lower in the afternoon than at night. Derwent et al. (2014) calculated exponential decreases in the concentrations of these VOCs at urban locations in the south-east of England, where Harwell is located, attributed to the effective control of evaporative and exhaust emissions from petrol-engined vehicles. Toluene has an atmospheric lifetime of ~1.9 days with respect to reaction with OH (Atkinson, 2000) so local daytime toluene emissions would not deplete substantially during transport to the monitoring site. The

observed decreasing trends at sites close to emission sources in the south-east of England suggest a decrease in the influence of local iso-pentane and toluene emissions in determining the diurnal profile of these VOCs at Harwell, and hence afternoon depletion of regionally-emitted toluene and iso-pentane was observed in 2010-2012.

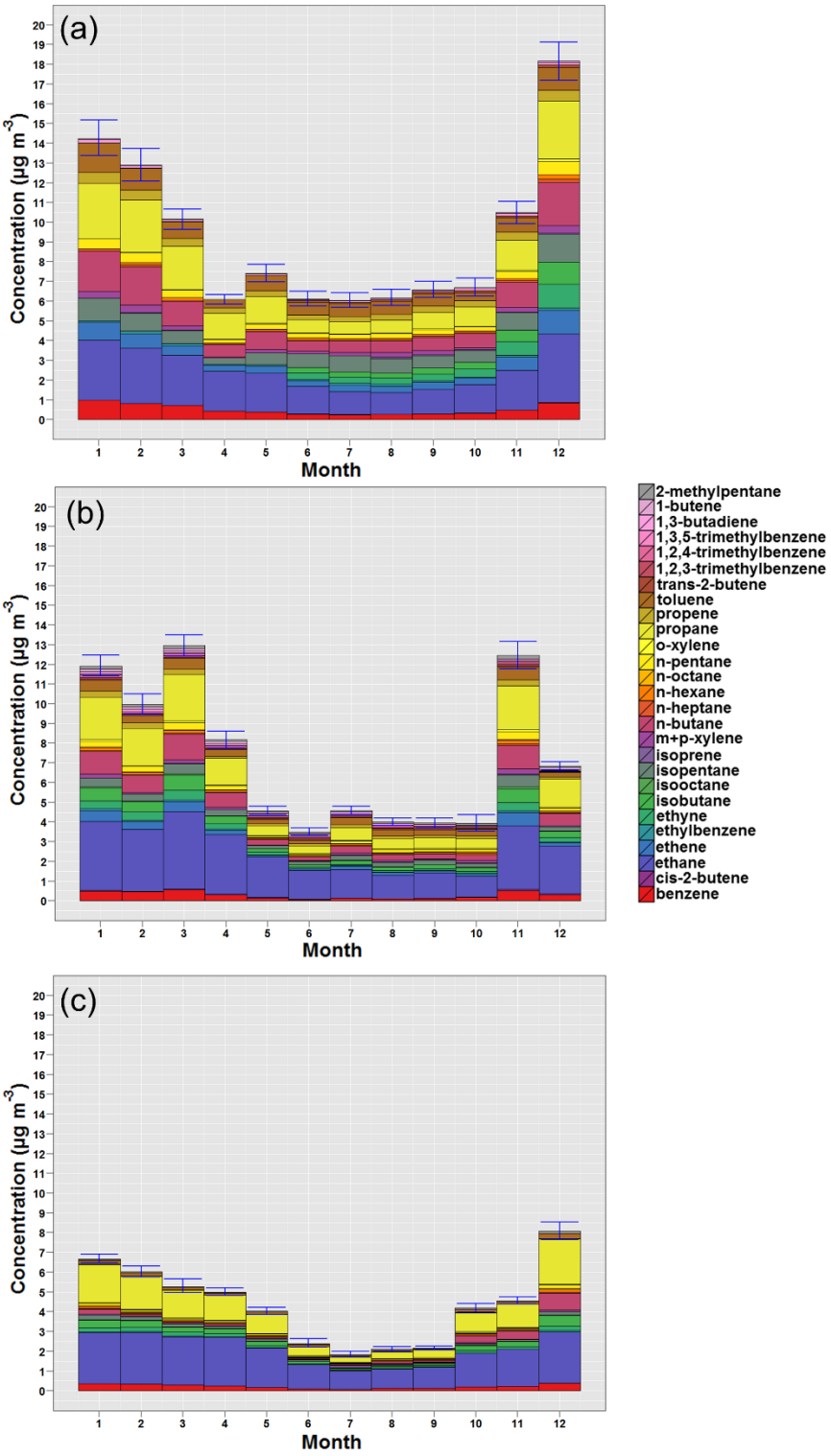

Figure 5.5: Stacked barchart of median VOC concentrations at (a) Harwell 2001, (b) Harwell 2011, and (c) Auchencorth 2012. The error bars show the sum of the 95th percentile confidence interval in the median VOC concentrations. This represents the error introduced by representing the dataset with the chosen fitted distribution (see text).

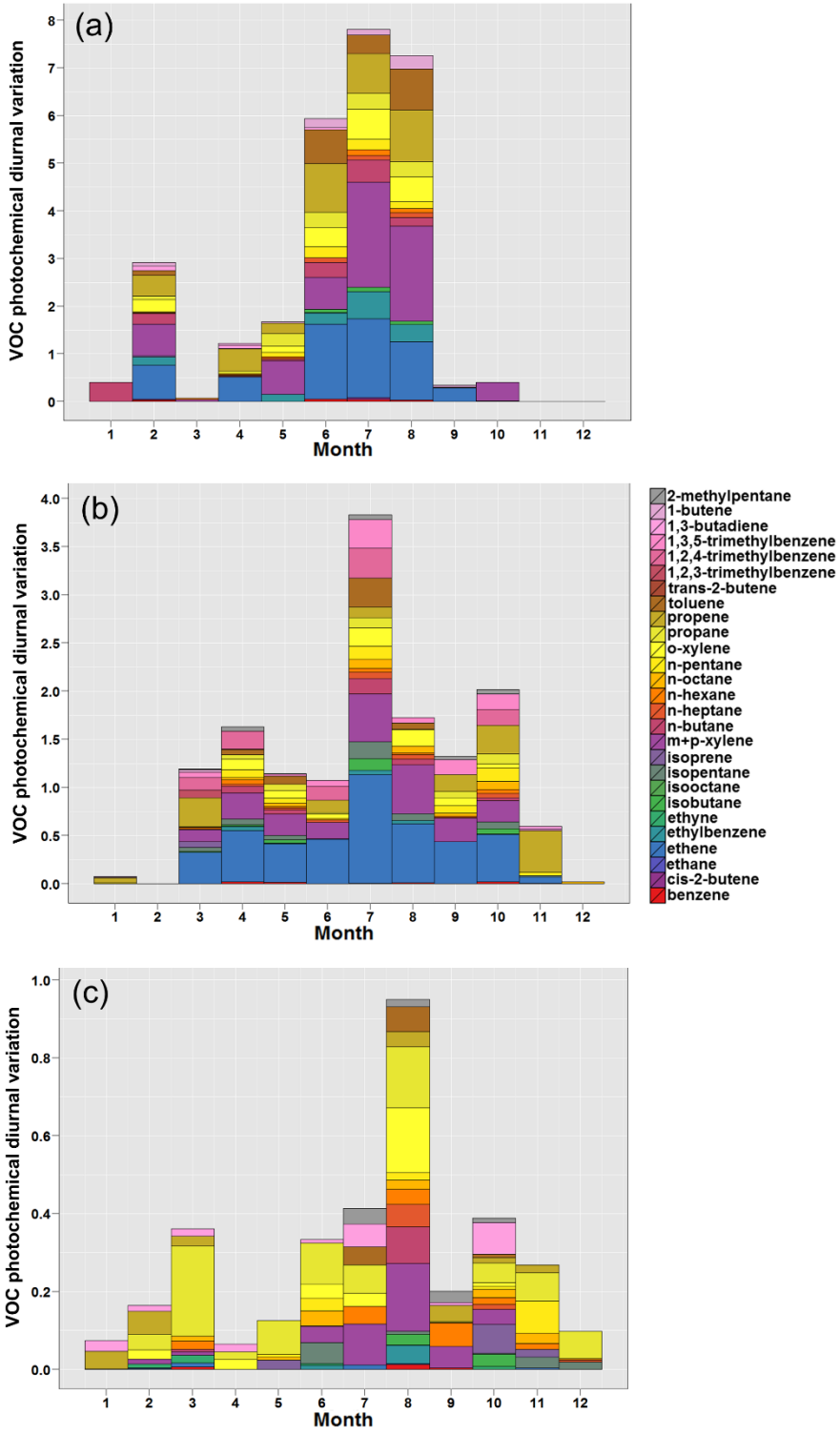

Figure 5.6: Monthly variation in VOC diurnal photochemical reactivity as defined by the difference between night (average of 1 am–5 am) and afternoon (1 pm–5 pm) POCP-weighted VOC/ethane ratios for (a) Harwell 2001, (b) Harwell 2011, and (c) Auchencorth 2011. Note the very different vertical scales.

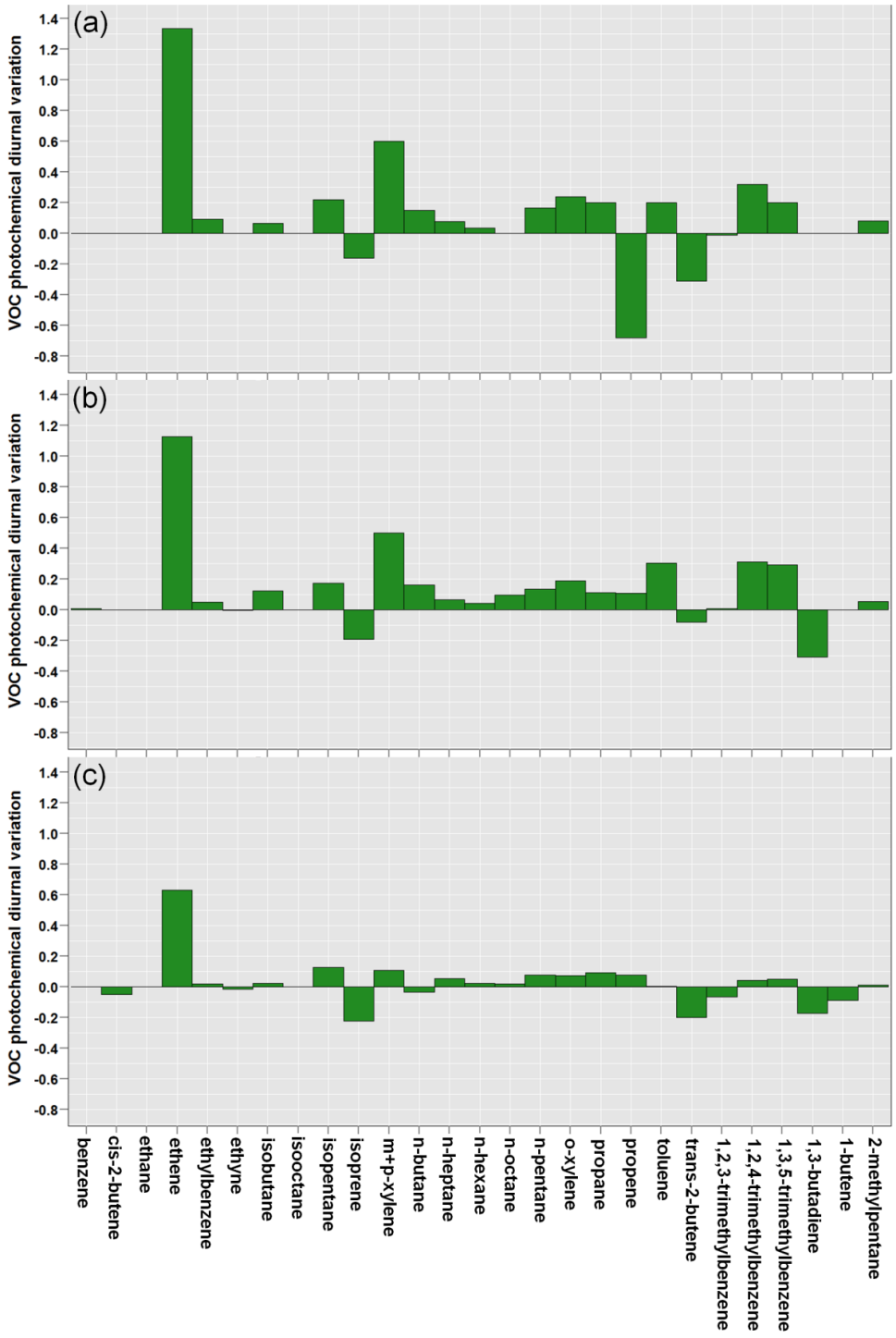

Figure 5.7: Individual VOC diurnal photochemical reactivity as defined by the difference between night (average of 1 am – 5 am) and afternoon (1 pm – 5 pm) POCP-weighted VOC/ethane ratios for (a) June 2010, (b) July 2011 and (c) July 2012, at Harwell. These months correspond to the periods of annual maximum regional O_3 increment at Harwell (see Figure 5.2).

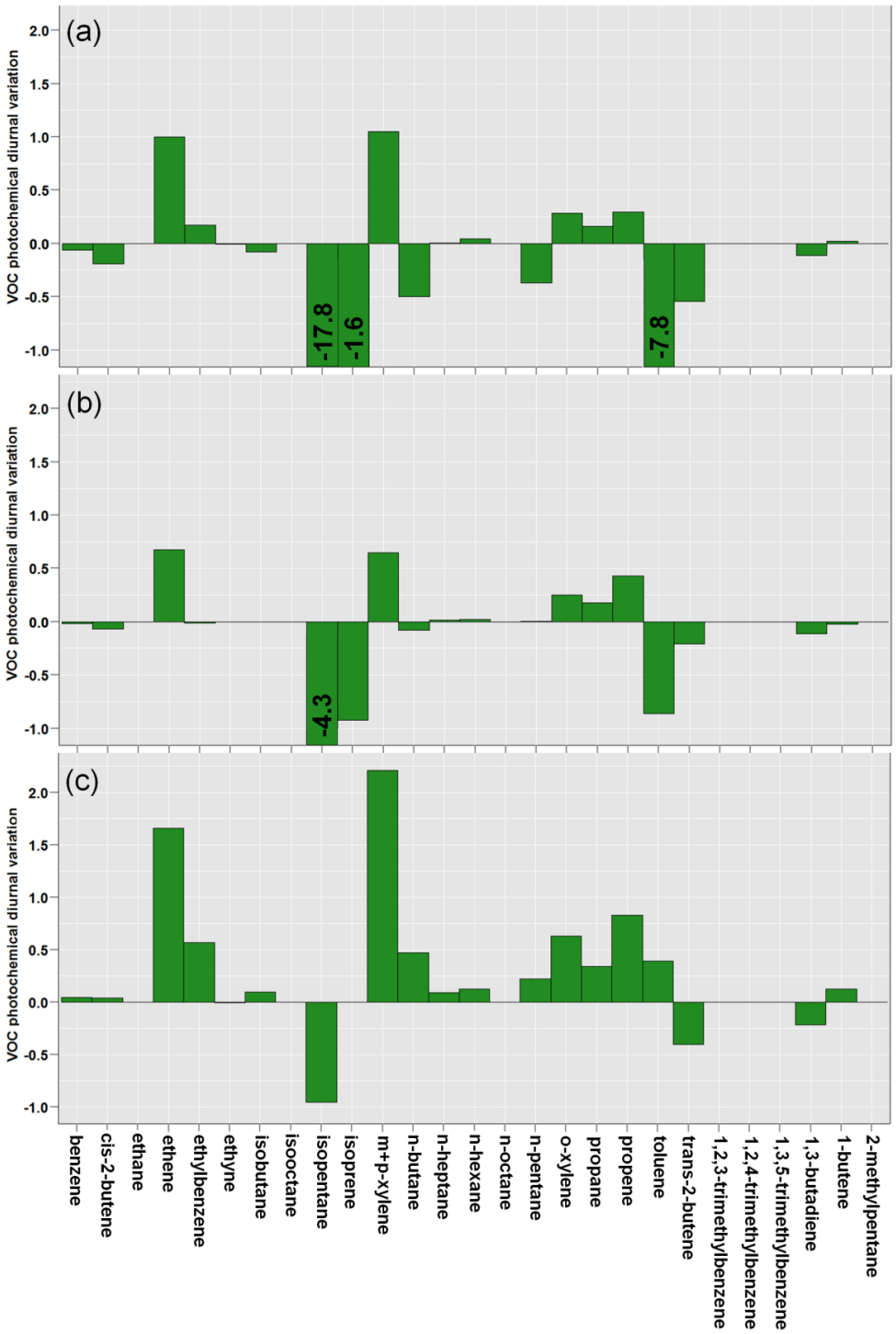

Figure 5.8: Individual VOC diurnal photochemical reactivity as defined by the difference between night (average of 1 am – 5 am) and afternoon (1 pm – 5pm) POCP-weighted VOC/ethane ratios in (a) July 1999, (b) July 2000 and (c) July 2001, at Harwell. These months correspond to the periods of annual maximum regional O_3 increment. To emphasise the positive contributions to VOC photochemical cycling, the negative values have been truncated.

5.3.3 Drivers of chemical climate state: Meteorology and emissions

5.3.3.1 Meteorology

The monthly-averaged meteorological data for the UK regions relevant for Harwell in 2001 and 2011 and Auchencorth in 2012 are shown in Figure 5.9. Variation in temperature and sunshine is often associated with spatio-temporal differences in VOC diurnal photochemical depletion and regional O_3 increment (Jenkin and Clemitshaw, 2000). For example, temperatures were generally lower in East Scotland than South East and Central South England but the number of hours of sunshine were comparable, although solar intensity is less in Scotland, hence a reduced VOC photochemical depletion and regional O_3 increment at Auchencorth. At Harwell in 2001, annual maximum VOC diurnal photochemical depletion occurred in July, coinciding with annual maximum monthly temperature, while in July 2011, a combination of relatively high temperature and hours of sunshine (although neither were annual maxima), coincided with annual maximum VOC diurnal photochemical depletion. These summers were typical of the 1999-2012 period; monthly mean temperatures were between −7% and +4% compared to the 1999-2012 average and hours of sunshine were between −14% to +11% compared to the average.

However, not all variation in VOC diurnal photochemical depletion and regional O_3 increment were associated with changes in meteorology. For example, at Harwell in April 2011, there was a larger regional O_3 increment compared with April 2001. This coincided with 4 °C higher mean temperature and 95 more hours of sunshine in South East and Central South England. In May 2011 the temperature and sunshine were similar to April 2011, but VOC diurnal photochemical depletion and the regional O_3 increment decreased. Hence other factors, such as the strength of VOC emission sources over which an air mass passes, also influence VOC diurnal photochemical depletion, and are discussed in Section 5.3.3.2.

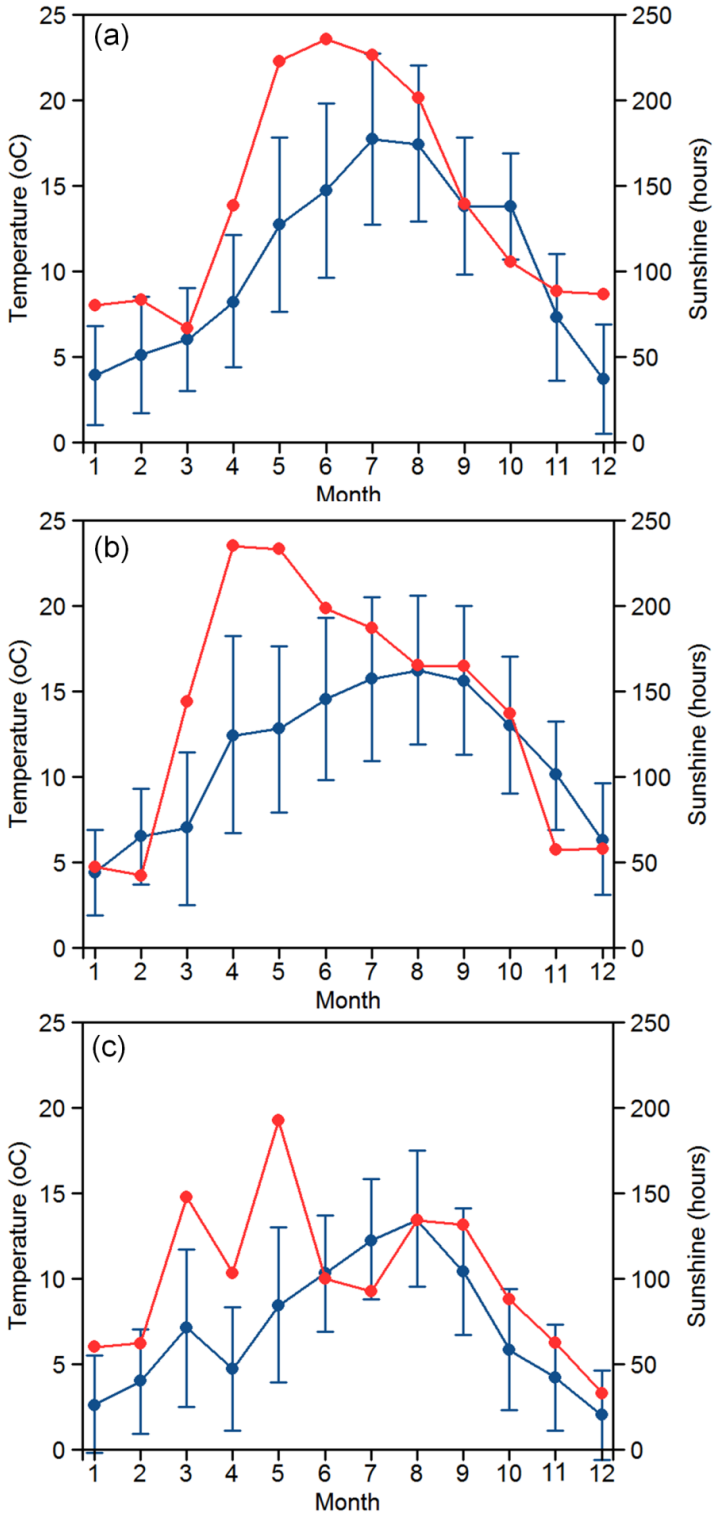

Figure 5.9: Average monthly mean temperatures (blue, maximum and minimum temperatures shown as whiskers) and hours of sunshine (red) from the UK Meteorological Office (http://www.metoffice.gov.uk/climate/uk/datasets/#) for (a) South East and Central South England 2001, (b) South East and Central South England 2011 and (c) East Scotland 2012.

5.3.3.2 Emissions

Variation in the monthly averaged European anthropogenic VOC trajectory emissions estimate (TEE) is shown in Figure 5.10. The VOC TEE is the sum of hourly emissions from the grid squares the trajectories passed over in the 96 hours prior to arrival at the supersites (units: Mg/96 hours), rather than a definitive quantification of the emissions directly impacting upon the measured atmospheric composition at the supersites. Compared with Harwell in 2001, the annual average VOC TEE, by mass, was 64% smaller in 2011 at Harwell, and 76% smaller in 2012 at Auchencorth. For the purposes of clarity the following assessment focuses on Harwell, where significant regional O_3 increment has been demonstrated (Section 5.3.1). The biggest change in contribution from the 11 SNAP sectors to average VOC TEE between 2001 and 2011 at Harwell was for SNAP 7 (road transport), which averaged 31 % of the total 10 VOC TEE in 2001, compared with 9 % in 2011 (Figure 5.10). The biggest change was for SNAP 7 (road transport), which averaged 31% of the total VOC TEE in 2001, compared to 9% in 2011. Emissions from SNAP 6 (solvents) were the largest contribution to the VOC TEE during both periods, contributing 50% of total emissions on average in 2011, compared to 34% in 2001. Emissions from SNAP 4 (production processes) were the second largest contributor on average in 2011 (11% of the total VOC TEE), followed by SNAP 7 (road transport), and SNAP 5 (extraction and distribution of fossil fuels), both contributing 9%.

Monthly variation in VOC TEE mirrors (during favourable meteorological conditions) that of VOC diurnal photochemical depletion and hence the magnitude of the regional O_3 increment. The period of April-July 2011 provides a useful case study to demonstrate the nature of the emissions driver. This period shows how variation in both the magnitude of the VOC TEE, as well as the proportion of emissions emitted closer to the receptor site (temporally) can influence the extent of VOC diurnal photochemical depletion and the magnitude of the regional O_3 increment. April and May 2011 have similar meteorological conditions (Figure 5.9), but VOC diurnal photochemical depletion was lower in May due to a 62% decrease in the VOC TEE

compared to April. The VOC TEE decreased in June, then increased in July. This latter increase, coupled with increased temperatures and solar intensity in summer, provided conditions conducive to producing the observed annual maximum in VOC diurnal photochemical depletion for 2011.

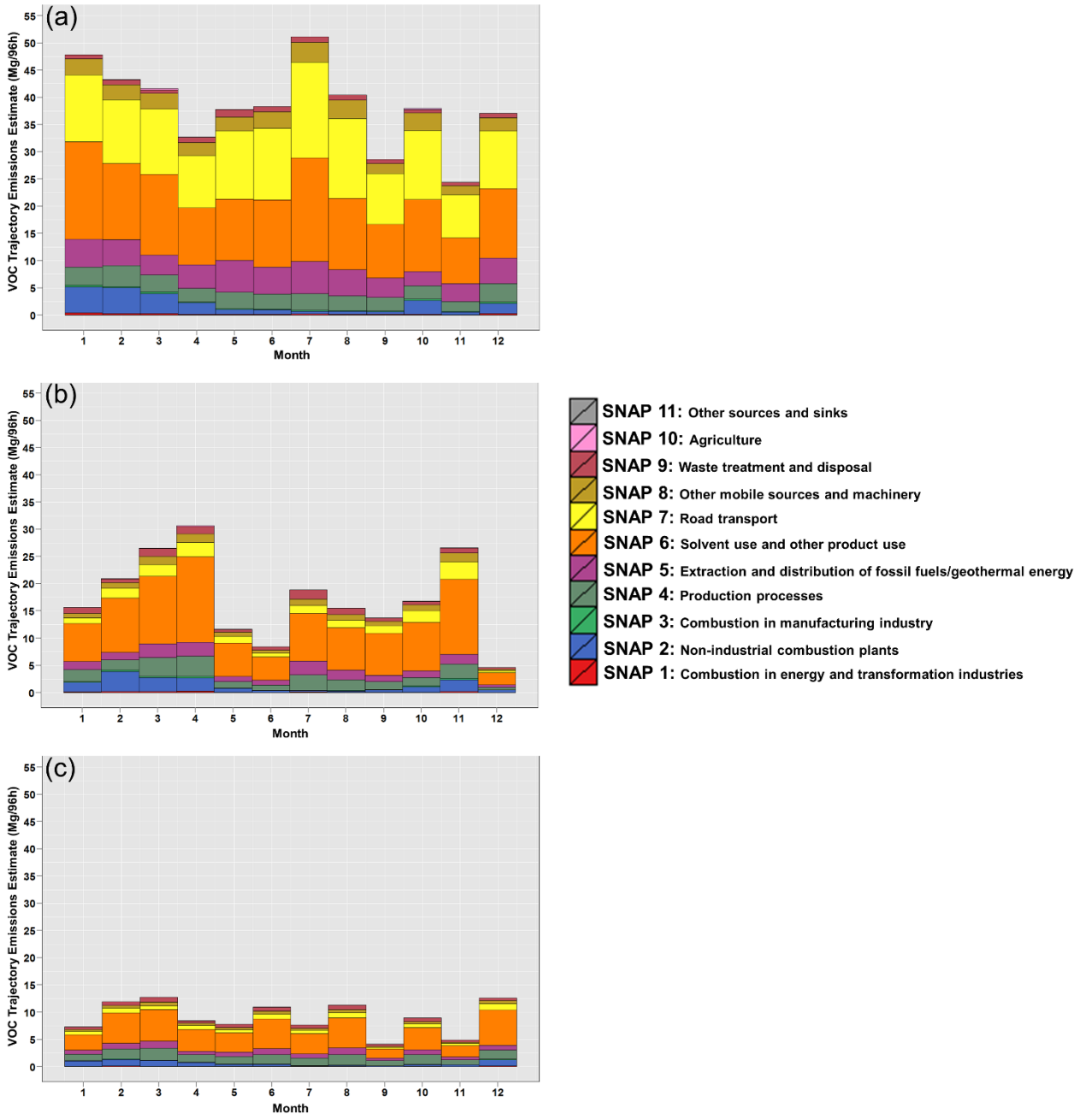

Figure 5.10: Monthly average VOC 96-hour back-trajectory emissions estimates prior to its arrival at the receptor site, disaggregated into 11 SNAP source sectors for (a) Harwell 2001, (b) 2011 Harwell, and (c) Auchencorth 2012.

The proportion of the total VOC TEE derived from the final 4 h prior to a trajectory's arrival, plus the hour of arrival, was labelled as the "final 4 h" VOC TEE to investigate the effect of variation in the proportion of emissions emitted closer to the monitoring site. In 2011 the final 4 hours was on average 28% of the total VOC TEE (Figure 5.11a). In May and June 2011 it was above average (36% and 44% respectively), and in April and July it was lower (17% and 20% respectively). While the 4-hour cut-off for this calculation was somewhat arbitrary, it was based on consideration of the average atmospheric lifetimes of the individual VOCs (Atkinson, 2000) which indicate that most VOCs emitted in the final 4 hours have insufficient time to form O_3. Between June and July 2011 there was a 32% increase in median VOC concentrations due to an increased VOC TEE (Figure 5.11b). However, there was a 275% increase in VOC diurnal photochemical depletion as a larger proportion of emissions were emitted earlier along the air-mass trajectory (Figure 5.11c). Hence in May and June, lower total VOC TEE compared to April and July, respectively, coupled with a larger proportion of VOCs emitted in the final 4 hours, resulted in the reduced regional O_3 increment impact (Figure 5.11d).

The speciated VOC monthly trajectory emissions estimates, based on a UK-specific speciation of the total VOC TEE for 9 SNAP sectors are shown in Figure 5.12 for July 2001 and 2011. Individual VOC trajectory emissions estimates were expressed as the percentage of the total POCP-weighted emissions and the comparison between 2001 and 2011 illustrates the contrast and similarities in contribution from individual VOCs to the VOC TEE during the months of maximum regional O_3 increment. The biggest decreases between 2001 and 2011 were for iso-pentane (4.1% total POCP emissions in 2001, 1.7% in 2011), and toluene (6.5% in 2001, 4.5% in 2011). These decreases mirror the absence of much greater POCP-weighted VOC/ethane ratios in the afternoon compared to night for toluene and isopentane in 2010–2012, which were observed in 1999–2001 and attributed to variation in local emissions (discussed in Section 5.3.2 and visualised as 'negative' VOC diurnal photochemical depletion in Figures 5.7 and 5.8).

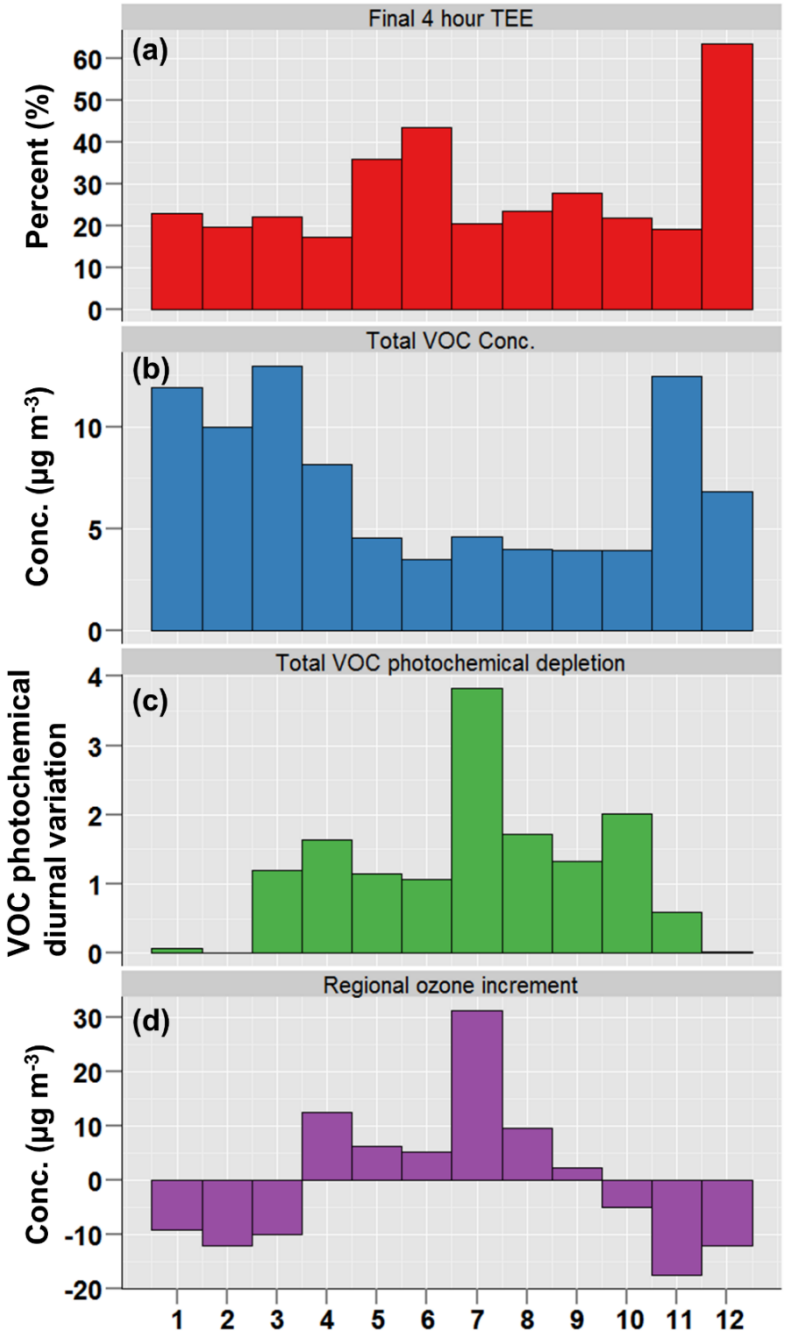

Figure 5.11: Summary of variables relevant to the assessment of the effect of variation in the proportion of emissions accumulated close (temporally) to the monitoring site: a) The final 4 hours TEE metric, i.e. the proportion of the TEE emitted into the air mass during the 4 hours prior to arrival at the site (defined in Section 5.3.3.2), b) Monthly average sum of measured VOCs, c) Monthly average sum of VOC diurnal photochemical depletion, d) Monthly maximum difference between hemispheric background concentrations and regional background concentrations (a positive value indicates additional regional O_3 production).

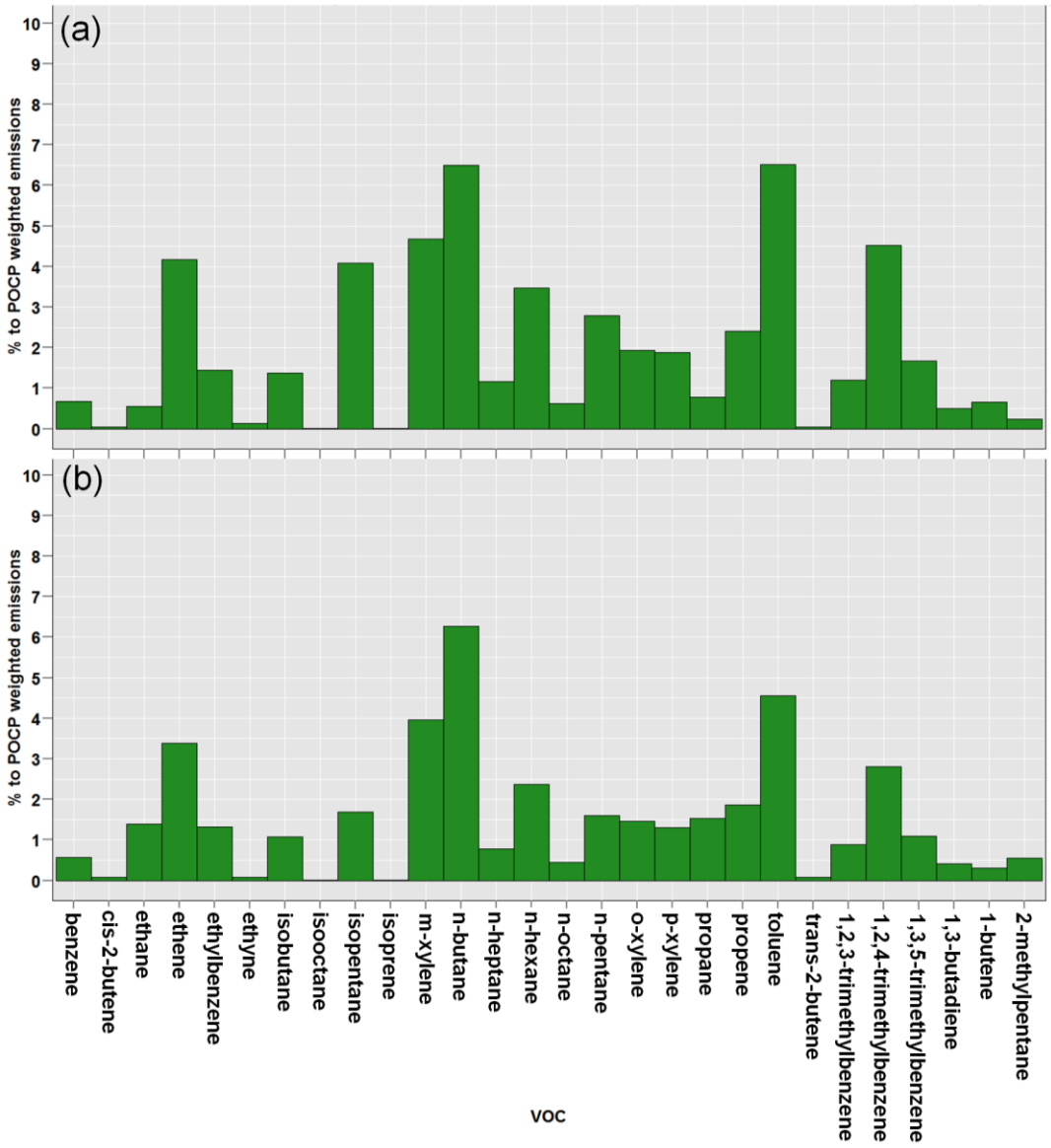

Figure 5.12: Speciation of average VOC back-trajectory emissions estimates in (a) July 2001, and (b) July 2011 at Harwell. The speciation was based on source profiles catalogued in Passant (2002) and the relative contribution of individual activities to annual total VOC emissions.

Monthly variation in the contribution of measured VOCs to the VOC TEE was not consistent with variation in the contribution of individual VOCs to total measured VOC diurnal photochemical depletion. This is in contrast to the observed changes between 2001 and 2011 in VOC contribution to TEE and VOC diurnal photochemical depletion, and is effectively illustrated using the April-July 2011 time period as an example. For example, in 2011, the VOC diurnal photochemical depletion peak in July

(Figure 5.6) was much greater than in April due to more intense sunshine and higher temperatures. This increase was not equally reflected across the measured VOCs, indicating differences in the speciation of the VOC TEEs prior to arrival at the site. For example, toluene was 4.2% of total VOC diurnal photochemical depletion in April, increasing to 9.6% in July and the 1,3,5-trimethylbenzene contribution increased from 0.1% in April to 8% in July. The monthly-averaged speciated VOC TEEs do not reflect these changes, and show little monthly variation within a given year.

The speciated VOC monthly TEE calculation assumes that the SNAP sector component activities (i.e. the activities for which speciated profiles are defined (Passant, 2002)) contribute similarly to the emissions exposure of the parent SNAP sector in each month of the year. For example, it is assumed that an *x*% increase in SNAP emissions results from an *x*% increase in emissions from all component activities. It is unlikely that the SNAP sector emissions in every region over which an air mass travels are similarly apportioned between component emissions activities. The inability of this method to account for these spatial differences will result in the underestimation of the TEE of some VOCs, and the overestimation of others. Currently, data are only available on changes in the contribution of more narrowly defined NFR codes to SNAP sector emissions at a country level and for annual VOC emissions. In 2011 the average contribution to monthly VOC TEE at Harwell from the UK was 62%, with France the second largest contributor at 14%. Comparing April and July 2011, the contributions from the UK to the VOC TEE were 50% and 95% respectively, with the other 50% in April resulting from contributions from Germany, France, Belgium and the Netherlands (Figure 5.13). These countries all have different relative contributions to total SNAP sector emissions from component NFR source sectors (EEA, 2014).

Highly-aggregated SNAP source sectors, and a constant contribution of component activities to SNAP emissions were identified as a potential contributing factor to inconsistencies between VOC contributions to TEE and VOC diurnal photochemical depletion. Disaggregation of the VOC TEEs into 91 NFR codes, based on country-

specific contributions of these NFR codes to annual VOC emissions in the 11 parent SNAP sectors, accounted for country-specific changes in NFR sector contributions to monthly VOC TEE at Harwell. The aim was to show that within each SNAP sector an increase in VOC SNAP emissions can result from an increase in a specific source activity (e.g. specific NFR code), rather than a general overall increase. Variability in the contribution of constituent activities to SNAP emissions could result in variation in the contribution of individual VOCs to those emissions. This would therefore demonstrate that the reporting of gridded VOC emissions in more disaggregated source sectors was required, so that more flexible VOC speciation profiles could be derived than those calculated for the 9 SNAP sectors in this study, and those calculated previously, e.g. Derwent et al. (2007c). For example, in 1999-2001, the large contribution from SNAP 7 (road transport, Figure 5.10) is more precisely attributed to NFR sectors 1A3bi (passenger cars) and 1A3bv (gasoline evaporation) which contributed 19% and 11% to the total VOC TEE in July 2001 (month of maximum regional O_3 increment) respectively, and 87% of the SNAP 7 emissions estimate. The next largest contribution was from 3D2 (domestic solvent use, 10%), a component of SNAP 6 (solvents). Between 2010 and 2012, SNAP 6 was the major contributor to the VOC TEE. During July 2011 SNAP 6 component NFR sectors, 3D2 (domestic solvent use) and 3D3 (other product use) contributed 18% and 12% of the total VOC TEE (65% of the SNAP 6 emissions estimate). The SNAP 4 (production processes) component 2D2 (food and drink) was the third largest contributor (10% in July 2011). The two road transport categories contributed 4% (1A3bi) and 1% (1A3bv) to the total VOC TEE in July 2011.

The difference between the contribution of 91 NFR codes to the average VOC TEE between April and July 2011 is shown in Figure 5.14 to demonstrate the variability in contribution of component activities to parent SNAP sector emissions. Between these months, the cumulative change in the contribution of the 9 SNAP sectors to the total VOC TEE was 13.4%, compared to a change of 15.9% for the 91 NFR codes. However, the changes in NFR code contributions were not equally spread between the constituent activities of a SNAP sector; they were concentrated in relatively few NFR

sectors. For example, between April and July 85% of the NFR change resulted from a decrease in 10 out of the 91 NFR sectors. The sectors ‘residential: stationary plant combustion’ and ‘industrial coating application’ show the greatest decrease, while sectors ‘food and drink’ and ‘venting and flaring’ show the largest increase (identified by stars on Figure 5.14). The disaggregation of SNAP sector VOC TEEs also illustrates changes of opposite sign in the contribution of component NFR sectors under the net changes in SNAP sector. For example, SNAP sector 4 (Production processes) increased in contribution between April and July by 2.7% (12.0 to 14.7%). Following disaggregation, this change was seen to result from a 3.4% increase in NFR sector 2D2 (food and drink) and a 0.76% decrease in 2B5 (other chemical industry). NFR sector level speciated profiles can therefore give much more specific information on the emissions source drivers of VOC diurnal photochemical depletion, though it is noted that the accuracy of many emission source speciation profiles is subject to discussion (Borbon et al., 2013). However, the changes in contribution of NFR sectors to the VOC TEE calculated here only account for country-level variation, not for variation in the contribution of NFR sectors to SNAP emissions on finer spatial scales, such as differences in NFR sector contribution to SNAP emissions in different 0.5° × 0.5° grid squares for which the SNAP sector gridded emissions are reported. Hence the future reporting of gridded emissions to NFR code level would more accurately represent the true nature of VOC emissions across Europe.

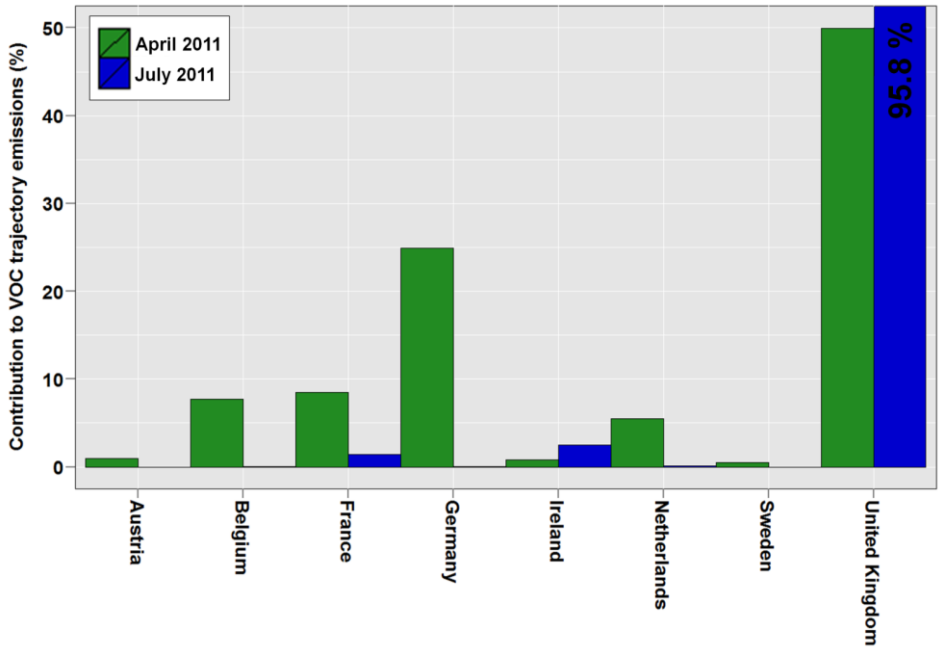

Figure 5.13: Contributions to the average VOC 96-hour back-trajectory emission estimates in April 2011 (green bars) and July 2011 (blue bars) from countries which contributed at least 0.5% during one of the months. The contribution of the UK in July 2011 was 95.8 %, and has been truncated in the plot.

5.3.4 Uncertainties and implications for future mitigation and monitoring

Two VOCs, ethene and m+p-xylene, consistently had larger contributions to total VOC diurnal photochemical depletion compared to the remaining VOC suite. Therefore a targeted reduction of these two VOCs (compared to other measured VOCs) would be most effective in reducing the regional O_3 increment. Further reduction of total measured VOC diurnal photochemical depletion would require a reduction across a larger number of the remaining measured VOCs. This could be achieved by lowering emissions from large VOC-emitting sources, rather than a focus on individual VOC species. As previously identified (Section 5.3.3), between 2010 and 2012, the largest VOC-emitting sources (NFR codes) were 3D2 (domestic solvent use including fungicides), 3D3 (other product use) and 2D2 (food and drink).

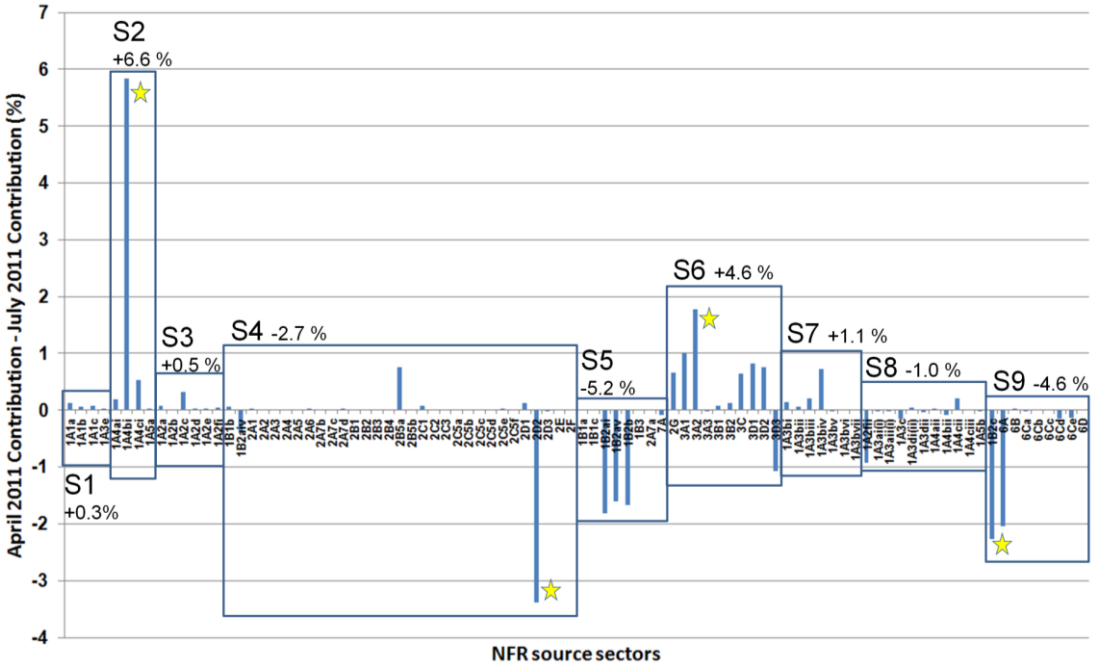

Figure 5.14: Difference between NFR source sector contributions to average VOC back trajectory emission estimates (VOC TEE) in April and July 2011 at Harwell. Also shown are the change in contribution of the SNAP source sectors. These were calculated from the VOC TEE prior to disaggregation, and do not represent the sum of the contribution changes of the constituent NFR source sectors. The source sectors identified by stars have the largest changes between April and July (Section 5.3.3.2).

The 27 measured VOCs studied here are a subset of the total VOC species emitted by a multitude of anthropogenic activities and biogenic processes. In 2011, 37.5% of the reported annual UK anthropogenic VOC emissions were emitted as one of the 27 measured VOCs, when speciated using the Passant (2002) speciation profiles. The UK biogenic VOC emissions estimate reported to EMEP for 2011 was 91.2 Gg (*c.f.* anthropogenic emissions of 752 Gg), but this value is uncertain and studies have estimated considerably higher UK annual biogenic VOC emissions, in excess of 200 Gg (Karl et al., 2009; Oderbolz et al., 2013). Biogenic VOC contributions to regional O_3 increments were not studied using this methodology. The estimate of 752 Gg of UK anthropogenic emissions is also subject to uncertainty associated with defining accurate activity rates and emissions factors for a large number of source activities (EEA, 2013). The UK National Atmospheric Emissions Inventory (NAEI) calculated the uncertainty in UK anthropogenic VOC emissions to be ± 10% (Misra et al., 2015).

Of the 62.5% of UK anthropogenic VOC emissions not emitted as one of the VOCs measured at the supersites, only the additional measurement of ethanol (13% of 2011 anthropogenic UK emissions), methanol (4%) and acetone (3%) would substantially increase the proportion of the UK VOC suite for which VOC diurnal photochemical depletion would be quantified. The measurement of these three VOCs would increase the proportion of UK anthropogenic emissions emitted as a measured VOC from 37.5% to 57.5%. Currently, ethanol, methanol and acetone constitute 35% of the unmeasured fraction of UK anthropogenic emissions. Contributions from the 40 unmeasured VOCs with the next highest emissions are required to make up the same percentage, and the remaining unmeasured emissions fraction comprises 464 VOCs. The large number of VOC contributing to the 'unmeasured' VOC emissions fraction supports the argument that the targeting of high VOC emitting sources would be more beneficial than reductions in individual VOCs from whatever their source(s). The large proportion of UK VOC emissions emitted as ethanol, methanol and acetone (mainly from SNAP6 (solvents), from which 39%, 97% and 91% of UK anthropogenic emissions of ethanol, methanol and acetone derived in 2011, and SNAP4 (production processes), which contributed 57% of ethanol emissions) suggests that, like ethene and m+p-xylene, they may have a disproportionately high contribution to VOC diurnal photochemical depletion, and hence to the magnitude of the regional O_3 increment. Measurement of these oxygenated VOCs at the supersites would allow their contribution to be quantified.

Other limitations, in addition to using measurements of a subset of the emitted VOC suite, include use of monthly-diurnal averages. Monthly-diurnal averages were required to use MLE to derive summary statistics, and to calculate hemispheric and regional background O_3 concentrations. Additionally, it is more appropriate to consider an ensemble of air-mass back trajectories to reduce the random uncertainty associated with their calculation. Hence the integration of air-mass back trajectories and gridded emissions inventories also benefitted from use of monthly averages. However, the contribution of VOCs to the average increase in regional O_3 increment

in a given month was evaluated, rather than any short term episodic regional O_3 increment increases.

An additional uncertainty is associated with the gridded emissions inventory itself. The derivation of the inventory requires accurate determination of emission factors and activity rates for a large number of source activities (EEA, 2013). Previous studies show the uncertainty associated with this process. For example, Koohkan et al. (2013) calculated VOC emissions across Europe using inverse modelling by data assimilation of measurements for 15 VOCs and comparison with the EMEP inventory showed an underestimation of emissions of some VOCs and an overestimation of others. Hence there is a requirement for improvement of emissions inventory derivation. However, this analysis shows that the future reporting of gridded VOC emissions in source sectors more highly disaggregated than currently (e.g. NFR codes) would also facilitate a more precise identification of those VOC sources most important to mitigation strategies, and increase the accuracy in calculating emissions of individual VOCs. For example, Derwent et al. (2007b) applied the POCP concept to calculate the contribution of 248 VOC source categories to regional O_3 production using a photochemical trajectory model with a near-explicit chemical mechanism which followed a 'worst case' 5-day trajectory bringing aged air masses from Europe to a location on the England-Wales border. A UK-derived VOC emissions speciation was derived and applied to total gridded VOC emissions estimates across north-west Europe. While the POCP concept provides an effective means of comparison between different source categories, source category POCPs were calculated without accounting for the spatial variation in the contribution of the different source categories to total VOC emissions.

The work presented here highlights the constraints of representing spatial variation of VOC emissions across Europe with 11 highly aggregated SNAP sectors in terms of accurately determining the suite of VOCs impacting atmospheric composition at a site. This results from a fixed contribution of component activities to the aggregated SNAP sector emissions spatially and temporally (see Section 5.3.3.2), although emissions

from different SNAP sectors can vary independently of one another. These constraints would be amplified with no disaggregation of gridded VOC emissions and a constant contribution from component activities spatially and temporally to total VOC emissions, i.e. emissions from each aggregated SNAP sector do not vary independently from one another. The effectiveness of the POCP concept in the determination of the strongest O_3-influencing VOC emission sources, and hence the most cost effective mitigation strategies, would be substantially improved by the reporting of gridded emissions at NFR sector level. Finally, the future measurement at supersites of VOCs which are distinct markers for source sectors (e.g. NFR codes) could be used to quantify the contribution from different VOC source sectors.

5.4 Conclusions

The chemical climatology methodology has been demonstrated, using measurement data at Harwell and Auchencorth, to successfully link the impact of regional O_3 increment to VOC photochemical depletion and spatially-gridded anthropogenic VOC emissions. The regional O_3 increment at Harwell in 2010-2012 was substantially larger than at Auchencorth, but substantially smaller than in 1999-2001. Of the 27 measured VOCs, ethene and m+p-xylene consistently contributed the most VOC photochemical depletion during regional O_3 production at Harwell, and therefore reductions in emissions of these VOCs would be most effective in reducing regional O_3 production. To reduce VOC diurnal photochemical depletion further, reductions across a larger number of the VOCs would be required. Of these, ethanol, methanol and acetone appear to be the most important, and measurement of these VOCs at the supersites would provide data for targeting future emissions reductions. Additionally, more detailed speciated measurement of biogenic VOCs at the supersite would also advance understanding of the relative contribution of anthropogenic vs biogenic VOCs in determining the regional O_3 increment.

Estimates of the integrated anthropogenic VOC emissions along back trajectories arriving at Harwell have decreased substantially between 1999-2001 and 2010-2012, due to decreases in emissions from SNAP source sector 7 (road transport). Currently, SNAP sector 6 (solvent and product use) provides most of the total VOC trajectory emissions estimate. The disaggregation of highly aggregated SNAP trajectory emissions estimates to NFR codes, accounting for country variation in the NFR sector contribution to parent SNAP sector, allowed the source sectors which determine the VOC contribution to the regional O_3 impact to be more precisely defined, i.e. NFR sectors 3D2 (domestic solvent use), 3D3 (other product use) and 2D2 (food and drink), which were the top three contributors to total VOC emissions exposure at Harwell (2010-2012) during the month of maximum regional O_3 increment. It is concluded that considerable additional benefits to the interpretation of measurement data, to modelling of future O_3 concentrations and hence to determining policy for abatement of detrimental O_3 impacts would be gained from the availability of gridded VOC emissions data reported in more narrowly defined source sectors such as the NFR codes.

References

Akaike, H., 1974. New look at statistical-model identification. IEEE T. Autom. Contr. 19, 716-723.

Atkinson, R., 2000. Atmospheric chemistry of VOCs and NOx. Atmos. Environ. 34, 2063-2101.

Borbon, A., Gilman, J. B., Kuster, W. C., Grand, N., Chevaillier, S., Colomb, A., Dolgorouky, C., Gros, V., Lopez, M., Sarda-Esteve, R., Holloway, J., Stutz, J., Petetin, H., McKeen, S., Beekmann, M., Warneke, C., Parrish, D. D., de Gouw, J. A., 2013. Emission ratios of anthropogenic volatile organic compounds in northern mid-latitude megacities: Observations versus emission inventories in Los Angeles and Paris. J. Geophys. Res-Atmos. 118, 2041-2057, doi:10.1002/jgrd.50059.

Bowman, F. M., 2005. A multi-parent assignment method for analyzing atmospheric chemistry mechanisms. Atmos. Environ. 39, 2519-2533.

Butler, T. M., Lawrence, M. G., Taraborrelli, D., Lelieveld, J., 2011. Multi-day ozone production potential of volatile organic compounds calculated with a tagging approach. Atmos. Environ. 45, 4082-4090.

Carslaw, D. C., Ropkins, K., 2012. openair - An R package for air quality data analysis. Environmental Modelling & Software 27-28, 52-61, doi:10.1016/j.envsoft.2011.09.008.

Clapp, L. J., Jenkin, M. E., 2001. Analysis of the relationship between ambient levels Of O-3, NO2 and NO as a function of NO chi in the UK. Atmos. Environ. 35, 6391-6405.

Dernie, J., Dumitrean, P., 2013. UK Hydrocarbon Network: Annual Report for 2012. Report No. ED47833 and ED46645 for Defra and the Devolved Administrations. Ricardo-AEA. http://uk-air.defra.gov.uk/assets/documents/reports/cat13/1311201446_Hydrocarbon_2012_FINAL_Issue_1.pdf.

Derwent, R. G., Simmonds, P. G., Manning, A. J., Spain, T. G., 2007a. Trends over a 20-year period from 1987 to 2007 in surface ozone at the atmospheric research station, Mace Head, Ireland. Atmos. Environ. 41, 9091-9098.

Derwent, R. G., Jenkin, M. E., Passant, N. R., Pilling, M. J., 2007b. Photochemical ozone creation potentials (POCPs) for different emission sources of organic compounds under European conditions estimated with a Master Chemical Mechanism. Atmos. Environ. 41, 2570-2579.

Derwent, R. G., Jenkin, M. E., Passant, N. R., Pilling, M. J., 2007c. Reactivity-based strategies for photochemical ozone control in Europe. Environ. Sci. Policy 10, 445-453.

Derwent, R. G., Jenkin, M. E., Pilling, M. J., Carter, W. P. L., Kaduwela, A., 2010. Reactivity Scales as Comparative Tools for Chemical Mechanisms. J. Air Waste Manage. 60, 914-924.

Derwent, R. G., Dernie, J. I. R., Dollard, G. J., Dumitrean, P., Mitchell, R. F., Murrells, T. P., Telling, S. P., Field, R. A., 2014. Twenty years of continuous high time

resolution volatile organic compound monitoring in the United Kingdom from 1993 to 2012. Atmos. Environ. 99, 239-247.

Dollard, G. J., Dumitrean, P., Telling, S., Dixon, J., Derwent, R. G., 2007. Observed trends in ambient concentrations of C-2-C-8 hydrocarbons in the United Kingdom over the period from 1993 to 2004. Atmos. Environ. 41, 2559-2569.

Draxler, R. R., Rolph, G. D., 2013. HYSPLIT (HYbrid Single-Particle Lagrangian Integrated Trajectory) Model access via NOAA ARL READY Website (http://www.arl.noaa.gov/HYSPLIT.php). NOAA Air Resources Laboratory, College Park, MD. .

EEA, 2013. EMEP/EEA air pollutant emission inventory guidebook 2013. EEA technical report No 12/2013. European Environment Agency. http://www.eea.europa.eu/publications/emep-eea-guidebook-2013.

EEA, 2014. EU emission inventory report 1990-2012 under the UNECE Convention on long-range transboundary air pollution (LRTAP). EEA technical report No 12/2014. European Environment Agency. http://www.eea.europa.eu//publications/lrtap-2014.

Gardner, M., 2012. Improving the interpretation of 'less than' values in environmental monitoring. Water Environ. J. 26, 285-290.

Gauss, M., Semeena, V., Benedictow, A., Klein, H., 2014. Transboundary air pollution by main pollutants (S, N, Ozone) and PM: The European Union. MSC-W Data Note
1/2014. http://emep.int/publ/reports/2014/Country_Reports/report_EU.pdf.

Hakami, A., Harley, R. A., Milford, J. B., Odman, M. T., Russell, A. G., 2004. Regional, three-dimensional assessment of the ozone formation potential of organic compounds. Atmos. Environ. 38, 121-134.

Helmig, D., Tanner, D. M., Honrath, R. E., Owen, R. C., Parrish, D. D., 2008. Nonmethane hydrocarbons at Pico Mountain, Azores: 1. Oxidation chemistry in the North Atlantic region. J. Geophys. Res. 113, doi:10.1029/2007jd008930.

Helsel, D. R., 2006. Fabricating data: How substituting values for nondetects can ruin results, and what can be done about it. Chemosphere 65, 2434-2439.

Honrath, R. E., Helmig, D., Owen, R. C., Parrish, D. D., Tanner, D. M., 2008. Nonmethane hydrocarbons at Pico Mountain, Azores: 2. Event-specific analyses of the impacts of mixing and photochemistry on hydrocarbon ratios. J. Geophysical Res. 113, doi:10.1029/2008jd009832.

Jenkin, M. E., 2008. Trends in ozone concentration distributions in the UK since 1990: Local, regional and global influences. Atmos. Environ. 42, 5434-5445.

Jenkin, M. E., Clemitshaw, K. C., 2000. Ozone and other secondary photochemical pollutants: chemical processes governing their formation in the planetary boundary layer. Atmos. Environ. 34, 2499-2527.

Jobson, B. T., McKeen, S. A., Parrish, D. D., Fehsenfeld, F. C., Blake, D. R., Goldstein, A. H., Schauffler, S. M., Elkins, J. C., 1999. Trace gas mixing ratio variability versus lifetime in the troposphere and stratosphere: Observations. J. Geophys. Res. 104, 16091-16113, doi:10.1029/1999jd900126.

Karl, M., Guenther, A., Koble, R., Leip, A., Seufert, G., 2009. A new European plant-specific emission inventory of biogenic volatile organic compounds for use in atmospheric transport models. Biogeosciences 6, 1059-1087.

Kaufman, L., Rousseeuw, P. J., 1990. Finding Groups in Data: An Introduction to ClusterAnalysis. Wiley, New York. Wiley, New York.

Koohkan, M. R., Bocquet, M., Roustan, Y., Kim, Y., Seigneur, C., 2013. Estimation of volatile organic compound emissions for Europe using data assimilation. Atmos. Chem. Phys. 13, 5887-5905, doi:10.5194/acp-13-5887-2013.

Lanz, V. A., Henne, S., Staehelin, J., Hueglin, C., Vollmer, M. K., Steinbacher, M., Buchmann, B., Reimann, S., 2009. Statistical analysis of anthropogenic non-methane VOC variability at a European background location (Jungfraujoch, Switzerland). Atmos. Chem. Phys. 9, 3445-3459.

Laurent, A., Hauschild, M. Z., 2014. Impacts of NMVOC emissions on human health in European countries for 2000-2010: Use of sector-specific substance profiles Atmos. Environ. 85, 247-255.

Luecken, D. J., Mebust, M. R., 2008. Technical challenges involved in implementation of VOC reactivity-based control of ozone. Environ. Sci. Technol. 42, 1615-1622.

Malley, C. S., Braban, C. F., Heal, M. R., 2014. New Directions: Chemical climatology and assessment of atmospheric composition impacts. Atmos. Environ. 87, 261-264.

Malley, C. S., Heal, M. R., Mills, G., Braban, C., 2015. Trends and drivers of ozone human health and vegetation impact metrics from UK EMEP supersite measurements (1990–2013). Atmos. Chem. Phys. Discuss. 15, 1869-1914.

Mangiameli, P., Chen, S. K., West, D., 1996. A comparison of SOM neural network and hierarchical clustering methods. Eur. J. Oper. Res. 93, 402-417.

Mareckova, K., Wankmueller, R., Whiting, R., Pinterits, M., 2013. Review of emission data reported under the LRTAP Convention and NEC Directive, Stage 1 and 2 review, Review of emission inventories from shipping, Status of Gridded and LPS data, EEA and CEIP technical report, 1/2013, ISBN 978-3-99004-248-9. Available at: http://www.ceip.at/review-of-inventories/review-2013/.

Martien, P. T., Harley, R. A., Milford, J. B., Russell, A. G., 2003. Evaluation of incremental reactivity and its uncertainty in Southern California. Environ. Sci. Technol. 37, 1598-1608.

Misra, A., Passant, N. R., Murrells, T. P., Pang, Y., Thistlethwaite, G., Walker, C., Broomfield, M., Wakeling, D., del Vento, S., Pearson, B., Hobson, M., Misselbrook, T., Dragosits, U., 2015. UK Informative Inventory Report (1990 to 2013): Annual Report for Submission under the UNECE-Convention on Long-Range Transboundary Air Pollution, available at: http://uk-air.defra.gov.uk/assets/documents/reports/cat07/1503131022_GB_IIR_2015_Final_v20.pdf.

Munir, S., Chen, H., Ropkins, K., 2013. Quantifying temporal trends in ground level ozone concentration in the UK. Sci. Total Environ. 458, 217-227.

Oderbolz, D. C., Aksoyoglu, S., Keller, J., Barmpadimos, I., Steinbrecher, R., Skjoth, C. A., Plass-Duelmer, C., Prevot, A. S. H., 2013. A comprehensive emission inventory of biogenic volatile organic compounds in Europe: improved seasonality and land-cover. Atmos. Chem. Phys. 13, 1689-1712.

Passant, N. R., 2002. Speciation of UK emissions of non-methane volatile organic compounds. AEA Technology Report ENV-0545, Culham, Abingdon, United Kingdom. http://uk-air.defra.gov.uk/reports/empire/AEAT_ENV_0545_final_v2.pdf.

Passant, N. R., Murrells, T. P., Pang, Y., Thistlewaite, G., H.L., V., Whiting, R., Walker, C., MacCarthy, J., Watterson, J., Hobson, M., Misselbrook, T., 2013. UK Informative Inventory Report (1980 to 2011). http://uk-air.defra.gov.uk/reports/cat07/1303261254_UK_IIR_2013_Final.pdf.

Perry, M., Hollis, D., 2005. The development of a new set of long-term climate averages for the UK. Int. J. Climatol. 25, 1023-1039, doi:10.1002/joc.1160.

R Core Development Team, 2008. R: A language and environment for statistical computing. R Foundation for Statistical Computing, Vienna, Austria. ISBN 3-900051-07-0, URL http://www.R-project.org. .

REVIHAAP, 2013. Review of evidence on health aspects of air pollution – REVIHAAP Project technical report. World Health Organization (WHO) Regional Office for Europe, Bonn. http://www.euro.who.int/__data/assets/pdf_file/0004/193108/REVIHAAP-Final-technical-report-final-version.pdf.

RoTAP, 2012. Review of Transboundary Air pollution: Acidification, Eutrophication, Ground Level Ozone and Heavy metals in the UK. Contract Report to the Department for Environment, Food and Rural Affairs. Centre for Ecology and Hydrology. http://www.rotap.ceh.ac.uk/sites/rotap.ceh.ac.uk/files/CEH%20RoTAP.pdf.

Sauvage, S., Plaisance, H., Locoge, N., Wroblewski, A., Coddeville, P., Galloo, J. C., 2009. Long term measurement and source apportionment of non-methane hydrocarbons in three French rural areas. Atmos. Environ. 43, 2430-2441.

Shao, M., Lu, S., Liu, Y., Xie, X., Chang, C., Huang, S., Chen, Z., 2009. Volatile organic compounds measured in summer in Beijing and their role in ground-level ozone formation. J. Geophys. Res. 114, doi:10.1029/2008jd010863.

Simpson, D., Benedictow, A., Berge, H., Bergstrom, R., Emberson, L. D., Fagerli, H., Flechard, C. R., Hayman, G. D., Gauss, M., Jonson, J. E., Jenkin, M. E., Nyiri, A., Richter, C., Semeena, V. S., Tsyro, S., Tuovinen, J. P., Valdebenito, A., Wind, P., 2012. The EMEP MSC-W chemical transport model - technical description. Atmos. Chem. Phys. 12, 7825-7865.

Tarasova, O. A., Brenninkmeijer, C. A. M., Joeckel, P., Zvyagintsev, A. M., Kuznetsov, G. I., 2007. A climatology of surface ozone in the extra tropics: cluster analysis of observations and model results. Atmos. Chem. Phys. 7, 6099-6117.

von Schneidemesser, E., Monks, P. S., Plass-Duelmer, C., 2010. Global comparison of VOC and CO observations in urban areas. Atmos. Environ. 44, 5053-5064.

von Schneidemesser, E., Monks, P. S., Gros, V., Gauduin, J., Sanchez, O., 2011. How important is biogenic isoprene in an urban environment? A study in London and Paris. Geophys. Res. Lett. 38, 7, doi:10.1029/2011gl048647.

Yates, E. L., Derwent, R. G., Simmonds, P. G., Greally, B. R., O'Doherty, S., Shallcross, D. E., 2010. The seasonal cycles and photochemistry of C-2-C-5 alkanes at Mace Head. Atmos. Environ. 44, 2705-2713.

Yuan, B., Shao, M., de Gouw, J., Parrish, D. D., Lu, S., Wang, M., Zeng, L., Zhang, Q., Song, Y., Zhang, J., Hu, M., 2012. Volatile organic compounds (VOCs) in urban air: How chemistry affects the interpretation of positive matrix factorization (PMF) analysis. J. Geophys. Res. 117, doi:10.1029/2012jd018236.

Chapter 6: Identifying mitigation strategies for the long-term human health impact of PM using the chemical climatology framework

6.1 Introduction

The first recorded fatalities from air pollutants occurred during short term 'episodes' of very high air pollution in Belgium (Meuse Valley), the USA (Donora) and the UK (London) in the late 1940s and early 1950s (Bell et al., 2004; Halliday, 1961; Heimann, 1961). These disasters led to an increased focus on mitigation of air pollution impacts through legislated air quality standards and the establishment of systemised monitoring networks to assess exposure (Clifton, 1964). It has since been shown that long-term exposure to air pollutants also results in negative health outcomes, in addition to short-term high concentration episodes (REVIHAAP, 2013, and references therein).

Particulate matter (PM) is one of those atmospheric constituents which has been associated with premature mortality and morbidity. The 'fine' fraction of PM is quantified by $PM_{2.5}$, while PM_{10} consists of both 'fine' and 'coarse' (PM_{10} - $PM_{2.5}$) particles. These metrics are defined as the aerodynamic diameter (2.5 μm and 10 μm for $PM_{2.5}$ and PM_{10} respectively) at which the collection efficiency for particles passing through a size-selective inlet is 50%. The concentrations of $PM_{2.5}$ and PM_{10} measured therefore do include particles with aerodynamic diameters greater than 2.5 μm and 10 μm, but these particles are collected with lower efficiency than those particles smaller than the respective diameters (Vincent, 2005). The WHO Review of

the Health Aspects of Air Pollution (REVIHAAP, 2013) concludes that the long-term health effects are not simply the sum of short-term effects, and risk estimates are much higher for long-term exposure studies. PM is comprised of various components with different chemical and physical properties with potentially different degrees of health effects (Heal et al., 2012). However, the WHO, and the UK Committee on the Medical Effects of Air Pollution (COMEAP) conclude that there is currently insufficient evidence to differentiate the constituents of $PM_{2.5}$ which are more closely associated with different health effects (COMEAP, 2015; REVIHAAP, 2013). REVIHAAP recommends that long-term human health-relevant PM exposure is quantified through annual average $PM_{2.5}$ and PM_{10} concentrations. Both fine and coarse fractions of PM have been associated with distinct health effects (Heal et al., 2012). REVIHAAP (2013) concludes that health benefits would result from any reduction in PM.

The UK Automatic Urban and Rural Network (AURN) has approximately 70 sites (Eaton, 2013), ranging from kerbside to rural background classifications, which make hourly measurements of both $PM_{2.5}$ and PM_{10} (AQEG, 2012). Harrison et al. (2012) and AQEG (2012) analysed temporal and spatial patterns of $PM_{2.5}$ concentrations across this network in 2009 and 2010 respectively, including covariance with other pollutants and with wind speed and direction. Harrison et al. (2012) showed that highest $PM_{2.5}$ concentrations generally occurred in winter, and high concentrations were associated with easterly winds transporting air masses from mainland European emission sources, rather than the direction of local traffic, demonstrating the substantial regional contribution to $PM_{2.5}$ concentrations in the UK. AQEG (2012) presented analysis in relation to annual mean $PM_{2.5}$ concentrations, i.e. the long-term impact on human health. Across sites in 2010, winter had the largest seasonal contribution to annual mean. Both wintertime and summertime high $PM_{2.5}$ episodes, produced by build-up of local emissions during stagnant conditions, and transport of secondary PM from continental Europe, respectively, also made a ‘not insignificant contribution’.

At the two rural UK European Monitoring and Evaluation Programme (EMEP) supersites, Harwell (SE England) and Auchencorth (SE Scotland), measurements of $PM_{2.5}$ and PM_{10} are supplemented by measurements of different PM constituents (summarised in Table 6.1), including 8 inorganic ions, organic and elemental carbon, heavy metals and polycyclic aromatic hydrocarbons (PAHs). These additional measurements allow further investigation of variation of different PM constituents and sources that result in variation in total PM_{10} and $PM_{2.5}$. The 8 inorganic ions include the secondary inorganic aerosol (SIA) components nitrate (NO_3^-), ammonium (NH_4^+) and sulphate (SO_4^{2-}), which are formed by the chemical transformation of gaseous NO_x, NH_3 and SO_2 emissions (Vieno et al., 2014). The other measured inorganic ions are components of sea salt, chloride (Cl^-), sodium (Na^+) and magnesium (Mg^{2+}), plus calcium (Ca^{2+}), which derives from dust emissions, and potassium (K^+) which is emitted from biomass burning and as a component of dust emissions (Pio et al., 2008; Viana et al., 2008). The carbonaceous components are elemental carbon (EC), which is emitted during the incomplete combustion of fossil fuels and biomass burning, and organic carbon (OC) which derives from both primary emission and secondary formation from volatile (and semi-volatile) organic compound emissions (Harrison and Yin, 2008). The measured heavy metals and PAHs have a diverse range of sources and measurements have been shown previously to be useful for source apportionment (Galarneau, 2008; Querol et al., 2007).

Some of these measurements have been analysed previously. For example, Twigg et al. (2015) showed that PM_{10} during high concentration episodes at Auchencorth was comprised predominantly of secondary inorganic aerosol components, whereas lower PM_{10} concentration periods had a substantially larger relative contribution from sea salt. The focus of this work is to integrate the measurements of total $PM_{2.5}$ and PM_{10} with the suite of PM component measurements using the chemical climatology framework so as to understand the severity and conditions producing the long-term human health impact of PM. The ‘impact’ in this study is quantified using the annual average PM_{10} and $PM_{2.5}$ metrics. The ‘state’ identifies the contributions from different PM concentrations, to understand the relative importance of infrequent high vs

frequent moderate concentrations. The monthly contribution, and the composition of PM during each of these concentrations, gives further insight into the pollutant variation giving rise to the health impact. The 'drivers' are investigated using 4-day air-mass back trajectories to quantify differences in the number of hours spent over different geographic regions. Principal component analysis (PCA) is used to assess the contribution of short vs long range transport in determining the contribution of the major PM constituents. Finally, variation in the concentrations of heavy metals in PM_{10} are used to indicate variation in the contribution from different source activities.

Table 6.1: PM constituents used in analysis of the long-term health impact of PM at Harwell and Auchencorth between 2010 and 2013, including annual data capture (N.M. indicates that the component was not measured during that year, while N.D. indicates that the data was not available). Data capture is calculated as the proportion of hours in the whole year with either a valid measurement, or a measurement below the limit of detection.

PM component	Freq.	Har 2013	Har 2012	Har 2011	Har 2010	Auch 2013	Auch 2012	Auch 2011	Auch 2010
PM_{10}	Hourly	53%	97%	80%	77%	59%	92%	80%	69%
$PM_{2.5}$	Hourly	57%	97%	94%	99%	61%	93%	99%	70%
Nitrate (NO_3^-) in PM_{10}	Hourly	87%	41%	N.D.	N.D.	83%	61%	N.D.	N.D.
Sulphate (SO_4^{2-}) in PM_{10}	Hourly	85%	47%	N.D.	N.D.	83%	61%	N.D.	N.D.
Ammonium (NH_4^+) in PM_{10}	Hourly	87%	68%	N.D.	N.D.	83%	67%	N.D.	N.D.
Chloride (Cl^-) in PM_{10}	Hourly	95%	50%	N.D.	N.D.	83%	56%	N.D.	N.D.
Sodium (Na^+) in PM_{10}	Hourly	93%	68%	N.D.	N.D.	79%	68%	N.D.	N.D.
Calcium (Ca^{2+}) in PM_{10}	Hourly	93%	68%	N.D.	N.D.	82%	70%	N.D.	N.D.
Magnesium (Mg^{2+}) in PM_{10}	Hourly	93%	68%	N.D.	N.D.	86%	70%	N.D.	N.D.
Potassium (K^+) in PM_{10}	Hourly	93%	67%	N.D.	N.D.	86%	70%	N.D.	N.D.
Nitrate (NO_3^-) in $PM_{2.5}$	Hourly	89%	41%	N.D.	N.D.	77%	55%	N.D.	N.D.
Sulphate (SO_4^{2-}) in $PM_{2.5}$	Hourly	86%	47%	N.D.	N.D.	73%	53%	N.D.	N.D.
Ammonium (NH_4^+) in $PM_{2.5}$	Hourly	89%	67%	N.D.	N.D.	62%	48%	N.D.	N.D.
Chloride (Cl^-) in $PM_{2.5}$	Hourly	96%	49%	N.D.	N.D.	81%	52%	N.D.	N.D.
Sodium (Na^+) in $PM_{2.5}$	Hourly	95%	66%	N.D.	N.D.	74%	60%	N.D.	N.D.
Calcium (Ca^{2+}) in $PM_{2.5}$	Hourly	95%	66%	N.D.	N.D.	70%	47%	N.D.	N.D.
Magnesium (Mg^{2+}) in $PM_{2.5}$	Hourly	95%	67%	N.D.	N.D.	77%	57%	N.D.	N.D.
Potassium (K^+) in $PM_{2.5}$	Hourly	95%	66%	N.D.	N.D.	74%	57%	N.D.	N.D.
Elemental Carbon (EC) in PM_{10}	Daily	87%	84%	86%	N.M.	N.M.	N.M.	N.M.	N.M.
Organic Carbon (OC) in PM_{10}	Daily	87%	84%	86%	N.M.	N.M.	N.M.	N.M.	N.M.
Elemental Carbon (EC) in $PM_{2.5}$	Weekly	88%	98%	N.M.	N.M.	90%	94%	N.M.	N.M.
Organic Carbon (OC) in $PM_{2.5}$	Weekly	88%	98%	N.M.	N.M.	90%	94%	N.M.	N.M.
25 Heavy Metals in PM_{10}	Weekly	100%	98%	93%	100%	92%	100%	98%	100%
25 Polycyclic Aromatic Hydrocarbons (PAHs)	Monthly	100%	100%	100%	100%	100%	100%	100%	100%

This chapter demonstrates the value added to measurement data when integrated together to investigate a specific impact and how it can be mitigated (It is noted that separate analyses of a subset of the measurements can also provide other useful conclusions, as shown by Twigg et al. (2015) and Harrison et al. (2012)). The interpretation of the less frequently monitored components (in terms of time resolution and number of measurement sites) places these measurements in a wider context. Across Europe, there is a greater density of sites which measure only PM_{10} and $PM_{2.5}$. A subset of the standard chemical climate statistics outlined in this work can be applied to those sites to spatially compare the conditions which produce the long-term PM health impact. Fewer measurement sites have concurrent measurements of PM and components. It is therefore important for these datasets to be integrated into the network-wide assessment of long term health impact of PM, as well as with the other measurements at the same monitoring site. Additional statistics use the PM composition measurements to assess the state of the chemical climate, and therefore incorporate the composition of PM with total mass PM measurements. A widespread derivation of the chemical climate statistics outlined here would increase the ability of monitoring networks to contribute to the understanding of the long term health impact of PM, and how it might most effectively be reduced.

6.2 Methods

The PM and constituent datasets were obtained from the publically available UK Department for Environment, Food and Rural Affairs (Defra) UK-Air (http://uk-air.defra.gov.uk/) and the Norwegian Institute for Air Research (NILU) maintained EBAS (ebas.nilu.no) data repositories. The measurement and data quality procedures are detailed in Braban et al. (2012), Brown et al. (2013b), Sarantaridis et al. (2013), and Eaton (2013). Chemical climate statistics were calculated on measurements, where available, between 2010 and 2013. The main focus was 2012 and 2013 due to the larger number of concurrent measurements. The data capture for the components of PM_{10} and $PM_{2.5}$ measured at Harwell and Auchencorth in 2012 and 2013 are listed in Table

6.1. At Harwell, there was low data capture for the inorganic ions in 2012, especially NO_3^-, and low data capture for PM_{10} (50%) and $PM_{2.5}$ (48%) in 2013. The inorganic ions make the largest contribution to total PM and therefore to effectively demonstrate the utility of the chemical climate statistics, concurrent measurements of PM and the inorganic ions were required. To achieve this, a proxy PM_{10} and $PM_{2.5}$ dataset was constructed for 2013 through comparison of PM measurements at Harwell and a nearby urban background site in Reading, approximately 20 km from Harwell. The data captures at Reading were 92% and 90% for PM_{10} and $PM_{2.5}$ respectively in 2013, and the linear regression equation for the Reading and Harwell data was statistically significant for PM_{10} and $PM_{2.5}$ (Figure 6.1). These equations were used to adjust the Reading dataset to estimate the PM_{10} and $PM_{2.5}$ concentrations at Harwell in 2013. At Auchencorth, PM_{10} and $PM_{2.5}$ data capture was substantially higher in 2012 than 2013, while the data capture of the inorganic ions was higher in 2013. In the absence of a suitable proxy site, 2012 was used as the example year at Auchencorth to ensure the accurate determination of chemical climate statistics derived using the PM_{10} and $PM_{2.5}$ time series. The following sections describe the impact (Section 6.2.1), state (Section 6.2.2) and drivers (Section 6.2.3) statistics of the long-term PM health chemical climate. A summary of the statistics used is given in Table 6.2.

6.2.1 Impact metric

The long-term health relevant PM metrics were the annual average PM_{10} and $PM_{2.5}$ concentrations, henceforth abbreviated to PM_{10AA} and $PM_{2.5AA}$ respectively. The measurement method, the TEOM-FDMS instrument, was limited by the fact that at low concentrations some measurements were recorded as negative values. The TEOM-FDMS instrument calculates the non-volatile and volatile components of PM separately in two measurement cycles. The volatile component of PM is calculated based on the mass lost from a filter sample during a 6-minute cycle. However, mass can also be adsorbed to the sample during that period, and at low PM concentrations this can exceed the volatile PM lost and result in a negative PM concentration (AQEG,

2012). This was most limiting for $PM_{2.5}$ measurements at Auchencorth (11% of measurements in 2012, as highlighted by Twigg et al. (2015)). The negative values were included in the calculation of the annual mean due to uncertainties (i.e. shifting the PM concentration distribution) introduced when attempting to account for the negative values by either excluding them or setting them to zero.

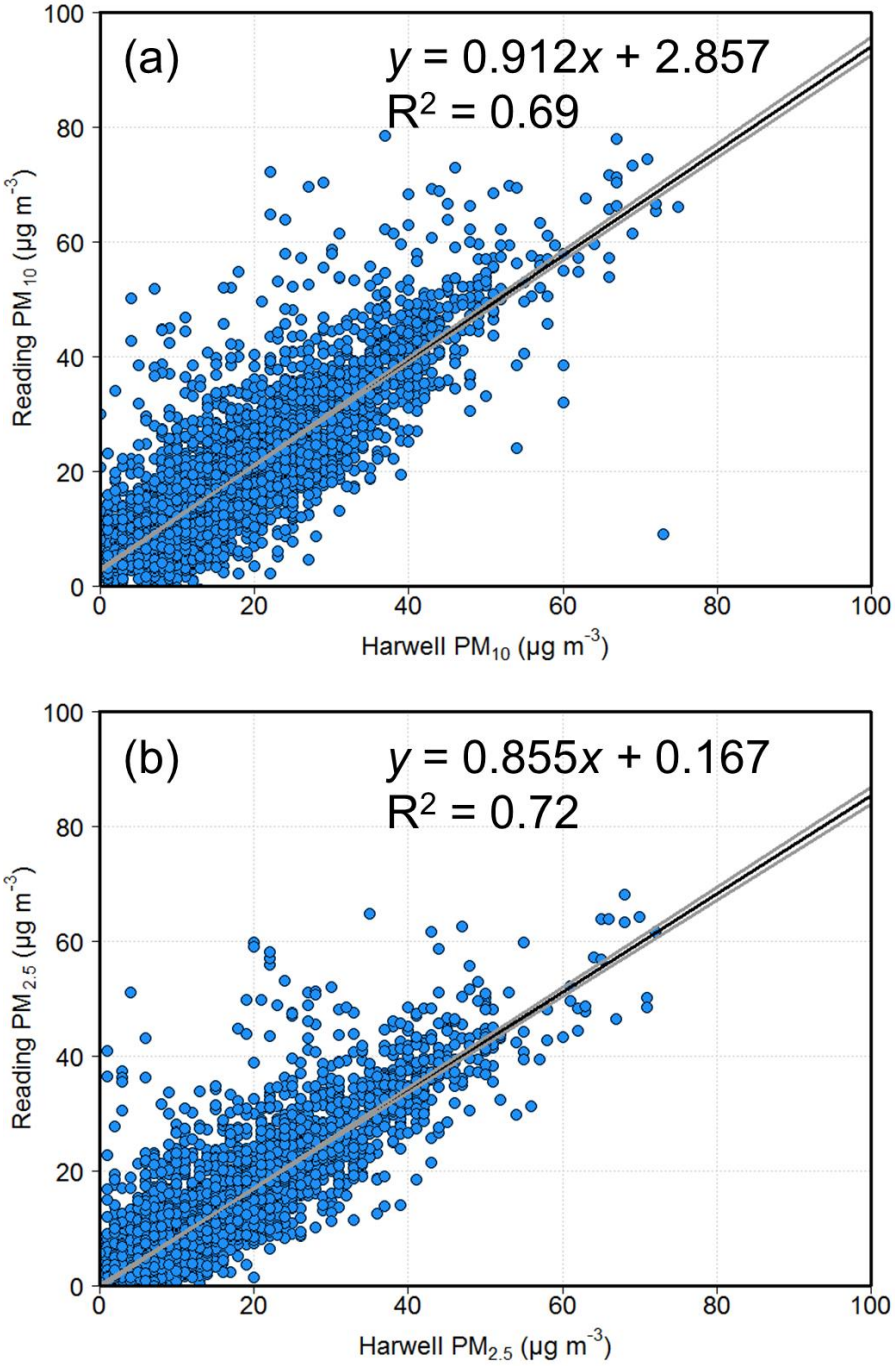

Figure 6.1: Correlation between a) Harwell PM_{10} vs Reading PM_{10} and b) Harwell $PM_{2.5}$ vs Reading $PM_{2.5}$. Hourly-averaged values in each case.

Table 6.2: Statistics derived to quantify the 'impact', 'state' and 'drivers' of the chemical climate specific to the long-term human health impact of PM.

Chemical Climate Component	Statistic	Further Description
Impact	Annual average PM_{10} (PM_{10AA}, μg m^{-3}) Annual average $PM_{2.5}$ ($PM_{2.5AA}$, μg m^{-3})	WHO REVIHAAP (2013) recommends quantification of long-term PM health impact using both PM_{10} and $PM_{2.5}$ size fractions due to distinct observed health impacts of fine and coarse PM
State	Contribution to PM_{10AA} and $PM_{2.5AA}$ for 20 × 5-percentile bins from 0-5th percentile to 95-100th percentile.	
	Contribution to PM_{10AA} and $PM_{2.5AA}$ from 1 μg m^{-3} concentration bins	
	Monthly contribution to PM concentrations in 1 μg m^{-3} concentration bins	
	Average PM composition for PM concentrations in 1 μg m^{-3} concentration bins	
Drivers	Contribution from geographic regions to PM concentrations in 1 μg m^{-3} concentration bins	Calculated using cluster analysis of 4-day back trajectories based on the number of hours each trajectory spent in Marine, UK, Ireland, Iceland, Eastern, Western, Northern, Southern Europe and Other regions.
	'Contribution distribution': Contribution of 1 μg m^{-3} PM_{10} and $PM_{2.5}$ concentration bins to annual average PM component concentrations. Contribution from each concentration bin separated by geographic region clusters.	
	Principal component analysis of inorganic ions	Identifies relative influence of short vs long-range transport in determining concentrations of major PM constituents
	Correlation matrix of 25 heavy metals	Groupings of highly correlated heavy metals indicate different source sectors

6.2.2 State

6.2.2.1 Total PM mass

The state statistics for PM_{10} and $PM_{2.5}$ measurements were calculated using the hourly data, as well as daily averages for comparison with measurements of EC and OC. The contributions from 20 × 5-percentile bins to PM_{10AA} and $PM_{2.5AA}$ was calculated to assess the contribution from different parts of the PM concentration distribution at each site. Secondly, the contributions of 1 μg m^{-3} concentration bins to PM_{10AA} and $PM_{2.5AA}$ was calculated to investigate the accumulation of the annual average across different absolute PM concentration ranges. Within each of the concentration bins, the proportion of those concentrations derived in each month of the year was calculated.

6.2.2.2 PM composition

For each chemical component measured at Harwell and Auchencorth (Table 6.1), the annual mean and contribution to PM_{10AA} or $PM_{2.5AA}$ was calculated. The fraction of SO_4^{2-} derived from sea salt (ss-SO_4^{2-}) was calculated using Equation 6.1 for each time step, while the non-sea salt SO_4^{2-} (nss-SO_4^{2-}) fraction was the difference between the measured SO_4^{2-} concentration and the ss-SO_4^{2-} concentration (Twigg, 2015). In the derivation of chemical climate statistics, ss-SO_4^{2-} and nss-SO_4^{2-} were treated at separate PM constituents.

$$[ssSO_4^{2-}] = 0.252\ x\ [Na^+] \quad (6.1)$$

A substantial number of the PM component time series had concentrations below the instrument limit of detection (LOD). Therefore the Kaplan-Meier (KM) method was used to estimate the distribution of component concentration within a given year, accounting for values below the limit of detection (She, 1997). The annual mean derived from the KM method was used as the annual mean. Similarly, the KM method

was used to calculate the average concentration for each component for each PM_{10} or $PM_{2.5}$ 1 µg m^{-3} concentration bin.

6.2.3 Drivers

The geographic drivers of this chemical climate were investigated using 4-day air-mass back trajectories arriving at hourly intervals at Harwell and at Auchencorth. Many studies have previously used cluster analysis to group trajectories based on the similarity of the trajectory pathway prior to arrival at the site (as reviewed by Fleming et al., 2012). However, small variation in the trajectory pathway can affect the source regions traversed. In this study cluster analysis was used to group air mass back trajectories, but each trajectory was described by the number of hours spent over different geographic regions, rather than the location of the trajectory at points along the pathway. For each trajectory (at each site), the number of hours spent above marine locations, the UK, Ireland, Iceland, Northern Europe, Eastern Europe, Southern Europe, Western Europe and Other (generally the USA and Canada for Harwell and Auchencorth) was recorded. The countries belonging to each region of Europe were defined using the United Nations Statistics Division (http://unstats.un.org/unsd/methods/m49/m49regin.htm), except that Ireland, Iceland and the UK were extracted to create their own geographic regions. For each year at each site, Ward's method hierarchical cluster analysis was used to group trajectories based on the similarity of the time spent over each geographic source region (Mangiameli et al., 1996; Ward, 1963). Trajectory separation was defined using the Euclidean distance (Kaufman and Rousseeuw, 1990). The aim of the clustering was to identify groups of trajectories which spend a distinctive number of hours within each geographic region compared to trajectories belonging to other clusters, and the dendrogram summarising the linkages between trajectories revealed five groupings. The number of hours (out of 96) spent in the different regions for each 'trajectory cluster' at Harwell in 2013 and at Auchencorth in 2012 are summarised in Figures 6.2 and 6.3 respectively. The five clusters arriving at Harwell in 2013 were named

'Marine', 'Marine-UK', 'Western Europe', 'UK' and 'Northern Europe'. At Auchencorth in 2012 the distinctive differences between trajectory clusters resulted in clusters named 'Marine', 'Marine-Other', 'UK', 'Western/Eastern Europe' and 'Northern Europe'. While the cluster names identify the geographic region which trajectories spend an anomalously high number of hours traversing for that cluster, Figures 6.2 and 6.3 show that some of the clusters have contributions from multiple regions. For example, at Harwell trajectories belonging to the Western Europe cluster also spend an average of 10 hours over the UK (Figure 6.2). The contribution of each trajectory cluster for concentrations in each 1 μg m^{-3} concentration bin was calculated. Additionally, for each PM constituent, the contribution to the component annual average from each cluster was calculated. This contribution was further separated into the contribution for each 1 μg m^{-3} PM_{10} or $PM_{2.5}$ concentration bin. This process yielded the different 'contribution distributions' for each PM constituent for each trajectory cluster.

Principal component analysis (PCA) was applied to the dataset of 9 inorganic ions (ss-SO_4^{2-} and nss-SO_4^{2-} were separate components). The aim of PCA is to reduce the dimensionality of the dataset and explain maximum variance in as few variables (Principal Components (PC)) as possible (e.g. Bro and Smilde, 2014). It has been used previously on PM composition data to identify the contribution of different sources (Belis et al., 2013). Firstly, the component time series were standardised so each explained an equal proportion of variance within the entire dataset. The components were positively skewed and were therefore natural-log transformed and standardised so that the mean was 0 and the variance 1. PCA was performed on this dataset using the R statistical software (R Core Team, 2014). The output from the PCA analysis was a set of 9 PCs, and a time series with a value for each of the PCs at each time step. Each PM constituent had a loading for each PC. The value of each PC determines the contribution of that PC to constituent concentrations at that time step. The relative loading of the PM constituents determines the level of correlation (and anti-correlation) between constituents for that PC. For example, a large value for a PC at a given time step will result in higher percentile concentrations for all those components

with high loadings for that PC. The first PC (PC1) explained the most variance, PC2 explained the most variance not explained by PC1 etc. The majority of the variability in the data at each site in each year was explained by PC1 and PC2. The loadings indicated that PC1 quantified the contribution to secondary inorganic aerosol (SIA) from short-range transport, and PC2 from long-range transport (this is further discussed in Section 6.3.3). To investigate the contribution of short and long-range transport during different trajectory clusters, the values of PC1 and PC2 at each time step were apportioned in 20 × 5-percentile bins. The proportion of values from each percentile bin for PC1 and PC2 during each trajectory cluster was calculated.

Heavy metals are constituents of PM which have been used as a method for source apportionment (Querol et al., 2007). Viana et al. (2008) summarise the characteristic PM composition from different source activities including 'vehicle exhaust', 'oil combustion' and 'mineral/city dust' which have heavy metal contributions. At Harwell and Auchencorth 25 heavy metals were measured at weekly time resolution between 2010 and 2013 (Brown et al., 2013b). Due to the substantially fewer annual measurement records from weekly sampling, the 2010-2013 period was analysed together to maximise the information derived from the time series. A correlation matrix was calculated using the Openair package in the R statistical software to identify distinct groups of heavy metals with high covariance between each other relative to the other heavy metals (Carslaw and Ropkins, 2012; R Core Team, 2014). Once identified, the conditions resulting in different concentrations of these heavy metals were calculated to investigate the conditions under which specific source activities may contribute to the long-term PM health impact. For each heavy metal, the range of concentrations were divided in 20 equal groups. In each of these concentration bins the following statistics were calculated: the contribution to the four-year average heavy metal concentration, the frequency of occurrence, the proportion occurring in each month, the average PM_{10} concentration, and the proportion of trajectory hours spent in each geographic region.

Polycyclic aromatic hydrocarbons were also measured at Harwell and Auchencorth, and their contribution to PM_{10AA} was calculated. Measurements of PAHs have previously been used for source apportionment based on characteristic ratios of PAHs associated with different source activities (Galarneau, 2008). However, it was not considered appropriate in this study given that measurements at Harwell and Auchencorth had monthly time resolution, and each site is classified as rural background. Hence over a monthly time scale at a rural background site, a large number of different source regions impact upon the atmospheric composition at the site. It was therefore not possible to extract contributions from individual source activities based on characteristic PAH ratios.

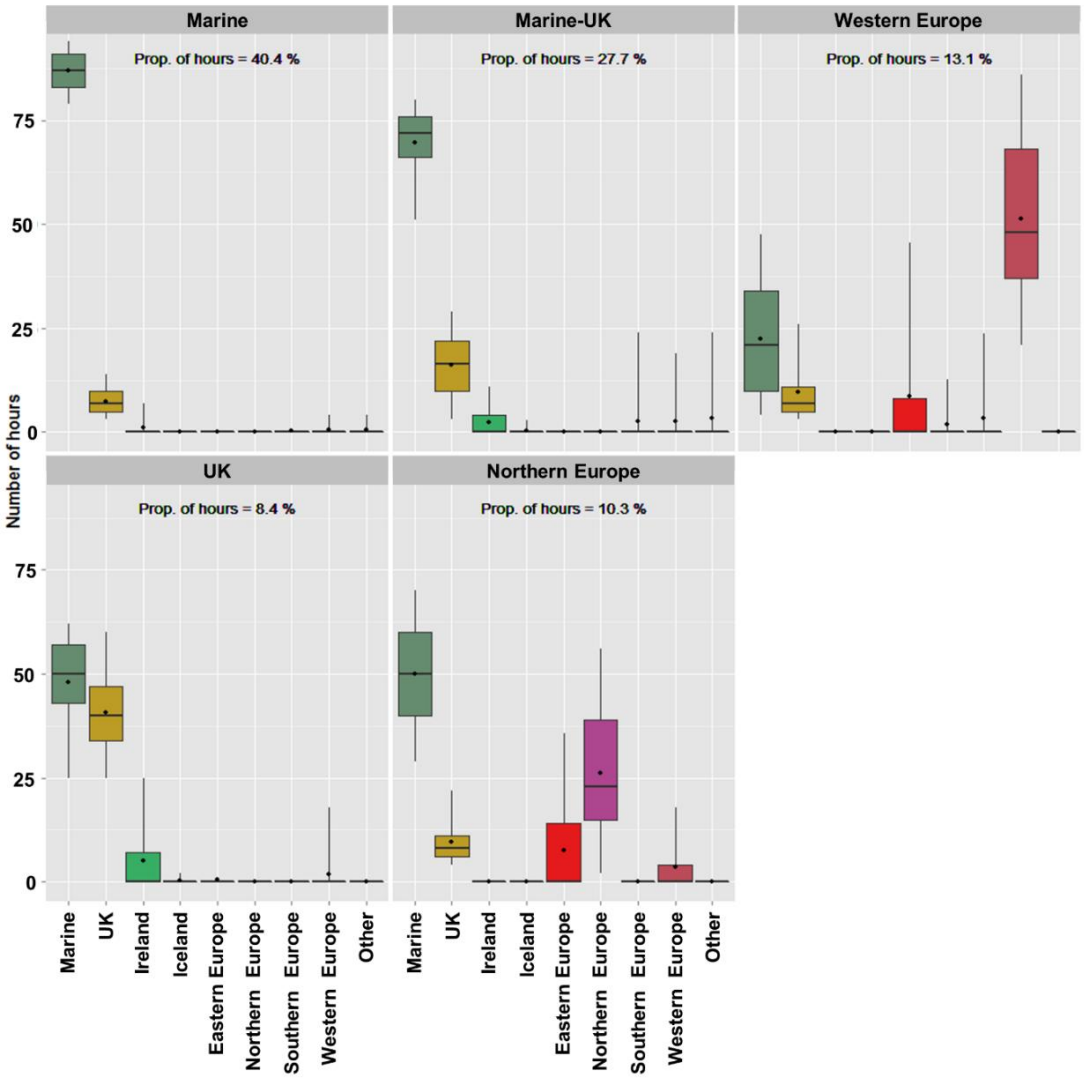

Figure 6.2: Number of hours spent in different geographic regions for each of the air-mass back trajectory clusters arriving at Harwell in 2013.

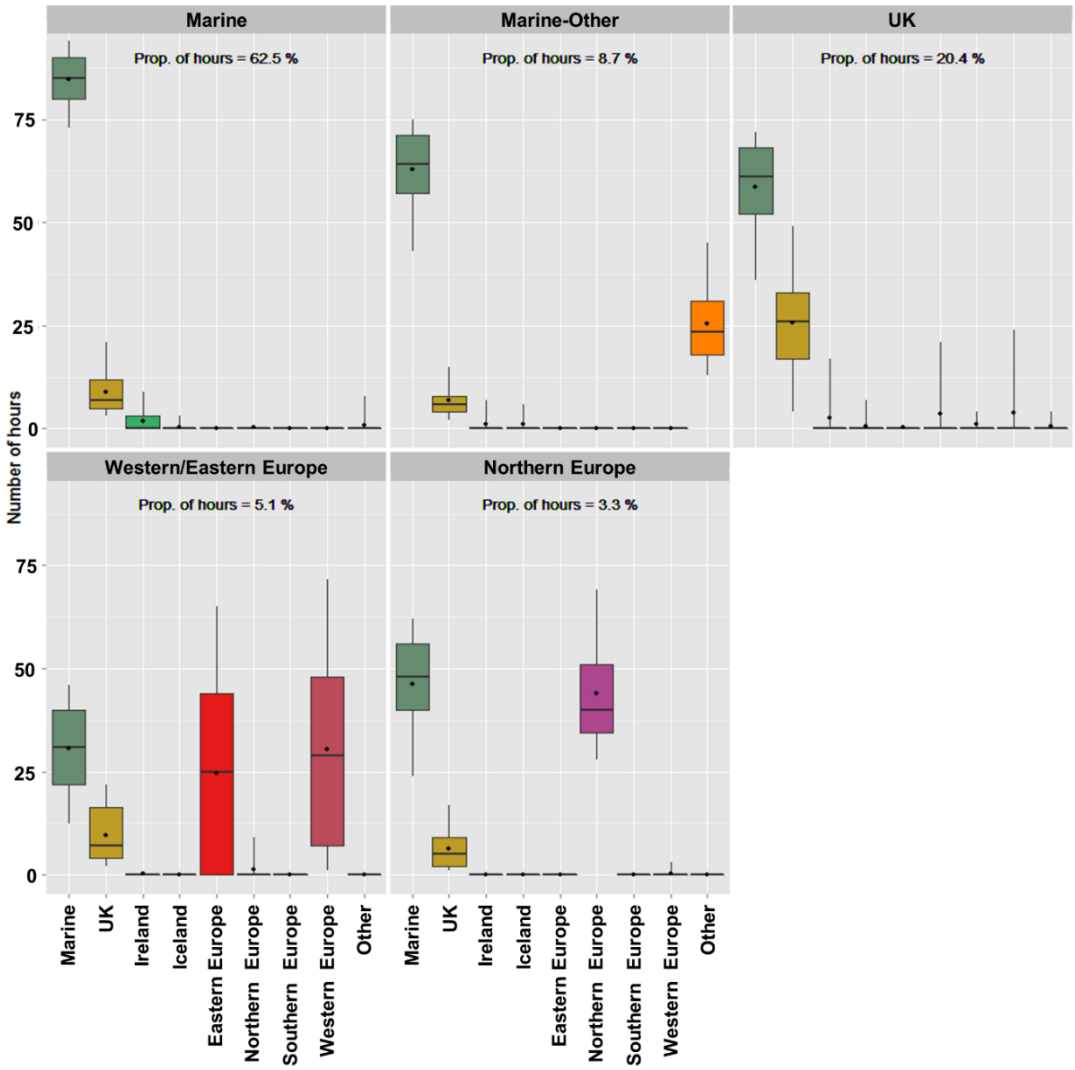

Figure 6.3: Number of hours spent in different geographic regions for each of the air-mass back trajectory clusters arriving at Auchencorth in 2012.

6.3 Results

6.3.1 Long-term PM health impact

The average ± 1 std. dev. annual average total PM_{10} and $PM_{2.5}$ (PM_{10AA} and $PM_{2.5AA}$ respectively) between 2010 and 2013 was 16.4 ± 1.4 µg m^{-3} and 11.9 ± 1.1 µg m^{-3} respectively at Harwell and 7.4 ± 0.4 µg m^{-3} and 4.1 ± 0.2 µg m^{-3} at Auchencorth (Table 6.3). As described previously, PM values at Harwell for 2013 were derived from adjusted PM concentrations from the nearby Reading monitoring site. The averages for Auchencorth includes years where data capture was below 75%. Whilst the inclusion of these years introduces uncertainty, given the small number of years available their inclusion was necessary to provide an indication of the variability in PM_{10AA} and $PM_{2.5AA}$. The $PM_{2.5AA}$ accounted for a larger proportion of PM_{10AA} at Auchencorth than at Harwell. The ratio of $PM_{2.5AA}/PM_{10AA}$ at Harwell was on average 0.73 ± 0.10 at Harwell compared to 0.55 ± 0.02 at Auchencorth. Additionally, the ratio of Harwell PM / Auchencorth PM was on average 2.23 ± 0.29 for PM_{10AA} and 2.93 ± 0.33 for $PM_{2.5AA}$. This indicates that the closer proximity of anthropogenic primary and secondary PM precursor emission sources to Harwell results in a greater increment in $PM_{2.5AA}$ than PM_{10AA} relative to Auchencorth, and hence a greater exacerbation of the health effects associated with $PM_{2.5}$. In comparison with annual average concentrations calculated at 60 sites across Europe (Putaud et al., 2010), the values calculated for Harwell were similar to other rural-background sites, while those at Auchencorth were closer to sites classified as ‘natural background’ located in Scandinavia.

Table 6.3: Annual average concentrations between 2010 and 2013 at Harwell and Auchencorth for PM_{10} and $PM_{2.5}$, and annual average contribution to PM_{10} and $PM_{2.5}$ for inorganic ions, total carbon (organic + elemental carbon), the sum of 25 heavy metals and the sum of 25 PAHs.

	PM	**NO_3^-**	**nssSO_4^{2-}**	**NH_4^+**	**Cl^-**	**Na^+**	**Ca^{2+}**	**ssSO_4^{2-}**	**Mg^{2+}**	**K^+**	**Total Carbon**	**Heavy Metals**	**PAH**
Harwell PM_{10}													
2013 annual average (µg m^{-3})	14.7	3.71	1.79	1.57	1.17	1.14	0.38	0.29	0.24	0.08	2.28	0.17	0.0018
Contribution to PM_{10} average		25.3%	12.2%	10.7%	8.0%	7.8%	2.6%	2.0%	1.6%	0.5%	15.5%	1.2%	0.01%
2012 annual average (µg m^{-3})	16.6	2.92	1.89	1.51	1.17	0.84	0.65	0.21	0.22	0.02	2.14	0.16	0.0019
Contribution to PM_{10} average		17.6%	11.3%	9.1%	7.0%	5.0%	3.9%	1.3%	1.3%	0.1%	12.9%	0.9%	0.01%
2011 annual average (µg m^{-3})	18.1										2.63	0.22	0.0008
Contribution to PM_{10} average											14.5%	1.2%	0.005%
2010 annual average (µg m^{-3})	16.0											0.16	0.0012
Contribution to PM_{10} average												1.0%	0.01%
Harwell $PM_{2.5}$													
2013 annual average (µg m^{-3})	12.5	3.34	1.84	1.57	0.61	0.60	0.22	0.15	0.14	0.06	1.49		
Contribution to $PM_{2.5}$ average		26.7%	14.7%	12.5%	4.8%	4.8%	1.7%	1.2%	1.1%	0.5%	11.9%		
2012 annual average (µg m^{-3})	12.8	2.00	1.51	1.04	0.50	0.41	0.38	0.10	0.12	0.01	1.38		
Contribution to $PM_{2.5}$ average		15.7%	11.8%	8.1%	3.9%	3.2%	3.0%	0.8%	0.9%	0.1%	10.8%		
2011 annual average (µg m^{-3})	11.9												
Contribution to $PM_{2.5}$ average													
2010 annual average (µg m^{-3})	10.3												
Contribution to $PM_{2.5}$ average													
Auchencorth PM_{10}													
2013 annual average (µg m^{-3})	7.94	1.28	0.98	0.74	1.15	0.73	0.06	0.18	0.08	0.07		0.12	0.0008
Contribution to PM_{10} average		16.2%	12.3%	9.3%	14.4%	9.2%	0.8%	2.3%	1.0%	0.8%		1.6%	0.01%
2012 annual average (µg m^{-3})	7.35	1.86	1.22	0.98	1.11	0.85	0.06	0.21	0.06	0.07		0.07	0.0012
Contribution to PM_{10} average		25.3%	16.6%	13.3%	15.1%	11.5%	0.9%	2.9%	0.8%	0.9%		0.9%	0.02%
2011 annual average (µg m^{-3})	7.06											0.08	0.0003
Contribution to PM_{10} average												1.17%	0.004%
2010 annual average (µg m^{-3})	7.12											0.09	0.0004
Contribution to PM_{10} average												1.29%	0.01%
Auchencorth $PM_{2.5}$													
2013 annual average (µg m^{-3})	4.40	1.09	0.88	0.67	0.69	0.45	0.05	0.11	0.05	0.04	0.66		
Contribution to $PM_{2.5}$ average		24.7%	20.0%	15.2%	15.6%	10.1%	1.1%	2.5%	1.1%	1.0%	15.0%		
2012 annual average (µg m^{-3})	3.82	1.58	1.13	0.89	0.62	0.49	0.05	0.12	0.04	0.05	0.66		
Contribution to $PM_{2.5}$ average		41.4%	29.6%	23.3%	16.3%	12.7%	1.2%	3.1%	1.0%	1.2%	17.4%		
2011 annual average (µg m^{-3})	4.01												
Contribution to $PM_{2.5}$ average													
2010 annual average (µg m^{-3})	4.03												
Contribution to $PM_{2.5}$ average													

6.3.2 State

Investigation of the 'state' of the PM human health chemical climate aims to link atmospheric composition variation relevant to the long-term PM health impact metrics (PM_{10AA} and $PM_{2.5AA}$) with causal drivers. These relevant composition variations were grouped into variations in the total PM mass measurements (Section 6.3.2.1), and in the PM chemical composition measurements (Section 6.3.2.2).

6.3.2.1 PM concentrations

The contribution to PM_{10AA} and $PM_{2.5AA}$ from 5-percentile bins in 2012 at Harwell and Auchencorth is shown in Figure 6.4. At each site, mass concentrations greater than the respective 95th percentile at each site contributed a larger proportion of $PM_{2.5AA}$ (17% at Harwell and 31% at Auchencorth in 2012) compared to PM_{10AA} (15% at Harwell and 20% at Auchencorth), and the contribution to both PM_{10AA} and $PM_{2.5AA}$ was larger at Auchencorth than at Harwell (see Figures 6.6-6.8 which detail the absolute concentration of 5th and 95th percentiles at each site). For $PM_{2.5AA}$ at Auchencorth, the negative contributions of the 0-15% bins (a consequence of negative values at low concentration) resulted in greater contribution from the higher percentiles. However, even when the negative values were excluded (which changed the 95th percentile contribution to $PM_{2.5}$ annual average at Auchencorth to 27%) or set to zero (29%), the 95th percentile contribution to $PM_{2.5AA}$ at Auchencorth was substantially larger than to PM_{10AA}.

Assessment of the contribution from absolute concentration ranges showed that the high frequency of moderate PM concentration resulted in a disproportionately high contribution from these concentrations to PM_{10AA} and $PM_{2.5AA}$. The contribution from 1 μg m^{-3} concentration bins to PM_{10AA} and $PM_{2.5AA}$ at Harwell and Auchencorth are shown in Figure 6.5. At Harwell, the largest contribution from a single concentration bin varied between 11-12 and 14-15 μg m^{-3} between 2010 and 2013 for PM_{10AA}, and

between 6-7 and 9-10 µg m^{-3} for $PM_{2.5AA}$. At Auchencorth, the largest contribution varied between 5-6 and 8-9 µg m^{-3} for PM_{10AA} and between 2-3 and 3-4 µg m^{-3} for $PM_{2.5AA}$. For PM_{10AA}, concentrations below 10 µg m^{-3} contributed between 44% and 56% of the annual average at Auchencorth, compared with 13-20% at Harwell. Concentrations below 20 µg m^{-3} accounted for 75-86% of the annual average at Auchencorth, compared to 48-58% at Harwell. Consequently the contribution from higher PM concentrations (> 40 µg m^{-3}) was higher at Harwell, between 10 and 17% compared to between 0.3 and 5% at Auchencorth. Hence, while the 95th percentile concentrations at Auchencorth contributed a larger portion of PM_{10AA} compared to Harwell, the magnitude of the highest concentrations was substantially smaller. For $PM_{2.5AA}$, the main difference compared to PM_{10AA} was a larger contribution from concentrations below 10 µg m^{-3}. At Harwell and Auchencorth the $PM_{2.5AA}$ / PM_{10AA} ratio of contribution from concentrations below 10 µg m^{-3} was on average 2.3 and 1.2 respectively, with 26-39% and 56-66% of the $PM_{2.5AA}$ accumulated below 10 µg m^{-3} at Harwell and Auchencorth. The decrease in $PM_{2.5AA}/PM_{10AA}$ ratio from Harwell to Auchencorth is consistent with the significant decreasing trend in this ratio with distance from the south-east corner of England using observations from a greater number of sites (Harrison et al., 2012).

The distribution of contributions across PM_{10} concentrations is 'flatter' compared with $PM_{2.5}$. The magnitude of the contribution from highest contributing concentration bins was larger at Auchencorth compared to Harwell, although the concentrations with highest contributions differed between sites (Figure 6.5). The single concentration bin with maximum contribution to PM_{10AA} contributed 5.9-8.3% at Auchencorth compared with 3.8-4.1% at Harwell, and 8.4-10.2% for $PM_{2.5AA}$ at Auchencorth compared with 3.7-6.9% at Harwell. Additionally, the contribution from the top five contributing 1 µg m^{-3} concentration bins was between 40% and 97% higher for PM_{10AA} at Auchencorth, and 18-153% higher for $PM_{2.5AA}$. There was also a larger contribution from the highest contributing concentrations to $PM_{2.5AA}$ compared with PM_{10AA}. In this case, the proportion of annual average contribution by the top five 1 µg m^{-3}

concentration bins was on average 15% and 17% greater for $PM_{2.5AA}$ at Harwell and Auchencorth respectively between 2010 and 2013.

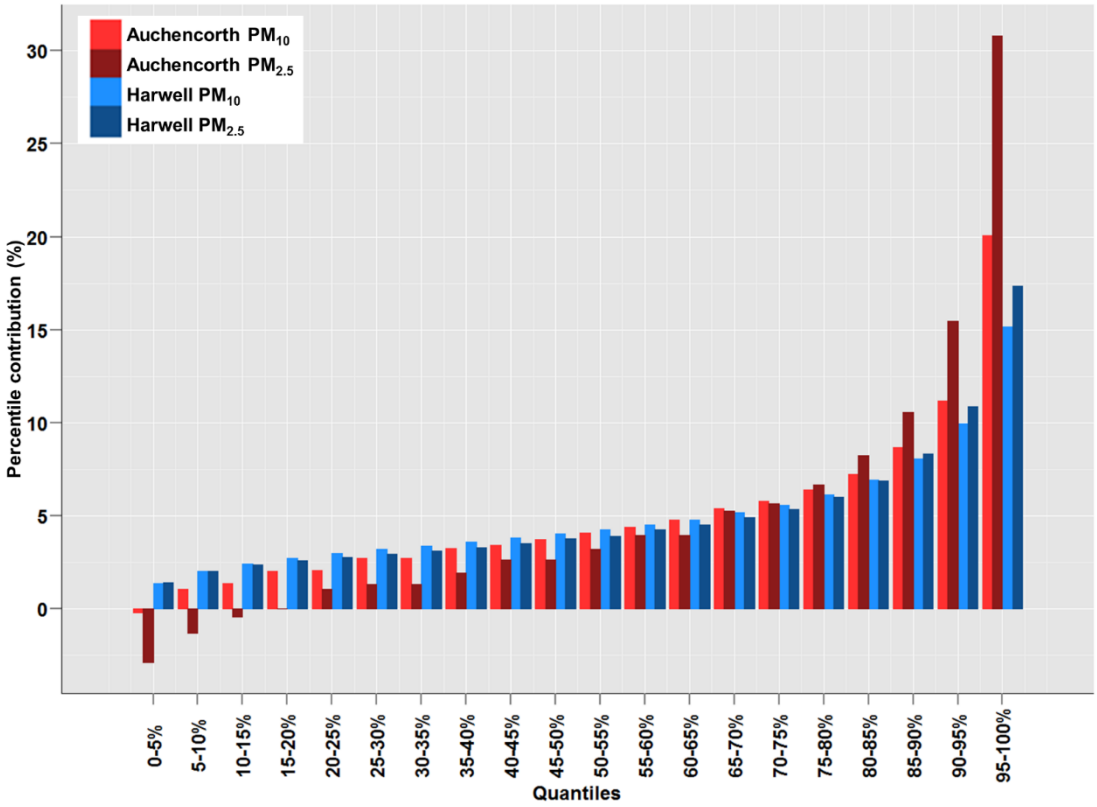

Figure 6.4: Contribution of 20 × 5-percentile bins to PM_{10AA} and $PM_{2.5AA}$ at Harwell and Auchencorth in 2012.

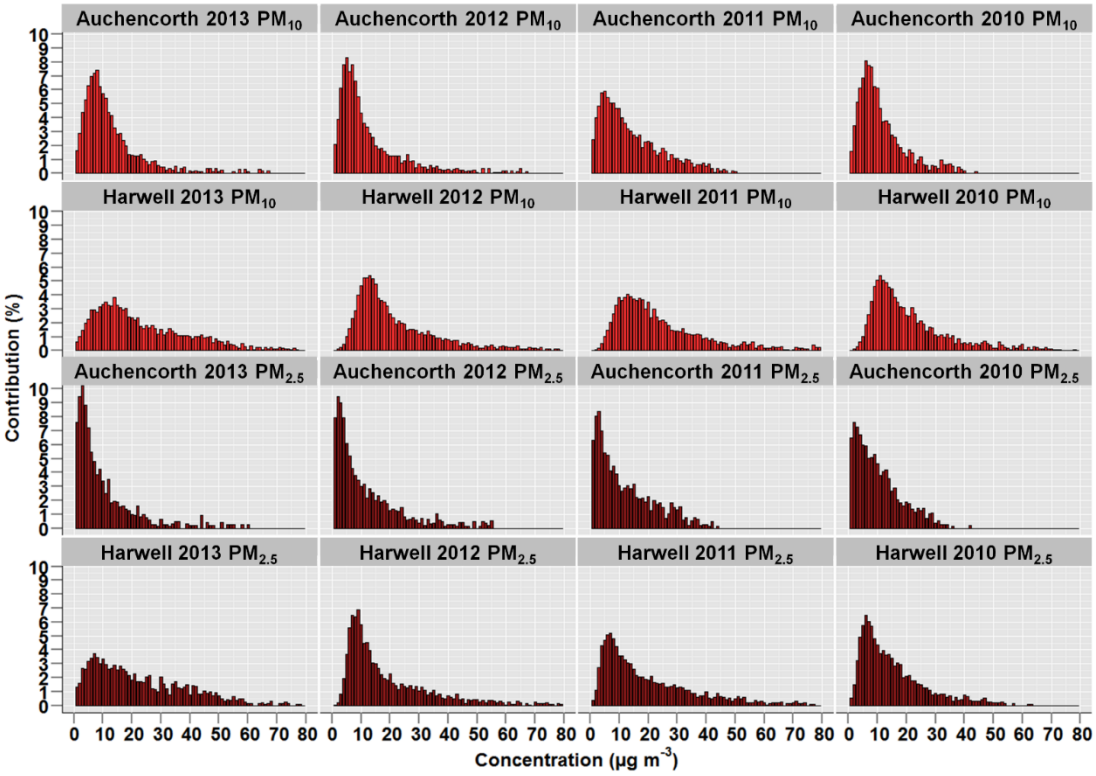

Figure 6.5: Contribution of 1 µg m^{-3} concentration bins to PM_{10AA} and $PM_{2.5AA}$ at Harwell and Auchencorth between 2010 and 2013.

Figures 6.6 and 6.7 summarise the 'state' of this chemical climate in 2013 at Harwell for PM_{10} and $PM_{2.5}$ respectively, and Figure 6.8 for PM_{10} Auchencorth in 2012, including the monthly contribution to measurements within each concentration bin. For the highest-contributing concentrations to PM_{10AA} and $PM_{2.5AA}$ at each site, there was a similar contribution across the year. At Harwell, the average contribution to PM_{10AA} and $PM_{2.5AA}$ from each season for the five highest contributing concentration bins was 28%, 20%, 28% and 24% for spring, summer, autumn and winter respectively for PM_{10} (Figure 6.6), and 21%, 30%, 27% and 21% for $PM_{2.5}$ (Figure 6.7). At Auchencorth, the average contribution to PM_{10AA} and $PM_{2.5AA}$ during the five highest contributing concentration bins was 18%, 31%, 29% and 22% for spring, summer, autumn and winter respectively for PM_{10} (Figure 6.8), and 24%, 35%, 20% and 21% for $PM_{2.5}$. At both sites, the contribution from summer months to the highest contributing concentrations was larger for $PM_{2.5AA}$ compared to PM_{10AA}. As concentrations increase, the contribution from spring, and winter became larger and the majority of the highest PM_{10} and $PM_{2.5}$ concentrations occurred in these seasons. This result supports work by Harrison et al. (2012), who calculated monthly-average concentrations for 37 sites across the UK in 2009. Winter and spring months had the highest concentrations across all UK regions.

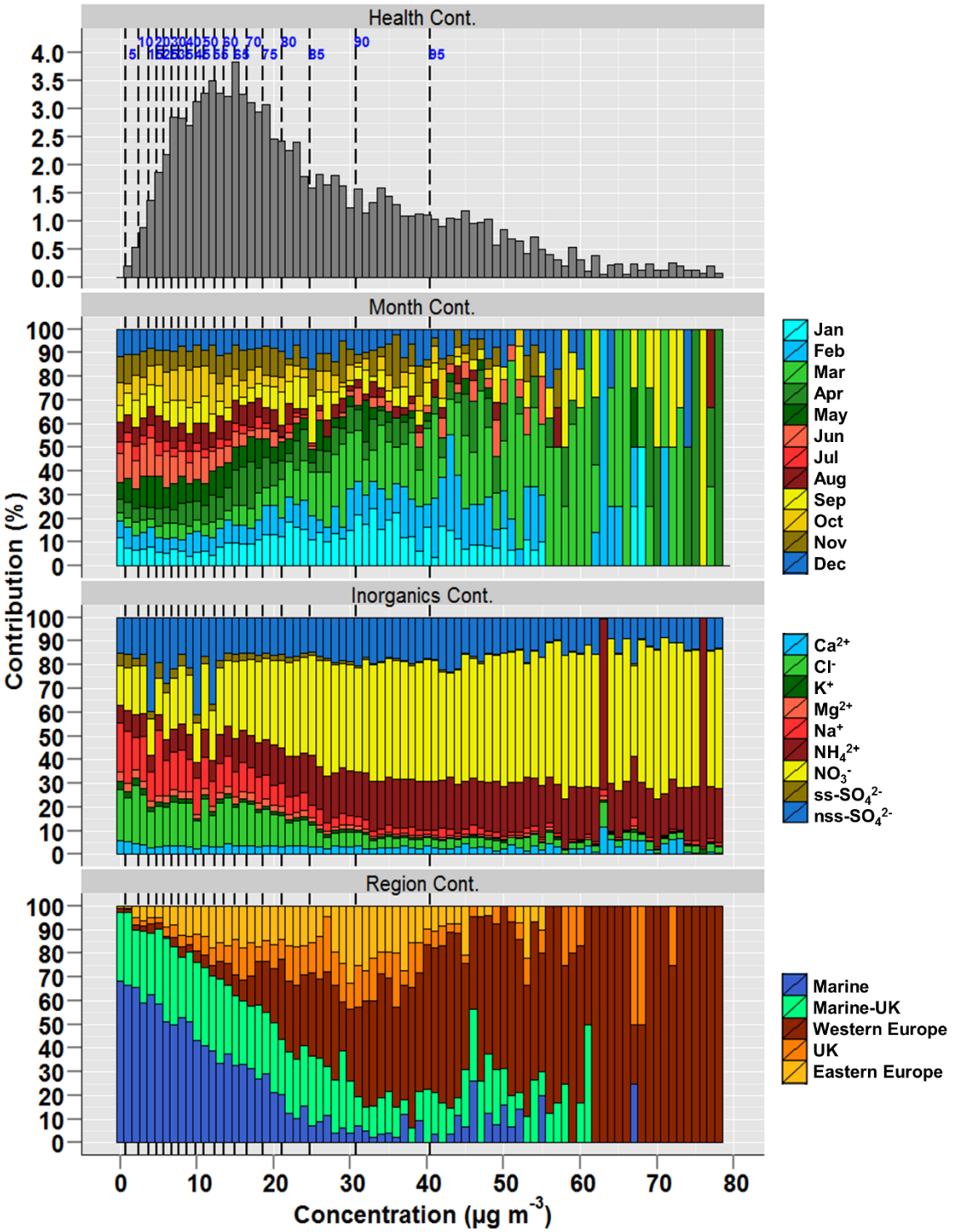

Figure 6.6: Contribution to annual average PM_{10} (PM_{10AA}) from PM_{10} concentrations segmented into 1 µg m^{-3} bins at Harwell in 2013. The vertical dashed lines indicate the concentrations of percentiles from the 5th to the 95th percentile in 5 percent steps. The proportion of concentrations within each bin from the different months of the year, the contribution from 9 inorganic ions to total inorganic ion concentrations and the contribution from different trajectory clusters are also shown.

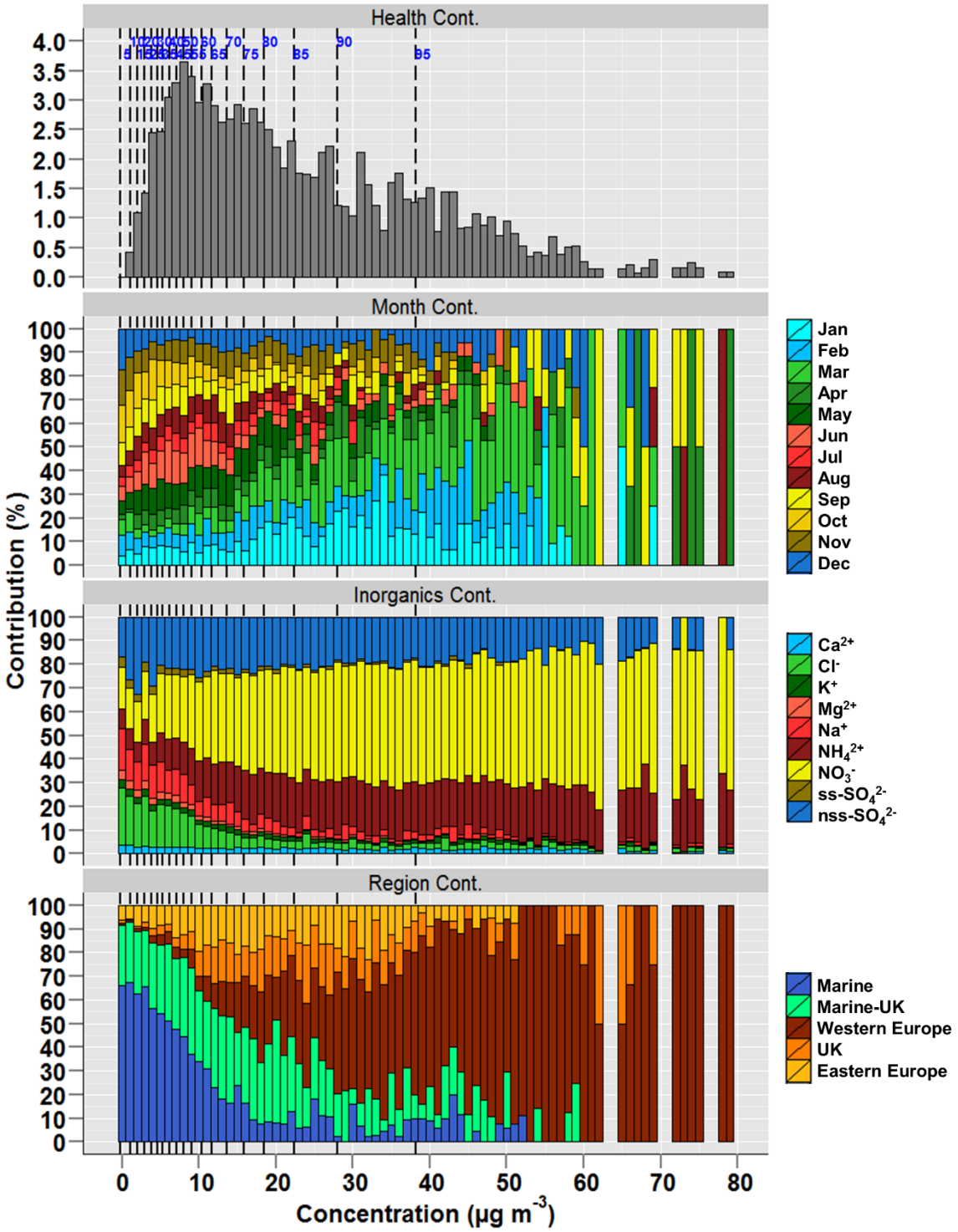

Figure 6.7: Contribution to annual average $PM_{2.5}$ ($PM_{2.5AA}$) concentrations segmented into 1 µg m^{-3} bins at Harwell in 2013. The vertical dashed lines indicate the concentrations of percentiles from the 5th to the 95th percentile in 5 percent steps. The proportion of concentrations within each bin from the different months of the year, the contribution from 9 inorganic ions to total inorganic ion concentrations and the contribution from different trajectory clusters are also shown.

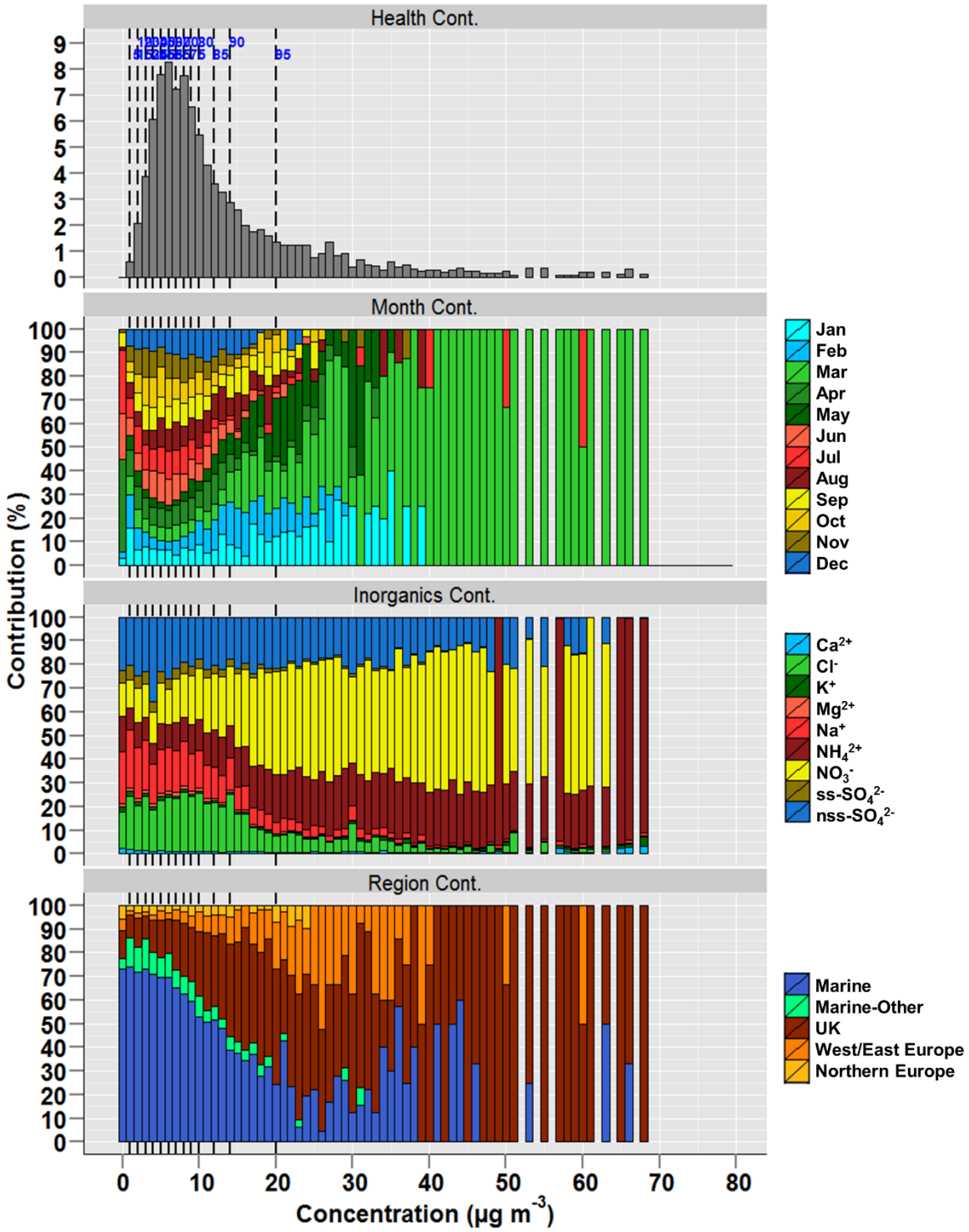

Figure 6.8: Contribution to annual average PM_{10} (PM_{10AA}) segmented into 1 µg m^{-3} bins at Auchencorth in 2012. The vertical dashed lines indicate the concentrations of percentiles from the 5th to the 95th percentile in 5 percent steps. The proportion of concentrations within each bin from the different months of the year, the contribution from 9 inorganic ions to total inorganic ion concentrations and the contribution from different trajectory clusters are also shown.

6.3.2.2 PM composition

The SIA components, NO_3^-, non-sea-salt SO_4^{2-} (nss-SO_4^{2-}) and NH_4^+ comprise the largest fraction of PM_{10AA} and $PM_{2.5AA}$ at Harwell and Auchencorth (Table 6.3). For example, the annual average sum of the SIA components account for 48% of PM_{10AA} and 54% of $PM_{2.5AA}$ at Harwell in 2013, and 60% of PM_{10AA} concentrations at Auchencorth. In comparison to a UK urban background site, the contribution from SIA to PM_{10} and $PM_{2.5}$ is greater at Harwell and Auchencorth, which may reflect the greater regional contribution to PM at rural UK sites, and less exposure to local sources of other constituents (Yin and Harrison, 2008). For $PM_{2.5}$ at Auchencorth, the SIA components accounted for 94% of $PM_{2.5AA}$. The sum of all measured components was substantially greater than $PM_{2.5AA}$, including when negative measurements were omitted. At Auchencorth, analysis of contributions of components of PM focussed on PM_{10}, as the higher PM_{10} concentrations are less affected by limitations of the TEOM-FDMS instrument during low concentrations.

The components of sea salt (Cl^-, Na^+, sea-salt SO_4^{2-} and Mg^{2+}) had the second largest combined contribution to PM_{10AA} and $PM_{2.5AA}$ (Table 6.3). For PM_{10} at Harwell in 2013, 19.4% of PM_{10AA} was made up of sea-salt components, compared to 11.9% for $PM_{2.5AA}$. At Auchencorth, 30.3% of PM_{10AA} in 2012 was accounted for by sea salt. These values are higher than those calculated at other rural sites in north-west Europe, where the contribution form sea salt was on average 12% (Putaud et al., 2010). Total carbon was the next largest component, and also accounted for a larger fraction in PM_{10AA} (15.5% in 2013 at Harwell) compared to $PM_{2.5AA}$ (11.9%). These values are substantially smaller than calculated at an urban background site in the UK, where total carbon accounted for 37% of $PM_{2.5}$ (Yin and Harrison, 2008). The additional contribution from carbon at this urban site could explain the relatively lower contribution of SIA compared to Harwell and Auchencorth. These three different fractions, SIA, sea-salt and carbon comprise the major mass fraction of both PM_{10AA} and $PM_{2.5AA}$ and therefore an assessment of the conditions giving rise to their

contributions would be most useful for consideration of mitigation of the long-term PM health impact.

The 25 heavy metals measured at Harwell and Auchencorth contributed approximately 1% of PM_{10AA} at both sites. Iron (on average 54 ± 4% of total heavy metal annual average at Harwell between 2010-2013, 47 ± 8% at Auchencorth), aluminium (23 ± 4% at Harwell, 34 ± 12% at Auchencorth), zinc (6% ± 0.7% at Harwell, 8 ± 2% at Auchencorth) and barium (5 ± 2% at Harwell, 1 ± 0.3% at Auchencorth) were the major components of the heavy metals contribution. The PAHs made a considerably smaller contribution to annual average concentrations, generally approximately 0.01%. Though not the focus for the long-term PM total mass health impact, it is noted that there is motivation for reduction in concentration of PAHs and heavy metals resulting from their individual, specific impacts (health or otherwise). For example, various PAHs have been shown to be carcinogenic (Kim et al., 2013), and analysis and interpretation of the variation in PAH measurements across the UK network has been undertaken previously (Brown et al., 2013a). Similarly individual heavy metals such as lead are neurotoxins, and have been linked to secondary impacts such as crime rate (aggravated assault) (Mielke and Zahran, 2012). These impacts are not addressed here.

Figures 6.6-6.9 show the contribution of inorganic ions to the sum of the 9 inorganic species within the different 1 µg m^{-3} concentration bins for PM_{10} and $PM_{2.5}$ at Harwell and PM_{10} at Auchencorth. At low concentrations (typically below 5 µg m^{-3}), the proportion of PM concentrations accounted for by the inorganic ions was generally above 100% due to a limitation in the TEOM-FDMS instrument which also resulted in negative mass measurements, i.e. an underestimation of the volatile PM component. At higher mass concentrations, the sum of the inorganic components was less than the PM mass and the fraction not accounted for by the inorganic ions could be calculated. However, it could not be precisely defined at which PM mass concentration this 'remaining' fraction accurately reflected the proportion of total PM mass not accounted for by the inorganic ions. Therefore to show how the composition of the inorganic ion fraction changes with PM concentrations, the contribution of each ion to

the total inorganic fraction was calculated. As a guide, the 'remaining' fraction was 29% and 32% of PM_{10AA} and $PM_{2.5AA}$ concentrations at Harwell, and 13% of PM_{10} annual average at Auchencorth. Above 20 µg m^{-3}, the remaining fraction fluctuated between 25 and 40% of composition for PM_{10} and $PM_{2.5}$ at Harwell, but did not show any trend with increasing concentration. At Auchencorth for PM_{10}, there were greater fluctuations in the extent of the remaining fraction, and for three size bins above 40 µg m^{-3} the sum of inorganic ions was greater than the measured, total mass concentration.

At both Harwell and Auchencorth, for PM_{10} and $PM_{2.5}$, the SIA contribution increases as PM concentration increases, and the sea-salt contribution decreases. At the 95th percentile concentrations for PM_{10} (41 µg m^{-3}) and $PM_{2.5}$ (38 µg m^{-3}) at Harwell, NO_3^-, nss-SO_4^{2-} and NH_4^+ comprised 50%, 18% and 21% of the inorganic fraction for PM_{10} (Figure 6.6), and 51%, 18% and 21% for $PM_{2.5}$ (Figure 6.7). These increases were also observed at urban locations (Yin and Harrison, 2008). In contrast, Cl^- and Na^+ comprised 4% and 2% for PM_{10} and 2% and 3% for $PM_{2.5}$. For the moderate concentrations with the largest contribution to PM_{10AA} and $PM_{2.5AA}$, there were contributions from a relatively larger number of components. For example, for PM_{10} in 2013 at Harwell, the contributions from NO_3^-, nss-SO_4^{2-} and NH_4^+ to total inorganic ions were 28%, 20% and 12% respectively, on average, for the five highest contributing concentration bins. The contribution of nss-SO_4^{2-} remained relatively constant for moderate and high concentrations, while contributions from NO_3^- and NH_4^+ were substantially larger at the moderate concentrations. For Cl^- and Na^+, the contributions for the five highest contributing concentrations were 17% and 12%. For $PM_{2.5}$ (Figure 6.7), the contribution from sea salt decreased more rapidly with increasing concentration than for PM_{10} (Figure 6.6). For example, the average contribution from Cl^- between 5 and 10 µg m^{-3} was similar, 18% and 16% for PM_{10} and $PM_{2.5}$ respectively, but the average contribution between 10 and 15 µg m^{-3} was 17% for PM_{10} and 8% for $PM_{2.5}$, and between 15 and 20 µg m^{-3} was 16% for PM_{10} and 4% for $PM_{2.5}$. Hence for $PM_{2.5}$ the relative contribution from SIA is larger at lower concentrations compared to PM_{10}.

At Auchencorth, the contribution from sea salt to the five highest contributing concentrations to PM_{10AA} was greater than at Harwell, and Cl^- and Na^+ contributed 23% and 18% to the total inorganic fraction (Figure 6.8). The contribution from SIA was therefore smaller, and NO_3^-, nss-SO_4^{2-} and NH_4^+ contributed 18%, 22% and 11%. The contribution from SIA increased at high concentrations. At the 95th percentile (20 µg m^{-3}), nss-SO_4^{2-} had a similar contribution as for moderate concentrations (22%), but the contributions from NO_3^- and NH_4^+ were substantially higher (43% and 20% respectively). These patterns were consistent with those calculated using Auchencorth measurements between 2006 and 2012 (Twigg et al., 2015).

The daily (PM_{10}, $PM_{2.5}$ and inorganic ions are measured at hourly time resolution) measurements of OC and EC at Harwell in PM_{10} were most suitable to assess the contribution of carbon to the state of this chemical climate compared with the lower time resolution weekly measurement of OC and EC in $PM_{2.5}$ at both sites. Total carbon accounted for 16% of PM_{10AA} at Harwell in 2013 (Table 6.3). Below 5 µg m^{-3}, the fraction of PM_{10} accounted for by either EC or OC was substantially larger (over 80% for the 1-2 µg m^{-3} concentration bin). Hence the change in carbon with changing PM_{10} concentrations was assessed as a change in contribution of organic and elemental carbon to total carbon at different PM_{10} concentrations (Figure 6.9). As a guide, above 5 µg m^{-3} the contribution of total carbon to PM concentration fluctuated around 15%, and showed no significant trend with PM_{10} concentration. At all PM_{10} concentrations, OC was the major fraction of total carbon, but as concentrations increased, the contribution of EC to total carbon also increased. The average contribution of EC to total carbon during daily average PM_{10} concentrations was 2% between 0 and 5 µg m^{-3}, 4% between 5 and 10 µg m^{-3}, 10% between 10 and 15 µg m^{-3}, 20% between 35 and 40 µg m^{-3}, and peaked at 31% between 50 and 55 µg m^{-3}. This is consistent with measurements detailed in Harrison and Yin (2008) for three sites in the UK.

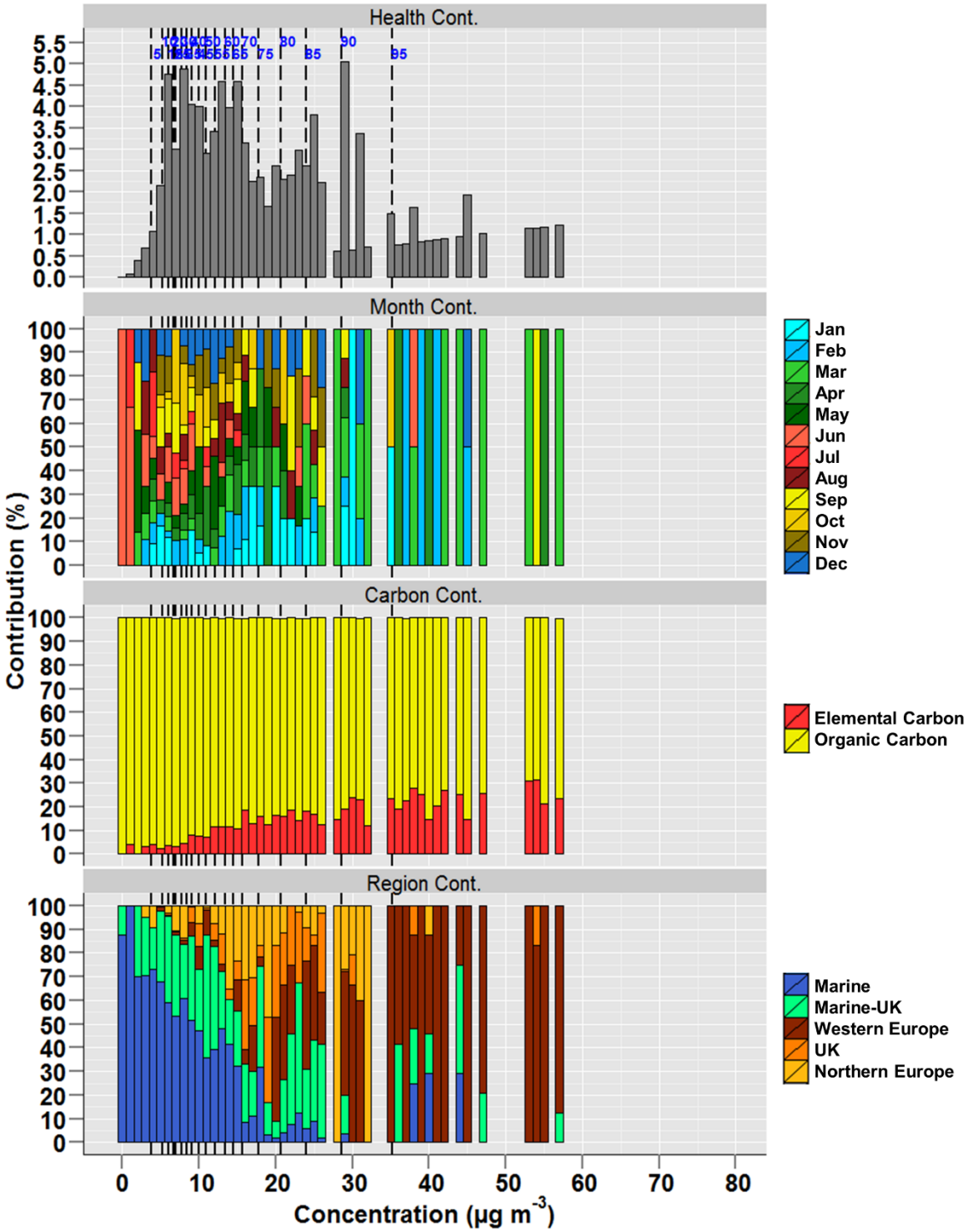

Figure 6.9: Contribution to annual average PM_{10} (PM_{10AA}) segmented into 1 µg m^{-3} bins at Harwell in 2013 based on daily averaged concentrations. The vertical dashed lines indicate the concentrations of percentiles from the 5th to the 95th percentile in 5 percent steps. The proportion of concentrations within each bin from the different months of the year, the contribution from elemental and organic carbon to total carbon concentrations and the contribution from different trajectory clusters are also shown.

6.3.3 Drivers

6.3.3.1 Air-mass back trajectories

The number of hours (out of 96) spent in the different regions for each 'trajectory cluster' at Harwell in 2013 and at Auchencorth in 2012, derived from the cluster analysis of air mass back trajectories, are summarised in Figures 6.2 and 6.3 respectively. The five clusters arriving at Harwell were named 'Marine', 'Marine-UK', 'Western Europe', 'UK' and 'Northern Europe' based on the major differences in geographic regions over which the trajectories traversed. The average proportion of hours during which trajectories belonging to each cluster arrived at Harwell for each concentration bin is shown in Figure 6.6 for PM_{10} and Figure 6.7 for $PM_{2.5}$. At low concentrations, 'Marine' and 'Marine-UK' clusters comprised the majority contribution for PM_{10} and $PM_{2.5}$. For example, below 5 µg m^{-3}, the average proportion of hours when 'Marine' and 'Marine-UK' trajectories arrived at Harwell was 64% and 26% respectively for $PM_{2.5}$. As concentrations increased, the contribution from the three 'terrestrial' clusters increased. For the 95th percentile $PM_{2.5}$ concentration, 'Western Europe' trajectories arrived during 60% of the hours. The transition from a Marine dominated trajectory cluster contribution to having large contribution from terrestrial trajectories occurred during the moderate concentrations which make the largest contribution to PM_{10AA} and $PM_{2.5AA}$. For $PM_{2.5}$, between 5-10 µg m^{-3}, 10-15 µg m^{-3} and 15-20 µg m^{-3} the 'Marine' cluster contributed 47%, 25% and 13% respectively, while the 'Western Europe' cluster contributed 5%, 11% and 25% respectively. Hence during those high frequency, moderate concentrations, there was a wide range of different geographic source regions influencing PM concentrations and composition at Harwell, while at extreme concentrations (high and low), a less diverse range of sources contributed.

At Auchencorth in 2012 the distinctive differences between trajectory clusters resulted in clusters named 'Marine', 'Marine-Other', 'UK', 'Western/Eastern Europe' and 'Northern Europe' (Figure 6.3). At low PM_{10} concentrations the 'Marine' cluster

dominated (on average 73% below 5 µg m^{-3}) (Figure 6.8). As concentrations increased, there was a larger contribution from terrestrial trajectory clusters, but the contribution from trajectories which traversed continental Europe was substantially lower compared with Harwell. For PM_{10}, between 5-10 µg m^{-3}, 10-15 µg m^{-3} and 15 and 20 µg m^{-3} the 'Marine' cluster contributed 65%, 48% and 34% respectively, while the 'UK' cluster contributed 19%, 33% and 47% respectively (Figure 6.8). The 'Western/Eastern Europe' trajectory contributed less than 13% for these concentration ranges. Hence during the highest-contributing concentrations to PM_{10AA} at Auchencorth, there was a substantial contribution from terrestrial and marine trajectories in determining atmospheric composition at the site, but the terrestrial air masses most commonly passed over the UK. At the highest PM_{10} concentrations at Auchencorth (>95^{th} percentile), the 'UK' trajectory cluster dominated, but the 'Western/Eastern Europe' trajectory cluster also contributed. AQEG (2012) showed the highest concentrations at Auchencorth in 2012 to be associated with trajectories which spent time over the south-east UK and north-west Europe.

The grouping of trajectories by geographic region was also used to assess the patterns of accumulation for PM constituents during different air-mass pathways. This is illustrated at Harwell in 2013 in Figure 6.10 which shows the proportion of annual average $PM_{2.5}$ NO_3^- accumulated in each trajectory cluster separated into contributions from different $PM_{2.5}$ concentrations. There was a disproportionately large contribution from the 'Western Europe' cluster to annual average $PM_{2.5}$ NO_3^- compared to the proportion of trajectories grouped in this cluster (36% despite these conditions occurring only 13% of the time). Elevated SIA component concentrations have previously been associated with transport of polluted air masses from continental Europe (Abdalmogith and Harrison, 2005; AQEG, 2012; Vieno et al., 2014). The proportion of annual average NO_3^- accumulated during 'UK' and 'Northern Europe' trajectory clusters was similarly greater than the proportion of trajectories classified in these groups. Conversely, the 'Marine' and 'Marine-UK' clusters constituted 68% of hours during 2013 combined, but contributed 35% NO_3^-. In the 'Marine' cluster, the majority (57%) of the contribution to annual average NO_3^- was accumulated below 10

µg m^{-3}. The 'Marine-UK' cluster annual average NO_3^- contribution was derived to a greater extent at higher concentrations compared to the 'Marine' cluster. The 10-20 µg m^{-3} and 20-30 µg m^{-3} concentrations ranges contributed 31% and 19% to the 'Marine-UK' cluster NO_3^- contribution compared with 21% and 7% for 'Marine'. The 'Northern Europe' cluster contribution distribution was similar to the 'Marine-UK' cluster. For the 'UK' cluster, there was a smaller contribution from low concentrations than for the 'Marine-UK cluster' (only 10% of the contribution was derived during concentrations below 10 µg m^{-3}), and the majority (63%) of the contribution was derived between 10 and 30 µg m^{-3}. The 'Western Europe' cluster contribution distribution was substantially different, with a small contribution from concentrations below 10 µg m^{-3} (3%), and similar (between 17% and 22%) contributions from 10-20 µg m^{-3}, 20-30 µg m^{-3}, 30-40 µg m^{-3} and 40-50 µg m^{-3} concentration ranges.

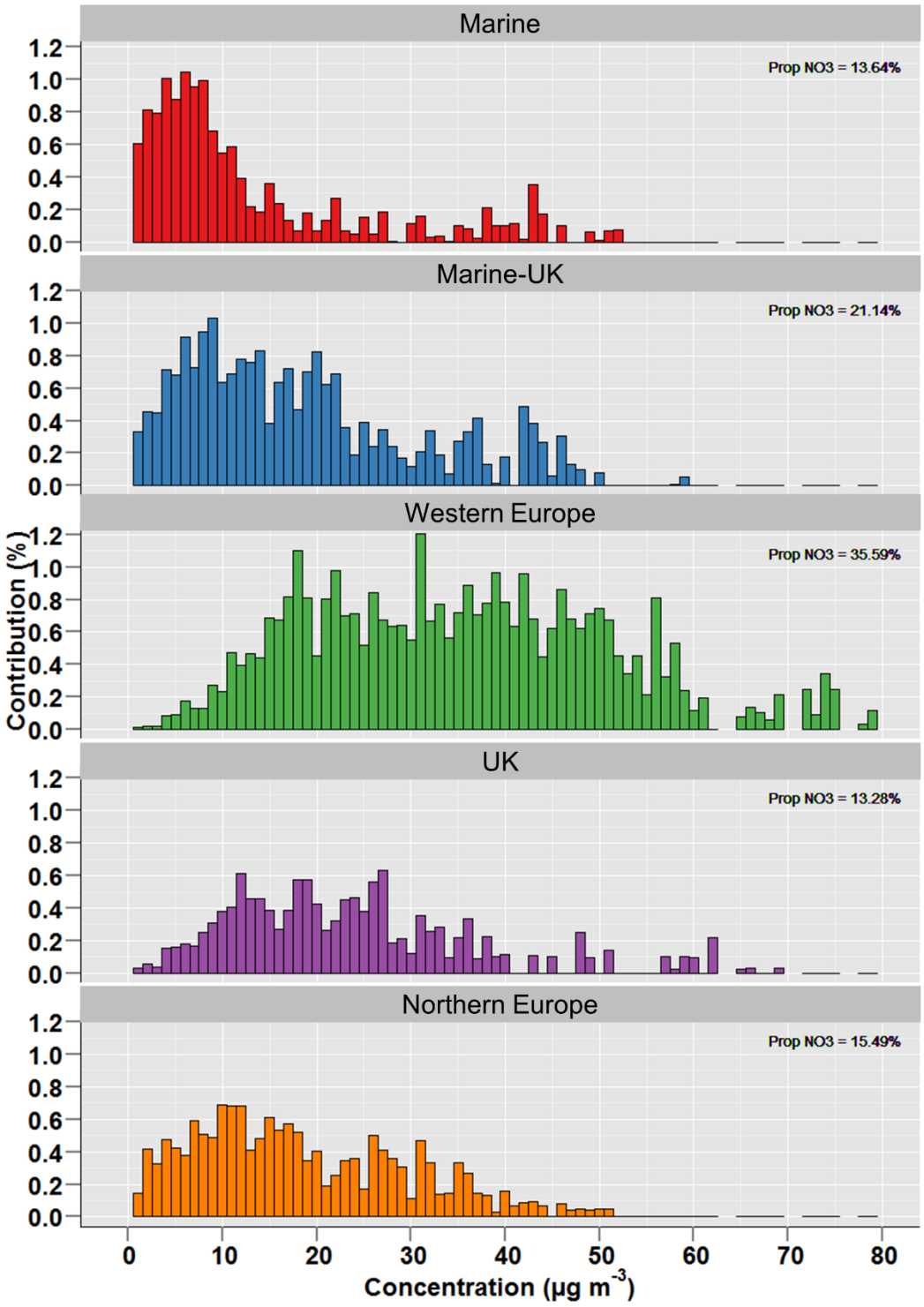

Figure 6.10: Contribution to annual average NO_3^- concentration in $PM_{2.5}$ at Harwell in 2013 separated into different $PM_{2.5}$ concentrations for each trajectory cluster. The 'Prop. NO_3' is the proportion of annual average NO_3^- in $PM_{2.5}$ contributed by each cluster, and is equal to the sum of all the bars in the respective panel.

The total contribution distribution for annual average $PM_{2.5}$ NO_3^- at Harwell in 2013 is shown in Figure 6.11a, with each contribution separated into the proportion derived by each cluster. The largest contribution to annual average NO_3^- occurred at the moderate $PM_{2.5}$ concentrations which also contributed most greatly to $PM_{2.5AA}$. The contribution distribution for NO_3^- was similar to that of $PM_{2.5}$ (Figure 6.5). The five highest contributing concentration bins contributed 14% of the annual average NO_3^- (Figure 6.11a) compared to 17% for $PM_{2.5AA}$ (Figure 6.5), and the concentrations above the $PM_{2.5}$ 95th percentile contributed 21% of annual average NO_3^- and $PM_{2.5AA}$. The contribution to annual average NO_3^- from high concentrations was dominated by the 'Western Europe' trajectory cluster (71% of the contribution from concentrations above the $PM_{2.5}$ 95th percentile concentration was derived during 'Western Europe' conditions, Figure 10 and Figure 11a). At the highest-contributing moderate $PM_{2.5}$ concentrations, there were substantial contributions from all trajectory clusters. For example, between 5 and 20 µg m^{-3}, which contributed 39% of the annual average NO_3^- (Figure 11a), the proportion derived during each trajectory cluster varied between 14% and 28%. Hence a wide range of geographic source regions made substantial contribution in determining the proportion of $PM_{2.5AA}$ accounted for by a single PM constituent (NO_3^-).

The corresponding plots to Figure 6.11a for NH_4^+, Cl^- and Ca^{2+} are shown in Figures 6.11b, c and d respectively. The contribution distributions for NH_4^+ was similar to that for NO_3^-, reflecting their linked formation pathways as components of SIA. The majority (68%) of the contribution to annual average Cl^- concentrations was derived below 10 µg m^{-3} and 'Marine' (65% of <10 µg m^{-3} contribution) and 'Marine-UK' (19%) trajectory clusters dominated (Figure 6.11c). Similar contribution distributions were calculated for other sea-salt components such as Na^+, and Mg^{2+}. The contribution of Ca^{2+} to $PM_{2.5}$ concentrations was minor, and the contribution distribution for Ca^{2+}, which derived mainly from mineral dust (Viana et al., 2008), was different to the SIA and sea salt components. The contribution from $PM_{2.5}$ concentrations below 10 µg m^{-3} (41%) to annual average Ca^{2+} and from 'Marine' (27% of annual average Ca^{2+}) was lower than for sea salt but higher than for SIA components (Figure 11d). Conversely,

the contribution from higher $PM_{2.5}$ concentrations (13% contributed from concentrations above $PM_{2.5}$ 95th percentile) and the 'Western Europe' (25%) cluster was lower than SIA, but higher than the sea salt distributions. The contribution distribution for K^+, which has a negligible contribution to $PM_{2.5}$ concentrations (Table 6.3), was similar in shape to that of Ca^{2+}, but the contribution to annual averages from 'UK' (18% of annual average K^+ compared to 8% of annual average Ca^{2+}) and 'Marine-UK' (26% for K^+, 22% for Ca^{2+}) trajectory clusters was larger for K^+ compared to Ca^{2+}. The corresponding lower contribution to annual average K^+ from 'Western Europe' (20% for K^+, 25% for Ca^{2-}) and 'Northern Europe' (4% for K^+, 14% for Ca^{2-}) suggests that there was a larger contribution from domestic emissions for K^+ compared to Ca^{2+}.

The contribution distributions for NO_3^-, NH_4^+, Cl^-, Ca^{2+} in PM_{10} at Harwell in 2013 are shown in Figure 6.12. For each of the four inorganic ions, the differences between the corresponding contribution distributions for $PM_{2.5}$ at Harwell was a shift in the largest contributing concentrations bins to higher, but still moderate PM_{10} concentrations. This was also the case for the contribution of PM concentrations to $PM_{2.5}$ and PM_{10} annual averages (Figures 6.6 and 6.7). For example, for NO_3^- and NH_4^+, the maximum contribution to the annual averages in $PM_{2.5}$ was at 12 µg m^{-3}, compared with 15 µg m^{-3} for PM_{10}. For Cl^-, there was a substantially larger contribution from concentrations between 10 and 20 µg m^{-3} to the PM_{10} Cl^- annual average (43%) compared with $PM_{2.5}$ (19%).

The corresponding contribution distributions for NO_3^-, NH_4^+, Cl^-, Ca^{2+} in PM_{10} at Auchencorth are shown in Figure 6.13. The main difference compared with Harwell was the larger contribution from UK-dominant trajectory clusters compared to European influenced trajectory clusters. For SIA, the moderate concentrations which make the largest contribution to annual averages had largest contributions from 'Marine' and 'UK' trajectory clusters, with a minor contribution from the 'Western/Eastern Europe' cluster. For example, 49%, 34% and 10% of the contribution from the five highest contributing PM_{10} concentrations was derived

during ‘Marine’, ‘UK’ and ‘Western/Eastern Europe’ clusters respectively. For the highest concentrations (>95th percentile), the largest proportion of the contribution from these concentrations was derived during ‘UK’ trajectory cluster conditions (54%), followed by ‘Marine’ (24%) and ‘Western/Eastern Europe’ (20%) clusters. Twigg et al. (2015) calculated a substantial increase in SIA component concentrations during trajectories which passed over the southern UK and north-west Europe based on concentrations at Auchencorth between 2006 and 2012. For Cl^- and Ca^{2+}, the ‘Marine’ cluster dominated (contributed 63% to Cl^- annual average and 57% for Ca^{2+}), and there was a larger contribution from the ‘UK’ cluster for Ca^{2+} (24% annual average contribution), which dominated at higher PM_{10} concentrations.

The corresponding contribution distributions for EC and OC in PM_{10} at Harwell in 2013 are shown in Figure 6.14. For OC, the maximum contribution was at 8 µg m^{-3} (daily averaged PM_{10} concentrations), which was dominated by the ‘Marine’ and ‘Marine-UK’ trajectory clusters. At higher concentrations (> 20 µg m^{-3}), which contributed 35% of annual average OC, the majority (54%) was derived during ‘Western Europe’ trajectory cluster conditions. As outlined in Figure 6.7, EC becomes a greater proportion of total carbon as PM_{10} concentrations increase. Hence PM_{10} concentrations above 20 µg m^{-3} made a larger contribution to EC annual average compared to OC (56% for EC, 35% for OC). A similar proportion of the contribution from PM_{10} concentrations above 20 µg m^{-3} was derived during ‘Western Europe’ trajectory cluster conditions (58%) for EC as for OC, and hence these conditions were more important to determining the EC annual average compared with OC.

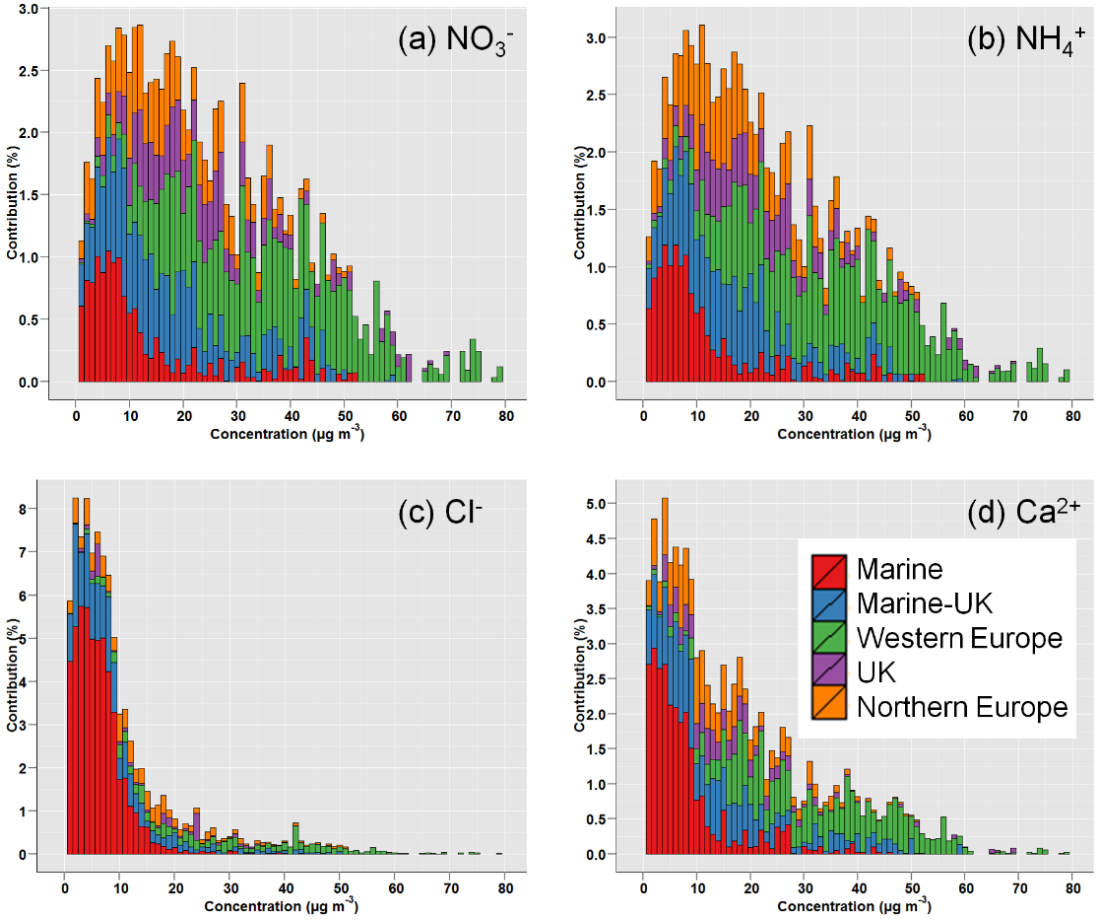

Figure 6.11: Contribution to annual average a) nitrate, b) ammonium, c) chloride, d) calcium concentrations in $PM_{2.5}$ at Harwell in 2013 from 1 µg m^{-3} $PM_{2.5}$ concentrations. The total contribution from each concentration bin is separated into the proportion derived during hours when each trajectory cluster arrived at the site.

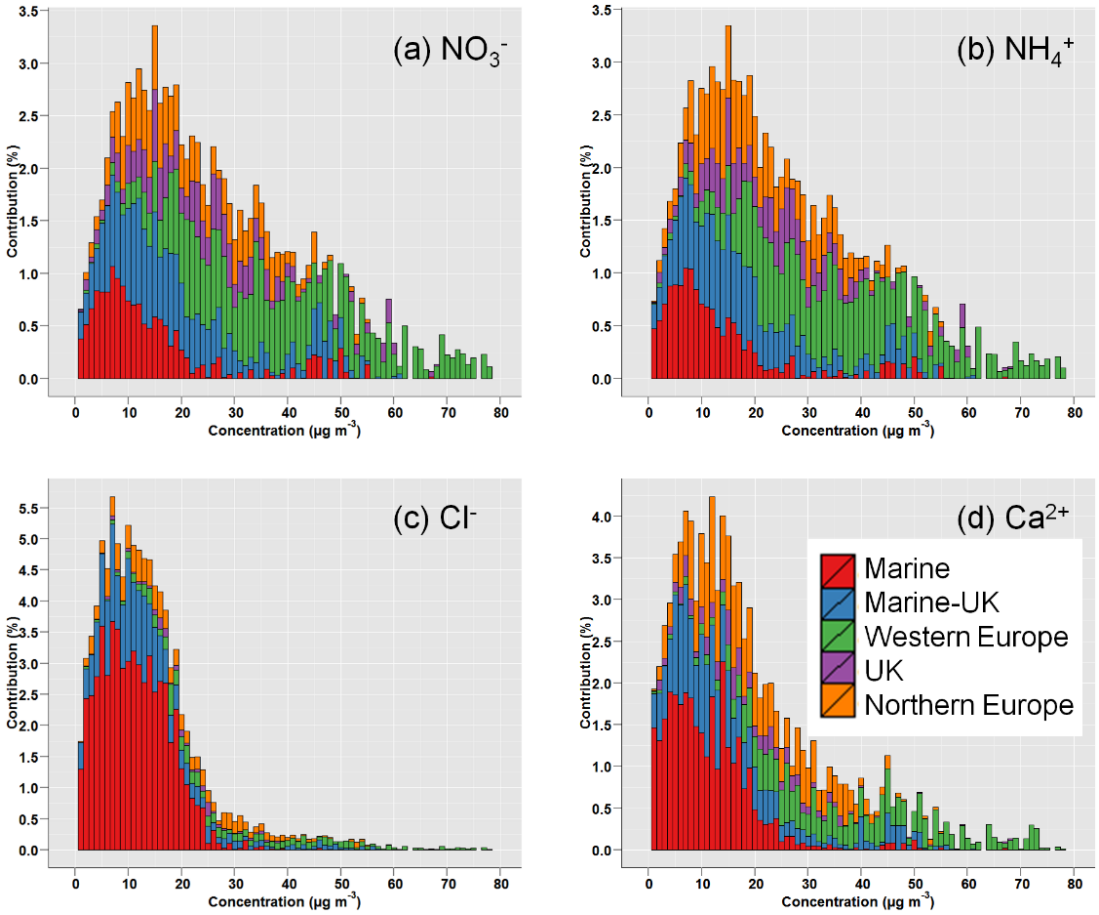

Figure 6.12: Contribution to annual average a) nitrate, b) ammonium, c) chloride, d) calcium concentrations in PM_{10} at Harwell in 2013 from 1 µg m^{-3} PM_{10} concentrations. The total contribution from each concentration bin is separated into the proportion derived during hours when each trajectory cluster arrived at the site.

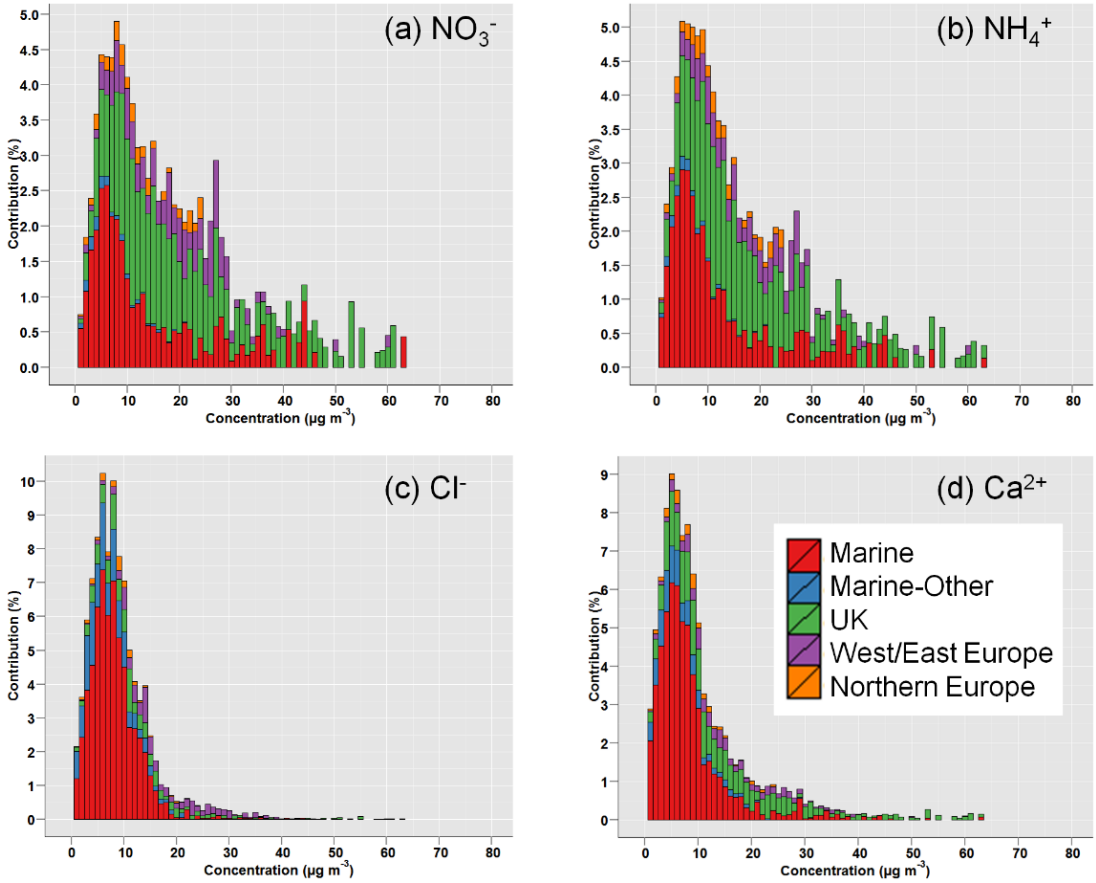

Figure 6.13: Contribution to annual average a) nitrate, b) ammonium, c) chloride, d) calcium concentrations in PM_{10} at Auchencorth in 2012 from 1 µg m^{-3} PM_{10} concentrations. The total contribution from each concentration bin is separated into the proportion derived during hours when each trajectory cluster arrived at the site.

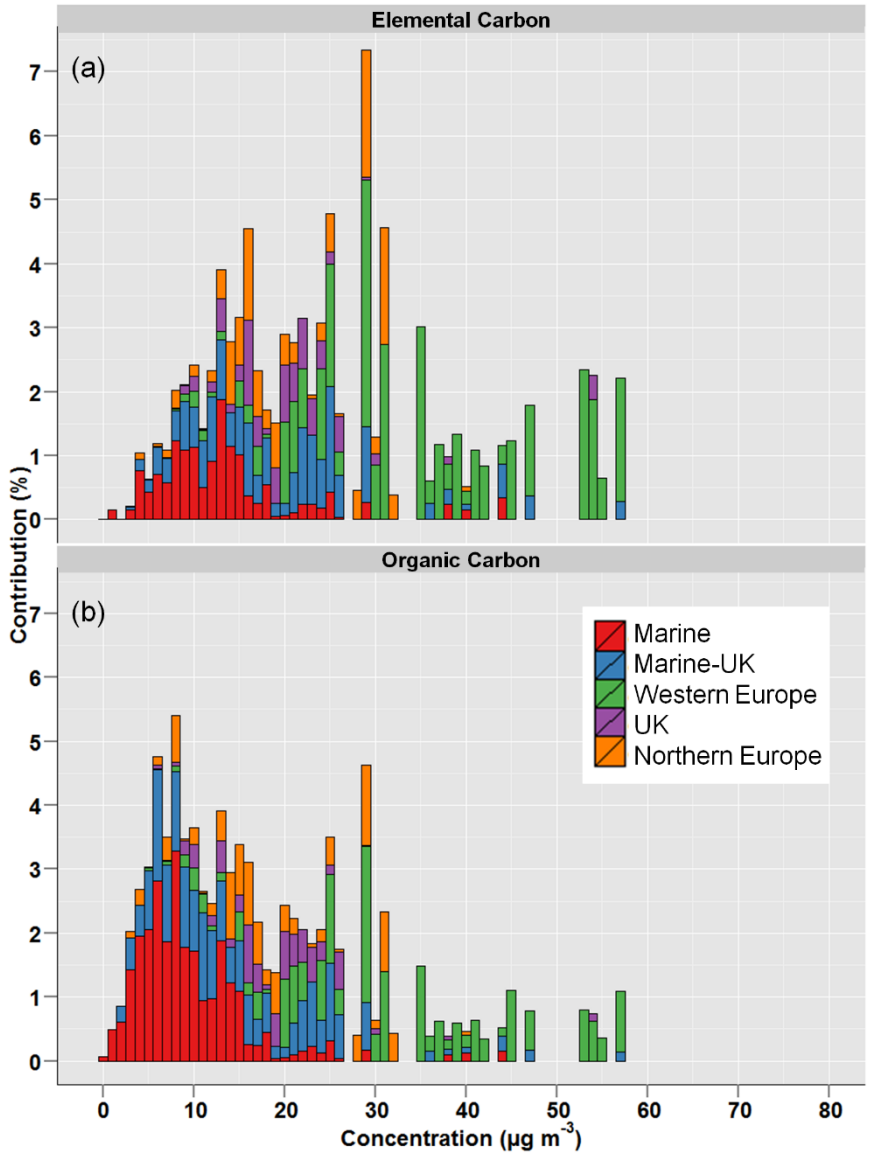

Figure 6.14: Contribution to annual average a) elemental carbon, b) organic carbon concentrations in PM_{10} at Harwell in 2013 from 1 µg m^{-3} PM_{10} concentrations. The total contribution from each concentration bin is separated into the proportion of hours during days when PM_{10} concentrations were within the concentration range when trajectories belonging to each trajectory cluster arrived at the site.

6.3.3.2 Principal Component Analysis (PCA)

The difference in contribution to annual average NO_3^-, NH_4^+ and nss-SO_4^{2-} from different PM concentrations and trajectory clusters demonstrates the variety of sources which determine the contribution of these SIA components to PM_{10AA} and $PM_{2.5AA}$. The PCA analysis investigates why the contribution from different clusters was derived in different ways. Figure 6.15 shows the loading for the first two PCs (which together explained 79% of variability) resulting from the application of PCA to the $PM_{2.5}$ inorganic ion time series in 2013 at Harwell. Similar magnitude and direction of a loading indicates high correlation between components, whilst similar magnitude but opposite direction of loading indicates anti-correlation between components. The SIA components, NO_3^-, NH_4^+ and nss-SO_4^{2-} had high correlation for PC1, and were anti-correlated with sea-salt components Cl^-, Na^+ and Mg^{2+}. The value of PC1 at an hourly time step therefore distinguishes between a relatively large contribution from SIA, and low contribution from sea salt, and vice versa. There was a correlation between all components for PC2, with the exception of K^+ which had a relatively low loading. Hence the value of PC2 determines whether there was a simultaneous increase in almost all inorganic components, both sea salt and SIA, at a given time step.

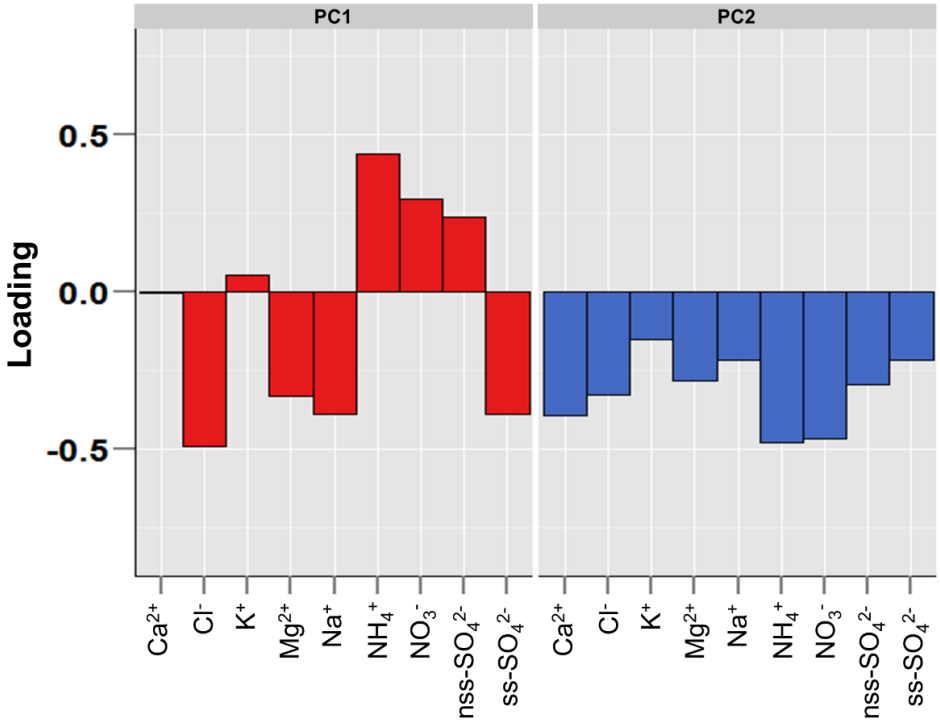

Figure 6.15: Loading of 9 inorganic ions for first two principal components (PCs) resulting from application of PCA to inorganic ion data set for $PM_{2.5}$ at Harwell in 2013.

In the context of SIA formation and the contribution of SIA to $PM_{2.5}$, the value of PC1 indicates the contribution from short-range transport to SIA formation, whilst PC2 indicates the contribution of long-range transport. For SIA, short-range transport is associated with an anti-correlation with sea salt because traversing over SIA precursor emissions sources (i.e. land) during the final hours of a trajectory means that less time is spent over marine environments and hence reduces the sea salt accumulated. For long-range transport, the longer time period means an air mass can pass over numerous SIA precursor emissions sources, as well as marine environments as the air mass proceeds to the receptor site (Figure 6.8 shows that even during 'Western Europe' trajectory conditions the air mass still spends on average 20 hours over water). Hence as the air mass travels towards the site over this longer time period (compared to short-range transport), the combination of traversing terrestrial and marine environments results in an increase in both SIA and sea-salt components. The loadings for Cl^- and Na^+ were 29% and 53% smaller than the loading for NO_3^+. Hence while SIA and sea-

salt components were correlated, a large PC2 value results in a higher percentile NO_3^+ and NH_4^+ concentration than Cl^- and Na^+.

The contribution from short-range transport and long-range transport in determining SIA concentrations during the five trajectory clusters is summarised in Figure 6.16 which shows, for each cluster, the proportion of hours with PC1 and PC2 values in 20 × 5-percentile bins. The majority of hours during 'Marine' cluster conditions had low-percentile PC1 and PC2 values. For the 'Marine-UK' there is a similar distribution of percentile contributions for PC2 as for the 'Marine' cluster, but an increase in the contribution from higher percentiles for PC1, i.e. an increase in the short-range transport indicator. While the top quantile of PC1 values contributed 11% during the 'Marine' cluster conditions, they contributed 27% of the values for 'Marine-UK'. For the 'UK' cluster, over 60% of PC1 values were in the top quantile, but there was no corresponding increase in contribution from high-percentile PC2 values. In the 'Northern Europe' cluster, the contribution from high-percentile PC2 values, i.e. the long range transport indicator, was much greater, and over 60% of the PC2 values are in the top quantile during the 'Northern Europe' conditions. Finally, for those hours with 'Western Europe' conditions, there was a large contribution from both high-percentile PC1 and PC2 values, comparable with those contributions for PC1 in the 'UK' cluster and PC2 for 'Northern Europe'. Hence the disproportionately large contribution to SIA from 'UK' and 'Northern Europe' compared to the number of hours in during which these conditions occurred resulted from an isolated increase in short-range transport and long-range transport respectively. For 'Western Europe', the even larger contribution to annual average SIA during these conditions resulted from the simultaneous increase in contribution from both short and long-range transport. Vieno et al. (2014) modelled the contribution from UK and European emissions sources to SIA across the UK between 2001 and 2010, and calculated that both continental European and UK emissions sources can have a large contribution to the magnitude of a high SIA episodic concentrations. These conclusions are also likely to extend to OC, which was previously shown to be correlated with secondary inorganic aerosol and identified as a regional pollutant (Charron et al., 2013).

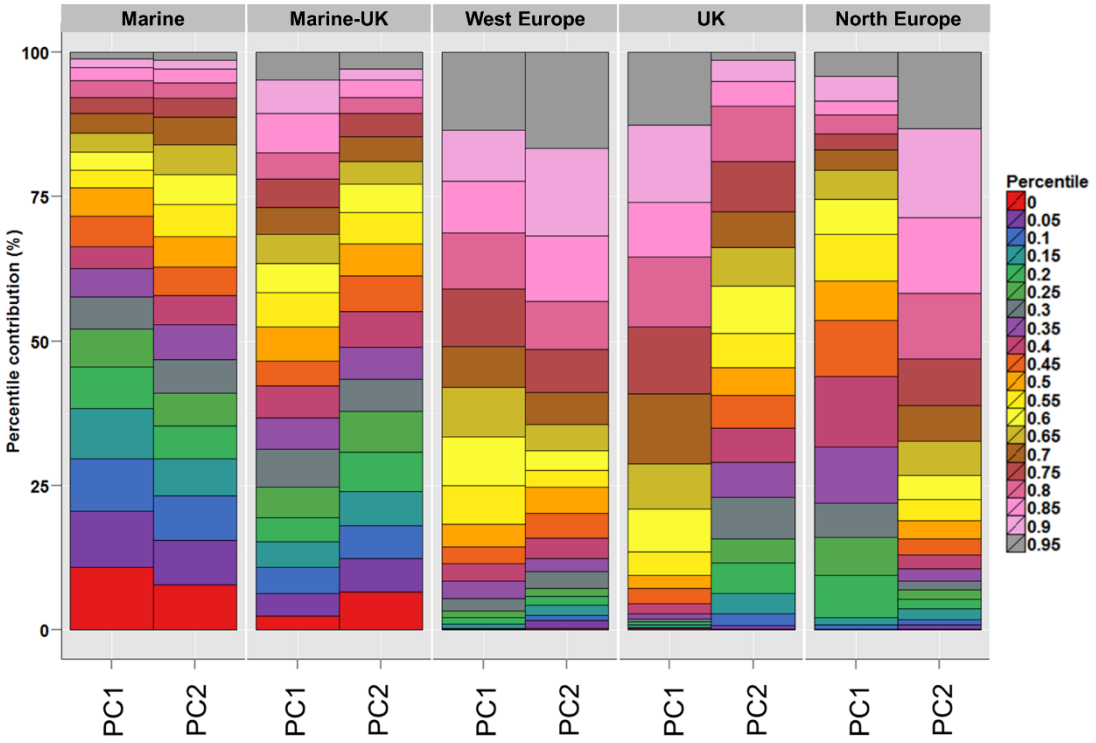

Figure 6.16: Proportion of hours in each cluster during which the value of PC1 and PC2 was within 20 × 5-percentile bins. For example, the larger the grey bar for a trajectory cluster, the more hours when there was a relatively high (i.e. 95th percentile) contribution from PC1/2, and the larger the red bar for a particular trajectory cluster, the more hours when there was a relatively low (i.e. 0-5th percentile) contribution from PC1/PC2.

6.3.3.3 Characteristic heavy metal source profiles

A correlation matrix for weekly heavy metal concentrations at Harwell between 2010 and 2013 is shown in Figure 6.17. Almost all heavy metals were positively correlated with each other, but there were distinct groupings which have higher correlation within each group. Aluminium (Al), lithium (Li), titanium (Ti), rubidium (Rb), iron (Fe) and manganese (Mn) all had high correlation with each other, as did arsenic (As), cadmium (Cd), lead (Pb), antimony (Sb), zinc (Zn), tin (Sn) and copper (Cu), but Sn and Cu also had relatively high correlation with Fe. Finally, vanadium (V) and nickel (Ni) were highly correlated. Viana et al. (2008) summarised characteristic PM constituents for different source activities, and Al and Fe were identified as

characteristic of 'mineral dust' or 'city dust' sources, Zn, Cu and Pb of 'vehicle exhaust' and V and Ni of 'Oil combustion' or 'Industry' (Viana et al., 2008).

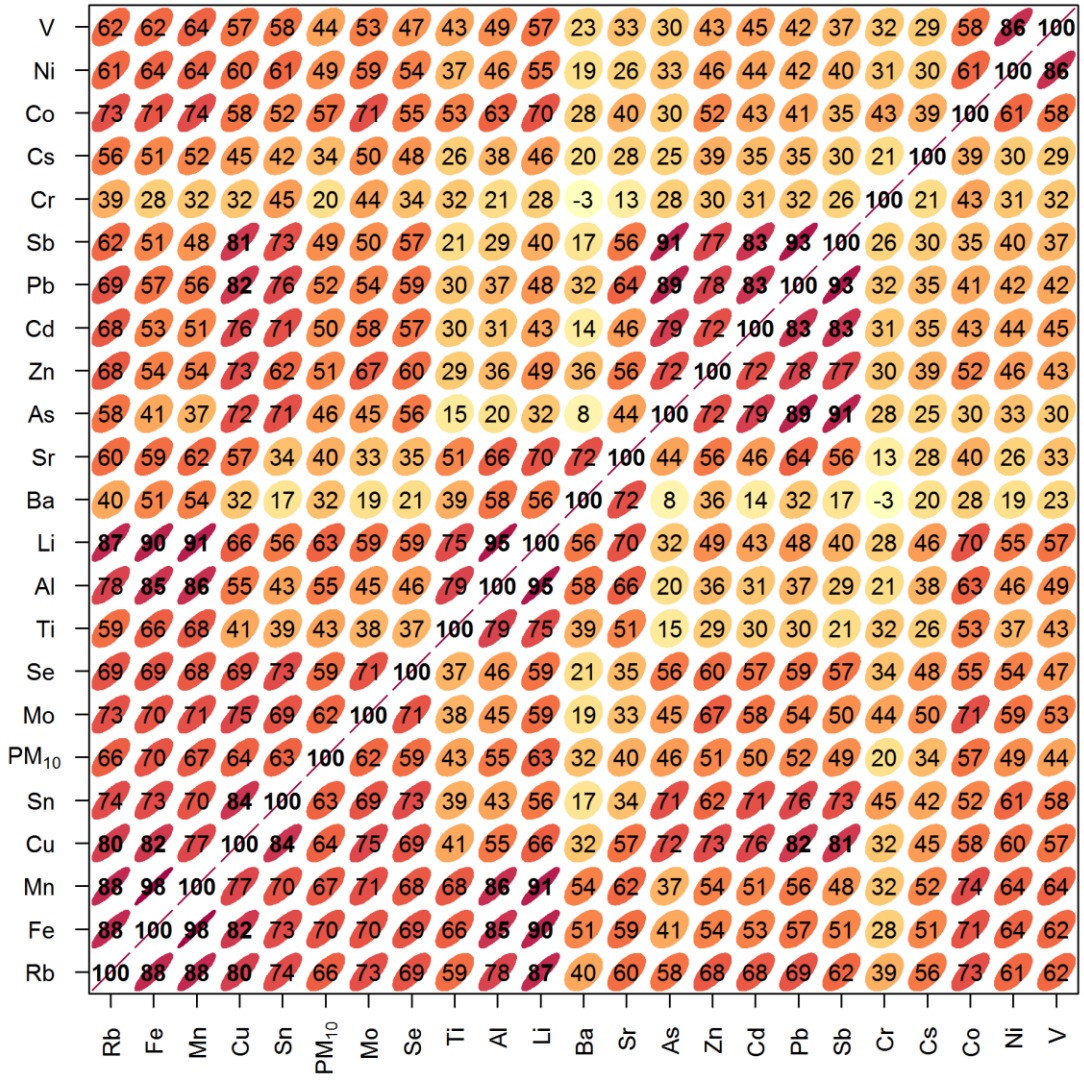

Figure 6.17: Correlation matrix of heavy metals in PM_{10} based on weekly average concentrations measured between 2010 and 2013.

Variation in the sources which the heavy metals had been previously identified as being characteristic of was summarised by the variation in Al, Fe, Zn and V (Figures 6.18-6.21). The entire 2010-2013 concentration range for each heavy metal was divided into 20 equally spaced concentration bins. Each figure shows the contribution of each bin to the 4-year average metal concentration, the proportion of weeks with concentrations in each bin, the contribution of each month to concentrations in each bin, the average PM_{10} concentration during that concentration bin and the proportion of hours trajectories spent over different geographic regions for concentrations in each bin. As expected, these parameters were similar for Al and Fe (Figures 6.18 and 6.19 respectively), both of which are characteristic of the 'dust' source. There was a peak in contribution to annual average Al and Fe of 12% and 14% respectively in the low concentration bins. The highest concentrations, i.e. highest contribution from dust, occurred during the spring. Finally, higher concentrations of these metals were also associated with increased time spent over western Europe and other terrestrial geographic regions.

The contribution to 4-year average Zn (representative of vehicle exhaust source, Figure 6.20) concentration was derived to a greater extent from the relatively lower concentrations compared with Al and Fe. There were fewer high Zn concentrations compared to Al and Fe, and a higher proportion of Zn concentrations occurred in the lowest concentration bin (35% for Zn compared to 14% for Fe and 25% for Al). Additionally, the ratio of the highest concentration bin concentration over the lowest concentrations bin concentration was 43 and 124 for Fe and Al respectively, but only 21 for Zn. Hence not only did relatively high concentrations occur less frequency for Zn (only 3 weeks had concentrations in the top 11 concentration bins), but the relative magnitude of the high concentrations was also smaller. This indicates that the vehicle exhaust source contribution to atmospheric composition at Harwell had less variation compared to the contribution from dust. The propensity for high concentrations was larger in summer for Al and Fe (Figure 6.18 and 6.19), as summer months mainly contributed to the lowest three concentration bins for Zn (Figure 6.20). Finally for V (oil combustion, Figure 6.21), there was also a lower propensity for the highest

concentrations compared to Al and Fe, but the range in concentrations was greater than for Zn. The ratio of highest concentration bin concentrations over lowest concentration bin concentration for V was 58, higher than for Fe and Zn. Increasing concentrations of V were also associated with higher concentrations of PM_{10}, with the exception of the four highest weekly V concentrations, which occurred in winter and were not associated with elevated PM_{10} concentrations (Figure 6.21). Similarly, the number of hours over western Europe also increased with increasing V concentrations, with the exception of these highest values.

The heavy metal source indicators show that the contribution from vehicle exhaust (Zn) had less variation in comparison to dust (Al and Fe) and oil combustion (V), while the high concentrations associated with oil combustion were less frequent, and therefore contributed less to the annual average concentration of V. High contributions from oil combustion and dust sources were also more associated with high concentrations of PM_{10} compared to vehicle exhaust. Measurement of heavy metals at higher time resolution would allow for a more in-depth assessment of the covariance between these source indicators and the major constituents of PM, and hence provide further evaluation of the conditions producing the long-term PM health impact.

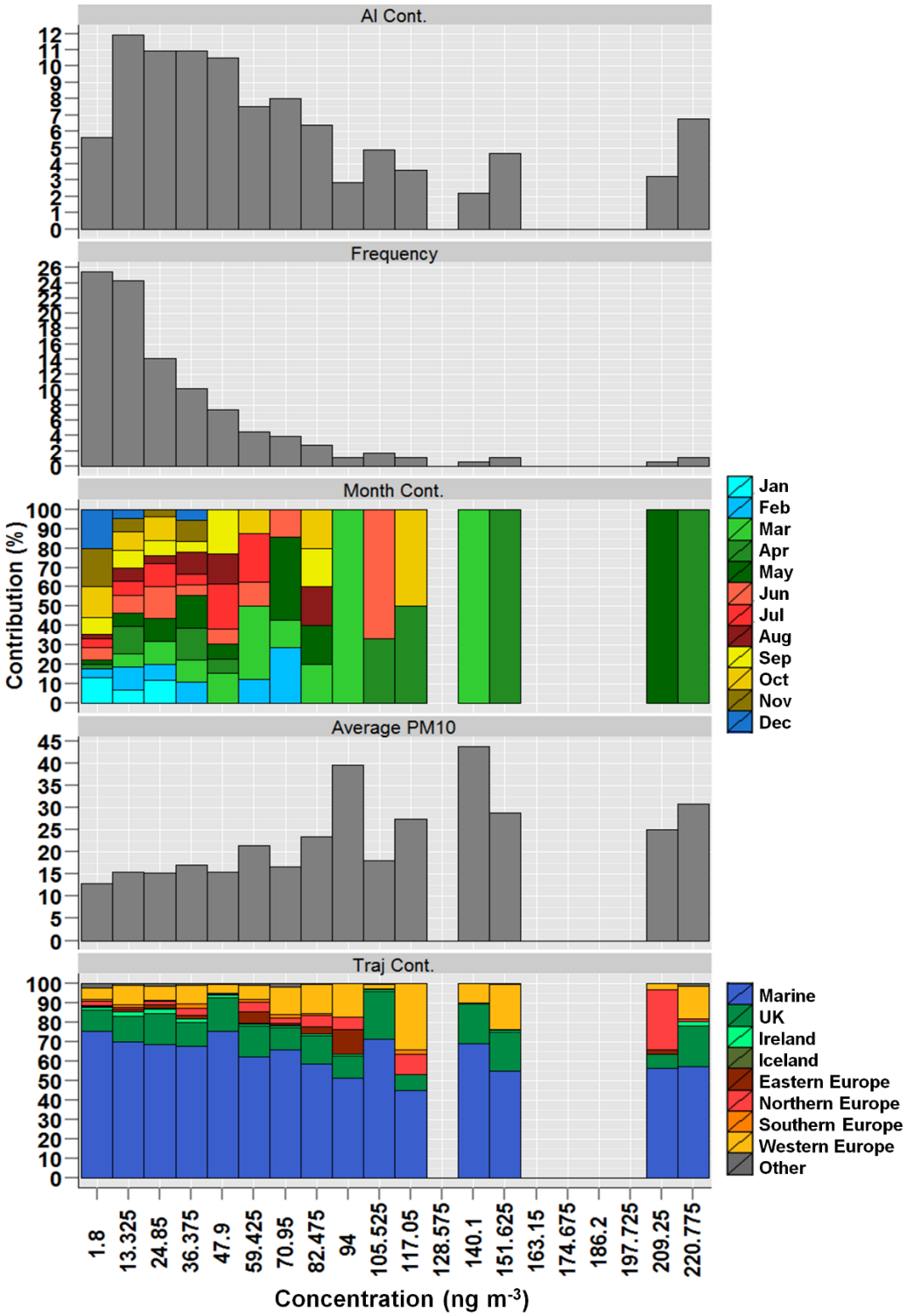

Figure 6.18: Summary of Al variation at Harwell, including the contribution from 20 equal concentration bins to the 4-year average, the frequency with which concentrations in each bin occur, the contribution from each month to concentrations in each bin, average PM_{10} concentration in each concentration bin and the proportion of time trajectories arriving for each concentration bin spent over different geographic regions.

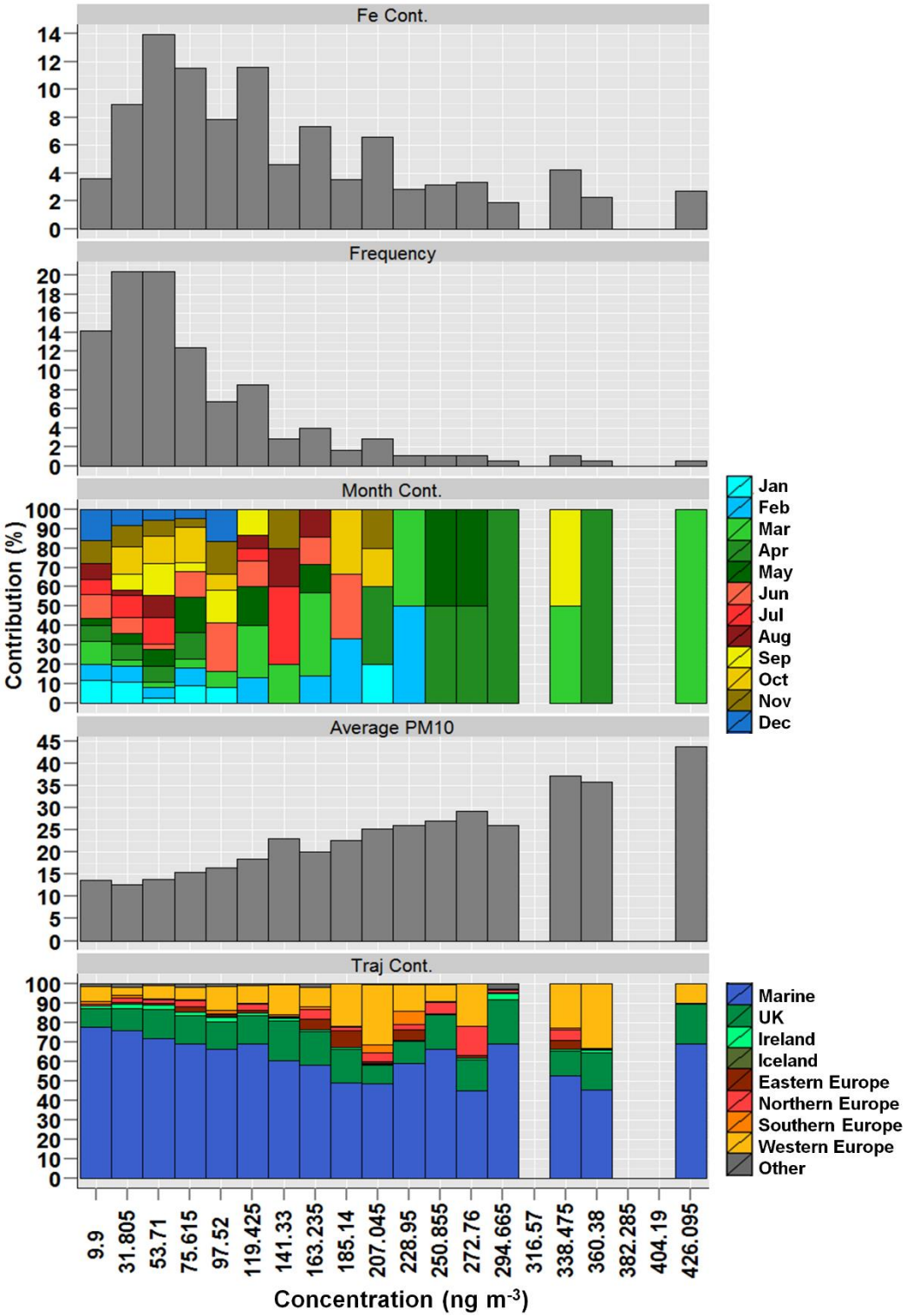

Figure 6.19: Summary of Fe variation at Harwell, including the contribution from 20 equal concentration bins to the 4-year average, the frequency with which concentrations in each bin occur, the contribution from each month to concentrations in each bin, average PM_{10} concentration in each concentration bin and the proportion of time trajectories arriving for each concentration bin spent over different geographic regions.

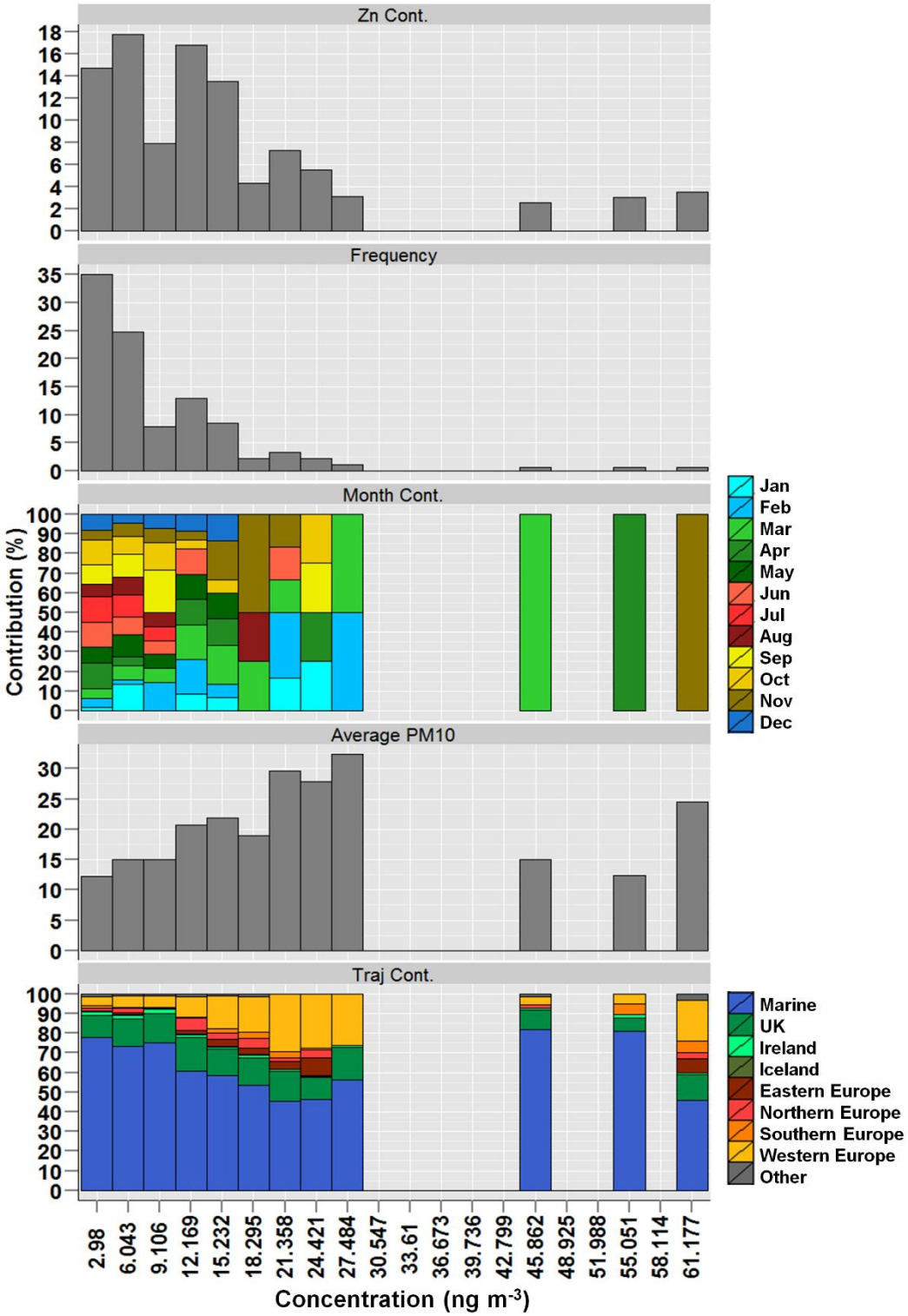

Figure 6.20: Summary of Zn variation, including the contribution from 20 equal concentration bins to the 4-year average, the frequency with which concentrations in each bin occur, the contribution from each month to concentrations in each bin, average PM_{10} concentration in each concentration bin and the proportion of time trajectories arriving for each concentration bin spent over different geographic regions.

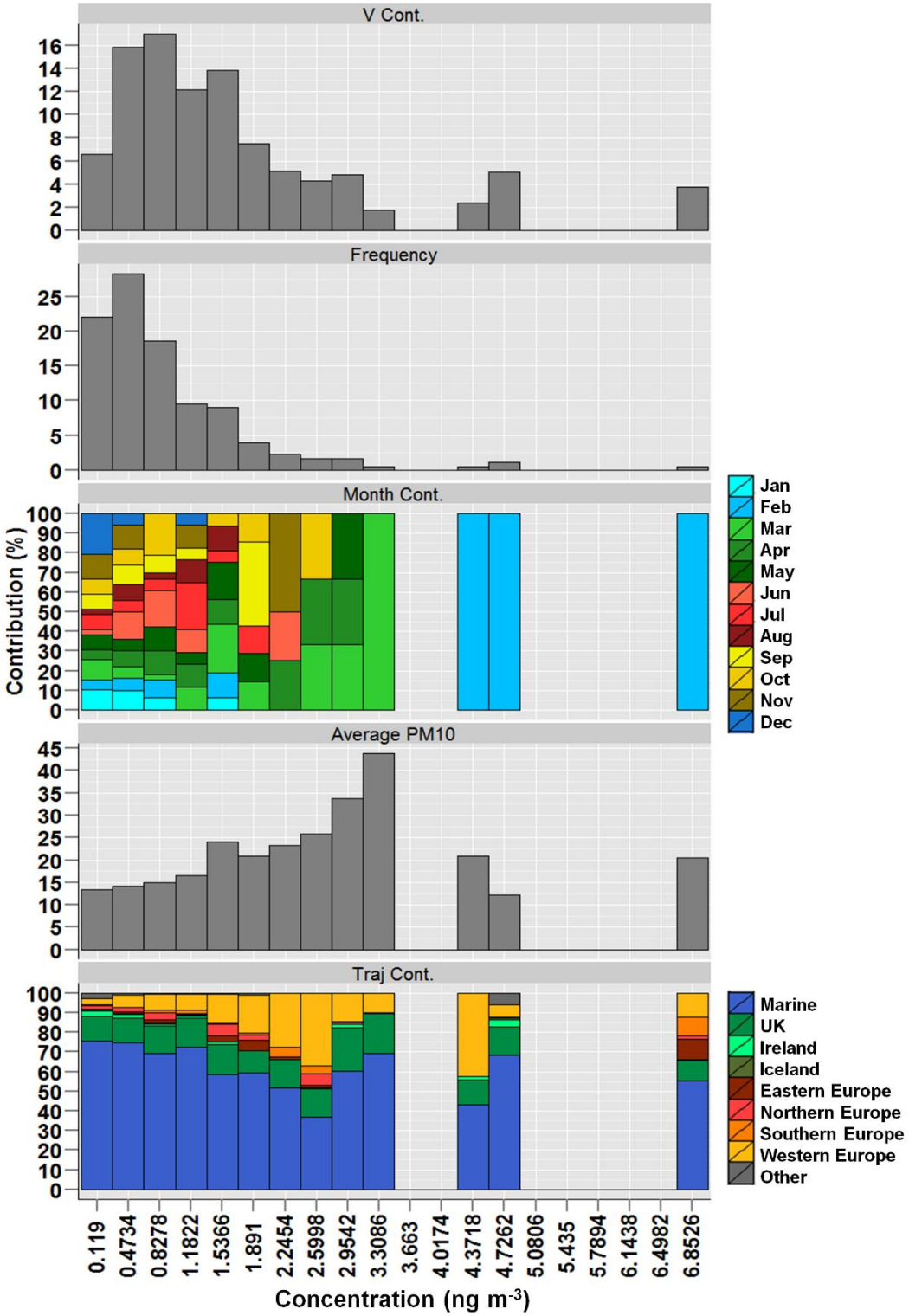

Figure 6.21: Summary of V variation, including the contribution from 20 equal concentration bins to the 4-year average, the frequency with which concentrations in each bin occur, the contribution from each month to concentrations in each bin, average PM_{10} concentration in each concentration bin and the proportion of time trajectories arriving for each concentration bin spent over different geographic regions.

6.4 Implications for the reduction of the long-term PM human health impact metric

The interpretation of PM_{10} and $PM_{2.5}$ measurements at Harwell and Auchencorth showed that a wide variety of conditions contribute to the long-term health impact of PM, and therefore should be taken into account during the formulation of mitigation strategies. It has been shown in numerous studies that the high concentrations episodes of PM_{10} and $PM_{2.5}$, as well as individual constituents across the UK are associated with transport of air pollutants from continental Europe emission sources (Abdalmogith and Harrison, 2005; Harrison et al., 2012; Twigg et al., 2015; Vieno et al., 2014). In this study it was calculated that the high concentration episodes at Harwell were associated with air mass pathways which traversed continental Europe, while at Auchencorth the highest concentrations resulted from air mass which spent a larger proportion of time over the UK. However, it was also shown that reduction of these highest concentrations would not be as effective at reducing the long-term PM health impact (quantified by PM_{10AA} and $PM_{2.5AA}$ metrics) as reduction in moderate concentrations which occur substantially more frequently and therefore have a larger contribution to PM_{10AA} and $PM_{2.5AA}$. The highest PM_{10} and $PM_{2.5}$ concentrations were primarily composed of secondary inorganic aerosol (SIA) constituents, NO_3^-, NH_4^+ and nss-SO_4^-, with a smaller contribution from elemental and organic carbon. The PCA analysis showed that during air masses which traversed western Europe prior to arrival at Harwell, there was an increase in both short and long-range transport of SIA components. Hence in order to reduce the SIA contribution to high PM concentrations, it is necessary to reduce SIA precursor emissions regionally, and also in closer proximity to the site/location of interest.

To reduce the moderate PM_{10} and $PM_{2.5}$ concentrations at both sites, which make the largest contribution to the health impact, there is a necessity to consider a wider variety of conditions compared with high concentration episodes. Moderate concentrations for $PM_{2.5}$ and PM_{10} occur at all times during the year and during all trajectory conditions. There were also a greater number of components with substantial contributions to

PM_{10} and $PM_{2.5}$ concentrations. Components of sea salt, and minor inorganic ions such as Ca^{2+} and K^{+} each have larger contributions to moderate concentrations compared to high concentrations, in addition to the contributions from SIA, EC and OC.

Additionally, there was a substantially wider variety of conditions resulting in the contribution of each individual PM constituent to moderate PM_{10} and $PM_{2.5}$ concentrations compared with the highest concentrations. For example, for NO_3^-, the largest individual contributing constituent, the contribution from different air masses was derived during different PM_{10} or $PM_{2.5}$ concentrations. The contribution from trajectories passing over western Europe was derived to a much larger extent during the highest PM_{10} or $PM_{2.5}$ concentrations, whereas the contribution from trajectories which spend the majority of time over marine environments was mainly derived during low PM concentrations. Hence during the moderate concentrations, the contribution of NO_3^- to total PM_{10} or $PM_{2.5}$ had substantial contributions from all air masses. The PCA analysis showed that the western Europe cluster had elevated short and long-range transport of SIA, Marine-dominated trajectories had relatively low short and long-range transport while UK and northern Europe-dominated trajectories had selective increases in short and long-range transport respectively. Hence reducing emissions from large SIA precursor emissions sources which were relatively infrequently traversed (the western Europe conditions occur 13% of the time and contribute 35% of annual average $PM_{2.5}$ NO_3^- at Harwell in 2013) would result in a reduction in the contribution of SIA to moderate PM concentrations. However, similar levels of benefit could be derived, in terms of reducing the SIA contribution to moderate concentrations with the largest contribution to the long term PM health metrics, from the reduction of smaller SIA precursor emissions sources which are substantially more frequently traversed.

6.5 Conclusions

The chemical climates outlined in this chapter provide a set of statistics for the interpretation of PM mass and component data which detail both the long-term PM health impact, and the conditions producing it. Their application to the measurements at the UK supersites showed a substantially larger long-term health impact metric for PM_{10} and $PM_{2.5}$ at Harwell than at Auchencorth. At both sites, the largest contribution to the long-term health metrics were the frequent moderate concentrations, rather than the relatively infrequent elevated, episodic PM concentrations. The method for reduction of these moderate concentrations is more complicated than the highest concentrations due to the larger number of months, air mass pathways and components which contribute. For example, the contribution of trajectories traversing western Europe to SIA component annual averages was derived mainly during high concentrations, while the contribution from marine-dominant air masses was derived during low concentrations. The SIA contribution to the moderate concentrations was derived to a similar extent from marine, UK and European air masses. Hence methods for the mitigation of the long-term PM health impact must consider that similar improvements in the contribution of SIA to the largest contributing concentrations could be achieved from both the reduction of frequently traversed, smaller emissions sources, and less frequently traversed, larger emissions sources.

The heavy metal components of PM made a small contribution to annual average PM_{10}. Therefore reduction in emissions of heavy metals would not result in significant improvement to annual average PM concentrations. Motivation for heavy metal reduction results from the human health impacts reported for those components individually. However, measurement of heavy metals at higher time resolution at the supersites would allow for a more in-depth assessment of the covariance between the heavy metals as source indicators and the major constituents of PM, and hence provide further evaluation of the conditions producing the long-term PM health impact.

The chemical climatology framework attempts to provide a method for the derivation of a standard set of statistics which link an impact to its causal drivers, and hence identify how it can be most effectively mitigated. The utility of this concept is dependent on the ability of the standardised set of statistics to be widely applied across monitoring sites and to other data sources (e.g. model output). Hence a subset of the chemical climate statistics derived here can be calculated at sites which only measure total PM mass as these sites are more numerous across the UK, Europe and on larger spatial scales than sites which also measure PM composition. The chemical climate statistics shown in this chapter therefore provide a template for a consistent assessment of spatial and temporal differences in the long-term PM health impact and the conditions producing it across monitoring networks. All relevant PM composition data can be integrated using the additional chemical climate statistics, and future work should focus on the application of these statistics across a large number, and diverse range of sites to identify commonalities and differences in the most effective methods for reduction of the long term PM health impact in different regions.

References

Abdalmogith, S. S., Harrison, R. M., 2005. The use of trajectory cluster analysis to examine the long-range transport of secondary inorganic aerosol in the UK. Atmospheric Environment 39, 6686-6695, doi:10.1016/j.atmosenv.2005.07.059.

AQEG, 2012. Fine particulate matter (PM2.5) in the United Kingdom, Air Quality Expert Group, Defra Publications, available at: http://uk-air.defra.gov.uk/assets/documents/reports/cat11/1212141150_AQEG_Fine_Particulate_Matter_in_the_UK.pdf.

Belis, C. A., Karagulian, F., Larsen, B. R., Hopke, P. K., 2013. Critical review and meta-analysis of ambient particulate matter source apportionment using receptor models in Europe. Atmos. Environ. 69, 94-108.

Bell, M. L., Davis, D. L., Fletcher, T., 2004. A retrospective assessment of mortality from the London smog episode of 1952: The role of influenza and pollution. Environ. Health Persp. 112, 6-8.

Braban, C., Tang, S., van Dijk, N., Leeson, S., Simmons, I., Leith, I., Leaver, D., Bealey, B., Sutton, M., Pereira, G., Davies, M., Woods, C., Ritchie, S., Knight, D., Vincent, K., Donovan, B., Kentisbeer, J., Twigg, M., Nemitz, E., Beith, S., Thacker, S., Poskitt, J., Lingard, J., Cape, N., 2012. UK Eutrophying and Acidifying Atmospheric Pollutants (UKEAP): Annual Report 2012, CEH Project nos: C04544, C04013, Defra.

Bro, R., Smilde, A. K., 2014. Principal component analysis. Anal. Method. 6, 2812-2831.

Brown, A. S., Brown, R. J. C., Coleman, P. J., Conolly, C., Sweetman, A. J., Jones, K. C., Butterfield, D. M., Sarantaridis, D., Donovan, B. J., Roberts, I., 2013a. Twenty years of measurement of polycyclic aromatic hydrocarbons (PAHs) in UK ambient air by nationwide air quality networks. Env. Sci. Process. Impact. 15, 1199-1215.

Brown, R. J. C., Butterfield, D. M., Goddard, S. L., Mustoe, C. L., Robins, C., Brown, S. A., Beccaceci, S., Whiteside, K. J., Bradshaw, C., Brennan, S., 2013b. Annual report for 2012 on the UK heavy metals monitoring network, National Physical Laboratory Report AS 79, available at: http://uk-air.defra.gov.uk/assets/documents/reports/cat13/1310031024_Heavy_Metals_Network_Annual_Report_2012_FINAL.pdf.

Carslaw, D. C., Ropkins, K., 2012. openair - An R package for air quality data analysis. Environ. Modell. Softw. 27-28, 52-61.

Charron, A., Degrendele, C., Laongsri, B., Harrison, R. M., 2013. Receptor modelling of secondary and carbonaceous particulate matter at a southern UK site. Atmos. Chem. Phys. 13, 1879-1894.

Clifton, M., 1964. The National Survey of air pollution. Proceedings of the Royal Society of Medicine-London 57, 1013-1015.

COMEAP, 2015. Statement on the evidence for differential health effects of particulate matter according to source or components. Committee on the Medical Effects of Air Pollution, available

from: https://www.gov.uk/government/uploads/system/uploads/attachment_data/file/411762/COMEAP_The_evidence_for_differential_health_effects_of_particulate_matter_according_to_source_or_components.pdf.

Eaton, S., 2013. QA/QC Data Ratification Report for the Automatic Urban and Rural Network, October-December 2012, and Annual Report 2012. Ricardo-AEA/R/3364 Issue 1. Contract Report to the Department for Environment, Food and Rural Affairs. Ricardo-AEA, available at: http://uk-air.defra.gov.uk/assets/documents/reports/cat05/1307171010_QAQC_Ricardo_Q4_2012_Issue_1.pdf.

Fleming, Z. L., Monks, P. S., Manning, A. J., 2012. Review: Untangling the influence of air-mass history in interpreting observed atmospheric composition. Atmospheric Research 104, 1-39.

Galarneau, E., 2008. Source specificity and atmospheric processing of airborne PAHs: Implications for source apportionment. Atmos. Environ. 42, 8139-8149.

Halliday, E. C., 1961. A Historical Review of Atmospheric Pollution. In: Air Pollution. World Health Organisation Monograph Series No. 46. Geneva, pp. 9-37.

Harrison, R. M., Yin, J. X., 2008. Sources and processes affecting carbonaceous aerosol in central England. Atmos. Environ. 42, 1413-1423.

Harrison, R. M., Laxen, D., Moorcroft, S., Laxen, K., 2012. Processes affecting concentrations of fine particulate matter (PM2.5) in the UK atmosphere. Atmos. Environ. 46, 115-124.

Heal, M. R., Kumar, P., Harrison, R. M., 2012. Particles, air quality, policy and health. Chem. Soc. Rev. 41, 6606-6630.

Heimann, H., 1961. Effects of Air Pollution on Human Health. In: Air Pollution. World Health Organisation Monograph Series No. 46. Geneva, pp. 159-220.

Kaufman, L., Rousseeuw, P. J., 1990. Finding Groups in Data: An Introduction to ClusterAnalysis. Wiley, New York. Wiley, New York.

Kim, K.-H., Jahan, S. A., Kabir, E., Brown, R. J. C., 2013. A review of airborne polycyclic aromatic hydrocarbons (PAHs) and their human health effects. Environ. Int. 60, 71-80.

Mangiameli, P., Chen, S. K., West, D., 1996. A comparison of SOM neural network and hierarchical clustering methods. Eur. J. Oper. Res. 93, 402-417.

Mielke, H. W., Zahran, S., 2012. The urban rise and fall of air lead (Pb) and the latent surge and retreat of societal violence. Environ. Int. 43, 48-55.

Pio, C. A., Legrand, M., Alves, C. A., Oliveira, T., Afonso, J., Caseiro, A., Puxbaum, H., Sanchez-Ochoa, A., Gelencser, A., 2008. Chemical composition of atmospheric aerosols during the 2003 summer intense forest fire period. Atmos. Environ. 42, 7530-7543.

Putaud, J. P., Van Dingenen, R., Alastuey, A., Bauer, H., Birmili, W., Cyrys, J., Flentje, H., Fuzzi, S., Gehrig, R., Hansson, H. C., Harrison, R. M., Herrmann, H., Hitzenberger, R., Hueglin, C., Jones, A. M., Kasper-Giebl, A., Kiss, G., Kousa, A., Kuhlbusch, T. A. J., Loeschau, G., Maenhaut, W., Molnar, A., Moreno, T., Pekkanen, J., Perrino, C., Pitz, M., Puxbaum, H., Querol, X., Rodriguez, S., Salma, I., Schwarz, J., Smolik, J., Schneider, J., Spindler, G., ten Brink, H., Tursic, J., Viana, M., Wiedensohler, A., Raes, F., 2010. A European aerosol phenomenology-3: Physical and chemical characteristics of

particulate matter from 60 rural, urban, and kerbside sites across Europe. Atmos. Environ. 44, 1308-1320, doi:10.1016/j.atmosenv.2009.12.011.

Querol, X., Viana, M., Alastuey, A., Amato, F., Moreno, T., Castillo, S., Pey, J., de la Rosa, J., de la Campa, A. S., Artinano, B., Salvador, P., Dos Santos, S. G., Fernandez-Patier, R., Moreno-Grau, S., Negral, L., Minguillon, M. C., Monfort, E., Gil, J. I., Inza, A., Ortega, L. A., Santamaria, J. M., Zabalza, J., 2007. Source origin of trace elements in PM from regional background, urban and industrial sites of Spain. Atmos. Environ. 41, 7219-7231.

R Core Team, 2014. R: A Language and Environment for Statistical Computing. R Foundation for Statistical Computing, Vienna, Austria, http://www.R-project.org/.

REVIHAAP, 2013. Review of evidence on health aspects of air pollution – REVIHAAP Project technical report. World Health Organization (WHO) Regional Office for Europe, Bonn. http://www.euro.who.int/__data/assets/pdf_file/0004/193108/REVIHAAP-Final-technical-report-final-version.pdf.

Sarantaridis, D., Goddard, S. L., Hussain, D., Whiteside, K. J., Hughey, P., Brown, A. S., Brown, R. J. C., Brennan, S., 2013. Annual Report for 2012 on the UK PAH Monitoring and Analysis Network, National Physical Laboratory Report AS 84, available at: http://uk-air.defra.gov.uk/assets/documents/reports/cat05/1402041506_Defra_PAH_Network_2012_annual_report_FINAL_v2.pdf.

She, N., 1997. Analyzing censored water quality data using a non-parametric approach. J. Am. Water Resour. As. 33, 615-624.

Twigg, M. M., Di Marco, C. F., Leeson, S., van Dijk, N., Jones, M. R., Leith, I. D., Morrison, E., Coyle, M., Proost, R., Peeters, A. N. M., Lemon, E., Frelink, T., Braban, C. F., Nemitz, E., Cape, J. N., 2015. Water soluble aerosols and gases at a UK background site – Part 1: Controls of PM2.5 and PM10 aerosol composition. Atmos. Chem. Phys. Discuss. 15, 3703-3743.

Viana, M., Kuhlbusch, T. A. J., Querol, X., Alastuey, A., Harrison, R. M., Hopke, P. K., Winiwarter, W., Vallius, A., Szidat, S., Prevot, A. S. H., Hueglin, C., Bloemen, H., Wahlin, P., Vecchi, R., Miranda, A. I., Kasper-Giebl, A., Maenhaut, W., Hitzenberger, R., 2008. Source apportionment of particulate matter in Europe: A review of methods and results. J. Aerosol Sci. 39, 827-849.

Vieno, M., Heal, M. R., Hallsworth, S., Famulari, D., Doherty, R. M., Dore, A. J., Tang, Y. S., Braban, C. F., Leaver, D., Sutton, M. A., Reis, S., 2014. The role of long-range transport and domestic emissions in determining atmospheric secondary inorganic particle concentrations across the UK. Atmos. Chem. Phys. 14, 8435-8447, doi:10.5194/acp-14-8435-2014.

Vincent, J. H., 2005. Health-related aerosol measurement: a review of existing sampling criteria and proposals for new ones. J. Environ. Monit. 7, 1037-1053.

Ward, J., 1963. Hierarchical Grouping to Optimize an Objective Function. J. Am. Stat. Assoc. 58, 236 - 244.

Yin, J. X., Harrison, R. M., 2008. Pragmatic mass closure study for PM1.0, PM2.5 and PM10 at roadside, urban background and rural sites. Atmos. Environ. 42, 980-988.

Chapter 7: The future application of chemical climatology

7.1 Introduction

The case studies in Chapters 4-6 provide conclusive evidence that the chemical climatology framework can enhance interpretation of monitoring site data. Specifically, it was shown to facilitate analysis of spatial and temporal changes in atmospheric composition impacts, comparison of different impacts, and consideration of multi-pollutant impacts. The Harwell and Auchencorth supersite measurements used in these studies represent only a small fraction of atmospheric composition data collected each year at thousands of sites globally. Hence substantially greater benefit could result from the extension of this chemical climatology concept at two monitoring sites to all sites within a monitoring network or between monitoring networks to improve their integration. To achieve this, standard sets of statistics that quantify the 'impact', 'state' and 'drivers', i.e. the chemical climate of distinct atmospheric composition impacts, should be developed which can then be consistently applied to data collected at a large number of monitoring sites. This chapter provides a practical demonstration of how this can be achieved, and highlights some of the resulting benefits such as assessment of the spatial applicability of mitigation strategies and identification and communication of linkages between anthropogenic atmospheric composition change and societal and economic impacts.

Chapter 1 outlined a chronology of atmospheric composition monitoring networks highlighting the benefits derived from increasing coordination and standardisation. Since the mid-1800s, and especially since the 1960s, standardisation in the context of monitoring networks has extended to site representativeness, measurement methods, data processing and data archiving. These advances have resulted in large increases in knowledge of atmospheric chemistry and its impacts (Seinfeld and Pandis, 2006).

However, in contrast there is a lack of standardisation in the interpretation of data across and between monitoring networks which limits the information obtained. For example, differences in air quality standards designed to protect human health or vegetation mean that these impacts cannot be compared consistently across different regions (van den Elshout et al., 2008). Hence the extension of monitoring network standardisation to data interpretation using sets of standard chemical climate statistics for different atmospheric composition impacts is proposed to further increase the information derived from monitoring networks.

Currently, public engagement with issues surrounding anthropogenic atmospheric composition change is relatively low compared with other societal issues, and the state of knowledge about the severity of these impacts. While a study calculated that a majority of the public agree action is required to tackle climate change (Brechin and Bhandari, 2011), climate change is also perceived as a threat distanced temporally and spatially from people's daily lives (Spence et al., 2012; Wolf and Moser, 2011). Many of the drivers of atmospheric composition impacts operate on regional and global scales, yet the public perception of air pollution is strongly influenced by the local setting (Bickerstaff and Walker, 2001). Hence when the environmental values, and associated actions taken by citizens of the EU, USA and globally are assessed, the probability of mitigation of these impacts and the transition to more sustainable practices is currently calculated as being low (Matutinovic, 2012). The lack of public engagement provides an additional motivating factor to increase the effectiveness of monitoring network data interpretation to communicate the wide range of consequences of anthropogenic atmospheric composition change, in addition to a general desire that the cost of monitoring networks yield maximum return.

When framed in the context of other issues, climate change was shown not to be the most important priority, including against specific societal issues (world poverty, crime, terrorism, war), other environmental issues (water pollution) and personal issues (health, finances and relationships) (Pidgeon, 2012). However, the number of societal areas which are linked with anthropogenic atmospheric composition change

is large and varied, including violence and conflict (Hsiang et al., 2013; Mielke and Zahran, 2012), human health (REVIHAAP, 2013), food security and agriculture (Bhatia et al., 2012; Burney and Ramanathan, 2014), unemployment, education, personal income (Branis and Linhartova, 2012), urbanisation (Duh et al., 2008), migration (Farbotko and Lazrus, 2012), tourism (Caric and Mackelworth, 2014), social deprivation and inequality (Padilla et al., 2014), poverty (Bell and Ebisu, 2012) and economic growth (Grossman and Krueger, 1995). These issues often have a greater degree of public engagement, and are more strongly linked to people's local environment and daily lives. The identification of linkages between atmospheric composition change and a diverse range of societal impacts would therefore be an effective strategy to improve public understanding of atmospheric composition impacts and increase support for their mitigation.

Consistent data interpretation applied across measurement sites has been shown previously to increase the useful information derived from a network, and the ability of networks to communicate the extent and risks of anthropogenic atmospheric composition change. The Köppen-Geiger (KG) climate classification scheme, originally derived in 1900 (Peel et al., 2007), demonstrates the successful application of standardised data interpretation to link meteorological measurements to a diverse range of impacts. Temperature and precipitation measurements at sites across the globe are subject to common interpretation to determine the 'climate zone' each site represents. In the past 5 years, KG climate classifications have linked the climate of a region to impacts in the fields of agriculture (Berg et al., 2013), census and survey collection (Wright et al., 2012), climate change (Zhang and Yan, 2014), construction (Wong et al., 2012), ecology (Vilizzi et al., 2015), energy (Li et al., 2014), forensics (corpse decomposition) (Meyer et al., 2013), forestry (Woodall et al., 2013), health (Hurrell et al., 2012), hydrology and drought (Punzet et al., 2012; Van Lanen et al., 2013), land use (Siqueira Neto et al., 2011), natural vegetation (Werier and Naczi, 2012), paleoclimate (Rey et al., 2013), sport (Walden et al., 2013), thermal comfort (Mishra and Ramgopal, 2013) and tourism (Hadwen et al., 2012).

There is no corresponding mechanism to the KG system applicable to atmospheric composition measurement sites. Hence monitoring network data are an underused resource in quantifying and communicating the link between anthropogenic atmospheric composition change and a diverse range of societal impacts, especially given the large volume of data collected at sites across the globe in a broad range of locations. The widespread application of the chemical climatology framework has the potential to address this by providing a common basis for the quantification of an impact of atmospheric composition (e.g. human health, vegetation or climate) which can then be linked to secondary societal impacts such as those outlined above. Additionally, the chemical climatology framework extends analysis from quantification of an impact using an appropriate metric by also outlining the conditions producing the impact through the calculation of state and drivers statistics. The aim of this chapter is to demonstrate how the potential advantages of a standardised interpretation of monitoring network data, specifically the chemical climatology framework, could be realised on a larger scale, i.e. across the entirety of a monitoring network. A standard set of statistics which quantify the human health O_3 chemical climate are applied to data from sites across Europe contributing to the European Monitoring and Evaluation Program (EMEP) network. The focus is not on the specific conclusions from this particular application of the chemical climatology framework. Instead, the emphasis is on the value added to these high quality measurements derived from calculation and visualisation of a standard set of chemical climate statistics.

7.2 Derivation of ozone health chemical climates across the EMEP network

7.2.1 Ozone health chemical climate statistics

The statistics used to derive the O_3 human health chemical climate at each rural EMEP site were based on those outlined Chapter 4, and are described in Table 7.1. The metrics used to quantify human health-relevant O_3 were the SOMO10 and SOMO35 (the annual sum of the positive differences between the daily maximum 8-h average and a threshold set at 10 and 35 ppb respectively), which are in line with the latest World Health Organisation (WHO) review (REVIHAAP, 2013). The state and drivers statistics describe the conditions which produce the metric values. To ensure chemical climates could be calculated at each site, and to maintain maximum transferability to other monitoring networks, the majority of statistics require only an annual time series of hourly O_3 concentrations and no other concurrent measurements. However, it is acknowledged that additional statistics utilising other measurements could provide substantial insight into the state and drivers of the chemical climate, for example measurements of ozone precursors and meteorological measurements.

The statistics which quantify the emissions drivers, i.e. the cumulative NO_x and VOC emissions along the pathway of air mass back trajectories during the 4 days prior to their arrival at the EMEP sites, required additional tools to just the O_3 time series. These statistics required the calculation of HYSPLIT air mass back trajectories (Draxler and Rolph, 2013) for the location of each EMEP site during the years of operation using NCEP-NCAR Reanalysis meteorological data (Kistler et al., 2001). The back trajectories were calculated in R, using an algorithm developed as part of the Openair project (Carslaw and Ropkins, 2012; R Core Team, 2014). For each year at each site 2920 4-day back trajectories arriving at 3-h intervals were calculated. The 2920 4-day back trajectories arriving each year were combined separately with reported gridded VOC and NO_x emissions obtained from the Centre for Emissions Inventories and Projections (CEIP, www.ceip.at), using the procedure outlined in

Chapter 4.2. The inclusion of these statistics allowed investigation of the emissions drivers of the O_3 health chemical climates. Back trajectories can be calculated for any location globally using the Openair algorithm, and the emissions map used allows calculation of these statistics at any European location. Other emissions maps could be used for other locations (Janssens-Maenhout et al., 2011; Lamarque et al., 2010), and hence the use of these non-O_3 time series tools in deriving the chemical climates do not present a serious limitation in the extension of this concept to other locations or larger spatial scales (e.g. other monitoring networks).

The O_3 data was downloaded from the EMEP data file archive (http://www.nilu.no/projects/ccc/emepdata.html), and statistics were calculated for each year a site was in operation between 1990 and 2011. The standardised method for processing and ensuring sufficient data quality are outlined in the EMEP Manual for Sampling and Analysis (EMEP, 2014). For a particular year at a particular site, it was necessary that data capture was greater than 75% in each month of the year for inclusion in the analysis. This ensured there was sufficient data capture across the year to accurately calculate important chemical climate statistics such as the monthly contribution to the impact metrics.

Table 7.1: Statistics derived to quantify the 'impact', 'state' and 'drivers' of the chemical climate specific to the human health impact of O_3 across the EMEP network.

Chemical Climate Component	Statistic	Further Description
Impact	SOMO10 (ppb.d) SOMO35 (ppb.d)	Annual sum of the positive difference between the daily maximum 8-h average O_3 concentration and 10 and 35 ppb
State	Monthly contribution to impact metric	
	Contribution from 5 ppb concentration bins (10-15 ppb to >70 ppb) to impact metric	
	Diurnal O_3 cycle amplitude on impact metric accumulation days (ADs) and non-accumulation days (NADs)	Diurnal cycle calculated as the difference between the maximum and minimum O_3 concentration within each calendar day
Drivers	NO_x trajectory emissions estimate on ADs and NADs (Mg $96h^{-1}$)	Integration of 0.5º x 0.5º gridded hourly NO_x emissions along the pathway of air mass trajectory during 96 h prior to arrival at the site. The daily NO_x trajectory emissions estimate is average emissions estimate of 8 trajectories arriving each day.
	VOC trajectory emissions estimate on ADs and NADs (Mg $96h^{-1}$)	Integration of 0.5º x 0.5º gridded hourly VOC emissions along the pathway of air mass trajectory during 96 h prior to arrival at the site. The daily VOC trajectory emissions estimate is average emissions estimate of 8 trajectories arriving each day.

7.3 Results and Discussion

Section 7.3.1 provides a brief overview of the O_3 human health chemical climate calculated at EMEP sites across Europe. The aim is to show the additional information gained from these measurements from the application of a standard interpretation of measurement data across a network, and the specific advantages of using the chemical climatology framework to achieve this. The full suite of chemical climate statistics calculated for SOMO10 and SOMO35 across 1990-2011 are viewable at https://chemclim.shinyapps.io/App-1/. This website was constructed using the R package, Shiny (Chang et al., 2015), and has interactive graphics which allow the user to select the chemical climate statistics in which they are most interested. Users can select a year and an impact metric to compare impact, state and drivers at all EMEP sites. Additionally, comparison can be made across the whole time series (1990-2011) either between two sites for the same impact, or for different impacts (i.e. SOMO10 and SOMO35) at the same site. This website is experimental, and intended only to show how the calculation of a large number of chemical climate statistics might be visualised for maximum benefit to the user. In the following sections, the spatial differences in European ozone health chemical climate are compared for an example year (2011) for the SOMO35 metric.

As outlined in Chapter 4, O_3 concentrations at a particular location are a product of processes occurring on three spatial scales (Jenkin, 2008). Hemispheric background concentrations are defined here as those concentrations produced with minimal influence from European emissions. These concentrations are therefore transported into a European domain where they are then modified by regional processes. Regional scale processes can enhance O_3 concentrations above hemispheric background levels through additional regional O_3 production, or deplete hemispheric background O_3 concentrations chemically through reaction with NO or through deposition. The balance between these O_3 forming and O_3 destruction processes determines whether there is a net increase or decrease in O_3 at the regional scale relative to the hemispheric background. Regional background O_3 concentrations are then modified at the local

scale, which can result in a further destruction of O_3 in high NO_x environments. The extent of the regional contribution to O_3 concentrations is determined by a number of factors, including the proximity of a location to emissions sources, meteorological conditions which influence the efficiency of photochemical O_3 production on the regional scale and the trajectory taken by the air mass arriving at a location.

Ozone concentrations, and the processes influencing O_3 concentrations on each of these scales, have been studied previously (Derwent et al., 2013; Jenkin, 2008; Wilson et al., 2012). The purpose of the application of a standard set of chemical climate statistics is to determine how processes on each of these scales contribute to health-relevant O_3. This information is required so that it can be determined what can be done on each spatial scale to reduce the impact of O_3 on human health. In Europe, action can be taken by member states, and the EU provides a regional regulatory framework to address these issues. Hence by interpreting O_3 measurement data across Europe similarly, it is possible to assess the extent to which national and regional cooperation can improve O_3 health impacts, and also what benefits would result from mitigation strategies agreed at a larger, hemispheric/global level.

7.3.1 European ozone health chemical climates in 2011

The chemical climate statistics are visualised in Figures 7.1-7.6. The SOMO35 values at the 92 EMEP sites with sufficient data capture are shown in Figure 7.1. The ‘state’ of the chemical climate is outlined by the number of days SOMO35 is accumulated at each site (Figure 7.2), the seasonal contribution to SOMO35 (Figure 7.3), the contribution from 5 ppb concentration ranges (Figure 7.4) and the ratio of the diurnal O_3 cycle amplitude on SOMO35 accumulation days (ADs) and non-accumulation days (NADs) (Figure 7.5). The larger the ratio, the larger the difference between daily maximum and minimum O_3 concentrations on SOMO35 ADs compared to NADs. The drivers are visualised as the ratio of the NO_x and VOC trajectory emissions estimate on SOMO35 ADs and NADs (Figures 7.6 and 7.7 for NO_x and VOCs respectively).

For these ratios, the closer the value is to 1, the more similar the trajectory emissions estimates are on average during SOMO35 ADs and NADs. However, a value of 1 does not indicate that VOC and NO_x emissions are not drivers for the O_3 health chemical climate at a particular site, but rather that additional drivers may also be important. For example, rather than variation in the trajectory emissions estimate determining O_3 variation at a site, meteorological conditions may be important in determining the extent to which precursor emissions react to form O_3 prior to the trajectories arrival at the site. The availability of representative meteorological measurements across the EMEP network precludes calculation of meteorological driver statistics, but the meteorological drivers are considered for the detailed O_3 health and vegetation chemical climate analysis at Harwell and Auchencorth detailed in Chapter 4.

The impact of O_3 on human health, quantified by the SOMO35 metric, across the EMEP sites ranged from 485 ppb.d at Pallas, Finland, to 6175 ppb.d at Ayia Marina, Cyprus (Figure 7.1). The 'state' and 'drivers' chemical climate statistics highlight the differences in contribution from hemispheric and regional processes in determining SOMO35 at each site. Three distinct chemical climate 'phases' (spatial domains with substantially different chemical climates, Chapter 2) are apparent from the division of sites into northern, central and southern Europe. The membership of each site to these domains is shown in Table 7.2 and was primarily based on the latitude of the stations. The division between phases was semi-arbitrary, and some sites exhibit intermediate behaviour (discussed below).

In northern Europe, including sites in Scandinavia, the UK, Ireland, and Baltic countries, SOMO35 in 2011 was generally lower than areas of Europe further south (Figure 7.1). The average SOMO35 in Northern Europe was 1279 ± 507 ppb.d compared to 2779 ± 1147 ppb.d and 3831 ± 1307 ppb.d in Central and Southern Europe respectively. The major contribution to SOMO35 at the northern sites was mainly in spring, on average 59%, up to 80% at some Finnish sites and at least 40% across all sites (Figure 7.3). The second largest season, in terms of SOMO35 accumulation was generally summer, on average 23% but ranging from 3% to 48%. Within this region,

the majority of SOMO35 was accumulated during concentrations in the range 35-55 ppb (Figure 7.4). Higher concentrations were less frequent and make a smaller contribution. An exception were sites in the south of the UK, such as Lullington Heath, where there was a larger contribution from high concentrations. At Lullington Heath in 2011, the contribution from concentrations above 60 ppb was 28%, compared to an average of just 8% across all sites in Northern Europe. Lullington Heath is closer to continental Europe, and may therefore represent an intermediate site between the two chemical climate phases. Similarly, the increase in diurnal O_3 cycle amplitude during SOMO35 accumulation days (ADs) compared with non-accumulation days (NADs) was larger at lower latitudes within Northern Europe, but lower than for Central European sites. The average increase was 24% at all Northern European sites, 42% at sites in south-east England, but 63% in Central Europe (Figure 7.5). Finally, the emissions drivers showed that in Northern Europe on average there was larger NO_x and VOC trajectory emissions estimates on NADs than ADs (Figure 7.6). Again, the main exceptions were sites in south-east England.

The chemical climate statistics for northern European sites suggest that SOMO35 was derived to a larger extent from hemispheric background concentrations than in other areas of Europe. Hemispheric background concentrations peak in spring (Derwent et al., 2013; Parrish et al., 2013), when contribution to SOMO35 was largest. Favourable conditions for regional photochemical O_3 production are most frequent during summer, and result in the highest O_3 concentrations, and greater diurnal variation (Jenkin, 2008). Hence the lower increase in diurnal O_3 cycle amplitude, and smaller contribution from high concentrations compared to other areas of Europe suggest regional O_3 production had a smaller relative contribution to health-relevant O_3 in northern Europe. Finally, the higher NO_x (and VOC) trajectory emissions estimates during NADs compared with ADs indicates that, on average, exposure to regional emissions resulted in depletion of hemispheric background O_3.

Table 7.2: Details of EMEP sites included in the O_3 health chemical climate analysis for 2011.

Site Code	Country	Site Name	Abbreviated Name	Lat-itude	Long-itude	Altitude (m)	Region of Europe
FI0096G	Finland	Pallas	pallas	68.000	24.150	340	Northern
FI0022R	Finland	Oulanka	oulanka	66.320	29.402	310	Northern
FI0037R	Finland	Ähtäri II	ahtari2	62.583	24.183	180	Northern
FI0017R	Finland	Virolahti	virolahti	60.527	27.686	4	Northern
FI0009R	Finland	Utö	uto	59.779	21.377	7	Northern
NO0015R	Norway	Tustervatn	tustervatn	65.833	13.917	439	Northern
NO0039R	Norway	Kårvatn	karvatn	62.783	8.883	210	Northern
NO0056R	Norway	Hurdal	hurdal	60.372	11.078	300	Northern
NO0052R	Norway	Sandve	sandve	59.200	5.200	15	Northern
NO0043R	Norway	Prestebakke	pbakke	59.000	11.533	160	Northern
EE0009R	Estonia	Lahemaa	lahemaa	59.500	25.900	32	Northern
EE0011R	Estonia	Vilsandi	vilsandi	58.383	21.817	6	Northern
SE0013R	Sweden	Esrange	esrange	67.883	21.067	475	Northern
SE0039R	Sweden	Grimsö	grimso	59.728	15.472	132	Northern
SE0012R	Sweden	Aspvreten	aspvreten	58.800	17.383	20	Northern
SE0032R	Sweden	Norra-Kvill	norrakvill	57.817	15.567	261	Northern
SE0014R	Sweden	Råö	rao	57.394	11.914	5	Northern
SE0011R	Sweden	Vavihill	vavihill	56.017	13.150	175	Northern
LT0015R	Latvia	Preila	preila	55.350	21.067	5	Northern
DK0031R	Denmark	Ulborg	ulborg	56.283	8.433	10	Northern
IE0031R	Ireland	Mace Head	macehead	53.167	-9.500	15	Northern
DE0001R	Germany	Westerland	westerland	54.926	8.310	12	Central
DE0009R	Germany	Zingst	zingst	54.433	12.733	1	Central
DE0007R	Germany	Neuglobsow	nglobsow	53.167	13.033	62	Central
DE0002R	Germany	Waldhof	waldhof	52.802	10.759	74	Central
DE0008R	Germany	Schmücke	schmucke	50.650	10.767	937	Central
DE0003R	Germany	Schauinsland	sland	47.915	7.909	1205	Central
NL0009R	Netherlands	Kollumerwaard	kward	53.334	6.277	1	Central
NL0091R	Netherlands	De Zilk	dezilk	52.300	4.500	4	Central
NL0007R	Netherlands	Eibergen	eibergen	52.083	6.567	20	Central
NL0010R	Netherlands	Vredepeel	vredepeel	51.541	5.854	28	Central
PL0004R	Poland	Leba	leba	54.750	17.533	2	Central
PL0002R	Poland	Jarczew	jarczew	51.817	21.983	180	Central
PL0003R	Poland	Sniezka	sniezka	50.733	15.733	1603	Central
GB0052R	UK	Lerwick	lerwick	60.139	-1.185	85	Northern
GB0033R	UK	Bush	bush	55.859	-3.205	180	Northern
GB0048R	UK	Auchencorth	auch	55.793	-3.245	260	Northern
GB0006R	UK	Lough Navar	lnavar	54.443	-7.870	126	Northern
GB0037R	UK	Ladybower	ladybower	53.399	-1.753	420	Northern
GB0031R	UK	Aston Hill	astonhill	52.504	-3.033	370	Northern
GB0039R	UK	Sibton	sibton	52.294	1.463	46	Northern
GB0050R	UK	St. Osyth	stosyth	51.778	1.082	8	Northern
GB0036R	UK	Harwell	harwell	51.573	-1.317	137	Northern
GB0038R	UK	Lullington Heath	lullington	50.793	0.179	120	Northern
BE0032R	Belgium	Eupen	eupen	51.458	6.003	295	Central
BE0001R	Belgium	Offagne	offagne	49.878	5.204	430	Central
CZ0001R	Czech Republic	Svratouch	svratouch	49.733	16.05	737	Central
CZ0003R	Czech Republic	Kosetice	kosetice	49.583	15.083	534	Central
FR0009R	France	Revin	revin	49.9	4.633	390	Central
FR0018R	France	La Coulonche	coulonche	48.633	-0.450	309	Central

FR0008R	France	Donon	donon	48.5	7.133	775	Central
FR0014R	France	Montandon	montandon	47.3	6.833	836	Central
FR0010R	France	Morvan	morvan	47.267	4.083	620	Central
FR0015R	France	La Tardière	tardiere	46.650	-0.750	133	Central
FR0016R	France	Le Casset	lecasset	45.000	6.467	1750	Central
FR0013R	France	Peyrusse Vieille	peyrusse	43.617	0.183	200	Central
AT0042R	Austria	Heidenreichstein	hrstein	48.879	15.047	570	Central
AT0045R	Austria	Dunkelsteinerwald	dswald	48.371	15.547	320	Central
AT0046R	Austria	Gänserdorf	ganserdorf	48.335	16.731	161	Central
AT0043R	Austria	Forsthof	forsthof	48.106	15.919	581	Central
AT0047R	Austria	Stixneusiedl	snsiedl	48.051	16.677	240	Central
AT0041R	Austria	Haunsberg	haunsberg	47.973	13.016	730	Central
AT0048R	Austria	Zoebelboden	zbboden	47.839	14.441	899	Central
AT0002R	Austria	Illmitz	illmitz	47.767	16.767	117	Central
AT0040R	Austria	Masenberg	masenberg	47.348	15.882	1170	Central
SK0006R	Slovakia	Starina	starina	49.050	22.267	345	Central
CH0003R	Switzerland	Tänikon	tanikon	47.480	8.905	539	Central
CH0005R	Switzerland	Rigi	rigi	47.068	8.464	1031	Central
CH0004R	Switzerland	Chaumont	chaumont	47.050	6.979	1137	Central
CH0002R	Switzerland	Payerne	payerne	46.813	6.945	489	Central
CH0001G	Switzerland	Jungfraujoch	jfjoch	46.548	7.985	3578	Central
SI0031R	Slovenia	Zarodnje	zarodnje	46.429	15.003	770	Central
SI0032R	Slovenia	Krvavec	krvavec	46.299	14.539	1740	Central
SI0033R	Slovenia	Kovk	kovk	46.129	15.114	600	Central
BG0053R	Bulgaria	Rojen Peak	rojenpeak	41.696	24.739	1750	Southern
IT0004R	Italy	Ispra	ispra	45.800	8.633	209	Central
IT0001R	Italy	Montelibretti	mbretti	42.100	12.633	48	Southern
ES0008R	Spain	Niembro	niembro	43.442	-4.850	134	Southern
ES0016R	Spain	O Saviñao	osavinao	43.231	-7.700	506	Southern
ES0005R	Spain	Noya	noya	42.728	-8.924	683	Southern
ES0010R	Spain	Cabo de Creus	cdcreus	42.319	3.317	23	Southern
ES0014R	Spain	Els Torms	elstorms	41.400	0.717	470	Southern
ES0013R	Spain	Penausende	psende	41.283	-5.867	985	Southern
ES0009R	Spain	Campisabalos	cbalos	41.281	-3.143	1360	Southern
ES0006R	Spain	Mahón	mahon	39.867	4.317	78	Southern
ES0001R	Spain	San Pablo	sanpablo	39.548	-4.349	917	Southern
ES0012R	Spain	Zarra	zarra	39.086	-1.102	885	Southern
ES0011R	Spain	Barcarrola	bcarrola	38.476	-6.923	393	Southern
ES0007R	Spain	Víznar	viznar	37.233	-3.533	1265	Southern
ES0017R	Spain	Doñana	donana	37.030	-6.332	5	Southern
CY0002R	Cyprus	Ayia Marina	ayiamar	35.039	33.058	532	Southern

In central Europe, regional O_3 production contributed to SOMO35 to a greater degree than in northern Europe, which resulted in the larger SOMO35 values on average at central European sites (Figure 7.1). A substantial proportion of SOMO35 was still accumulated in spring (on average 49%), but the contribution from summer was greater at sites in Central Europe (on average 36%) than sites in Northern Europe (23%) (Figure 7.3). The contribution from high O_3 concentrations was greater in Central Europe (on average 27% compared to 8% in northern Europe, Figure 7.4), as

was the increase in diurnal O_3 cycle amplitude on ADs which, for some sites, was double that on NADs (Figure 7.5). Finally, the majority of sites in Central Europe had larger NO_x and VOC trajectory emissions estimates on SOMO35 ADs compared with NADs (Figure 7.6). On average, there was a 6% increase in NO_x trajectory emissions estimate on ADs compared to NADs, and there was an increase at 81% of central European sites. This provides clear demarcation between Central and Northern European sites, where on average there was a 9% decrease in NO_x trajectory emissions estimates on ADs, and 77% of sites showing a decrease. Hence for Central European sites, during those hours when air masses passed over regions with greater NO_x and VOC emissions, on average regional O_3 production and an increase in O_3 over hemispheric background concentrations occurred which resulted in accumulation of SOMO35.

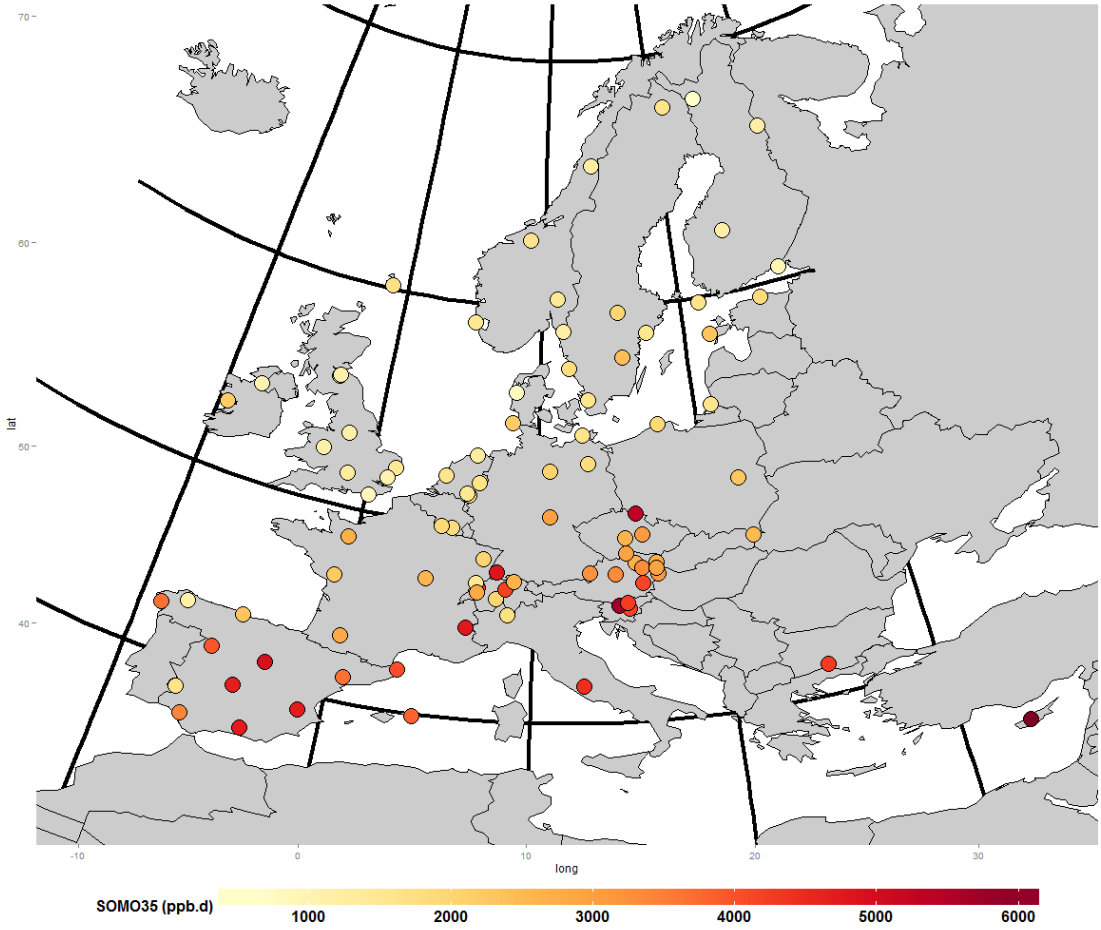

Figure 7.1: Human health relevant O_3 quantified by SOMO35 across EMEP sites in 2011.

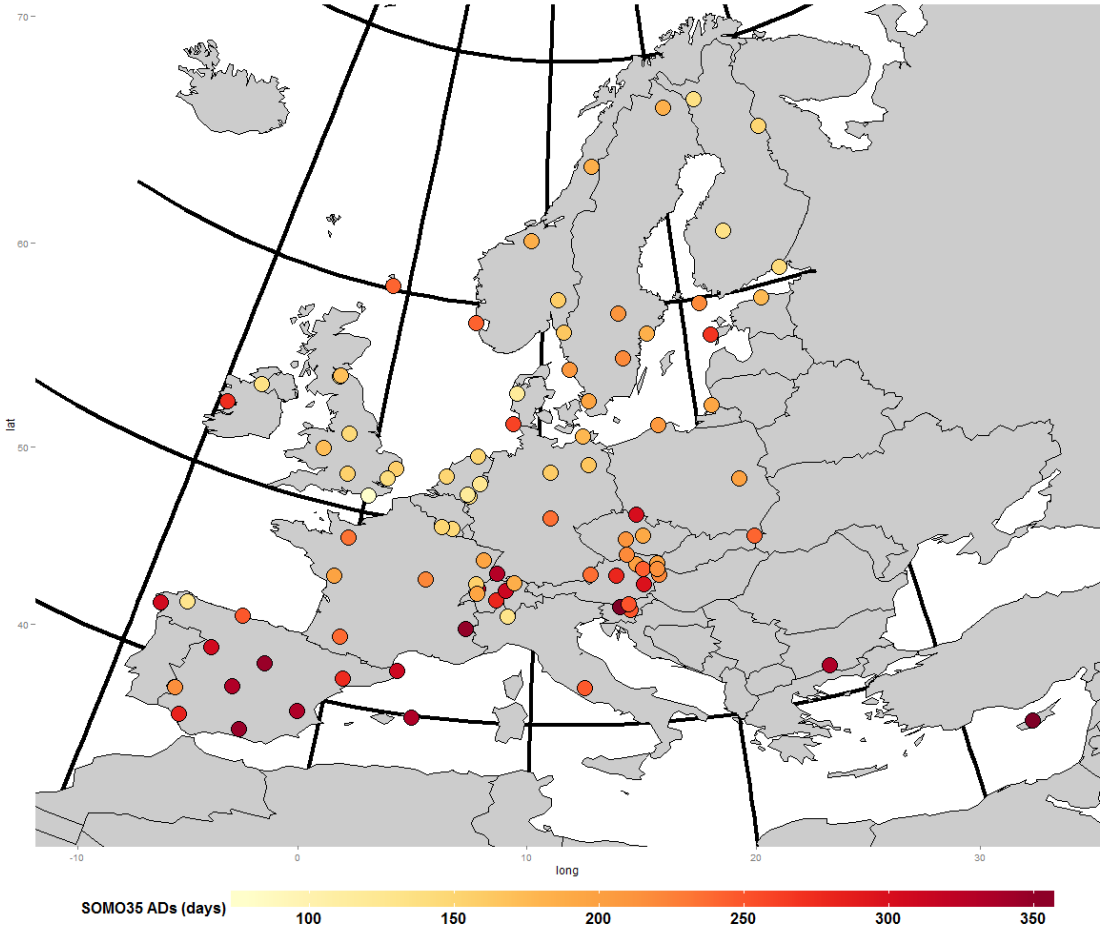

Figure 7.2: Number of SOMO35 accumulation days (ADs) at each EMEP site in 2011.

In Southern Europe SOMO35 was also elevated compared with Northern Europe (Figure 7.1). The southerly latitude has conditions more frequently favourable for photochemical O_3 production compared with other European regions (Fernandez-Fernandez et al., 2011), and consequently the contribution to SOMO35 was largest in summer at many Southern European sites (Figure 7.3). Additionally, the average contribution from spring to SOMO35 (35%) was lower than both Northern and Central European site averages, indicating that at these lower latitudes regional O_3 production had a relatively larger contribution to SOMO35 compared with Northern Europe. However, the contribution from different concentration bins, as well as the ratio of diurnal O_3 cycle amplitude on SOMO35 ADs and NADs indicates that regional O_3 episodes were less frequent than in central Europe. In Southern Europe, the major

contribution from different concentrations was the intermediate elevated concentrations (45-60 ppb), on average 62% across southern European sites (Figure 7.4). This was higher than for Central European sites, where on average 53% was accumulated in this range (47% for Northern European sites). Conversely, the contribution from higher concentrations (>60 ppb) was greater at Central European sites (27% on average for Central European sites compared to 18% in Southern Europe). The increase in diurnal O_3 cycle amplitude on SOMO35 AD and NADs was also lower in Southern Europe, on average 37% higher on ADs compared with 63% in Central Europe. It is noted that the increases at Montelibretti, Italy (84%), and Ayia Marina, Cyprus (73%), were more similar to the average of sites in Central Europe, but the low site density in these countries precludes assessment of the representativeness of these values. The number of days over which SOMO35 was accumulated in Southern Europe (293 days y^{-1} on average) was also greater than in Central Europe (218 days y^{-1}) (Figure 7.2).

These statistics indicate that while regional O_3 production makes a relatively large contribution to SOMO35 at both Southern and Central European sites, the pattern of accumulation, and therefore the strategy for mitigation, is different. In Southern Europe, the lower latitude provides more frequently favourable conditions for regional O_3 production, hence there were more SOMO35 accumulation days and a larger number of intermediate concentrations contributing to SOMO35. However, sites in Southern Europe tend to be further from major sources of O_3 precursor emissions. For example, at Southern European sites, the average NO_x trajectory emissions estimate during SOMO35 ADs (27 Mg $96h^{-1}$) was substantially lower than at Central European sites (47 Mg $96h^{-1}$). Hence there was a lower frequency at Southern European sites of high concentration (>60 ppb) regional O_3 episodes compared with Central Europe. Reduction in the frequency and severity of these episodes would therefore be of greater benefit to health-relevant O_3 in Central Europe compared with Southern Europe, where more frequent modest regional O_3 production dominated the SOMO35 metric. Similar patterns have been shown previously during investigation of the spatial distribution of high percentile O_3 concentrations (EEA, 2013).

The identification of these three chemical climate phases highlights regions of Europe for which health-relevant O_3 is determined to greater extents by hemispheric background concentrations (Northern Europe), and two different types of regional O_3 production (Central and Southern Europe). However this division of EMEP sites into three spatial domains is only one analysis to interpret the chemical climate statistics. For example, comparison of different types of sites, e.g. elevated vs non-elevates sites, could also yield conclusions about differences in the accumulation of health-relevant O_3, and potential mitigation strategies. There are also important differences within each region, and within individual countries. For example in the UK there was a division between northern UK sites where O_3 concentrations are less influenced from hemispheric background, and southern UK sites, where SOMO35 has a larger contribution from regional O_3 production.

Additionally, the utility of the chemical climates derived across networks is dependent on the quality of the data used to derive the set of statistics. The data used to derive the O_3 health chemical climates were measurements from national and regional databases, as well as official emission inventories, therefore representing the best estimate of both the concentrations of O_3 at each location, and of the spatial variability of emissions across Europe. However, the chemical climates would be improved from the reduction in the uncertainty associated with the O_3 measurements. The O_3 analysers used by the UK Automatic Urban and Rural Network are calibrated with an uncertainty of ±3.5% (AQEG, 2009). The NO_x and VOC gridded emissions inventories also have uncertainties associated with them, as they are derived from estimations of activity rates and emission factors for a wide range of diverse sources (discussed in Chapter 5). Misra et al. (2015) estimated the uncertainty in UK NO_x and VOC emissions to be ±10%. In addition, the co-location of a greater number of pollutant measurements at a greater number of measurement sites would allow more state and driver statistics to be calculated relating to variation in the concentrations of O_3 precursors (VOCs and NO_x), and the nature of the meteorological driver (e.g. temperature, solar radiation) respectively. Finally, the metric used to quantify the impact can have a large effect on the conditions producing the impact, and hence on the most effective mechanisms for

impact reduction. Other metrics, which focus on high percentile O_3 concentrations are also used to quantify health-relevant O_3 (a comparison between SOMO10, SOMO35 and high percentile metrics is outlined in Chapter 4), and therefore continued evaluation of the nature of an air pollutant impact and the most appropriate metric would also increase the utility of the chemical climatology framework.

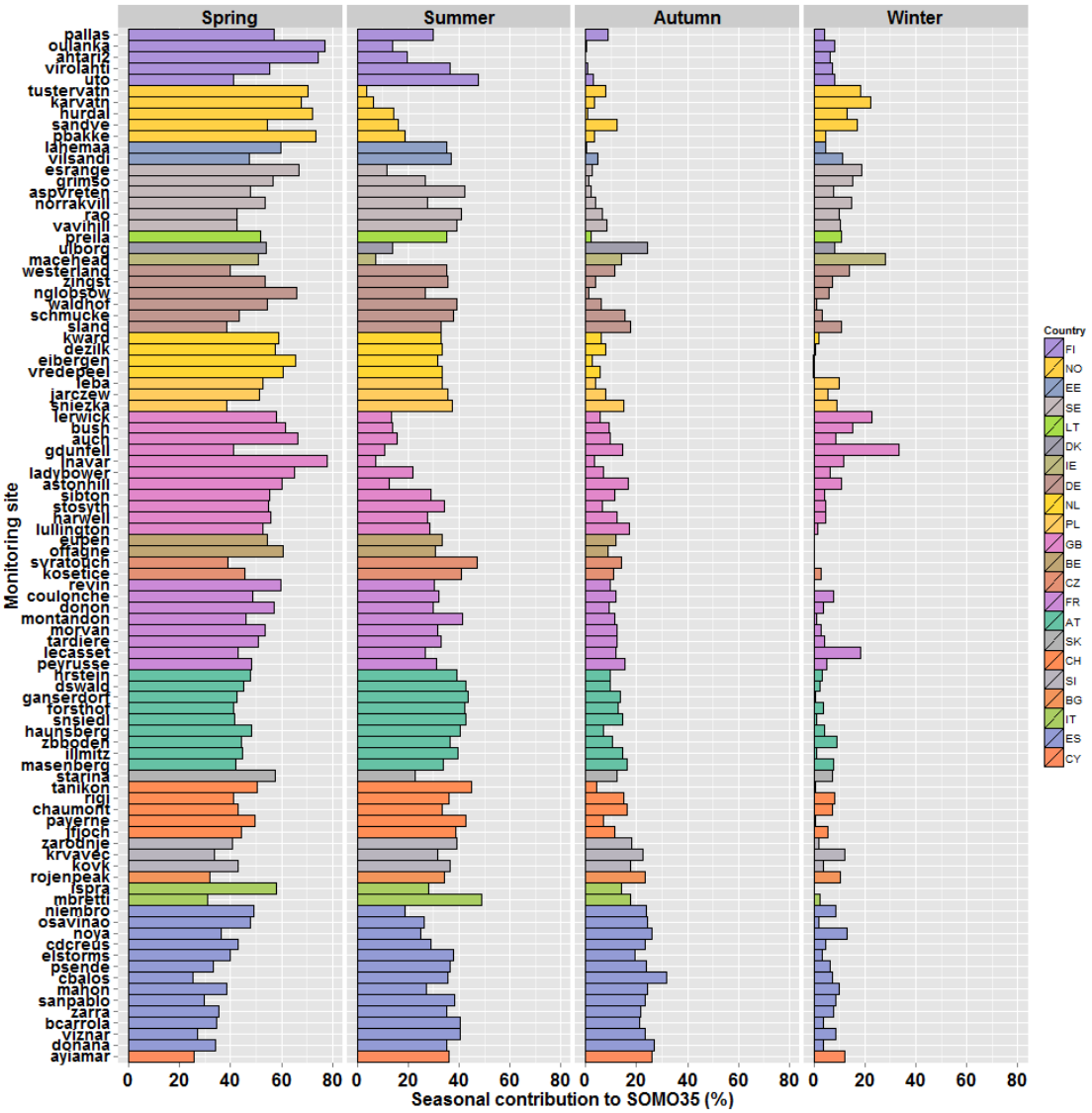

Figure 7.3: Seasonal contributions to SOMO35 metric in 2011. Sites are grouped by country, and within each country sites are ordered by latitude. Countries are ordered by the latitude of the capital city.

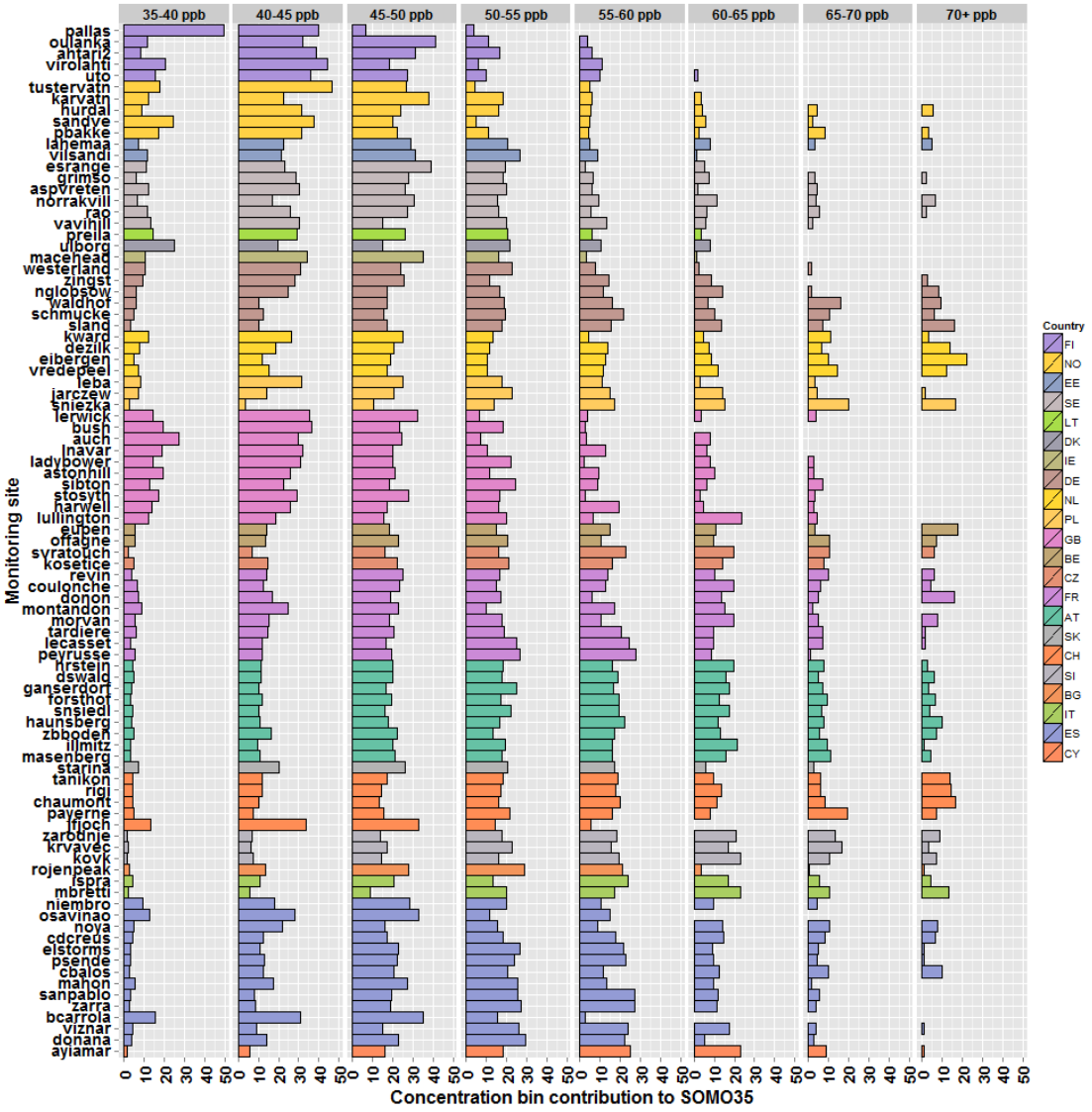

Figure 7.4: Contributions from 5 ppb concentration bins to SOMO35 in 2011. Sites are grouped by country, and within each country sites are ordered by latitude. Countries are ordered by the latitude of the capital city.

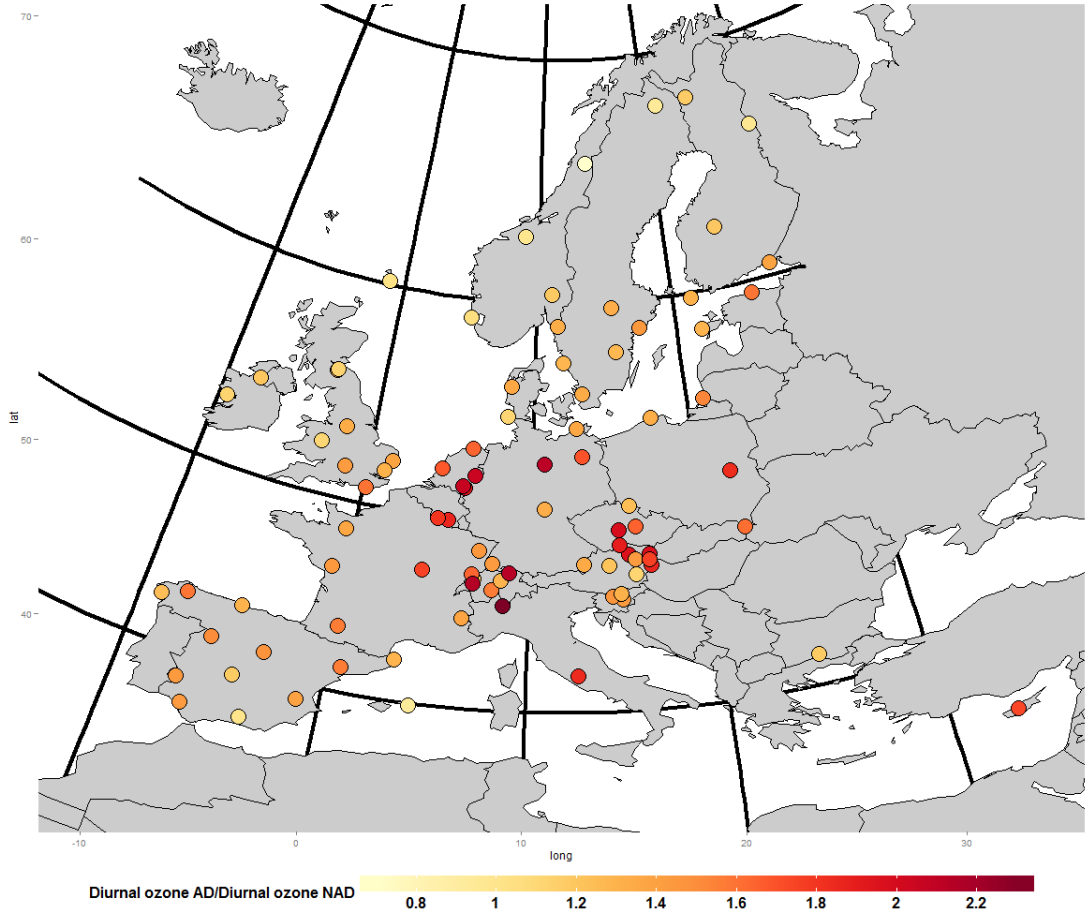

Figure 7.5: Ratios between diurnal O_3 amplitude on SOMO35 accumulation days (ADs) and non-accumulation days (NADs) in 2011.

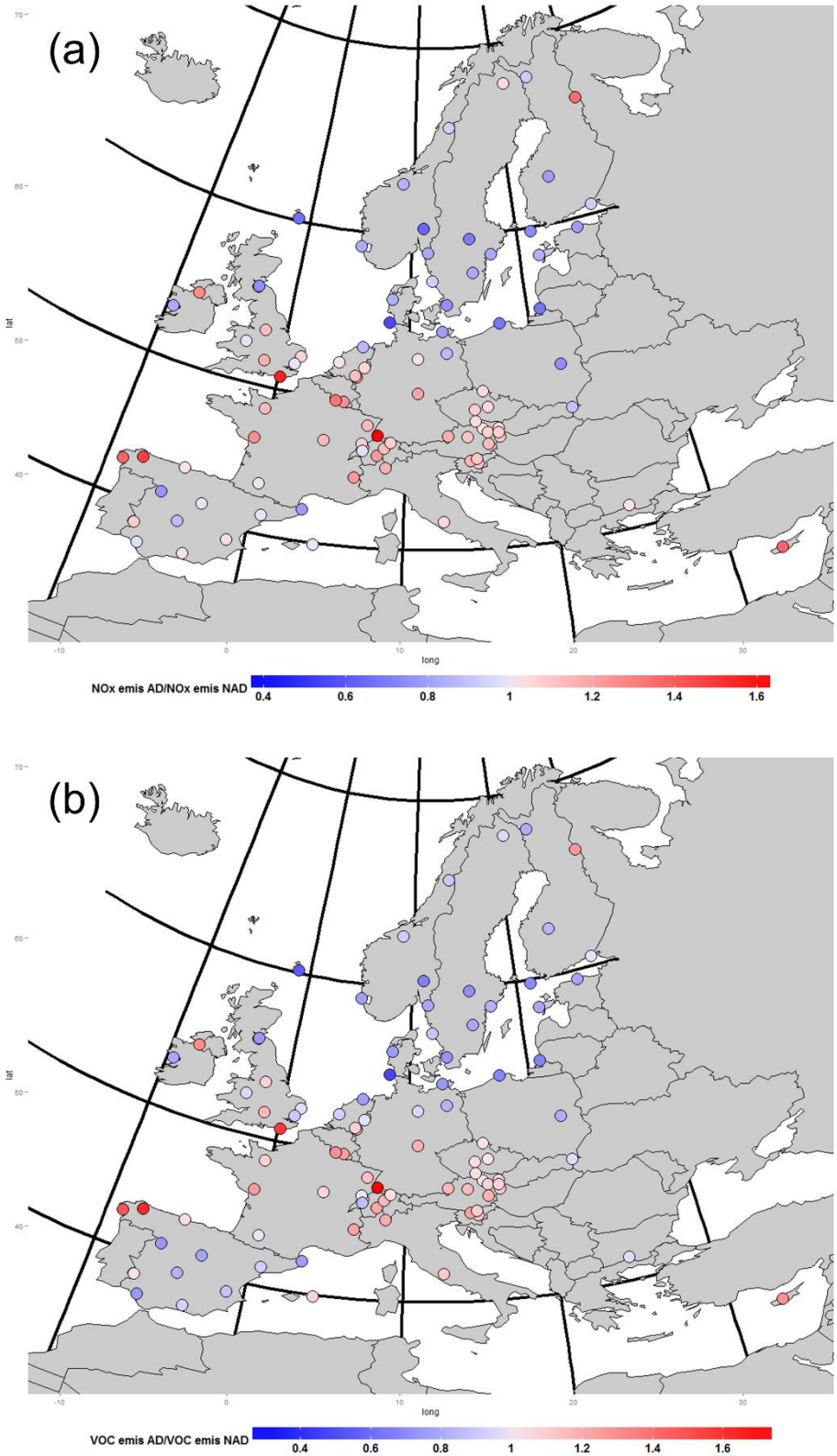

Figure 7.6: Ratios between SOMO35 accumulation days (ADs) and non-accumulation days (NADs) in 2011: a) amplitude of the NO_x trajectory emissions estimates (b) amplitude of the VOC trajectory emissions estimates.

7.3.2 Advantages and policy-relevance of the chemical climatology framework

The application of the standard set of chemical climate statistics provided a consistent assessment of health-relevant O_3 across a large spatial domain, and provides a basis for further investigation. An advantage of a standardised interpretation of measurement data such as this is the potential for the identification of linkages between atmospheric composition change and societal impacts. Monitoring networks are not typically used to identify these linkages. However, a standardised interpretation of monitoring network data could extend the identification of the linkage between atmospheric composition and societal impacts from an isolated study in a single location to other regions/cities/populations etc. An advantage of identifying these linkages within the chemical climatology framework is that the conditions producing the impacts are also derived through the state and drivers statistics. Therefore not only is atmospheric composition linked to societal issues, but the necessary information is also derived on how these impacts might be reduced. Examples of societal issues to which anthropogenic atmospheric composition change could be linked through the application of chemical climatology to monitoring networks include:

Health: The health-relevant O_3 quantified by the SOMO35 metric can be converted into an increase in mortality and morbidity through the application of Equation 7.1, as calculated in Heal et al. (2013) and Stedman and Kent (2008).

$$Mortality\ (or\ Morbidity) = [O_3]\ x\ concentration\ response\ coefficient\ x\ baseline\ mortality\ (or\ morbidity)\ rate\ x\ population \quad (7.1)$$

In Heal et al. (2013), the increase in mortality was calculated daily, using model-derived daily maximum 8-h average O_3 concentrations for the UK and a daily baseline mortality rate, whereas Stedman and Kent (2008) calculate annual increase in mortality using the annual average daily maximum 8-h with various thresholds (SOMO35 is

equivalent to the annual average daily maximum 8-h concentration multiplied by the number of days in the year). Concentration-response relationships were based on WHO (2004). Hence the O_3 health chemical climate could be extended to quantify the effect on mortality and morbidity within the area of representativeness of each monitoring site providing there were sufficient mortality/morbidity statistics available. Chemical climates for the health impact of other pollutants could similarly be linked to specific health outcomes, e.g. using concentration response relationships summarised in REVIHAAP (2013). There is also scope for further linkage such as that between air pollution and societal issues resulting from quantification of a specific health outcome.

Economic: Heal et al. (2013) calculated an increase in morbidity based on increase in emergency respiratory hospital admissions. The cost of all emergency admissions per year is £1.42 billion across the National Health Service (NHS) in England, with higher costs associated with under-5s and over-75s, population subgroups also more susceptible to the effects of air pollution (Tian et al., 2012). It was also shown that 70% of hospital bed days are occupied by emergency admissions, and that more efficient use of these beds could save the NHS £1 billion a year (Poteliakhoff and Thompson, 2011). Hence an increase in morbidity due to the effects of O_3 exposure could be converted into the cost to the NHS resulting from these increased emergency admissions, or into the potential benefit in terms of savings which would result from O_3 reduction strategies.

Economic impacts also result from other atmospheric composition impacts. For example, Mills et al. (2011a) calculated the flux-based vegetation impact metric (POD_Y) for crops and calculated that for the UK there were potential losses of £359 million in 2006 and £253 million in 2008 resulting from exposure to O_3. The calculation of the economic impact of O_3 through vegetation yield loss was based on reported concentration response relationships which quantify the yield loss of different crops for a particular accumulated O_3 flux (Mills et al., 2011b), maps of crop distribution across the UK, and modelled stomatal flux of O_3 based on model-derived

O_3 concentrations and meteorology across the UK. Monitoring network data could also be used to derive the economic impact of O_3 on crops through extension of the O_3 chemical climates derived in Chapter 4 to sites across a monitoring network.

Migration: Changes in the population distribution across a country/region have implications for the exposure of populations to air pollution. For example, the difference between the number of EU migrants living in a country and the number of people from that country living in other EU countries provides an indication of net-changes in the distribution of EU citizens across the EU. In 2010, the difference was most positive (i.e. more EU migrants than citizens living in another EU country) for Germany (2.2 million), Spain (1.7 million), France (1.4 million) and the UK (0.7 million), and most negative for Romania (-2.2 million), Poland (-1.6 million), Portugal (-1.1 million), and Italy (-0.5 million) (Vargas-Silva, 2012). Hence the net movement of EU citizens increases the number of people exposed to the health relevant O_3 chemical climates derived at German, Spanish, French and UK sites. Further analysis could therefore indicate whether migration has resulted in a change to the number of people for which health-relevant O_3 is determined predominantly through hemispheric background concentrations, or through regional O_3 production. Similar analyses could be undertaken through the development and application across monitoring networks of chemical climate statistics for the impact of other pollutants (PM or NO_2) on human health. The common basis with which monitoring site data is interpreted allows the effects of these changes to be consistently analysed across the spatial domain of interest.

Crime: While the impact of O_3 on human health or vegetation might not be directly related to crime, Mielke and Zahran (2012) showed that atmospheric lead concentrations were highly correlated with aggravated assault rates with a 22-year lag. This study estimated ‘air-Pb’ based on a number of different drivers, including gasoline usage, traffic volume, fuel consumption and gasoline lead content. The availability of measurements of atmospheric concentrations of lead (and application of existing measurements) would allow the conclusions from this study to be extended

to other locations, including the identification of regions where the impact of lead concentrations on crime may still be a problem.

The chemical climatology approach also facilitates the identification of common drivers between atmospheric composition impacts and societal issues, and hence the identification of co-beneficial policies. Figure 7.7 shows the contribution from 11 different Selected Nomenclature for Air Pollution (SNAP) sources sectors to the NO_x trajectory emissions estimates. At the majority of EMEP sites, the contribution to NO_x trajectory emissions estimates during SOMO35 ADs was dominated by SNAP 7: Road Transport and SNAP8: Non-Road Transport sectors. Reduction in emissions from road transport has benefits in other areas. For example, eliminating short car journeys was shown to improve health (decrease mortality) through both a reduction in short car journeys and increased physical activity, which would have an associated economic benefit, and would also reduce emissions of greenhouse gases (Grabow et al., 2012). Reduced NO_x emissions from road transport would therefore not only reduce O_3 downwind of emissions sources (close to emissions sources O_3 concentrations may increase with reduced NO_x emissions), but if this reduction was achieved through fewer car journeys, benefits in other areas would also result.

Other advantages of the standardised calculation of chemical climate statistics across monitoring networks is that it allows the relevance of conclusions from isolated studies to be expanded to larger spatial domains and populations. For example, monitoring networks which measure atmospheric lead concentrations could be used to assess the similarity in lead chemical climates between the 6 cities in the Mielke and Zahran (2012) study, and those in other locations. The studies of mortality and morbidity increases from O_3 exposure carried out by Heal et al. (2013) and Stedman and Kent (2008) both require the availability of statistics which accurately represent spatial population distribution and spatial differences in the base rate of the mortality/morbidity statistic. This may not be available or comparable in all locations. The calculation of the set of chemical climate statistics quantifying the impact of O_3 on human health using an appropriate metric like SOMO35 allows for a comparison

of health-relevant O_3 with the spatial domains of these studies (i.e. the UK), and other locations. Using the chemical climates across Europe in 2011 (Figures 7.1-7.6), it appears that the increase in mortality and morbidity for the UK is lower than would be expected in areas of central and southern Europe.

Other studies provide valuable insight into a specific component of atmospheric composition variation. For example, Derwent et al. (2013) estimated hemispheric background O_3 concentrations from measurements at Mace Head, on the west coast of Ireland, while Gerasopoulous et al. (2006) concluded that entrainment of the free troposphere has a substantial influence on O_3 variation at Finokalia, a site on the island of Crete, Greece. These studies are valuable analyses of O_3 variation at these sites, but the calculation of chemical climate statistics allows the conclusions from these studies to gain wider relevance, and an assessment of what the effect of substantial influence of hemispheric background and free tropospheric entrainment is at the respective sites on health relevant O_3. For example, at Mace Head in 2011, SOMO35 was 2127 ppb.d. This was double the average value for sites in the neighbouring UK, but the increase in the diurnal O_3 cycle amplitude on SOMO35 ADs was smaller, 12% compared to an average of 27% at UK sites. Hence the lower modification of hemispheric background concentrations at Mace Head results in an increase in health-relevant O_3 in comparison to other sites in the UK and Ireland which have more regional modification. Data capture at Finokalia was insufficient to be included in the 2011 analysis, but Ayia Marina, Cyprus, is similarly located and had the highest SOMO35 in 2011. Hence entrainment of the free troposphere could contribute substantially to health relevant O_3 at Mediterranean coastal locations.

The standardised interpretation of data using the chemical climatology framework has benefit for both well-established sites and monitoring networks which have relatively higher site density and also for newer sites and networks which have less abundance of data. For example, the relatively high site density across the central and western European portion of the EMEP domain allowed the identification of the key spatial differences in O_3 health chemical climate. However, there is potentially greater benefit

for sites which are not as well established or have lower spatial density. For example, Rojen Peak, Bulgaria is the only sites in south-eastern continental Europe with sufficient O_3 measurements in 2011. However, due to the consistent method of data interpretation, this isolated site can be compared with those in areas of Europe with higher spatial density. It is shown that the O_3 health chemical climate at Rojen Peak was similar to those in Spain and other areas of southern Europe. Hence policies implemented to reduce O_3 exposure in Spain could also be of relevance to mitigating O_3 health impacts in Bulgaria.

The calculation of standard chemical climate statistics allows comparison of atmospheric composition impacts between different monitoring networks in even more diverse regions of the world. Currently this is in many cases limited due to the focus of many networks on compliance monitoring, with different air quality objectives in different regions (Chow and Watson, 2008). This is particularly important for those regions where there is currently a low spatial density of sites, or where networks are less well established, e.g. the Male Directive network in South East Asia (Nordberg and Hicks, 2013). The application of chemical climate statistics to measurements from these sites immediately facilitates comparison with longer time series in other location. Therefore, the future utility of the chemical climatology framework and the derived standard chemical climate statistics would be substantially enhanced through increased monitoring (in terms of spatial density of sites, range of constituents measured and time resolution of measurements) across as diverse range of regions as possible.

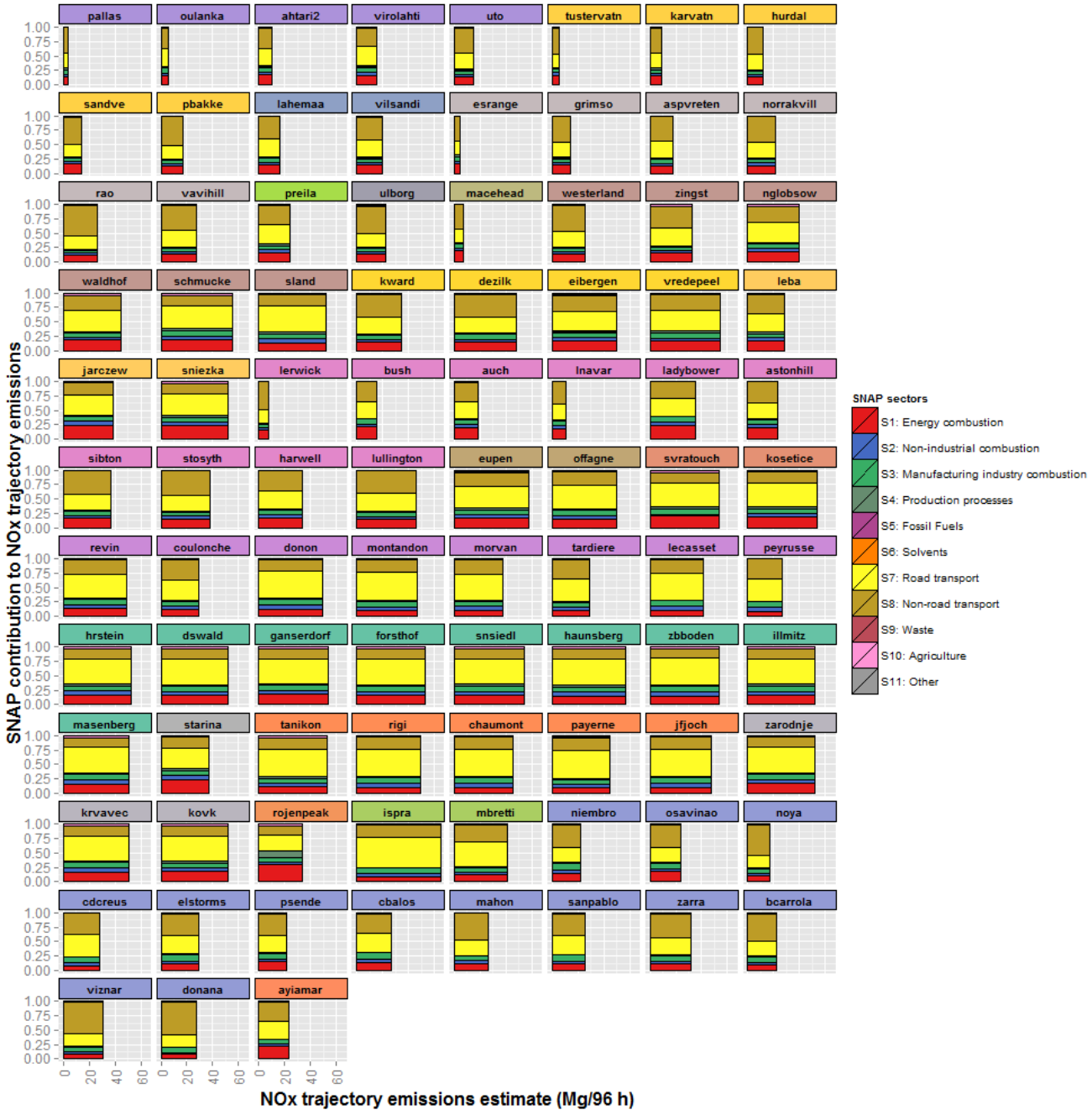

Figure 7.7: The NO_x trajectory emissions estimate at each EMEP site in 2011. The width of the bar represents the magnitude of the total emissions estimate, while the stacked bars are the proportion from 11 SNAP sources sectors.

7.4 Conclusions

The consistent calculation of a standard set of chemical climate statistics across the EMEP network specific to the health impact of O_3 highlighted the spatial pattern of impact severity across rural Europe. The common quantification of an impact in this manner could facilitate the linkage of this impact, and spatial changes in its severity, to societal issues such as health, migration, economic costs/benefits. The increase in knowledge of atmospheric composition change and its impacts has not been associated with an increase in public engagement with these impacts, and hence linkage between atmospheric composition impacts and societal issues with higher engagement could be successful in raising awareness of the multiple benefits which would result from decreased anthropogenic influence on the atmosphere.

The chemical climatology approach not only quantifies an impact, but the 'state' and 'drivers' statistics outline the conditions which produce it. The calculation of the state and drivers statistics for the O_3 health chemical climates identified differences over the domain of the monitoring network in contributions from hemispheric and regional O_3. Across Europe there are common protocols implemented to reduce the human health effects of O_3 but the differences in chemical climate 'phase' across Europe require consideration of different mitigation strategies, i.e. a greater focus on reduction of hemispheric background O_3 concentrations in northern Europe and regional O_3 at more southerly latitudes. Hence using the standard chemical climate statistics allows for consideration of the most effective mitigation strategies, as well as identification of spatial differences and similarities in appropriate mitigation approaches.

References

AQEG, 2009. Ozone in the United Kingdom: Air Quality Expert Group, Defra Publications,
London. http://www.defra.gov.uk/environment/quality/air/airquality/publications/ozone/documents/aqeg-ozone-report.pdf.

Bell, M. L., Ebisu, K., 2012. Environmental Inequality in Exposures to Airborne Particulate Matter Components in the United States. Environ. Health Persp. 120, 1699-1704.

Berg, A., de Noblet-Ducoudre, N., Sultan, B., Lengaigne, M., Guimberteau, M., 2013. Projections of climate change impacts on potential C4 crop productivity over tropical regions. Agr. Forest Meteorol. 170, 89-102.

Bhatia, A., Tomer, R., Kumar, V., Singh, S. D., Pathak, H., 2012. Impact of tropospheric ozone on crop growth and productivity - a review. J. Sci. Ind. Res. India 71, 97-112.

Bickerstaff, K., Walker, G., 2001. Public understandings of air pollution: the 'localisation' of environmental risk. Global Environ. Change 11, 133-145.

Branis, M., Linhartova, M., 2012. Association between unemployment, income, education level, population size and air pollution in Czech cities: Evidence for environmental inequality? A pilot national scale analysis. Health Place 18, 1110-1114.

Brechin, S. R., Bhandari, M., 2011. Perceptions of climate change worldwide. WIREs Clim. Change 2, 871-885.

Burney, J., Ramanathan, V., 2014. Recent climate and air pollution impacts on Indian agriculture. P. Natl. Acad. Sci. USA 111, 16319-16324.

Caric, H., Mackelworth, P., 2014. Cruise tourism environmental impacts - The perspective from the Adriatic Sea. Ocean Coast. Manage. 102, 350-363.

Carslaw, D. C., Ropkins, K., 2012. openair - An R package for air quality data analysis. Environ. Modell. Softw. 27-28, 52-61.

Chang, W., Cheng, J., Allaire, J., Xie, Y., McPherson, J., 2015. shiny: Web Application Framework for R. R package version 0.11.1. http://CRAN.R-project.org/package=shiny

Chow, J. C., Watson, J. G., 2008. New directions: Beyond compliance air quality measurements. Atmos. Environ. 42, 5166-5168.

Derwent, R., Manning, A., Simmonds, P., Gerard Spain, T., O'Doherty, S., 2013. Analysis and interpretation of 25 years of ozone observations at the Mace Head Atmospheric Research Station on the Atlantic Ocean coast of Ireland from 1987 to 2012. Atmos. Environ. 80, 361-368.

Draxler, R. R., Rolph, G. D., 2013. HYSPLIT (HYbrid Single-Particle Lagrangian Integrated Trajectory) Model access via NOAA ARL READY Website (http://www.arl.noaa.gov/HYSPLIT.php). NOAA Air Resources Laboratory, College Park, MD. .

Duh, J.-D., Shandas, V., Chang, H., George, L. A., 2008. Rates of urbanisation and the resiliency of air and water quality. Sci. tot. environ. 400, 238-56.

EEA, 2013. Air pollution by ozone across Europe during summer 2012: Overview of exceedances of EC ozone threshold values for April–September 2012. EEA Technical Report No. 3/2013, European Environment Agency, available at: http://www.eea.europa.eu/publications/air-pollution-by-ozone-across-EU-2012/download.

EMEP, 2014. Manual for Sampling and Analysis. EMEP/CCC Report 1/2014, Co-operative programme for monitoring and evaluation of the transmission of air pollutants in Europe, available at: http://www.nilu.no/projects/ccc/manual/index.html.

Farbotko, C., Lazrus, H., 2012. The first climate refugees? Contesting global narratives of climate change in Tuvalu. Global Environ. Chang. 22, 382-390.

Fernandez-Fernandez, M. I., Gallego, M. C., Garcia, J. A., Acero, F. J., 2011. A study of surface ozone variability over the Iberian Peninsula during the last fifty years. Atmos. Environ. 45, 1946-1959.

Gerasopoulos, E., Kouvarakis, G., Vrekoussis, M., Donoussis, C., Mihalopoulos, N., Kanakidou, M., 2006. Photochemical ozone production in the eastern Mediterranean. Atmos. Environ. 40, 3057-3069.

Grabow, M. L., Spak, S. N., Holloway, T., Stone, B., Jr., Mednick, A. C., Patz, J. A., 2012. Air Quality and Exercise-Related Health Benefits from Reduced Car Travel in the Midwestern United States. Environ. Health Persp. 120, 68-76.

Grossman, G. M., Krueger, A. B., 1995. Economic Growth and the Environment Q. J. Econ. 110, 353-377.

Hadwen, W. L., Boon, P. I., Arthington, A. H., 2012. Not for all seasons: why timing is critical in the design of visitor impact monitoring programs for aquatic sites within protected areas. Australas. J. Environ. 19, 241-254.

Heal, M. R., Heaviside, C., Doherty, R. M., Vieno, M., Stevenson, D. S., Vardoulakis, S., 2013. Health burdens of surface ozone in the UK for a range of future scenarios. Environ. Int. 61, 36-44.

Hsiang, S. M., Burke, M., Miguel, E., 2013. Quantifying the Influence of Climate on Human Conflict. Science 341, 1212-+.

Hurrell, J. M., Genta, R. M., Dellon, E. S., 2012. Prevalence of Esophageal Eosinophilia Varies by Climate Zone in the United States. Am. J. Gastroenterol. 107, 698-706.

Janssens-Maenhout, G., Dentener, F., van Aardenne, J., Monni, S., Pagliari, V., Orlandini, L., Klimont, Z., Kurokawa, J., Akimoto, H., Ohara, T., Wankmuller, R., Battye, B., Grano, D., Zuber, A., Keating, T., 2011. EDGAR-HTAP: a harmonized gridded air pollution emission dataset based on national inventories. JRC Scientific and Technical Reports, EUR 25229 EN, available at: http://edgar.jrc.ec.europa.eu/htap/EDGAR-HTAP_v1_final_jan2012.pdf.

Jenkin, M. E., 2008. Trends in ozone concentration distributions in the UK since 1990: Local, regional and global influences. Atmos. Environ. 42, 5434-5445.

Kistler, R., Kalnay, E., Collins, W., Saha, S., White, G., Woollen, J., Chelliah, M., Ebisuzaki, W., Kanamitsu, M., Kousky, V., van den Dool, H., Jenne, R., Fiorino, M., 2001. The NCEP-NCAR 50-year reanalysis: Monthly means CD-ROM and documentation. B. Am. Meteorol. Soc. 82, 247-267.

Lamarque, J. F., Bond, T. C., Eyring, V., Granier, C., Heil, A., Klimont, Z., Lee, D., Liousse, C., Mieville, A., Owen, B., Schultz, M. G., Shindell, D., Smith, S. J., Stehfest, E., Van Aardenne, J., Cooper, O. R., Kainuma, M., Mahowald, N., McConnell, J. R., Naik, V., Riahi, K., van Vuuren, D. P., 2010. Historical (1850-2000) gridded anthropogenic and biomass burning emissions of reactive gases and aerosols: methodology and application. Atmos. Chem. Phys. 10, 7017-7039.

Li, D. H. W., Pan, W., Lam, J. C., 2014. A comparison of global bioclimates in the 20th and 21st centuries and building energy consumption implications. Build. Environ. 75, 236-249.

Matutinovic, I., 2012. The prospects of transition to sustainability from the perspective of environmental values and behaviors in the EU 27 and globally. Int. J. Sust. Dev. World 19, 526-535.

Meyer, J., Anderson, B., Carter, D. O., 2013. Seasonal Variation of Carcass Decomposition and Gravesoil Chemistry in a Cold (Dfa) Climate. J. Forensic Sci. 58, 1175-1182.

Mielke, H. W., Zahran, S., 2012. The urban rise and fall of air lead (Pb) and the latent surge and retreat of societal violence. Environ. Int. 43, 48-55.

Mills, G., Hayes, F., Norris, D., Hall, J., Coyle, M., Cambridge, H., Cinderby, S., Abbott, J., Cooke, S., Murrells, T., 2011a. Impacts of Ozone Pollution on Food Security in the UK: a Case Study for Two Contrasting Years, 2006 and 2008. Defra contract AQ0816, London.

Mills, G., Pleijel, H., Braun, S., Bueker, P., Bermejo, V., Calvo, E., Danielsson, H., Emberson, L., Gonzalez Fernandez, I., Gruenhage, L., Harmens, H., Hayes, F., Karlsson, P.-E., Simpson, D., 2011b. New stomatal flux-based critical levels for ozone effects on vegetation. Atmos. Environ. 45, 5064-5068.

Mishra, A. K., Ramgopal, M., 2013. Field studies on human thermal comfort - An overview. Build. Environ. 64, 94-106.

Misra, A., Passant, N. R., Murrells, T. P., Pang, Y., Thistlethwaite, G., Walker, C., Broomfield, M., Wakeling, D., del Vento, S., Pearson, B., Hobson, M., Misselbrook, T., Dragosits, U., 2015. UK Informative Inventory Report (1990 to 2013): Annual Report for Submission under the UNECE-Convention on Long-Range Transboundary Air Pollution, available at: http://uk-air.defra.gov.uk/assets/documents/reports/cat07/1503131022_GB_IIR_2015_Final_v20.pdf.

Nordberg, L., Hicks, K., 2013. Male Declaration 1998-2013: a Synthesis: Progress and Opportunities. Male Declaration Report, available at: http://www.rrcap.ait.asia/male/uploadedfiles/file/Synthesis%20Report.pdf.

Padilla, C. M., Kihal-Talantikite, W., Vieira, V. M., Rossello, P., Le Nir, G., Zmirou-Navier, D., Deguen, S., 2014. Air quality and social deprivation in four French metropolitan areas-A localized spatio-temporal environmental inequality analysis. Environ. Res. 134, 315-324.

Parrish, D. D., Law, K. S., Staehelin, J., Derwent, R., Cooper, O. R., Tanimoto, H., Volz-Thomas, A., Gilge, S., Scheel, H. E., Steinbacher, M., Chan, E., 2013. Lower tropospheric ozone at northern midlatitudes: Changing seasonal cycle. Geophys. Res. Lett. 40, 1631-1636.

Peel, M. C., Finlayson, B. L., McMahon, T. A., 2007. Updated world map of the Koppen-Geiger climate classification. Hydrol. Earth Syst. Sc. 11, 1633-1644.

Pidgeon, N., 2012. Public understanding of, and attitudes to, climate change: UK and international perspectives and policy. Clim. Policy 12, S85-S106.

Poteliakhoff, E., Thompson, J., 2011. Emergency bed use: what the numbers tell us. Data Briefing, The King's Fund, available at: http://www.kingsfund.org.uk/sites/files/kf/data-briefing-emergency-bed-use-what-the-numbers-tell-us-emmi-poteliakhoff-james-thompson-kings-fund-december-2011.pdf.

Punzet, M., Voss, F., Voss, A., Kynast, E., Baerlund, I., 2012. A Global Approach to Assess the Potential Impact of Climate Change on Stream Water Temperatures and Related In-Stream First-Order Decay Rates. J. Hydrometeorol. 13, 1052-1065.

R Core Team, 2014. R: A Language and Environment for Statistical Computing. R Foundation for Statistical Computing, Vienna, Austria, http://www.R-project.org/.

REVIHAAP, 2013. Review of evidence on health aspects of air pollution – REVIHAAP Project technical report. World Health Organization (WHO) Regional Office for Europe, Bonn. http://www.euro.who.int/__data/assets/pdf_file/0004/193108/REVIHAAP-Final-technical-report-final-version.pdf.

Rey, K., Amiot, R., Lecuyer, C., Koufos, G. D., Martineau, F., Fourel, F., Kostopoulos, D. S., Merceron, G., 2013. Late Miocene climatic and environmental variations in northern Greece inferred from stable isotope compositions (delta O-18, delta C-13) of equid teeth apatite. Palaeogeogr. Palaeocl. 388, 48-57.

Seinfeld, J. H., Pandis, S. N., 2006. Atmospheric Chemistry and Physics: From Air Pollution to Climate Change, Wiley-Blackwell.

Siqueira Neto, M., Piccolo, M. d. C., Costa Junior, C., Cerri, C. C., Bernoux, M., 2011. Emissão de gases do efeito estufa em diferentes usos da terra no bioma Cerrado. Rev. Bras. Cienc. Solo 35, 63-76.

Spence, A., Poortinga, W., Pidgeon, N., 2012. The Psychological Distance of Climate Change. Risk Anal. 32, 957-972.

Stedman, J. R., Kent, A. J., 2008. An analysis of the spatial patterns of human health related surface ozone metrics across the UK in 1995, 2003 and 2005. Atmos. Environ. 42, 1702-1716.

Tian, Y., Dixon, A., Gao, H., 2012. Emergency hospital admissions for ambulatory care-sensitive conditions: identifying the potential for reductions. Data Briefing, The King's Fund, available at: http://www.kingsfund.org.uk/sites/files/kf/field/field_publication_file/data-briefing-emergency-hospital-admissions-for-ambulatory-care-sensitive-conditions-apr-2012.pdf.

van den Elshout, S., Leger, K., Nussio, F., 2008. Comparing urban air quality in Europe in real time - A review of existing air quality indices and the proposal of a common alternative. Environ. Int. 34, 720-726.

Van Lanen, H. A. J., Wanders, N., Tallaksen, L. M., Van Loon, A. F., 2013. Hydrological drought across the world: impact of climate and physical catchment structure. Hydrol. Earth Syst. Sc. 17, 1715-1732.

Vargas-Silva, C., 2012. Briefing: EU Migrants in other EU Countries: An Analysis of Bilateral Migrant Stocks. The Migration Observatory at the University of Oxford, available at: http://www.migrationobservatory.ox.ac.uk/briefings/eu-migrants-other-eu-countries-analysis-bilateral-migrant-stocks.

Vilizzi, L., Ekmekci, F. G., Tarkan, A. S., Jackson, Z. J., 2015. Growth of common carp *Cyprinus carpio* in Anatolia (Turkey), with a comparison to native and invasive areas worldwide. Ecol. Freshw. Fish. 24, 165-180.

Walden, M., Hagglund, M., Orchard, J., Kristenson, K., Ekstrand, J., 2013. Regional differences in injury incidence in European professional football. Scand. J. Med. Sci. Spor. 23, 424-430.

Werier, D. A., Naczi, R. F. C., 2012. Carex Secalina (Cyperaceae), an introduced sedge new to North America. Rhodora 114, 349-365.

WHO, 2004. Meta-analysis of time-series studies and panel studies of particulate matter and ozone. Report No. EUR/04/5042688, World Health Organisation, available at: http://www. euro.who.int/document/e82792.pdf.

Wilson, R. C., Fleming, Z. L., Monks, P. S., Clain, G., Henne, S., Konovalov, I. B., Szopa, S., Menut, L., 2012. Have primary emission reduction measures reduced ozone across Europe? An analysis of European rural background ozone trends 1996-2005. Atmos. Chem. Phys. 12, 437-454.

Wolf, J., Moser, S. C., 2011. Individual understandings, perceptions, and engagement with climate change: insights from in-depth studies across the world. WIREs Clim. Change 2, 547-569.

Wong, S. L., Wan, K. K. W., Yang, L., Lam, J. C., 2012. Changes in bioclimates in different climates around the world and implications for the built environment. Build. Environ. 57, 214-222.

Woodall, C. W., Domke, G. M., Riley, K. L., Oswalt, C. M., Crocker, S. J., Yohe, G. W., 2013. A Framework for Assessing Global Change Risks to Forest Carbon Stocks in the United States. Plos One 8, 8.

Wright, J. A., Yang, H., Walker, K., 2012. Do international surveys and censuses exhibit 'Dry Season' bias? Popul. Space Place 18, 116-126.

Zhang, X., Yan, X., 2014. Spatiotemporal change in geographical distribution of global climate types in the context of climate warming. Clim. Dynam. 43, 595-605.

Chapter 8: Conclusions and Future Work

The aim of this thesis was to identify and demonstrate how improvements in monitoring network outputs could be realised. A historical assessment of the development of monitoring networks showed that increases in their utility were associated with step changes in network coordination and standardisation. For example, the standardisation of networks with respect to site representativeness, measurement methods, data quality and data archiving have increased confidence that measurements made at different sites within a network are comparable (Chapter 1). However, limitations with the current state of monitoring networks have also been identified, including an over emphasis on compliance monitoring (Chow and Watson, 2008) and the need for greater linkage between emissions and exposure (Brook et al., 2009). The process of increased network standardisation is not complete, and one method which could be used to improve network output is the advancement of network standardisation to data interpretation.

In this thesis a method, called 'chemical climatology' has been outlined and demonstrated to be useful in the derivation of standard interpretations of atmospheric composition data across monitoring networks. Using the chemical climatology framework, standard sets of statistics are derived which link an 'impact' of atmospheric composition, through the 'state' of atmospheric composition variation to the causal 'drivers'. The derivation of these chemical climate statistics are distinct for different impacts, and provide a common basis for the consistent comparison of both a specific atmospheric composition impact across the spatial domain of a network, and the conditions producing the impact (Chapter 2). The application of derived chemical climate statistics to measurements from the Harwell (SE England) and Auchencorth (SE Scotland) UK EMEP supersites has resulted in important scientific and policy-relevant conclusions which demonstrate the benefits which could result from a broader application of the chemical climatology concept.

8.1 Conclusions

Firstly, chemical climates at Harwell and Auchencorth specific to the impacts of ozone on human health and vegetation were derived (Chapter 4). The 'impact' was quantified using the SOMO10/SOMO35 and flux-based POD_Y metrics for human health and vegetation respectively. The 'state' statistics assessed monthly, diurnal and the contribution from different parts of the ozone concentration distribution while the 'drivers' assessed included air mass history and meteorology. Long term trends in these statistics were calculated at Harwell between 1990 and 2013, while calculation at Auchencorth between 2007 and 2013 provided spatial comparison between two sites representative of UK background O_3 varation (Chapter 3).

Between 1990 and 2013 at Harwell, the distinct state and drivers statistics linked to the impact metrics showed a significant decrease in the contribution of regionally (European) derived O_3 in determining the severity of human health and vegetation-relevant O_3 exposure, associated with European precursor emissions reductions (EEA, 2014a). The analysis highlighted the differences in response to this decrease from the different impact metrics. For human health-relevant O_3, improvement at Harwell was calculated for SOMO35, but not for SOMO10, due to the lower threshold for accumulation for SOMO10. The relative contribution of high percentile O_3 concentrations was lower for SOMO10 compared to SOMO35, and the decrease in these concentrations associated with reduced regional O_3 production therefore had less effect on SOMO10. Additionally, any decrease in SOMO10 from reduction in high O_3 concentrations was offset by an increase in contribution from O_3 concentrations below 35 ppb (which do not contribute to SOMO35), as a result of increases in hemispheric background O_3 concentrations and a lower NO_x environment. However, both metrics show health-relevant O_3 in south-east England is being determined to a greater extent by hemispheric background concentrations, reducing the degree of improvement which can be obtained from further European O_3 precursor emission reductions, and increasing the need for coordinated hemispheric action.

There was no significant reduction in any of the four vegetation POD_Y metrics (wheat, potato, beech and Scots pine) at Harwell resulting from reduced regional O_3 production. The timing of regional photochemical O_3 episodes frequently coincided with plant conditions that reduced O_3 accumulation by vegetation, hence limiting any benefit from reduction of regional O_3 precursor emissions. Reduction of the moderate O_3 concentrations, determined to a greater extent by hemispheric background concentrations, which occur during more favourable plant conditions are required to reduce POD_Y. The work highlights the necessity to formulate impact mitigation strategies using appropriate metrics. The crop-relevant concentration-based AOT40 metric, decreased significantly between 1990 and 2013 at Harwell, indicating an improvement in vegetation-relevant O_3 resulting from regional emissions controls which is not calculated when meteorological and plant conditions which modify the O_3 uptake ability of the plant are accounted for.

At Auchencorth between 2007 and 2013 O_3 concentrations were determined to a greater extent by hemispheric background concentrations compared with Harwell. Consequently, the relative magnitude of health-relevant O_3 was dependent on whether SOMO10 (similar between both sites and less sensitive to high O_3 concentrations produced during regional O_3 production) or SOMO35 (higher at Harwell, and determined to a greater extent by regional O_3 production) was chosen for comparison. Larger POD_Y was calculated at Auchencorth for vegetation types with lower exceedance thresholds and longer growing seasons. Additionally, during periods of regional O_3 production, there was a greater prevalence of plant conditions which enhance O_3 uptake (e.g. high soil moisture) at Auchencorth. Hence despite Auchencorth being further from major O_3 precursor emissions sources compared with Harwell, there was greater potential for exacerbation of the vegetation impacts at Auchencorth during regional photochemical O_3 episodes. Therefore further reductions of O_3 precursor emissions on the European scale would result in greater improvement in vegetation impact at Auchencorth compared with Harwell. This particular application of the chemical climatology framework highlights the capability of the

methodology to evaluate the effect of particular emission reduction strategies. In this case the need for control of O_3 on a much larger (hemispheric) scale is emphasised.

Secondly, the chemical climate associated with the regional O_3 increment 'impact' at Harwell and Auchencorth was derived (Chapter 5). The chemical climate state quantified the 'chemical loss' of 27 VOCs measured at Harwell and Auchencorth through calculation of the diurnal photochemical depletion. This resulted in a relative contribution to the production of the regional O_3 increment from the measured anthropogenic VOCs. Finally, the drivers investigated in this study were meteorology and spatially gridded VOC emissions. The latter were integrated with air mass back trajectories to quantify the VOC emissions emitted along the air mass pathway prior to arrival at the supersite. These emissions of total VOC were then speciated to estimate emissions of individual VOCs impacting atmospheric composition at the receptor sites. This chemical climate effectively integrates numerous methods and tools which have previously been applied separately to investigate atmospheric composition (including calculation of hemispheric background (Derwent et al., 2013), and regional background O_3 concentrations (Clapp and Jenkin, 2001), air mass back trajectories (Yates et al., 2010) and emissions inventories (EEA, 2014a)). When utilised together to investigate the impact of VOCs on the regional O_3 increment, the derived chemical climate highlights the most effective strategies for reduction of the regional component of O_3 concentrations, as well as limitations in the current suite of tools used to investigate VOC variation across Europe.

At Harwell between 2010 and 2012, during the month of maximum regional O_3 increment, ethene and m+p-xylene had the largest diurnal photochemical depletion, i.e. chemical loss, and therefore in comparison to the other measured VOCs, a targeted reduction of ethene and m+p-xylene emissions would be most effective in reducing the magnitude of the regional O_3 increment. The smaller contribution from the remaining measured VOC indicates that for further benefit emissions reduction of a larger number of VOCs is required. To achieve this, it may be more effective to target specific large VOC emissions sources, regardless of the VOC composition. The 27

VOC measured at each site are a small number of the hundreds of VOCs emitted. Analysis of the unmeasured portion of anthropogenic UK VOC emissions showed a few VOCs with large emissions, specifically ethanol, methanol and acetone. Specifically targeting emissions reductions for these VOCs may therefore also be beneficial to the reduction of the regional O_3 increment, but measurements of these VOCs are necessary in order to quantify their relative contribution. The remaining fraction of unmeasured VOC emissions was speciated between over 400 indiviudal VOCs, and therefore this supports a strategy of targeting high VOC emitting sources to reduce the regional O_3 increment further.

In addition, the use of gridded VOC emissions to investigate VOC variation in both measurement and modelling applications is limited by the reporting of these emissions in highly aggregated source sectors (11 SNAP sectors). Substantial benefit would result from the reporting of VOC gridded emissions in disaggregated source sectors such as the NFR codes used to report annual VOC emissions for EU Member States (EEA, 2014a). The disaggregation of source sectors would allow for spatial variation in the relative strength of emissions from two sources (e.g. NFR sectors) contributing to the same SNAP sector to be accounted for. Hence the strength of VOC emission sources in a particular grid square could be more accurately represented. If this was combined with improved accuracy of VOC source speciation profiles (highlighted in Borbon et al. (2013)), this would lead to a more accurate representation of the suite of anthropogenic VOCs emitted from that grid square, and hence impacting upon atmospheric composition at a receptor site.

The final chemical climate calculated only using data from Harwell and Auchencorth focussed on the long term health impact of PM, quantified by the annual average PM_{10} and $PM_{2.5}$ metrics (Chapter 6). The contribution from 1 µg m^{-3} concentration bins to annual average PM_{10} and $PM_{2.5}$ concentrations was calculated, as well as the monthly contribution, and average composition at each of these concentration bins. The drivers were assessed using air mass back trajectories, grouped based on the time spent over geographic regions, and by the application of Principal Component Analysis (PCA) to

the hourly measurements of 8 inorganic ions. This produced two Principal Components (PCs) which quantified the contribution of short vs long range transport during a particular time step. These chemical climates demonstrate the effectiveness of this framework in integrating a large number of datasets to investigate an impact. In this case measurements of total PM_{10} and $PM_{2.5}$, secondary inorganic arerosol components, sea salt components, elemental and organic carbon, heavy metals and polycyclic aromatic hydrocarbons are all integrated and used to calculate the impact, state or drivers statistics based on the suitability of the dataset. For example, total PM_{10} and $PM_{2.5}$ measurements were used to calculate the impact metrics, the PM components were used to calculate the state statistics and the inorganic ion measurements were also used with PCA to quantify the chemical climate drivers.

The key conclusion was that the frequent moderate PM_{10} and $PM_{2.5}$ concentrations at both Harwell and Auchencorth make a substantially larger contribution to the long term health metric compared to the infrequent high percentile concentrations. To reduce the long term health impact of PM, it is necessary to consider a large number of different factors and emission source regions. The frequent moderate concentrations occurred in similar proportions during all months of the year, during a variety of trajectory conditions (including Marine, UK-based and continental air masses) and with substantial contributions secondary inorganic aerosol, sea salt, elemental and organic carbon and calcium. Additionally, for nitrate, the single largest component of PM_{10} and $PM_{2.5}$, a similar proportion of annual average nitrate was accumulated during trajectories classified as ‘Marine’ and ‘Western Europe’. Hence frequently traversing smaller emissions sources as trajectories arrive at Harwell from the Atlantic Ocean results in a similar proportion of the nitrate contribution to total PM as the less frequent traversing of larger emission sources over continental Europe. In comparison the majority of the highest concentrations were measured in winter and spring, during continental air masses and the majority of the total mass was accounted for by secondary inorganic aerosol components.

Lastly, the O_3 human health chemical climate statistics were calculated across the EMEP network of European rural background sites. This demonstrated the enhancement of monitoring network output gained from the standardised interpretation of a large number of time series (hourly O_3 data from 100 sites between 1990 and 2011) using the chemical climatology framework. The common basis for comparison of the O_3 health impact, and the conditions producing it resulted in the identification of three distinct, broad spatial domains which potentially require different mitigation strategies for reduction of the health-relevant O_3 due to differences in the pattern of accumulation. For the SOMO35 metric, sites in northern Europe had lower SOMO35 compared to sites in central and southern Europe, and was derived to a greater extent by hemispheric background concentrations. For those sites in central and southern Europe, the larger SOMO35 compared to northern Europe resulted from increased regional O_3 production. At central European sites, the number of days when SOMO35 was accumulated was lower than at southern European sites, and the increase in the amplitude of the diurnal O_3 cycle on accumulation days compared to non-accumulation days was greater. The NO_x and VOC emissions along trajectories arriving at central European sites were also elevated compared to southern Europe. Hence health-relevant O_3 in central Europe was determined to a greater extent by regional photochemical O_3 episodes whereas in southern Europe SOMO35 was derived through more frequent, smaller exceedance of the 35 ppb threshold.

Across Europe there are common protocols implemented to reduce the human health effects of O_3 (EEA, 2014b). The application of the chemical climatology framework in this example highlights differences in chemical climate spatial 'phases' across Europe which require consideration of different mitigation strategies, and in the effectiveness of current efforts, i.e. the benefit for health-relevant O_3 from reduction of European O_3 precursor emissions is less in northern Europe compared to central and southern Europe.

8.2 Future work and development

Together, the case studies contained within this thesis provide clear examples of how the chemical climatology framework can be used to derive statistics which effectively link a specific impact of atmospheric composition to the conditions producing it to: a) investigate spatial and temporal trends in an impact, b) investigate multi-pollutant impacts through integrate of numerous datasets, and c) consistently compare different impacts.

The future success of the chemical climatology concept relies on its widespread application for a large number of impacts at a large number of sites to enhance the capability of networks to produce outputs which address the three elements listed above. To extend the chemical climatology framework, analogous standard chemical climate statistics are required for a range of atmospheric composition impacts. Potential impacts for which this approach should be extended include: health impacts (acute and chronic) of particulate matter (fine and coarse modes), nitrogen dioxide and sulphur dioxide, and environmental impacts resulting from wet and dry deposition of reactive (oxidised and reduced) nitrogen, sulphur and heavy metals. The quantification of these impacts and the conditions producing them using a common method will facilitate the consideration of co-beneficial impact reduction strategies, as well as identifying where trade-offs may be required. Finally, these chemical climate statistics should be applied to a large number of sites in a diverse range of regions, so that sites across the globe can be integrated with those from other locations to give a consistent comparison of impacts. Additionally, application at a large number of diverse locations will facilitate assessment of whether the standard statistics derived to investigate impacts at Harwell and Auchencorth are equally appropriate for assessment of the same impacts in other locations. This could result in the development of additional useful statistics which increase the comparability of impacts, and the conditions producing them across different regions, site classifications and time periods.

A specific example of a future chemical climate which could result in substantial benefit is for the impact on human health of NO_2. Health impacts associated with air pollution have been calculated to increase substantially when the health impact of NO_2 is included. Walton et al. (2015) calculated that the mortality burden of NO_2 in London for the year 2010 was up to 5900 deaths, higher than the 3500 deaths for anthropogenic $PM_{2.5}$, although the NO_2 figure was calculated with less certainty. Hence it is necessary for the protection of public health across the UK to understand the linkage between the impact of NO_2 on human health, and the conditions producing the impact so that mitigation strategies can be properly developed. Currently, across the UK NO_2 is measured at 119 sites as part of the Automatic Urban and Rural Network (Eaton, 2015). The development and derivation of standard chemical climate statistics at these sites would increase the effectiveness of the large volume of network measurements in advancing understanding of the spatial variation in NO_2 health impact and the factors producing it.

The WHO Review of the Evidence on the Health Aspects of Air Pollution (REVIHAAP) report recommends assessment of the short term impact of NO_2 on human health based on a 1 hour exposure period (REVIHAAP, 2013), and the EU Air Quality standards for NO_2 have a 1 hour (200 µg m^{-3}) and 1 year (40 µg m^{-3}) averaging period (http://ec.europa.eu/environment/air/quality/standards.htm). These values could be used as the health impact metrics for the chemical climate, and 'state' statistics which summarise the monthly and diurnal variation as well as contribution from different parts of the NO_2 concentration distribution to the health metrics would provide information on the specific conditions during which the health impact is accumulated. Statistics which quantify the strength of meteorological, emissions and air mass history 'drivers' could be used to determine how the impact might most effectively be reduced. As has been shown for the impacts of ozone and PM on human health (Chapter 4 and Chapter 6 respectively) and ozone on vegetation (Chapter 4), this method of specifically linking the NO_2 health impact to the causal drivers could provide insight into the necessary measures required for impact reduction. The development of the standard set of statistics also provides a resource for use at sites in

other locations facilitating comparison of both impact severity, and the commonality of conditions producing the impact and hence the spatial applicability of different mitigation strategies.

Additional, general developments in the field of atmospheric composition research would benefit the derivation of chemical climate statistics to quantify impact, state and drivers.

Impact: For many atmospheric composition impacts there are multiple impact metrics which have been and continue to be used for quantification of that impact. Different metrics quantifying the same impact can result in substantial differences in both the spatial pattern of impact severity, as well as the conditions resulting in impact accumulation (see for example Chapter 4 for discussion of differences in impact severity and timing between SOMO10/35 and metrics with higher thresholds). Future work should focus on the assimilation of air pollution effects data to ensure that the most robust metrics are developed and then used as the basis for derivation of the associated chemical climate. Where this is not possible, it should be ensured that the scientific basis for the selection of a particular metric is clearly defined, so that those using the derived chemical climate (e.g. the research or policy community) understand what the impact being quantified by the metric is, and therefore what benefits could results from the curtailment of the identified 'drivers'.

State: The calculation of statistics which summarise the state of atmospheric composition variation relevant to a specific impact necessarily require measurements or model output of atmospheric composition concentrations. For atmospheric composition measurements, a more accurate calculation of a chemical climate state would result from measurement of a wider variety of atmospheric constituents across a larger number of locations and at higher time resolution. For example, while the chemical climates derived in Chapters 4 and 5 integrated time series of ozone and ozone precursors NO_x and VOCs, the chemical climate state could be further improved from measurement of other components. For example, production of ozone results

from OH-initiated VOC degradation (Jenkin and Clemitshaw, 2000). The photolysis of HONO has been shown during certain conditions to contribute to the reservoir of OH radicals (Villena et al., 2011). The measurement of HONO (and/or OH) with the suite of other measurements could allow for its incorporation into the chemical climate state to quantify the contribution of HONO to ozone formation (and impact accumulation). Depending on the strength of the HONO source of OH, this could reveal potentially important new mitigation strategies for the reduction of ozone impacts.

Additionally, as outlined in Chapter 5, the measurement of a wider variety of VOCs would allow for the quantification of the contribution of a wider variety of VOCs to the production of the regional O_3 increment. In particular, the measurement and integration of biogenic VOCs into the assessment of the conditions producing the regional O_3 increment is particularly important to investigate the relative contribution of biogenic vs anthropogenic VOCs in producing the regional O_3 production and hence the capacity for improvement from anthropogenic VOC emission reductions. Currently Harwell and Auchencorth measure isoprene concentrations, which provide a starting point for such an analysis. In Chapter 6 the chemical climate statistics for the long term health impact of PM were outlined such that a subset could be calculated at the majority of sites which only measure total PM_{10} or $PM_{2.5}$. The more widespread measurement of PM components would yield substantial benefit to the characterisation of the spatial differences in the state of the PM long term health climate in terms of which components need to be targeted in different regions to yield maximum improvement to the impact.

Drivers: Emissions inventories are a key method for evaluating the nature of the emissions drivers of the chemical climates outlined in this thesis. However, Chapter 5 showed that for VOCs, spatially gridded emissions inventories are limited through their reporting in highly aggregated source sectors. The improvement gained through reporting of gridded emissions in narrower source sectors is not limited to VOCs, and would allow for a more precise determination of the source activities which require

attention, regardless of the atmospheric component that is of interest. Specifically for VOCs, greater harmonisation between anthropogenic and biogenic emissions inventories would allow the relative contribution of each to ozone, peroxyacetyl nitrate (PAN) or secondary organic aerosol production to be more easily quantified.

Additionally, meteorological drivers are often key to understanding the accumulation of a particular impact. At the majority of measurements sites there are not concurrent measurements of meteorological parameters such as temperature or solar radiation. The routine measurement of meteorological parameters at atmospheric composition monitoring sites would increase the precision with which the nature of the meteorological driver could be evaluated.

References

Borbon, A., Gilman, J. B., Kuster, W. C., Grand, N., Chevaillier, S., Colomb, A., Dolgorouky, C., Gros, V., Lopez, M., Sarda-Esteve, R., Holloway, J., Stutz, J., Petetin, H., McKeen, S., Beekmann, M., Warneke, C., Parrish, D. D., de Gouw, J. A., 2013. Emission ratios of anthropogenic volatile organic compounds in northern mid-latitude megacities: Observations versus emission inventories in Los Angeles and Paris. J. Geophys. Res-Atmos. 118, 2041-2057, doi:10.1002/jgrd.50059.

Brook, J. R., Demerjian, K. L., Hidy, G., Molina, L. T., Pennell, W. I., Scheffe, R., 2009. New Directions: Results-oriented multi-pollutant air quality management. Atmos. Environ. 43, 2091-2093.

Chow, J. C., Watson, J. G., 2008. New directions: Beyond compliance air quality measurements. Atmos. Environ. 42, 5166-5168.

Clapp, L. J., Jenkin, M. E., 2001. Analysis of the relationship between ambient levels Of O-3, NO2 and NO as a function of NO chi in the UK. Atmos. Environ. 35, 6391-6405.

Derwent, R., Manning, A., Simmonds, P., Gerard Spain, T., O'Doherty, S., 2013. Analysis and interpretation of 25 years of ozone observations at the Mace Head Atmospheric Research Station on the Atlantic Ocean coast of Ireland from 1987 to 2012. Atmos. Environ. 80, 361-368.

Eaton, S., 2015. QA/QC Report for the Automatic Urban and Rural Network, October-December 2014, and Annual Review 2014. ED60071-2014-Q4 Issue 1. Contract Report to the Department for Environment, Food and Rural Affairs. Ricardo-AEA.

EEA, 2014a. EU emission inventory report 1990-2012 under the UNECE Convention on long-range transboundary air pollution (LRTAP). EEA technical report No 12/2014. European Environment Agency. http://www.eea.europa.eu//publications/lrtap-2014.

EEA, 2014b. Air Quality in Europe - 2014 Report. EEA Report No 5/2014, European Environment Agency, available at: http://www.eea.europa.eu/publications/air-quality-in-europe-2014.

Jenkin, M. E., Clemitshaw, K. C., 2000. Ozone and other secondary photochemical pollutants: chemical processes governing their formation in the planetary boundary layer. Atmos. Environ. 34, 2499-2527.

REVIHAAP, 2013. Review of evidence on health aspects of air pollution – REVIHAAP Project technical report. World Health Organization (WHO) Regional Office for Europe, Bonn. http://www.euro.who.int/__data/assets/pdf_file/0004/193108/REVIHAAP-Final-technical-report-final-version.pdf.

Villena, G., Wiesen, P., Cantrell, C. A., Flocke, F., Fried, A., Hall, S. R., Hornbrook, R. S., Knapp, D., Kosciuch, E., Mauldin, R. L., III, McGrath, J. A., Montzka, D., Richter, D., Ullmann, K., Walega, J., Weibring, P., Weinheimer, A., Staebler, R. M., Liao, J., Huey, L. G., Kleffmann, J., 2011. Nitrous acid (HONO) during polar spring in Barrow, Alaska: A net source of OH radicals?

Journal of Geophysical Research-Atmospheres 116, doi:10.1029/2011jd016643.

Walton, H., Dajnak, D., Beevers, S., Williams, M., Watkiss, P., Hunt, A., 2015. Understanding the Health Impacts of Air Pollution in London, King's College London, Report TFL 90419 Task 5, available at: https://www.london.gov.uk/sites/default/files/HIAinLondon_KingsReport_14072015_final_0.pdf.

Yates, E. L., Derwent, R. G., Simmonds, P. G., Greally, B. R., O'Doherty, S., Shallcross, D. E., 2010. The seasonal cycles and photochemistry of C-2-C-5 alkanes at Mace Head. Atmos. Environ. 44, 2705-2713.

Appendix I: Supplementary Information for Chapter 4

This supplementary information contains 12 datasheets, summarising the statistics outlined in Chapter 4.2 for the derivation of chemical climates relating to the impact of O_3 exposure on human health and on four vegetation types at Harwell (1990-2013) and Auchencorth (2007-2013).

Tables S4.1 and S4.2: the chemical climates for the O_3 exposure associated with impact on human health (characterised using the SOMO10 and SOMO35 metrics) for Harwell and Auchencorth respectively.
Tables S4.3 and S4.4: the chemical climates for the impact of O_3 on potato (characterised using the POD_Y metric) at Harwell and Auchencorth respectively.
Tables S4.5 and S4.6: the chemical climates for the impact of O_3 on wheat (characterised using the POD_Y metric) at Harwell and Auchencorth respectively.
Tables S4.7 and S4.8: the chemical climates for the impact of O_3 on crops (characterised using the AOT40 metric) at Harwell and Auchencorth respectively.
Tables S4.9 and S4.10: the chemical climates for the impact of O_3 on beech (characterised using the POD_Y metric) at Harwell and Auchencorth respectively.
Tables S4.11 and S4.12: the chemical climates for the impact of O_3 on Scots pine (characterised using the POD_Y metric) at Harwell and Auchencorth respectively.

Table S4.1: Chemical climate datasheet summarising the O_3 exposure associated with human health impact at Harwell.

Impact

Acute ozone human health impact

Respiratory effects: Increased mortality, decreased lung function, coughing, throat irritation, shortness of breath, inflammation of airways, increased asthma attacks (REVIHAAP, 2013).

Metric

REVIHAAP (2013) recommends:
1. Assessment of the O_3 health impact using all year coefficients based on daily maximum 8-hour average O_3 concentrations.
2. A linear concentration-response relationship for short term exposure
3. 2 thresholds: 10 ppb and 35 ppb

Hence health impact evaluated using annual SOMO10 and SOMO35 metrics (sum of max daily 8h means above 10ppb and 35ppb).

Years	SOMO10 (ppb)	SOMO35 (ppb)
1990-1993	8058	1661
1994-1997	8249	1676
1998-2001	8322	1134
2002-2005	9094	1657
2006-2009	7738	985
2010-2013	8512	1088

Spatial domain

Harwell
EMEP level 2 Supersite,
lat: 51.571078
long: -1.32528

Representivity

S and SE UK
(Malley et al., 2014a)
AURN classification:
Rural Background

Temporal Domain

O_3 data: 1990-2013
NO_x data: 1996-2013

State

No. of exceedance days/year

	SOMO10	SOMO35
1990-1993	312	138
1994-1997	323	147
1998-2001	347	143
2002-2005	346	185
2006-2009	337	129
2010-2013	358	148

Ozone Variation (ppb)

	Mean	3rd Quartile	Max
1990-1993	25.0	33.3	111.8
1994-1997	24.6	33.3	107.3
1998-2001	25.8	33.3	89.3
2002-2005	27.3	35.8	88.8
2006-2009	25.2	32.8	85.0
2010-2013	26.7	33.5	77.9

Seasonal contribution to no. of exceedance days

	Spring		Summer		Autumn		Winter	
	SOMO10	SOMO35	SOMO10	SOMO35	SOMO10	SOMO35	SOMO10	SOMO35
1990-1993	29%	46%	29%	36%	25%	9%	17%	9%
1994-1997	27%	41%	27%	39%	24%	9%	22%	12%
1998-2001	24%	42%	26%	34%	26%	10%	24%	14%
2002-2005	27%	40%	27%	31%	23%	13%	24%	16%
2006-2009	22%	46%	27%	30%	27%	9%	24%	15%
2010-2013	25%	50%	26%	28%	25%	8%	24%	14%

	Spring		Summer		Autumn		Winter	
	SOMO10	SOMO35	SOMO10	SOMO35	SOMO10	SOMO35	SOMO10	SOMO35
1990-1993	34.1%	38.3%	35.8%	52.4%	17.7%	7.9%	12.4%	1.4%
1994-1997	30.6%	31.0%	36.8%	63.4%	16.6%	3.1%	16.1%	2.5%
1998-2001	29.0%	41.2%	30.9%	47.0%	20.6%	7.0%	19.4%	4.8%
2002-2005	31.6%	43.0%	30.6%	40.1%	19.2%	9.6%	18.6%	7.3%
2006-2009	28.7%	46.9%	30.8%	43.3%	21.1%	4.0%	19.5%	5.8%
2010-2013	32.7%	56.5%	28.0%	32.1%	19.5%	6.3%	19.9%	5.0%

Mean diurnal variation: SOMO10/35 exceedance (non-exceedance) days (ppb)

	O_3		NO		NO_2	
	SOMO10	SOMO35	SOMO10	SOMO35	SOMO10	SOMO35
1990-1993	27.6 (6.9)	36.8 (19.3)	-	-	-	-
1994-1997	26.8 (8.1)	34.0 (19.1)	8.9 (55.2)	5.4 (19.1)	14.5 (18.4)	12.1 (16.8)
1998-2001	22.8 (8.3)	27.7 (18.9)	6.3 (43.8)	4.6 (9.1)	11.9 (16.0)	10.2 (13.2)
2002-2005	24.2 (9.3)	27.5 (19.6)	5.6 (42.0)	3.5 (10.3)	10.8 (15.4)	9.5 (12.5)
2006-2009	20.8 (8.6)	24.8 (17.9)	4.4 (38.6)	2.8 (6.9)	9.2 (17.5)	7.6 (10.4)
2010-2013	19.9 (9.8)	23.7 (17.0)	4.0 (27.1)	2.5 (5.7)	9.2 (15.0)	7.3 (10.6)

Contribution to SOMO10/35 from different daily max 8h concentrations

Concentration	90-93		94-97		98-01		02-05		06-09		10-13	
range (ppb)	10	35	10	35	10	35	10	35	10	35	10	35
10-20 ppb	2%	-	2%	-	2%	-	1%	-	3%	-	2%	-
20-30 ppb	15%	-	15%	-	18%	-	12%	-	23%	-	18%	-
30-35 ppb	20%	-	18%	-	24%	-	19%	-	21%	-	24%	-
35-40 ppb	18%	7%	21%	9%	21%	14%	23%	14%	22%	15%	21%	14%
40-50 ppb	21%	29%	19%	25%	23%	44%	29%	46%	22%	46%	26%	52%
50-60 ppb	8%	17%	10%	22%	7%	21%	8%	21%	4%	21%	7%	24%
60-70 ppb	6%	16%	4%	12%	4%	14%	3%	10%	3%	11%	1%	6%
>70 ppb	10%	32%	10%	32%	2%	8%	4%	10%	2%	7%	1%	4%

Drivers

Meteorology: Av. Temp on exceedance (non-exceedance) days (°C)

	SOMO10	SOMO35
1990-1993	10.8 (2.8)	12.6 (8.7)
1994-1997	10.3 (3.4)	12.3 (8.0)
1998-2001	10.4 (3.4)	12.0 (9.1)
2002-2005	10.8 (3.9)	12.0 (8.8)
2006-2009	10.7 (1.3)	11.9 (9.6)
2010-2013	10.0 (4.0)	11.3 (9.0)

Air Mass origin: Percentage of trajectories from 4 geographical groupings on exceedance (non-exceedance) days

SOMO10	Northerly	Easterly	Southerly	Westerly
1990-1993	25% (25%)	20% (64%)	28% (9%)	27% (2%)
1994-1997	23% (19%)	17% (69%)	21% (8%)	40% (3%)
1998-2001	19% (21%)	19% (65%)	26% (6%)	35% (9%)
2002-2005	24% (20%)	19% (58%)	21% (20%)	36% (3%)
2006-2009	21% (23%)	18% (71%)	23% (3%)	38% (3%)
2010-2013	21% (2%)	19% (66%)	19% (32%)	40% (1%)

SOMO35	Northerly	Easterly	Southerly	Westerly
1990-1993	22% (26%)	28% (20%)	27% (28%)	22% (26%)
1994-1997	27% (19%)	15% (24%)	19% (20%)	39% (37%)
1998-2001	19% (20%)	19% (21%)	28% (25%)	35% (35%)
2002-2005	23% (25%)	19% (20%)	21% (22%)	37% (33%)
2006-2009	19% (23%)	22% (18%)	20% (23%)	39% (35%)
2010-2013	24% (19%)	19% (20%)	19% (20%)	38% (41%)

Emissions: Av. hourly emissions along 96 hour back trajectory path arriving on POD_Y exceedance (non-exceedance) days (Mg)

	SOMO10	SOMO35
1990-1993	57 (138)	67 (61)
1994-1997	49 (116)	52 (55)
1998-2001	38 (100)	39 (39)
2002-2005	35 (91)	35 (39)
2006-2009	27 (92)	27 (30)
2010-2013	23 (72)	24 (24)

Table S4.2: Chemical climate datasheet summarising the O_3 exposure associated with human health impact at Auchencorth.

Impact

Acute ozone human health impact

Respiratory effects: Increased mortality, decreased lung function, coughing, throat irritation, shortness of breath, inflammation of airways, increased asthma attacks (REVIHAAP, 2013).

Metric

REVIHAAP (2013) recommends:
1. Assessment of the O_3 health impact using all year coefficients based on daily maximum 8-hour average O_3 concentrations.
2. A linear concentration-response relationship for short term exposure
3. 2 thresholds: 10 ppb and 35 ppb

Hence health impact evaluated using annual SOMO10 and SOMO35 metrics (sum of max daily 8h means above 10ppb and 35ppb).

Years	SOMO10 (ppb)	SOMO35 (ppb)
2007	8762	816
2008	9111	1379
2009	8137	750
2010	8517	680
2011	8456	676
2012	8312	673
2013	8820	799

Spatial domain

Auchencorth
EMEP level 2 Supersite,
lat: 55.792160
long: -3.242900

Representivity

Central/northern UK (Malley et al., 2014a)
AURN classification: Rural Background

Temporal Domain

O_3 statistics: 2007-2013
NO_x statistics: 2007-2013
(data from proxy site Bush)

State

No. of exceedance days/year

	SOMO10	SOMO35
2007	363	166
2008	361	160
2009	360	125
2010	365	129
2011	365	131
2012	366	123
2013	364	144

Ozone Variation (ppb)

	Mean	3rd Quartile	Max
2007	29.1	35.0	59.0
2008	30.1	36.0	71.0
2009	27.8	34.0	64.0
2010	28.1	34.0	70.0
2011	28.2	33.0	71.0
2012	28.2	33.0	56.0
2013	29.8	34.5	54.5

Seasonal contribution to no. of exceedance days

	Spring		Summer		Autumn		Winter	
	SOMO10	SOMO35	SOMO10	SOMO35	SOMO10	SOMO35	SOMO10	SOMO35
2007	25%	52%	25%	16%	25%	11%	24%	21%
2008	24%	53%	25%	24%	25%	3%	25%	20%
2009	25%	64%	26%	14%	25%	7%	25%	15%
2010	25%	59%	25%	17%	25%	14%	25%	10%
2011	25%	55%	25%	17%	25%	11%	25%	18%
2012	25%	63%	25%	24%	25%	4%	25%	9%
2013	25%	56%	25%	17%	25%	7%	24%	20%

	Spring		Summer		Autumn		Winter	
	SOMO10	SOMO35	SOMO10	SOMO35	SOMO10	SOMO35	SOMO10	SOMO35
2007	33%	72%	24%	16%	21%	3%	22%	9%
2008	35%	74%	24%	16%	19%	1%	22%	9%
2009	34%	75%	24%	17%	19%	2%	23%	6%
2010	31%	63%	24%	19%	23%	9%	22%	9%
2011	32%	66%	23%	16%	22%	10%	24%	9%
2012	33%	78%	24%	15%	22%	4%	21%	3%
2013	33%	77%	23%	11%	21%	2%	24%	11%

Mean diurnal variation: SOMO10/35 exceedance (non-exceedance) days (ppb)

	O_3		NO		NO_2	
	SOMO10	SOMO35	SOMO10	SOMO35	SOMO10	SOMO35
2007	15.7 (10.0)	17.0 (14.7)	3.8 (33.6)	3.6 (4.2)	9.0 (12.8)	8.8 (9.1)
2008	16.1 (-)	18.4 (14.3)	3.4 (-)	1.9 (4.7)	8.7 (-)	7.3 (9.9)
2009	14.9 (16)	17.6 (13.6)	3.2 (12.8)	2.1 (3.9)	7.9 (11.7)	7.6 (8.1)
2010	16.3 (-)	18.8 (15.0)	4.3 (-)	2.3 (5.4)	9.5 (-)	7.6 (10.5)
2011	15.4 (-)	18.3 (13.8)	2.6 (-)	1.9 (3.1)	6.9 (-)	5.9 (7.4)
2012	14.5 (-)	17.3 (13.1)	2.4 (-)	1.3 (2.8)	7.4 (-)	5.8 (7.9)
2013	13.8 (-)	15.2 (12.9)	2.4 (-)	1.6 (2.9)	7.6 (-)	6.8 (8.1)

Contribution to SOMO10/35 from different daily max 8h concentrations

Concentration	2007		2008		2009		2010		2011		2012		2013	
range (ppb)	10	35	10	35	10	35	10	35	10	35	10	35	10	35
10-20 ppb	0%	-	0%	-	1%	-	0%	-	0%	-	1%	-	0%	-
20-30 ppb	19%	-	20%	-	28%	-	21%	-	23%	-	26%	-	16%	-
30-35 ppb	24%	-	20%		23%	-	33%	-	30%	-	28%		33%	-
35-40 ppb	32%	27%	15%	8%	18%	15%	25%	30%	26%	27%	21%	21%	23%	21%
40-50 ppb	21%	58%	32%	56%	27%	72%	19%	60%	17%	55%	22%	67%	25%	71%
50-60 ppb	3%	15%	9%	25%	3%	13%	1%	6%	2%	10%	2%	12%	2%	8%
60-70 ppb	0%	0%	3%	11%	0%	0%	1%	4%	1%	8%	0%	0%	0%	0%

Drivers

Meteorology: Av. Temp on exceedance (non-exceedance) days (ºC)

	SOMO10	SOMO35
2007	9.6 (-1.9)	9.1 (9.9)
2008	9.0 (-)	9.4 (8.7)
2009	9.3 (11.8)	8.5 (9.7)
2010	8.1 (-)	9.2 (7.5)
2011	9.6 (-)	9.6 (9.6)
2012	8.6 (-)	9.1 (8.4)
2013	9.0 (-)	8.2 (9.6)

Air Mass origin: Percentage of trajectories from 4 geographical groupings on exceedance (non-exceedance) days

SOMO10	Northerly	Easterly	Southerly	Westerly
2007	25% (0%)	17% (100%)	12% (0%)	46% (0%)
2008	20% (-)	20% (-)	9% (-)	52% (-)
2009	19% (6%)	22% (0%)	25% (50%)	34% (44%)
2010	22% (-)	24% (-)	34% (-)	21% (-)
2011	19% (-)	13% (-)	43% (-)	26% (-)
2012	20% (-)	18% (-)	28% (-)	34% (-)
2013	20% (-)	23% (-)	29% (-)	28% (-)

SOMO35	Northerly	Easterly	Southerly	Westerly
2007	24% (26%)	19% (16%)	11% (12%)	46% (46%)
2008	18% (21%)	28% (13%)	9% (9%)	45% (56%)
2009	16% (21%)	32% (16%)	23% (25%)	28% (37%)
2010	23% (21%)	23% (24%)	34% (33%)	19% (21%)
2011	15% (21%)	16% (11%)	40% (44%)	30% (24%)
2012	25% (17%)	29% (13%)	17% (33%)	28% (37%)
2013	19% (20%)	30% (19%)	29% (29%)	22% (32%)

Emissions: Av. hourly emissions along 96 hour back trajectory path arriving on POD_Y exceedance (non-exceedance) days (Mg)

	SOMO10	SOMO35
2007	15 (87)	12 (17)
2008	16 (-)	14 (17)
2009	14 (17)	14 (14)
2010	13 (-)	12 (14)
2011	15 (-)	14 (15)
2012	12 (-)	12 (13)
2013	10 (-)	9 (11)

Table S4.3: Chemical climate datasheet summarising the impact of O_3 on potato at Harwell.

Impact

Ozone impact on POTATO

Critical levels for O_3 impact on potato based on reduction in tuber size (LRTAP Convention, 2010).

Metric

Phytotoxic O_3 Dose above a flux threshold of Y nmol m^{-2} s^{-1} (POD_Y) calculates accumulated stomatal flux of O_3 into the plant across growing season (1130°C days after plant emergence (26th May)). Critical level POD_6 = 2 corresponds to 5% tuber reduction.

Annual PODy 1990-2013

Theil Sen trend estimate is not statistically signiciant (p = 0.05)

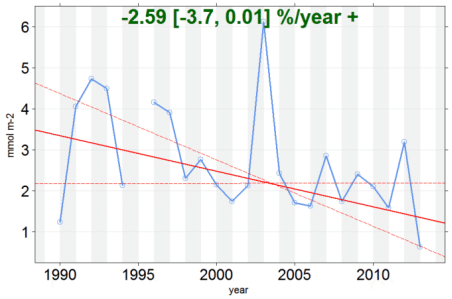

Average annual PODy and % yield reduction

Averaged period	POD_Y (mmol m^{-2})	Yield reduction
1990-1993	3.62 ± 1.62	4.7%
1994-1997	2.87 ± 1.38	3.7%
1998-2001	2.24 ± 1.35	2.9%
2002-2005	3.09 ± 2.04	4.0%
2006-2009	2.15 ± 0.58	2.8%
2010-2013	1.88 ± 1.07	2.4%

Spatial domain

Harwell
EMEP level 2 Supersite,
lat: 51.571078
long: -1.32528

Representivity

S and SE UK
(Malley et al., 2014a)
AURN classification:
Rural Background

Temporal Domain

O_3 data: 1990-2013
NO_x data: 1996-2013

State

Annual and monthly no. of POD_Y exceedance days

	annual	5	6	7
1990-1993	27	2	16	8
1994-1997	25	2	19	3
1998-2001	26	3	19	5
2002-2005	23	3	19	1
2006-2009	27	2	19	6
2010-2013	25	2	20	3

Monthly % contribution to POD_Y

	5	6	7
1990-1993	20%	57%	24%
1994-1997	6%	89%	5%
1998-2001	10%	87%	3%
2002-2005	12%	87%	1%
2006-2009	6%	90%	4%
2010-2013	9%	86%	5%

Mean diurnal O_3 variation: POD_Y exceedance (non-exceedance) days (ppb)

	5	6	7
1990-1993	46.5 (35.7)	39.2 (24.0)	39.2 (25.2)
1994-1997	36.9 (30.8)	37.0 (23.0)	63.6 (39.2)
1998-2001	39.3 (27.0)	32.9 (19.9)	31.7 (27.7)
2002-2005	38.8 (23.3)	29.4 (20.5)	26.4 (28.0)
2006-2009	32.0 (25.8)	30.8 (23.3)	28.8 (24.4)
2010-2013	20.3 (22.6)	22.7 (19.2)	40.2 (21.9)

Mean diurnal NO variation: POD_Y exceedance (non-exceedance) days (ppb)

	5	6	7
1990-1993	-	-	-
1994-1997	8.5 (6.0)	4.8 (3.1)	- (3.4)
1998-2001	4.5 (5.7)	5.6 (3.8)	8.0 (3.9)
2002-2005	3.7 (2.6)	2.2 (1.5)	1.4 (2.7)
2006-2009	4.4 (3.9)	3.5 (4.5)	1.9 (2.5)
2010-2013	0.9 (2.2)	2.1 (2.0)	2.2 (1.7)

Mean diurnal NO_2 variation: POD_Y exceedance (non-exceedance) days (ppb)

	5	6	7
1990-1993	-	-	-
1994-1997	12.7 (11.3)	12.7 (8.6)	- (7.9)
1998-2001	9.5 (12.1)	11.7 (8.1)	11.7 (8.6)
2002-2005	11.1 (7.7)	7.6 (6.9)	5.6 (7.2)
2006-2009	10.9 (8.9)	8.1 (8.2)	3.8 (6.5)
2010-2013	4.4 (6.4)	6.5 (6.0)	11.5 (4.9)

Drivers

Meteorology: Av. Temp on exceedance (non-exceedance) days (°C)

	5	6	7
1990-1993	15.0 (11.7)	15.5 (13.0)	17.3 (16.3)
1994-1997	13.8 (10.2)	15.3 (13.0)	17.9 (17.3)
1998-2001	14.1 (12.1)	15.3 (13.5)	16.2 (16.7)
2002-2005	14.9 (11.4)	16.2 (14.3)	15.4 (16.7)
2006-2009	14.7 (12.5)	16.0 (14.8)	17.5 (16.9)
2010-2013	15.4 (11.2)	14.9 (13.8)	18.0 (16.8)

Av. Global radiation on exceedance (non-exceedance) days (W m^{-2})

	5	6	7
1990-1993	233 (182)	226 (121)	121 (262)
1994-1997	365 (241)	330 (201)	201 (250)
1998-2001	271 (185)	239 (151)	151 (216)
2002-2005	264 (186)	243 (152)	152 (275)
2006-2009	249 (187)	244 (180)	180 (196)
2010-2013	310 (233)	259 (191)	191 (311)

Emissions: Av. hourly emissions along 96 hour back trajectory path arriving on POD_Y exceedance (non-exceedance) days (Mg)

	5	6	7
1990-1993	79 (68)	107 (62)	52 (49)
1994-1997	55 (61)	52 (35)	67 (47)
1998-2001	66 (39)	47 (35)	46 (41)
2002-2005	43 (28)	34 (30)	39 (28)
2006-2009	42 (31)	45 (34)	23 (24)
2010-2013	16 (23)	19 (21)	55 (18)

Air Mass origin: Percentage of trajectories from 4 geographical groupings on exceedance (non-exceedance) days

	Northerly	Easterly	Southerly	Westerly
1990-1993	22% (28%)	35% (15%)	21% (27%)	22% (29%)
1994-1997	38% (27%)	6% (13%)	20% (17%)	35% (43%)
1998-2001	21% (20%)	17% (16%)	27% (27%)	35% (36%)
2002-2005	23% (26%)	11% (16%)	21% (18%)	45% (40%)
2006-2009	26% (24%)	25% (14%)	18% (25%)	30% (38%)
2010-2013	25% (24%)	14% (6%)	21% (19%)	40% (51%)

Table S4.4: Chemical climate datasheet summarising the impact of O_3 on potato at Auchencorth.

Impact

Ozone impact on POTATO

Critical levels for O_3 impact on potato based on reduction in tuber size (LRTAP Convention, 2010).

Metric

Phytotoxic O_3 Dose above a flux threshold of Y nmol m^{-2} s^{-1} (POD_Y) calculates accumulated stomatal flux of O_3 into the plant across growing season (1130ºC days after plant emergence (26th May)). Critical level POD_6 = 2 corresponds to 5% tuber reduction.

Annual PODy 2007-2013.

Theil Sen trend estimate is not statistically significant (p = 0.05)

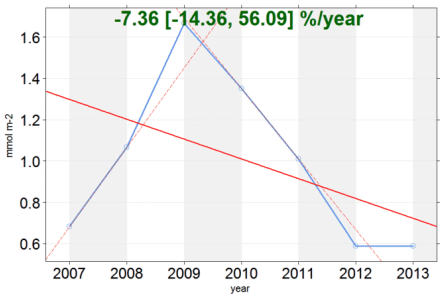

Average annual PODy and % yield reduction for quartile groups

Year	POD_Y (mmol m^{-2})	Yield reduction
2007	0.7	0.8%
2008	1.1	1.4%
2009	1.7	2.2%
2010	1.4	1.7%
2011	1.0	1.3%
2012	0.6	0.8%
2013	0.6	0.8%

Spatial domain

Auchencorth
EMEP level 2 Supersite,
lat: 55.792160
long: -3.242900

Representivity

Central/northern UK
(Malley et al., 2014a)
AURN classification:
Rural Background

Temporal Domain

O_3 statistics: 2007-2013
NO_x statistics: 2007-2013
(data from proxy site Bush)

State

Annual and monthly no. of POD_Y exceedance days

	Annual	5	6	7
2007	24	0	11	13
2008	36	2	22	12
2009	23	3	13	7
2010	20	0	17	3
2011	23	0	9	14
2012	18	3	11	4
2013	17	2	14	1

Monthly % contribution to POD_Y

	5	6	7
2007	-	80%	20%
2008	27%	53%	20%
2009	20%	39%	42%
2010	-	100%	-
2011	-	30%	70%
2012	50%	47%	3%
2013	2%	96%	2%

Mean diurnal O_3 variation: POD_Y exceedance (non-exceedance) days (ppb)

	5	6	7
2007	- (18.0)	27.1 (15.9)	17.1 (16.1)
2008	44.5 (22.4)	17.4 (21.3)	23.3 (16.1)
2009	24.7 (15.5)	19.3 (12.8)	23.7 (12.7)
2010	- (20.0)	22.4 (16.5)	19.0 (13.6)
2011	- (16.0)	20.2 (15.9)	22.1 (15.9)
2012	24.0 (18.7)	18.9 (15.4)	20.5 (13.9)
2013	23.8 (16.6)	21.3 (16.0)	17.0 (18.9)

Mean diurnal NO variation: POD_Y exceedance (non-exceedance) days (ppb)

	5	6	7
2007	- (3.2)	6.6 (5.0)	2.8 (3.5)
2008	0.8 (3.3)	1.1 (2.0)	3.1 (2.5)
2009	1.3 (0.6)	3.5 (1.2)	- (0.6)
2010	- (2.6)	2.0 (2.1)	1.3 (1.4)
2011	- (1.5)	1.3 (2.1)	1.9 (2.4)
2012	1.6 (2.8)	1.5 (1.1)	6.4 (0.9)
2013	1.6 (1.4)	2.0 (1.7)	0.8 (1.5)

Mean diurnal NO_2 variation: POD_Y exceedance (non-exceedance) days (ppb)

	5	6	7
2007	- (8.3)	14.9 (11.1)	5.6 (5.0)
2008	8.2 (11.0)	4.9 (7.2)	7.7 (5.8)
2009	7.6 (3.8)	9.0 (5.7)	- (3.7)
2010	- (7.8)	6.4 (7.1)	3.2 (3.8)
2011	- (3.8)	4.0 (5.5)	5.4 (6.3)
2012	5.3 (8.4)	4.9 (5.2)	10.2 (3.8)
2013	5.6 (6.5)	6.3 (4.9)	1.6 (5.9)

Drivers

Meteorology: Av. Temp on exceedance (non-exceedance) days (ºC)

	5	6	7
2007	- (10.2)	14.7 (11.6)	14.6 (13.5)
2008	15.3 (11.2)	13.3 (11.5)	15.4 (14.7)
2009	15.6 (10.3)	14.6 (11.8)	17.0 (14.5)
2010	- (10.2)	15.2 (13.8)	16.4 (14.9)
2011	- (10.9)	13.8 (11.7)	14.6 (14.0)
2012	14.8 (8.7)	13.5 (11.1)	15.5 (13.2)
2013	13.6 (9.9)	13.8 (12.6)	17.3 (16.7)

Av. Global radiation on exceedance (non-exceedance) days (W m^{-2})

	5	6	7
2007	- (195)	171 (138)	217 (174)
2008	287 (185)	223 (147)	206 (144)
2009	295 (208)	230 (206)	221 (171)
2010	- (277)	350 (220)	366 (219)
2011	- (307)	306 (173)	363 (258)
2012	499 (269)	313 (217)	248 (234)
2013	360 (274)	370 (289)	487 (327)

Emissions: Av. hourly emissions along 96 hour back trajectory path arriving on POD_Y exceedance (non-exceedance) days (Mg)

	5	6	7
2007	- (10)	30 (14)	13 (10)
2008	36 (19)	11 (13)	21 (16)
2009	16 (7)	14 (7)	17 (13)
2010	- (8)	14 (12)	7 (8)
2011	- (13)	11 (12)	16 (10)
2012	8 (11)	12 (15)	23 (7)
2013	6 (9)	12 (8)	5 (11)

Air Mass origin: Percentage of trajectories from 4 geographical groupings on exceedance (non-exceedance) days

	Northerly	Easterly	Southerly	Westerly
2007	24% (33%)	30% (16%)	24% (5%)	22% (46%)
2008	21% (19%)	14% (20%)	10% (14%)	55% (47%)
2009	15% (21%)	52% (13%)	24% (26%)	10% (40%)
2010	21% (19%)	9% (15%)	56% (40%)	14% (26%)
2011	47% (33%)	5% (4%)	34% (34%)	13% (28%)
2012	29% (28%)	23% (11%)	38% (32%)	10% (28%)
2013	25% (19%)	8% (7%)	36% (34%)	31% (40%)

Table S4.5: Chemical climate datasheet summarising the impact of O_3 on wheat at Harwell.

Impact

Ozone impact on WHEAT

Critical levels for O_3 impact on wheat based on reduction in grain yield (LRTAP Convention, 2010).

Metric

Phytotoxic O_3 Dose above a flux threshold of Y nmol m^{-2} s^{-1} (POD_Y) calculates accumulated stomatal flux of O_3 into the plant across growing season (200°C before anthesis - 700 °C after anthesis)). Critical level POD_6 = 1 corresponds to 5% yield reduction.

Annual PODy 1990-2013

Theil Sen trend estimate is not statistically signiciant (p = 0.05)

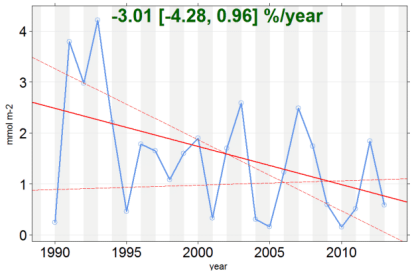

Average annual PODy and % yield reduction

Averaged period	POD_Y (mmol m^{-2})	Yield reduction
1990-1993	2.81 ± 1.78	10.7%
1994-1997	1.53 ±0.74	5.8%
1998-2001	1.23 ±0.60	4.7%
2002-2005	1.19 ± 1.16	4.5%
2006-2009	1.52 ± 0.80	5.8%
2010-2013	0.77 ±0.74	2.9%

Spatial domain

Harwell
EMEP level 2 Supersite,
lat: 51.571078
long: -1.32528

Representivity

S and SE UK
(Malley et al., 2014a)
AURN classification:
Rural Background

Temporal Domain

O_3 data: 1990-2013
NO_x data: 1996-2013

State

Annual and monthly no. of POD_Y exceedance days

	Annual	6	7
1990-1993	24	14	10
1994-1997	18	13	5
1998-2001	20	14	7
2002-2005	15	11	4
2006-2009	22	14	8
2010-2013	19	15	4

Monthly % contribution to POD_Y

	6	7
1990-1993	74%	26%
1994-1997	83%	17%
1998-2001	90%	10%
2002-2005	92%	8%
2006-2009	90%	10%
2010-2013	97%	3%

Mean diurnal O_3 variation: POD_Y exceedance (non-exceedance) days (ppb)

	6	7
1990-1993	40.5 (27.3)	38.2 (26.5)
1994-1997	35.6 (27.0)	58.9 (26.7)
1998-2001	31.9 (24.7)	29.5 (26.6)
2002-2005	29.2 (26.2)	35.0 (26.7)
2006-2009	27.0 (30.0)	29.9 (24.0)
2010-2013	20.9 (20.8)	27.4 (22.7)

Mean diurnal NO variation: POD_Y exceedance (non-exceedance) days (ppb)

	6	7
1990-1993	-	-
1994-1997	5.1 (3.6)	2.8 (3.1)
1998-2001	5.6 (4.7)	5.4 (3.7)
2002-2005	1.4 (2.0)	3.5 (2.5)
2006-2009	3.9 (4.2)	2.1 (2.5)
2010-2013	1.7 (2.3)	2.9 (1.7)

Mean diurnal NO_2 variation: POD_Y exceedance (non-exceedance) days (ppb)

	6	7
1990-1993	-	-
1994-1997	12.1 (10.4)	6.1 (7.1)
1998-2001	11.1 (9.8)	10.1 (8.3)
2002-2005	7.2 (7.7)	7.8 (6.9)
2006-2009	7.8 (9.0)	4.9 (6.3)
2010-2013	5.1 (7.7)	6.2 (5.5)

Drivers

Meteorology: Av. Temp on exceedance (non-exceedance) days (°C)

	6	7
1990-1993	15.4 (13.5)	17.4 (16.4)
1994-1997	15.1 (13.6)	17.9 (17.2)
1998-2001	15.2 (14.0)	16.4 (16.6)
2002-2005	16.5 (15.1)	16.3 (16.7)
2006-2009	15.7 (15.4)	17.5 (16.8)
2010-2013	14.2 (14.4)	16.4 (17.0)

Av. Global radiation on exceedance (non-exceedance) days (W m^{-2})

	6	7
1990-1993	228 (147)	251 (158)
1994-1997	324 (238)	224 (252)
1998-2001	236 (177)	214 (199)
2002-2005	236 (187)	222 (180)
2006-2009	233 (213)	190 (199)
2010-2013	247 (222)	279 (258)

Emissions: Av. hourly emissions along 96 hour back trajectory path arriving on POD_Y exceedance (non-exceedance) days (Mg)

	6	7
1990-1993	122 (59)	52 (53)
1994-1997	53 (39)	76 (43)
1998-2001	49 (38)	43 (40)
2002-2005	34 (35)	35 (26)
2006-2009	40 (41)	28 (23)
2010-2013	17 (21)	16 (20)

Air Mass origin: Percentage of trajectories from 4 geographical groupings on exceedance (non-exceedance) days

	Northerly	Easterly	Southerly	Westerly
1990-1993	28% (27%)	33% (25%)	21% (23%)	19% (25%)
1994-1997	37% (30%)	3% (16%)	15% (21%)	45% (33%)
1998-2001	23% (23%)	13% (24%)	28% (23%)	35% (29%)
2002-2005	18% (29%)	15% (13%)	30% (14%)	37% (44%)
2006-2009	33% (18%)	11% (27%)	23% (21%)	22% (16%)
2010-2013	27% (27%)	13% (16%)	33% (33%)	38% (41%)

Table S4.6: Chemical climate datasheet summarising the impact of O_3 on wheat at Auchencorth.

Impact

Ozone impact on WHEAT

Critical levels for O_3 impact on wheat based on reduction in grain yield (LRTAP Convention, 2010).

Metric

Phytotoxic O_3 Dose above a flux threshold of Y nmol m^{-2} s^{-1} (POD_Y) calculates accumulated stomatal flux of O_3 into the plant across growing season (200°C before anthesis - 700 °C after anthesis)). Critical level POD_6 = 1 corresponds to 5% yield reduction.

Annual PODy 2007-2013

Theil Sen trend estimate is not statistically signiciant (p = 0.05)

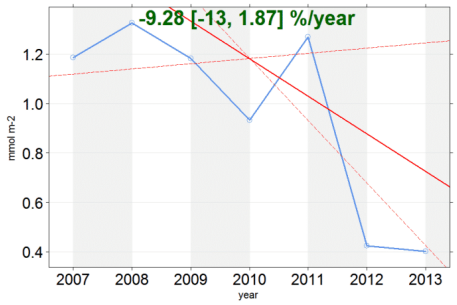

Average annual PODy and % yield reduction

Year	POD_Y (mmol m^{-2})	Yield reduction
2007	1.2	4.5%
2008	1.3	5.0%
2009	1.2	4.5%
2010	0.9	3.6%
2011	1.3	4.8%
2012	0.4	1.6%
2013	0.4	1.5%

Spatial domain

Auchencorth
EMEP level 2 Supersite,
lat: 55.792160
long: -3.242900

Representivity

Central/northern UK
(Malley et al., 2014a)
AURN classification:
Rural Background

Temporal Domain

O_3 statistics: 2007-2013
NO_x statistics: 2007-2013
(data from proxy site Bush)

State

Annual and monthly no. of POD_Y exceedance days

	Annual	6	7
2007	33	11	22
2008	40	23	17
2009	29	14	15
2010	22	15	7
2011	31	10	21
2012	22	15	7
2013	13	12	1

Monthly % contribution to POD_Y

	6	7
2007	61%	39%
2008	64%	36%
2009	42%	58%
2010	90%	10%
2011	20%	80%
2012	80%	20%
2013	99%	1%

Mean diurnal O_3 variation: POD_Y exceedance (non-exceedance) days (ppb)

	6	7
2007	27.0 (16.0)	16.9 (15.6)
2008	17.0 (23.0)	20.4 (17.0)
2009	18.2 (13.3)	17.5 (13.0)
2010	19.1 (21.2)	17.3 (13.3)
2011	17.5 (17.1)	20.8 (14.2)
2012	18.3 (15.1)	17.6 (13.9)
2013	20.8 (16.9)	17.0 (18.9)

Mean diurnal NO variation: POD_Y exceedance (non-exceedance) days (ppb)

	6	7
2007	8.1 (4.2)	3.2 (2.8)
2008	1.1 (2.1)	2.5 (3.0)
2009	1.3 (2.3)	0.3 (0.8)
2010	1.9 (2.3)	0.9 (1.5)
2011	1.2 (2.2)	2.1 (2.3)
2012	1.4 (1.0)	3.8 (1.1)
2013	1.7 (1.9)	0.8 (1.5)

Mean diurnal NO_2 variation: POD_Y exceedance (non-exceedance) days (ppb)

	6	7
2007	14.5 (11.4)	5.3 (5.3)
2008	5.0 (7.0)	7.0 (5.9)
2009	6.2 (7.0)	2.2 (5.1)
2010	5.5 (8.0)	2.4 (4.2)
2011	3.9 (5.6)	5.7 (6.2)
2012	4.7 (5.5)	6.5 (4.1)
2013	6.2 (5.1)	1.6 (5.9)

Drivers

Meteorology: Av. Temp on exceedance (non-exceedance) days (°C)

	6	7
2007	14.3 (11.8)	14.3 (13.2)
2008	13.2 (11.7)	15.4 (14.6)
2009	13.6 (12.4)	15.9 (14.3)
2010	15.4 (13.8)	16.2 (14.6)
2011	12.9 (12.1)	14.5 (13.6)
2012	13.0 (11.0)	15.2 (13.0)
2013	13.8 (12.8)	17.3 (16.7)

Av. Global radiation on exceedance (non-exceedance) days (W m^{-2})

	6	7
2007	179 (134)	209 (148)
2008	219 (147)	187 (144)
2009	217 (214)	211 (155)
2010	332 (261)	270 (223)
2011	271 (184)	355 (200)
2012	320 (184)	253 (230)
2013	354 (309)	487 (327)

Emissions: Av. hourly emissions along 96 hour back trajectory path arriving on POD_Y exceedance (non-exceedance) days (Mg)

	6	7
2007	23 (18)	12 (10)
2008	10 (15)	21 (15)
2009	13 (7)	12 (15)
2010	11 (16)	6 (8)
2011	11 (12)	15 (9)
2012	13 (15)	15 (8)
2013	13 (8)	5 (11)

Air Mass origin: Percentage of trajectories from 4 geographical groupings on exceedance (non-exceedance) days

	Northerly	Easterly	Southerly	Westerly
2007	35% (25%)	23% (31%)	17% (7%)	25% (36%)
2008	25% (20%)	12% (39%)	10% (15%)	53% (26%)
2009	33% (13%)	33% (26%)	20% (25%)	14% (37%)
2010	19% (22%)	2% (14%)	55% (37%)	25% (27%)
2011	56% (25%)	4% (18%)	27% (32%)	14% (25%)
2012	38% (41%)	17% (24%)	34% (16%)	11% (20%)
2013	11% (25%)	23% (10%)	40% (32%)	26% (34%)

Table S4.7: Chemical climate datasheet summarising the impact of O_3 on crops at Harwell using the AOT40 metric.

Impact

Ozone impact on crops

Impact of O_3 crops and wild plants are summarised in (Royal Society, 2008), and include decreased crop yields, nutritional quality, tree growth and photosynthesis rates.

Metric: AOT40

Accumulated annual exposure of hourly O_3 concentrations over a threshold of 40 ppb. Gothenburg Protocol 1999 sets long term critical value for the protection of crops at 3000 ppb.h for the sum of daylight hourly concentrations between May and July (typical growing season).

Averaging period	AOT40 (ppb.h)
1990-1993	6533
1994-1997	6463
1998-2001	3483
2002-2005	3688
2006-2009	3433
2010-2013	2623

Spatial domain

Harwell
EMEP level 2 Supersite,
lat: 51.571078
long: -1.32528

Representivity

S and SE UK
(Malley et al., 2014a)
AURN classification:
Rural Background

Temporal Domain

O_3 data: 1990-2013
NO_x data: 1996-2013)

State

Monthly contribution to AOT40

	May	June	July
1990-1993	32%	31%	37%
1994-1997	28%	27%	45%
1998-2001	38%	36%	26%
2002-2005	39%	31%	30%
2006-2009	38%	36%	26%
2010-2013	44%	21%	35%

Monthly average diurnal O_3 cycle (ppb)

	May	June	July
1990-1993	26.8	22.9	23.8
1994-1997	22.5	22.5	30.4
1998-2001	17.3	18.2	20.8
2002-2005	15.5	19.5	21.3
2006-2009	16.5	20.6	20.3
2010-2013	15.7	14.7	18.8

Monthly average diurnal NO cycle (ppb)

	May	June	July
1990-1993	-	-	-
1994-1997	3.4	2.3	2.7
1998-2001	2.9	2.4	1.8
2002-2005	1.7	0.9	1.6
2006-2009	1.9	1.8	1.5
2010-2013	1.6	1.1	1.4

Monthly average diurnal NO_2 cycle (ppb)

	May	June	July
1990-1993	-	-	-
1994-1997	4.1	5.0	4.4
1998-2001	5.2	4.4	3.8
2002-2005	3.2	2.9	2.5
2006-2009	2.6	2.7	2.2
2010-2013	2.8	2.5	2.3

Drivers

Meteorology: Monthly average temperature (°C)

	May	June	July
1990-1993	12.2	14.4	16.7
1994-1997	10.6	14.4	17.4
1998-2001	12.5	14.6	16.5
2002-2005	11.8	15.6	16.7
2006-2009	12.6	15.4	17.2
2010-2013	11.5	14.5	17.1

Air Mass origin: Percentage of trajectories from 4 geographical groupings during growing season (May-July)

	Northerly	Easterly	Southerly	Westerly
1990-1993	27%	27%	14%	32%
1994-1997	32%	13%	20%	35%
1998-2001	23%	23%	24%	30%
2002-2005	29%	11%	15%	45%
2006-2009	21%	25%	17%	38%
2010-2013	28%	15%	17%	40%

Emissions: Average hourly emissions along 96 hour back trajectory path during each month of growing season (Mg)

	May	June	July
1990-1993	70.6	78.3	53.8
1994-1997	61.6	46.5	49.6
1998-2001	41.9	42.3	40.8
2002-2005	29.6	32.7	28.3
2006-2009	30.1	39.1	22.0
2010-2013	22.6	19.7	21.4

Annual crop AOT40 1990-2013

Theil Sen trend estimate is statistically signiciant (p = 0.001)

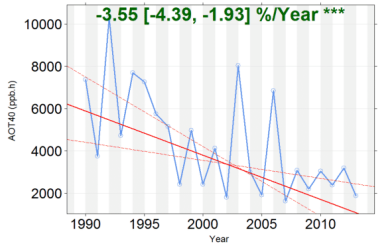

Table S4.8: Chemical climate datasheet summarising the impact of O_3 on crops at Auchencorth using the AOT40 metric.

Impact

Ozone impact on crops

Impact of O_3 crops and wild plants are summarised in (Royal Society, 2008), and include decreased crop yields, nutritional quality, tree growth and photosynthesis rates.

Metric: AOT40

Accumulated annual exposure of hourly O_3 concentrations over a threshold of 40 ppb. Gothenburg Protocol 1999 sets long term critical value for the protection of crops at 3000 ppb.h for the sum of daylight hourly concentrations between May and July (typical growing season).

Years	AOT40 (ppb.h)
2007	896
2008	4555
2009	1332
2010	963
2011	925
2012	1085
2013	694

Spatial domain

Auchencorth
EMEP level 2 Supersite,
lat: 55.792160
long: -3.242900

Representivity

Central/northern UK
(Malley et al., 2014a)
AURN classification:
Rural Background

Temporal Domain

O_3 statistics: 2007-2013
NO_x statistics: 2007-2013
(data from proxy site Bush)

State

Monthly contribution to AOT40

	May	June	July
2007	42%	57%	1%
2008	82%	11%	7%
2009	57%	23%	20%
2010	39%	61%	0%
2011	61%	10%	30%
2012	96%	3%	1%
2013	73%	13%	14%

Monthly average diurnal O_3 cycle (ppb)

	May	June	July
2007	8.4	7.4	10.2
2008	14.0	12.0	11.3
2009	10.1	11.4	10.8
2010	12.7	13.8	7.0
2011	8.7	10.6	13.7
2012	11.4	8.4	8.0
2013	7.0	11.2	11.9

Monthly average diurnal NO cycle (ppb)

	May	June	July
2007	1.9	3.5	1.7
2008	1.5	0.5	1.4
2009	0.3	1.1	0.3
2010	1.6	1.1	0.8
2011	0.8	1.3	1.5
2012	2.0	0.8	1.1
2013	0.7	1.2	1.0

Monthly average diurnal NO_2 cycle (ppb)

	May	June	July
2007	3.3	3.5	2.1
2008	4.3	1.2	2.3
2009	1.5	2.9	1.4
2010	2.6	2.0	1.5
2011	0.9	1.6	1.9
2012	3.8	1.6	1.6
2013	2.2	1.8	2.0

Drivers

Meteorology: Monthly average temperature (°C)

	May	June	July
2007	10.2	12.7	14.0
2008	11.4	12.9	15.0
2009	11.0	13.1	15.3
2010	10.2	14.5	15.0
2011	10.9	12.5	14.3
2012	9.3	12.0	13.5
2013	10.1	13.2	16.8

Air Mass origin: Percentage of trajectories from 4 geographical groupings during growing season (May-July)

	Northerly	Easterly	Southerly	Westerly
2007	27%	32%	11%	30%
2008	22%	32%	12%	34%
2009	19%	31%	20%	30%
2010	20%	14%	43%	24%
2011	34%	11%	32%	23%
2012	40%	24%	17%	19%
2013	24%	13%	31%	32%

Emissions: Av. hourly emissions along 96 hour back trajectory path arriving on POD_y exceedance (non-exceedance) days (Mg)

	May	June	July
2007	9.7	19.9	11.2
2008	20.4	11.6	18.1
2009	7.8	10.1	13.5
2010	8.0	13.5	7.6
2011	13.4	11.7	13.1
2012	10.4	13.9	9.3
2013	8.4	9.9	10.5

Annual crop
AOT40
1990-2013

Theil Sen trend estimate is not statistically signiciant ($p = 0.05$)

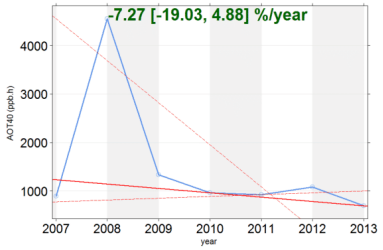

Table S4.9: Chemical climate datasheet summarising the impact of O_3 on beech at Harwell.

Impact

Ozone impact on BEECH

Critical levels for O_3 impact on beech based on reduction in whole tree biomass (LRTAP Convention, 2010).

Metric

Phytotoxic O_3 Dose above a flux threshold of Y nmol m^{-2} s^{-1} (POD_Y) calculates accumulated stomatal flux of O_3 into the plant across growing season (19th April-20th October)). Critical level POD_1 = 4 corresponds to 4% biomass reduction.

Annual PODy 1990-2013

Theil Sen trend estimate is not statistically signiciant (p =0.05)

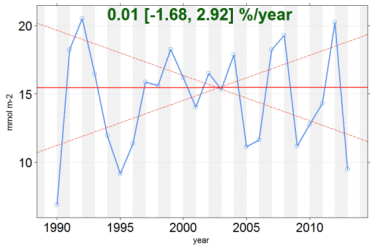

Average annual PODy and % yield reduction for quartile groups

Averaged period	POD_Y (mmol m^{-2})	Biomass reduction
1990-1993	15.5 ± 6.0	17.1%
1994-1997	12.0 ±2.8	13.3%
1998-2001	16.0 ±3.3	17.6%
2002-2005	15.2 ±2.9	16.7%
2006-2009	15.1 ±4.3	16.6%
2010-2013	14.2 ±4.5	15.6%

Spatial domain

Harwell
EMEP level 2 Supersite,
lat: 51.571078
long: -1.325283

Representivity

S and SE UK
(Malley et al., 2014a)
AURN classification:
Rural Background

Temporal Domain

O_3 data: 1990-2013
NO_x data: 1996-2013

State

No. of POD_Y exceedance days & monthly contribution

	Annual	4	5	6	7	8	9
90-93	154	8	29	29	27	26	25
94-97	148	8	27	28	29	24	20
98-01	170	8	30	30	30	30	30
02-05	166	10	31	30	31	30	29
06-09	165	8	29	29	30	30	29
10-13	162	8	31	29	29	29	28

Monthly % contribution to POD_Y

	4	5	6	7	8	9
90-93	3%	33%	23%	16%	16%	7%
94-97	3%	35%	34%	12%	7%	8%
98-01	3%	27%	28%	15%	14%	11%
02-05	3%	34%	30%	13%	11%	9%
06-09	3%	29%	29%	15%	13%	9%
10-13	3%	33%	25%	12%	12%	14%

Mean diurnal O_3 variation: POD_Y exceedance (non-exceedance) (ppb)

	4	5	6	7	8	9
90-93	31.5 (24.0)	36.7 (14.9)	33.7 (21.5)	33.6 (8.8)	36.4 (13.1)	31.5 (10.8)
94-97	28.6 (27.9)	32.2 (2.5)	32.4 (-)	40.6 (22.0)	42.5 (17.7)	24.1 (14.8)
98-01	28.5 (21.9)	28.1 (-)	27.9 (-)	28.1 (-)	30.0 (13.5)	24.5 (6.0)
02-05	26.7 (29.5)	25.2 (-)	26.8 (-)	28.2 (17.0)	32.5 (15.8)	28.9 (13.3)
06-09	24.6 (24.5)	26.2 (-)	28.4 (-)	24.8 (11.0)	20.5 (19.0)	21.0 (5)
10-13	22.6 (18.5)	22.8 (-)	21.4 (-)	24.1 (16.9)	21.6 (15.6)	19 (13)

Mean diurnal NO variation: POD_Y exceedance (non-exceedance) (ppb)

	4	5	6	7	8	9
90-93	-	-	-	-	-	-
94-97	2.1 (8.9)	6.2 (-)	4.1 (-)	3.4 (-)	-	3.4 (3.6)
98-01	4.2 (3.6)	5.7 (-)	5.0 (-)	4.1 (-)	4.8 (6.2)	5.5 (-)
02-05	3.1 (4.1)	2.8 (-)	1.8 (-)	2.6 (6.4)	3.9 (6.4)	6.0 (3.5)
06-09	2.7 (2.9)	4.0 (-)	3.8 (-)	2.5 (0)	2.2 (1.2)	4.4 (1.8)
10-13	2.7 (1.8)	2.1 (-)	2.0 (-)	1.8 (1.3)	1.9 (2.5)	3.9 (1.2)

Mean diurnal NO_2 variation: POD_Y exceedance (non-exceedance) (ppb)

	4	5	6	7	8	9
90-93	-	-	-	-	-	-
94-97	9.7 (18.4)	11.6 (-)	11.2 (-)	7.9 (-)	-	10.6 (7.4)
98-01	10.0 (10.3)	11.9 (-)	10.2 (-)	8.8 (-)	11.1 (11.7)	10.5 (-)
02-05	11.0 (12.7)	8.2 (-)	7.3 (-)	7.0 (9.0)	13.2 (11.8)	11.8 (9.7)
06-09	9.0 (8.2)	9.0 (-)	8.1 (-)	6.1 (2.1)	4.6 (9.0)	9.0 (6.6)
10-13	7.5 (6.5)	6.3 (-)	6.3 (-)	5.4 (5.0)	6.5 (7.8)	7.8 (5.6)

Drivers

Meteorology: Av. Temp on exceedance (non-exceedance) days (°C)

	4	5	6	7	8	9
90-93	9.8 (7.9)	11.9 (11.2)	14.5 (12.9)	17.0 (15.3)	16.8 (15.6)	13.5 (11.3)
94-97	10.4 (7.3)	10.7 (5.4)	14.5 (-)	17.4 (17.9)	18.0 (18.0)	12.1 (14.3)
98-01	9.9 (6.5)	12.4 (-)	14.6 (-)	16.7 (-)	16.5 (14.3)	14.6 (11.8)
02-05	10.9 (8.2)	11.8 (-)	15.6 (-)	16.7 (14.1)	17.4 (17.6)	14.5 (14.5)
06-09	10.6 (8.2)	12.7 (-)	15.6 (-)	17.2 (16.4)	16.2 (17.6)	14.3 (14.5)
10-13	10.6 (8.4)	11.5 (-)	14.6 (-)	16.9 (18.9)	16.3 (16.4)	13.9 (13.1)

Av. Global radiation on exceedance (non-exceedance) days (W m^{-2})

	4	5	6	7	8	9
90-93	150 (138)	194 (9)	198 (11)	209 (39)	185 (83)	130 (24)
94-97	221 (192)	257 (-)	278 (-)	269 (159)	247 (180)	151 (82)
98-01	170 (112)	194 (-)	206 (-)	206 (-)	182 (35)	119 (9)
02-05	161 (154)	193 (-)	211 (-)	190 (57)	177 (155)	135 (36)
06-09	173 (148)	190 (-)	224 (-)	211 (147)	164 (177)	131 (24)
10-13	166 (141)	242 (-)	239 (-)	269 (221)	251 (135)	146 (60)

Emissions: Average hourly NO_x emissions along 96 hour back trajectory path arriving on POD_Y exceedance (non-exceedance) days (Mg)

	4	5	6	7	8	9
90-93	74 (55)	68 (106)	81 (69)	55 (33)	58 (35)	68 (66)
94-97	49 (61)	60 (65)	47 (-)	49 (19)	59 (36)	38 (54)
98-01	38 (45)	41 (-)	42 (-)	43 (-)	40 (28)	43 (21)
02-05	47 (45)	30 (-)	33 (-)	28 (39)	38 (33)	40 (25)
06-09	31 (30)	32 (-)	40 (-)	22 (6)	19 (22)	29 (15)
10-13	28 (27)	23 (-)	19 (-)	22 (8)	17 (9)	19 (25)

Air Mass origin: Percentage of trajectories from 4 geographical groupings on exceedance (non-exceedance) days

	Northerly	Easterly	Southerly	Westerly
90-93	28% (29%)	23% (18%)	25% (27%)	24% (27%)
94-97	29% (23%)	15% (22%)	20% (21%)	36% (34%)
98-01	19% (20%)	20% (17%)	27% (35%)	33% (28%)
02-05	27% (19%)	16% (42%)	18% (20%)	39% (19%)
06-09	21% (28%)	20% (15%)	22% (22%)	37% (35%)
10-13	20% (15%)	15% (16%)	19% (20%)	43% (41%)

Table S4.10: Chemical climate datasheet summarising the impact of O_3 on beech at Auchencorth.

Impact

Ozone impact on BEECH

Critical levels for O_3 impact on beech based on reduction in whole tree biomass (LRTAP Convention, 2010).

Metric

Phytotoxic O_3 Dose above a flux threshold of Y nmol m^{-2} s^{-1} (POD_Y) calculates accumulated stomatal flux of O_3 into the plant across growing season (26th April-10th October)). Critical level POD_1 = 4 corresponds to 4% biomass reduction.

Annual PODy 2007-2013.

Theil Sen trend estimate is not statistically signiciant (p = 0.05)

Average annual PODy and % yield reduction for quartile groups

Averaged period	POD_Y (mmol m^{-2})	Biomass reduction
2007	16.9	18.6%
2008	19.1	21.0%
2009	16.5	18.1%
2010	17.8	19.6%
2011	16.1	17.7%
2012	15.8	17.4%
2013	14.6	16.0%

Spatial domain

Auchencorth
EMEP level 2 Supersite,
lat: 55.792160
long: -3.242900

Representivity

Central/northern UK (Malley et al., 2014a)
AURN classification: Rural Background

Temporal Domain

O_3 statistics:
2007-2013
NO_x statistics:
2007-2013
(data from proxy site Bush)

State

Annual and monthly no. of POD_Y exceedance days

	Annual	5	6	7	8	9
2007	159	31	30	31	31	30
2008	157	31	30	31	31	30
2009	156	29	30	31	31	29
2010	160	31	30	31	31	30
2011	155	31	28	31	31	30
2012	155	31	30	29	31	30
2013	155	31	30	31	31	29

Monthly % contribution to POD_Y

	5	6	7	8	9
2007	21%	23%	23%	19%	14%
2008	30%	25%	21%	15%	9%
2009	25%	25%	22%	18%	10%
2010	21%	27%	19%	19%	15%
2011	25%	21%	26%	14%	14%
2012	25%	23%	18%	21%	13%
2013	25%	28%	15%	22%	10%

Mean diurnal O_3 variation: POD_Y exceedance (non-exceedance) (ppb)

	5	6	7	8	9
2007	18.0 (-)	20.0 (-)	16.5 (-)	16.8 (-)	13.4 (-)
2008	23.8 (-)	18.4 (-)	18.9 (-)	15.7 (-)	16.0 (-)
2009	16.4 (-)	15.5 (-)	15.2 (-)	13.3 (-)	13.1 (5)
2010	20.0 (-)	20.1 (-)	14.2 (-)	15.6 (-)	16.8 (-)
2011	16.0 (-)	17.5 (8)	18.7 (-)	14.4 (-)	14.2 (-)
2012	19.2 (-)	16.7 (-)	15.1 (4)	17.3 (-)	12.8 (-)
2013	17.1 (-)	18.5 (-)	18.8 (-)	14.3 (-)	14.1 (17.0)

Mean diurnal NO variation: POD_Y exceedance (non-exceedance) (ppb)

	5	6	7	8	9
2007	3.2 (-)	5.6 (-)	3.1 (-)	3.3 (-)	2.0 (-)
2008	3.1 (-)	1.3 (-)	2.7 (-)	1.5 (-)	2.6 (-)
2009	0.7 (-)	2.0 (-)	0.6 (-)	1.5 (-)	1.6 (7.2)
2010	2.6 (-)	2.1 (-)	1.4 (-)	2.4 (-)	3.0 (-)
2011	1.5 (-)	1.6 (8.8)	2.2 (-)	2.6 (-)	1.6 (-)
2012	2.6 (-)	1.2 (-)	1.9 (0)	1.1 (-)	1.4 (-)
2013	1.4 (-)	1.8 (-)	1.5 (-)	2.8 (-)	2.6 (27.2)

Mean diurnal NO_2 variation: POD_Y exceedance (non-exceedance) (ppb)

	5	6	7	8	9
2007	8.3 (-)	12.5 (-)	5.3 (-)	6.1 (-)	5.7 (-)
2008	10.8 (-)	5.5 (-)	6.5 (-)	5.8 (-)	7.7 (-)
2009	4.2 (-)	6.7 (-)	3.7 (-)	3.3 (-)	5.3 (8.5)
2010	7.8 (-)	6.6 (-)	3.8 (-)	6.3 (-)	7.6 (-)
2011	3.8 (-)	4.4 (22.9)	5.9 (-)	5.7 (-)	3.8 (-)
2012	7.9 (-)	5.1 (-)	5.0 (0.5)	4.4 (-)	4.1 (-)
2013	6.5 (-)	5.5 (-)	5.7 (-)	5.9 (-)	6.6 (17.6)

Drivers

Meteorology: Av. Temp on exceedance (non-exceedance) days (ºC)

	5	6	7	8	9
2007	10.2 (-)	12.7 (-)	14.0 (-)	14.1 (-)	12.6 (-)
2008	11.4 (-)	12.8 (-)	15.0 (-)	14.9 (-)	12.4 (-)
2009	10.9 (-)	13.0 (-)	15.1 (-)	15.5 (-)	13.3 (10.4)
2010	10.2 (-)	14.7 (-)	15.0 (-)	14.0 (-)	12.9 (-)
2011	10.9 (-)	12.3 (13.4)	14.2 (-)	13.7 (-)	13.5 (-)
2012	9.3 (-)	12.0 (-)	13.6 (11.0)	14.8 (-)	11.8 (-)
2013	10.1 (-)	13.2 (-)	16.8 (-)	15.3 (-)	12.5 (13.6)

Av. Global radiation on exceedance (non-exceedance) days (W m^{-2})

	5	6	7	8	9
2007	195 (-)	150 (-)	192 (-)	208 (-)	117 (-)
2008	192 (-)	202 (-)	168 (-)	122 (-)	94 (-)
2009	217 (-)	216 (-)	182 (-)	231 (-)	154 (116)
2010	277 (-)	299 (-)	234 (-)	215 (-)	156 (-)
2011	307 (-)	223 (-)	305 (-)	190 (-)	183 (-)
2012	291 (-)	252 (-)	230 (388)	232 (-)	178 (-)
2013	280 (-)	327 (-)	333 (-)	232 (-)	106 (27)

Emissions: Average hourly NO_x emissions along 96 hour back trajectory path arriving on POD_Y exceedance (non-exceedance) days (Mg)

	5	6	7	8	9
2007	10 (-)	20 (-)	11 (-)	8 (-)	6 (-)
2008	20 (-)	12 (-)	18 (-)	16 (-)	23 (-)
2009	8 (-)	10 (-)	13 (-)	7 (-)	7 (18)
2010	8 (-)	13 (-)	8 (-)	6 (-)	14 (-)
2011	13 (-)	12 (9)	13 (-)	17 (-)	13 (-)
2012	10 (-)	14 (-)	9 (9)	15 (-)	5 (-)
2013	8 (-)	10 (-)	10 (-)	10 (-)	7 (36)

Air Mass origin: Percentage of trajectories from 4 geographical groupings on exceedance (non-exceedance) days

	Northerly	Easterly	Southerly	Westerly
2007	28% (43%)	23% (3%)	7% (13%)	42% (42%)
2008	18% (38%)	27% (2%)	12% (0%)	42% (60%)
2009	20% (19%)	20% (10%)	23% (40%)	38% (31%)
2010	21% (0%)	14% (31%)	41% (67%)	23% (2%)
2011	30% (19%)	11% (0%)	35% (46%)	24% (35%)
2012	28% (58%)	17% (7%)	27% (0%)	27% (36%)
2013	21% (32%)	13% (13%)	31% (31%)	34% (25%)

Table S4.11: Chemical climate datasheet summarising the impact of O_3 on Scots pine at Harwell.

Impact

Ozone impact on PINE

Critical levels for coniferous trees based on whole tree biomass reductions. Scots pine representative tree for 'atlantic central Europe' (LRTAP Convention, 2010).

Metric

Phytotoxic O_3 Dose above a flux threshold of Y nmol m^{-2} s^{-1} (POD_Y) calculates accumulated stomatal flux of O_3 into the plant across growing season (year round when daily mean temperature >0 °C).

Annual PODy 1990-2013

Theil Sen trend estimate is not statistically signiciant (p = 0.05)

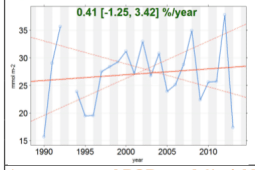

Average annual PODy and % yield reduction for quartile groups

Averaged period	POD_Y (mmol m^{-2})	Biomass reduction
1990-1993	27.1 ±8.3	Response function not available for Scots pine.
1994-1997	22.6 ±3.8	
1998-2001	29.0 ±4.9	
2002-2005	28.6 ±4.0	
2006-2009	27.8 ±5.4	
2010-2013	26.6 ±8.4	

Spatial domain

Harwell
EMEP level 2 Supersite,
lat: 51.571078
long: -1.325283

Representivity

S and SE UK (Malley et al., 2014a)
AURN classification: Rural Background

Temporal Domain

O_3 data: 1990-2013
NO_x data: 1996-2013

State

Annual and monthly no. of POD_Y exceedance days

	Annual	3	4	5	6	7	8	9
90-93	291	31	28	29	30	28	27	25
94-97	294	28	30	27	28	29	24	20
98-01	325	29	22	30	30	30	30	30
02-05	324	30	30	31	30	31	31	29
06-09	316	23	23	29	29	30	30	30
10-13	316	28	24	31	29	28	30	29

Monthly % contribution to POD_Y

	3	4	5	6	7	8	9
90-93	11%	17%	20%	14%	12%	10%	4%
94-97	10%	20%	23%	19%	6%	4%	5%
98-01	8%	11%	20%	18%	9%	8%	7%
02-05	11%	18%	24%	16%	7%	7%	3%
06-09	8%	13%	20%	17%	10%	9%	6%
10-13	9%	14%	21%	14%	7%	8%	6%

Mean diurnal O_3 variation: POD_Y exceedance (non-exceedance) (ppb)

	3	4	5	6	7	8	9
90-93	23.7 (30.0)	26.6 (7.3)	38.7 (9.2)	30.6 (16.0)	36.8 (12.8)	38.8 (24.0)	32.5 (12.4)
94-97	22.4 (18.0)	28.1 (23.0)	32.2 (2.5)	32.4 (-)	40.4 (25.3)	42.0 (17.7)	24.1 (14.8)
98-01	21.2 (20.4)	26.6 (4.0)	28.1 (-)	27.9 (-)	28.1 (-)	30.0 (13.5)	24.5 (6.0)
02-05	25.4 (17.3)	28.5 (-)	25.2 (-)	26.8 (-)	28.2 (17.0)	32.4 (19.0)	28.8 (13.5)
06-09	18.6 (9.5)	24.3 (4.0)	26.2 (-)	28.4 (-)	24.8 (11.0)	20.4 (21.0)	20.7 (11.0)
10-13	21.9 (10.5)	20.4 (-)	22.8 (-)	21.4 (-)	24.2 (16.4)	21.2 (34.6)	19.3 (10.6)

Mean diurnal NO variation: POD_Y exceedance (non-exceedance) (ppb)

	3	4	5	6	7	8	9
90-93	-	-	-	-	-	-	-
94-97	12.2 (17.4)	6.6 (28.0)	6.2 (-)	4.1 (-)	3.4 (-)	-	3.4 (3.6)
98-01	8.2 (20.9)	3.9 (0)	5.7 (-)	5.0 (-)	4.1 (-)	4.8 (6.2)	5.5 (-)
02-05	9.6 (20.3)	4.0 (-)	2.8 (-)	1.8 (-)	2.6 (6.4)	4.0 (2.0)	5.9 (4.8)
06-09	2.7 (2.2)	2.9 (0)	4.0 (-)	3.8 (-)	2.5 (0)	2.1 (1.4)	4.3 (1.6)
10-13	6.7 (10.2)	2.1 (-)	2.1 (-)	2.0 (-)	1.8 (1.0)	1.9 (0.5)	3.8 (0)

Mean diurnal NO_2 variation: POD_Y exceedance (non-exceedance) (ppb)

	3	4	5	6	7	8	9
90-93	-	-	-	-	-	-	-
94-97	17.0 (18.0)	15.7 (28.7)	11.6 (-)	11.2 (-)	7.9 (-)	-	10.6 (7.4)
98-01	13.8 (22.3)	10.4 (2.1)	11.9 (-)	10.2 (-)	8.8 (-)	11.1 (11.7)	10.5 (-)
02-05	15.0 (17.2)	12.0 (-)	8.2 (-)	7.3 (-)	7.0 (9.0)	9.4 (6.6)	11.8 (8.6)
06-09	7.6 (5.9)	9.2 (0)	9.0 (-)	8.1 (-)	6.1 (2.1)	6.2 (5.3)	8.9 (10.6)
10-13	12.7 (10.7)	6.9 (-)	6.3 (-)	6.3 (-)	5.4 (4.4)	5.6 (3.9)	7.8 (2.1)

Drivers

Meteorology: Av. Temp on exceedance (non-exceedance) days (ºC)

	3	4	5	6	7	8	9
90-93	7.9 (5.7)	8.2 (5.8)	12.0 (12.2)	14.0 (14.6)	17.2 (17.0)	17.6 (17.4)	13.9 (12.8)
94-97	6.3 (4.3)	8.2 (4.7)	10.7 (5.4)	14.5 (-)	17.4 (17.3)	18.0 (17.9)	12.1 (14.3)
98-01	7.0 (5.7)	8.5 (-0.8)	12.4 (-)	14.6 (-)	16.7 (-)	16.5 (14.3)	14.6 (11.8)
02-05	6.9 (6.2)	9.1 (-)	11.8 (-)	15.6 (-)	16.7 (14.1)	17.4 (21.0)	14.5 (14.3)
06-09	6.1 (4.1)	9.6 (8.1)	12.7 (-)	15.6 (-)	17.2 (16.4)	16.2 (18.7)	14.4 (14.7)
10-13	5.6 (3.3)	9.1 (8.3)	11.5 (-)	14.6 (-)	16.9 (18.8)	16.3 (20.3)	13.9 (13.6)

Av. Global radiation on exceedance (non-exceedance) days (W m^{-2})

	3	4	5	6	7	8	9
90-93	92 (36)	149 (0)	196 (1)	182 (0)	210 (58)	184 (166)	135 (26)
94-97	131 (40)	202 (58)	257 (2)	278 (-)	268 (261)	247 (180)	151 (82)
98-01	92 (35)	156 (0)	194 (-)	206 (-)	206 (-)	182 (35)	119 (9)
02-05	98 (28)	156 (-)	193 (-)	211 (-)	190 (57)	177 (126)	134 (41)
06-09	108 (5)	160 (0)	190 (-)	224 (-)	211 (147)	163 (206)	129 (51)
10-13	139 (51)	163 (-)	242 (-)	239 (-)	271 (239)	246 (304)	144 (71)

Emissions: Average hourly NO_x emissions along 96 hour back trajectory path arriving on POD_Y exceedance (non-exceedance) days (Mg)

	3	4	5	6	7	8	9
90-93	51 (61)	60 (55)	74 (89)	72 (76)	64 (40)	62 (30)	67 (40)
94-97	54 (89)	56 (108)	60 (65)	47 (-)	49 (24)	59 (36)	38 (54)
98-01	42 (68)	40 (21)	41 (-)	42 (-)	43 (-)	40 (28)	43 (21)
02-05	47 (88)	45 (-)	30 (-)	33 (-)	28 (39)	38 (11)	40 (24)
06-09	19 (13)	28 (109)	32 (-)	40 (-)	22 (6)	19 (21)	29 (15)
10-13	33 (41)	25 (-)	23 (-)	19 (-)	22 (13)	17 (15)	19 (29)

Air Mass origin: Percentage of trajectories from 4 geographical groupings on exceedance (non-exceedance) days

	Northerly	Easterly	Southerly	Westerly
90-93	29% (15%)	18% (33%)	26% (21%)	27% (22%)
94-97	23% (22%)	15% (44%)	21% (13%)	41% (21%)
98-01	18% (27%)	18% (38%)	27% (16%)	36% (18%)
02-05	24% (28%)	18% (42%)	21% (18%)	38% (12%)
06-09	22% (25%)	17% (35%)	23% (19%)	38% (21%)
10-13	22% (18%)	15% (52%)	20% (16%)	43% (14%)

Table S4.12: Chemical climate datasheet summarising the impact of O_3 on Scots pine at Auchencorth.

Impact

Ozone impact on PINE

Critical levels for coniferous trees based on whole tree biomass reductions. Scots pine representative coniferous tree for 'atlantic central Europe' (LRTAP Convention, 2010).

Metric

Phytotoxic O_3 Dose above a flux threshold of Y nmol m^{-2} s^{-1} (POD_Y) calculates accumulated stomatal flux of O_3 into the plant across growing season (year round when daily mean temperature >0 °C).

Annual PODy 2007-2013. Theil Sen trend estimate is not statistically signiciant (p = 0.05)

Average annual PODy and % yield reduction for quartile groups

Year	POD_Y (mmol m^{-2})	Biomass reduction
2007	39.7	Response function not available for Scots pine.
2008	39.7	
2009	35.6	
2010	36.1	
2011	37.2	
2012	34.9	
2013	30.1	

Spatial domain

Auchencorth
EMEP level 2 Supersite,
lat: 55.792160
long: -3.242900

Representivity

Central/northern UK (Malley et al., 2014a)
AURN classification: Rural Background

Temporal Domain
O_3 statistics:
2007-2013
NO_x statistics:
2007-2013
(data from proxy site Bush)

State

Annual and monthly no. of POD_Y exceedance days

	Annual	3	4	5	6	7	8	9	10
2007	351	31	30	31	30	31	31	30	31
2008	330	25	30	31	30	31	31	30	30
2009	322	28	30	29	30	31	31	30	31
2010	317	31	30	31	30	31	31	30	31
2011	346	31	30	31	28	31	31	30	31
2012	345	31	30	31	30	29	31	30	31
2013	343	24	30	31	30	31	31	30	31

Monthly % contribution to POD_Y

	3	4	5	6	7	8	9	10
2007	7%	15%	15%	14%	14%	11%	9%	7%
2008	6%	12%	22%	17%	14%	10%	8%	5%
2009	8%	16%	17%	16%	14%	11%	8%	5%
2010	7%	15%	16%	17%	12%	12%	11%	6%
2011	7%	15%	18%	18%	15%	9%	10%	6%
2012	10%	11%	18%	18%	12%	13%	10%	5%
2013	4%	15%	20%	20%	7%	12%	8%	7%

Mean diurnal O_3 variation: POD_Y exceedance (non-exceedance) (ppb)

	3	4	5	6	7	8	9	10
2007	14.6 (-)	18.9 (-)	18.0 (-)	20.0 (-)	16.5 (-)	16.8 (-)	13.4 (-)	16.3 (-)
2008	15.9 (-)	19.3 (-)	23.8 (-)	18.4 (-)	18.9 (-)	15.7 (-)	16.0 (-)	11.8 (-)
2009	13.6 (-)	20.8 (-)	16.4 (-)	15.5 (-)	15.2 (-)	13.3 (-)	12.9 (-)	14.4 (-)
2010	18.6 (-)	18.8 (-)	20.0 (-)	20.1 (-)	14.2 (-)	15.6 (-)	16.8 (-)	13.5 (-)
2011	17.2 (-)	20.8 (-)	16.0 (-)	17.5 (8)	18.7 (-)	14.4 (-)	14.2 (-)	13.0 (-)
2012	16.2 (-)	14.9 (-)	19.2 (-)	16.7 (-)	15.1 (4)	17.3 (-)	12.8 (-)	16.5 (-)
2013	13.4 (8.6)	14.9 (-)	17.1 (-)	18.5 (-)	18.8 (-)	14.3 (-)	14.2 (-)	11.6 (-)

Mean diurnal NO variation: POD_Y exceedance (non-exceedance) (ppb)

	3	4	5	6	7	8	9	10
2007	3.2 (-)	5.3 (-)	3.2 (-)	5.6 (-)	3.1 (-)	3.3 (-)	2.0 (-)	5.1 (-)
2008	1.2 (-)	2.7 (-)	3.1 (-)	1.3 (-)	2.7 (-)	1.5 (-)	2.6 (-)	1.5 (-)
2009	2.1 (-)	3.2 (-)	0.7 (-)	2.0 (-)	0.6 (-)	1.5 (-)	1.8 (-)	4.7 (-)
2010	3.8 (-)	2.9 (-)	2.6 (-)	2.1 (-)	1.4 (-)	2.4 (-)	3.0 (-)	1.8 (-)
2011	3.4 (-)	2.9 (-)	1.5 (-)	1.6 (8.8)	2.2 (-)	2.6 (-)	1.6 (-)	1.3 (-)
2012	- (-)	0.9 (-)	2.6 (-)	1.2 (-)	1.9 (-)	1.1 (-)	1.4 (-)	4.3 (-)
2013	3.1 (1.3)	1.3 (-)	1.4 (-)	1.5 (-)	1.5 (-)	2.8 (-)	3.5 (-)	2.6 (-)

Mean diurnal NO_2 variation: POD_Y exceedance (non-exceedance) (ppb)

	3	4	5	6	7	8	9	10
2007	9.0 (-)	8.3 (-)	8.3 (-)	12.5 (-)	5.3 (-)	6.1 (-)	5.7 (-)	10.5 (-)
2008	6.0 (-)	9.7 (-)	10.8 (-)	5.5 (-)	6.5 (-)	5.8 (-)	7.7 (-)	7.0 (-)
2009	5.4 (-)	9.6 (-)	4.2 (-)	6.7 (-)	3.7 (-)	3.3 (-)	5.4 (-)	9.7 (-)
2010	11.3 (-)	8.4 (-)	7.8 (-)	6.6 (-)	3.8 (-)	6.3 (-)	7.6 (-)	6.8 (-)
2011	8.3 (-)	6.9 (-)	3.8 (-)	4.4 (22.8)	5.9 (-)	5.7 (-)	3.8 (-)	6.0 (-)
2012	- (-)	7.4 (-)	7.9 (-)	5.1 (-)	5.0 (0.5)	4.5 (-)	4.1 (-)	11.1 (-)
2013	11.4 (5.5)	7.2 (-)	6.5 (-)	5.5 (-)	5.7 (-)	5.9 (-)	7.0 (-)	8.2 (-)

Drivers

Meteorology: Av. Temp on exceedance (non-exceedance) days (°C)

	3	4	5	6	7	8	9	10
2007	6.3 (-)	10.1 (-)	10.2 (-)	12.7 (-)	14.0 (-)	14.1 (-)	12.6 (-)	10.6 (-)
2008	4.9 (-)	7.1 (-)	11.4 (-)	12.8 (-)	15.0 (-)	14.9 (-)	12.4 (-)	8.8 (-)
2009	6.5 (-)	9.1 (-)	10.9 (-)	13.0 (-)	15.1 (-)	15.5 (-)	13.2 (-)	10.7 (-)
2010	5.3 (-)	8.4 (-)	10.2 (-)	14.7 (-)	15.0 (-)	14.0 (-)	12.9 (-)	9.8 (-)
2011	6.1 (-)	10.3 (-)	10.9 (-)	12.3 (-)	14.2 (-)	13.7 (-)	13.5 (-)	11.2 (-)
2012	8.2 (-)	6.4 (-)	9.3 (-)	12.0 (-)	13.6 (11.0)	14.8 (-)	11.8 (-)	7.4 (-)
2013	2.7 (1.2)	6.6 (-)	10.1 (-)	13.2 (-)	16.8 (-)	15.3 (-)	12.6 (-)	11.2 (-)

Av. Global radiation on exceedance (non-exceedance) days (W m^{-2})

	3	4	5	6	7	8	9	10
2007	115 (-)	171 (-)	195 (-)	150 (-)	192 (-)	208 (-)	117 (-)	69 (-)
2008	97 (-)	139 (-)	192 (-)	202 (-)	168 (-)	122 (-)	94 (-)	65 (-)
2009	106 (-)	138 (-)	217 (-)	216 (-)	182 (-)	231 (-)	153 (-)	61 (-)
2010	89 (-)	212 (-)	277 (-)	299 (-)	234 (-)	215 (-)	156 (-)	79 (-)
2011	140 (-)	258 (-)	307 (-)	223 (-)	305 (-)	190 (-)	183 (-)	83 (-)
2012	158 (-)	194 (-)	291 (-)	252 (-)	230 (388)	232 (-)	178 (-)	96 (-)
2013	130 (42)	253 (-)	280 (-)	326 (-)	333 (-)	232 (-)	104 (-)	76 (-)

Emissions: Average hourly NO_x emissions along 96 hour back trajectory path arriving on POD_Y exceedance (non-exceedance) days (Mg)

	3	4	5	6	7	8	9	10
2007	9.6 (-)	15.3 (-)	9.7 (-)	19.9 (-)	11.2 (-)	7.8 (-)	5.7 (-)	29.9 (-)
2008	8.2 (-)	13.6 (-)	20.4 (-)	11.6 (-)	18.1 (-)	15.7 (-)	23.0 (-)	7.7 (-)
2009	9.2 (-)	23.9 (-)	8.1 (-)	10.1 (-)	13.5 (-)	7.2 (-)	7.0 (-)	25.1 (-)
2010	17.5 (-)	13.6 (-)	8.0 (-)	13.5 (-)	7.6 (-)	6.2 (-)	13.7 (-)	11.1 (-)
2011	17.8 (-)	12.8 (-)	13.4 (-)	11.9 (-)	13.1 (-)	17.5 (-)	13.5 (-)	18.7 (-)
2012	18.4 (-)	11.7 (-)	10.4 (-)	13.9 (-)	9.4 (8.7)	14.5 (-)	5.5 (-)	12.2 (-)
2013	14.0 (-)	7.0 (-)	8.4 (-)	9.9 (-)	10.5 (-)	10.2 (-)	7.6 (-)	12.8 (-)

Air Mass origin: Percentage of trajectories from 4 geographical groupings on exceedance (non-exceedance) days

	Northerly	Easterly	Southerly	Westerly
2007	25% (13%)	16% (58%)	12% (8%)	47% (21%)
2008	19% (22%)	19% (23%)	8% (14%)	53% (42%)
2009	19% (23%)	20% (36%)	25% (21%)	37% (19%)
2010	22% (24%)	19% (59%)	37% (7%)	22% (11%)
2011	18% (24%)	13% (10%)	43% (35%)	26% (31%)
2012	19% (26%)	16% (53%)	29% (9%)	35% (12%)
2013	20% (12%)	20% (74%)	30% (10%)	30% (5%)

Appendix II: Publication

This appendix contains the peer-review publication which in part formed the basis for Chapter 2.

Malley, C. S., Braban, C. F., & Heal, M. R. (2014). New Directions: Chemical climatology and assessment of atmospheric composition impacts. *Atmospheric Environment, 87*, 261-264. 10.1016/j.atmosenv.2014.01.027.

Atmospheric Environment 87 (2014) 261–264

Contents lists available at ScienceDirect

Atmospheric Environment

journal homepage: www.elsevier.com/locate/atmosenv

New Directions: Chemical climatology and assessment of atmospheric composition impacts☆

Many atmospheric composition studies measure or model the concentration of *X* at place *Y* at time *t*, but fewer studies synthesise these measurements in the context of the full chemical environment and specific impacts. In contrast, the first systematic study of air pollution, by Victorian chemist Robert Angus Smith (1817–1884), had this explicit aim. From his experiences with the Health of Towns Commission and as Chief Inspector of the Alkali Act (1863), Angus Smith investigated the link between atmospheric composition and human health impacts in urban areas. In his 1872 book *'Air and Rain: The beginnings of a chemical climatology'*, not only did Angus Smith coin the phrase 'chemical climatology', but he utilised methodologies recognisable today including monitoring networks with site classification, the analysis of temporal trends, and basic source apportionment (Angus Smith, 1872). Perhaps the most important legacy was his philosophy of seeking to link the atmospheric state to both causal factors and to pollution impacts. Subsequently, the term chemical climatology was used only sporadically. Recently, however, published literature containing phrases such as 'chemical climatology', 'aerosol climatology' and 'ozone climatology' have increased, but with widely varying context.

We propose that an impact-centred approach to defining chemical climatology, based on the legacy of Angus Smith, would be beneficial to establishing both relevant linkages between impacts and their drivers, and consistent syntheses of atmospheric composition studies for the research community and policy makers. To achieve this, we propose a framework that defines any climate (chemical, or otherwise, for example meteorological or political) as consisting of three elements –the **'impact'**, the **'state'** and the **'drivers'**, contained within specified spatial and temporal boundaries (Fig. 1, Table 1). It is noted that some studies do fulfil the chemical climatology framework laid out here (e.g. Derwent et al., 2013). This framework is consistent with modern interpretations of a meteorological climate. For example Bryson (1997) defined meteorological climate as *'the thermodynamic/hydrodynamic status of the global boundary conditions that determine the current array of weather patterns'*. In this definition a climate 'state' determines the possible weather patterns (impacts) and is itself produced by drivers e.g. solar variability.

In the atmospheric chemical climatology context:

- **Impact** is an identified effect or metric of atmospheric composition, for which it is sought to determine the underlying contributing sources and processes. Different impacts (e.g. different metrics of the same component or of different components) are associated with different chemical climates.
- **State** is the description of the 'what', 'when' and 'where' of atmospheric composition producing the identified impact. This includes consideration of atmospheric constituents and their temporal and spatial variations relevant to the impact (metric), for example diurnal, annual, peak over threshold, etc. An individual chemical climate contains one state, incorporating all relevant variation.
- **Drivers** are the sources and influences on the atmospheric composition that determine the state, and hence the impact (metric). Assessment of the relative importance of each driver should explain 'why' and 'how' the composition variation detailed in the state occurs, and hence identify the dominant processes in producing instances of the impact.

The chemical climatology framework can be applied to measured or modelled data. The chemical climate is the holistic characterisation within clearly demarcated boundaries in space and time. Further, the concept of a 'phase' of a chemical climate (Fig. 1) demarcates significant change in the drivers and state leading to significant change in the impact (metric). Phases may be identified through the segmentation of the temporal or spatial domain of a chemical climate derived using all available data, or by merging climates derived separately for a given impact over smaller temporal or spatial domains into a single climate of separate phases.

Six practical steps to define a chemical climate are summarised in Table 1, and an example template for its presentation is shown in Table 2. Step 1 identifies the impact; for example, studies link acute exposure to elevated ozone concentrations and respiratory conditions (WHO, 2006). Step 2 defines the relevant metric; e.g. maximum daily 8-h average concentration above 70 μg m^{-3}, which is associated with a statistically significant increase in mortality (Amann et al., 2008). Step 3 defines the temporal and spatial boundaries to the dataset. Step 4 is the description of the state. This involves relevant temporal and spatial patterns of ozone variation above 70 μg m^{-3}, e.g. diurnal and seasonal variation, and covariance with precursor molecules. Step 5 identifies drivers, for example the relative importance of local, regional and hemispheric transport, and source activities emitting ozone precursors.

☆ Something to say? Comments on this article, or suggestions for other topics, are welcome. Please contact: new.directions@uea.ac.uk, or go to atmos_env@uea.ac.uk http://www.elsevier.com/wps/find/journaldescription.cws_home/246/authorinstructionsfor further details.

1352-2310/$ – see front matter
http://dx.doi.org/10.1016/j.atmosenv.2014.01.027

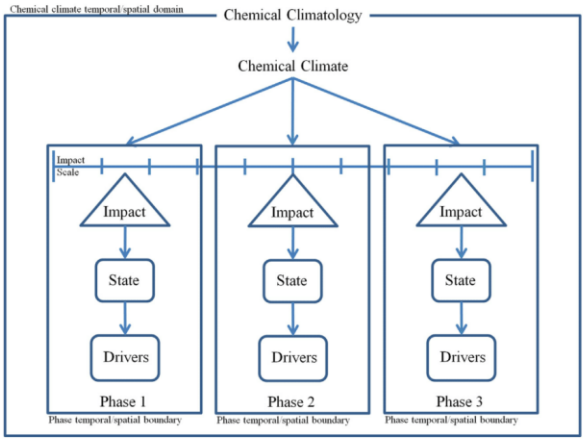

Fig. 1. An illustration of the chemical climatology framework. For a particular chemical climate description, only a single phase might be identified.

Step 6 assesses the presence of different phases within the chemical climate e.g. significantly different patterns of ozone metric exceedance in different regions, or significant changes to ozone precursor emissions over time. Different phases may be identified during steps 2–5 or through independent application of steps 2–5 for different spatial/temporal domains, followed by collation into a single chemical climate. Were a different impact being investigated, for example the ozone impact on vegetation (assessed by a cumulative deposition flux over a season), the state and drivers would be different, and a separate chemical climate would be derived.

Table 1 highlights the chemical climatology steps covered by four illustrative studies concerning ground-level ozone. Derwent et al. (2013) is a good recent example of a study featuring full chemical climates assessing the contribution of a driver (hemispheric baseline ozone concentrations) to different ozone impacts (vegetation and human health). Three examples of the majority of studies which assess a subset of the steps are also included in Table 1. WHO (2006) assess the health impact of ozone and define a relevant metric (steps 1 and 2), but do not evaluate the state and drivers of ozone variation in particular locations; Malley et al. (2014) describe changes in ozone variation at rural sites across Europe (steps 3 and 4), but do not link to ozone impacts or causal drivers; Gerasopoulos et al. (2006) assess the state and drivers of ozone variation at Finokalia, Crete (steps 4 and 5), but do not link this variation to ozone impacts, nor evaluate the temporal and spatial representativeness of ozone variation at the location. Covering a subset of the chemical climatology steps is not a shortcoming of studies, and neither should every investigation aim to cover every step in the chemical climatology framework. However, increased awareness of the steps within the framework covered by isolated studies means that they can be combined to produce full impact-led chemical climate assessments focussing on relevant local, regional and global scale issues. This would better facilitate consideration of impact mitigation strategy development where needed. A standard output from chemical climate studies (Table 2) summarises the statistical features of the chemical climate, as well as the temporal and spatial boundaries and scientific uncertainties. This could allow collation and linkage between chemical climates.

Table 1
Chemical climatology framework: component steps and a few example studies identifying which component steps were described.

Step	Description	Example chemical climatology	Example studies			
		Ozone	Gerasopoulos et al. (2006)	WHO (2006)	Derwent et al. (2013)	Malley et al. (2014)
1	Identify **impact**	Human health; Vegetation damage		✓	✓	
2	Define relevant chemical climate metric(s) for the **impact**	Sum of means over 35 ppb (SOMO35); Accumulated ozone over 40 ppb (AOT40)		✓	✓	
3	Define the chemical climate's temporal and spatial boundaries	Representivity of time period and location			✓	✓
4	Describe the chemical climate **state**	Statistical analysis of measured/modelled dataset	✓		✓	✓
5	Identify the chemical climate **driver(s)**	Relative contribution of meteorology, source apportionment, atmospheric chemistry	✓		✓	
6	Assess for phases within the chemical climate	Significant temporal/spatial changes in impact severity			✓	

Table 2
Chemical climate datasheet template. The example is for the human health impact of ozone at Harwell, a monitoring site in south east England.

Impact	Spatial domain	Drivers	State	Key uncertainties
Ozone human health impact Respiratory effects: Increased mortality, decreased lung function, coughing, throat irritation, shortness of breath, inflammation of airways, increased asthma attacks, (WHO, 2006). World Health Organization (WHO) 8-hour daily max ozone concentration above which there is a significant increased mortality risk: 35 ppb (Amann et al., 2008). Severity of exceedance characterised by SOMO35 metric: Sum of daily max 8-hour mean ozone concentration in excess of 35 ppb.	**Harwell:** EMEP level II Supersite, lat: 51.571078 long: -1.325283 **Temporal Domain**	**Representivity** S and SE UK (Malley et al., 2014) AURN classification: Rural Background **Phases**	**Meteorology** **Temperature** **Prevailing Wind Direction** **Atmospheric chemistry** **Air transport patterns (back trajectories grouped using hierarchical cluster analysis):** **Hemispheric/Regional/Local influences:** **Source proximity:** Data source: EU27 NO_x emissions (Gg) UK NO_x emissions (% EU27) EU27 VOC emissions (Gg) UK VOC emissions (% EU27) **Major sources: NO_x** **Major sources: VOCs**	**1990-1995** **1996-2001** **2002-2006** **2007-2011**	**Data source:** **Ozone Variation** Mean | 3rd Quartile | Max No. exceedances | SOMO35 **% exceedances by season** Spring | Summer | Autumn | Winter 07-11 02-06 96-01 90-95 **% SOMO35 by season** Spring | Summer | Autumn | Winter 07-11 02-06 96-01 90-95 **Diurnal ozone cycle** Non-exceedance | Exceedance 07-11 02-06 96-01 90-95 **Covariance with NO_x (mean NO_x during ozone exceedance/non-exceedance (ppb))** NO non-ex | NO ex | NO_2 non-ex | NO_2 ex 07-11 02-06 96-01	

Acknowledgements

C.S. Malley acknowledges the University of Edinburgh School of Chemistry, the NERC Centre for Ecology & Hydrology (CEH) and the UK Department for Environment, Food and Rural Affairs (Defra) for funding.

References

Amann, M., Derwent, D., Forsberg, B., Hanninen, O., Hurley, F., Krzyzanowski, M., de Leeuw, F., Liu, S., Mandin, C., Schneider, J., Schwarze, P., Simpson, D., 2008. World Health Organization: Health Risks of Ozone from Long-range Transboundary Air Pollution. WHO Regional Office for Europe. http://www.euro.who.int/__data/assets/pdf_file/0005/78647/E91843.pdf.

Angus Smith, R., 1872. Air and Rain: the Beginnings of a Chemical Climatology. Longmans, Green and Co., London.

Bryson, R.A., 1997. The paradigm of climatology: an essay. Bull. Am. Meteorol. Soc. 78, 449–455.

Derwent, R., Manning, A., Simmonds, P., Gerard Spain, T., O'Doherty, S., 2013. Analysis and interpretation of 25 years of ozone observations at the Mace Head Atmospheric Research Station on the Atlantic Ocean coast of Ireland from 1987 to 2012. Atmos. Environ. 80, 361–368.

Gerasopoulos, E., Kouvarakis, G., Vrekoussis, M., Donoussis, C., Mihalopoulos, N., Kanakidou, M., 2006. Photochemical ozone production in the eastern Mediterranean. Atmos. Environ. 40, 3057–3069.

Malley, C.S., Braban, C.F., Heal, M.R., 2014. The application of hierarchical cluster analysis and non-negative matrix factorization to European atmospheric monitoring site classification. Atmos. Res. 138, 30–40.

WHO, 2006. Air Quality Guidelines. Global Update 2005. Particulate Matter, Ozone, Nitrogen Dioxide and Sulfur Dioxide. World Health Organisation Regional Office for Europe, Copenhagen, ISBN 92 890 2192 6. http://whqlibdoc.who.int/hq/2006/WHO_SDE_PHE_OEH_06.02_eng.pdf.

Christopher S. Malley*
NERC Centre for Ecology & Hydrology, Bush Estate, Penicuik EH26 0QB, UK

School of Chemistry, University of Edinburgh, West Mains Road, Edinburgh EH9 3JJ, UK

Christine F. Braban
NERC Centre for Ecology & Hydrology, Bush Estate, Penicuik EH26 0QB, UK

Mathew R. Heal
School of Chemistry, University of Edinburgh, West Mains Road, Edinburgh EH9 3JJ, UK

* Corresponding author. School of Chemistry, University of Edinburgh, West Mains Road, Edinburgh EH9 3JJ, UK. Tel.: +44 7578 725402.
E-mail address: C.Malley@sms.ed.ac.uk (C.S. Malley).

12 September 2013
Available online 22 January 2014

Appendix III: Publication

This appendix contains the peer-review publication which formed the basis for Chapter 3.

Malley, C. S., Braban, C. F., & Heal, M. R. (2014). The application of hierarchical cluster analysis and non-negative matrix factorization to European atmospheric monitoring site classification. *Atmospheric research*, *138*, 30-40. 10.1016/j.atmosres.2013.10.019.

Atmospheric Research 138 (2014) 30–40

Contents lists available at ScienceDirect

Atmospheric Research

journal homepage: www.elsevier.com/locate/atmos

The application of hierarchical cluster analysis and non-negative matrix factorization to European atmospheric monitoring site classification

Christopher S. Malley [a,b,*], Christine F. Braban [a], Mathew R. Heal [b]

[a] NERC, Centre for Ecology & Hydrology, Bush Estate, Penicuik EH26 0QB, UK
[b] School of Chemistry, University of Edinburgh, West Mains Road, Edinburgh EH9 3JJ, UK

ARTICLE INFO

Article history:
Received 25 July 2013
Received in revised form 22 October 2013
Accepted 28 October 2013

Keywords:
Ozone
EMEP monitoring sites
Cluster analysis
Non-negative matrix factorisation

ABSTRACT

The effective classification of atmospheric monitoring sites within a network allows conclusions from measurements to be extrapolated beyond the confines of the site itself and applied to larger areas or populations. This is especially important for the European EMEP 'supersites' because these are relatively few in number yet are subject to much investment in composition monitoring capability. Here, the representativeness of the two UK EMEP supersites, Auchencorth and Harwell, was evaluated using the hierarchical cluster analysis (HCA) of all available EMEP monitoring sites based on measured ozone concentration datasets for the period 1991–2010. A novel feature was to apply non-negative matrix factorization (NMF) to order the sites within the HCA dendrograms according to the relative anthropogenic influence on ozone. The ordered dendrograms enabled UK sites to be placed more precisely in a European context. For 2007–2010, all 19 UK EMEP sites were assigned to two of the site classification clusters, with 17 of the sites grouping closely with each other in each cluster. Auchencorth clustered with the sites characterised by less modification of hemispheric background ozone levels, whilst Harwell grouped with the sites showing a more polluted regime. A similar grouping of sites occurred between 1991 and 2010, with relatively closer clustering of Polluted UK sites compared with Remote UK sites due to the larger, transboundary spatial domain for which the Remote UK sites are representative. This tight clustering of the majority of the other UK ozone monitoring sites with either one of the supersites, shows that UK background ozone conditions are well represented by Auchencorth and Harwell, and gives confidence that more extensive chemical climatologies developed for the two supersites will have wider geographical relevance.

1. Introduction

The European Monitoring and Evaluation Programme (EMEP, www.emep.int) provides governments with scientific information to inform policy regarding the long-range, transboundary transport of air pollution (Torseth et al., 2012). The programme has three core strands: collation of atmospheric emissions inventories; modelling of atmospheric transport and deposition; and measurement of atmospheric composition at locations where the impact of local pollutant emission sources should be low. The EMEP guidance (EMEP/CCC-Report 1/95) outlines methods intended to ensure that air sampled at a monitoring site is representative of air not directly affected by local emission sources. These include: 50 km from major pollution sources (towns, power plants, etc.), 2 km from the application of manure, and consideration of meteorological and topographical features. EMEP Level I sites are designed to capture basic atmospheric composition, whilst Level II and III sites (often referred to as EMEP supersites) measure a wider range of atmospheric constituents at higher time resolution than Level I (see Torseth et al. (2012)).

Monitoring sites in a network are usually classified into different groups that internally share similar chemical climatologies, i.e. similar atmospheric composition, drivers of that

* Corresponding author at: School of Chemistry, University of Edinburgh, West Mains Road, Edinburgh EH9 3JJ, UK. Tel.: +44 7578 725402.
E-mail address: C.Malley@sms.ed.ac.uk (C.S. Malley).

0169-8095/$ – see front matter © 2013 Elsevier B.V. All rights reserved.
http://dx.doi.org/10.1016/j.atmosres.2013.10.019

composition, and impacts due to that composition. A balance is required which captures the major variations in composition and drivers across the network but in as few groups as possible so as to retain the ability to generalise. Various grouping methodologies have been applied (Joly and Peuch, 2012). These range from the relatively subjective use of metadata (Spangl et al., 2007), traditionally used in monitoring networks, to more objective techniques such as rankings based on statistical indicators (Kovac-Andric et al., 2010), linear discriminant analysis (Joly and Peuch, 2012), principal component analysis (Lau et al., 2009), and non-hierarchical (Ignaccolo et al., 2008) and hierarchical cluster analyses (Flemming et al., 2005; Henne et al., 2010; Tarasova et al., 2007). The latter is a multivariate approach that encompasses many separation/agglomeration techniques which aims to identify natural groupings, or clusters, amongst objects in a dataset through minimisation of the within-cluster variance and maximisation of the between-cluster variance (Kaufman and Rousseeuw, 1990). Clustering methods require user-defined parameters which may impact the objectivity of the analysis. For example, a method for calculating 'distance' between individual members needs to be specified (Dabboor et al., 2013), as must a method for calculating the separation between different groups of members (Mangiameli et al., 1996). Nevertheless, as cited above, clustering techniques have been widely applied to grouping atmospheric monitoring sites.

The aim of this study was to assess whether the locations of the two Level II UK supersites, at Auchencorth in south-east Scotland and Harwell in southern England, are representative of UK background conditions, even though they do not fully meet the EMEP criteria for non-locally influenced "background" sites (this is the case at other EMEP sites, as acknowledged in Torseth et al. (2012)): Auchencorth is located 17 km from Edinburgh, although prevailing winds mean that it is predominantly upwind from the city, whilst Harwell is 7 km from a 1360 MW natural gas power station. Effective site classification is particularly important for EMEP Level II 'supersites' because these are considerably few in number yet subject to much investment in composition monitoring capability.

In this work, sites across the EMEP domain were classified according to the annual and daily patterns in ground-level ozone concentrations. Ozone was chosen for two reasons. First, it is the most widely measured constituent across the EMEP network — between 2007 and 2010, 113 sites measured hourly ozone concentrations and 49 sites have continuous ozone time series since 1991. Second, measured ozone concentrations are a result of the combination of a wide variety of drivers which are also relevant to many aspects of atmospheric composition, including precursor emissions, photochemistry, deposition, meteorological and climatic conditions and long-range transport (AQEG, 2009; Royal Society, 2008). A major driver of temporal ozone variation is hemispheric background concentrations (AQEG, 2009). Regional and local-scale processes lead to modification of these values. Under suitable conditions, efficient photochemical processing of NO_x and volatile organic compounds (VOCs) lead to additional ozone formation and high ozone episodes, whilst local-scale depletion of ozone occurs due to reaction with NO, an effect which increases with higher NO concentrations (Jenkin, 2008).

Hierarchical clustering was applied to the monthly-diurnal ozone concentrations (average diurnal cycle for each month of the year) at each EMEP site over 4-year periods. Although hierarchical clustering has been applied previously to monitoring site classification (Tarasova et al., 2007), the novelty here was the subsequent application of non-negative matrix factorisation (NMF) (Lee and Seung, 2001) to order the sites across the dendrogram according to an extracted factor. In this case, the factor represented the extent of anthropogenic influence on ozone concentrations. Hierarchical cluster analysis was chosen in preference to non-hierarchical techniques as the robustness and suitability of the cluster assignment are more objectively investigated through the resulting dendrogram, particularly when this is combined with NMF. By using NMF, the ozone concentrations at the two UK EMEP supersites were placed more precisely in the European context. The analysis was carried out separately for five 4-year periods spanning 1991–2010 to assess the consistency of site representativeness over time.

2. Methodology

Data arrays of 4-year averaged monthly-diurnal ozone concentrations were calculated for each EMEP site, i.e. 288 (=24 h × 12 months) ozone concentrations per site where, for example, the ozone concentration for 'Jan-00.00' was the average of the 00.00–01.00 hourly ozone on all days in January in the 4-year period under consideration (1991–1994, 1995–1998, 1999–2002, 2003–2006 and 2007–2010) (measured data from http://ebas.nilu.no). Four-year averages of monthly-diurnal concentrations were considered a reasonable compromise between long enough to smooth out inter-annual variability and short enough to avoid incorporation of long term trends. The number of sites included in each time period and the number of countries within which these sites are located are summarised in Table 1. 154 sites contributed ozone data to at least one 4-year period, of which 49 contributed to every 4-year time period.

The choice of clustering parameters can impact the clustering result. In this study, the standard Euclidean distance between two n-dimensional data arrays was used and in this case $n = 288$ (Eq. (1)).

$$d(x,y) = \sqrt{\sum_{i=1}^{n}(x_i - y_i)^2} \quad (1)$$

In hierarchical clustering, each object (here each site's monthly-diurnal ozone concentrations) initially constitutes its own cluster. The two nearest clusters are then combined

Table 1
Number of sites used in cluster analysis for each four year period. The increasing number of countries with sites indicates the increasing geographical coverage across Europe with time. 49 sites are common to all time periods.

Time period	No. of sites	No. of countries
1991–1994	76	14
1995–1998	100	20
1999–2002	117	27
2003–2006	117	27
2007–2010	113	26

and this process is continued until there is one cluster containing all objects. The process of agglomeration is summarised in a dendrogram. Hierarchical clustering techniques differ in how the separation of clusters is quantified, and hence how the linkages of the dendrogram are constructed. A number of linkage methods can be applied, e.g. single, complete, average or centroid linkage, or Ward's method (Kaufman and Rousseeuw, 1990). Mangiameli et al. (1996) applied these linkage methods to model datasets of known cluster assignments to assess their effectiveness under a range of conditions, e.g. with dispersed datasets and large disparities in cluster density. In general, Ward's method resulted in a higher percentage of objects assigned to their correct cluster. Ward's method has also been used previously with pollutant concentration data (e.g. Dillner et al. (2005) and Lu et al. (2006)) and was chosen here. At each step, Ward's method calculates the within-cluster sum of squares (WCSS) for every cluster (Kaufman and Rousseeuw, 1990; Ward, 1963), where WCSS is the squared Euclidean distance between an object in the cluster (x_j) and the mean of that cluster ($\bar{x}$), summed over all (m) objects in that cluster (Eq. (2)).

$$\mathrm{WCSS} = \sum_{j=1}^{m} \left(x_j - \bar{x}\right)^2 \tag{2}$$

The two clusters, merged at that step, are those which after merging produce the smallest increase in the sum of WCSS over all clusters.

The branches of the dendrogram are rotatable, allowing the members to be weighted and reordered according to those weightings within the confines of the dendrogram branches. Here, non-negative matrix factorisation (NMF) was used to reorder the monitoring sites based on the range of monthly-diurnal ozone profiles observed across Europe. The 288 ozone concentrations for all monitoring sites are combined into a $n \times m$ matrix, **V**, where n is the number of dimensions (288), and m is the number of monitoring sites (113 for 2007–2010). NMF decomposes **V** into two output matrices, an $n \times r$ matrix, **W**, and an $r \times m$ matrix, **H**, whose product **WH** approximates the input matrix **V** (Fig. 1). This approximation is achieved such that the Euclidean distance between the input matrix and output matrix product (i.e. $(\mathbf{V} - \mathbf{WH})^2$) is minimised. Variable r is the number of factors with which to simplify **V**, **H** contains the contribution of each factor at each monitoring site, and **W** details the composition of each factor (Lee and Seung, 1999). Although a locally minimised Euclidean distance between **V** and **WH** resulted from the NMF algorithm, and therefore **W** and **H** varied between runs, this did not cause significant variation in dendrogram reordering results (Lee and Seung, 2001).

Two factors were used in the NMF here; hence **W** described two ozone monthly-diurnal cycles (visualised in Fig. 2), from which the monthly-diurnal cycle at each site is reconstructed by considering the contribution of each from **H**. The appearance of the monthly-diurnal cycle of Factor 1 is consistent with an air mass significantly influenced by anthropogenic emissions of ozone precursor/depleting species. It features pronounced diurnal (max ~40 μg m^{-3}) and annual (max ~40 μg m^{-3}) ozone variation, and a summer maximum in ozone concentration, consistent with regional-scale ozone production, as shown in Jenkin (2008). Factor 2 exhibits greater uniformity in ozone concentrations. The choice of two factors was semi-arbitrary, but allows an estimation of the anthropogenic influence at each site to be encapsulated via the contribution from a single factor (Factor 1). Each site was weighted with this contribution, and at each node in the dendrogram, where two branches meet, the mean weight of sites on each branch was calculated. The branch with the higher value was placed on the right hand side of the node, producing a dendrogram reordered based on each site's relative pollution levels.

The hierarchical cluster analysis, NMF and map plotting were undertaken with the R statistical software (R Core Development Team, 2008), using respectively the 'NMFN' (Liu, 2012), 'cluster' (Maechler et al., 2013) and 'openair' (Carslaw and Ropkins, 2013) packages.

3. Results

Fig. 3 shows the dendrogram for the EMEP sites recording ozone data for the period 2007–2010. The progression of the average monthly-diurnal ozone cycles across the dendrogram is shown across the bottom of the diagram for selected sites, and illustrates the dramatic change in characteristics of these cycles. Fig. 4 shows the proportion of explained within-cluster variance as a function of the number of clusters, and ranges from 100% when all sites were located in individual clusters to zero when all sites were located in one cluster. In selecting the optimal number of clusters, the aim is to

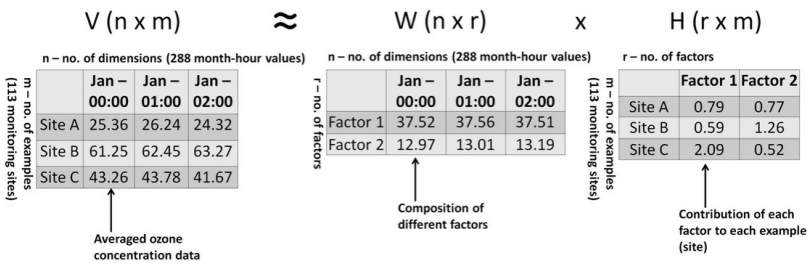

Fig. 1. Illustration of the process of non-negative factorization as applied to the ozone data in this work.

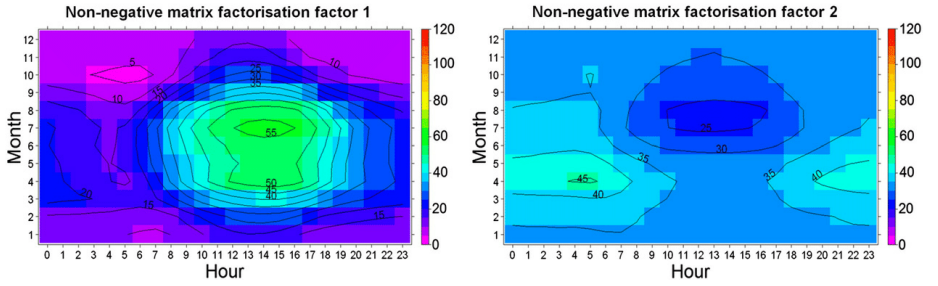

Fig. 2. Average ozone monthly-diurnal cycles of two factors produced during non-negative matrix factorisation of data for 2007–2010. Concentrations are μg m^{-3}.

maximise the explained inter-site ozone variability using a small number of clusters, allowing key features of ozone variation across Europe to be summarised. The statistics in Fig. 4 clearly show that decreasing from 113 to 4 clusters yields relatively small decreases in explained variance (four clusters still explains 75% of within cluster variance) but that a further decrease in cluster number results in substantial disbenefit to explained variance. The natural break into four clusters is also clearly evident in the dendrogram of Fig. 3. These four clusters were designated as Remote, Polluted, Elevated and Mountain going from left to right across the dendrogram. The average monthly-diurnal cycles and locations of sites in each cluster are shown in Figs. 5 and 6 respectively.

The Remote cluster's average monthly-diurnal cycle comprised an annual maximum in April (~85 μg m^{-3}) and a diurnal maximum during the early afternoon (Fig. 5). However, diurnal and annual variations in ozone concentrations were not large. The minimum ozone concentration was ~44 μg m^{-3} and maximum amplitudes in diurnal and annual ozone variation were 23 and 37 μg m^{-3} respectively. The majority of the sites in the Remote cluster are on the north and west fringes of Europe, predominantly in Scandinavia and the UK (Fig. 6). In comparison, the Polluted cluster contained significantly more ozone concentration variation. Maximum average ozone concentrations (96 μg m^{-3}) occurred in April and elevated afternoon concentrations persisted through summer before decreasing in August and September. Maximum amplitudes in diurnal and annual ozone variation of 49 and 59 μg m^{-3}, respectively, produced the lowest concentrations across all clusters (minimum concentration: 27 μg m^{-3}). Sites contributing to this cluster were predominantly in central and southern Europe, including central and eastern England (Fig. 6). The majority of sites in the Elevated and Mountain clusters are located at altitude. The Mountain cluster contained a greater proportion of mountain-top sites, as opposed to the mix of mountain-top, mountain-side and valley sites found in the Elevated cluster. Diurnal ozone variation was considerably lower in these two clusters than in the Remote and Polluted clusters (maximum amplitude of Mountain cluster diurnal cycle = 5 μg m^{-3}), and the Mountain cluster showed highest ozone concentrations (maximum 119 μg m^{-3}). The average ozone monthly-diurnal cycle of the Elevated cluster had similar features to that of the Mountain cluster, but with lower concentrations and greater annual/diurnal ozone variation. These statistics summarise variation for the period 2007–2010; however, due to numerous factors, including long-term trends and inter-annual variability, these values vary for the other four time periods spanning 1990–2006.

Though the four major clusters explained 75% of the variability in monthly-diurnal ozone variation between EMEP sites for 2007–2010, application of NMF dendrogram reordering allowed the remaining 25% to be investigated. From left to right in Fig. 3 sites within each cluster are ordered according to increasing anthropogenic influence. All 19 UK EMEP sites (which are highlighted in Fig. 3 and shown geographically in Fig. 7) were apportioned to the Remote and Polluted clusters. Of these, 17 sites grouped closely with each other within the two clusters (Fig. 3). The two exceptions were Lerwick and Weybourne. Lerwick, on the Shetland Islands, is much further north and double the distance from a city than any other UK site and was ordered in the dendrogram as considerably more remote than other UK sites in the Remote cluster, i.e. significantly less anthropogenically influenced. Weybourne, on England's east coast, was clustered midway between the two groupings of UK sites, suggesting the site experienced both types of ozone regimes. The Auchencorth EMEP supersite was in the middle of the grouping of twelve UK sites within the Remote cluster, whilst the Harwell supersite grouped with the five UK sites in the Polluted cluster, and was the least anthropogenically influenced of this grouping (Fig. 3). It is a highly relevant result that the cluster analysis showed two dominant ozone regimes in the UK and each was well represented by one of the two UK EMEP supersites.

For the other four 4-year periods spanning 1991–2006, sites were included in the clustering if monitor data was available for the 4-year period under consideration. The number of clusters produced for each 4-year time period were not fully consistent. The periods 2007–2010 and 1999–2002 yielded a Remote, Polluted, Elevated, Mountain cluster set. For 2003–2006, the nine least anthropogenically-influenced Remote cluster sites formed an additional, distinct cluster. For 1995–1998, four clusters were produced, but three of these groups were of non-elevated sites, with Mountain and Elevated sites combined into one cluster. For 1991–1994 there were only three clusters: a Remote, Polluted and combined Mountain and Elevated cluster.

The Harwell EMEP supersite was consistently amongst the least anthropogenically-influenced sites of the Polluted

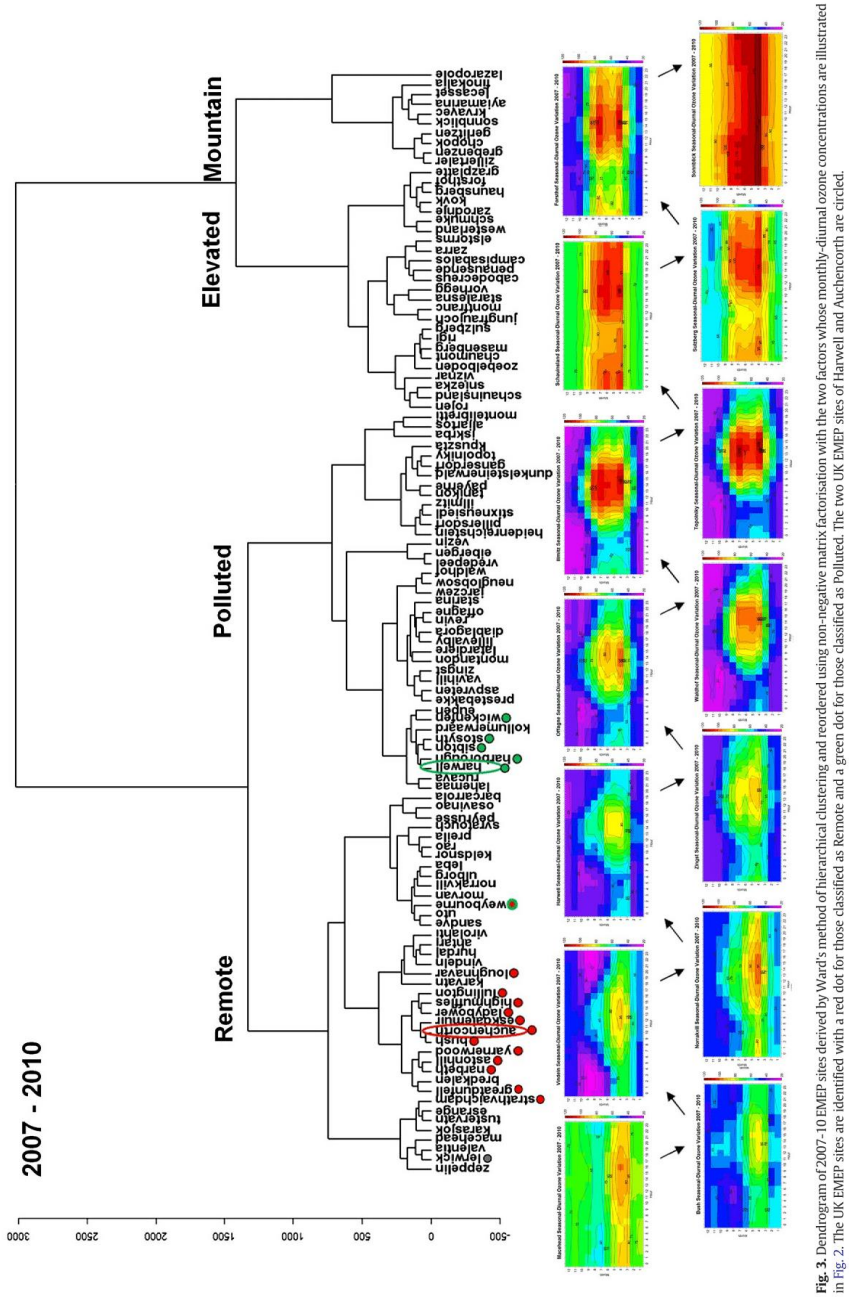

Fig. 3. Dendrogram of 2007–10 EMEP sites derived by Ward's method of hierarchical clustering and reordered using non-negative matrix factorisation with the two factors whose monthly-diurnal ozone concentrations are illustrated in Fig. 2. The UK EMEP sites are identified with a red dot for those classified as Remote and a green dot for those classified as Polluted. The two UK EMEP sites of Harwell and Auchencorth are circled.

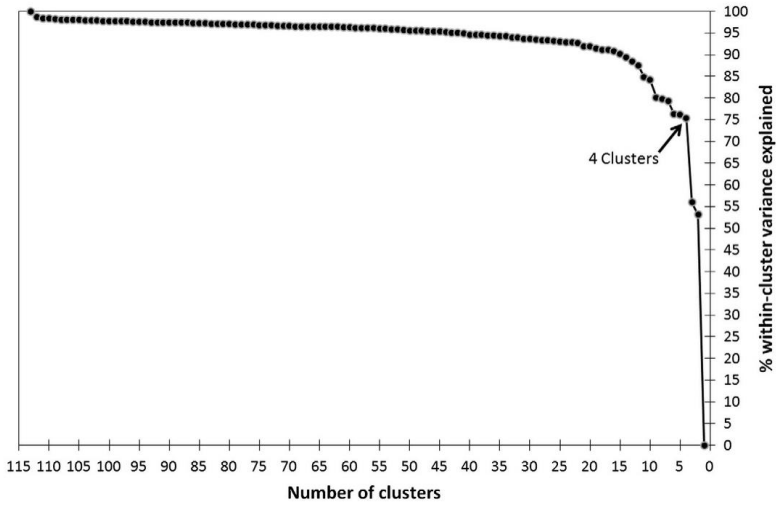

Fig. 4. The proportion of within-cluster variance explained as a function of number of clusters (2007–2010 dataset).

cluster in every 4-year period except 2003–2006 (see Fig. 3 for 2007–2010). For 2003–2006, the clustering assigned Harwell to the Remote cluster. This shift in classification also occurred for the four other UK sites which clustered tightly with Harwell in 2007–2010 (Market Harborough, Sibton, St Osyth and Wicken Fen). This indicated a change in this UK ozone regime, relative to ozone variation across Europe. This regime, for which Harwell was representative, was characterised by greater diurnal and annual ozone variation than the rest of the UK, and its spatial domain

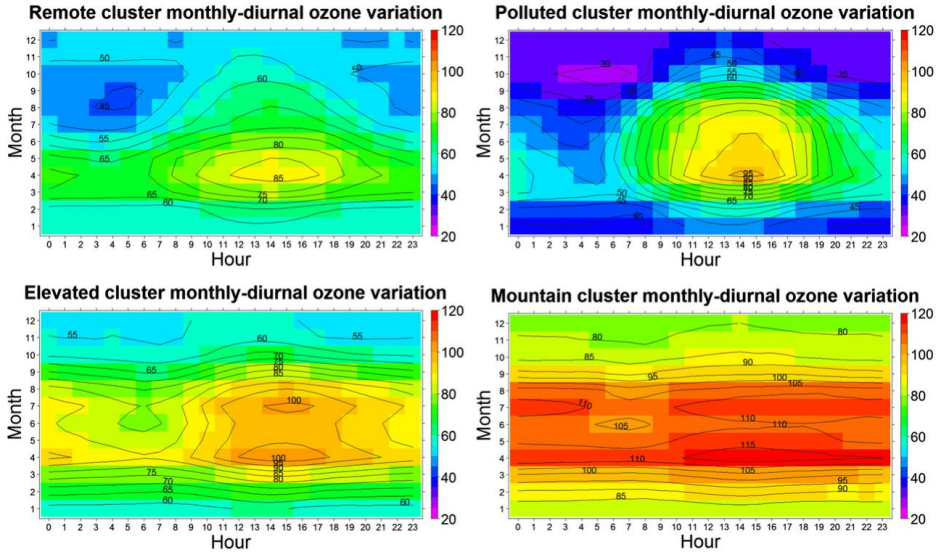

Fig. 5. Average ozone monthly-diurnal cycle for the four clusters assigned for 2007–2010. Concentrations are μg m^{-3}.

encompassed sites within 120 km of London. In a European context, however, this regime was not the most anthropogenically influenced.

Data submission to EMEP for Auchencorth commenced in 2006, so ozone concentrations from a neighbouring site at Bush, only 8 km from Auchencorth, were used as a proxy for Auchencorth prior to 2006. Whilst small changes to the state and drivers of atmospheric composition can result in relatively large changes in ozone variation, both sites are south of Edinburgh and similarly influenced by local and regional-scale meteorology. In 2011, hourly wind direction between the two sites differed by more than 45° only 3% of the time. For the period 2007–2010, Auchencorth and Bush grouped immediately adjacent in the dendrogram (Fig. 3), and the mean difference in hourly ozone concentrations was 6.48 μg m^{-3}. Bush maintained a consistent assignment across the 20-year period, grouping immediately after sites including Zeppelin (on the Arctic island of Svalbard), Mace Head (on the west coast of Ireland), and other more Remote sites. However, the other Remote UK sites exhibited greater variability in their position relative to Bush with time than was the case for the other UK Polluted sites relative to Harwell. For example, in

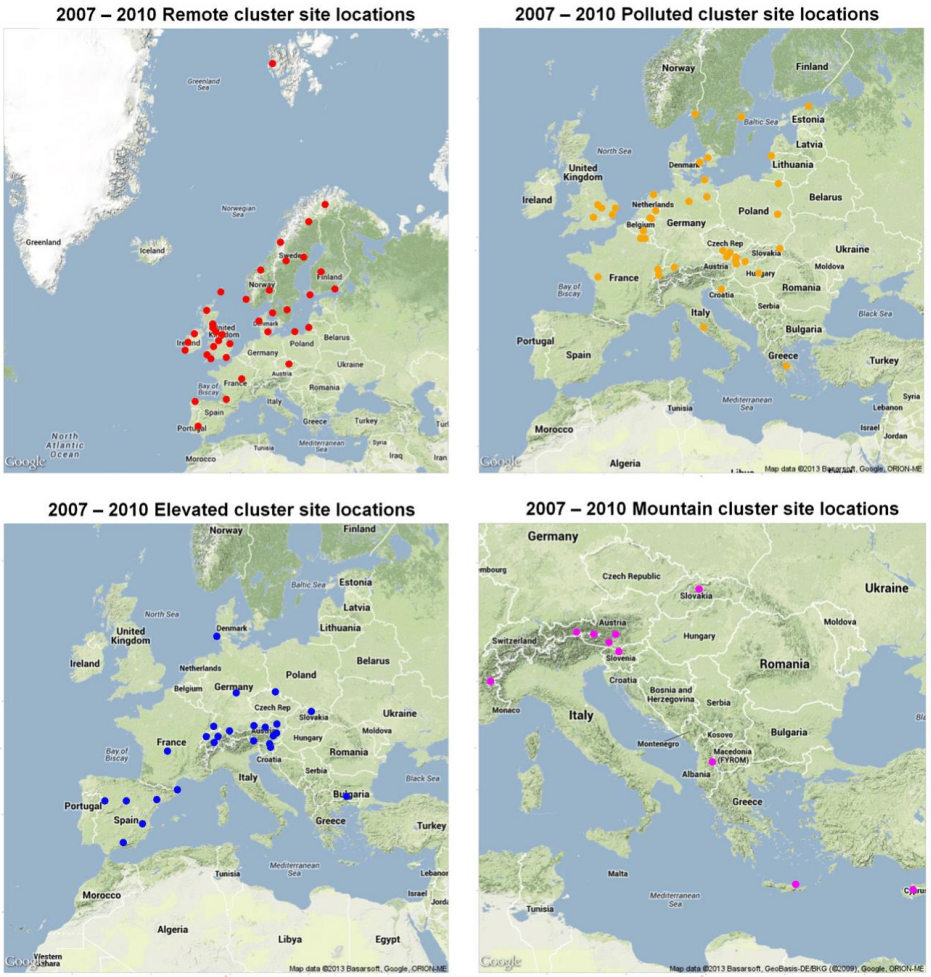

Fig. 6. Locations of the 113 EMEP sites separated according to the four clusters assigned for 2007–2010 monthly-diurnal ozone cycles (Map data: Google, Basarsoft, GeoBasis-DE/BKG, ORION-ME).

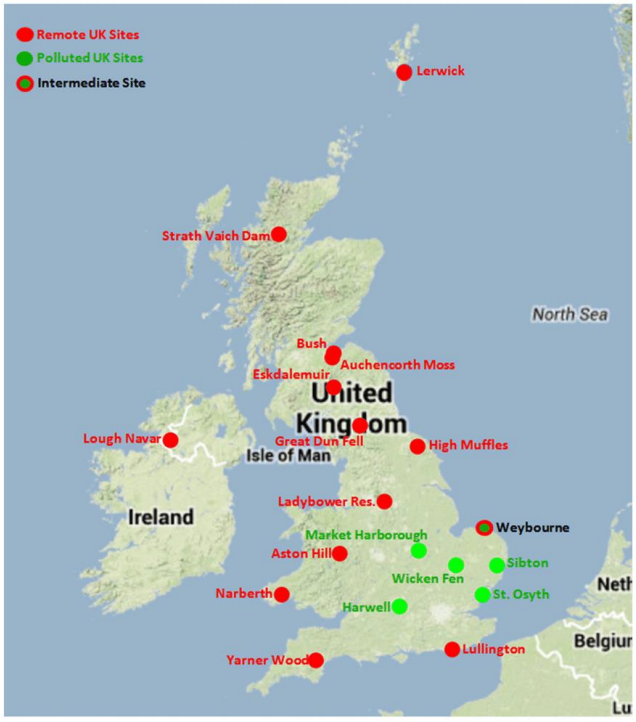

Fig. 7. Location of UK EMEP sites operational for 2007–2010. Sites clustered as Remote are shown in red, and those clustered as Polluted are shown in green (Map data: Google, GeoBasis-DE/BKG).

2003–2006, five UK sites grouped with Bush, however, four were less tightly grouped but remained assigned to the Remote cluster, and one site, (Lullington Heath) was assigned to the Polluted cluster. Similar variability was found for the remaining time periods. The Remote UK sites were located in the north and west of the UK, with the exception of Lullington Heath on England's south coast.

4. Discussion

Sites within the Remote cluster are further from the largest sources of ozone precursor (NO_x) and depleting (NO) species as shown by their locations predominantly on the north-west fringe of Europe. This leads to lower perturbation of larger scale, continental and hemispheric background ozone levels, and hence relatively low amplitude monthly-diurnal ozone cycles. Ozone variation in the Polluted cluster shows greater diurnal and annual variation, and sites are closer to major sources of ozone precursor/depleting species which facilitate greater photochemical production during the day and removal at night through deposition and reaction with NO. In the Elevated and Mountain clusters, higher concentrations and less diurnal variability are observed due to ozone transport in the free troposphere. Ozone formed in polluted areas with high concentrations of VOCs and NO_x ventilates from the boundary layer to the free troposphere where lower temperatures reduce ozone loss through reaction with species such as NO (Guo et al., 2013). The greater atmospheric motions at altitude also rapidly replenish any ozone loss by deposition. The lower average altitude of sites in the Elevated cluster possibly leads to a greater degree of local ozone production/depletion, increasing diurnal variability compared with the Mountain cluster.

These results reflect previous analysis of ozone spatial trends across the UK and Europe. Tarasova et al. (2007) used cluster analysis to group 114 extra-tropical sites globally based on ozone variation between 1990 and 2004. Of the six clusters derived, European sites were assigned to five, with only a 'polar/remote' classification not found in Europe. The additional cluster in Tarasova et al. (2007) compared to this study was because sites assigned to the Remote cluster (for 2007–2010) were separated into Clean Background and Rural clusters. Inspection of Figs. 3 and 4 shows that this subsidiary separation is not borne out by the application of the clustering algorithm applied here. Ozone variation at monitoring sites in North America, Japan and Argentina was classified in the five

clusters containing European sites. Henne et al. (2010) reported an 'observation-independent' Ward's method hierarchical cluster analysis to differentiate 34 rural European sites. Parameters characterising emissions, deposition and transport were included and six clusters ranging from 'generally remote' to 'agglomeration' were identified. The Harwell site grouped in the most polluted 'agglomeration' cluster along with Weybourne. The clustering result explained 55% of the inter-site variability in daily median ozone concentrations, compared with 75% of inter-site variability explained by the methodology adopted here. Comparison of the results from Henne et al. (2010) with the results obtained in this study shows one main difference. In the former clustering there was no differentiation between elevated sites (e.g. Jungfraujoch, Switzerland, 3578 m) and non-elevated remote sites. A study of 97 'non-urban' US sites used principal component analysis to identify 14 groups of sites with similar summer ozone variation (Chan and Vet, 2010). Comparison of the monthly ozone variation revealed a spectrum of sites similar to that found in the cluster analysis of European sites, from those with high summer concentrations and a strong influence of regional photochemistry, to those without such regional photochemical influences.

Variation in the clusters produced for each four-year period may be a result of numerous factors. One is long-term trends in ozone variation from the curtailment of ozone precursor emissions, as recently highlighted across 158 EMEP sites by Wilson et al. (2012), and globally by Parrish et al. (2013) who found long-term shifts in seasonal ozone cycles at sites in Europe and North America. Another factor is changes in the number and distribution of EMEP monitoring sites (Table 1). In 1991–1994, there was only one site in southern Europe (Portugal) and in Eastern Europe (Czech Republic). The rest were located in central Europe, Scandinavia and the UK. Hence there was less variability in monthly-diurnal ozone variation overall and only three major clusters formed. By 2010, more sites had been established in Mediterranean regions and Eastern Europe providing data across a more varied ozone landscape. A third factor is anomalous characteristics for some time periods. In one 4-year period, 2003–2006, half of the years (2003 and 2006), contained periods when 'heat-wave' conditions affected significant areas across Europe. Lee et al. (2006) detail the significant increase in photochemical activity during these conditions, including an approximate doubling of VOC reactivity with the OH radical. Hence this change in drivers provides another potential method for changes in site classification. In the cluster results from 2003 to 2006, nine Remote sites formed an additional cluster, suggesting that ozone variation at these sites was more different from the other Remote sites than at any other time between 1991 and 2010. Similarly, Polluted UK sites, including Harwell, grouped in the Remote cluster, and therefore showed most difference in ozone variation compared to Polluted sites in central and southern Europe during this period. Conversely, Lullington Heath, on England's south coast, clustered in the Polluted cluster. Its closer proximity to mainland Europe, relative to other UK sites may have led to a greater exposure to the anomalous ozone variation during the two 'heat-wave' periods in 2003 and 2006.

AQEG (2009) reported that annual mean ozone concentrations were highest in the north and west UK, but the propensity for prolonged exceedance of health-based ozone metrics was higher in the south and east. This is explained by a greater influence of hemispheric background levels in the UK towards the north-west (Jenkin, 2008), and leads to the separation of UK EMEP sites found in this analysis. Modification of hemispheric background ozone concentrations occurs through formation of additional ozone on a regional scale due to reaction of NO_x and VOCs, and local-scale depletion of ozone by reaction with NO. Remote UK sites, generally towards the north and west UK are less susceptible to transport of primary emissions from major pollution sources such as southern England and continental Europe (RoTAP, 2012). Hence lower NO concentrations at Remote UK sites lead to less ozone depletion, and greater influence of hemispheric background concentrations. Ozone concentrations at many EMEP sites across Europe, such as in Scandinavia, are similarly influenced by hemispheric background concentrations. The geographic domain for which monthly-diurnal ozone variation at Auchencorth is representative is therefore large and transboundary in nature. Non-UK sites falling within this international domain also cluster tightly with Auchencorth, leading to greater variability in the position of UK Remote sites relative to Auchencorth within the ordered dendrograms.

Conversely, Polluted UK sites, in south-east England, are closer to major sources of VOCs and NO_x and have higher diurnal and annual variability due to greater modification of hemispheric background ozone concentrations. Higher NO concentrations facilitate greater ozone depletion, whilst the proximity of ozone precursor sources increases the prevalence of regional-scale, elevated ozone episodes. Ozone variation within the entire Polluted cluster is less homogeneous than in the Remote cluster due to the differences in emission patterns and other drivers (e.g. solar intensity) between sites. For example, the southern UK has a variety of different drivers determining ozone concentrations compared with sites in central Europe. Depending on meteorological conditions air masses entering this region can contain relatively high or low concentrations of ozone formation and loss species (see e.g. Jenkin, 2008). Hence these UK sites, in close proximity to London, cluster more tightly with Harwell between 1991 and 2010. Harwell is therefore representative of a smaller geographic area than Auchencorth. UK EMEP sites provide an excellent case study for this effect, due to their large number (19) and density. However it is also apparent elsewhere: for example, six sites within 120 km of Vienna all cluster tightly together in the 2007–2010 dendrogram, along with Topolniky, Slovakia, a similar distance from Vienna. These sites (Heidenreichstein, Pillersdorf, Ganserndorf, Stixneusiedl, Illmitz, Dunkelsteinerwald and Topolniky) are located at the more anthropogenically influenced end of the Polluted cluster.

Europe-wide, the clustering produced a number of anomalous classifications. For example, Finokalia, a coastal site on Crete, grouped in the Mountain cluster (Fig. 3). It has been shown that significant incursion and entrainment of the free troposphere into the boundary layer occurs at Finokalia producing a monthly-diurnal ozone profile typically found at sites at much higher elevations (Gerasopoulos et al., 2005, 2006). Other coastal sites, such as Westerland, Denmark and Cabo de Creus, Spain, were grouped in the Elevated cluster. The NMF reordering facilitated evaluation of other

anomalous sites. For example, Lazaropole in Macedonia was a member of the mountain cluster, but the classification was relatively weak and it could be construed as its own cluster. Ozone concentrations at Lazaropole were significantly higher than the 112 other sites in the analysis, with 51% of the monthly–hourly averaged concentrations exceeding 120 μg m^{-3}. The source of this anomaly remains unexplained. There are no other EMEP sites within 300 km of Lazaropole, and only two sites within 500 km, so to examine the geographic extent of the high ozone concentrations reported at Lazaropole, and the ozone regime across south Eastern Europe in general, require a greater number of sites.

Few pollutants are monitored as widely as ozone, with some not routinely measured at all, making pollutant-specific site representativeness studies impractical. For example, peroxyacetyl nitrates (PAN), which provide a mechanism for NO_x storage and long range transport, are not continuously monitored at EMEP sites (McFadyen and Cape, 2005), but it is nevertheless important to assess the spatial relevance of conclusions of sporadic PAN measurement. Since ozone is influenced by a wide variety of drivers, site classifications based on ozone may be anticipated to be representative for many other atmospheric species — particularly secondary components, including PAN. Hence, as a consequence of demonstrating the representativeness of the UK EMEP supersites based on ozone variation, comprehensive chemical climatologies derived for the impacts of other atmospheric components at the sites can be placed in a European context. Application of this methodology to different pollutant datasets could be used to assess changes in site classification as a function of pollutant. For example, a recent study applies a k-means clustering algorithm to differentiate US sites based on five-year averaged concentrations of $PM_{2.5}$ components (Austin et al., 2013).

5. Conclusions

Two major ground-level ozone regimes over the UK have been identified through the use of hierarchical cluster analysis of monthly-diurnal ozone datasets from 154 EMEP monitoring sites across Europe. The application of non-negative matrix factorization (NMF) reordered the summary dendrogram based on the relative anthropogenic influence on ozone at each site. This allows the 25% within-cluster variability in ozone concentrations across Europe not explained by the identification of four major clusters to be interpreted. For 2007–2010, all 19 UK EMEP sites were assigned to two of the Europe-wide clusters, with 17 sites apportioned into 2 groups in these two clusters. One cluster is comparatively less anthropogenically influenced, with ozone concentrations featuring less modification from hemispheric background levels; the other cluster is of sites closer to ozone precursor/depleting emissions and features more pronounced diurnal and annual ozone cycles. The UK EMEP supersites of Auchencorth and Harwell grouped tightly with the other UK sites in these 'Remote' and 'Polluted' clusters respectively. For the other four, four-year periods considered between 1991 and 2006, a similar separation of UK sites occurred, with relatively tighter clustering of Polluted UK sites to Harwell than Remote UK sites to Auchencorth/Bush due to the larger, transboundary spatial domain for which Auchencorth is representative. Hence the UK background ozone conditions are well represented by the location of the UK EMEP supersites at Auchencorth and Harwell. Both supersites currently monitor 120 different chemicals in air, precipitation and particulate matter; this work shows that conclusions derived from interpretation of these large datasets are likely appropriately applied to a wider geographic area.

Acknowledgements

C. S. Malley acknowledges the University of Edinburgh, School of Chemistry, the NERC Centre for Ecology & Hydrology (CEH) and the UK Department for Environment, Food and Rural Affairs (Defra) for funding. The authors gratefully acknowledge EMEP for the availability of the ozone datasets.

References

AQEG, 2009. Ozone in the United Kingdom: Air Quality Expert Group. Defra Publications, London (http://www.defra.gov.uk/environment/quality/air/airquality/publications/ozone/documents/aqeg-ozone-report.pdf).
Austin, E., Coull, B., Zanobetti, A., Koutrakis, P., 2013. A framework to spatially cluster air pollution monitoring sites in US based on the PM2.5 composition. Environ. Int. 59, 244–254.
Carslaw, D.C., Ropkins, K., 2013. Openair: open-source tools for the analysis of air pollution data. R Package Version 0.8-5.
Chan, E., Vet, R.J., 2010. Baseline levels and trends of ground level ozone in Canada and the United States. Atmos. Chem. Phys. 10, 8629–8647.
Dabboor, M., Yackel, J., Hossain, M., Braun, A., 2013. Comparing matrix distance measures for unsupervised POLSAR data classification of sea ice based on agglomerative clustering. Int. J. Remote Sens. 34, 1492–1505.
Dillner, A.M., Schauer, J.J., Christensen, W.F., Cass, G.R., 2005. A quantitative method for clustering size distributions of elements. Atmos. Environ. 39, 1525–1537.
EMEP/CCC-Report 1/95, Revision 1/2002, 2002. EMEP Manual for Sampling and Chemical Analysis. NILU, Norway (http://www.nilu.no/projects/ccc/manual/).
Flemming, J., Stern, R., Yamartino, R.J., 2005. A new air quality regime classification scheme for O-3, NO2, SO2 and PM10 observations sites. Atmos. Environ. 39, 6121–6129.
Gerasopoulos, E., Kouvarakis, G., Vrekoussis, M., Kanakidou, M., Mihalopoulos, N., 2005. Ozone variability in the marine boundary layer of the eastern Mediterranean based on 7-year observations. J. Geophys. Res. 110, D15309. http://dx.doi.org/10.1029/2005JD005991.
Gerasopoulos, E., Kouvarakis, G., Vrekoussis, M., Donoussis, C., Mihalopoulos, N., Kanakidou, M., 2006. Photochemical ozone production in the eastern Mediterranean. Atmos. Environ. 40, 3057–3069.
Guo, H., Ling, H., Cheung, K., Jiang, F., Wang, D.W., Simpson, I.J., Barletta, B., Meinardi, S., Wang, T.J., Wang, X.M., Saunders, S.M., Blake, D.R., 2013. Characterization of photochemical pollution at different elevations in mountainous areas in Hong Kong. Atmos. Chem. Phys. 13, 3881–3898.
Henne, S., Brunner, D., Folini, D., Solberg, S., Klausen, J., Buchmann, B., 2010. Assessment of parameters describing representativeness of air quality in-situ measurement sites. Atmos. Chem. Phys. 10, 3561–3581.
Ignaccolo, R., Ghigo, S., Giovenali, E., 2008. Analysis of air quality monitoring networks by functional clustering. Environmetrics 19, 672–686.
Jenkin, M.E., 2008. Trends in ozone concentration distributions in the UK since 1990: local, regional and global influences. Atmos. Environ. 42, 5434–5445.
Joly, M., Peuch, V.H., 2012. Objective classification of air quality monitoring sites over Europe. Atmos. Environ. 47, 111–123.
Kaufman, L., Rousseeuw, P.J., 1990. Finding Groups in Data: An Introduction to Cluster Analysis. Wiley, New York.
Kovac-Andric, E., Sorgo, G., Kezele, N., Cvitas, T., Klasinc, L., 2010. Photochemical pollution indicators-an analysis of 12 European monitoring stations. Environ. Monit. Assess. 165, 577–583.
Lau, J., Hung, W.T., Cheung, C.S., 2009. Interpretation of air quality in relation to monitoring station's surroundings. Atmos. Environ. 43, 769–777.
Lee, D.D., Seung, H.S., 1999. Learning the parts of objects by non-negative matrix factorization. Nature 401, 788–791.
Lee, D.D., Seung, H.S., 2001. Algorithms for non-negative matrix factorization. Adv. Neural Inf. Process. Syst. 13, 556–562.
Lee, J.D., Lewis, A.C., Monks, P.S., Jacob, M., Hamilton, J.F., Hopkins, J.R., Watson, N.M., Saxton, J.E., Ennis, C., Carpenter, L.J., Carslaw, N., Fleming,

Z., Bandy, B.J., Oram, D.E., Penkett, S.A., Slemr, J., Norton, E., Rickard, A.R., Whalley, L.K., Heard, D.E., Bloss, W.J., Gravestock, T., Smith, S.C., Stanton, J., Pilling, M.J., Jenkin, M.E., 2006. Ozone photochemistry and elevated isoprene during the UK heatwave of August 2003. Atmos. Environ. 40, 7598–7613.

Liu, S., 2012. NMFN: non-negative matrix factorization. R Package Version 2.0. (http://CRAN.R-project.org/package=NMFN).

Lu, H.C., Chang, C.L., Hsieh, J.C., 2006. Classification of PM10 distributions in Taiwan. Atmos. Environ. 40, 1452–1463.

Maechler, M., Rousseeuw, P., Struyf, A., Hubert, M., Hornik, K., 2013. Cluster: cluster analysis basics and extensions. R Package Version 1.14.4.

Mangiameli, P., Chen, S.K., West, D., 1996. A comparison of SOM neural network and hierarchical clustering methods. Eur. J. Oper. Res. 93, 402–417.

McFadyen, G.G., Cape, J.N., 2005. Peroxyacetyl nitrate in eastern Scotland. Sci. Total Environ. 337, 213–222.

Parrish, D.D., Law, K.S., Staehelin, J., Derwent, R., Cooper, O.R., Tanimoto, H., Volz-Thomas, A., Gilge, S., Scheel, H.E., Steinbacher, M., Chan, E., 2013. Lower tropospheric ozone at northern midlatitudes: changing seasonal cycle. Geophys. Res. Lett. 40, 1631–1636.

R Core Development Team, 2008. R: A Language and Environment for Statistical Computing. R Foundation for Statistical Computing, Vienna, Austria (ISBN 3-900051-07-0, URL http://www.R-project.org).

RoTAP, 2012. Review of transboundary air pollution: acidification, eutrophication, ground level ozone and heavy metals in the UK. Contract Report to the Department for Environment, Food and Rural Affairs. Centre for Ecology and Hydrology. (http://www.rotap.ceh.ac.uk/sites/rotap.ceh.ac.uk/files/CEH%20RoTAP.pdf).

Royal Society, 2008. Ground-level Ozone in the 21st Century: Future Trends, Impacts and Policy Implications. The Royal Society, London ((Science Policy, 15/08) http://royalsociety.org/uploadedFiles/Royal_Society_Content/policy/publications/2008/7925.pdf).

Spangl, W., Schneider, J., Moosmann, L., Nagi, C., 2007. Representativeness and classification of air quality monitoring stations. Umweltbundesamt Report. (http://www.umweltbundesamt.at/fileadmin/site/publikationen/REP0121.pdf).

Tarasova, O.A., Brenninkmeijer, C.A.M., Joeckel, P., Zvyagintsev, A.M., Kuznetsov, G.I., 2007. A climatology of surface ozone in the extra tropics: cluster analysis of observations and model results. Atmos. Chem. Phys. 7, 6099–6117.

Torseth, K., Aas, W., Breivik, K., Fjaeraa, A.M., Fiebig, M., Hjellbrekke, A.G., Myhre, C.L., Solberg, S., Yttri, K.E., 2012. Introduction to the European Monitoring and Evaluation Programme (EMEP) and observed atmospheric composition change during 1972–2009. Atmos. Chem. Phys. 12, 5447–5481.

Ward, J., 1963. Hierarchical grouping to optimize an objective function. J. Am. Stat. Assoc. 58, 236–244.

Wilson, R.C., Fleming, Z.L., Monks, P.S., Clain, G., Henne, S., Konovalov, I.B., Szopa, S., Menut, L., 2012. Have primary emission reduction measures reduced ozone across Europe? An analysis of European rural background ozone trends 1996–2005. Atmos. Chem. Phys. 12, 437–454.

Appendix IV: Publication

This appendix contains the peer-review publication which formed the basis for Chapter 4.

Malley, C. S., Heal, M. R., Mills, G., & Braban, C. F. (2015). Trends and drivers of ozone human health and vegetation impact metrics from UK EMEP supersites measurements (1990-2013). *Atmospheric Chemistry & Physics*, 15, 4025-4042. 10.5194/acp-15-4025-2015.

Atmos. Chem. Phys., 15, 4025–4042, 2015
www.atmos-chem-phys.net/15/4025/2015/
doi:10.5194/acp-15-4025-2015

Atmospheric Chemistry and Physics Open Access

Trends and drivers of ozone human health and vegetation impact metrics from UK EMEP supersite measurements (1990–2013)

C. S. Malley[1,2], **M. R. Heal**[1], **G. Mills**[3], **and C. F. Braban**[2]

[1]School of Chemistry, University of Edinburgh, Edinburgh, UK
[2]NERC Centre for Ecology & Hydrology, Penicuik, UK
[3]NERC Centre for Ecology & Hydrology, Environment Centre Wales, Bangor, UK

Correspondence to: C. S. Malley (c.malley@sms.ed.ac.uk)

Received: 5 November 2014 – Published in Atmos. Chem. Phys. Discuss.: 20 January 2015
Revised: 18 March 2015 – Accepted: 26 March 2015 – Published: 16 April 2015

Abstract. Analyses have been undertaken of the spatial and temporal trends and drivers of the distributions of ground-level O_3 concentrations associated with potential impacts on human health and vegetation using measurements at the two UK European Monitoring and Evaluation Program (EMEP) supersites of Harwell and Auchencorth. These two sites provide representation of rural O_3 over the wider geographic areas of south-east England and northern UK respectively. The O_3 exposures associated with health and vegetation impacts were quantified respectively by the SOMO10 and SOMO35 metrics and by the flux-based POD_Y metrics for wheat, potato, beech and Scots pine. Statistical analyses of measured O_3 and NO_x concentrations were supplemented by analyses of meteorological data and NO_x emissions along air-mass back trajectories.

The findings highlight the differing responses of impact metrics to the decreasing contribution of regional O_3 episodes in determining O_3 concentrations at Harwell between 1990 and 2013, associated with European NO_x emission reductions. An improvement in human health-relevant O_3 exposure observed when calculated by SOMO35, which decreased significantly, was not observed when quantified by SOMO10. The decrease in SOMO35 is driven by decreases in regionally produced O_3 which makes a larger contribution to SOMO35 than to SOMO10. For the O_3 vegetation impacts at Harwell, no significant trend was observed for the POD_Y metrics of the four species, in contrast to the decreasing trend in vegetation-relevant O_3 exposure perceived when calculated using the crop AOT40 metric. The decreases in regional O_3 production have not decreased POD_Y as climatic and plant conditions reduced stomatal conductance and uptake of O_3 during regional O_3 production.

Ozone concentrations at Auchencorth (2007–2013) were more influenced by hemispheric background concentrations than at Harwell. For health-related O_3 exposures this resulted in lower SOMO35 but similar SOMO10 compared with Harwell; for vegetation POD_Y values, this resulted in greater impacts at Auchencorth for vegetation types with lower exceedance ("Y") thresholds and longer growing seasons (i.e. beech and Scots pine). Additionally, during periods influenced by regional O_3 production, a greater prevalence of plant conditions which enhance O_3 uptake (such as higher soil water potential) at Auchencorth compared to Harwell resulted in exacerbation of vegetation impacts at Auchencorth, despite being further from O_3 precursor emission sources.

These analyses indicate that quantifications of future improvement in health-relevant O_3 exposure achievable from pan-European O_3 mitigation strategies are highly dependent on the choice of O_3 concentration cut-off threshold, and reduction in potential health impact associated with more modest O_3 concentrations requires reductions in O_3 precursors on a larger (hemispheric) spatial scale. Additionally, while further reduction in regional O_3 is more likely to decrease O_3 vegetation impacts within the spatial domain of Auchencorth compared to Harwell, larger reductions in vegetation impact could be achieved across the UK from reduction of hemispheric background O_3 concentrations.

Published by Copernicus Publications on behalf of the European Geosciences Union.

Figure 1. Map of the United Kingdom and Ireland showing the location of the two UK EMEP supersites (purple circles) at Auchencorth and Harwell, as well as the location of the UK Met Office stations from which meteorological data were used (green circles).

1 Introduction

As part of the European Monitoring and Evaluation Program (EMEP) monitoring network, the UK operates two level II "supersites" at Harwell (80 km west of London, Fig. 1) and Auchencorth (17 km south of Edinburgh, Fig. 1) (Tørseth et al., 2012). The utility of the supersite concept as part of a strategy to address air quality research issues through concurrent measurements of a suite of atmospheric constituents has recently been reinforced (Kuhlbusch et al., 2014). The distinct impacts of one of the constituents measured at Harwell and Auchencorth, ground-level ozone (O_3), on human health and vegetation have been widely studied (REVIHAAP, 2013; RoTAP, 2012), but changes in the recommended metrics by which O_3 exposure relevant to these impacts is quantified (see below) necessitates new analyses of supersite measurement data.

The analyses in this study are based on the chemical climatology concept introduced by chemist Robert Angus Smith in "Air and rain: The beginnings of a chemical climatology" (Angus Smith, 1872). A chemical climatology approach comprises three elements (Malley et al., 2014a): (i) an "impact" of the atmospheric composition, often characterised through a metric; (ii) the "state" of relevant atmospheric composition variation (temporal, spatial and covariance) producing instances of the impact; and (iii) the "drivers" of this state, which could include meteorology, source proximity and emission profiles. A chemical climate has temporal boundaries (time period) and spatial boundaries (geographical extent); where there is identification of a significant change in the impact resulting from significant change to the drivers and state, these may be classified as different phases of the chemical climate.

In this study the six steps in the construction of a chemical climate described in Fig. 2 and outlined in Malley et al. (2014a) were applied to characterise the exposure of ground-level O_3 concentrations measured at Harwell and Auchencorth relevant to human health and four vegetation types. The O_3 measured at these sites has been shown to be representative of rural O_3 concentrations in the larger geographical areas of south-east England and northern UK respectively (Malley et al., 2014b).

Ozone exposure relevant to health impacts is quantified using the SOMO10 and SOMO35 metrics, which are the annual sums of daily maximum running 8 h average O_3 concentrations above 10 and 35 ppb thresholds respectively. These metrics are in line with the recent World Health Organisation "Review of evidence on health aspects of air pollution" (REVIHAAP, 2013) report which recommends quantifying acute O_3 health impacts using both these measures of daily O_3 concentration and across the full year. In earlier syntheses of human health effects of O_3, importance was attached to the peak O_3 concentrations (WHO, 2006). The recent REVIHAAP synthesis shows important O_3 effects on human health down to very small concentrations and a suggestion that there is no specific threshold for effects. The inclusion of SOMO10 reflects this recent synthesis. To quantify vegetation impacts of O_3, the species-specific metric of phytotoxic O_3 dose above a threshold flux Y (POD_Y) is used (LRTAP Convention, 2010). This parameter represents the modelled accumulated stomatal uptake of O_3 over a fixed time period based on hourly variations in climate (temperature (T), vapour pressure deficit (VPD), photosynthetically active radiation (PAR)), soil moisture (soil water potential (SWP) or plant available water (PAW)), O_3 and plant phenology (Emberson et al., 2000). Stomatal flux metrics are increasingly used to assess O_3 vegetation impacts, as they more accurately reflect the spatial pattern of O_3 damage across Europe than concentration-based metrics such as AOT40 (Mills et al., 2011b; RoTAP, 2012). Statistical analyses of O_3 and NO_x variation provide characterisation of the "state" of atmospheric composition at the two sites for the different impacts, while analysis of meteorology, air-mass history and NO_x emissions provide insight into the relevant "drivers" of the chemical climates.

The focus of this study is to characterise the variation in O_3 impacts, temporally at Harwell and spatially between Har-

well and Auchencorth, and the contributions of regional and hemispheric O_3-modifying processes in determining each impact. Hemispheric background O_3 concentrations are defined here as O_3 formed from anthropogenic and natural precursor emissions outside of Europe (Derwent et al., 2013). Superimposed on this, regional net O_3 production or loss derives from the balance of processes such as emissions, deposition and meteorological conditions occurring on a regional scale. Photochemical reactions between NO_x and volatile organic compounds (VOCs) emitted in Europe produce O_3 regionally, but high NO_x environments (regionally and locally) limit O_3 formation (Jenkin, 2008; Munir et al., 2013). Spatial and temporal variation of these processes in the UK context have been discussed previously (AQEG, 2009). Studies have also quantified both human health (EMEP, 2014; Stedman and Kent, 2008; Gauss et al., 2014; Guerreiro et al., 2014) and vegetation O_3 impacts (Mills et al., 2011a; RoTAP, 2012) within the spatial domain of each supersite. However, consideration of both impacts at each site using a common chemical climatology approach links the impact studies with the analyses of temporal and spatial O_3 variation and allows identification of differences and similarities in the drivers of each impact, which inform the development of co-beneficial O_3 mitigation strategies.

An important aspect of this study is to also compare impacts quantified through the updated metrics with previously used metrics. For the health impact the contrast is between health-relevant exposure quantified by SOMO10 and SOMO35 and that quantified using the higher thresholds of the WHO guideline (50 ppb) and the EU target value (60 ppb) (Derwent et al., 2013; EEA, 2014b). For the vegetation impact the contrast is between the POD_Y metric and the concentration-based crop AOT40 metric, the sum of hourly O_3 concentrations above 40 ppb during daylight hours during the growing season (Coyle et al., 2002; Klingberg et al., 2014; Jenkin, 2014). In addition, a comparison is made between POD_Y calculated using on-site measured O_3 and meteorological data (used in this study and previously in Karlsson et al., 2007) and analyses which have used gridded modelled O_3 and meteorological data to calculate POD_Y (Emberson et al., 2007; Klingberg et al., 2011; Mills et al., 2011a, b; Simpson et al., 2007).

The ambition to integrate data (such as measured concentrations) with knowledge (such as the adverse impacts of O_3) to advance both science and policy is currently an area of intense research interest (Schmale et al., 2014; Abbatt et al., 2014; Kuhlbusch et al., 2014). This current work, using the chemical climatology concept, presents a clear methodology for achieving this and shows a simple categorisation for summarising information which could be more widely adopted.

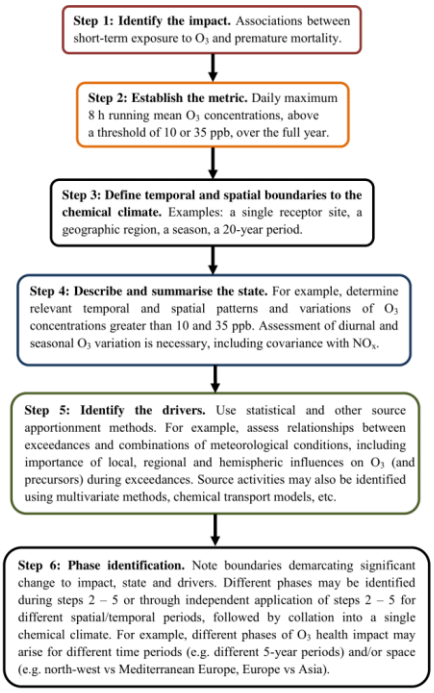

Figure 2. Practical steps for derivation of a chemical climate. The impact of premature mortality associated with short-term exposure to O_3 is used as an example. Text in the chemical climate data sheets is coloured the same as the step which gave rise to the statistic. The details of application of these six steps to the focus of this study are described in Sect. 2.

2 Methods

A chemical climate is based on an identified impact (Fig. 2, Step 1), which is linked to atmospheric composition variation through a suitable metric (Step 2). For assessment of O_3 acute health impact, REVIHAAP (2013) recommends the use of all-year metrics based on the value by which the daily maximum 8 h average O_3 concentration exceeds either 10 or 35 ppb. The annual sum of the daily exceedances of these thresholds yields the SOMO10 and SOMO35 metrics respectively. The POD_Y metric for the vegetation chemical climates was calculated using the DO_3SE model version 3.0.5 (http://www.sei-international.org/do3se; Emberson et al., 2000). POD_Y values were calculated for two crops (wheat and potato) and two forest trees (beech and Scots pine),

accumulated across their respective growing seasons. The length of the growing seasons and phenological limitation on stomatal conductance throughout the growing season were derived according to methods detailed in LRTAP Convention (2010). The growing seasons for wheat (late April–early August) and potato (late May–early September) were calculated by accumulated temperature and therefore varied interannually based on meteorological conditions. For beech, the growing season was calculated using a latitude model (19 April–20 October at Harwell, 26 April–10 October at Auchencorth). The Scots pine growing season was the full year.

The DO_3SE model calculates the stomatal flux for each species using parameterisations which quantify the sensitivity of each species to modification of stomatal conductance due to the effects of phenology, O_3, PAR, T, VPD and soil moisture (SWP for potato, beech and Scots pine and PAW for wheat; LRTAP Convention, 2010). For this study, the DO_3SE model used hourly measured O_3 concentrations at Harwell and Auchencorth as input, and the following hourly meteorological data from the Met Office stations closest to each monitoring site: wind speed, rainfall, vapour pressure deficit, temperature, global radiation and pressure (UK Meteorological Office, 2012). For Harwell, the station in Benson (SRC ID: 613) at a 13 km distance, provided all meteorological data except global radiation, which was obtained from Bracknell (SRC ID: 838, 1990–2002) and Rothamsted (SRC ID: 471, 2003–2013). For Auchencorth, all meteorological data were obtained from the station in Gogarbank (SRC ID: 19260) at a 14 km distance. All archived data from these stations undergo documented quality control procedures (http://badc.nerc.ac.uk/data/ukmo-midas/ukmo_guide.html). The DO_3SE model calculated hourly O_3 concentrations at the top of the canopy and stomatal conductance for each vegetation type (LRTAP Convention, 2010; Emberson et al., 2000). SWP and PAW were calculated in the DO_3SE model using the measured meteorological data based on the Penman–Monteith model of evapotranspiration (Büker et al., 2012). In addition to meteorological conditions, the evaporation of moisture from soil is dependent on the hydraulic properties of the soil texture. Statistics were therefore calculated for four different soil textures: sandy loam (soil texture classification = coarse), silt loam (medium coarse), loam (medium) and clay loam (fine). The properties of these soil textures are detailed in Büker et al. (2012).

POD_Y was accumulated when this stomatal flux was above a plant-specific threshold flux set at 6 nmol m^{-2} s^{-1} for crops and 1 nmol m^{-2} s^{-1} for forest trees. Response functions were applied to wheat, potato and beech to convert POD_Y into grain yield, tuber weight and whole-tree biomass reduction estimates respectively (Mills et al., 2011c). As the representative coniferous species in the "Atlantic central Europe" geographic zone (LRTAP Convention, 2010), Scots pine was included despite no published response function, with increasing POD_Y assumed to indicate increasing potential damage. In addition, the crop-specific AOT40 metric for May–July was calculated (Fuhrer et al., 1997) to allow for comparison with previous studies that used AOT40 to estimate the impact of O_3 on crops (e.g. Derwent et al., 2013; Jenkin, 2014).

The spatial domain (Fig. 2, Step 3) in this analysis was the area of representativeness of each monitoring site. In the context of European O_3 variation evaluated across all EMEP sites measuring O_3, Harwell was shown to be representative of rural sites within 120 km of London, and Auchencorth was representative of rural locations in a larger domain including the rest of the UK (Malley et al., 2014b). The temporal domain investigated was 1990–2013 for Harwell (NO_x data available from 1996) and 2007–2013 for Auchencorth. The NO_x and O_3 measurements were co-located at Harwell, but the NO_x data for analyses at Auchencorth were obtained from Bush (UK-AIR ID: UKA00128), 8 km from Auchencorth. The suitability of Bush as a proxy site for Auchencorth has been outlined previously, and O_3 variation was found to be similar at both sites (Malley et al., 2014b). The chemical data were downloaded from the UK-Air data repository (http://uk-air.defra.gov.uk) and the Automatic Urban and Rural Network (AURN) reports provide further details on these measurements (Eaton and Stacey, 2012).

A minimum data capture of 75 % across the year for SOMO10/35 calculations, and across the relevant growing season for POD_Y and AOT40 calculations, was imposed for inclusion in the summary statistics. This resulted only in the exclusion of statistics at Harwell for potato in 1995 and Scots pine in 1993. As data capture was generally very high, no adjustment of summary statistics for missing data was applied. At Harwell, average annual data capture for 1990–2013 was 94 %. The lowest annual data capture was 76 % (1993). When the missing hourly O_3 data were estimated through linear interpolation, 1993 SOMO35 and SOMO10 increased by no more than 2 % compared to no interpolation. For the four vegetation types, the 1990–2013 average data capture during the respective growing seasons at Harwell was between 92 and 94 %. Sensitivity to missing O_3 and meteorological data during the years of lowest data capture (above 75 %) for wheat (1994, 75 %), potato (1993, 80 %), beech (1995, 82 %) and pine (2007, 81 %) was also evaluated through linear interpolation. POD_Y values were 19, 19 and 18 % higher for wheat, beech and pine respectively, compared to no linear interpolation, and 6 % lower for potato. These sensitivities illustrate an estimate of the greatest extent of impact metrics not included due to missing data. For the majority of years, biases will be much smaller, as data capture was substantially higher. As estimation of missing data introduces new sources of uncertainty, the impacts calculated using measured data only are considered here.

The state (Fig. 2, Step 4) of the human health chemical climates was characterised using the following statistics for the SOMO10 and SOMO35 metrics: the number of accumulation days (ADs), i.e. days on which the maximum 8 h O_3

concentration exceeded 10 or 35 ppb; percentage contribution per season to annual number of ADs; the percentage contribution per season to SOMO10/35; the average diurnal amplitudes in O_3, NO and NO_2 concentrations on ADs and non-accumulation days (NADs); and the contributions from 13 daily maximum 8 h O_3 concentration bins (between 10 and > 70 ppb in 5 ppb groups) to SOMO10/35. The state for the vegetation chemical climates was characterised by the following statistics for the POD_Y metric for each vegetation type: the number of POD_Y accumulation days; the percentage monthly contributions to POD_Y across the growing season; the contributions from 15 hourly O_3 concentration bins (between 0 and > 70 ppb in 5 ppb groups) to POD_Y; and the average diurnal amplitudes of O_3, NO and NO_2 on ADs and NADs. For the AOT40 metric, the contributions from May, June and July were calculated as well as the average diurnal amplitudes in May, June and July of O_3, NO and NO_2.

Three potential drivers of the state (Step 5) were investigated. First, the effect of temperature was investigated using data from Benson (SRC ID: 613), 13 km from Harwell, and Gogarbank (SRC ID: 19260), 14 km from Auchencorth (UK Meteorological Office, 2012). The mean daily temperature on ADs and NADs for SOMO10/35 and POD_Y were compared. Monthly averaged temperatures during the AOT40 growing season were calculated. Second, the association of the state (Step 4) with air-mass history was investigated by grouping back trajectories based on the similarity of their pathway. The proportion of trajectories arriving from each group during SOMO10/35 and POD_Y ADs and NADs, as well as over the AOT40 growing season, was then compared. Pre-calculated 4-day HYSPLIT air-mass back trajectories arriving at 3 h intervals (2920 trajectories per year) (Draxler and Rolph, 2013; Carslaw and Ropkins, 2013; R Core Development Team, 2008) were grouped using Ward's linkage hierarchical cluster analysis which has been shown through simulations to perform effectively (Mangiameli et al., 1996). The similarity between trajectories was quantified using the measure of their "angle" from the receptor (Eq. 1):

$$d_{1,2} = \frac{1}{n}\sum_{i=1}^{n}\cos^{-1}\left(0.5\frac{A_i + B_i + C_i}{\sqrt{A_i B_i}}\right), \quad (1)$$

where

$$A_i = (X_1(i) - X_0)^2 + (Y_1(i) - Y_0)^2,$$

$$B_i = (X_2(i) - X_0)^2 + (Y_2(i) - Y_0)^2,$$

$$C_i = (X_2(i) - X_1(i))^2 + (Y_2(i) - Y_1(i))^2,$$

$d_{1,2}$ is the variance between trajectory 1 and trajectory 2, X_0 and Y_0 are the latitude and longitude coordinates of the origin of the back trajectory (i.e. the supersite) and X_1, Y_1 and X_2, Y_2 are the coordinates of back trajectories 1 and 2 respectively at a common time point i along the trajectory. In Ward's method each object (back trajectory) initially constitutes its own cluster. At each step, the two clusters are merged that give the smallest increase in total within-cluster variance. This process is repeated until all trajectories are located in one cluster (Kaufman and Rousseeuw, 1990). The summary dendrogram was then "cut" to produce a set of four clusters in which the back trajectories were predominantly "westerly", "easterly", "northerly" and "southerly".

Third, the 2920 4-day back trajectories arriving each year were combined with reported gridded NO_x emissions to investigate the contribution of NO_x emissions as a chemical climate driver. Each 1 h time point along a trajectory was associated with the relevant $0.5° \times 0.5°$ grid square NO_x emissions reported by EMEP (Mareckova et al., 2013; Simpson et al., 2012). This grid encompasses the region 30.25°–75.25° N and 29.75° W–60.25° E. The associated annual NO_x gridded emissions were adjusted using month, day of week and hour of day time factors (Simpson et al., 2012) to obtain an estimate of the hourly NO_x emissions during the hour in which the trajectory passed over the grid cell. The 96-hourly emission estimates for each trajectory were summed, and averaged across the eight trajectories arriving each day, producing a daily average trajectory NO_x emission estimate which was compared on SOMO10/35 and POD_Y ADs and NADs. The monthly average trajectory NO_x emission estimate was calculated for the May–July AOT40 growing season.

The chemical climate statistics derived were compared between Harwell and Auchencorth for evidence of different spatial phases in the O_3 impacts (Fig. 2, Step 6). Evidence for a different temporal phase in the O_3 impact chemical climate at Harwell was investigated by Theil–Sen trend analysis of the 24-year time series of chemical climate statistics. This non-parametric test selects the median of all the slopes between pairs of points in a time series as the estimate of the trend and calculates statistical significance using bootstrap re-sampling (Carslaw and Ropkins, 2013). The 7-year data set from Auchencorth was of insufficient duration to evaluate significant changes in either the health or vegetation impacts.

The terminology spring, summer, autumn and winter refer to the 3-month periods Mar–Apr–May, Jun–Jul–Aug, Sep–Oct–Nov and Dec–Jan–Feb respectively.

3 Results and discussion

The chemical climate statistics derived for the O_3 human health and vegetation impacts at Harwell and Auchencorth are presented as data sheets in Tables S1–S12 in the Supplement. For Harwell, the statistics are averaged across six time periods (1990–1993, 1994–1997, 1998–2001, 2002–2005, 2006–2009, 2010–2013). These tables have a lot of statistics and exemplify a resource which could be replicated and collated for different impacts, locations and time periods to identify key linkages between chemical climates and aid in the development of more holistically considered mitigation strategies. The main features which support the key

conclusions from the human health and vegetation O_3 chemical climates at the UK supersites are presented in Figs. 3–14 and discussed in the following subsections.

3.1 O_3 human-health-impact chemical climates

The detailed statistics describing the O_3 human health chemical climates at Harwell and Auchencorth are presented in Tables S1 and S2 respectively. This section presents two analyses of the impact, state and drivers of the chemical climatology framework (Fig. 2, steps 1–5): specifically, changes in chemical climate phase (Fig. 2, Step 6) temporally at Harwell between 1990 and 2013 (Sect. 3.1.1) and spatially between Auchencorth and Harwell (Sect. 3.1.2).

3.1.1 Long-term changes at Harwell

When characterised by the SOMO35 metric, the O_3 exposure associated with human health impact at Harwell decreased significantly between 1990 and 2013 (Fig. 3), with a median trend of $-2.2\,\%\,y^{-1}$ ($p = 0.001$). The annual number of SOMO35 accumulation days did not vary significantly during this period, averaging 148 ± 28 days y^{-1}. In contrast, when characterised by the SOMO10 metric, O_3 exposure associated with human health impact at Harwell showed no statistically significant trend (1990–2013 mean ($\pm$ SD) $= 8329 \pm 802$ ppb d) (Fig. 3). However, the annual number of SOMO10 ADs has increased significantly with a median trend of $+1.7$ days y^{-1} ($p = 0.01$). In more recent years, the additional ADs occurred in winter, and SOMO10 was accumulated on almost every day of the year (Table S1).

The majority of SOMO35 accumulation at Harwell occurred in spring and summer (Fig. 4). Between 1990 and 2013 the spring contribution to SOMO35 increased significantly ($+1.1\,\%\,y^{-1}$, $p = 0.01$), whilst the summer contribution decreased significantly ($-1.2\,\%\,y^{-1}$, $p = 0.01$). The spring and summer contributions to SOMO35 values were considerably larger and showed larger interannual variation compared to those for SOMO10 (Fig. 4). Between 1990 and 2013 there was a significant decrease in contribution to SOMO10 during summer (trend $-0.4\,\%\,y^{-1}$, $p = 0.01$) and a significant increase during winter ($+0.3\,\%\,y^{-1}$, $p = 0.001$).

Figure 5 shows the contributions from 13 5 ppb daily maximum 8 h O_3 concentration bins to SOMO10 and SOMO35 at Harwell. The majority of SOMO10 was accumulated on days when the O_3 concentration was between 25 and 45 ppb (Fig. 5a). Contributions to SOMO10 from days with the highest concentrations (60–70 ppb and > 70 ppb) decreased significantly between 1990 and 2013 (-0.2 and $-0.4\,\%\,y^{-1}$ respectively), while contributions from more moderate O_3 concentrations (20–30 and 40–50 ppb) increased significantly ($+0.3$ and $+0.2\,\%\,y^{-1}$ respectively). Ozone concentrations between 10 and 35 ppb, i.e. included in SOMO10 but not in SOMO35, contributed on average $40 \pm 8\,\%$ across the

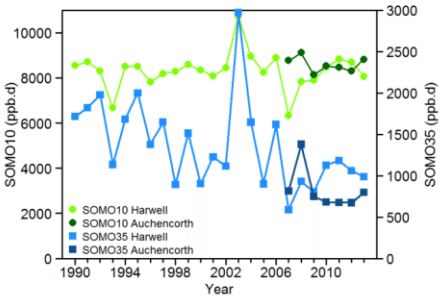

Figure 3. Human health-relevant exposure to O_3 at Harwell (1990–2013) and Auchencorth (2007–2013), as characterised by the SOMO10 and SOMO35 metrics.

whole 24-year period. The contribution to SOMO35 from the higher concentration bins was larger than for SOMO10 but also decreased significantly (Fig. 5b): the 1990–2013 trends in SOMO35 contributions from O_3 concentrations between 60–70 and > 70 ppb were -0.4 and $-1.4\,\%\,y^{-1}$ respectively. There were significant increases in contributions to SOMO35 from concentrations between 35 and 50 ppb (trends in the range 0.4–1.5 $\%\,y^{-1}$). At Harwell the amplitude of the diurnal O_3 cycle was consistently greater (by 7–18 ppb) on SOMO35 ADs compared to SOMO35 NADs (Table S1), while the diurnal NO and NO_2 cycles were substantially lower on ADs than on NADs. Figure 6 shows that the mean diurnal amplitudes of O_3, NO_2 and NO on SOMO35 ADs decreased significantly between 1990 and 2013 (trends of -1.8, -2.8 and $-3.6\,\%\,y^{-1}$ respectively). There was also a significant decrease in mean diurnal cycle amplitudes of O_3, NO_2 and NO on SOMO10 ADs (trends of -1.4, -2.6 and $-3.9\,\%\,y^{-1}$ respectively; NO_x data only from 1996). Trends of decreasing diurnal amplitudes were also observed on SOMO35 NADs (note that SOMO10 NADs were rare, and during 2010–2013 there were essentially no SOMO10 NADs).

The largest change in the O_3 human health chemical climate drivers between 1990 and 2013 at Harwell was the decrease in the estimated daily averaged NO_x emissions along the air-mass back trajectories (Fig. 7). For SOMO35 ADs and NADs, the decreases were -3.1 and $-3.0\,\%\,y^{-1}$ respectively, while the decrease on SOMO10 ADs was $-2.9\,\%\,y^{-1}$ (all $p = 0.001$). For SOMO10 and SOMO35, temperatures on NADs were lower than on ADs. For SOMO35, the average temperature was 2.3 ± 1.5 °C higher on ADs than on NADs between 2010 and 2013, smaller than the corresponding differential of 3.9 ± 1.3 °C between 1990 and 1993. The median trend in this temperature differential was $-2.5\,\%\,y^{-1}$ ($p = 0.001$). The proportion of air-mass back trajectories classified into the four geographic groupings through cluster

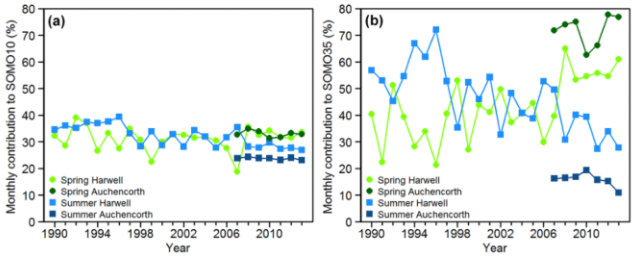

Figure 4. Relative annual contributions from spring (MAM) and summer (JJA) to **(a)** SOMO10 and **(b)** SOMO35.

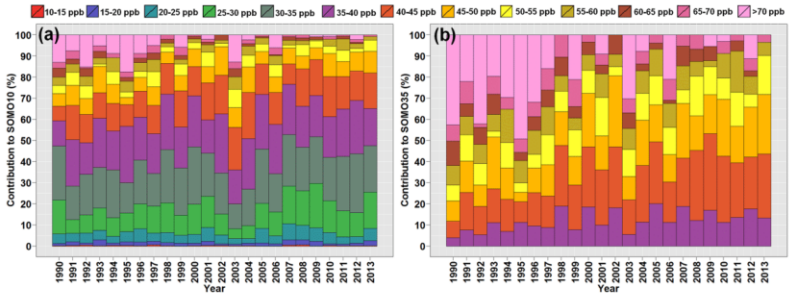

Figure 5. Relative annual contributions to **(a)** SOMO10 and **(b)** SOMO35 at Harwell from different O_3 concentration bins. Concentrations are separated into 13 5 ppb bins spanning daily maximum 8 h mean O_3 concentrations between 10 and > 70 ppb. Note: these concentration bins are contributing to a decreasing long-term trend in SOMO35 and to a constant trend in SOMO10, as illustrated in Fig. 3.

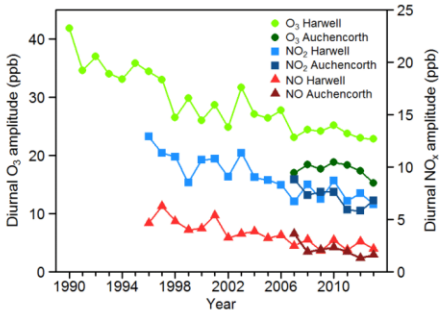

Figure 6. Amplitude of the diurnal O_3, NO_2 and NO cycles at Harwell and Auchencorth during SOMO35 accumulation days (ADs).

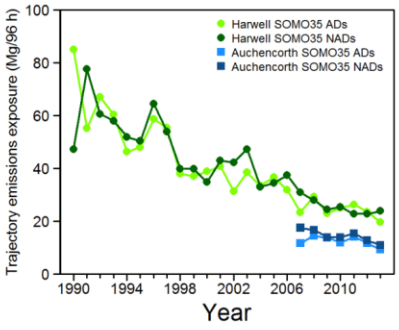

Figure 7. Estimate of the hourly European NO_x emissions emitted from the EMEP 0.5° grids over which 96 h back trajectories passed prior to arrival at Harwell and Auchencorth for SOMO35 accumulation days (ADs) and non-accumulation days (NADs).

analysis did not vary significantly between ADs and NADs for SOMO35 or across the whole 1990–2013 period. In 2003, the effects of long-term changes in the emission drivers were temporarily offset and SOMO10 and SOMO35 values were elevated (Fig. 3). This was due to the "heat-wave" period experienced across south-east England during the summer of that year. The elevated temperatures enhanced O_3 concentrations by leading to greater biogenic VOC emissions, increased reactivity of VOCs with OH and reduced O_3 dry deposition (Lee et al., 2006; Vieno et al., 2010).

The trends and differences in the statistics presented for the SOMO10 and SOMO35 metrics for 1990–2013 at Harwell reveal changes in the relative importance to O_3 concentrations of hemispheric, regional and local-scale processes in determining the health-relevant O_3 exposure at Harwell. Hemispheric background levels of O_3 over Europe feature a pronounced spring maximum and summer minimum (Derwent et al., 2013; Parrish et al., 2013). Hence during spring the SOMO35 threshold is exceeded on the majority of days. Derwent et al. (2013) analysed O_3 concentrations in non-European influenced air masses and found an increasing trend up to 2008, most strongly observed in winter and spring, followed by a levelling off and decrease. Wilson et al. (2012) also calculated a significant positive trend between 1996 and 2005 in monthly fifth percentile O_3 concentrations, taken as a measure of background concentrations, at 82 out of 158 European monitoring sites, including the majority of sites in the UK. This increase in hemispheric background concentrations has led to the increases in the number of winter SOMO10 ADs and in the spring contribution to SOMO35.

Regional O_3 production is greatest in summer when solar intensity and temperatures are highest, so the contribution to the O_3 exposure associated with the health impact during summer is predominantly of European origin (Jenkin, 2008). Autumn and winter have far fewer SOMO35 ADs because of lower hemispheric background levels and lower solar intensity for regional production; however, the consistent exceedance of 10 ppb during autumn and winter leads to a significant contribution to SOMO10 (approximately 40 % in 2010–2013; Table S1). The decrease in summer contribution to SOMO35 results from reduced regionally produced O_3 episodes. This is evidenced by the reduced contribution from the highest O_3 concentration days, the decreased amplitude of diurnal O_3 variation during SOMO35 and SOMO10 ADs and the decreased temperature difference between SOMO35 AD and NADs (regionally generated O_3 exhibits a pronounced diurnal cycle due to its photochemical production and is therefore determined to a greater extent by European meteorological conditions than is hemispheric background O_3). Jenkin (2008) and Munir et al. (2013) likewise attributed long-term decreases in high percentile O_3 concentrations at UK monitoring sites to reduced regional photochemical O_3 episodes and increases in lower percentile concentrations to increased hemispheric background.

The decrease in regional O_3 production is due to the decreasing trend in precursor emissions affecting Harwell (Fig. 7). The European Environment Agency (EEA) estimates that, across the EU28 countries, NO_x emissions have decreased by 51 % between 1990 and 2012 and VOC emissions have decreased by 60 % (EEA, 2014a). Unlike SOMO35, the SOMO10 metric did not decline between 1990 and 2013 because of the lower contribution to SOMO10 from the highest O_3 concentrations, which derive from regional photochemical episodes. SOMO10 was therefore less sensitive to decreases in the magnitude of these episodes, and the decrease was offset by an increase in contribution from 20 to 30 ppb daily maximum 8 h ADs, which were not included in SOMO35.

In summary, whether or not it can be concluded that there has been a decline in O_3 exposure associated with human health impact between 1990 and 2013 at Harwell depends on the choice of a 35 or 10 ppb threshold, both of which are recommended in the recent WHO review (REVIHAAP, 2013). Although the absolute health impact apportioned to O_3 is sensitive to the choice of threshold (Stedman and Kent, 2008; Heal et al., 2013), the analyses presented here have shown that, irrespective of whether a 35 or 10 ppb threshold is selected, the extent, timing and severity of the human health impact of O_3 is increasingly driven by more frequent, modest exceedances of the respective threshold rather than short-lived extreme episodic exceedances.

3.1.2 Spatial differences between Auchencorth and Harwell (2007–2013)

In the comparison of Auchencorth (representative of much of the rural west and north of the UK) and Harwell (representative of south-east England), annual mean and 75th percentile O_3 concentrations were greater at Auchencorth between 2007 and 2013, while maximum values were substantially greater at Harwell (Tables S1 and S2). Between 2007 and 2013, the average SOMO35 was 14 % lower at Auchencorth, while the average SOMO10 was 7 % higher than Harwell. The proportion of SOMO10 accumulated in spring was similar at both sites, but the proportion accumulated in summer was on average 5.3 ± 2.9 % lower at Auchencorth. The contribution to SOMO35 from spring was greater at Auchencorth but smaller for summer compared to Harwell (Fig. 4). Auchencorth also had a smaller contribution from days with > 60 ppb daily maximum 8 h O_3 concentrations (Table S2). Mean amplitudes of diurnal O_3 variation on SOMO10 and SOMO35 ADs were also smaller at Auchencorth than at Harwell (see Fig. 6 for the data relating to SOMO35 ADs). In addition, the difference in mean amplitudes of diurnal O_3, NO_2 and NO variation on SOMO10/35 ADs and NADs was smaller at Auchencorth than at Harwell. For example, diurnal O_3 amplitude was 2.2–4.5 ppb greater on SOMO35 ADs than on NADs at Auchencorth (Table S2), which was smaller

than the 5.6–8.2 ppb differential at Harwell between 2007 and 2013 (Table S1).

The estimated daily averaged NO_x emissions along the airmass back trajectories were substantially lower at Auchencorth than at Harwell (Fig. 7) and generally lower (13 ± 9 % on average in 2007–2013) on SOMO35 ADs than NADs. The temperature difference between SOMO35 ADs and NADs at Auchencorth was less than at Harwell, ranging between 1.7 °C higher on average on ADs in 2010 to 1.4 °C lower on ADs in 2013. Elevated SOMO10 (6 % above 2007–2013 average) and SOMO35 (67 %) values in 2008 at Auchencorth (as also reported by Gauss et al. (2014) using the EMEP/MSC-W model) resulted from an increased contribution from days with maximum 8 h concentrations above 50 ppb (12 and 36 % contributions to SOMO10 and SOMO35 respectively). In addition, 28 % of trajectories were grouped in an "easterly" cluster on SOMO35 ADs in 2008 compared to 13 % on NADs. Patterns were similar in 2009, 2012 and 2013 but without the elevated SOMO35 compared to 2008. The larger O_3 and NO_2 diurnal amplitudes on SOMO10 and SOMO35 ADs in 2008 and the elevated temperatures on SOMO35 ADs (Table S2) suggest regional O_3 production was a substantially stronger driver of SOMO35 in 2008 compared to other years at Auchencorth.

The chemical climate state and driver statistics for Auchencorth indicate that O_3 concentrations at this location are less modified from the hemispheric background than at Harwell, consistent with spatial patterns reported in Jenkin (2008). The larger contribution from spring to SOMO35 at Auchencorth compared to Harwell shows that the hemispheric spring maximum in O_3 produces the majority of SOMO35, and the lower contribution from high O_3 concentration ADs indicates lower influence from regional photochemical O_3 production. Since SOMO10 is determined to a lesser extent by high O_3 concentration ADs, this explains why calculated SOMO35 are lower at Auchencorth, yet SOMO10 values are similar at Auchencorth and Harwell.

3.1.3 Comparison between SOMO10/SOMO35 and higher threshold metrics

In spite of these spatial differences between the SOMO10 and SOMO35 metrics, both provide a substantially different picture of the extent (proportion of year over which impact metric is accumulated), timing (particular periods when impact metric is accumulated) and severity (magnitude of impact metric) of human health-relevant O_3 exposure at Harwell and Auchencorth compared with use of higher threshold metrics such as the WHO air quality guideline (50 ppb) or the EU target value (60 ppb). For example, in 2013 the extent of exceedance of the 60 ppb EU target value across the UK was only 19 days (at least 1 of 81 UK sites exceeding threshold), and the timing of these exceedances was mainly in summer (EEA, 2014b). In contrast, at Harwell in 2013 there were 356 and 130 ADs for SOMO10 and SOMO35 respectively, of which only 27 and 28 % was accumulated in summer. In respect to severity, during 2010–2013 at Harwell on average 91 and 66 % of SOMO10 and SOMO35 respectively was accumulated on days with maximum 8 h O_3 concentrations below the WHO guideline of 50 ppb, compared to 76 and 38 % in 1990–1993 (Table S1). At Auchencorth, an even larger proportion of SOMO10 and SOMO35 were accumulated below 50 ppb, on average 96 and 84 % respectively, during the 2007–2013 monitoring period (Table S2).

The overall impression from these statistics showing a decline in exposure to concentrations in excess of 35 ppb is that the threat to human health has declined between 1990 and 2013 in south-east England. The comments from the EEA (2014b) on the very few episodes in excess of 50 or 60 ppb in 2013 are consistent with this view. However, the recent REVIHAAP (2013) synthesis shows that the lower percentiles of O_3 are also important and it is hard to define a precise threshold below which O_3 is not harmful. Thus the dose of O_3 to humans through respiration may be the more important guide to the potential threat, and as the SOMO10 (and the mean values) have changed little with time, the suggested improvement in air quality from the EEA may be more apparent than real. An important policy implication of these trends is the degree to which local, regional or global policies are required to decrease the threat to human health from O_3. In the case of exposures to O_3 in excess of 60 ppb, controls at the European and national scales can be effective, as the measurements demonstrate. However, if the mean or lower percentiles are important, as suggested in recent syntheses, then controls at much larger (hemispheric) scales are required.

3.2 O_3 vegetation-impact chemical climates

The detailed statistics describing the impacts of O_3 on crops at Harwell and Auchencorth, as derived using the POD_Y metric, are presented in Tables S3 and S4 for potato and Tables S5 and S6 for wheat, and as derived using the generic crop AOT40 metric for a May–July growing season in Tables S7 and S8. The statistics for the POD_Y metric for forest trees are presented in Tables S9 and S10 for beech, and Tables S11 and S12 for Scots pine. The POD_Y statistics presented in Tables S5–S12, and Figs. 8–13 were calculated for the loam (medium) soil texture (Büker et al., 2012). The representativeness of the conclusions derived from the interpretation of these statistics to other soil textures is discussed in Sect. 3.2.1 and 3.2.2. This section presents two analyses of the impact, state and drivers of the chemical climatology framework (Fig. 2, steps 1–5); specifically, changes in chemical climate phase (Fig. 2, Step 6) temporally at Harwell between 1990 and 2013 (Sect. 3.2.1) and spatially between Auchencorth and Harwell (Sect. 3.2.2).

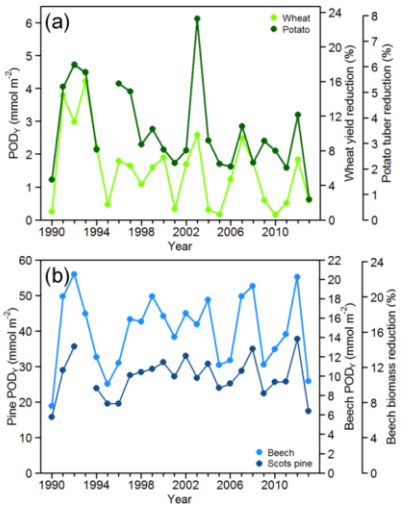

Figure 8. Impact of O_3 characterised by the POD_Y metric (and associated response) for **(a)** wheat (grain yield reduction), potato (tuber weight reduction), **(b)** beech (biomass reduction) and Scots pine at Harwell between 1990 and 2013.

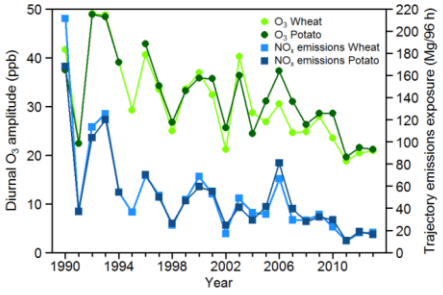

Figure 9. Amplitude of the diurnal O_3 cycle at Harwell during June POD_Y accumulation days for wheat and potato and hourly European NO_x emission estimate for the EMEP 0.5° grids over which 96 h back trajectories passed prior to arrival at Harwell during June POD_Y accumulation days for wheat and potato.

3.2.1 Long-term changes in vegetation impact at Harwell (1990–2013)

Figure 8 shows the impact of O_3 on vegetation at Harwell, as quantified by the relevant POD_Y and response (grain yield for wheat, tuber weight for potato and biomass reduction for beech). The 1990–2013 average POD_Y values calculated using sandy loam (coarse), silt loam (medium coarse), loam (medium) and clay loam (fine) soil texture properties are shown in Table 1. The ratio between the largest and smallest average POD_Y due to differences in soil moisture for the different soil textures was 1.57 (wheat), 1.32 (potato), 1.14 (beech) and 1.10 (Scots pine), but the annual pattern of POD_Y accumulation was consistent across the four soil textures. The statistics in the following sections are those calculated for the loam soil texture, unless otherwise stated, which has intermediate hydraulic properties compared with the three other soil textures.

For crops, there has not been a statistically significant change in POD_Y between 1990 and 2013, across all soil textures. Using the critical levels for adverse vegetation damage agreed by the UN Convention on Long-range Transboundary Air Pollution (LRTAP; Mills et al., 2011c), O_3 has a greater impact on wheat than potato at Harwell, with 13 of the 24 years exceeding the 5 % yield reduction critical level for wheat, compared to 6 years exceeding the 5 % tuber weight reduction critical level for potato. Mills et al. (2011a), using modelled O_3 and meteorological data to assess the impact of O_3 on vegetation across the UK in 2006 and 2008, also reported a smaller impact on potato than wheat, due to the lower sensitivity of potato to O_3.

The majority of POD_Y accumulation for potato and wheat occurred in June (Tables S3 and S5). Between 1990 and 2013 there were significant decreases in diurnal O_3, NO_2 and NO amplitudes on June ADs (Fig. 9, Tables S3 and S5). The median trend in diurnal O_3 amplitude on June ADs was -2.0 and $-2.4\,\%\,y^{-1}$ for potato and wheat respectively ($p = 0.001$), and, in the latter period (2010–2013), the difference in diurnal O_3 amplitude between June ADs and NADs was small (Tables S3 and S5). Figure 10 shows the percentage of POD_Y accumulated during different measured hourly O_3 concentration ranges. There were significant decreasing trends in the contribution from the highest concentration bins (65–70 ppb and > 70 ppb) for potato (-0.4–$-1.4\,\%\,y^{-1}$) and from the 55–60 and 65–70 ppb concentrations bins for wheat. In contrast, there were increasing trends in POD_Y contribution from the 25–45 ppb O_3 concentration bins for potato (0.1–$0.8\,\%\,y^{-1}$) and from the 30–45 ppb concentration bins for wheat (0.5–$1.1\,\%\,y^{-1}$). These trends were due to a decreasing frequency of hours with O_3 concentrations in the range between 55 and > 70 ppb during the growing seasons of potato (-3.0–$-4.3\,\%\,y^{-1}$) and wheat (-2.1–$-4.8\,\%\,y^{-1}$) and increasing frequency of hourly O_3 concentrations in the range 25–45 ppb (wheat) and 20–35 ppb (potato). For both crops, the estimated back-trajectory NO_x emissions on ADs decreased significantly in the period 1990–2013 for each month of the growing season (Fig. 9 shows this decrease for ADs in June), with trends ranging from -2.5 to $-4.3\,\%\,y^{-1}$. Other drivers such as temperature, global radia-

Table 1. Average ± SD wheat, potato, beech and Scots pin POD_Y calculated for four different soil textures (see Bueker et al., 2012, for a description of their hydraulic properties) over the monitoring periods at Harwell and Auchencorth.

	Sandy loam (coarse)	Silt loam (medium coarse)	Loam (medium)	Clay loam (fine)
Harwell 1990–2013 average				
Wheat POD_Y (mmol m^{-2}) (grain yield % reduction)	1.21 ± 1.07 (4.61 %)	1.75 ± 1.19 (6.64 %)	1.51 ± 1.14 (5.72 %)	1.90 ± 1.19 (7.22 %)
Potato POD_Y (mmol m^{-2}) (tuber yield % reduction)	2.35 ± 1.27 (3.03 %)	3.10 ± 1.42 (3.99 %)	2.64 ± 1.32 (3.40 %)	3.10 ± 1.46 (4.00 %)
Beech POD_Y (mmol m^{-2}) (biomass % reduction)	14.0 ± 3.7 (15.4 %)	16.0 ± 3.5 (17.6 %)	14.7 ± 3.7 (16.2 %)	16.1 ± 3.4 (17.7 %)
Pine POD_Y (mmol m^{-2})	26.2 ± 5.5	28.7 ± 5.3	27.0 ± 5.6	28.8 ± 5.3
Auchencorth 2007–2013 average				
Wheat POD_Y (mmol m^{-2}) (grain yield % reduction)	0.85 ± 0.45 (3.23 %)	1.01 ± 0.38 (3.86 %)	0.96 ± 0.39 (3.65 %)	1.05 ± 0.37 (3.99 %)
Potato POD_Y (mmol m^{-2}) (tuber yield % reduction)	0.95 ± 0.41 (1.22 %)	1.08 ± 0.46 (1.39 %)	0.99 ± 0.41 (1.28 %)	1.09 ± 0.47 (1.40 %)
Beech POD_Y (mmol m^{-2}) (biomass % reduction)	16.6 ± 1.6 (18.3 %)	16.9 ± 1.2 (18.6 %)	16.7 ± 1.5 (18.4 %)	16.9 ± 1.2 (18.6 %)
Pine POD_Y (mmol m^{-2})	35.9 ± 3.6	36.5 ± 2.7	36.2 ± 3.3	36.6 ± 2.7

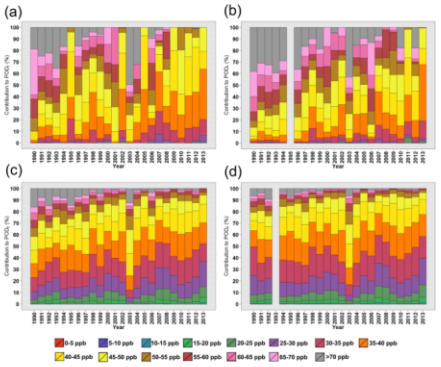

Figure 10. Relative annual contributions to **(a)** wheat POD_Y, **(b)** potato POD_Y, **(c)** beech POD_Y and **(d)** Scots pine POD_Y at Harwell from different O_3 concentration bins. Concentrations are separated into 15 5 ppb groups spanning hourly O_3 concentrations between 0 ppb and > 70 ppb. Note: these concentration bins are contributing to constant trends in POD_Y for each vegetation type – see Fig. 7.

tion and back-trajectory pathway did not change significantly between 1990 and 2013 (Tables S3 and S5).

For beech and Scots pine, there was no significant trend in POD_Y between 1990 and 2013 across all soil types (Fig. 8). The average POD_Y for beech (Table 1) was 4 times the critical level (Mills et al., 2011c). Beech and Scots pine POD_Y values were substantially higher than for the crops, due to a lower threshold for exceedance, a longer growing season and other differences in the stomatal conductance response to T, PAR, VPD and SWP. The average beech POD_Y value calculated here is comparable with the estimate for beech POD_Y modelled by Simpson et al. (2007) for the south-east of England (8–16 mmol m^{-2}), but both values were higher than the values estimated in Emberson et al. (2007) for three European climate regions (not including UK) in 1997.

The low 1 nmol m^{-2} s^{-1} threshold for POD_Y accumulation for beech and Scots pine was exceeded during the majority of days during the respective growing seasons. The major contributions by month to POD_Y were consistently May and June for beech and April, May and June for Scots pine (Tables S9 and S11). During 1990–2013 diurnal O_3 amplitude decreased significantly on beech and Scots pine ADs between May and September, with median monthly AD trends between −1.5 and −2.3 % y^{-1} for beech and −1.3 and −2.4 % y^{-1} for Scots pine. Across the 24-year period there was a more consistent major contribution to POD_Y during hourly O_3 concentrations in the range 25–50 ppb compared to wheat and potato, especially for Scots pine (Fig. 10c and d). For beech and Scots pine, the trends in contribution from different concentration bins were smaller compared to crops. Decreasing trends in POD_Y contribution were significant for concentration bins between 50 and > 70 ppb (−0.1–−0.4 % y^{-1} for beech and −0.1–−0.2 % y^{-1} for Scots pine), and significant increasing trends in more moderate concen-

tration bins (25–40 ppb) were only apparent for beech. During the growing season of each tree, the frequency of high O_3 concentrations (between 55 and > 70 ppb) decreased significantly (-2.5–$-5.3\,\%\,y^{-1}$ for both trees), and there was an increase in the frequency of concentrations between 25 and 35 ppb ($+1.4$–$+2.2\,\%\,y^{-1}$ for both trees). Karlsson et al. (2007) calculated a similar result for Norway Spruce in Sweden, where between 2002–2004 approximately 80 % of POD_Y was accumulated during O_3 concentrations between 30 and 50 ppb. The estimated NO_x emissions into the air-mass trajectories also decreased significantly during beech and Scots pine ADs, with median monthly trends ranging from -3.2 to $-3.6\,\%\,y^{-1}$ for beech and -1.9 to $-3.7\,\%\,y^{-1}$ for Scots pine.

The significant trends in state (pollutant diurnal variation and concentration bin contributions) and drivers (trajectory emission estimates) for the four vegetation types (Fig. 9 and Tables S3, S5, S9 and S11) indicate an increase in the relative importance of hemispheric background O_3 concentrations in determining POD_Y. Despite this change POD_Y values have not decreased, in contrast to SOMO35, for which decreased contribution from high O_3 concentrations (produced during regional O_3 episodes) resulted in a decreasing trend. This was due to non-O_3 factors such as stomatal response to VPD and soil moisture which also determine the severity of a vegetation impact by limiting the O_3 flux during high O_3 concentration episodes, reducing the sensitivity of POD_Y values to decreases in regional O_3 production. For example, during the potato growing season the median stomatal conductance during hours with O_3 concentrations in the ranges 60–65, 65–70 and > 70 ppb were 86, 90 and 65 mmol $m^{-2}\,s^{-1}$ respectively (median across 1990–2013). These are significantly lower than the maximum stomatal conductance for potato of 750 mmol $m^{-2}\,s^{-1}$ (LRTAP Convention, 2010) and similar to the median stomatal conductances calculated during more moderate O_3 concentrations, such as 35–40 ppb (54 mmol $m^{-2}\,s^{-1}$), 40–45 ppb (68 mmol $m^{-2}\,s^{-1}$) and 45–50 ppb (87 mmol $m^{-2}\,s^{-1}$).

Soil water potential is a soil-texture-dependent determinant of potato stomatal conductance in the DO_3SE model, which decreases when SWP is lower than -0.5 MPa (LRTAP Convention, 2010; Büker et al., 2012). The 1990–2013 average SWP during hours when O_3 concentrations at Harwell were in the concentration ranges 60–65, 65–70 and > 70 ppb were -1.50 ± 1.32 MPa, -1.14 ± 0.93 MPa and -1.10 ± 0.90 MPa respectively for the clay loam (fine) soil texture. The average SWP during these O_3 concentration ranges were lower and even more limiting for the other three soil textures. These are substantially lower than the average SWP for the O_3 concentration ranges between 25 and 50 ppb, all of which are above the -0.5 MPa cut-off except 45–50 ppb for sandy loam, silt loam and loam soil textures (average SWP of -0.65, -0.52 and -0.58 MPa respectively). Across all soil textures, reduction in the frequency of elevated O_3 concentrations produced during regional photochemical episodes has therefore not reduced POD_Y, as these elevated O_3 concentrations coincided with other factors (e.g. SWP) which limit stomatal conductance and hence any potential increase in O_3 accumulation resulting from increased O_3 concentrations. Decreasing regional O_3 production resulted in the largest change in concentration bin contributions for potato POD_Y (Fig. 10b). This is due to a later growing season than wheat and a shorter accumulation period and higher maximum stomatal conductance than forest trees (150 and 180 mmol $m^{-2}\,s^{-1}$ for beech and Scots pine respectively compared to 750 mmol $m^{-2}\,s^{-1}$ for potato), limiting the O_3 flux during high O_3 episodes.

These non-O_3 factors, such as SWP, also determine the annual pattern of POD_Y accumulation. For example, between 2010 and 2013 at Harwell the average SWP on potato ADs in June was -0.11 MPa compared to -0.72 MPa on NADs (loam soil texture). Hence in June O_3 concentrations were sufficient that, when plant conditions were favourable, accumulation of POD_Y occurred. In July, SWP was substantially higher due to increased temperatures (2010–2013 average SWP on potato ADs was -1.02 MPa). This, combined with decreasingly favourable potato and wheat phenology and reduced potato and wheat stomatal conductance, led to a smaller contribution to total POD_Y in July than in June. Higher O_3 concentrations were therefore needed to accumulate POD_Y; these occurred during regional photochemical O_3 production, hence the larger difference between diurnal O_3 amplitude on AD and NADs in July than in June for the two crops.

For beech and Scots pine, the proportion of POD_Y accumulated in May and June was higher than in July and August, despite no change in phenology used in the DO_3SE model from May to August, and exceedance of the 1 mmol $m^{-2}\,s^{-1}$ threshold on the majority of days. For beech, reduction in stomatal conductance occurs when SWP is lower than -0.8 MPa (LRTAP Convention, 2010). Between 2010 and 2013, across the four soil textures, on average 0 and 0–9 % of hourly SWP values in May and June respectively were below this value, compared to 23–51 and 18–31 % in July and August respectively. The effect of SWP on stomatal conductance begins at -0.7 MPa for Scots pine and therefore has a larger limiting effect. SWP was also found to be one of the most important limiting factors in determining the impact of O_3 on forests across Europe (Emberson et al., 2007). Clay loam had the highest SWP of the four soil textures and therefore the lowest limitation to stomatal conductance, followed by silt loam, loam and sandy loam. However, the variation in soil moisture between different soil textures due to differences in the extent of evaporation is sufficiently small that the lack of long-term trend in POD_Y and annual pattern of accumulation is consistent across the soil textures.

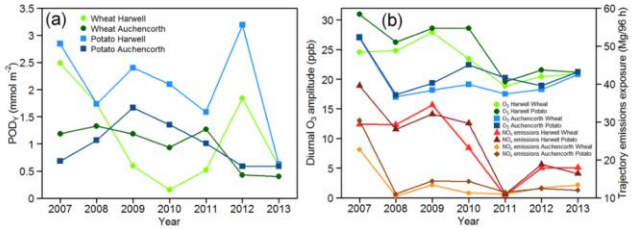

Figure 11. Comparison of O_3 vegetation impact chemical climates for wheat and potato 2007–2013: **(a)** annual POD_Y for wheat and potato, **(b)** diurnal O_3 amplitude during June accumulation days (ADs) at Harwell and Auchencorth and trajectory NO_x emission estimates at Harwell and Auchencorth.

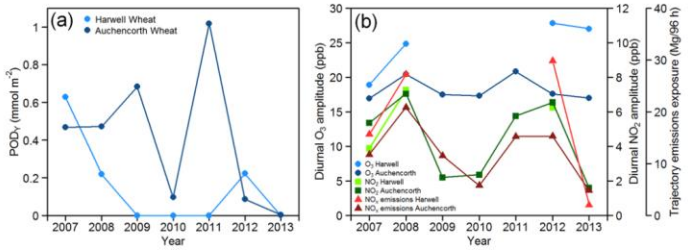

Figure 12. (a) Wheat POD_Y accumulated during July at Harwell and at Auchencorth, 2007–2013. **(b)** Diurnal cycle amplitude of O_3 and NO_2 and back-trajectory NO_x emission estimates during wheat accumulation days (ADs) in July at Harwell and at Auchencorth, 2007–2013.

3.2.2 Spatial differences between Auchencorth and Harwell (2007–2013)

The 2007–2013 average POD_Y calculated for the four soil textures is shown in Table 1, and the variation between soil textures is less than at Harwell. The ratio between the largest and smallest average POD_Y due to differences in soil moisture for the different soil textures was 1.24 (wheat), 1.15 (potato), 1.02 (beech) and 1.02 (Scots pine). The pattern of accumulation, as well as spatial differences between Harwell and Auchencorth, were consistent across soil textures. Annual POD_Y for potato at Auchencorth (Table S4) was consistently lower than at Harwell, while POD_Y for wheat were higher at Auchencorth (Table S6) for 3 of the 7 years. The LRTAP critical level for impact (Mills et al., 2011c) was only exceeded at this site in 2008 for wheat (5.04 % yield reduction). These observations, determined using measured O_3 and meteorological data, are consistent with the spatial patterns identified by Mills et al. (2011a) in which modelled O_3 and meteorological variables were used to model POD_Y in 10×10 km grids across the UK. However, the calculated 2008 tuber weight reduction of 1.4 % for potato at Auchencorth is higher than the 0 % reduction estimated for the grids containing Auchencorth. Simpson et al. (2007) also modelled wheat POD_Y across Europe for 2000 and calculated POD_Y in south-east Scotland at 0.5–1 mmol m^{-2} and in south-east England at 1–3 mmol m^{-2}, which are similar values to those determined here using the measurement data at Harwell and Auchencorth. In general, diurnal amplitudes of O_3, NO_2 and NO and back-trajectory NO_x emission estimates were lower at Auchencorth (shown in Fig. 11b for wheat and potato POD_Y ADs in June), which indicates a greater importance of hemispheric background concentrations in determining the O_3 impact at Auchencorth on wheat and potato.

Periods with elevated regional O_3 influence at Auchencorth can lead to a larger effect on POD_Y compared to Harwell. For example, in 2008 across all soil textures July contributed 0.47 mmol m^{-2} (36 % total) to wheat POD_Y (Fig. 12a). In this month, O_3 concentrations at Auchencorth had a significant regional photochemical contribution, evidenced by elevated diurnal O_3 and NO_2 variation and 71 % higher back-trajectory NO_x emissions on ADs compared to the 2007–2013 average (Fig. 12b). POD_Y in July 2011 at Auchencorth was also influenced by regional O_3 production. Diurnal O_3 amplitude in July 2011 was 6 ppb higher on ADs than on NADs and global radiation during ADs was 26% higher than the AD average. July 2011 contributed 80 % of the annual wheat POD_Y at Auchencorth across all soil tex-

tures. At Harwell in July 2008, wheat POD_Y was less than half the Auchencorth value, and in July 2011 there was no POD_Y accumulation despite elevated regional O_3 influence in both cases. These two examples demonstrate that elevated regional photochemical O_3 production can have a larger crop impact, characterised through POD_Y, in south-east Scotland than in south-east England, despite being further from major sources of O_3 precursor emissions. The meteorological conditions conducive to regional photochemical O_3 production (higher temperature and global radiation) at Harwell resulted in unfavourable conditions for high O_3 stomatal conductance in crops compared to Auchencorth. The median daytime O_3 stomatal conductance was 58 and 63 mmol m^{-2} s^{-1} in July 2008 and 2011 respectively for loam soil texture at Harwell, compared to 94 and 95 mmol m^{-2} s^{-1} at Auchencorth. Average SWP in July 2008 and 2011 was respectively −0.03 and −0.02 MPa at Auchencorth and −0.63 and −1.17 MPa at Harwell. In addition, lower temperatures at Auchencorth result in a longer accumulated temperature growing season. In July 2008 and 2011, the phenological limitation on wheat stomatal conductance was similar for the first 3 weeks of the month at both sites but diverged in the final week and was substantially more limiting at Harwell at the end of July (40 and 50 % lower in 2008 and 2011 respectively), also resulting in less favourable conditions for POD_Y accumulation in south-east England.

Between 2007 and 2013, Scots pine and beech POD_Y were on average 27–37 and 5–19 % higher at Auchencorth compared to Harwell across the soil textures (Table 1 and Fig. 13a). These larger values were due to larger contributions from July and August at Auchencorth (Tables S10 and S12). In these months, higher temperatures at Harwell produced conditions which reduced stomatal conductance. For example, during 2007–2013 at Harwell for loam soil texture, SWP was on average 59 % higher in July and 82 % higher in August than at Auchencorth.

Elevated regional photochemical O_3 production also had varying impacts on forest trees at the two sites. In May 2008 across all soil textures, accumulated POD_Y was elevated at Auchencorth for both Scots pine and beech (Fig. 13b). Larger diurnal O_3 variation (28 % higher than the 2007–2013 average) and back-trajectory NO_x emissions (53 % higher) during May 2008 indicate regional photochemical O_3 production made a significant contribution to measured O_3 concentrations at Auchencorth (Fig. 13c). Despite larger increases in these variables at Harwell, the accumulated POD_Y in May 2008 was 14 and 29 % less than at Auchencorth for beech and Scots pine respectively across all soil textures (Fig. 13b), and the frequency of hours with high POD_Y accumulation was lower at Harwell. For example, the maximum hourly POD_Y accumulated at Harwell and Auchencorth in May 2008 were 0.027 and 0.033 mmol m^{-2} respectively and there were 21 fewer hours when hourly POD_Y accumulated was above 0.02 mmol m^{-2} compared to Auchencorth. Hence the conditions during this regional O_3 episode at Harwell, e.g. a 12 % increase in monthly average temperature, also produced less favourable plant conditions for POD_Y accumulation.

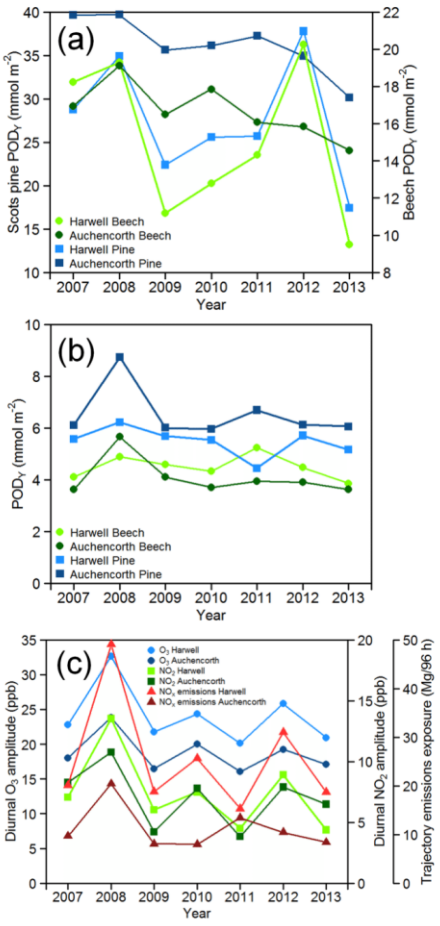

Figure 13. Comparison of O_3 vegetation-impact chemical climates for beech and Scots pine 2007–2013 at Harwell and Auchencorth: **(a)** annual POD_Y for beech and Scots pine; **(b)** POD_Y accumulated in May for beech and Scots pine; **(c)** May monthly average diurnal amplitude of O_3 and NO_2 and back-trajectory NO_x emission estimates.

3.2.3 Comparison between POD_Y and AOT40

The chemical climates based on the AOT40 metric (Tables S7 and S8) were derived for the crop-based AOT40 definition and are therefore most comparable with the wheat and potato POD_Y chemical climates. At Harwell, there was a significant long-term decrease in AOT40 from an average of 6533 ppbh during 1990–1993 to an average of 2623 ppbh during 2010–2013 (trend: $-3.6\,\%\,y^{-1}$, $p = 0.001$, Fig. 14, Table S7). This decrease in AOT40 is in contrast to the trends in wheat and potato POD_Y at Harwell, which showed no significant trend across the 24-year period (Fig. 8a). However, the AOT40 climate showed similar decreases in diurnal pollutant amplitudes and back-trajectory NO_x emission estimates compared to the crop POD_Y climates, indicating increased importance of hemispheric background concentrations. This is in line with Derwent et al. (2013), who reported an increase between 1989 and 2012 in AOT40 when selecting hemispheric background air arriving at Mace Head, Ireland. AOT40 at Auchencorth was lower than at Harwell, and the magnitude of the difference was much larger than for POD_Y. This was similar to the spatial differences in Jenkin (2014), in which estimated regional background AOT40 was twice as large at Harwell compared to a rural site in central Scotland (EMEP site GB0033R: Bush).

The spatial difference between sites was less for POD_Y because AOT40 does not account for modification of stomatal conductance, especially during summer months when SWP at Harwell can be low. Hence the average contribution from July 2010–2013 to AOT40 was 35 % but for wheat POD_Y only 3 % (Tables S5 and S7). Conversely, the contribution from July to AOT40 at Auchencorth is lower than the contribution to wheat and potato POD_Y (Tables S6 and S8), indicating that O_3 concentrations below the 40 ppb threshold determine the wheat and potato POD_Y to a large extent during this month. The limitations of the fixed growing season in the AOT40 concept have been detailed previously (RoTAP, 2012; Coyle et al., 2003), including the observation that there can be significant impact on vegetation below the 40 ppb threshold. For forest trees, Gauss et al. (2014) reported forest-based AOT40 across the UK from 2007 to 2012 to be between 5 and 50 % lower than that calculated in 2000. In addition, Klingberg et al. (2014) found a much smaller decline in forest-specific POD_Y than AOT40 between 1960 and 2100 using modelled O_3 and meteorological data at 14 sites across Europe.

In summary, the crop-based AOT40 trend at Harwell showed an improvement in O_3 crop impact which is not shown when the interaction between plant and O_3 climates are modelled using biologically more relevant POD_Y metric.

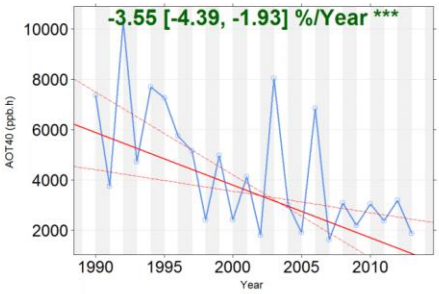

Figure 14. Crop-relevant AOT40 (calculated between May and July) at Harwell for the period 1990–2013. The Theil–Sen trend estimate of median trend (shown in red) is $-3.6\,\%\,y^{-1}$ ($p = 0.001$).

4 Conclusions

A chemical climatology framework was applied to characterise O_3 exposure associated with human health and vegetation impacts using measured data at the Harwell and Auchencorth UK EMEP supersites. These sites have been shown to be representative of rural O_3 over the wider geographic areas of south-east England and northern UK respectively.

At Harwell, each chemical climate analysis indicated a decrease over the period 1990–2013 in the relative importance of regional photochemical O_3 production, associated with NO_x emission reductions, and an increase in relative importance of hemispheric background concentrations. However, trends in the human health and vegetation metrics associated with these changes were different.

As quantified by the SOMO35 metric, the human health-relevant O_3 exposure at Harwell decreased significantly over the period 1990–2013 ($-2.2\,\%\,y^{-1}$), while quantification using the SOMO10 metric showed no trend due to its lower dependence on the highest O_3 concentrations, which have decreased due to declining regional photochemical production. Hence the choice of these two O_3 concentration thresholds, both recommended by WHO REVIHAAP for health impact assessments, determines both the perceived annual pattern of health burden and whether there has been improvement in time. The policy significance of these findings is important since the regional policies adopted to date, regarding controls on NO_x and VOC emissions in Europe, have been effective in reducing peak concentrations and exposure. The growth in these emissions elsewhere has increased the importance of background contribution to O_3 exposure in the UK. The effective controls for background O_3 would be controls at hemispheric scales on O_3 precursors and in methane emissions especially.

The POD_Y metrics used to quantify the impact of O_3 on vegetation showed no change over the period 1990–2013 at

Harwell for wheat and potato crops and beech and Scots pine trees, in contrast to a decreasing trend in potential impact when quantified by the crop AOT40 metric. The contrast highlights the need to model vegetation impacts using the biologically more relevant POD_Y metrics. The potential reductions in vegetation impact (i.e. POD_Y), due to decreases in regional photochemical O_3 production decreases (as reflected in the decrease in crop AOT40 at Harwell), did not occur due to the other factors that reduce plant stomatal conductance and hence accumulated O_3 uptake (e.g. changing plant phenology and low soil water potential). Thus the long-term decrease in regional O_3 production evident at Harwell led to a lower beneficial effect on POD_Y than on SOMO35.

The chemical climates indicate a greater influence of hemispheric background concentrations at Auchencorth compared to Harwell (for the period 2007–2013). SOMO10 values were similar at both sites, but SOMO35 was lower at Auchencorth. POD_Y values were larger for vegetation species with longer growing seasons and lower thresholds for exceedance compared to Harwell (i.e. for beech and Scots pine). In addition, more favourable plant conditions (higher SWP, longer accumulated temperature-derived growing season) during periods of elevated regional O_3 production resulted in exacerbation of vegetation impacts at Auchencorth compared to Harwell. Hence the potential for O_3 vegetation impact reduction from future reductions in regional O_3 is greater at Auchencorth than at Harwell, despite being further from the major sources of O_3 precursors. However, the policies required to substantially reduce exposure of vegetation in the UK to damage from O_3, like those for human health, are measures that reduce the background O_3 concentrations – hence the need for hemispheric control measures on O_3 precursors.

The Supplement related to this article is available online at doi:10.5194/acp-15-4025-2015-supplement.

Acknowledgements. C. S. Malley acknowledges the University of Edinburgh School of Chemistry, the NERC Centre for Ecology & Hydrology (NERC-CEH studentship funding project no. NEC04544) and the UK Department for Environment, Food and Rural Affairs (Defra, grant no. AQ0647) for funding. Defra contractors Ricardo-AEA, Bureau Veritas and NERC Centre for Ecology & Hydrology and their field teams are acknowledged for operating the UK EMEP Supersites. Particular acknowledgement goes to Mhairi Coyle for valuable discussion regarding AOT40 calculation and to David Fowler for insightful discussion regarding POD_Y vegetation assessment and for helpful guidance on the policy relevancy of this work.

Edited by: P. Monks

References

Abbatt, J., George, C., Melamed, M., Monks, P., Pandis, S., and Rudich, Y.: New Directions: Fundamentals of atmospheric chemistry: Keeping a three-legged stool balanced, Atmos. Environ., 84, 390–391, 2014.

Angus Smith, R.: Air and Rain: The Beginnings of a Chemical Climatology, Longmans, Green and Co., London, 1872.

AQEG: Ozone in the United Kingdom: Air Quality Expert Group, Defra Publications, London, available at: http://uk-air.defra.gov.uk/assets/documents/reports/aqeg/aqeg-ozone-report.pdf (last access: 19 January 2015), 2009.

Büker, P., Morrissey, T., Briolat, A., Falk, R., Simpson, D., Tuovinen, J. P., Alonso, R., Barth, S., Baumgarten, M., Grulke, N., Karlsson, P. E., King, J., Lagergren, F., Matyssek, R., Nunn, A., Ogaya, R., Peñuelas, J., Rhea, L., Schaub, M., Uddling, J., Werner, W., and Emberson, L. D.: DO3SE modelling of soil moisture to determine ozone flux to forest trees, Atmos. Chem. Phys., 12, 5537–5562, doi:10.5194/acp-12-5537-2012, 2012.

Carslaw, D. C. and Ropkins, K.: Openair: Open-source tools for the analysis of air pollution data, R package version 0.8-5, 2013.

Coyle, M., Smith, R. I., Stedman, J. R., Weston, K. J., and Fowler, D.: Quantifying the spatial distribution of surface ozone concentration in the UK, Atmos. Environ., 36, 1013–1024, 2002.

Coyle, M., Fowler, D., and Ashmore, M.: New directions: Implications of increasing tropospheric background ozone concentrations for vegetation, Atmos. Environ., 37, 153–154, 2003.

Derwent, R., Manning, A., Simmonds, P., Gerard Spain, T., and O'Doherty, S.: Analysis and interpretation of 25 years of ozone observations at the Mace Head Atmospheric Research Station on the Atlantic Ocean coast of Ireland from 1987 to 2012, Atmos. Environ., 80, 361–368, 2013.

Draxler, R. R. and Rolph, G. D.: HYSPLIT (HYbrid Single-Particle Lagrangian Integrated Trajectory) Model access via NOAA ARL READY Website, NOAA Air Resources Laboratory, available at: http://www.arl.noaa.gov/HYSPLIT.php (last access: 19 January 2015), College Park, MD., 2013.

Eaton, S. and Stacey, B.: QA / QC Data Ratification Report for the Automatic Urban and Rural Network, October–December 2011, and Annual Report 2011, AEAT/ENV/R/3284 Issue 1. Contract Report to the Department for Environment, Food and Rural Affairs, AEA, available at: http://uk-air.defra.gov.uk/assets/documents/reports/cat05/1207040912_AURN_2011_Q4_Issue_1.pdf (last access: 19 January 2015), 2012.

EEA: Overview of exceedances of EC ozone threshold values: April–September 2013. EEA technical report No 3/2014, European Environment Agency, available at: http://www.eea.europa.eu/publications/air-pollution-by-ozone-across-1, 2014a.

EEA: EU emission inventory report 1990-2012 under the UNECE Convention on long-range transboundary air pollution (LRTAP). EEA technical report No 12/2014, European Environment Agency, available at: http://www.eea.europa.eu/publications/eu-emission-inventory-report-lrtap, 2014b.

Emberson, L. D., Ashmore, M. R., Cambridge, H. M., Simpson, D., and Tuovinen, J. P.: Modelling stomatal ozone flux across Europe, Environ. Pollut., 109, 403–413, 2000.

Emberson, L. D., Buker, P., and Ashmore, M. R.: Assessing the risk caused by ground level ozone to European forest trees: A case

study in pine, beech and oak across different climate regions, Environ. Pollut., 147, 454–466, 2007.

EMEP: Transboundary particulate matter, photo-oxidants, acidifying and eutrophying components. EMEP Status Report 1/2014. European Monitoring and Evaluation Programme, available at: http://emep.int/publ/reports/2014/EMEP_Status_Report_1_2014.pdf (last access: 19 January 2015), 2014.

Fuhrer, J., Skarby, L., and Ashmore, M. R.: Critical levels for ozone effects on vegetation in Europe, Environ. Pollut., 97, 91–106, 1997.

Gauss, M., Semeena, V., Benedictow, A., and Klein, H.: Transboundary air pollution by main pollutants (S, N, Ozone) and PM: The United Kingdom. MSC-W Data Note 1/2014, available at: http://www.emep.int/publ/reports/2012/Country_Reports/report_GB.pdf (last access: 19 January 2015), 2014.

Guerreiro, C. B. B., Foltescu, V., and de Leeuw, F.: Air quality status and trends in Europe, Atmos. Environ., 98, 376–384, 2014.

Heal, M. R., Heaviside, C., Doherty, R. M., Vieno, M., Stevenson, D. S., and Vardoulakis, S.: Health burdens of surface ozone in the UK for a range of future scenarios, Environ. Int., 61, 36–44, 2013.

Jenkin, M.: Trends in ozone concentration distributions in the UK since 1990: Local, regional and global influences, Atmos. Environ., 42, 5434–5445, 2008.

Jenkin, M.: Investigation of an oxidant-based methodology for AOT40 exposure assessment in the UK, Atmos. Environ., 94, 332–340, 2014.

Karlsson, P. E., Tang, L., Sundberg, J., Chen, D., Lindskog, A., and Pleijel, H.: Increasing risk for negative ozone impacts on vegetation in northern Sweden, Environ. Pollut., 150, 96–106, 2007.

Kaufman, L. and Rousseeuw, P. J.: Finding Groups in Data: An Introduction to ClusterAnalysis, Wiley, New York, Wiley, New York, 1990.

Klingberg, J., Engardt, M., Uddling, J., Karlsson, P. E., and Pleijel, H.: Ozone risk for vegetation in the future climate of Europe based on stomatal ozone uptake calculations, Tellus A, 63, 174–187, 2011.

Klingberg, J., Engardt, M., Karlsson, P. E., Langner, J., and Pleijel, H.: Declining ozone exposure of European vegetation under climate change and reduced precursor emissions, Biogeosciences, 11, 5269–5283, doi:10.5194/bg-11-5269-2014, 2014.

Kuhlbusch, T., Quincey, P., Fuller, G., Kelly, F., Mudway, I., Viana, M., Querol, X., Alastuey, A., Katsouyanni, K., Weijers, E., Borowiak, A., Gehrig, R., Hueglin, C., Bruckmann, P., Favez, O., Sciare, J., Hoffmann, B., EspenYttri, K., Tørseth, K., Sager, U., Asbach, C., and Quass, U.: New Directions: The future of European urban air quality monitoring, Atmos. Environ., 87, 258–260, 2014.

Lee, J. D., Lewis, A. C., Monks, P. S., Jacob, M., Hamilton, J. F., Hopkins, J. R., Watson, N. M., Saxton, J. E., Ennis, C., Carpenter, L. J., Carslaw, N., Fleming, Z., Bandy, B. J., Oram, D. E., Penkett, S. A., Slemr, J., Norton, E., Rickard, A. R., Whalley, L. K., Heard, D. E., Bloss, W. J., Gravestock, T., Smith, S. C., Stanton, J., Pilling, M. J., and Jenkin, M. E.: Ozone photochemistry and elevated isoprene during the UK heatwave of August 2003, Atmos. Environ., 40, 7598–7613, 2006.

LRTAP Convention: Chapter 3 of the LRTAP Convention Manual of Methodologies for Modelling and Mapping Effects of Air Pollution, edited by: Mills, G., Pleijel, H., Büker, P., Braun, S., Emberson, L., Harmens, H., Simpson, D., Grünhage, L., Karlsson, P., Danielsson, H., Bermejo, V., and Gonzalez-Fernandez, I., available at: http://icpvegetation.ceh.ac.uk/ (last access: 19 January 2015), 2010.

Malley, C. S., Braban, C. F., and Heal, M. R.: The application of hierarchical cluster analysis and non-negative matrix factorization to European atmospheric monitoring site classification., Atmos. Res., 138, 30–40, 2014a.

Malley, C. S., Braban, C. F., and Heal, M. R.: New Directions: Chemical climatology and assessment of atmospheric composition impacts, Atmos. Environ., 87, 261–264, 2014b.

Mangiameli, P., Chen, S. K., and West, D.: A comparison of SOM neural network and hierarchical clustering methods, Eur. J. Oper. Res., 93, 402–417, 1996.

Mareckova, K., Wankmueller, R., Whiting, R., and Pinterits, M.: Review of emission data reported under the LRTAP Convention and NEC Directive, Stage 1 and 2 review, Review of emission inventories from shipping, Status of Gridded and LPS data, EEA and CEIP technical report, 1/2013, ISBN 978-3-99004-248-9, available at: http://www.ceip.at/review-of-inventories/review-2013/ (last access: 19 January 2015), 2013.

Mills, G., Hayes, F., Norris, D., Hall, J., Coyle, M., Cambridge, H., Cinderby, S., Abbott, J., Cooke, S., and Murrells, T.: Impacts of Ozone Pollution on Food Security in the UK: a Case Study for Two Contrasting Years, 2006 and 2008, Defra contract AQ0816, London, 2011a.

Mills, G., Hayes, F., Simpson, D., Emberson, L., Norris, D., Harmens, H., and Büker, P.: Evidence of widespread effects of ozone on crops and (semi-)natural vegetation in Europe (1990–2006) in relation to AOT40-and flux-based risk maps, Global. Change. Biol., 17, 592–613, 2011b.

Mills, G., Pleijel, H., Braun, S., Bueker, P., Bermejo, V., Calvo, E., Danielsson, H., Emberson, L., Gonzalez Fernandez, I., Gruenhage, L., Harmens, H., Hayes, F., Karlsson, P.-E., and Simpson, D.: New stomatal flux-based critical levels for ozone effects on vegetation, Atmos. Environ., 45, 5064–5068, 2011c.

Munir, S., Chen, H., and Ropkins, K.: Quantifying temporal trends in ground level ozone concentration in the UK, Sci. Total Environ., 458, 217–227, 2013.

Parrish, D. D., Law, K. S., Staehelin, J., Derwent, R., Cooper, O. R., Tanimoto, H., Volz-Thomas, A., Gilge, S., Scheel, H. E., Steinbacher, M., and Chan, E.: Lower tropospheric ozone at northern midlatitudes: Changing seasonal cycle, Geophys. Res. Lett., 40, 1631–1636, 2013.

R Core Development Team: R: A language and environment for statistical computing, R Foundation for Statistical Computing, Vienna, Austria, ISBN 3-900051-07-0, available at: http://www.R-project.org. (last access: 19 January 2015), 2008.

REVIHAAP: Review of evidence on health aspects of air pollution – REVIHAAP Project technical report. World Health Organization (WHO) Regional Office for Europe, Bonn, available at: http://www.euro.who.int/__data/assets/pdf_file/0004/193108/REVIHAAP-Final-technical-report-final-version.pdf (last access: 19 January 2015), 2013.

RoTAP: Review of Transboundary Air pollution: Acidification, Eutrophication, Ground Level Ozone and Heavy metals in the UK, Contract Report to the Department for Environment, Food and Rural Affairs, Centre for Ecology and Hydrol-

ogy, available at: http://www.rotap.ceh.ac.uk/sites/rotap.ceh.ac.uk/files/CEHRoTAP.pdf (last access: 19 January 2015), 2012.

Schmale, J., van Aardenne, J., and von Schneidemesser, E.: New Directions: Support for integrated decision-making in air and climate policies – Development of a metrics-based information portal, Atmos. Environ., 90, 146–148, 2014.

Simpson, D., Ashmore, M. R., Emberson, L., and Tuovinen, J. P.: A comparison of two different approaches for mapping potential ozone damage to vegetation. A model study, Environ. Pollut., 146, 715–725, 2007.

Simpson, D., Benedictow, A., Berge, H., Bergström, R., Emberson, L. D., Fagerli, H., Flechard, C. R., Hayman, G. D., Gauss, M., Jonson, J. E., Jenkin, M. E., Nyíri, A., Richter, C., Semeena, V. S., Tsyro, S., Tuovinen, J. P., Valdebenito, Á., and Wind, P.: The EMEP MSC-W chemical transport model – technical description, Atmos. Chem. Phys., 12, 7825–7865, doi:10.5194/acp-12-7825-2012, 2012.

Stedman, J. R. and Kent, A. J.: An analysis of the spatial patterns of human health related surface ozone metrics across the UK in 1995, 2003 and 2005, Atmos. Environ., 42, 1702–1716, 2008.

Tørseth, K., Aas, W., Breivik, K., Fjæraa, A. M., Fiebig, M., Hjellbrekke, A. G., Lund Myhre, C., Solberg, S., and Yttri, K. E.: Introduction to the European Monitoring and Evaluation Programme (EMEP) and observed atmospheric composition change during 1972–2009, Atmos. Chem. Phys., 12, 5447–5481, doi:10.5194/acp-12-5447-2012, 2012.

UK Meteorological Office: Met Office Integrated Data Archive System (MIDAS) Land and Marine Surface Stations Data (1853–current), (Internet), NCAS British Atmospheric Data Centre, 2014, available at: http://catalogue.ceda.ac.uk/uuid/220a65615218d5c9cc9e4785a3234bd0 (last access: 19 January 2015), 2012.

Vieno, M., Dore, A. J., Stevenson, D. S., Doherty, R., Heal, M. R., Reis, S., Hallsworth, S., Tarrason, L., Wind, P., Fowler, D., Simpson, D., and Sutton, M. A.: Modelling surface ozone during the 2003 heat-wave in the UK, Atmos. Chem. Phys., 10, 7963–7978, doi:10.5194/acp-10-7963-2010, 2010.

WHO: Air Quality Guidelines. Global update 2005. Particulate matter, ozone, nitrogen dioxide and sulfur dioxide., World Health Organisation Regional Office for Europe, Copenhagen, ISBN 92 890 2192 6, available at: http://www.euro.who.int/__data/assets/pdf_file/0005/78638/E90038.pdf (last access: 19 January 2015), 2006.

Wilson, R. C., Fleming, Z. L., Monks, P. S., Clain, G., Henne, S., Konovalov, I. B., Szopa, S., and Menut, L.: Have primary emission reduction measures reduced ozone across Europe? An analysis of European rural background ozone trends 1996–2005, Atmos. Chem. Phys., 12, 437–454, doi:10.5194/acp-12-437-2012, 2012.

Appendix V: Publication

This appendix contains the peer-review publication which formed the basis for Chapter 5.

Malley, C. S., Braban, C. F., Dumitrean, P., Cape, J.N., and Heal, M.R. (2015). The impact of speciated VOCs on regional ozone increment derived from measurements at the UK EMEP supersites between 1999 and 2012. *Atmospheric Chemistry & Physics Discussions*, 15, 7267-7308. 10.5194/acpd-15-7267-2015.

Atmos. Chem. Phys. Discuss., 15, 7267–7308, 2015
www.atmos-chem-phys-discuss.net/15/7267/2015/
doi:10.5194/acpd-15-7267-2015

Atmospheric Chemistry and Physics Discussions

The impact of speciated VOCs on regional ozone increment derived from measurements at the UK EMEP supersites between 1999 and 2012

C. S. Malley[1,2], C. F. Braban[1], P. Dumitrean[3], J. N. Cape[1], and M. R. Heal[2]

[1]NERC Centre for Ecology & Hydrology, Edinburgh, UK
[2]School of Chemistry, University of Edinburgh, Edinburgh, UK
[3]Ricardo-AEA, Didcot, UK

Received: 21 January 2015 – Accepted: 2 March 2015 – Published: 10 March 2015

Correspondence to: C. S. Malley (c.malley@sms.ed.ac.uk)

Published by Copernicus Publications on behalf of the European Geosciences Union.

Abstract

The impact of 27 volatile organic compounds (VOC) on the regional O_3 increment was investigated using measurements made at the UK EMEP supersites Harwell (1999–2001 and 2010–2012) and Auchencorth (2012). Ozone at these sites is representative of rural O_3 in south-east England and northern UK, respectively. Monthly-diurnal regional O_3 increment was defined as the difference between the regional and hemispheric background O_3 concentrations, respectively derived from oxidant vs. NO_x correlation plots, and cluster analysis of back trajectories arriving at Mace Head, Ireland. At Harwell, which had substantially greater regional ozone increments than at Auchencorth, variation in the regional O_3 increment mirrored afternoon depletion of VOCs due to photochemistry (after accounting for diurnal changes in boundary layer mixing depth, and weighting VOC concentrations according to their photochemical ozone creation potential). A positive regional O_3 increment occurred consistently during the summer, during which time afternoon photochemical depletion was calculated for the majority of measured VOCs, and to the greatest extent for ethene and m + p-xylene. This indicates that, of the measured VOCs, ethene and m + p-xylene emissions reduction would be most effective in reducing the regional O_3 increment, but that reductions in a larger number of VOCs would be required for further improvement.

The VOC diurnal photochemical depletion was linked to the sources of the VOC emissions through the integration of gridded VOC emissions estimates over 96 h air-mass back trajectories. This demonstrated that the effectiveness of VOC gridded emissions for use in measurement and modelling studies is limited by the highly aggregated nature of the 11 SNAP source sectors in which they are reported, as monthly variation in speciated VOC trajectory emissions did not reflect monthly changes in individual VOC diurnal photochemical depletion. Additionally, the major VOC emission source sectors during elevated regional O_3 increment at Harwell were more narrowly defined through disaggregation of the SNAP emissions to 91 NFR codes (i.e. sectors 3D2 (domestic solvent use), 3D3 (other product use) and 2D2 (food and drink)). However, spa-

ACPD
15, 7267–7308, 2015

The impact of speciated VOCs on regional ozone increment derived from measurements

C. S. Malley et al.

Title Page
Abstract Introduction
Conclusions References
Tables Figures
◀◀ ▶▶
◀ ▶
Back Close
Full Screen / Esc
Printer-friendly Version
Interactive Discussion

tial variation in the contribution of NFR sectors to parent SNAP emissions could only be accounted for at the country level. Hence, the future reporting of gridded VOC emissions in source sectors more highly disaggregated than currently (e.g. to NFR codes) would facilitate a more precise identification of those VOC sources most important for mitigation of the impact of VOCs on O_3 formation.

In summary, this work presents a clear methodology for achieving a coherent VOC regional-O_3-impact chemical climate using measurement data and explores the effect of limited emission and measurement species on the understanding of the regional VOC contribution to O_3 concentrations.

1 Introduction

Production of ground-level ozone (O_3) is dependent on concentrations of NO_x (NO and NO_2), methane, carbon monoxide, and volatile organic compounds (VOCs) (Jenkin and Clemitshaw, 2000). The formation of O_3 causes substantial deleterious human health and environmental impacts worldwide (RoTAP, 2012; REVIHAAP, 2013). Development of policies for the mitigation of these impacts requires understanding of the influences on O_3 concentrations from local, regional and hemispheric scale processes. The range in VOC atmospheric lifetimes from a few hours to several days (Atkinson, 2000) means that the major fraction of the VOC impact on O_3 production occurs on the regional scale of air-mass movements. At the regional scale, Gauss et al. (2014) modelled the reductions in O_3 impact across Europe on human health (using the SOMO35 metric) and vegetation (using the deciduous forest POD_Y metric) resulting from 15 % reductions in EU27 NO_x and VOC emissions and showed that VOC emissions reductions were more effective than NO_x emissions reductions in reducing the O_3 impact metrics across much of north-west Europe. Hence knowledge of the contribution of individual VOCs to O_3 production on the European (regional) scale will enable targeting of the most effective VOC reductions for reducing regionally-derived O_3 exposure relevant to O_3 impacts.

ACPD
15, 7267–7308, 2015

Within Europe, the European Monitoring and Evaluation Programme (EMEP) makes in situ atmospheric composition measurements at sites considered to have minimal influence from local emissions sources (Torseth et al., 2012). The UK operates two EMEP Level II monitoring sites (or "supersites"), Auchencorth and Harwell, at which hourly concentrations of O_3, NO_x and 27 VOCs are measured. In this work, chemical climates (defined in Malley et al. (2014a)) are derived to quantify the impact of the measured VOCs on the regional increment of O_3 concentrations (the difference between regional background and hemispheric background O_3 concentrations) measured at Harwell and Auchencorth. Full definitions of each of these O_3 quantities are given in Sect. 2.1. Monthly-diurnal O_3 variation at the EMEP supersites has previously been shown to be representative of wider geographical areas, namely rural background air of south-east England and northern UK for the Harwell and Auchencorth UK supersites, respectively (Malley et al., 2014b).

The interpretation of VOC measurements at rural sites has previously been undertaken using Positive Matrix Factorisation (PMF) (Lanz et al., 2009), trajectory analysis (Sauvage et al., 2009), VOC variability as a measure of source proximity (Jobson et al., 1999), winter/summer VOC ratios to indicate changing emissions sources (Jobson et al., 1999), and the ratio of VOCs with similar reactivity to highlight changes in emission sources (Yates et al., 2010). These studies identified VOC emissions sources based on measured VOC concentrations. However, the "state" of atmospheric composition variation producing a regional O_3 increment above hemispheric background concentrations is more rigorously evaluated by considering the chemical loss of the measured VOCs, since it is the VOC chemical loss in the air mass that drives the production of a regional O_3 increment, not the VOC concentration remaining in the air mass. In urban environments, the chemical loss of VOCs has been calculated by estimating OH exposure of the VOC suite, allowing calculation of the initial emission ratio of two VOCs (Shao et al., 2009; Yuan et al., 2012). This method is not appropriate for rural studies since it assumes that local sources dominate emissions.

Discussion Paper | Discussion Paper | Discussion Paper | Discussion Paper |

ACPD
15, 7267–7308, 2015

The impact of speciated VOCs on regional ozone increment derived from measurements

C. S. Malley et al.

Title Page
Abstract | Introduction
Conclusions | References
Tables | Figures
◀| |▶
◀ ▶
Back | Close
Full Screen / Esc
Printer-friendly Version
Interactive Discussion

In this work, monthly-averaged diurnal variations of individual VOC concentrations relative to ethane were used to assess the photochemical loss of each VOC and its contribution to the regional O_3 increment at Harwell and Auchencorth. The magnitude of VOC chemical loss at each site was linked to emissions by estimating the integrated VOC emissions along 96 h air-mass back trajectories. These emissions, from the 11 Selected Nomenclature for Air Pollution (SNAP; EEA, 2013) source sectors, were speciated to compare observed VOC variation with an estimate of individual VOC integrated back-trajectory emissions. Integration of emissions, VOC chemistry and O_3 production has been reported previously for one location in the UK using a photochemical trajectory model with a near-explicit chemical mechanism for a large suite of VOCs (Derwent et al., 2007b, a). The advantage of the methodology presented here, based on measurement data, is that uncertainties associated with the speciation of VOC emission source categories can be identified. A country-specific disaggregation of emissions into 91 more narrowly defined Nomenclature for Reporting (NFR; EEA, 2013) source sectors was used to determine more precisely the activities contributing to VOC back-trajectory emissions estimates. This current work presents a clear methodology for achieving a coherent VOC regional-O_3-impact chemical climate and explores the effect of limited emission and measurement species on the understanding of the regional contribution to O_3 concentrations.

2 Methodology

The methodology is separated into the three elements of a chemical climate, the impact (here, the regional O_3 increment), state (VOC diurnal photochemical depletion) and drivers (meteorology and emissions) as defined in Malley et al. (2014a). Analyses were undertaken for the periods 1999–2001 and 2010–2012 at Harwell and 2010–2012 at Auchencorth. Measured data were obtained from UK-AIR (http://uk-air.defra.gov.uk/) and EMEP (http://ebas.nilu.no/). For each year, the monthly-averaged diurnal cycles of each atmospheric component were calculated, i.e. $24 \cdot 12 = 288$ values year^{-1}.

2.1 Regional O_3 increment impact

The regional O_3 increment is defined as the regional background O_3 concentrations minus the hemispheric background O_3 concentration. Here, regional background O_3 concentration is defined as that which is imported into a local spatial domain, such as the two shown previously to be represented by the O_3 measurements at Auchencorth and Harwell (Malley et al., 2014b), following the modification of hemispheric background O_3 concentrations by European emissions. The hemispheric background O_3 concentration is in turn defined as that which is imported into the European domain, with minimal influence from European emissions.

Hemispheric background O_3 concentrations were derived by applying Ward's method hierarchical cluster analysis to pre-calculated 96 h air-mass back trajectories arriving at 3 h intervals at Mace Head, Ireland (R Core Development Team, 2008; Carslaw and Ropkins, 2012; Draxler and Rolph, 2013), to identify periods with no European influence. The discrimination achieved by cluster analysis may be influenced by user choices but the method used here was shown to be the most accurate of commonly used clustering techniques (Mangiameli et al., 1996). In Ward's method, each object (back trajectory) initially constitutes its own cluster. The algorithm then calculates which two clusters, when merged, gives the smallest increase in total within-cluster variance. The process is repeated until all trajectories are located in one cluster (Kaufman and Rousseeuw, 1990). The dendrogram summarising the cluster merging process is then "cut" at an appropriate level to produce the cluster set. The aim is to maximise explained inter-trajectory variability using a small number of clusters to highlight major distinctions between trajectory paths. The distance between a trajectory and its cluster mean was quantified using the two-dimensional "angle" of each trajectory (or cluster mean trajectory) from the origin (i.e. the supersite) at common time points along the trajectory:

$$d_{1,2} = \frac{1}{n}\sum_{i=1}^{n}\cos^{-1}\left(0.5\frac{A_i + B_i + C_i}{\sqrt{A_i B_i}}\right) \quad (1)$$

ACPD
15, 7267–7308, 2015

The impact of speciated VOCs on regional ozone increment derived from measurements

C. S. Malley et al.

ACPD
15, 7267–7308, 2015

The impact of speciated VOCs on regional ozone increment derived from measurements

C. S. Malley et al.

Title Page
Abstract | Introduction
Conclusions | References
Tables | Figures
◀| |▶
◀ ▶
Back | Close
Full Screen / Esc
Printer-friendly Version
Interactive Discussion

ACPD
15, 7267–7308, 2015

where

$$A_i = (X_1(i) - X_0)^2 + (Y_1(i) - Y_0)^2$$
$$B_i = (X_2(i) - X_0)^2 + (Y_2(i) - Y_0)^2$$
$$C_i = (X_2(i) - X_1(i))^2 + (Y_2(i) - Y_1(i))^2$$

$d_{1,2}$ is the distance between trajectory 1 and trajectory 2, X_0,Y_0 are the latitude and longitude coordinates of the origin of the trajectory, and $X_1(i)$,$Y_1(i)$, and $X_2(i)$,$Y_2(i)$ are the coordinates at time i of trajectories 1 and 2 respectively. The 2920 back trajectories arriving at Mace Head each year were separated into four clusters. The monthly-diurnal cycles of O_3 concentrations for the westerly trajectory cluster were used as the estimate of hemispheric background O_3. These values showed excellent agreement with the monthly average hemispheric background estimates derived by Derwent et al. (2007c) using Mace Head O_3 data and a combination of pollutant tracers and atmospheric modelling to select "clean" air masses ($r = 0.93$, $p < 0.001$, Fig. 1).

Regional background O_3 concentrations were estimated using the method of Clapp and Jenkin (2001). In the region of south-east England characterised by the Harwell supersite nine locations, ranging from rural background to kerbside, had hourly measurements of O_3, NO and NO_2. The y intercept of the linear fit to a total oxidant (O_3 + NO_2) vs. NO_x ($NO + NO_2$) plot yields the NO_x-independent oxidant contribution, interpreted as the regional background O_3 concentration, i.e. the contribution to O_3 within south-east England from processes occurring outside south-east England. Extraction of the y intercept from an oxidant vs. NO_x plot for each of the 288 "month-hour" averages yielded the monthly-diurnal cycle of regional background O_3 variation in south-east England. The difference between the hemispheric background and regional background O_3 concentrations provided the magnitude and direction of the regional modification to hemispheric background O_3 concentration.

The spatial domain for which Auchencorth is representative does not have sufficient co-located NO_x and O_3 monitoring sites to derive regional background O_3 concentrations by the above method. The regional O_3 increment at Auchencorth was therefore

Discussion Paper | Discussion Paper | Discussion Paper | Discussion Paper |

ACPD
15, 7267–7308, 2015

The impact of speciated VOCs on regional ozone increment derived from measurements

C. S. Malley et al.

Title Page
Abstract Introduction
Conclusions References
Tables Figures
◀◀ ▶▶
◀ ▶
Back Close
Full Screen / Esc
Printer-friendly Version
Interactive Discussion

estimated by subtracting the Mace Head hemispheric background estimates directly from the Auchencorth monthly-averaged diurnal concentrations.

2.2 State

VOC concentrations were determined by automated gas chromatography (Dernie and Dumitrean, 2013). For 2010–2012, data were available for 27 species; for 1999–2001 (at Harwell), data were available for only 21 of these VOCs. Concentrations of 6 VOCs at Auchencorth were not above the reported limit of detection (LOD) so their contribution to the regional O_3 increment was not evaluated.

The VOC datasets had extensive periods in which concentrations were below LOD, particularly at Auchencorth. Therefore maximum likelihood estimation (MLE) was used to fit three positively-skewed distributions (lognormal, gamma and Weibull) to the dataset for each VOC (Helsel, 2006; Gardner, 2012). The Akaike Information Criterion (AIC) was then used to select the distribution which best fitted the data; this provides a relative estimate of the information lost when a given distribution is used to represent a dataset (Akaike, 1974). This process was performed on data for each month of the year, and separately for the 288 monthly-diurnal time periods. The fitted distributions estimated the probability that a "non-detect" (below the LOD) was a concentration in the range 0 µg m^{-3} to the LOD. When non-detects occurred for all VOCs in a particular hour, these were excluded from the MLE analysis on the assumption that this was due to instrument failure. To avoid the unnecessary omission of valid concentration measurements, all other data were used, and consequently all remaining non-detects were assumed to be values below LOD. A number of non-detects due to the selective failure of the instrument to measure a particular VOC may be falsely considered to be below the LOD. However, the following evidence indicates that any bias introduced is likely to be small. Annual medians were calculated twice using MLE for Harwell in 2011, first, with the non-detects unique to each VOC, secondly with their omission (i.e. assuming all these non-detects were due to reasons other than LOD). The increase when omitted was below 10 % for 11 of the 27 VOCs, including the VOCs with concentrations

consistently well above the LOD. For example, the 5th percentile concentrations (of all valid concentrations) of propane, ethane and toluene were 1200, 800 and 175 % above the LOD, and consequently the number of unique non-detects was relatively low (4, 2 and 1 % of values respectively). The increase when the unique non-detects were omitted was 10, 8 and 3 % for propane, ethane and toluene respectively. Other VOCs had a 5th percentile concentration much closer to the LOD, increasing the likelihood of periods during which concentrations were below LOD. For nine of the 10 VOCs with the largest annual median increase, the 5th percentile concentration was the LOD. In summary, for those VOCs with few unique non-detects, the potential inclusion of non-LOD related non-detects results in a small change in calculated concentration, while VOCs with a larger proportion of non-detects have concentrations more frequently close to the LOD, increasing the likelihood that the unique non-detects result from concentrations below the LOD. Intra-annual and monthly-diurnal variation in VOC concentrations were summarised using the monthly median concentrations and the 24 hourly median concentrations for each month from the best-fit distributions respectively.

For each VOC, each of the 288 median monthly-diurnal concentrations was multiplied by the corresponding model-derived Photochemcial Ozone Creation Potential (POCP) (Derwent et al., 2007b), to weight the observed diurnal variation of VOCs according to their different propensities for O_3 formation. Multiple studies have calculated reactivity scales of O_3 production potential (OPP) for a range of VOCs using incremental reactivity methods (Luecken and Mebust, 2008; Derwent et al., 2007b; Hakami et al., 2004; Martien et al., 2003), multi-parent assignment (Bowman, 2005) and "tagging" of VOC degradation sequences (Butler et al., 2011). These varying methods were shown to be generally well correlated (Butler et al., 2011; Luecken and Mebust, 2008; Derwent et al., 2010). The Derwent et al. (2007b) POCPs are appropriate to use in this study as they were calculated under simulated north-western European conditions.

The diurnal variation of individual VOCs due to photochemical depletion was summarised by calculating the ratio of each POCP-weighted VOC concentration to the POCP-weighted ethane concentration. Ethane has the second smallest POCP of the

ACPD
15, 7267–7308, 2015

measured VOCs, 87 % smaller than the average, and 20 % smaller than the next smallest POCP (benzene), so using this ratio removed the effect on diurnal VOC concentration of changes in boundary layer mixing depth. It is also assumed that the magnitude of VOC emissions which determine VOC concentrations measured at the sites do not differ substantially between day and night. This can be evaluated from the monthly median VOC emissions emitted along the path of 96 h trajectories (outlined in Sect. 2.3) arriving at night (3 a.m.) and afternoon (3 p.m.), which were generally similar. For example at Harwell in 2011, night trajectory VOC emissions were ±12 % compared to afternoon. Hence a daytime decrease in POCP-weighted VOC/ethane ratio indicates greater photochemical depletion of the VOC relative to ethane. The magnitude of diurnal photochemical variability for each VOC was derived from the difference between the average POCP-weighted VOC/ethane ratio at night (1–5 a.m.) and in the afternoon (1–5 p.m.). A positive value indicates daytime photochemical depletion of the VOC relative to ethane.

At Auchencorth, the analysis of VOC diurnal photochemical depletion was not possible in 2010 and 2011 due to low data capture which compromises the ability of MLE to accurately estimate median VOC concentrations. This is particularly important for ethane, as a large error in the fitted distribution for ethane propagates to all VOC/ethane ratios. In 2011, the average proportion of non-detects for the measured VOCs was 56 % when the 6 VOCs with no measurements above LOD were excluded (34 % for ethane). In 2012 this decreased to 34 % (10 % for ethane), and VOC diurnal photochemical depletion was calculated. For comparison, at Harwell, there were on average 26 % non-detects for each VOC species in 2011 (7 % for ethane).

2.3 Drivers

The two main drivers producing the "state" of this chemical climate, i.e. VOC diurnal photochemical depletion, which are considered here are meteorology and VOC emissions. The meteorology was characterised by monthly mean, maximum and minimum temperature, and number of hours of sunshine for Harwell and Auchencorth obtained

ACPD
15, 7267–7308, 2015

The impact of speciated VOCs on regional ozone increment derived from measurements

C. S. Malley et al.

Title Page
Abstract | Introduction
Conclusions | References
Tables | Figures
◂◂ | ▸▸
◂ | ▸
Back | Close
Full Screen / Esc
Printer-friendly Version
Interactive Discussion

from the UK Met Office climate summaries for "South East and Central South England" and "East Scotland", respectively (http://www.metoffice.gov.uk/climate/uk/datasets/#) (Perry and Hollis, 2005).

To investigate geographical emissions sources, the locations of each of the 96 hourly time points of the 2920 HYSPLIT 96 h back trajectories arriving at 3 h intervals per year were mapped to the 0.5° × 0.5° gridded VOC emissions reported by EMEP and used in the EMEP model (Mareckova et al., 2013; Simpson et al., 2012). This grid encompasses the region 30.25–75.25° N and 29.75° W–60.25° E, and the emissions in each grid square are disaggregated into 11 SNAP source sectors (http://ceip.at/ms/ceip_home1/ceip_home/webdab_emepdatabase/emissions_emepmodels/).When the location of the trajectory during a particular hour fell within the gridded domain, the annual emissions and country of the grid square over which the trajectory was located were assigned to that time point. Emissions were assigned to the country which had the greatest emissions when the grid square straddled an international border. Annual emissions were modified by prescriptive month, day-of-week and hour-of-day time factors (Simpson et al., 2012) to obtain an estimate of the hourly emissions from each SNAP sector during the hour in which the trajectory passed over the grid cell. The monthly average hourly SNAP emission estimates at each of the 96 1 h time points were summed to give the average European VOC emissions estimate of all the trajectories arriving in that month (henceforth the VOC trajectory emissions estimate (TEE)), and the proportions derived from individual countries.

The total VOC TEE from the 11 SNAP sectors were speciated using the 114 VOC speciated profiles from Passant (2002) to quantify the proportion of emissions emitted as one of the 27 measured VOCs. The profiles were first applied to UK annual emissions to obtain speciated profiles for each SNAP sector which could be applied to the VOC TEEs. Each year, at the most disaggregated level, the UK National Atmospheric Emissions Inventory (NAEI) reports total VOC emissions for 337 source activities (http://naei.defra.gov.uk/data/) (Passant et al., 2013). In Passant (2002), each of these activities is assigned one of the 114 speciation profiles which in total consider the

ACPD
15, 7267–7308, 2015

contribution from 630 VOCs, including aggregated groups of VOCs, for example, "C7 alkanes". The total annual UK emissions for each activity were apportioned between the VOCs in the assigned profile. This resulted in a matrix of 337 columns of source activities, and 630 rows of VOCs. Activities were then grouped into the 55 NFR codes used by NAEI, and then into SNAP sectors 1–9 based on the NFR-SNAP conversion recommended by the EMEP Centre for Emission Inventories and Projections (CEIP, http://www.ceip.at/fileadmin/inhalte/emep/pdf/nfr09_to_snap.pdf). There were no reported VOC emissions from activities falling under SNAP 10 (agriculture) and SNAP 11 (other). The relative contribution of each VOC to total annual UK SNAP emissions was calculated to provide speciated emissions profiles which were used to speciate the monthly SNAP sector VOC TEEs. This produced an estimate of the contribution to total monthly VOC TEE from 630 VOCs. This contribution was then multiplied by the VOC's POCP to weight it according to O_3 formation potential.

The EU emissions inventory disaggregates annual emissions from SNAP sectors 1–9 into 91 NFR codes for each EU member state (EEA, 2014). The monthly change in the SNAP sector VOC TEE was attributed to changes in the contribution from the more narrowly defined NFR codes, based on the country-specific contributions of each NFR sector to annual SNAP sector emissions. The VOC TEE from each of the 91 NFR codes for each country were summed across all countries to obtain the contribution of each NFR code to the total VOC TEE for each month.

The emission inventories used in this study have several sources of uncertainty (EEA, 2013). The 0.5° × 0.5° grid squares mean that numerous distinct sources, each with uncertainties in emission factors and activity rates, are aggregated together to produce the estimate of emissions from a particular SNAP or NFR source sector. The size of the grid square also does not necessarily reflect the size of the area from which emissions influence the atmospheric composition of the trajectory air mass as it passes over. The VOC TEE is therefore used as a relative comparison spatially and temporally, rather than a definitive quantification of the VOC emissions emitted into an air mass. In addition, there are uncertainties in the speciation of total VOC emissions to individual

Discussion Paper | Discussion Paper | Discussion Paper | Discussion Paper |

ACPD
15, 7267–7308, 2015

The impact of speciated VOCs on regional ozone increment derived from measurements

C. S. Malley et al.

Title Page
Abstract Introduction
Conclusions References
Tables Figures
◀◀ ▶▶
◀ ▶
Back Close
Full Screen / Esc
Printer-friendly Version
Interactive Discussion

components (Borbon et al., 2013). However, the emissions inventories used here are the best estimate of the spatial distribution of anthropogenic VOC emissions across Europe.

3 Results and discussion

3.1 Impact: regional O_3 production/destruction assessment

The difference between hemispheric background O_3 concentrations and regional background O_3 concentrations relevant for Harwell for 2001 (representative of 1999–2001), 2011 (representative of 2010–2012) and for Auchencorth in 2012 is shown in Fig. 2. Although there was inter-annual variability within each time period, the data for these years illustrate the main differences between three different phases of the regional O_3 increment chemical climate both temporally at Harwell (1999–2001 vs. 2010–2012) and spatially (Harwell vs. Auchencorth). At Harwell in 2001, a positive regional O_3 increment occurred in each month between May and September (Fig. 2a). The annual maximum regional O_3 increment (i.e. the difference between hemispheric background and regional background O_3 concentrations) occurred in the afternoon in July 2001 ($42\,\mu g\,m^{-3}$), while monthly regional O_3 increments peaked in excess of $20\,\mu g\,m^{-3}$ in June and August, and in excess of $10\,\mu g\,m^{-3}$ in May and September. In 2011 at Harwell positive regional O_3 increments occurred between April and September (Fig. 2b), but their magnitudes were reduced compared with the 1999–2001 phase. Only two months, April and July, had maximum regional O_3 increments $> 10\,\mu g\,m^{-3}$ (11 and $32\,\mu g\,m^{-3}$, respectively). In 2012, the monthly regional O_3 increment exceeded $10\,\mu g\,m^{-3}$ in May ($12\,\mu g\,m^{-3}$), July ($28\,\mu g\,m^{-3}$) and August ($11\,\mu g\,m^{-3}$), and occurred more modestly in April, June and September. In 2010, the regional O_3 increment in June was $24\,\mu g\,m^{-3}$, which then decreased in July ($19\,\mu g\,m^{-3}$). Reductions in regional O_3 have been reported in the UK previously, using high percentile O_3 concentrations as an indicator of regionally-derived episodes, rather than calculation of the average

monthly-diurnal regional O_3 increment. For example, Munir et al. (2013) attributed negative trends in highest O_3 concentrations calculated at 22 UK monitoring sites (13 sites with significant trends) to regional reduction in O_3 precursor emissions between 1993 and 2011.

The regional O_3 increments at Auchencorth were substantially lower than at Harwell. Between 2010 and 2012, the maximum regional O_3 increment observed was $14\,\mu g\,m^{-3}$ in July 2011. In 2012 (Fig. 2c), the maximum regional O_3 increment was $4\,\mu g\,m^{-3}$. The spatial differences in the extent of regional contribution to O_3 variation at Harwell and Auchencorth are consistent with a previous study of rural UK O_3 spatial variability (Jenkin, 2008).

3.2 State: VOC concentration and chemical depletion

The monthly median concentrations of the 27 VOCs measured at Harwell and Auchencorth have a pronounced seasonal cycle with highest total summed VOC concentrations in winter at each site, albeit with concentrations at Auchencorth substantially lower than at Harwell (Fig. 3 shows an example year for each of the three periods). Monthly variation was lower at Auchencorth: the difference between minimum and maximum monthly total VOC concentrations at Auchencorth in 2012 was $6.2\,\mu g\,m^{-3}$, compared with 9.5 and $13.1\,\mu g\,m^{-3}$ at Harwell in 2011 and 2001 respectively. Monthly median total VOC concentrations at Harwell in 1999–2001 and 2010–2012 were similar in winter months (January, February, December), and generally ranged between 6 and $18\,\mu g\,m^{-3}$. In summer (June, July, August) between 1999 and 2001, total VOC concentrations were between 5 and $13\,\mu g\,m^{-3}$, but between 2010 and 2012, concentrations were lower, between 3 and $6\,\mu g\,m^{-3}$, and only June 2010 had higher total VOC concentrations than the summer month in 1999–2001 with the lowest total VOC concentration. In 2001 six VOCs were not measured, and these constituted between 2.1 and 7.4 % of monthly total measured VOC concentrations in 2011.

ACPD
15, 7267–7308, 2015

ACPD
15, 7267–7308, 2015

The impact of speciated VOCs on regional ozone increment derived from measurements

C. S. Malley et al.

Title Page
Abstract | Introduction
Conclusions | References
Tables | Figures
◀◀ | ▶▶
◀ | ▶
Back | Close
Full Screen / Esc
Printer-friendly Version
Interactive Discussion

The relative composition of total measured VOCs showed differences between 2001 and 2011. Ethane, propane and n-butane had the largest measured concentrations. Ethane contributed on average 22 % of total monthly measured VOC concentrations in 2001, compared with 33 % in 2011 (annual average monthly measured ethane concentration had a small increase from 2.0 $\mu g\,m^{-3}$ in 2001 to 2.3 $\mu g\,m^{-3}$ in 2011), while the relative contribution from propane did not vary (15 % in each year, average monthly concentrations in 2001 and 2011 were 1.5 and 1.2 $\mu g\,m^{-3}$ respectively) and that from n-butane decreased from 11 to 8 % (1.1 $\mu g\,m^{-3}$ in 2001 and 0.6 $\mu g\,m^{-3}$ in 2011). Although these differences are not large, they may result from differences in the reduction of VOC emission sources between 1999–2001 and 2010–2012. The aim of this work, however, was not the determination of long-term trends in absolute VOC concentrations, and the reader is referred to Dollard et al. (2007), von Schneidemesser et al. (2010) and Derwent et al. (2014) which have undertaken analyses of trends in VOC concentrations at multiple UK sites, including Harwell and Auchencorth.

The extent of diurnal photochemical loss of VOCs over the year is shown in Fig. 4. At Harwell, periods of increased VOC diurnal photochemical depletion mirror the monthly magnitude of regional O_3 increments (Fig. 2 c.f. Fig. 4). In 2001, both the regional O_3 increment and VOC diurnal photochemical depletion increased from June to July, before declining in August. In 2011, there was a local maximum in the regional O_3 increment in April, followed by the annual maximum in July, mirrored by VOC diurnal photochemical depletion. During 2012 the regional O_3 increment was minimal at Auchencorth, and the magnitude of VOC diurnal photochemical depletion was low, with a small peak in August.

The contributions of each measured VOC to total VOC diurnal photochemical depletion during the month of maximum regional O_3 increment in 2010, 2011 and 2012 at Harwell are shown in Fig. 5. Ethene had the largest contribution during these months (34, 29 and 45 % of total measured VOC diurnal reactivity in 2010, 2011 and 2012 respectively). The sum of m + p-xylene also made a major positive contribution during 2010 (15 %) and 2011 (13 %). The majority of the remaining measured VOCs made

Discussion Paper | Discussion Paper | Discussion Paper | Discussion Paper |
ACPD
15, 7267–7308, 2015
The impact of speciated VOCs on regional ozone increment derived from measurements
C. S. Malley et al.
Title Page
Abstract Introduction
Conclusions References
Tables Figures
◀ ▶
Back Close
Full Screen / Esc
Printer-friendly Version
Interactive Discussion

smaller, positive contributions. In July 2011, 71 % of the remaining VOCs contributed on average 3.4 ± 2.5 % to total positive VOC diurnal variation. In July 2012, the maximum regional O_3 increment was 12 % lower than July 2011, and only 58 % of remaining VOCs made positive contributions. In June 2010, the maximum regional O_3 increment was 25 % lower, and 54 % of the remaining VOCs contributed. VOCs with larger VOC/ethane ratios in the afternoon included isoprene, which is predominantly of biogenic origin (von Schneidemesser et al., 2011). Laurent and Hauschild (2014) modelled the impact on O_3 formation of speciated VOC emissions from 31 countries, and also reported m-xylene and ethene to have the largest impact of 270 VOCs on regional O_3 formation.

Figure 6 is the analogous plot to Fig. 5 for 1999–2001 at Harwell. In 1999–2001, m + p-xylene had the largest diurnal photochemical depletion, followed by ethene. However, there were much larger negative VOC/ethane diurnal variations for some anthropogenic VOCs compared to 2010–2012 (Fig. 5). Iso-pentane had the largest negative difference, but had a consistent positive contribution in 2010–2012. Toluene also had a negative value in 1999 and 2000. Therefore from 1999–2001 to 2010–2012 there was a change in the balance between emissions of iso-pentane and toluene and their photochemical removal to the point where photochemical depletion dominated during the day, and VOC/ethane ratios were lower in the afternoon than at night. Derwent et al. (2014) calculated exponential decreases in the concentrations of these VOCs at urban locations in the south-east of England, where Harwell is located, attributed to the effective control of evaporative and exhaust emissions from petrol-engined vehicles. Toluene has an atmospheric lifetime of ∼ 1.9 days with respect to reaction with OH (Atkinson, 2000) so local daytime toluene emissions would not deplete substantially during transport to the monitoring site. The observed decreasing trends at sites close to emission sources in the south-east of England suggest a decrease in the influence of local iso-pentane and toluene emissions in determining the diurnal profile of these VOCs at Harwell, and hence afternoon depletion of regionally-emitted toluene and iso-pentane was observed in 2010–2012.

3.3 Drivers of chemical climate state: meteorology and emissions

3.3.1 Meteorology

The monthly-averaged meteorological data for the UK regions relevant for Harwell in 2001 and 2011 and Auchencorth in 2012 is shown in Fig. 7. Variation in temperature and sunshine is often associated with spatio-temporal differences in VOC diurnal photochemical depletion and regional O_3 increment. For example, temperatures were generally lower in East Scotland than South East and Central South England but the number of hours of sunshine were comparable, although solar intensity is less in Scotland, hence a reduced VOC photochemical depletion and regional O_3 increment at Auchencorth. At Harwell in 2001, annual maximum VOC diurnal photochemical depletion occurred in July, coinciding with annual maximum monthly temperature, while in July 2011, a combination of relatively high temperature and hours of sunshine (although neither were annual maxima), coincided with annual maximum VOC diurnal photochemical depletion. These summers were typical of the 1999–2012 period; monthly mean temperatures were between −7 and +4 % compared to the 1999–2012 average and hours of sunshine were between −14 to +11 % compared to the average.

At Harwell in April 2011, there was a larger regional O_3 increment compared with April 2001. This coincided with 4 °C higher mean temperature and 95 more hours of sunshine in South East and Central South England. However, other factors, such as the strength of VOC emission sources over which an air mass passes, also influence VOC diurnal photochemical depletion, and in May 2011 the temperature and sunshine were similar to April 2011, but VOC diurnal photochemical depletion and the regional O_3 increment decreased.

3.3.2 Emissions

Variation in the monthly averaged European anthropogenic VOC trajectory emissions estimate (TEE) is shown in Fig. 8. The VOC TEE is the sum of hourly emissions from

the grid squares the trajectories passed over in the 96 h prior to arrival at the supersites (units: Mg 96 h^{-1}), rather than a definitive quantification of the emissions directly impacting upon the measured atmospheric composition at the supersites. Compared with Harwell in 2001, the annual average VOC TEE, by mass, was 64 % smaller in 2011 at Harwell, and 76 % smaller in 2012 at Auchencorth. For the purposes of clarity the following assessment focuses on Harwell, where significant regional O_3 increment has been demonstrated (Sect. 3.1). The change in contribution from the 11 SNAP sectors to average VOC TEE between 2001 and 2011 at Harwell is shown in Fig. 8. The biggest change was for SNAP 7 (road transport), which averaged 31 % of the total VOC TEE in 2001, compared to 9 % in 2011. Emissions from SNAP 6 (solvents) were the largest contribution to the VOC TEE during both periods, contributing 50 % of total emissions on average in 2011, compared to 34 % in 2001. Emissions from SNAP 4 (production processes) were the second largest contributor on average in 2011 (11 % of the total VOC TEE), followed by SNAP 7 (road transport), and SNAP 5 (extraction and distribution of fossil fuels), both contributing 9 %.

Monthly variation in VOC TEE mirrors that of VOC diurnal photochemical depletion and hence the magnitude of the regional O_3 increment. The period of April–July 2011 provides a useful case study to demonstrate the nature of the emissions driver. April and May 2011 have similar meteorological conditions (Fig. 7), but VOC diurnal photochemical depletion was lower in May due to a 62 % decrease in the VOC TEE compared to April. The VOC TEE decreased in June, then increased in July. This latter increase, coupled with increased temperatures and solar intensity in summer, provided conditions conducive to producing the observed annual maximum in VOC diurnal photochemical depletion for 2011.

The proportion of the total VOC TEE derived from the final 4 h prior to a trajectory's arrival, plus the hour of arrival, was labelled as the "final 4 h" VOC TEE. In 2011 the final 4 h was on average 28 % of the total VOC TEE (Fig. 9). In May and June 2011 it was above average (36 and 44 % respectively), and in April and July it was lower (17 and 20 % respectively). While the 4 h cut-off for this calculation was somewhat arbitrary,

ACPD
15, 7267–7308, 2015

The impact of speciated VOCs on regional ozone increment derived from measurements

C. S. Malley et al.

ACPD
15, 7267–7308, 2015

The impact of speciated VOCs on regional ozone increment derived from measurements

C. S. Malley et al.

Title Page
Abstract | Introduction
Conclusions | References
Tables | Figures
◀| |▶
◀ ▶
Back | Close
Full Screen / Esc
Printer-friendly Version
Interactive Discussion

it was based on consideration of the average atmospheric lifetimes of the individual VOCs (Atkinson, 2000) which indicate that most VOCs emitted in the final 4 h have insufficient time to form O_3. Between June and July 2011 there was a 32 % increase in median VOC concentrations due to an increased VOC TEE. However, there was a 275 % increase in VOC diurnal photochemical depletion as a larger proportion of emissions were emitted earlier along the air-mass trajectory. Hence in May and June, lower total VOC TEE compared to April and July, respectively, coupled with a larger proportion of VOCs emitted in the final 4 h, resulted in the reduced regional O_3 increment impact.

The speciated VOC monthly trajectory emissions estimates, based on a UK-specific speciation of the total VOC TEE for 9 SNAP sectors are shown in Fig. 10 for July 2001 and 2011. Individual VOC trajectory emissions estimates were expressed as the percentage of the total POCP-weighted emissions. The biggest decreases between 2001 and 2011 were for iso-pentane (4.1 % total POCP emissions in 2001, 1.7 % in 2011), and toluene (6.5 % in 2001, 4.5 % in 2011). These decreases mirror the absence of the large negative VOC diurnal photochemical depletion of the two VOCs in 2010–2012, which were observed in 1999–2001 (Figs. 5 and 6). However, monthly variation in the contribution of measured VOCs to the VOC TEE was not consistent with variation in the contribution of individual VOCs to total measured VOC diurnal photochemical depletion. For example, in 2011, the VOC diurnal photochemical depletion peak in July (Fig. 4) was much greater than in April due to more intense sunshine and higher temperatures. This increase was not equally reflected across the measured VOCs, indicating differences in the speciation of the VOC TEEs prior to arrival at the site. For example, toluene was 4.2 % of total VOC diurnal photochemical depletion in April, increasing to 9.6 % in July and the 1,3,5-trimethylbenzene contribution increased from 0.1 % in April to 8 % in July. The monthly-averaged speciated VOC TEEs do not reflect these changes, and show little monthly variation within a given year. The speciated VOC monthly TEE calculation assumes that the SNAP sector component activities (i.e. the activities for which speciated profiles are defined (Passant, 2002)) contribute simi-

larly to the emissions exposure of the parent SNAP sector in each month of the year. For example, it is assumed that an x % increase in SNAP emissions results from an x % increase in emissions from all component activities. It is unlikely that the SNAP sector emissions in every region over which an air mass travels are similarly apportioned between component emissions activities. The inability of this method to account for these spatial differences will result in the underestimation of the TEE of some VOCs, and the overestimation of others. Currently, data are only available on changes in the contribution of more narrowly defined NFR codes to SNAP sector emissions at a country level and for annual VOC emissions. In 2011 the average contribution to monthly VOC TEE at Harwell from the UK was 62 %, with France the second largest contributor at 14 %. Comparing April and July 2011, the contributions from the UK to the VOC TEE were 50 and 95 % respectively, with the other 50 % in April resulting from contributions from Germany, France, Belgium and the Netherlands (Fig. 11). These countries all have different relative contributions to total SNAP sector emissions from component NFR source sectors (EEA, 2014).

Disaggregation of the VOC TEEs into 91 NFR codes, based on country-specific contributions of these NFR sectors to annual VOC emissions in the 11 parent SNAP sectors, accounted for country-specific changes in NFR sector contributions to monthly VOC TEE at Harwell. The increase in VOC emissions from a SNAP sector in a specific country can result from an increase in a specific source activity (e.g. specific NFR code), rather than a general overall increase. For example, in 1999–2001, the large contribution from SNAP 7 (road transport, Fig. 8) is more precisely attributed to NFR sectors 1A3bi (passenger cars) and 1A3bv (gasoline evaporation) which contributed 19 and 11 % to the total VOC TEE in July 2001 (month of maximum regional O_3 increment) respectively, and 87 % of the SNAP 7 emissions estimate. The next largest contribution was from 3D2 (domestic solvent use, 10 %), a component of SNAP 6 (solvents). Between 2010 and 2012, SNAP 6 was the major contributor to the VOC TEE. During July 2011 SNAP 6 component NFR sectors, 3D2 (domestic solvent use) and 3D3 (other product use) contributed 18 and 12 % of the total VOC TEE (65 % of the

ACPD
15, 7267–7308, 2015

Discussion Paper | Discussion Paper | Discussion Paper | Discussion Paper |

ACPD
15, 7267–7308, 2015

The impact of speciated VOCs on regional ozone increment derived from measurements

C. S. Malley et al.

Title Page
Abstract Introduction
Conclusions References
Tables Figures
◀◀ ▶▶
◀ ▶
Back Close
Full Screen / Esc
Printer-friendly Version
Interactive Discussion

SNAP 6 emissions estimate). The SNAP 4 (production processes) component 2D2 (food and drink) was the third largest contributor (10 % in July 2011). The two road transport categories contributed 4 % (1A3bi) and 1 % (1A3bv) to the total VOC TEE in July 2011.

The difference between the contribution of 91 NFR codes to the average VOC TEE between April and July 2011 is shown in Fig. 12. Between these months, the cumulative change in the contribution of the 9 SNAP sectors to the total VOC TEE was 13.4 %, compared to a change of 15.9 % for the 91 NFR codes. However, the changes in NFR code contributions were not equally spread between the constituent activities of a SNAP sector; they were concentrated in relatively few NFR sectors. For example, between April and July 85 % of the NFR change resulted from a decrease in 10 out of the 91 NFR sectors. The sectors "residential: stationary plant combustion" and "industrial coating application" show the greatest decrease, while sectors "food and drink" and "venting and flaring" show the largest increase (identified by stars on Fig. 12). The disaggregation of SNAP sector VOC TEEs also illustrates changes of opposite sign in the contribution of component NFR sectors under the net changes in SNAP sector. For example, SNAP sector 4 (production processes) increased in contribution between April and July by 2.7 % (12.0 to 14.7 %). Following disaggregation, this change was seen to result from a 3.4 % increase in NFR sector 2D2 (food and drink) and a 0.76 % decrease in 2B5 (other chemical industry). NFR sector level speciated profiles can therefore give much more specific information on the emissions source drivers of VOC diurnal photochemical depletion, though it is noted that the accuracy of many emission source speciation profiles is subject to discussion (Borbon et al., 2013). However, the changes in contribution of NFR sectors to the VOC TEE calculated here only account for country-level variation, not for variation in the contribution of NFR sectors to SNAP emissions on finer spatial scales, such as differences in NFR sector contribution to SNAP emissions in different $0.5^{\circ} \times 0.5^{\circ}$ grid squares for which the SNAP sector gridded emissions are reported. Hence the future reporting of gridded emissions to NFR

code level would more accurately represent the true nature of VOC emissions across Europe.

3.3.3 Uncertainties and implications for future mitigation and monitoring

Two VOCs, ethene and m + p-xylene, consistently had larger contributions to total VOC diurnal photochemical depletion compared to the remaining VOC suite. Therefore a targeted reduction of these two VOCs (compared to other measured VOCs) would be most effective in reducing the regional O_3 increment. Further reduction of total measured VOC diurnal photochemical depletion would require a reduction across a larger number of the remaining measured VOCs. This could be achieved by lowering emissions from large VOC emitting sources, rather than a focus on individual VOC species. As previously identified (Sect. 3.3), between 2010 and 2012, the largest VOC emitting sources (NFR codes) were 3D2 (domestic solvent use including fungicides), 3D3 (other product use) and 2D2 (food and drink).

The 27 measured VOCs studied here are a subset of the total VOC species emitted by a multitude of anthropogenic activities and biogenic processes. In 2011, 37.5 % of the reported annual UK anthropogenic VOC emissions were emitted as one of the 27 measured VOCs, when speciated using the Passant (2002) speciation profiles. The UK biogenic VOC emissions estimate reported to EMEP for 2011 was 91.2 Gg (c.f. anthropogenic emissions of 752 Gg), but this value is uncertain and studies have estimated considerably higher UK annual biogenic VOC emissions, in excess of 200 Gg (Karl et al., 2009; Oderbolz et al., 2013). Biogenic VOC contributions to regional O_3 increments were not studied using this methodology. Of the 62.5 % of UK anthropogenic VOC emissions not emitted as one of the VOCs measured at the supersites, only the additional measurement of ethanol (13 % of 2011 anthropogenic UK emissions), methanol (4 %) and acetone (3 %) would substantially increase the proportion of the UK VOC suite for which VOC diurnal photochemical depletion would be quantified. These three VOCs constitute 35 % of the unmeasured fraction of UK anthropogenic emissions. Contributions from the 40 unmeasured VOCs with the next highest emis-

ACPD
15, 7267–7308, 2015

ACPD
15, 7267–7308, 2015

The impact of speciated VOCs on regional ozone increment derived from measurements

C. S. Malley et al.

Title Page
Abstract | Introduction
Conclusions | References
Tables | Figures
◀| |▶
◀ ▶
Back | Close
Full Screen / Esc
Printer-friendly Version
Interactive Discussion

sions are required to make up the same percentage, and the remaining unmeasured emissions fraction comprises 464 VOCs. The large number of VOC contributing to the "unmeasured" VOC emissions fraction supports the argument that the targeting of high VOC emitting sources would be more beneficial than reductions in individual VOCs from whatever sources. The large proportion of UK VOC emissions emitted as ethanol, methanol and acetone (mainly from SNAP6 (solvents), from which 39, 97 and 91 % of UK anthropogenic emissions of ethanol, methanol and acetone derived in 2011, and SNAP4 (production processes), which contributed 57 % of ethanol emissions) suggests that, like ethene and m + p-xylene, they may have a disproportionately high contribution to VOC diurnal photochemical depletion, and hence to the magnitude of the regional O_3 increment. Measurement of these oxygenated VOCs at the supersites would allow their contribution to be quantified.

The future reporting of gridded VOC emissions in source sectors more highly disaggregated than currently (e.g. NFR codes) would facilitate a more precise identification of those VOC sources most important to mitigation strategies. For example, Derwent et al. (2007a) applied the POCP concept to calculate the contribution of 248 VOC source categories to regional O_3 production using a photochemical trajectory model with a near-explicit chemical mechanism which followed a "worst case" 5 day trajectory bringing aged air masses from Europe to a location on the England–Wales border. A UK-derived VOC emissions speciation was derived and applied to total gridded VOC emissions estimates across north-west Europe. While the POCP concept provides an effective means of comparison between different source categories, source category POCPs were calculated without accounting for the spatial variation in the contribution of the different source categories to total VOC emissions. The work presented here highlights the constraints of representing spatial variation of VOC emissions across Europe with 11 highly aggregated SNAP sectors, and these constraints would be amplified with no disaggregation of gridded VOC emissions. The effectiveness of the POCP concept in the determination of the strongest O_3-influencing VOC emission sources, and hence the most cost effective mitigation strategies, would be substantially improved by the

ACPD
15, 7267–7308, 2015

reporting of gridded emissions at NFR sector level. Finally, the future measurement at supersites of VOCs which are distinct markers for source sectors (e.g. NFR codes) could be used to quantify the contribution from different VOC source sectors.

4 Conclusions

A methodology has been demonstrated using measurement data at the two UK EMEP supersites (Harwell and Auchencorth) which links the impact of regional O_3 increment to VOC photochemical depletion. The regional O_3 increment at Harwell in 2010–2012 was substantially larger than at Auchencorth, but substantially smaller than in 1999–2001. Of the 27 measured VOCs, ethene and m + p-xylene consistently contributed the most VOC photochemical depletion during regional O_3 production at Harwell, and therefore reductions in emissions of these VOCs would be most effective in reducing regional O_3 production. To reduce VOC diurnal photochemical depletion further, reductions across a larger number of the VOCs would be required. Of these, ethanol, methanol and acetone appear to be the most important, and measurement of these VOCs at the supersites would provide data for targeting future emissions reductions. Additionally, more detailed speciated measurement of biogenic VOCs at the supersite would also advance understanding of the relative contribution of anthropogenic vs. biogenic VOCs in determining the regional O_3 increment.

Estimates of the integrated VOC emissions along back trajectories arriving at Harwell have decreased substantially between 1999–2001 and 2010–2012, due to decreases in emissions from SNAP source sector 7 (road transport). Currently, SNAP sector 6 (solvent and product use) provides most of the total VOC trajectory emissions estimate. The disaggregation of highly aggregated SNAP trajectory emissions estimates to NFR codes, accounting for country variation in the NFR sector contribution to parent SNAP sector, allowed the source sectors which determine the VOC contribution to the regional O_3 impact to be more precisely defined, i.e. NFR sectors 3D2 (domestic solvent use), 3D3 (other product use) and 2D2 (food and drink), which were the top three

Discussion Paper | Discussion Paper | Discussion Paper | Discussion Paper |

ACPD
15, 7267–7308, 2015

The impact of speciated VOCs on regional ozone increment derived from measurements

C. S. Malley et al.

Title Page
Abstract Introduction
Conclusions References
Tables Figures
◀◀ ▶▶
◀ ▶
Back Close
Full Screen / Esc
Printer-friendly Version
Interactive Discussion

contributors to total VOC emissions exposure at Harwell (2010–2012) during the month of maximum regional O_3 increment. It is concluded that considerable additional benefits to the interpretation of measurement data, to modelling of future O_3 concentrations and hence to determining policy for abatement of detrimental O_3 impacts would be gained from the availability of gridded VOC emissions data reported in more narrowly defined source sectors such as the NFR codes.

Acknowledgements. C. S. Malley acknowledges the University of Edinburgh School of Chemistry, the NERC Centre for Ecology & Hydrology (NERC-CEH studentship funding project no. NEC04544) and the UK Department for Environment, Food and Rural Affairs (Defra Grant no. AQ0647) for funding. Defra contractors Ricardo-AEA, Bureau Veritas and NERC Centre for Ecology & Hydrology and their field teams are acknowledged for operating the UK EMEP Supersites.

References

Akaike, H.: New look at statistical-model identification, IEEE T. Automt. Contr., 19, 716–723, 1974.

Atkinson, R.: Atmospheric chemistry of VOCs and NO_x, Atmos. Environ. 34, 2063–2101, 2000.

Borbon, A., Gilman, J. B., Kuster, W. C., Grand, N., Chevaillier, S., Colomb, A., Dolgorouky, C., Gros, V., Lopez, M., Sarda-Esteve, R., Holloway, J., Stutz, J., Petetin, H., McKeen, S., Beekmann, M., Warneke, C., Parrish, D. D., and de Gouw, J. A.: Emission ratios of anthropogenic volatile organic compounds in northern mid-latitude megacities: observations versus emission inventories in Los Angeles and Paris, J. Geophys. Res.-Atmos., 118, 2041–2057, doi:10.1002/jgrd.50059, 2013.

Bowman, F. M.: A multi-parent assignment method for analyzing atmospheric chemistry mechanisms, Atmos. Environ. 39, 2519–2533, 2005.

Butler, T. M., Lawrence, M. G., Taraborrelli, D., and Lelieveld, J.: Multi-day ozone production potential of volatile organic compounds calculated with a tagging approach, Atmos. Environ. 45, 4082–4090, 2011.

Carslaw, D. C. and Ropkins, K.: openair – an R package for air quality data analysis, Environ. Modell. Softw. 27–28, 52–61, doi:10.1016/j.envsoft.2011.09.008, 2012.

Clapp, L. J. and Jenkin, M. E.: Analysis of the relationship between ambient levels Of O_3, NO_2 and NO as a function of NO chi in the UK, Atmos. Environ. 35, 6391–6405, 2001.

Dernie, J. and Dumitrean, P.: UK Hydrocarbon Network: Annual Report for 2012, Report No. ED47833 and ED46645 for Defra and the Devolved Administrations, Ricardo-AEA, available at: http://uk-air.defra.gov.uk/assets/documents/reports/cat13/1311201446_Hydrocarbon_2012_FINAL_Issue_1.pdf, 2013.

Derwent, R. G., Jenkin, M. E., Passant, N. R., and Pilling, M. J.: Photochemical ozone creation potentials (POCPs) for different emission sources of organic compounds under European conditions estimated with a Master Chemical Mechanism, Atmos. Environ. 41, 2570–2579, 2007a.

Derwent, R. G., Jenkin, M. E., Passant, N. R., and Pilling, M. J.: Reactivity-based strategies for photochemical ozone control in Europe, Environ. Sci. Policy, 10, 445–453, 2007b.

Derwent, R. G., Simmonds, P. G., Manning, A. J., and Spain, T. G.: Trends over a 20-year period from 1987 to 2007 in surface ozone at the atmospehric research station Mace Head, Ireland, Atmos. Environ. 41, 9091–9098, 2007c.

Derwent, R. G., Jenkin, M. E., Pilling, M. J., Carter, W. P. L., and Kaduwela, A.: Reactivity scales as comparative tools for chemical mechanisms, J. Air Waste Manage., 60, 914–924, 2010.

Derwent, R. G., Dernie, J. I. R., Dollard, G. J., Dumitrean, P., Mitchell, R. F., Murrells, T. P., Telling, S. P., and Field, R. A.: Twenty years of continuous high time resolution volatile organic compound monitoring in the UK from 1993 to 2012, Atmos. Environ. 99, 239–247, 2014.

Dollard, G. J., Dumitrean, P., Telling, S., Dixon, J., and Derwent, R. G.: Observed trends in ambient concentrations of C-2–C-8 hydrocarbons in the UK over the period from 1993 to 2004, Atmos. Environ. 41, 2559–2569, 2007.

Draxler, R. R. and Rolph, G. D.: HYSPLIT (HYbrid Single-Particle Lagrangian Integrated Trajectory) Model access via NOAA ARL READY Website, available at: http://www.arl.noaa.gov/HYSPLIT.php, NOAA Air Resources Laboratory, College Park, MD, 2013.

EEA: EMEP/EEA Air Pollutant Emission Inventory Guidebook 2013, EEA Technical Report No 12/2013, available at: http://www.eea.europa.eu/publications/emep-eea-guidebook-2013, European Environment Agency, 2013.

EEA: EU Emission Inventory Report 1990–2012 under the UNECE Convention on Long-Range Transboundary Air Pollution (LRTAP), EEA Technical Report No 12/2014, available at: http://www.eea.europa.eu//publications/lrtap-2014, European Environment Agency, 2014.

Discussion Paper | Discussion Paper | Discussion Paper | Discussion Paper |

ACPD
15, 7267–7308, 2015

The impact of speciated VOCs on regional ozone increment derived from measurements

C. S. Malley et al.

Title Page
Abstract Introduction
Conclusions References
Tables Figures
◀I ▶I
◀ ▶
Back Close
Full Screen / Esc
Printer-friendly Version
Interactive Discussion

Gardner, M.: Improving the interpretation of "less than" values in environmental monitoring, Water Environ. J., 26, 285–290, 2012.
Gauss, M., Semeena, V., Benedictow, A., and Klein, H.: Transboundary Air Pollution by Main Pollutants (S, N, Ozone) and PM: The European Union, MSC-W Data Note 1/2014, available at: http://emep.int/publ/reports/2014/Country_Reports/report_EU.pdf, 2014.
Hakami, A., Harley, R. A., Milford, J. B., Odman, M. T., and Russell, A. G.: Regional, three-dimensional assessment of the ozone formation potential of organic compounds, Atmos. Environ. 38, 121–134, 2004.
Helsel, D. R.: Fabricating data: how substituting values for nondetects can ruin results, and what can be done about it, Chemosphere, 65, 2434–2439, 2006.
Jenkin, M. E.: Trends in ozone concentration distributions in the UK since 1990: local, regional and global influences, Atmos. Environ. 42, 5434–5445, 2008.
Jenkin, M. E. and Clemitshaw, K. C.: Ozone and other secondary photochemical pollutants: chemical processes governing their formation in the planetary boundary layer, Atmos. Environ. 34, 2499–2527, 2000.
Jobson, B. T., McKeen, S. A., Parrish, D. D., Fehsenfeld, F. C., Blake, D. R., Goldstein, A. H., Schauffler, S. M., and Elkins, J. C.: Trace gas mixing ratio variability versus lifetime in the troposphere and stratosphere: observations, J. Geophys. Res., 104, 16091–16113, doi:10.1029/1999jd900126, 1999.
Karl, M., Guenther, A., Köble, R., Leip, A., and Seufert, G.: A new European plant-specific emission inventory of biogenic volatile organic compounds for use in atmospheric transport models, Biogeosciences, 6, 1059–1087, doi:10.5194/bg-6-1059-2009, 2009.
Kaufman, L. and Rousseeuw, P. J.: Finding Groups in Data: An Introduction to ClusterAnalysis, Wiley, New York, 1990.
Lanz, V. A., Henne, S., Staehelin, J., Hueglin, C., Vollmer, M. K., Steinbacher, M., Buchmann, B., and Reimann, S.: Statistical analysis of anthropogenic non-methane VOC variability at a European background location (Jungfraujoch, Switzerland), Atmos. Chem. Phys., 9, 3445–3459, doi:10.5194/acp-9-3445-2009, 2009.
Laurent, A. and Hauschild, M. Z.: Impacts of NMVOC emissions on human health in European countries for 2000–2010: use of sector-specific substance profiles, Atmos. Environ. 85, 247–255, 2014.
Luecken, D. J. and Mebust, M. R.: Technical challenges involved in implementation of VOC reactivity-based control of ozone, Environ. Sci. Technol., 42, 1615–1622, 2008.

Malley, C. S., Braban, C. F., and Heal, M. R.: New directions: chemical climatology and assessment of atmospheric composition impacts, Atmos. Environ. 87, 261–264, 2014a.
Malley, C. S., Braban, C. F., and Heal, M. R.: The application of hierarchical cluster analysis and non-negative matrix factorization to European atmospheric monitoring site classification, Atmos. Res., 138, 30–40, 2014b.
Mangiameli, P., Chen, S. K., and West, D.: A comparison of SOM neural network and hierarchical clustering methods, Eur. J. Oper. Res., 93, 402–417, 1996.
Mareckova, K., Wankmueller, R., Whiting, R., and Pinterits, M.: Review of Emission Data Reported under the LRTAP Convention and NEC Directive, Stage 1 and 2 Review, Review of Emission Inventories from Shipping, Status of Gridded and LPS data, EEA and CEIP technical report, 1/2013, ISBN 978-3-99004-248-9, available at: http://www.ceip.at/review-of-inventories/review-2013/, 2013.
Martien, P. T., Harley, R. A., Milford, J. B., and Russell, A. G.: Evaluation of incremental reactivity and its uncertainty in southern California, Environ. Sci. Technol., 37, 1598–1608, 2003.
Munir, S., Chen, H., and Ropkins, K.: Quantifying temporal trends in ground level ozone concentration in the UK, Sci. Total Environ., 458, 217–227, 2013.
Oderbolz, D. C., Aksoyoglu, S., Keller, J., Barmpadimos, I., Steinbrecher, R., Skjøth, C. A., Plaß-Dülmer, C., and Prévôt, A. S. H.: A comprehensive emission inventory of biogenic volatile organic compounds in Europe: improved seasonality and land-cover, Atmos. Chem. Phys., 13, 1689–1712, doi:10.5194/acp-13-1689-2013, 2013.
Passant, N. R.: Speciation of UK Emissions of Non-Methane Volatile Organic Compounds, AEA Technology Report ENV-0545, available at: http://uk-air.defra.gov.uk/reports/empire/AEAT_ENV_0545_final_v2.pdf, Culham, Abingdon, UK, 2002.
Passant, N. R., Murrells, T. P., Pang, Y., Thistlewaite, G., H. L., V., Whiting, R., Walker, C., MacCarthy, J., Watterson, J., Hobson, M., and Misselbrook, T.: UK Informative Inventory Report (1980 to 2011), available at: http://uk-air.defra.gov.uk/reports/cat07/1303261254_UK_IIR_2013_Final.pdf, 2013.
Perry, M. and Hollis, D.: The development of a new set of long-term climate averages for the UK, Int. J. Climatol., 25, 1023–1039, doi:10.1002/joc.1160, 2005.
R Core Development Team: R: a Language and Environment for Statistical Computing, ISBN 3-900051-07-0, http://www.R-project.org, R Foundation for Statistical Computing, Vienna, Austria, 2008.

ACPD
15, 7267–7308, 2015

ACPD
15, 7267–7308, 2015

The impact of speciated VOCs on regional ozone increment derived from measurements

C. S. Malley et al.

Title Page
Abstract | Introduction
Conclusions | References
Tables | Figures
◂◂ | ▸▸
◂ | ▸
Back | Close
Full Screen / Esc
Printer-friendly Version
Interactive Discussion

REVIHAAP: Review of Evidence on Health Aspects of Air Pollution – REVIHAAP Project Technical Report, available at: http://www.euro.who.int/__data/assets/pdf_file/0004/193108/REVIHAAP-Final-technical-report-final-version.pdf, World Health Organization (WHO) Regional Office for Europe, Bonn, 2013.

RoTAP: Review of Transboundary Air Pollution: Acidification, Eutrophication, Ground Level Ozone and Heavy Metals in the UK, Contract Report to the Department for Environment, Food and Rural Affairs, Centre for Ecology and Hydrology, available at: http://www.rotap.ceh.ac.uk/sites/rotap.ceh.ac.uk/files/CEH%20RoTAP.pdf, 2012.

Sauvage, S., Plaisance, H., Locoge, N., Wroblewski, A., Coddeville, P., and Galloo, J. C.: Long term measurement and source apportionment of non-methane hydrocarbons in three French rural areas, Atmos. Environ. 43, 2430–2441, 2009.

Shao, M., Lu, S., Liu, Y., Xie, X., Chang, C., Huang, S., and Chen, Z.: Volatile organic compounds measured in summer in Beijing and their role in ground-level ozone formation, J. Geophys. Res., 114, D00G06, doi:10.1029/2008jd010863, 2009.

Simpson, D., Benedictow, A., Berge, H., Bergström, R., Emberson, L. D., Fagerli, H., Flechard, C. R., Hayman, G. D., Gauss, M., Jonson, J. E., Jenkin, M. E., Nyíri, A., Richter, C., Semeena, V. S., Tsyro, S., Tuovinen, J.-P., Valdebenito, Á., and Wind, P.: The EMEP MSC-W chemical transport model – technical description, Atmos. Chem. Phys., 12, 7825–7865, doi:10.5194/acp-12-7825-2012, 2012.

Tørseth, K., Aas, W., Breivik, K., Fjæraa, A. M., Fiebig, M., Hjellbrekke, A. G., Lund Myhre, C., Solberg, S., and Yttri, K. E.: Introduction to the European Monitoring and Evaluation Programme (EMEP) and observed atmospheric composition change during 1972–2009, Atmos. Chem. Phys., 12, 5447–5481, doi:10.5194/acp-12-5447-2012, 2012.

von Schneidemesser, E., Monks, P. S., and Plass-Duelmer, C.: Global comparison of VOC and CO observations in urban areas, Atmos. Environ. 44, 5053–5064, 2010.

von Schneidemesser, E., Monks, P. S., Gros, V., Gauduin, J., and Sanchez, O.: How important is biogenic isoprene in an urban environment? A study in London and Paris, Geophys. Res. Lett., 38, L19804, doi:10.1029/2011gl048647, 2011.

Yates, E. L., Derwent, R. G., Simmonds, P. G., Greally, B. R., O'Doherty, S., and Shallcross, D. E.: The seasonal cycles and photochemistry of C-2–C-5 alkanes at Mace Head, Atmos. Environ. 44, 2705–2713, 2010.

Yuan, B., Shao, M., de Gouw, J., Parrish, D. D., Lu, S., Wang, M., Zeng, L., Zhang, Q., Song, Y., Zhang, J., and Hu, M.: Volatile organic compounds (VOCs) in urban air: how chemistry affects the interpretation of positive matrix factorization (PMF) analysis, J. Geophys. Res., 117, D24302, doi:10.1029/2012jd018236, 2012.

ACPD
15, 7267–7308, 2015

The impact of speciated VOCs on regional ozone increment derived from measurements

C. S. Malley et al.

Title Page
Abstract Introduction
Conclusions References
Tables Figures
◀◀ ▶▶
◀ ▶
Back Close
Full Screen / Esc
Printer-friendly Version
Interactive Discussion

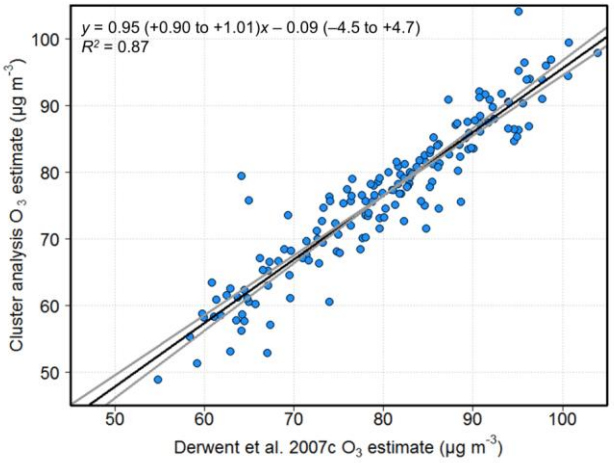

Figure 1. Correlation between monthly hemispheric background O_3 concentrations derived by Derwent et al. (2007c) using pollutant tracers and atmospheric modelling to select "clean" air masses, and derived by the method described in Sect. 2.1 using cluster analysis. Black regression line is calculated by the ordinary least squares (OLS) method, with confidence intervals (95th percent) shown in grey.

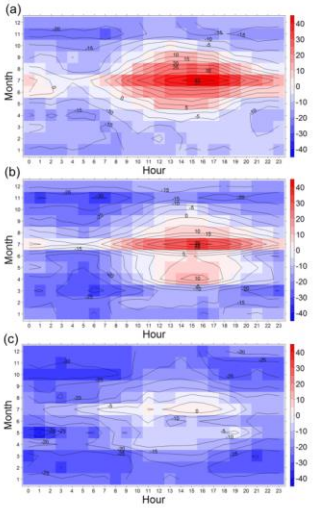

Figure 2. Monthly-hourly average differences between hemispheric background O_3 and regional background O_3 concentrations ($\mu g\,m^{-3}$) for **(a)** 2001 and **(b)** 2011 in south-east England, the area for which Harwell is representative, and **(c)** the difference between hemispheric and measured O_3 concentrations for 2012 at Auchencorth.

Discussion Paper | Discussion Paper | Discussion Paper | Discussion Paper |
ACPD
15, 7267–7308, 2015
The impact of speciated VOCs on regional ozone increment derived from measurements
C. S. Malley et al.
Title Page
Abstract Introduction
Conclusions References
Tables Figures
◀I ▶I
◀ ▶
Back Close
Full Screen / Esc
Printer-friendly Version
Interactive Discussion

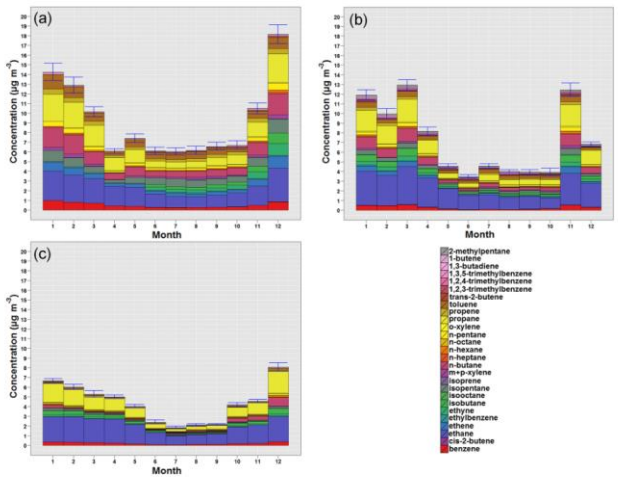

Figure 3. Stacked barchart of median VOC concentrations at **(a)** Harwell 2001, **(b)** Harwell 2011, and **(c)** Auchencorth 2012. The error bars show the sum of the 95th percentile confidence interval in the median VOC concentrations. This represents the error introduced by representing the dataset with the chosen fitted distribution (see text).

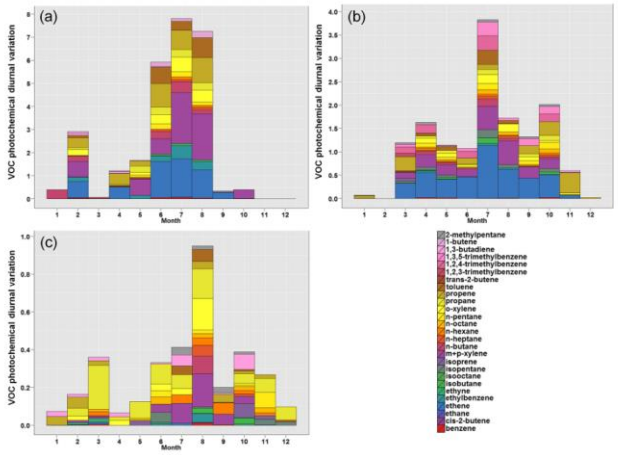

Figure 4. Monthly variation in VOC diurnal photochemical reactivity as defined by the difference between night (average of 1–5 a.m.) and afternoon (1–5 p.m.) POCP-weighted VOC/ethane ratios for **(a)** Harwell 2001, **(b)** Harwell 2011, and **(c)** Auchencorth 2011. Note the very different vertical scales.

ACPD
15, 7267–7308, 2015

The impact of speciated VOCs on regional ozone increment derived from measurements

C. S. Malley et al.

ACPD
15, 7267–7308, 2015

The impact of speciated VOCs on regional ozone increment derived from measurements

C. S. Malley et al.

Title Page
Abstract | Introduction
Conclusions | References
Tables | Figures
◀| |▶
◀ ▶
Back | Close
Full Screen / Esc
Printer-friendly Version
Interactive Discussion

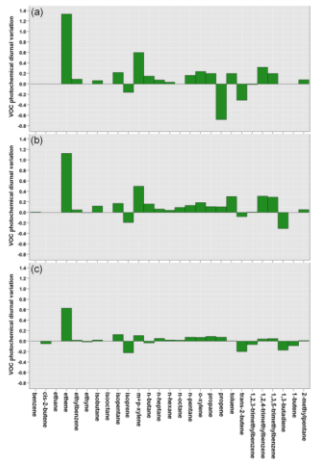

Figure 5. Individual VOC diurnal photochemical reactivity as defined by the difference between night (average of 1–5 a.m.) and afternoon (1–5 p.m.) POCP-weighted VOC/ethane ratios for **(a)** June 2010, **(b)** July 2011 and **(c)** July 2012, at Harwell. These months correspond to the periods of annual maximum regional O_3 increment at Harwell (see Fig. 2).

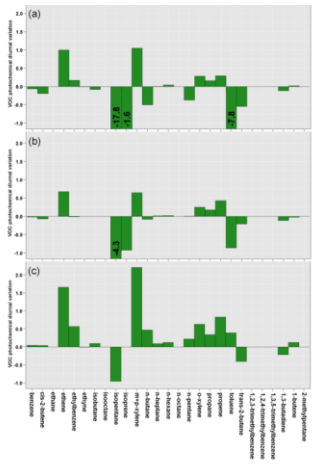

Figure 6. Individual VOC diurnal photochemical reactivity as defined by the difference between night (average of 1–5 a.m.) and afternoon (1–5 p.m.) POCP-weighted VOC/ethane ratios in **(a)** July 1999, **(b)** July 2000 and **(c)** July 2001, at Harwell. These months correspond to the periods of annual maximum regional O_3 increment. To emphasise the positive contributions to VOC photochemical cycling, the negative values have been truncated.

ACPD
15, 7267–7308, 2015

ACPD
15, 7267–7308, 2015

The impact of speciated VOCs on regional ozone increment derived from measurements

C. S. Malley et al.

Title Page
Abstract | Introduction
Conclusions | References
Tables | Figures
◀| |▶
◀ ▶
Back | Close
Full Screen / Esc
Printer-friendly Version
Interactive Discussion

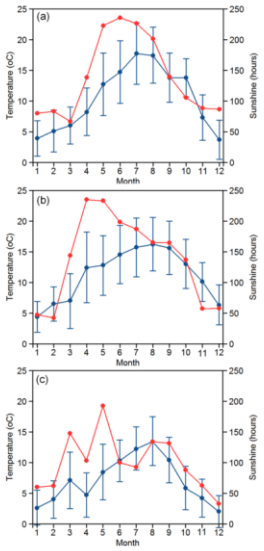

Figure 7. Average monthly mean temperatures (blue, maximum and minimum temperatures shown as whiskers) and hours of sunshine (red) from the UK Meteorological Office (http://www.metoffice.gov.uk/climate/uk/datasets/#) for **(a)** South East and Central South England 2001, **(b)** South East and Central South England 2011 and **(c)** East Scotland 2012.

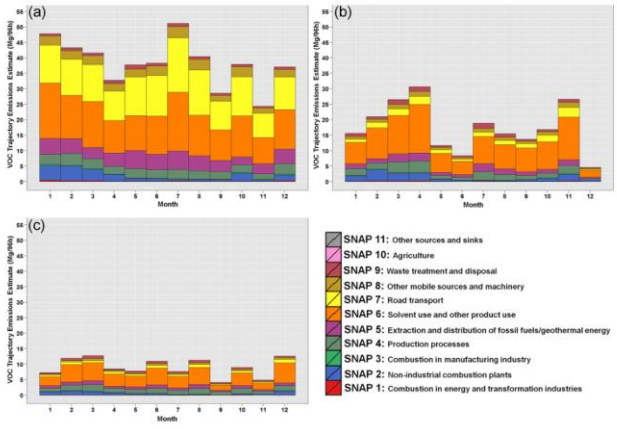

Figure 8. Monthly average VOC 96 h back-trajectory emissions estimates prior to its arrival at the receptor site, disaggregated into 11 SNAP source sectors for **(a)** Harwell 2001, **(b)** 2011 Harwell, and **(c)** Auchencorth 2012.

ACPD
15, 7267–7308, 2015

ACPD
15, 7267–7308, 2015

The impact of speciated VOCs on regional ozone increment derived from measurements

C. S. Malley et al.

Title Page
Abstract | Introduction
Conclusions | References
Tables | Figures
◀◀ | ▶▶
◀ | ▶
Back | Close
Full Screen / Esc
Printer-friendly Version
Interactive Discussion

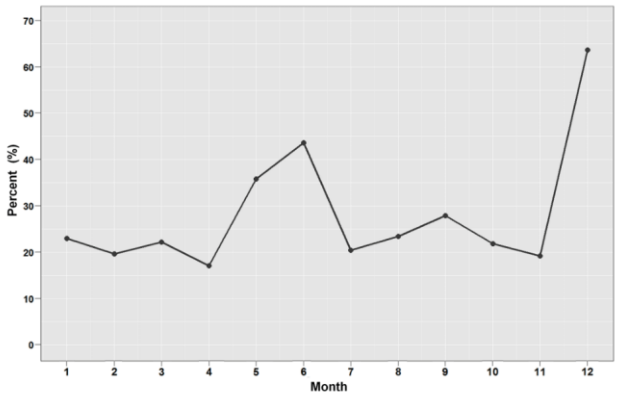

Figure 9. Proportion of average VOC 96 h back-trajectory emissions estimate for Harwell, 2011, emitted in the final 4 h before arrival over the emission grid containing Harwell.

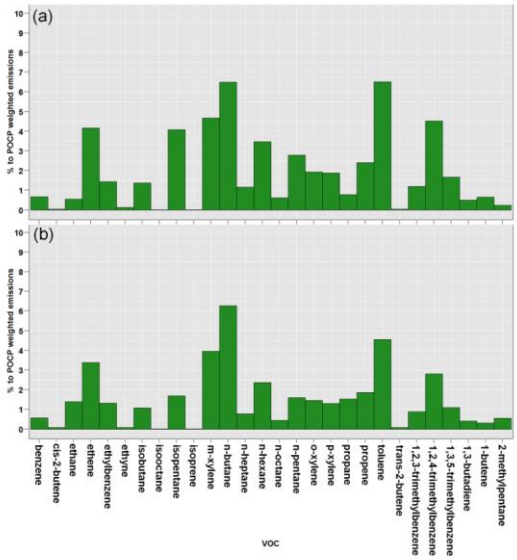

Figure 10. Speciation of average VOC back-trajectory emissions estimates in **(a)** July 2001, and **(b)** July 2011 at Harwell. The speciation was based on source profiles catalogued in Passant (2002) and the relative contribution of individual activities to annual total VOC emissions.

ACPD
15, 7267–7308, 2015

The impact of speciated VOCs on regional ozone increment derived from measurements

C. S. Malley et al.

Title Page
Abstract Introduction
Conclusions References
Tables Figures
◀| |▶
◀ ▶
Back Close
Full Screen / Esc
Printer-friendly Version
Interactive Discussion

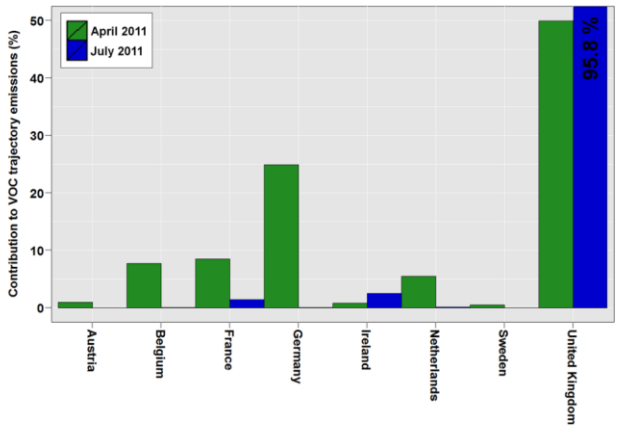

Figure 11. Contributions to the average VOC 96 h back-trajectory emission estimates in April 2011 (green bars) and July 2011 (blue bars) from countries which contributed at least 0.5 % during one of the months. The contribution of the UK in July 2011 was 95.8 %, and has been truncated in the plot.

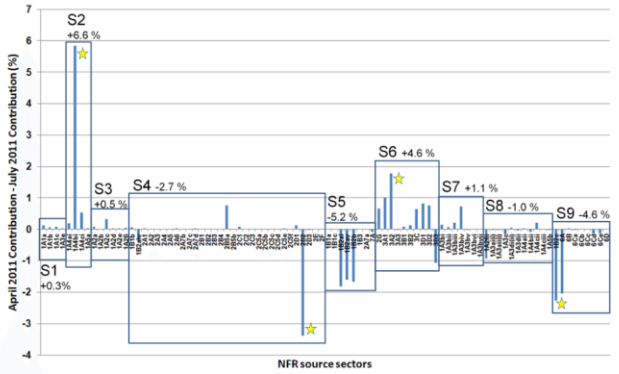

Figure 12. Difference between NFR source sector contributions to average VOC back trajectory emission estimates (VOC TEE) in April and July 2011 at Harwell. Also shown are the changes in contribution of the SNAP source sectors. These were calculated from the VOC TEE prior to disaggregation, and do not represent the sum of the contribution changes of the constituent NFR source sectors. The source sectors identified by stars have the largest changes between April and July (Sect. 3.3.2).

ACPD
15, 7267–7308, 2015

ACPD
15, 7267–7308, 2015

The impact of speciated VOCs on regional ozone increment derived from measurements

C. S. Malley et al.

Title Page
Abstract | Introduction
Conclusions | References
Tables | Figures
◀| |▶
◀ ▶
Back | Close
Full Screen / Esc
Printer-friendly Version
Interactive Discussion